37

NUSC Technical Report 4331

The Response of Cable-Moored Axisymmetric Buoys To Ocean Wave Excitation

KIRK T. PATTON
Ocean Science Department

15 June 1972

NAVAL UNDERWATER SYSTEMS CENTER

Details of illustrations in this document may be better studied on microfiche

Approved for public release; distribution unlimited.

Hob

ADMINISTRATIVE INFORMATION

This study was prepared originally as a dissertation in partial fulfillment of the requirements for the degree of Doctor of Philosophy in Mechanical Engineering at the University of Rhode Island. The work was accomplished under NUSC Project No. A-071-00-00, "Buoy Dynamics," Principal Investigator, K. T. Patton (Code TA12), and Navy Subproject and Task No. ZR-001-01-611-1N, Program Manager, Dr. J. H. Huth (DLP/MAT 03L4).

REVIEWED AND APPROVED: 15 June 1972

W. A. Von Winkle
Director of Science and Technology

Inquiries concerning this report may be addressed to the author,
New London Laboratory, Naval Underwater Systems Center,
New London, Connecticut 06320

UNCLASSIFIED
Security Classification

DOCUMENT CONTROL DATA - R & D

(Security classification of title, body of abstract and indexing annotation must be entered when the overall report is classified)

1. ORIGINATING ACTIVITY (Corporate author) Naval Underwater Systems Center Newport, Rhode Island 02840	2a. REPORT SECURITY CLASSIFICATION UNCLASSIFIED 2b. GROUP

3. REPORT TITLE

THE RESPONSE OF CABLE-MOORED AXISYMMETRIC BUOYS TO OCEAN WAVE EXCITATION

4. DESCRIPTIVE NOTES (Type of report and inclusive dates)

Research Report

5. AUTHOR(S) (First name, middle initial, last name)

Kirk T. Patton

6. REPORT DATE	7a. TOTAL NO. OF PAGES	7b. NO. OF REFS
15 June 1972	402	87

8a. CONTRACT OR GRANT NO.	9a. ORIGINATOR'S REPORT NUMBER(S)
b. PROJECT NO. A-071-00-00	4331
c. ZR-011-01-01-611-1N	9b. OTHER REPORT NO(S) (Any other numbers that may be assigned this report)
d.	

10. DISTRIBUTION STATEMENT

Approved for public release; distribution unlimited

11. SUPPLEMENTARY NOTES	12. SPONSORING MILITARY ACTIVITY
	Department of the Navy

13. ABSTRACT

Forces and motions imposed upon a moored buoy system by the oceanic environment are investigated using numerical methods on a digital computer. Equations of motion for axisymmetric buoys are developed for six degrees of freedom including cross-coupled hydrostatic and hydrodynamic forces. Equations of motion for the mooring cable are developed to allow simultaneous axial and transverse wave propagation. A unique method of characteristics numerical technique is shown for digital computer simulation of cable dynamics. The equations of motion for the buoy and its mooring cable are coupled and are excited by winds, currents, and a quasi-random wind wave model. Simulated buoy system parameter response characteristics are compared with response characteristics observed from actual oceanographic buoy system moorings. This comparison indicates that steady state buoy system forces and configurations can be predicted within 5 percent and that dynamic motions can be predicted within 50 percent using the digital computer simulation.

DD FORM 1473 (PAGE 1)
1 NOV 65

S/N 0102-014-6600

UNCLASSIFIED
Security Classification

14 KEY WORDS	LINK A		LINK B		LINK C	
	ROLE	WT	ROLE	WT	ROLE	WT
Ocean Buoys						
Axisymmetric Buoys						
Moored Buoys						

ABSTRACT

Motions and dynamic forces imposed upon a moored buoy system by the oceanic environment are of vital interest to the user of the system. If instrumentation for monitoring the environment is motion sensitive, it is of little value if its response to platform motion is greater than its response to the changing environment. The buoy system designer is also concerned with motions and forces in buoy systems in order to design for the highest probability of system survival under extreme conditions.

In response to these needs, this study investigates digital computer simulation of buoy system dynamics for simple buoy systems, i.e., a surface buoy moored on a single mooring line. The buoy system can be excited by winds, waves, and currents. Winds can act from any compass direction, and currents can vary in strength and direction as a function of depth in the water column. Wind waves are simulated by first computing their properties with the Sverdrup-Munk-Bretschneider method and then by using Borgman's energy partitioning scheme on a two-parameter Bretschneider spectrum to compute component sine wave amplitudes and frequencies. Since the component Stokesian waves are linear, the principle of superposition can be used to sum component magnitudes in order to compute water particle motions.

Equations of motion for the buoy are developed for six degrees of freedom--three translational and three rotational. Hydrostatic and hydrodynamic forces

and moments acting on an oblate spheroid moving on the free surface of an infinite body of water are investigated in detail. The set of integro-differential equations for buoy motions are reduced to a set of nonlinear, ordinary differential equations with nonconstant coefficients by using the Haskind hypothesis to evaluate the hydrodynamic force and moment integrals and to represent them as frequency dependent coefficients. Buoy motions are coupled through hydrostatic, hydrodynamic, and mooring line forces.

Cable dynamics are also investigated. A set of coupled, hyperbolic, partial differential equations for cable motions are developed, and characteristic equations are derived to effect a method of characteristics solution. A unique numerical method of characteristics technique, based upon Hartree's method, is developed for the solution of the cable equations in the time-space domain. Buoy motions, which are dependent upon the cable tensions, serve as the upper boundary conditions. Lower boundary conditions are prescribed at the anchor, where there can be no motion.

For certain buoy systems, where many mass discontinuities exist along the cable, or for shallow water moorings, where slack cable conditions can exist, a lumped-mass method of computing cable dynamics is developed as opposed to the finite-difference method just described. In general, for cable dynamics the lumped-mass numerical method is an order of magnitude faster in computation time than the finite difference method.

The equations of motion developed for the buoy were solved numerically in the time domain using a fourth-order, Runge-Kutta integration method. Cable equations can be solved either by finite-difference methods or by integrating with the Runge-Kutta algorithm for the lumped-mass model.

In order to validate the numerical models developed, two buoy systems were instrumented and deployed in Block Island Sound. The motion data from these experiments, along with data published in the literature, are compared with simulated buoy motion data. This comparison indicates that steady-state buoy system forces and configurations can be predicted within approximately 5 percent and that buoy system dynamics can be predicted within approximately 50 percent. There are some indications that the surge and sway hydrodynamic forces acting on the buoy are being underestimated by the computer model.

ACKNOWLEDGMENTS

I am grateful to the Faculty of the Mechanical Engineering and Applied Mechanics Department and of the Ocean Engineering Department at the University of Rhode Island for their continuing inspiration and guidance. In particular, I would like to thank my advisor, Dr. Rodger B. Dowdell and the members of my dissertation committee, Drs. Charles D. Nash and Everett E. McEwen.

This research would not have been possible without the support of my colleagues at the Naval Underwater Systems Center. Many helpful discussions were held with Dr. Robert G. Williams, Messrs. Stanley L. Rupinski, Louis F. DiRienzo, and Gary T. Griffin. The instrumentation and telemetry circuitry were designed and constructed by Mr. George F. Battista. Field support was offered by Messrs. Hector F. Bernier and Carl T. Milner, of the BIFI acoustic range.

The buoys were installed and removed through the efforts of Lt. Robert B. Doughty, Master, and the crew of the U.S. Coast Guard buoy tender, REDWOOD. The many trips required to inspect and service the buoys were made possible by Dr. Andrew J. Nalwalk, of the University of Connecticut, and Oram A. Campbell, Master of the R/V UCONN and his crew.

I am thankful for the support I received from the Naval Underwater Systems Center under the Advanced Professional Development Program and from my supervisor, Mr. Kenneth L. Moothart. Support for the research was furnished by NUSC Project A-071-00-00, "Buoy Dynamics," Principal Investigator, Kirk T. Patton (Code TA12), and Navy Subproject and Task ZR-011-01-01-611-1N, Program Manager, Dr. J. H. Huth (DLP/MAT 03L4).

TABLE OF CONTENTS

TABLE OF CONTENTS (Cont'd)

LIST OF TABLES

LIST OF ILLUSTRATIONS

LIST OF ILLUSTRATIONS (Cont'd)

LIST OF ILLUSTRATIONS (Cont'd)

LIST OF ILLUSTRATIONS (Cont'd)

LIST OF ILLUSTRATIONS (Cont'd)

LIST OF ILLUSTRATIONS (Cont'd)

LIST OF SYMBOLS AND NOTATIONS

Buoy Dynamics

a	Spheroid minor half-diameter
a	Frequency parameter
A	Transform matrix from inertial to cable coordinates
A_H	Plan area of immersed buoy volume
A_s	Profile area of immersed buoy volume
A_1	Buoy windage — profile area above free surface
A_2	Plan area of buoy
b	Spheroid major half-diameter
B	Hydrostatic force vector
C_D	Buoy hull drag coefficient
CV	Current component in y direction
CW	Current component in z direction
C_L	Buoy hull lift coefficient
d	Spheroid buoyant force moment arm
d	Viscous drag force component
D	Viscous drag force vector
D	Wind duration
$\overline{D}$	Dimensionless duration parameter
e	2.7182 . . .

Buoy Dynamics (Cont'd)

F	Fetch
F_D	Force vector on an immersed body B
$\overline{F}$	Dimensionless fetch parameter
F_1	Dimensionless wave height parameter for Bretschneider spectra
F_2	Dimensionless wave period parameter for Bretschneider spectra
g	Gravitation constant
G	Gravity vector
G_D	Moments on an immersed body B
H	Hydrodynamic force vector
H_D	Buoy draft
H	Angular wave damping coefficient
H_{CB}	Height of center of buoyancy below free surface
H_{CG}	Height of center of gravity
H_{CP}	Height of center of pressure
H_{ML}	Height of the center of gravity of the buoy above mooring line termination
H_w	Height of wind center of pressure from center of gravity
$H_{1/3}$	Significant wave height
$\overline{H}$	Dimensionless significant wave height parameter
i	$\sqrt{-1}$
I	Structural mass moment of inertia
I	Hydrodynamic mass moment of inertia coefficient
I^A	Area of the intersection of a body B with the free surface

Buoy Dynamics (Cont'd)

I_x^A, I_y^A	Moments of I^A about vertical planes
J_o	Bessel function of first kind of order 0
K	Wave number
L	Wind lift force
m	Structural mass of the buoy
M	Structural mass matrix
M	Hydrodynamic mass coefficient
M_h	Hydrodynamic mass dyadic
M_β	Pitch buoyant moment
M_γ	Roll buoyant moment
n	Unit normal to immersed surface of body B
N	Wave damping coefficient
N	Wave damping dyadic
P_k	Components of unit normal n
q_k	Components of moment of n about center of gravity of body B
Q	Displacement vector of the buoy center of gravity
$\bar{r}$	Position vector of a point on the immersed surface of body B
R	Coordinate system center
Re	Reynold's number
S	Immersed surface of body B
S_o	Struve function of order 0
t	Time
T	Mooring line tension vector

Buoy Dynamics (Cont'd)

u_j	Pressure function
u, v, w	Velocity components of the buoy center of gravity
V	Wind velocity vector.
W	Wind force vector
W_D	Wind drag force on buoy
W_L	Wind lift force on buoy
WV	Wind velocity components
x, y, z	Spatial coordinates
Yo	Bessel function of second kind of order 0
α	Yaw angle
β	Pitch angle
β	Dimensionless frequency
γ	Roll angle
ϵ	Wave component phase angle
η	Instantaneous free surface height below mean free surface
θ	Cable tilt angle
θ	Rotation vector
θ', θ'', θ'''	Angular displacements of body B
λ	Wavelength
μ	Absolute viscosity
ν	Kinematic viscosity
ξ	Instantaneous wave surface slope
π	3.1416 . . .

Buoy Dynamics (Cont'd)

ρ	Fluid mass density
ρ_A	Air mass density
σ	Angular frequency of buoy motion
$\tau_{1/3}$	Significant wave period
$\bar{\tau}$	Dimensionless significant period parameter
ϕ	Cable transverse tilt angle
$\Phi(s, y, z; t)$	Velocity potential
ω	Angular frequency of wind waves
Ω	Buoy rotation matrix

Subscripts

d	Viscous drag
D	Drag
h	Hydrodynamic
i	Coordinate system
L	Lift
max.	Maximum
min.	Minimum
o	Static position
og	Static position of center of gravity
S	Surface
w	Wave
x, y, z	Coordinate directions
α, β, γ	Buoy rotations
1/3	Statistically significant

Cable Dynamics

a	Cable section radius
A	Transform matrix from inertial to cable coordinates
C_{DN}	Normal drag coefficient
C_{DT}	Tangential drag coefficient
Ch	Characteristic velocity
C_s	Current velocity vector
d	Cable diameter
D	Viscous drag
F_H	Hydrodynamic inertia force
g	Gravitational constant
G	Cable loading function
h	Node separation in grid
H	Cable loading function
$\hat{i}, \hat{j}, \hat{k}$	Direction indices
I	Cable loading function
k	Time step size in grid
K	Linearized tension - strain derivative
m_h	Hydrodynamic mass
$\vec{Q}$	Force vector on a cable segment
$\vec{r}$	Vector from origin to point on cable
Re	Reynolds number
S	Stokes number
t	Time
$\vec{T}$	Tension vector

Cable Dynamics (Cont'd)

U, V, W	Velocity components
w_c	Cable in-water weight per unit length
x, y, z	Spatial coordinates
X, Y, Z	Force components on cable
ϵ	Strain
θ	Cable tilt angle
λ	Characteristic velocities
μ	Cable structural mass per unit length
ν	Kinematic viscosity
π	3.1416 . . .
ρ	Fluid mass density
ϕ	Cable transverse tilt angle
ω	Angular frequency of oscillation

Subscripts

A	Point (i, j) in time-space grid
B	Point (i-1, j) in time-space grid
B	Buoy
C	Point (i-1, j-1) in time-space grid
D	Point (i+1, j) in time-space grid
E	Point (i, j-1) in time-space grid
F	Point i+1, j-1) in time-space grid
H	High
i	Space

Subscripts (Cont'd)

j	Time
L	Low
N	Normal
P_1	Point between B-A in grid for tensile characteristic
P_2	Point between A-D in grid for tensile characteristic
Q_1	Point between B-A in grid for transverse characteristic
Q_2	Point between A-D in grid for transverse characteristic
R	Point (i, j+1) in time-space grid
S	Current velocity
T	Tangential

I. INTRODUCTION

Clean, green, windy billows notching out the sky,
Grey clouds tattered into rags, sea-winds blowing high,
And the ships under topsails, beating, thrashing by,
    And the mewing of the herring gulls.

Dancing, flashing green seas shaking white locks,
Boiling in blind eddies over hidden rocks,
And the wind in the rigging, the creaking of the blocks,
    And the straining of the timber hulls.

John Masefield
"Cardigan Bay"

This study is concerned with the analysis and simulation of the dynamics of simple oceanic buoy systems. The analysis must include the effect of the significant forces that act on the buoy system and are imposed by the ocean environment — wind, waves, and currents. Because of the highly nonlinear nature of the problem, numerical methods are favored in order to provide a realistic simulation.

Buoys have been employed by mariners for centuries as aids to navigation and to support mooring chains. In this country, navigational buoys were in service in the Delaware River in 1767 and in Boston Harbor by 1808. At present, the United States Coast Guard maintains over 24,000 buoys in the navigable waters of the United States and its possessions. Navigational buoy system design is largely a matter of employing "rules of thumb" evolved over decades of experience with these buoys. The vast majority of navigational buoys are moored in waters less than 100 ft deep, and the most common cause of failure is collision with a vessel. Thus, these buoy systems are characterized by massive steel buoys moored with heavy chain to large concrete clumps. They are serviced on a regular basis and are recovered and overhauled annually.

In recent years, oceanographers have used buoy systems to support current meters, thermistor chains, and other oceanographic instrumentation. The state of the art in oceanography has advanced to the point where oceanographers are no longer satisfied with data taken at a single point over a rather short time duration. Multiple measurements to be made simultaneously over wide areas of the ocean or long-duration measurements are made most economically with a buoy system equipped with self-recording or telemetering instrumentation. This economy can be realized only if the buoy system is designed to have a life on station greater than the desired measurement time.

The basic design philosophy of deep-sea oceanographic buoy systems is quite different from that of the navigational buoys. Oceanographic vessels are usually small and are not equipped for handling heavy objects over the side at sea; thus, the buoys and mooring line components must be of relatively light weight. The mooring lines are miles long and thus preclude the use of heavy chains (except at the bottom) and tend to be made up of light, high-strength wire ropes or of synthetic fiber ropes. Designers of oceanographic buoy systems are faced with the near-impossible task of designing a lightweight, highly compliant structure to survive for periods of a year or more in one of the harshest environments known to man.

Isaacs[1] describes a mean time between failure (MTBF) of 121 days for the taut-moored Scripps Institution of Oceanography "Catamaran" buoys. The observed system failures were due to parting of the nylon mooring line near the surface. The writers hypothesize that high tensile loads in the nylon line are caused by tensile waves propagating up and down the cable. Richardson[2] of theWoods Hole Oceanographic Institution (WHOI), anchored 106 buoy systems between Cape Cod and Bermuda. The MTBF for these systems was found to be about 90 days. The WHOI buoy system failures were attributed to mooring line failures, fish bite of synthetic mooring lines, and theft. In 1967, WHOI[3] set nine long term buoy moorings of which only one was recovered on station after 60 days. Three of these were found adrift. WHOI was more successful in 1968,[4] when only 3 of 14 long-term buoy moorings failed.

All the oceanographic buoy systems described above were taut-moored systems, the majority of which utilized synthetic rope in their mooring lines. Their short life on station and their low recovery rate indicate a need for an accurate engineering method of computing the dynamic response of the buoy system to the ocean environment.

Slack moored buoy systems have a much greater MTBF and are more reliable. The catenary of the mooring line provides the necessary compliance; thus, dynamic tensions in the mooring line are reduced. Navigational buoy systems are slack moored and are very reliable. Smith[5] cites a long history of successful moorings in the Gulf of Mexico for the NOMAD buoy system. Over a 5-year period, a number of the NOMAD buoys were kept on station for periods of a year or more. Smith also describes fifteen, 25-ton barges that were slack moored for 8 months in water depths over 12,000 ft with no failures.

Oceanographers are also concerned with the effects of buoy system motions on their instrumentation. For example, instrumentation fastened to the mooring line of a slack-moored system will undergo depth excursions that are dependent on the current structure. Webster[6,7] discusses errors in self-recording current meter data due to buoy system motion. Webster shows a current energy spectrum developed from a current meter that is attached to the mooring line of a buoy system (figure 1). The energy introduced into the current data by the buoy system motions is far greater than the energy of the currents themselves.

Marcus[8] compared anemometer data taken from a NOMAD buoy in the Gulf of Mexico with other meteorological observations in the area over a 6-month period. The mean error of the wind speed data was 0.2 knot with a standard deviation of the error of ± 4.67 knots. Huff[9] shows a power spectrum of anemometer data taken from another NOMAD buoy system moored off Bermuda. This spectrum (figure 2) indicates that a large amount of energy was introduced into the spectrum by the motion of the buoy. Huff also shows an increase in the average wind speed deviation from the mean with increasing mean wind speed that levels out at high wind speeds. This variation is characteristic of sea surface slopes, which have an upper limit due to gravity. This upper limit implies that the wind speed error is due to the pitch and roll motions of the buoy. Day[10] found that wind data sampled every 10 min from a

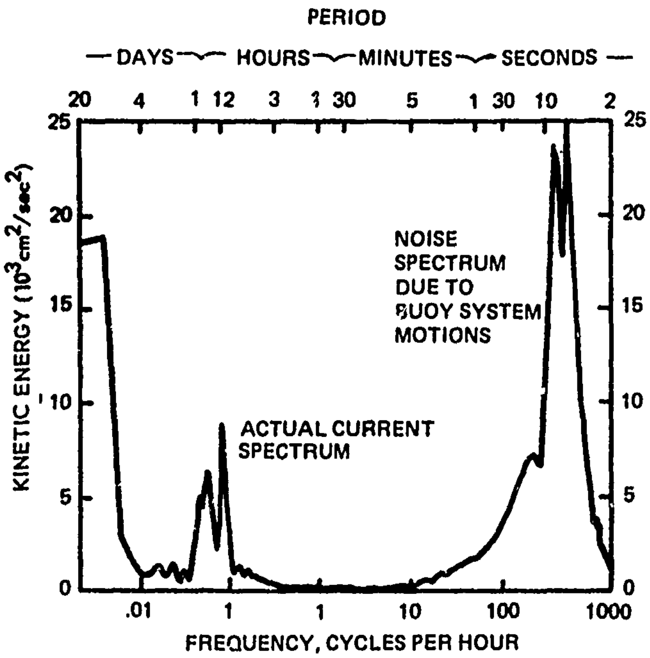

Figure 1. A Current Meter Energy Spectrum
(From Webster, reference 7.)

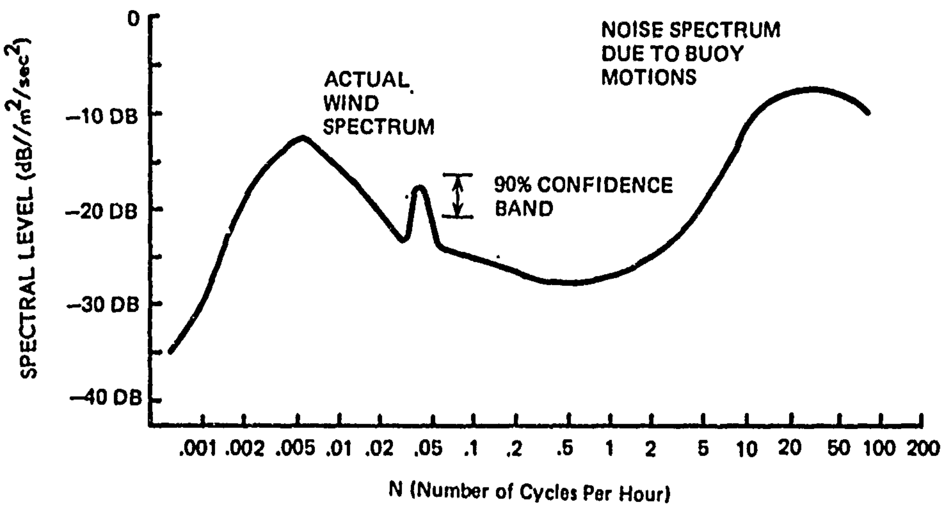

Figure 2. An Anemometer Power Spectrum
(From Webster, reference 9.)

buoy-mounted anemometer had to be time averaged over a 2-hr period to remove errors due to buoy motions.

The two-dimensional, steady-state configurations of buoy cable systems have been investigated by Wilson.[11,12] Wilson constrained the upper end of the cable to be at the mean ocean surface and did not consider cable elasticity. Patton,[13] as part of this dissertation research, developed a numerical method to determine the equilibrium configuration of buoy cable systems. The three-dimensional configuration for any current structure (currents may vary in strength and direction as a function of depth), as well as the buoy draft, is computed. The elasticity of the cable is considered and the stretch is also computed. Martin[14] developed a numerical method similar to Patton's, but it is restricted to two dimensions. Martin also experimentally investigated the elastic properties of nylon rope and the drag of buoy models. Smith[5] presented a graphical method for two-dimensional buoy system configurations but neglected tangential drag and elasticity.

The study of the motions of bodies floating on the ocean surface and being excited by waves originated in 1749 with Euler[15] in his classic work, Scientia Navalis. Froude[16] was concerned with the rolling and roll stability of ships. Froude recognized the nonlinearity of the problem and included viscous resistance in the equations of motion. Kriloff[17] investigated ship motions and wrote coupled equations of motion. Both Froude and Kriloff assumed that the ship did not influence the waves, which allowed them to treat the hydrodynamic properties of the ship as a body oscillating on a free surface. By far, the single greatest problem in ship dynamics is the description of the hydrodynamic forces acting on the ship. Lewis[18] introduced the "strip theory" in 1929,wh... allowed computation of three-dimensional hydrodynamic characteristics from two-dimensional theory. Haskind[19,21] assumed that the hydrodynamic equations could be linearized in such a manner that velocity potentials could be superimposed. This method allowed the use of three velocity potentials: (1) incident wave potential, i.e., the velocity potential of the waves alone; (2) diffracted wave potential, i.e., the velocity potential of the body fixed on a free surface exposed to waves; and (3) forced heave potential, i.e., the velocity potential of the body oscillating in still water. Naval architects currently favor the Haskind hypothesis as opposed to the earlier Froude-Kriloff hypothesis, which assumes that body dimensions are small compared with the waves.

John[22,23] wrote complete sets of coupled equations of motion for floating bodies in harmonic waves and considered the influence of the body on the waves (after Haskind). John also included an external force term that could be used to describe a mooring cable. Heave and surge motions of a sphere were computed for various wave frequencies.

St. Denis and Pierson[24] linearized the decoupled equations of motion for a ship and investigated ship motions in confused seas by summing the ship's responses to sine wave seas of different frequencies. Korvin-Kroukovsky[25-27] used the "strip" method to compute the hydrodynamic characteristics of the ship and included cross-coupled hydrodynamic forces. A complete discussion of the state of the art in the prediction of ship motions is presented in the proceedings of the fifth symposium on naval hydrodynamics.[28] Current research indicates that cross-coupled hydrodynamic forces are the same order of magnitude as other hydrodynamic forces and can not be neglected.

A large oceanographic buoy was built in 1965 by General Dynamics/ Convair Division. As part of the design process,[29] model tests were conducted in a towing tank for various buoy hull shapes, and buoy motions were simulated on an analog computer. The analog computer simulation considered the dynamics of the planar motions of the buoy alone; the mooring line was treated as an elastic spring. The following quote is from reference 29:

> The simulation was not fully successful; some results are considered inconclusive. Due to the difficulty in obtaining reasonable agreement with the model data, the analog computer study was terminated short of its goal.

The 40-ft-diameter "MONSTER" buoy described in reference 29 has proven to be a successful ocean data station. At sea motions of this buoy are described by Devereux[30] and Uyeda.[31] Gaul and Brown[32] correlated buoy heave acceleration power spectra from the "MONSTER" buoy and from a small wave sensing buoy.

Paquette[33] developed a two-dimensional, lumped-mass analog computer model for buoy system dynamics. The buoy was assumed to follow an elliptical orbit (major axis vertical and equal to the wave height), and its motions were not integrated as part of the system dynamics. The lumped-mass cable elements were acted upon by tensions on adjacent elements, weight and buoyancy forces, and velocity-squared drag forces. Cable hydrodynamic masses and linear damping forces were neglected. Paquette concluded that at least ten mass elements are needed for a deep-sea mooring line to adequately describe the system dynamics in the band of ocean wave frequencies that were considered (0 to 0.5 Hz). The coupling of tensile waves into transverse waves due to the steady-state curvature of the cable was also noted.

Bivens and Swann[34] also developed a two-dimensional, lumped-mass simulation of buoy system dynamics but included the buoy dynamics. However, hydrodynamic cross-coupled terms were neglected. Rudnick[35] measured motions of the "FLIP" spar buoy at sea and compared motion power spectra with the power spectra predicted from a linear, decoupled buoy motion model. Blumberg and Osborn[36] developed a digital computer simulation for submerged buoy motions. The mooring line was considered to be a rigid, massless, and dragless link. Hydrodynamic forces acting on the buoy included no cross-coupled terms, and the equations of motion were linearized. Millard[37] describes tension measurements made at sea as part of the Woods Hole Oceanographic Institution buoy reliability program. Tension amplitudes were correlated with recorded currents and wind speeds. Millard's data indicate that the tension amplitudes are attenuated with length down the mooring cable. A very comprehensive study of buoy system dynamics has been conducted by Prof. Nath, of Oregon State University.[38] The two-dimensional motions of a buoy and its mooring cable were considered. Buoy motions were solved by use of recurrence formulas and served as boundary conditions for the cable. Cable dynamics were solved by using a numerical method of characteristics solution.

Hydrodynamic forces acting on the buoy and cable were included,and nonlinear stress-strain properties of the cable were used. Transfer functions between wave spectra and line tension spectra along the cable were developed and compared with MONSTER buoy data.

Hsu and Blenkarn[39] utilized momentum flux equations to compute the hydrodynamic forces acting on a moored ship. Equations of motion were solved numerically, and the mooring lines were considered as elastic springs. Each wave was assumed to impart an impulse; thus, the forcing function was composed of a series of impulses acting on the ship. Burke[40] assumed that a set of linear response functions for the vessel were known and developed sets of statistical relations for vessel motions in a random sea. This technique was applied to predict drilling vessel motions, and the results were compared with drilling vessel motions recorded at sea.

The present investigation has produced a three-dimensional, numerical model for buoy system dynamics. The model includes cross-coupled hydrodynamic forces and can be excited by wind, current, and wave forces. Cable dynamics are investigated with both finite-element (lumped masses) and finite-difference (distributed mass) methods. In this study, finite-element methods were found to be attractive because of their relative economy with regard to numerical computational time. Finite-difference methods, while more rigorous, are more involved numerically and require relatively large amounts of computer time.

The deterministic model is excited by a numerical wave model having the same spectral characteristics as the ocean waves. The computed buoy system response is then sampled to provide motion spectra by using Fast Fourier Transform (FFT) techniques.

To validate the model, two oceanographic buoys were equipped with motion sensing instrumentation and installed in Block Island Sound. Buoy motions were monitored and recorded for various wind, current, and wave conditions. These data are compared with buoy motions computed with the numerical model for the same environmental conditions.

II. PROCEDURE

In order to predi^t the response of the buoy system (figure 3) to the ocean environment, a deterministic model of the system dynamics must be constructed and excited by a random model of the oceanic conditions. The two major structural components of the system (the buoy and the mooring line) are treated separately and then are combined to form the deterministic buoy system model.

2.1 System Dynamics

Buoy motions can be described by the equations of motion for a body with six degrees of freedom floating on the free surface of a fluid.[28] The major problem encountered in the solution of the set of six, coupled, elliptical, differential equations of motion is the description of the hydrodynamic forces acting on the buoy. In their most rigorous form, the buoy equations of motion would be integro-differential equations since the dynamic pressures must be integrated over the immersed surface of the buoy. Analytical solution of these equations of motion for an arbitrary body in a random sea state has not been accomplished up to this time. If the hydrodynamic forces can be expressed as variable coefficients in the equations of motion, the equations can be written as a set of six, ordinary differential equations that can be solved by using the approximate methods of numerical techniques. The problem now is to define the variable hydrodynamic coefficients. If the fluid is assumed to be incompressible and

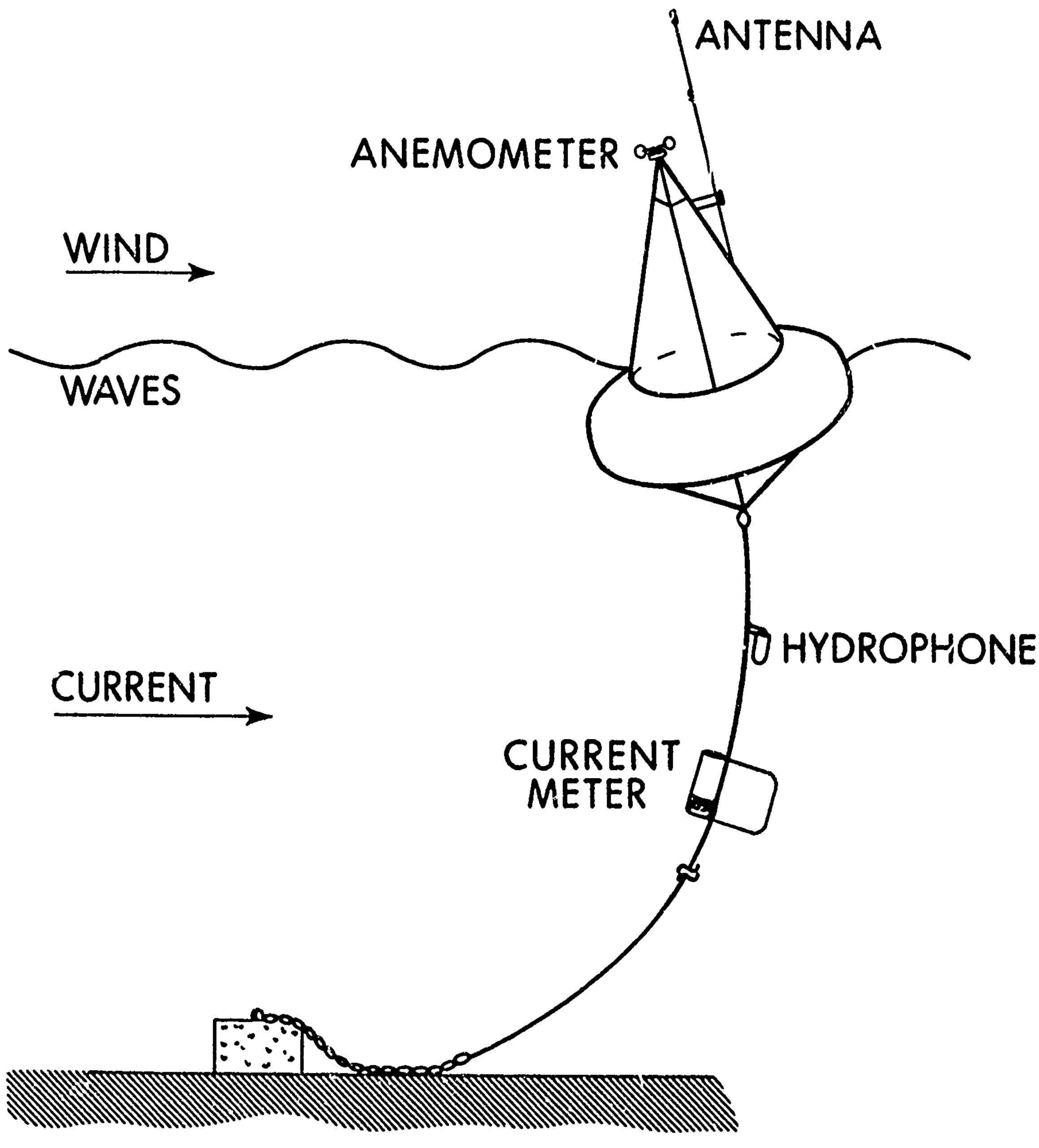

Figure 3. A Simple Buoy System

irrotational, the hydrodynamic properties of certain simple two- and three-dimensional bodies can be computed. Also, if the waves on the free surface of the fluid are deterministic and linear, the velocity potentials for various body motion modes can be superimposed to construct the case of a body floating on a free surface and responding to waves propagating on that free surface.

This study employs the technique described above. Equations of motion are written as a set of six, coupled, ordinary differential equations with variable coefficients; hydrodynamic coefficients are computed by assuming that the fluid is incompressible and irrotational and that velocity potentials can be superimposed; aerodynamic and hydrodynamic viscous forces are assumed to follow a velocity-squared law; and the body is assumed to be axisymmetric about a vertical axis (as are most oceanographic and navigational buoys), which simplifies the computation of the hydrodynamic coefficients.

Dynamics of cables are investigated and simulated. The most direct approach, i.e., solution of the cable equations of motion by a finite-difference method, is developed first. Since the cable equations are a set of nonlinear, hyperbolic, partial differential equations, analytical solutions are intractable, and a numerical method of solution is devised. Although more accurate, the finite-difference method can be very expensive with regard to digital computer time. A lumped-mass simulation of cable dynamics is also investigated and developed. Lumped-mass methods offer significant savings in computational time at the expense of truncation of the higher frequency cable dynamics.

The buoy equations of motion and the two sets of cable equations (finite-difference and lumped-mass) are then coupled and solved numerically on a

UNIVAC 1108 digital computer. A numerical model of ocean waves is used to excite the buoy system dynamics model. Steady-state buoy system configurations are solved as the zeroth-order case of buoy system dynamics.

2.2 Experimental Validation

In order to validate the computer model, two oceanographic buoys were equipped with motion sensing instrumentation and were monitored. The recorded buoy motion data have been reduced in statistical form and will be correlated with buoy motions predicted from the computer models. Also, buoy motion data reported in the literature have been used to validate the computer models.

III. ANALYTICAL DEVELOPMENT AND DISCUSSION

3.1. Buoy Dynamics

Consider an axisymmetric buoy having six degrees of freedom, floating on the free surface of a fluid, constrained by a mooring line, and exposed to wind, waves, and currents (figure 4). The buoy is being acted on by the following:

Inertial forces and moments

Hydrostatic forces and moments

Hydrodynamic forces and moments

Wind forces

Mooring line tensions.

The inertial forces can be separated into those due to gravity (weight) and those due to the motion of the buoy. Hydrostatic forces can be obtained by integration of the hydrostatic pressure acting on the submerged surface of the buoy. Likewise, hydrodynamic forces can be obtained by integration of the hydrodynamic pressures acting on the submerged surface of the buoy. Hydrodynamic forces are classified as inertial or dissipative. Energy is being dissipated through viscous effects, radiation of pressure waves, and radiation of surface waves generated by the motion of the buoy. Energy is introduced to the system through hydrostatic and hydrodynamic forces due to currents and surface waves.

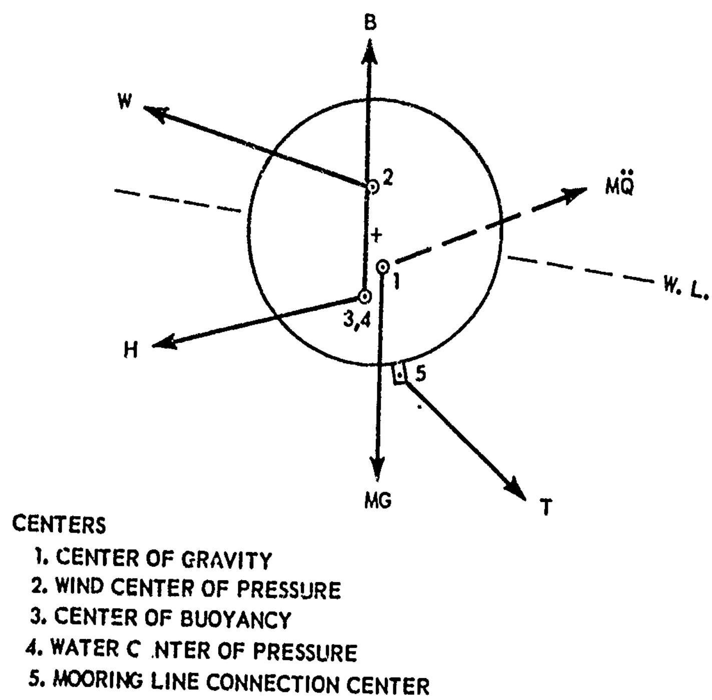

A FREE BODY OF THE BUOY

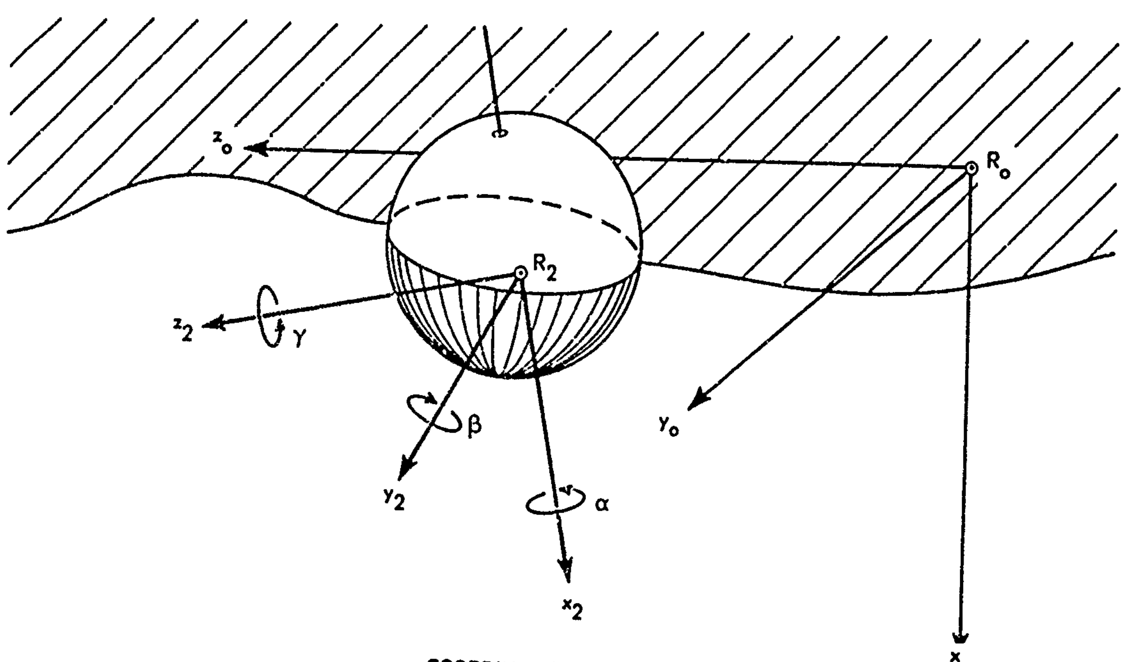

COORDINATE SYSTEMS

Figure 4. Buoy Coordinate Systems

Wind forces acting on the exposed surface of the buoy also introduce energy into the system. Mooring line tensions indicate a path of energy removal from the system. If the buoy were treated as a "black box" that transforms energy from one form to another, we can draw a schematic as shown in figure 5.

From figure 4, it is seen that four sets of coordinates must be considered. It is desired to solve for the coordinates of the center of gravity of the buoy in inertial coordinates, (x_{og}, y_{og}, z_{og}), but the hydrostatic and hydrodynamic forces and moments are due to fluid motions relative to the buoy. Any point in space has coordinates x_i, y_i, z_i relative to R_i ($i = 0, 1, 2, 3$); therefore,

$$x_o = x_{og} + x_i$$

$$y_o = y_{og} + y_i$$

$$z_o = z_{og} + z_i \; .$$

The only difference between R_1 and R_2 is a space rotation about the axes of the buoy. Thus, we have

$$\begin{bmatrix} X_2 \\ Y_2 \\ Z_2 \end{bmatrix} = \Omega \cdot \begin{bmatrix} X_1 \\ Y_1 \\ Z_1 \end{bmatrix} , \tag{1}$$

where Ω is a 3-by-3 orthogonal rotation matrix,

$$\Omega = \begin{bmatrix} \cos\gamma\cos\beta & -\cos\gamma\sin\beta\sin\alpha + \sin\gamma\cos\alpha & \cos\gamma\sin\beta\cos\alpha + \sin\gamma\sin\alpha \\ -\sin\gamma\cos\beta & \sin\gamma\sin\beta\sin\alpha + \cos\gamma\cos\alpha & -\sin\gamma\sin\beta\cos\alpha + \cos\gamma\sin\alpha \\ -\sin\beta & -\cos\beta\sin\alpha & \cos\beta\cos\alpha \end{bmatrix} . \tag{2}$$

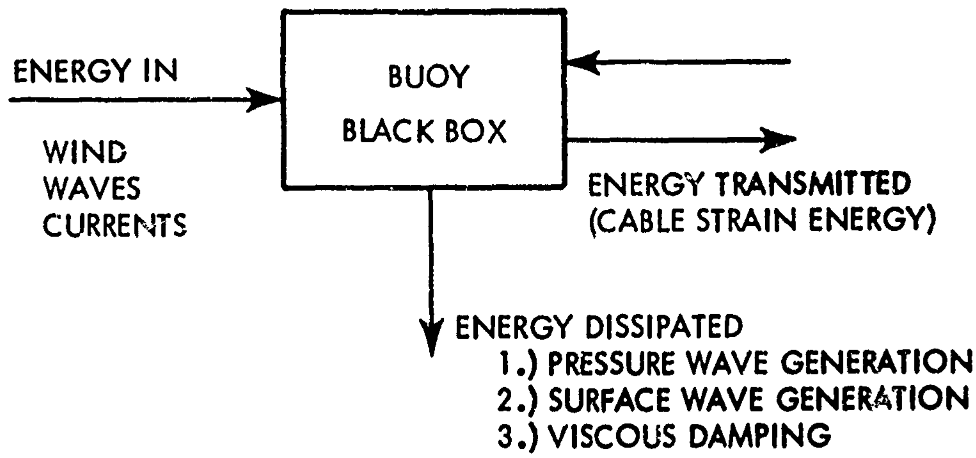

MATRIX EQUATIONS OF MOTION

$$M\ddot{Q} = MG - B - H + W - T$$

WHERE:

- M - MASS MATRIX
- $\ddot{Q}$ - ACCELERATION VECTOR
- G - GRAVITY VECTOR
- B - HYDROSTATIC FORCE & MOMENT VECTOR
- H - HYDRODYNAMIC FORCE & MOMENT VECTOR
- W - WIND FORCE VECTOR
- T - CABLE TENSION VECTOR

Figure 5. Energy Flow in Buoy System

Since Ω is orthogonal, we see that $\Omega^{-1} = \Omega^{T}$; thus,

$$\Omega^{-1} = \begin{bmatrix} \cos\gamma\cos\beta & -\sin\gamma\cos\beta & -\sin\beta \\ -\cos\gamma\sin\beta\sin\alpha + \sin\gamma\cos\alpha & \sin\gamma\sin\beta\sin\alpha + \cos\gamma\cos\alpha & -\cos\beta\sin\alpha \\ \cos\gamma\sin\beta\cos\alpha + \sin\gamma\sin\alpha & -\sin\gamma\sin\beta\cos\alpha + \cos\gamma\sin\alpha & \cos\beta\cos\alpha \end{bmatrix} . \tag{3}$$

The spatial coordinates become

$$X_0 = X_{0g} + X_2\cos\gamma\cos\beta - Y_2\sin\gamma\cos\beta - Z_2\sin\beta , \tag{4A}$$

$$Y_0 = Y_{0g} + X_2(-\cos\gamma\sin\beta\sin\alpha + \sin\gamma\cos\alpha) + Y_2(\sin\gamma\sin\beta\cos\alpha + \cos\gamma\sin\alpha) + Z_2(-\cos\beta\sin\alpha) , \tag{4B}$$

and

$$Z_0 = Z_{0g} + X_2(\cos\gamma\sin\beta\cos\alpha + \sin\gamma\sin\alpha) + Y_2(-\sin\gamma\sin\beta\cos\alpha + \cos\gamma\sin\alpha) + Z_2(\cos\beta\cos\alpha). \tag{4C}$$

The center of the coordinate system, which is aligned with the waterplane area, is located directly above the center of gravity of the buoy. Motions of fluid particles due to waves are described relative to this coordinate system. The dynamical equations of motion will be written in buoy coordinates, but displacements will be transformed to the R_0 coordinate system in order to solve for cable tensions.

Using the free body of the buoy (figure 4) and applying Newton's Second Law, we can develop the equations of motion for the buoy. In matrix form, the equations of motion for the buoy are

$$\mathcal{M}\ddot{Q} = \mathcal{M}G - B - H - W - T \, , \tag{5}$$

where

$\mathcal{M}$ is the structural mass matrix

$\ddot{Q}$ is the acceleration vector

G is the gravitational acceleration vector

B is the hydrostatic force vector

H is the hydrodynamic force vector

W is the wind force vector

T is the mooring line tension vector.

Each of these forces will be considered in turn.

Using a coordinate system with the origin located at the center of gravity of the buoy and including moments and products of inertial, we can write the structural mass matrix as

$$\mathcal{M} = \begin{bmatrix} m & 0 & 0 & 0 & 0 & 0 \\ 0 & m & 0 & 0 & 0 & 0 \\ 0 & 0 & m & 0 & 0 & 0 \\ 0 & 0 & 0 & I_{\alpha\alpha} & I_{\alpha\beta} & I_{\alpha\gamma} \\ 0 & 0 & 0 & I_{\beta\alpha} & I_{\beta\beta} & I_{\beta\gamma} \\ 0 & 0 & 0 & I_{\gamma\alpha} & I_{\gamma\beta} & I_{\gamma\gamma} \end{bmatrix} . \tag{6}$$

If the coordinate system is aligned with the principal axes of the buoy, the structural mass matrix is

$$M = \begin{bmatrix} m & 0 & 0 & 0 & 0 & 0 \\ 0 & m & 0 & 0 & 0 & 0 \\ 0 & 0 & m & 0 & 0 & 0 \\ 0 & 0 & 0 & I_{\alpha\alpha} & 0 & 0 \\ 0 & 0 & 0 & 0 & I_{\beta\beta} & 0 \\ 0 & 0 & 0 & 0 & 0 & I_{\gamma\gamma} \end{bmatrix} . \tag{7}$$

The acceleration vectors are

$$\ddot{Q} = \begin{bmatrix} \ddot{x} \\ \ddot{y} \\ \ddot{z} \\ \ddot{\alpha} \\ \ddot{\beta} \\ \ddot{\gamma} \end{bmatrix} \quad \text{and} \quad G = \begin{bmatrix} g \cos\gamma \cos\beta \\ -g \sin\gamma \cos\beta \\ -g \sin\beta \\ 0 \\ 0 \\ 0 \end{bmatrix} . \tag{8}$$

3.1.1 Wind Forces

The wind force vector is now considered. For an axisymmetric buoy about the x_2 axis and assuming a velocity-squared viscous drag, the drag and lift forces acting on the body are given by

$$D = \frac{1}{2} \rho_a C_D A_1 WV^2 \tag{9}$$

and

$$L = \frac{1}{2} \rho_A C_L A_2 WV^2, \tag{10}$$

where

D is the drag force

L is the lift force

ρ_A is the air density

C_D is the drag coefficient (subcritical, $\frac{WV\, h\, \rho_A}{\mu_A} < 5 \times 10^5$)

C_L is the lift coefficient (subcritical, $\frac{WV\, h\, \rho_A}{\mu_A} < 5 \times 10^5$)

A_1 is the vertical projected area

A_2 is the horizontal projected area

WV is the wind velocity

μ_A is the absolute viscosity of the air

h is the buoy width .

Because of the axial symmetry, the drag and lift coefficients of the buoy are the same in the y_2 and z_2 directions. Given wind velocity components WV_{yo} and WV_{zo} in the R_o coordinate system and assuming that the wind velocities are an order of magnitude greater than the displacement velocities of the buoy, we can transform to the R_2 coordinate system and can compute the wind forces and moments. For forces acting on a point that lies on the axis of symmetry of the buoy, the transform from inertial coordinates to buoy coordinates is independent of α rotations.

The wind components in the R_2 coordinate system are

$$\begin{bmatrix} WV_{x2} \\ WV_{y2} \\ WV_{z2} \end{bmatrix} = \Omega \cdot \begin{bmatrix} 0 \\ WV_{y0} \\ WV_{z0} \end{bmatrix} . \tag{11}$$

Neglecting the small wind velocity component acting along the axis of symmetry, the magnitude of the wind velocity in the R_2 coordinate system is

$$WV_{R_2} = \sqrt{WV_{y2}^2 + WV_{z2}^2} , \tag{12}$$

and the wind forces become

$$W_{D_2} = \frac{1}{2} \rho_H C_D A_1 WV_{R_2} \left| WV_{R_2} \right| \tag{13}$$

and

$$W_{L_2} = \frac{1}{2} \rho_H C_L A_2 WV_{R_2} \left| WV_{R_2} \right| . \tag{14}$$

(Note that velocities squared is written as the product of the velocity and its absolute value in order to maintain the sign convention.) Resolving the wind drag force into y_2 and z_2 components, we find that

$$W_{y2} = \frac{WV_{y2}}{WV_{R_2}} \cdot W_{D2} \tag{15}$$

and

$$W_{z_2} = \frac{WV_{z_2}}{WV_{R_2}} \cdot W_{D_2} \cdot \tag{16}$$

The wind moments are computed by usi·.g the wind forces and the moment arm:

$$W_{\alpha_2} = 0 \tag{17A}$$

$$W_{\beta_2} = -W_{z_2} \cdot H_w \tag{17B}$$

and

$$W_{\gamma_2} = -W_{Y_2} \cdot H_w \tag{17C}$$

where H_w is the height from $C.$ of $G.$ to the wind force center of pressure.

In the R_2 coordinate system, the wind forces and moments are

$$W_{R_2} = \begin{bmatrix} -W_{X_2} \\ W_{Y_2} \\ W_{Z_2} \\ 0 \\ W_{\beta_2} \\ W_{\gamma_2} \end{bmatrix} . \tag{18}$$

3.1.2 Mooring Line Forces

Mooring line tensions are acting on the buoy at the mooring line termination point. This point is taken to be below the center of gravity and along the axis of symmetry a distance H_{ML} from the center of gravity. If the space orientation of the cable is described by angles θ and ϕ relative to the R_o coordinate system (figure 4), we can develop a 3-by-3 orthogonal rotation matrix to transform from inertial to cable coordinates. The inverse of the matrix can be used to compute the tension components acting on the buoy. This rotation matrix, (A), is developed in the next section on cable dynamics but is used here.

The tension components at the buoy end of the cable are

$$T_{B_o} = A^{-1} \begin{bmatrix} T \\ 0 \\ 0 \end{bmatrix} = \begin{bmatrix} T_{x_o} \\ T_{y_o} \\ T_{z_o} \end{bmatrix}. \tag{19}$$

In the R_2 coordinate system, they become

$$T_{B_2} = \Omega \cdot T_{B_o} = \begin{bmatrix} T_{x_2} \\ T_{y_2} \\ T_{z_2} \end{bmatrix}. \tag{20}$$

The moments due to the mooring line tension are

$$T_{\alpha_2} = 0 \tag{21A}$$

$$T_{\beta_2} = T_{z_2} \cdot H_{ML} \tag{21B}$$

$$T_{\gamma_2} = T_{y_2} \cdot H_{ML} \, . \tag{21C}$$

The forces and moments due to cable tensions are then

$$T = \begin{bmatrix} T_{x_2} \\ T_{y_2} \\ T_{z_2} \\ 0 \\ T_{\beta_2} \\ T_{\gamma_2} \end{bmatrix} . \tag{22}$$

3.1.3 Hydrostatic Forces

The hydrostatic forces are considered next. If the displacements of an elemental volume of fluid just below the free surface and in the immediate vicinity of the buoy are given relative to the inertial coordinates (η), and if the slope of the free surface above this particle is also given (ξ), the buoyant forces and moments can be computed. The assumptions that the buoy diameter is small relative to the wavelength and that the presence of the buoy does not influence the shape of the free surface (Froude-Kriloff hypothesis) allow representation of the sea surface as a plane intersecting with the body volume.

Most oceanographic buoys have axial symmetry, and their shape can be approximated by an oblate spheroid. Consider an ellipsoid of revolution (figure 6) with a major diameter of 2b and a minor diameter of 2a. The equation of the surface is

$$\frac{X_b^2}{A^2} + \frac{Y_b^2}{b^2} + \frac{Z_b^2}{b^2} = 1 . \tag{23}$$

Let a plane intersect the oblate spheroid at a height H_d from the geometric center at an angle β'. The intercepts of the plane are

$$X = -H_D$$
$$Y = \infty$$
$$Z = -H_D / \tan \beta' .$$

The equation of the plane becomes

$$\frac{X_b}{-H_D} + \frac{Z_b}{-H_D / \tan \beta'} = 1 \tag{24}$$

or

$$X_b + Z_b \tan \beta' + H_D = 0 . \tag{24A}$$

The intersection of the body and the plane is therefore given by

$$\frac{X_b^2}{A^2} + \frac{Y_b^2}{b^2} + \frac{Z_b^2}{b^2} - 1 = X_b + Z_b \tan \beta' + H_D \tag{25}$$

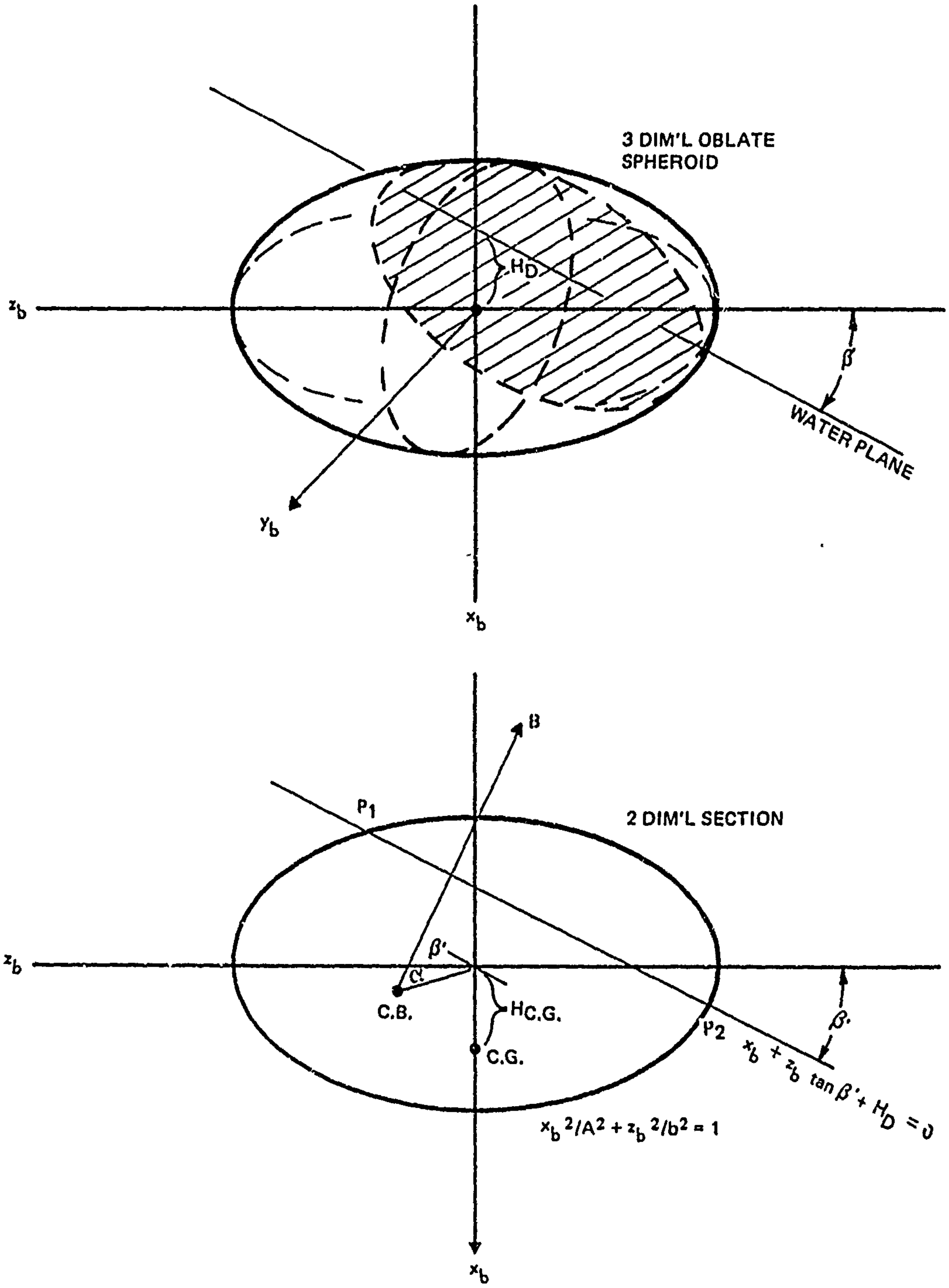

Figure 6. Immersed Volume of an Oblate Spheroid

or

$$\frac{X_b^2}{A^2} + \frac{Y_b^2}{b^2} + \frac{Z_b^2}{b^2} - X_b - Z_b \tan\beta' - H_D - 1 = 0 , \tag{25A}$$

which is an ellipse. In order to compute the volume of the "cut" oblate spheroid, the area of any section parallel to the cutting plane must be defined. In the $x_b - z_b$ plane, we find that on the ellipse

$$X_b^2 = A^2 - \frac{A^2}{b^2} \cdot Z_b^2 \tag{26}$$

and on the line

$$X_b^2 = Z_b^2 \tan^2\beta' + 2 H_D Z_b \tan\beta' + H_D^2 . \tag{27}$$

Equating (26) and (27), we can compute the z coordinates of intersecting points P_1 and P_2 by

$$\left(\tan^2\beta + A^2/b^2\right) Z_b^2 + 2 Z_b H_D \tan\beta' + \left(H_D^2 - A^2\right) = 0 . \tag{28}$$

Solving for z_b, we find

$$Z_b = \frac{-H_D \tan\beta' \pm A/b \sqrt{b^2 \tan^2\beta' + A^2 - H_D^2}}{\left(\tan^2\beta' + A^2/b^2\right)} \tag{29}$$

For P_1, the coordinates are

$$Z_{b_1} = \frac{-H_D \tan\beta' + A/b \sqrt{b^2 \tan^2\beta' + A^2 - H_D^2}}{\left(\tan^2\beta' + A^2/b^2\right)} \tag{30}$$

and

$$X_{b_1} = -Z_{b_1} \tan \beta' - H_D \; ; \tag{31}$$

for P_2 , the coordinates are

$$Z_{b_2} = \frac{-H_D \tan \beta' - A/b \sqrt{b^2 \tan^2 \beta' + A^2 - H_D^2}}{\left(\tan^2 \beta' + A^2/b^2\right)} \tag{32}$$

and

$$X_{b_2} = -Z_{b_2} \tan \beta' - H_D \; ; \tag{33}$$

thus,

$$Z_{b_1} - Z_{b_2} = \frac{2 \, A/b \sqrt{b^2 \tan^2 \beta' + A^2 - H_D^2}}{\left(\tan^2 \beta' + A^2/b^2\right)} \, . \tag{34}$$

The b' axis of the intersecting ellipse is

$$b' = \frac{1}{2} \frac{(Z_{b_1} - Z_{b_2})}{\cos \beta'} \, .$$

From equation (34), we substitute and find

$$b' = \frac{A/b \sqrt{b^2 \tan^2 \beta' + A^2 - H_D^2}}{\cos \beta' \left(\tan^2 \beta' + A^2/b^2\right)} \, . \tag{35}$$

The z coordinate of the center of the elliptical section is

$$Z_c = Z_{b_1} - b' \cos \beta' = \frac{-H_D \tan \beta'}{\left(\tan^2 \beta' + A^2/b^2\right)} \, . \tag{36}$$

The x coordinate of the center of the elliptical section is

$$X_c = \frac{H_D \tan^2 \beta'}{(\tan^2 \beta' + a^2/b^2)} - H_D \quad . \tag{37}$$

The dimension of the a' axis of the intersecting ellipse is one-half the y dimension at the center. The y dimension at the center is

$$Y_b = \pm \sqrt{b^2 - \frac{H_D^2 \tan^2 \beta'}{(\tan^2 \beta' + a^2/b^2)^2} - \frac{b^2}{a^2}\left(\frac{H_D \tan^2 \beta'}{(\tan^2 \beta' + a^2/b^2)} - H_D\right)^2} \ , \tag{38}$$

and the axis length is

$$a' = \sqrt{b^2 - \frac{H_D^2}{(\tan^2 \beta' + a^2/b^2)}} \ . \tag{39}$$

The area of the intersecting ellipse is

$$A = \pi a' b' = \pi \sqrt{b^2 - \frac{H_D^2}{(\tan^2 \beta' + a^2/b^2)}} \cdot \frac{a/b \sqrt{b^2 \tan^2 \beta' + a^2 - H_D^2}}{\cos \beta' (\tan^2 \beta' + a^2/b^2)}$$

or

$$A = \frac{\pi a b}{\cos \beta'} \left(\frac{1}{(\tan^2 \beta' + a^2/b^2)^{1/2}} - \frac{H_D^2}{b^2 (\tan^2 \beta' + a^2/b^2)^{3/2}} \right) . \tag{40}$$

The volume of the "cut" oblate spheroid is given by

$$V = \int_{-H_{LO}}^{H_D'} A \, dH' \ . \tag{41}$$

The lower limit of the integral can be found by setting the area of the cutting plane equal to zero $(A = 0)$. The deepest draft is

$$H_{LO} = \sqrt{b^2 \tan^2 \beta' + A^2} \;; \tag{42}$$

thus, with this lower limit, the volume is

$$V = \int_{-\cos\beta'\sqrt{b^2\tan^2\beta' + A^2}}^{H_D \cos\beta'} \frac{\pi A b}{\cos\beta'} \left(\frac{1}{(\tan^2\beta' + A^2/b^2)^{1/2}} - \frac{H'^2/\cos^2\beta'}{b^2(\tan^2\beta' + A^2/b^2)^{3/2}} \right) dH' \;,$$

or, when integrating, it becomes

$$V = \pi A b^2 \left[\frac{2}{3} + \frac{H_D}{(b^2 \tan^3\beta' + A^2)^{1/2}} - \frac{H_D^3}{3(b^2\tan^2\beta' + A^2)^{3/2}} \right] . \tag{43}$$

The location of the centroid is given by

$$H'_{CB} = \frac{\int H' \, dV}{V} \;.$$

Expanding, we find

$$H'_{CB} = \frac{1}{V} \int_{-\cos\beta'\sqrt{b^2\tan^2\beta' + A^2}}^{H_D \cos\beta'} \frac{\pi A b}{\cos\beta'} \left(\frac{1}{(\tan^2\beta' + A^2/b^2)^{1/2}} - \frac{H'^2/\cos^2\beta'}{b^2(\tan^2\beta' + A^2/b^2)^{3/2}} \right) H' \, dH' \;.$$

Thus, carrying out the integration, we see that the centroid location becomes

$$H'_{CB} = \frac{\dfrac{\cos\beta'}{2} \left[H_D^2 - \dfrac{(b^2\tan^2\beta' + A^2)}{2} - \dfrac{H_D^4}{2(b^2\tan^2\beta' + A^2)} \right]}{\left[\dfrac{2}{3}\sqrt{b^2\tan^2\beta' + A^2} + H_D - \dfrac{H_D^3}{3(b^3\tan^2\beta' + A^2)} \right]} \;. \tag{44}$$

The H dimension of the centroidal plane is

$$H_{CB} = \frac{\frac{1}{2}\left[\frac{H_D^4}{2(b^2\tan^2\beta' + A^2)} - H_D^2 + \frac{(b^2\tan^2\beta' + A^2)}{2}\right]}{\left[\frac{2}{3}\sqrt{b^2\tan^2\beta' + A^2} + H_D - \frac{H_D^3}{3(b^2\tan^2\beta' + A^2)}\right]} . \tag{45}$$

The x coordinate of the centroid is

$$X_{CB} = \left(\frac{\tan^2\beta'}{(\tan^2\beta' + A^2/b^2)} - 1\right) \cdot H_{CB} . \tag{46}$$

The z coordinate of the centroid is

$$Z_{CB} = \left(\frac{-\tan\beta'}{(\tan^2\beta' + A^2/b^2)}\right) \cdot H_{CB} . \tag{47}$$

The moment arm for the buoyant force is

$$d = d_1 + d_2 ,$$

where the distances d_1 and d_2 are given by

$$d_1 = \sqrt{X_{CB}^2 + Z_{CB}^2} \cdot \cos(\alpha' + \beta') ,$$

or

$$d_1 = Z_{CB} \cos\beta' + X_{CB} \sin\beta' ,$$

and

$$d_2 = H_{CG} \sin\beta' .$$

The angle α' is defined as

$$\alpha' = \tan^{-1}\frac{X_{CB}}{Z_{CB}} .$$

The moment arm is

$$d = Z_{CB} \cos\beta' + (H_{CG} - X_{CB}) \sin\beta' . \tag{48}$$

For the special case of a sphere of radius A , the immersed volume is

$$V = \pi A^3 \left[\frac{2}{3} + \frac{H_D}{A}\cos\beta' - \frac{H_D^3}{3A^3}\cos^3\beta'\right] . \tag{49}$$

The height of the plane intersecting the center of buoyancy is

$$H_{CB} = \frac{3\left[\frac{H_D^4}{A^2}\cos^2\beta' - 2H_D^2 + A^2\sec^2\beta'\right]}{4\left[2A\cdot\sec\beta' + 3H_D - \frac{H_D^3}{A^2}\cos^2\beta'\right]} . \tag{50}$$

The coordinates of the center of buoyancy are

$$X_{CB} = -\cos^2\beta' \cdot H_{CB} \tag{51}$$

and

$$Z_{CB} = -\sin\beta'\cos\beta' \cdot H_{CB} . \tag{52}$$

The buoyancy moment arm is then

$$d = Z_{CB} \cos\beta' + (H_{CG} - X_{CB}) \sin\beta' . \tag{53}$$

If the buoy is pitched and rolled with angles β and γ and the sea surface slope at the buoy is β_w and γ_w, the slope of the sea surface relative to buoy coordinates is $\beta_s = \beta - \beta_w$ and $\gamma_s = \gamma - \gamma_w$. The angle between the sea surface plane and the buoy vertical axis is $\beta' = \cos^{-1}(\cos\gamma_s \cos\beta_s)$. With the buoy tilt angle defined, along with the location of the buoy center of gravity relative to the sea surface, the buoyant force and moment can be computed for an oblate spheroid. The buoyant force B acts normal to the plane of the sea surface through the center of buoyancy. In buoy coordinates, the buoyant force vector is

$$B_{R_2} = \begin{bmatrix} -B\cos\gamma_s\cos\beta_s \\ -B\sin\gamma_s \\ -B\cos\gamma_s\sin\beta_s \end{bmatrix}. \tag{54}$$

The β buoyant moment becomes

$$M_\beta = (B\cos\gamma_s\cos\beta_s)(Z_{CB}\cos\alpha) - (H_{CG} - X_{CB})(B\cos\gamma_s\sin\beta_s), \tag{55}$$

and the γ buoyant moment becomes

$$M_\gamma = (B\cos\gamma_s\cos\beta_s)(Z_{CB}\sin\alpha) - (H_{CG} - X_{CB})(B\sin\gamma_s). \tag{56}$$

The same transformations as used above can be applied to any axisymmetric buoy if the buoyancy can be defined as a function of the draft and tilt angle of the buoy. The angular stability of axisymmetric buoy hulls, as defined by the locations of the centers of buoyancy and gravity, is discussed in appendix A.

3.1.4 Hydrodynamic Forces

The hydrodynamic forces acting on the buoy that are due to the waves incident on the buoy and the motion of the buoy in the fluid must be included in the equations of motion. Ideally, the computation of these forces should be made for a buoy moving in a viscous fluid exposed to a random sea state. However, the solution to this general problem is not tractable and the forces acting on a buoy moving sinusoidally in an ideal fluid is considered in this study. These forces are considered as being composed of two components — inertial and dissipative. Energy is dissipated from the buoy, which is moving in an ideal fluid, by the generation of surface waves that radiate cylindrically to infinity. Dissipative forces due to viscosity will be included in the equations of motion as separate force components.

The separation of dissipative forces into those due to surface wave generation and those due to viscous drag is supported by Havelock,[41] who concluded through dimensional analysis of the decay of oscillations of a prism on a free surface that the viscous damping is an order of magnitude less than the damping due to surface wave generation. Ogilvie[28] cites other model experiments which support Havelock's conclusions. Ogilvie also lists generalized equations of motion for ships in a seaway in which the viscous damping is either neglected or included as a separate force term, which is the current practice among naval architects.

The analysis of the motion of floating bodies conducted by John[22,23] illustrates the computation of the hydrodynamic forces. Consider a mechanical system consisting of a liquid and a partly immersed body B. The liquid is assumed to be incompressible and to have irrotational motion. The free surface extends to infinity in all directions (figure 7). The body B is assumed to be rigid and to describe a forced motion under the influence of external forces. The state of the liquid is described by the velocity potential $\phi(x, y, z; t)$, which satisfies LaPlace's equation. The boundary condition that the normal velocity of the particles along with the pressure is continuous across the surface must be satisfied. In addition, the pressure on the free surface is assumed constant and equal to the atmospheric pressure. Under these conditions, energy is gained or lost by the system only through waves arriving or departing at infinity or through the external forces.

The difficulties arising from the fact that the velocity potential, ϕ, is a solution of the potential equation determined by nonlinear boundary conditions on a variable boundary force linearization of the problem in order to make it tractable. Restricting the analysis to infinitesimal motions, note that the boundary conditions become linear conditions for the potential function ϕ on fixed surfaces corresponding to the rest or equilibrium position. The average free surface lies in a horizontal plane, and the average immersed surface S^o for the body B is for a position of equilibrium for B. On the average free surface, $y = 0$, the wave equation is

$$\phi_{tt} + g\phi_y = 0. \qquad (57)$$

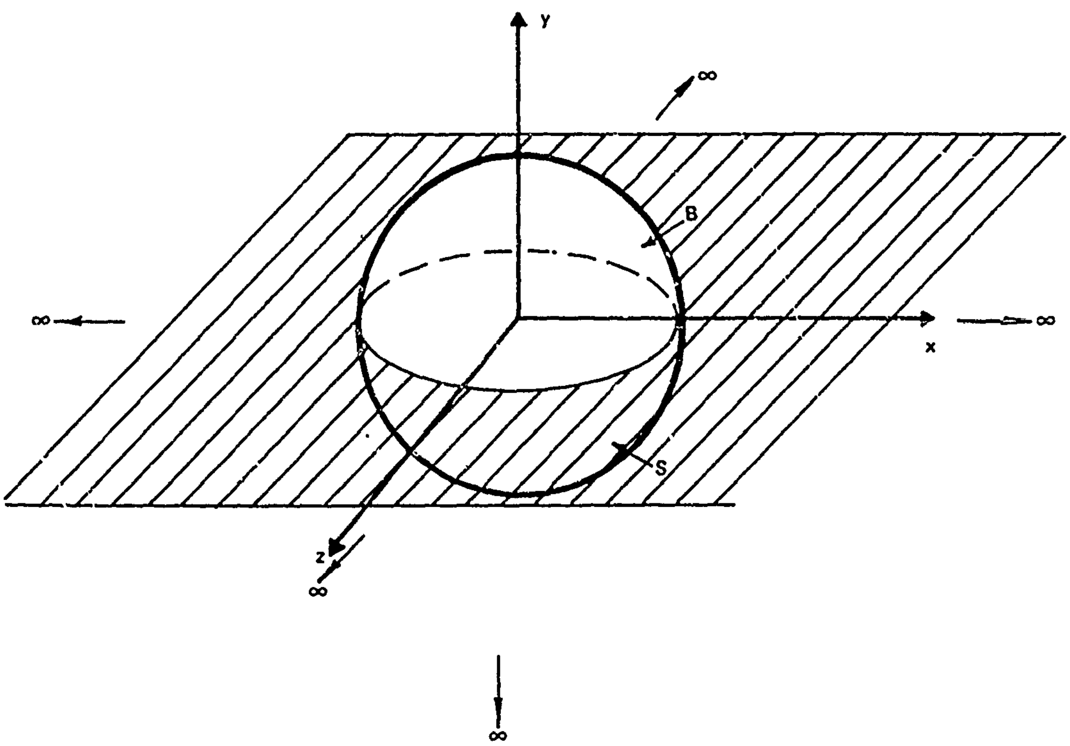

Figure 7. An Object on a Free Surface

On the average immersed surface, we find

$$\frac{\partial\phi}{\partial n} = X_t p_1 + Y_t p_2 + Z_t p_3 + \theta_t' g_1 + \theta_t'' g_2 + \theta_t''' g_3 \, , \tag{58}$$

where

X, Y, Z are the coordinates of the center of gravity of B

$\theta', \theta'', \theta'''$ are the angular displacements of B

n is the unit normal of S°

p_k are the components of n

g_k are the components of the moment of n about the center of gravity.

Six differential equations of motion for B must also be written. For small perturbations, they are linear, second-order differential equations in x , y , z , $\theta', \theta'', \theta'''$ with constant coefficients and integrals of ϕ in the inhomogeneous part. They are of the form

$$\frac{M}{\rho} Y_{tt} = -\iint_{S^\circ} \phi_t \, p_2 \, dS - g\left[I^A(Y - Y_0) + I_x^A \theta''' - I_z^A \theta'\right], \tag{59}$$

where

M is the mass of B

ρ is the fluid density

I^A is the area of A , the intersection of the body and free surface

I_x^A, I_z^A are the moments of A about vertical planes

g is the acceleration of gravity.

The integral expresses the hydrodynamic forces, whereas the right-hand term represents the hydrostatic forces.

For a buoy undergoing simple harmonic oscillations, ϕ can be defined as

$$\phi(\bar{x},\bar{y},\bar{z};t) = Re\left[V(\bar{x},\bar{y},\bar{z})\, e^{-i\sigma t}\right] , \tag{60}$$

where

σ is the angular frequency of the oscillation.

For an incompressible fluid, V is a solution to

$$\nabla^2 V(\bar{x},\bar{y},\bar{z}) = 0 \quad \text{in } \bar{y} < 0 ,$$

where V is complex valued. For small oscillations of the buoy, the amplitude of induced wave motion will be small compared with the wavelength. Thus, the linearized dynamic condition for ϕ on the free surface is

$$g\bar{\eta}(\bar{x},\bar{z};t) + \phi_t(\bar{x},0,\bar{z};t) = 0 , \tag{61}$$

where

$\bar{\eta}$ is the free surface elevation.

Equation (61) with the linearized kinematic condition,

$$\phi_{\bar{y}}(\bar{x},0,\bar{z};t) = \bar{\eta}_t(\bar{x},\bar{z};t) \quad \text{, yields}$$

$$\frac{\partial}{\partial y} V(\bar{x},0,\bar{z}) - kV(\bar{x},0,\bar{z}) = 0 \quad \text{on } \bar{y} = 0 , \tag{62}$$

where

k is the wave number, $k = \sigma^2/g = 2\pi/\bar{\lambda}$,

$\bar{\lambda}$ is the free wavelength.

The normal velocity across the immersed surface of the buoy is continuous; thus, we find

$$\frac{\partial}{\partial \bar{n}} \phi(\bar{x}, \bar{y}, \bar{z}; t) = (\dot{\bar{Q}} + \dot{\theta} \times \bar{r}) \cdot n \, , \tag{63}$$

which is equation (58) restated in vector form where

$\bar{Q}$ is the position vector of the body C. of G. ; $\bar{Q} = X p_1 + Y p_2 + Z p_3$,

θ is the rotation vector of body B ; $\theta = \theta' q_1 + \theta'' q_2 + \theta''' q_3$,

$\bar{r}$ is the position vector of some point on the immersed surface of the body.

The kinematic condition is to be satisfied on the immersed surface in the undisturbed position, i.e.,

$$\frac{\partial}{\partial \bar{n}} V(\bar{x}, \bar{y}, \bar{z}) = \sum_{j=1}^{6} \frac{\partial}{\partial n} V_j(\bar{x}, \bar{y}, \bar{z}) = -i\sigma\left[\bar{Q}^{\circ} \cdot n + \theta^{\circ} (\bar{r} \times n)\right] \tag{64}$$

Applying a Sommerfeld radiation condition at infinity, we find that a disturbance in the finite region should only produce an outgoing wave at a large distance:

$$V(\bar{d}, \psi, \bar{y}) - A(\psi)\, \bar{d}^{-\frac{1}{2}} e^{k\bar{y} + ik\bar{d}} \longrightarrow 0 \text{ as } \bar{d} \to \infty \, , \tag{65}$$

where

$$\bar{d} = (\bar{x}^2 + \bar{z}^2)^{1/2}$$
$$\psi = \tan^{-1}(\bar{z}/\bar{x}) \, .$$

To put the equations in dimensionless form, let

$$a = \bar{a}K \qquad \text{the frequency}$$

$$\begin{aligned} x &= \bar{x}/a \\ y &= \bar{y}/a \\ z &= \bar{z}/a \end{aligned} \qquad \text{space variables}$$

$$Q = \bar{Q}/a \qquad \text{the space parameters,}$$

where a is a typical buoy dimension. Introduce the pressure function u_j by

$$i\sigma V_j(\bar{x},\bar{y},\bar{z})/g\bar{a}\,Q_j^0 = a\,u_j(x,y,z) \qquad j=1,2,3 \tag{66A}$$

and

$$i\sigma V_j(\bar{x},\bar{y},\bar{z})/g\bar{a}\,\theta_j^0 = a\,u_j(x,y,z) \qquad j=4,5,6 \tag{66B}$$

The boundary value problem is to find a potential $u_j(x,y,z)$, $j=1,2,\cdots,6$ that is continuous in the fluid space in such a manner that

$$\nabla^2 u_j(x,y,z) = 0 \quad \text{in } y<0 ,$$

$$\frac{\partial}{\partial y} u_j(x,0,z) - a\,u_j(x,0,z) = 0 \quad \text{outside } S^0 ,$$

$$\frac{\partial}{\partial n} u_j(x,y,z) = h_j(x,y,z) \quad \text{on } S^0 ,$$

$$u_j(d,\psi,y) - A_j(\psi)\,d^{-\frac{1}{2}}e^{ay+iad} \longrightarrow 0 \quad \text{as } d\to\infty ,$$

where h_j represents the prescribed function that depends on the mode of oscillation. The h_j are given as

$$\begin{aligned} h_1(x,y,z) &= n_x & \qquad h_4(x,y,z) &= y n_z - z n_y \\ h_2(x,y,z) &= n_y & \qquad h_5(x,y,z) &= z n_x - x n_z \\ h_3(x,y,z) &= n_z & \qquad h_6(x,y,z) &= x n_y - y n_x . \end{aligned}$$

The source potentials G of unit strength in the lower half-space which satisfy the sets of boundary conditions are

$$G(x,y,z;\xi,\eta,\zeta) = R^{-1} + R'^{-1} - \pi A\, e^{A(y+\eta)}\left[S_0(A\bar{\omega}) + Y_0(A\bar{\omega}) - i2J_0(A\bar{\omega})\right]$$
$$- 2A e^{A(y+\eta)} \int_{y+\eta}^{0} e^{-A\mu}(\mu^2+\bar{\omega}^2)^{-\frac{1}{2}} d\mu \,, \qquad (67)$$

where

$$\bar{\omega} = \left[(x-\xi)^2 + (y-\eta)^2\right]^{\frac{1}{2}} \,, \qquad \bar{\omega}' = \left[(x-\xi)^2 + (y+\eta)^2\right]^{\frac{1}{2}} \,,$$

$$R = \left[\bar{\omega}^2 + (z-\zeta)^2\right]^{\frac{1}{2}} \,, \qquad R' = \left[\bar{\omega}'^2 + (z-\zeta)^2\right]^{\frac{1}{2}} \,.$$

$S_0(A\bar{\omega})$ is the Struve function of order 0

$J_0(A\bar{\omega}), Y_0(A\bar{\omega})$ is the Bessel functions of first and second kind of order 0 .

The solution to the boundary value problem is now in the form

$$u_j(x,y,z) = \frac{1}{4\pi}\iint_S f_j(\xi,\eta,\zeta)\, G(x,y,z;\xi,\eta,\zeta)\, dS \,, \qquad (68)$$

where f is the strength of the distributed sources over the immersed surface and is a continuous complex function. If the forces and moments are written as components in phase with the acceleration and velocity, we find that

$$F_i = -\rho \bar{A}^3 M \ddot{Q}_j - \rho \sigma \bar{A}^3 N \dot{Q}_j \qquad j = 1,2,3 \,. \qquad (69)$$

For simple harmonic motions, the body vectors become

$$Q_j(t) = \mathrm{Re}\left[\bar{Q}_j^o(t)\, e^{-i\sigma t} \right] \qquad j = 1,2,3$$

and

$$\Theta_j(t) = \mathrm{Re}\left[\Theta_j^o(t)\, e^{-i\sigma t} \right] \qquad j = 4,5,6 \,. \tag{70}$$

The moments are

$$G_d = -\rho \bar{A}^4 I\, \ddot{\theta}_j - \rho\sigma \bar{A}^4 H\, \dot{\theta}_j \qquad j = 4,5,6 \,.$$

Then, M and N are the hydrodynamic mass and the linear damping coefficients, and I and H are the hydrodynamic mass moment of inertia and rotational damping coefficients. The dimensionless coefficients are

$$M = \frac{\bar{M}}{\rho \bar{A}^3} = \mathrm{Re}\left[\iint_S u_j(x,y,z)\, n\, dS \right] \qquad j = 1,2,3 \,, \tag{71}$$

$$N = \frac{\bar{N}}{\rho\sigma \bar{A}^3} = \mathrm{Im}\left[\iint_S u_j(x,y,z)\, n\, dS \right] \qquad j = 1,2,3 \,, \tag{72}$$

$$I = \frac{\bar{I}}{\rho \bar{A}^4} = \mathrm{Re}\left[\iint_S u_j(x,y,z)\cdot(r\times n)\, dS \right] \qquad j = 4,5,6 \,, \tag{73}$$

and

$$H = \frac{\bar{H}}{\rho\sigma \bar{A}^4} = \mathrm{Im}\left[\iint_S u_j(x,y,z)\cdot(r\times n)\, dS \right] \qquad j = 4,5,6 \,. \tag{74}$$

Kim[42] has evaluated these integrals numerically for spheroids of various aspect ratios and has plotted the dimensionless hydrodynamic coefficients versus the frequency parameter. Barakat[43] evaluated the Fredholm integrals with an approximate analytical solution for the case of a sphere on the free surface. Kim's data are shown in figures 8, 9, and 10. A curve-fitting program (CURFIT) built into the Government Services Administration remote terminal

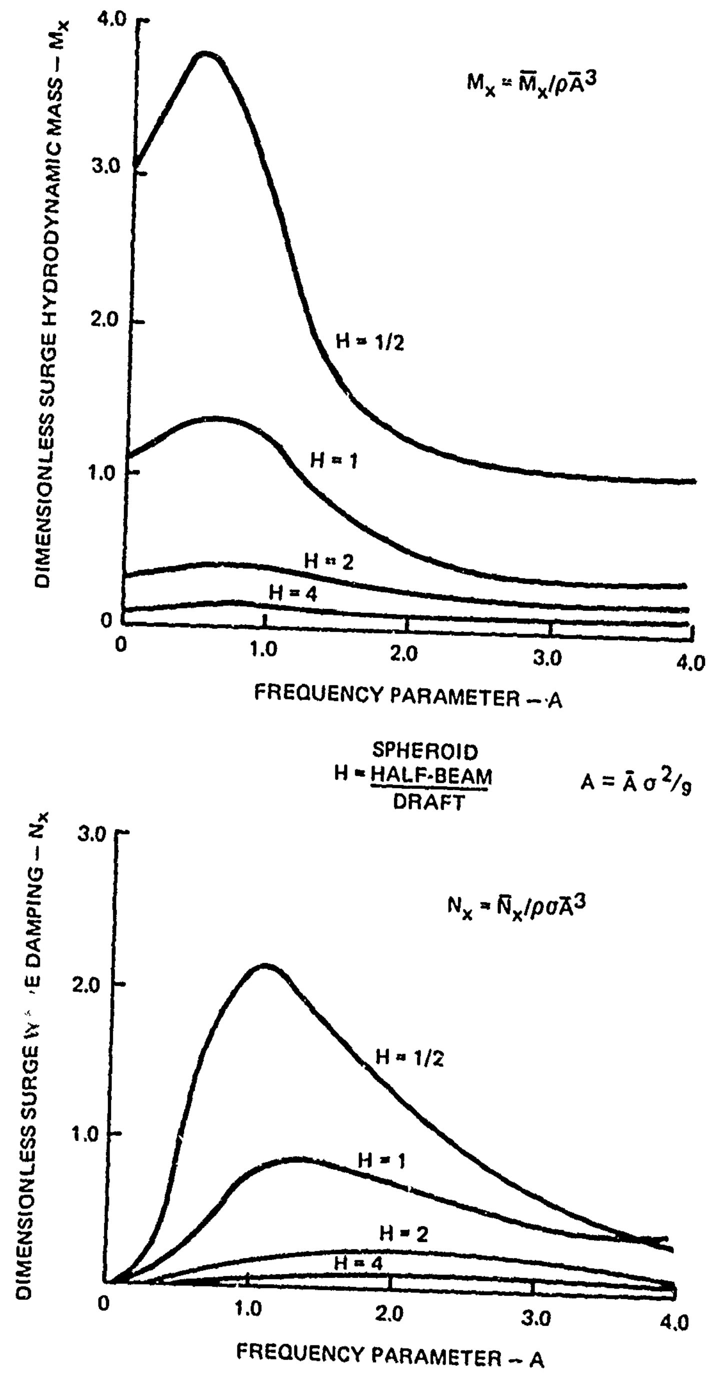

Figure 8. Hydrodynamic Mass and Wave Damping for Swaying or Surging Oblate Spheroids

(From Kim, reference 42.)

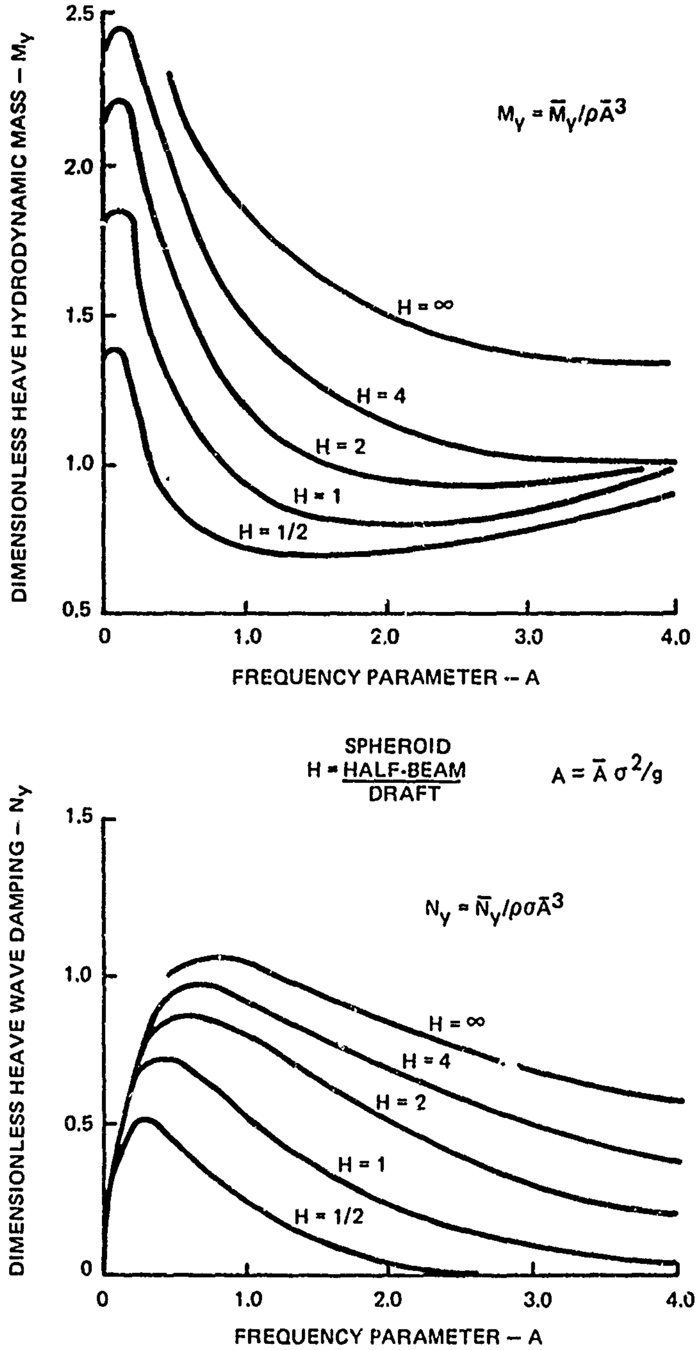

Figure 9. Hydrodynamic Mass and Wave Damping for Heaving Oblate Spheroids

(From Kim, reference 42.)

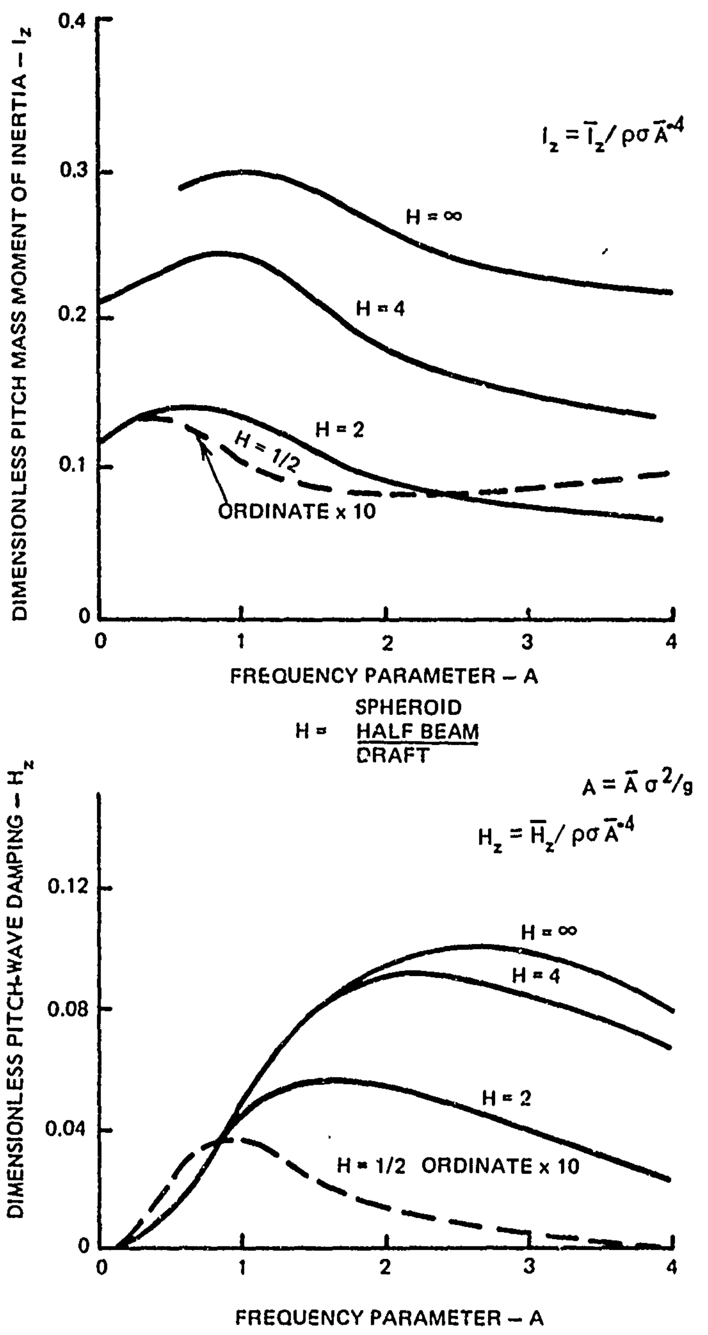

Figure 10. Hydrodynamic Mass Moment of Inertia For Pitching or Rolling Oblate Spheroids

(From Kim, reference 42.)

computer system was used to develop approximate equations for Kim's data for a sphere. Program CURFIT fits six curves to the data by a least-squares fit of the candidate curve's linear transform. The six curves are of the following types:

$$Y = A + B \cdot X$$
$$Y = A e^{BX}$$
$$Y = A X^{B}$$
$$Y = A + B/X$$
$$Y = 1/(A + B \cdot X)$$
$$Y = X/(A + B \cdot X) .$$

Coefficients for each curve and an index of determination (best fit) are computed. Kim's data for the sphere are approximated by the following functions:

<u>Sway-Surge</u>

HYDRODYNAMIC MASS

$$M_z = M_x = 1.089 + 0.529\,\kappa' \qquad 0 < \kappa' < 0.74 \qquad (75A)$$
$$= 1/(-0.0318 + 0.954\,\kappa') \qquad 0.74 < \kappa' < 3.4 \qquad (75B)$$

DAMPING

$$N_z = N_x = 0 \qquad 0 < \kappa' < 0.1 \qquad (76A)$$
$$= -0.069 + 0.71\,\kappa' \qquad 0.1 < \kappa' < 1.37 \qquad (76B)$$
$$= 1.595\, e^{-0.415\,\kappa'} \qquad 1.37 < \kappa' < 3.4 \qquad (76C)$$

<u>Heave</u>

HYDRODYNAMIC MASS

$$M_y = 1.85 \qquad 0 < \kappa' < 0.1 \qquad (77A)$$
$$= 1.02 \cdot \kappa'^{\,-0.256} \qquad 0.1 < \kappa' < 3.4 \qquad (77B)$$

DAMPING

$$N_y = 0.126 + 1.7\,A' \qquad 0 < A' < 0.4 \qquad \text{(78A)}$$

$$= 1.18\, e^{-0.83A'} \qquad 0.4 < A' < 3.4 \quad . \qquad \text{(78B)}$$

Dimensionless hydrodynamic mass and wave damping coefficients for a sphere based upon Kim's study along with the above approximate curves are shown in figure 11. The set of approximate functions will be used in the computer simulation of buoy dynamics for a spherical buoy.

Birkoff[44] has investigated the influence of body symmetry on the hydrodynamic mass dyadic. An oblate spheroid possessing an axis of symmetry has five hydrodynamic mass values along the main diagonal: heave, surge, sway (same as surge), pitch, and roll (same as pitch). For an ideal fluid, the yaw hydrodynamic mass is zero. However, Lamb[45] studied the rotational motion of a sphere in a viscous fluid and identifies a force proportional to angular acceleration that can be considered as a yaw hydrodynamic mass. For a fully immersed oblate spheroid in an ideal fluid with the centers of gravity and pressure coincident, all the off-diagonal terms would be zero. However, for a half-immersed oblate spheroid, the following hydrodynamic forces are coupled:

Surge-Pitch

Sway-Roll

Pitch-Surge

Roll-Sway.

Thus far, hydrodynamic mass and wave damping have been computed for heave, sway, surge, pitch, and roll. Using Lamb's analysis for a rotating sphere, we can approximate the yaw hydrodynamic mass for an oblate spheroid

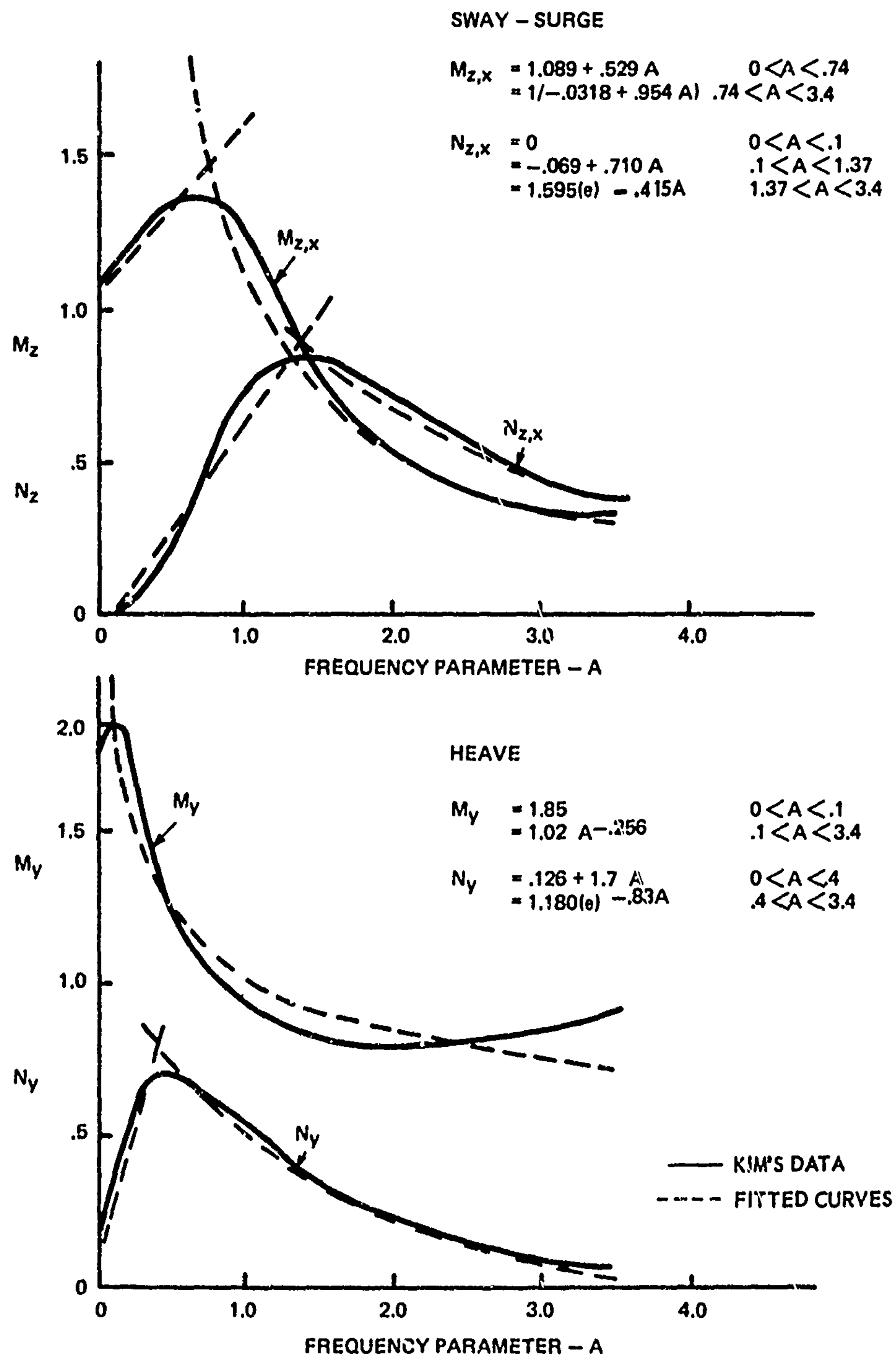

Figure 11. Least-Squares Fits to Kim's Parameters

in a viscous fluid:

$$M_{\alpha\alpha} = \frac{4}{3}\pi\rho A^5 \cdot \frac{1+\beta A}{1+2\beta A+2\beta^2 A^2} \tag{79}$$

The viscous damping in yaw is

$$N_{\alpha\alpha} = \frac{4}{3}\pi\mu A^3 \cdot \frac{3+6\beta A+6\beta^2 A^2+2\beta^3 A^3}{1+2\beta A+2\beta^2 A^2}, \tag{80}$$

where

A is the major diameter

ρ is the fluid density

μ is the viscosity

ν is the kinematic viscosity

β is defined as $\sqrt{\sigma/2\nu}$

σ is the angular frequency of oscillatory motion.

Since the center of pressure and center of gravity of the buoy do not necessarily coincide, force components due to hydrodynamic mass or damping will induce moments about the center of gravity. The projected area of an oblate spheroid in the y-x or z-x body planes is a semiellipse. For $H_D < 0$, i.e., less than half immersion, the center of pressure is located a distance

$$H_{cp} = \frac{2}{3}\frac{b}{A}\sqrt{(A^2-H_D^2)^3} \tag{81}$$

below the centroid of the oblate spheroid. For $H_D > 0$, i.e., more than half immersion, the center of pressure is located a distance

$$H_{CP} = \frac{\left(\frac{\pi}{2} A b - \frac{b}{A} H_D \sqrt{A^2 - H_D^2} - A b \sin^{-1}\frac{H_D}{|A|}\right)\left(\frac{2}{3}\frac{b}{A}\sqrt{(A^2 - H_D^2)^3}\right)}{\frac{\pi}{2} A b + \frac{b}{A} H_D \sqrt{A^2 - H_D^2} + A b \sin^{-1}(H_D/|A|)} \tag{82}$$

below the centroid.

In the coordinate system shown, a positive y acceleration will induce a negative γ moment and, conversely, a positive γ acceleration will induce a negative y force if the center of gravity is below the center of pressure. Thus, the coupled roll-sway hydrodynamic mass moment of inertia is

$$M_{h_{\gamma y}} = M_{h_{y\gamma}} = -M_{h_{yy}}\left(H_{CG} - H_{CP}\right). \tag{83}$$

Also, a positive z acceleration will induce a positive β moment and vice versa. Thus, the coupled pitch-surge moment is

$$M_{h_{\beta z}} = M_{h_{z\beta}} = M_{h_{zz}}\left(H_{CG} - H_{CP}\right) \quad . \tag{84}$$

Summarizing the inertial hydrodynamic force coefficients, i.e., the elements of the hydrodynamic mass dyadic for a half-immersed oblate spheroid, we find

$$M_h = \begin{bmatrix} m_{h_{xx}} & 0 & 0 & 0 & 0 & 0 \\ 0 & m_{h_{yy}} & 0 & 0 & 0 & m_{h_{y\gamma}} \\ 0 & 0 & m_{h_{zz}} & 0 & m_{h_{z\beta}} & 0 \\ 0 & 0 & 0 & I_{h_{\alpha\alpha}} & 0 & 0 \\ 0 & 0 & m_{h_{\beta z}} & 0 & I_{h_{\beta\beta}} & 0 \\ 0 & m_{h_{\gamma y}} & 0 & 0 & 0 & I_{h_{\gamma\gamma}} \end{bmatrix} . \tag{85}$$

For the special case of a sphere, the elements of the dyadic are

$$m_{h_{xx}} = 1.85\,\rho A^3 \qquad 0 < A' < 0.1$$

$$\quad = (1.02\,A'^{-0.256})\,\rho A^3 \qquad 0.1 < A' < 3.4$$

$$m_{h_{yy}} = m_{h_{zz}} = (1.089 + 0.529\,A')\,\rho A^3 \qquad 0 < A' < 0.74$$

$$\quad = (1.0/(-0.0318 + 0.954\,A'))\,\rho A^3 \qquad 0.74 < A' < 3.4$$

$$I_{h_{\alpha\alpha}} = I_{h_{\beta\beta}} = I_{h_{\gamma\gamma}} = \frac{4}{3}\pi\rho A^5 \cdot \frac{1 + \beta A}{1 + 2\beta A + 2\beta^2 A^2}$$

$$m_{h_{y\gamma}} = m_{h_{\gamma y}} = -m_{h_{yy}}\,(H_{CG} - H_{CP})$$

$$m_{h_{z\beta}} = m_{h_{\beta z}} = m_{h_{zz}}\,(H_{CG} - H_{CP}) ,$$

where .

A' is defined as $\frac{A\sigma^2}{g}$

A is the sphere radius

σ is the angular frequency

ρ is the fluid density

β is defined as $\sqrt{\sigma/2\nu}$

ν is the kinematic viscosity

H_{CG}, H_{CP} are locations of centers of gravity and pressure.

In a similar fashion, the dissipative force coefficients due to surface wave generation are

$$N = \begin{bmatrix} n_{xx} & 0 & 0 & 0 & 0 & 0 \\ 0 & n_{yy} & 0 & 0 & 0 & n_{y\gamma} \\ 0 & 0 & n_{zz} & 0 & n_{z\beta} & 0 \\ 0 & 0 & 0 & 0 & 0 & 0 \\ 0 & 0 & n_{\beta z} & 0 & n_{\beta\beta} & 0 \\ 0 & n_{\gamma y} & 0 & 0 & 0 & n_{\gamma\gamma} \end{bmatrix} \qquad (86)$$

.

Again, for the special case of a sphere, the elements of the dyadic are

$$
\begin{aligned}
n_{xx} &= (0.126 + 1.7 \cdot a')\rho\sigma a^3 && 0 < a' < 0.4 \\
&= (1.18\, e^{-0.13 a'})\rho\sigma a^3 && 0.4 < a' < 3.4 \\
n_{yy} = n_{zz} &= 0 && 0 < a' < 0.1 \\
&= (-0.069 + 0.71 a')\rho\sigma a^3 && 0.1 < a' < 1.37 \\
&= (1.595\, e^{-0.415 a'})\rho\sigma a^3 && 1.37 < a' < 3.4 \\
n_{\beta\beta} &= n_{\gamma\gamma} = 0 \\
n_{y\gamma} &= n_{\gamma y} = -n_{yy}(H_{CG} - H_{CP}) \\
n_{z\beta} &= n_{\beta z} = n_{zz}(H_{CG} - H_{CP}) \, .
\end{aligned}
$$

Dissipative forces due to viscosity are assumed to follow a velocity-squared drag law. There is some question as to the validity of representing an unsteady force with a coefficient based upon steady flow experimental measurements. Martin[46] has found that the mean drag coefficient for a plate started impulsively from rest is an order of magnitude greater than for steady flow. However, there is no general, analytical method available to compute the viscous forces for a fully turbulent, oscillatory flow. Schlicting[47] cites use of a method of successive approximations for unsteady laminar flow. Since viscous forces, $f(a^2)$, are an order of magnitude less than hydrodynamic inertia and wave damping forces, $f(a^3)$, and because steady currents are acting on the buoy, the viscous forces are assumed to follow a velocity-squared drag law for subcritical Reynold's numbers.

Analagous to the hydrodynamic mass dyadic, the viscous force matrix will contain ten elements. The viscous force coefficient matrix is

$$
\mathbb{D} = \begin{bmatrix} d_{xx} & 0 & 0 & 0 & 0 & 0 \\ 0 & d_{yy} & 0 & 0 & 0 & d_{y\gamma} \\ 0 & 0 & d_{zz} & 0 & d_{z\beta} & 0 \\ 0 & 0 & 0 & d_{\alpha\alpha} & 0 & 0 \\ 0 & 0 & d_{\beta z} & 0 & d_{\beta\beta} & 0 \\ 0 & d_{\gamma y} & 0 & 0 & 0 & d_{\gamma\gamma} \end{bmatrix} , \tag{87}
$$

where

$$
d_{xx} = \frac{\rho}{2} C_{DH} A_H
$$

$$
d_{yy} = d_{zz} = \frac{\rho}{2} C_{DS} A_S
$$

$$
d_{\alpha\alpha} = d_{\beta\beta} = d_{\gamma\gamma} = \frac{4}{3} \pi \mu A^3 \cdot \frac{3 + 6\beta A + 6\beta^2 A^2 + 2\beta^3 A^3}{1 + 2\beta A + 2\beta^2 A^2}
$$

$$
d_{y\gamma} = d_{\gamma y} = -d_{yy} (H_{CG} - H_{CP})
$$

$$
d_{z\beta} = d_{\beta z} = d_{zz} (H_{CG} - H_{CP}) .
$$

The projected area in heave is

$$
A_H \cong \pi b^2 \tag{88}
$$

and in surge or sway is

$$
A_S = \frac{\pi}{2} A b + \frac{b}{A} H_D \sqrt{A^2 - H_D^2} + A b \sin^{-1} \frac{H_D}{|A|} . \tag{89}
$$

For half-immersed spheroids, Hoerner[42] shows plots of drag coefficient (surge or sway) versus the ratio of vertical to horizontal axis dimensions.

Hoerner's plot for a subcritical drag coefficient is fitted by the function

$$C_{DS} = 0.354\ a/b \qquad Re < 10^5; \quad \text{subcritical}$$

for various spheroids. The drag coefficient in heave is approximated with one-half the value for a sphere, $C_{DH} = 0.3$.

3.1.5 Ocean Waves

In order to compute the magnitude of the hydrodynamic forces with the coefficients just derived, the relative motion of the fluid surrounding the buoy, relative to the buoy, must be computed. A mathematical model of the sea state must be developed.

The following hypothesis offered by St. Denis and Pierson[24] in 1953 has been verified by Dalzell,[49,50] Gerritsma,[51] and others for the motions of ships in a random seaway:

1. Assume that the sea can be represented as the linear sum of elementary waves, each traveling in the manner described by the classical Airy formulas of linearized water wave theory. Each component wave train will have random phase.

2. Weight the component waves to have the same spectral characteristics as the observed sea state.

3. Assume that the body response to a random sea is the sum of its responses to the various frequency components.

Within the constraints imposed by the assumptions made in the derivation of the hydrodynamic coefficients, i.e., body dimensions are small compared with a wavelength, the St. Denis-Pierson hypothesis should be better suited to the case of a buoy, with dimensions on the order of 10 ft, than to ships, with dimensions on the order of 100 ft. (For example, as a worst case, a 10-ft buoy in waves with 100-ft wavelengths would only cause a peak error of 3.3 percent in the computed elevation of the mean waterplane. This error will decrease as the wavelengths become longer.)

From the Airy formulas, water particle motions in deep water for waves traveling along the z axis are described as follows:

Wave Height

$$X_w = A_w \sin(kz - \sigma t) \tag{90A}$$

Vertical Velocity Component

$$\dot{X}_w = -\frac{A_w g k}{\sigma} \cos(kz - \sigma t) \tag{90B}$$

Horizontal Velocity Component

$$\dot{Z}_w = \frac{A_w g k}{\sigma} \sin(kz - \sigma t) \tag{90C}$$

Vertical Acceleration Component

$$\ddot{X}_w = -A_w g k \sin(kz - \sigma t) \tag{90D}$$

Horizontal Acceleration Component

$$\ddot{Z}_w = -A_w g k \cos(kz - \sigma t) \tag{90E}$$

Wave Slope

$$\beta_w = -\tan^{-1}\left(A_w k \cos(kz - \sigma t)\right)$$
$$\cong -A_w k \cos(kz - \sigma t) \tag{90F}$$

Angular Velocity of Free Surface

$$\dot{\beta}_w \cong -A_w k \sigma \sin(kz - \sigma t) \tag{90G}$$

Angular Acceleration of Free Surface

$$\ddot{\beta}_w \cong A_w k \sigma^2 \cos(kz - \sigma t) \tag{90H}$$

where

k is the wave number $(k = 2\pi / L_o)$

L_o is the wavelength

σ is the angular frequency

t is the time.

The assumption that body dimensions are small compared with wavelengths implies that body displacements are small compared with wavelengths. Thus, we find that

$$X_w \cong -A_w \sin \sigma t \quad , \tag{91A}$$

$$\dot{X}_w \cong -A_w \sigma \cos \sigma t \quad , \tag{91B}$$

$$\dot{z}_w \cong -A_w \sigma \sin \sigma t \quad , \tag{91C}$$

$$\ddot{X}_w \cong A_w \sigma^2 \sin \sigma t \;, \tag{91D}$$

$$\ddot{Z}_w \cong -A_w \sigma^2 \cos \sigma t \;, \tag{91E}$$

$$\beta_w \cong A_w k \cos \sigma t \;, \tag{91F}$$

$$\dot{\beta}_w \cong -A_w k \sigma \sin \sigma t \;, \tag{91G}$$

and

$$\ddot{\beta}_w \cong -A_w k \sigma^2 \cos \sigma t \;. \tag{91H}$$

Transforming the water mass velocities and accelerations to body coordinates, we see that the velocities are

$$\begin{bmatrix} \dot{X}_{w2} \\ \dot{Y}_{w2} \\ \dot{Z}_{w2} \end{bmatrix} = \Omega \cdot \begin{bmatrix} \dot{X}_w \\ 0 \\ \dot{Z}_w \end{bmatrix} \;, \tag{92A}$$

and that the accelerations are

$$\begin{bmatrix} \ddot{X}_{w2} \\ \ddot{Y}_{w2} \\ \ddot{Z}_{w2} \end{bmatrix} = \Omega \cdot \begin{bmatrix} \ddot{X}_w \\ 0 \\ \ddot{Z}_w \end{bmatrix} \;. \tag{92B}$$

The location of the intersection of the free surface and the "vertical" axis of the buoy is

$$H_D = X_{0G} \cos\beta \cos\gamma + X_2 - X_W \cos\beta \cos\gamma \ . \tag{93}$$

In order to develop a random wave model, the statistical properties of the sea state must be described. The development of wind waves on a body of water is either limited by the distance to land in the direction from which the wind blows (fetch limited) or by the length of time during which the wind acts on the water surface (duration limited). For the fetch limited case, Bretschneider[52] normalized the original wind wave forecasting relations of Sverdrup and Munk[53] and included much additional data. Bretschneider's dimensionless curves have been approximated by piecewise linear functions by Patton.[54] The approximate functions are as follows:

Significant Period

$$\bar{T}_{1/3} = 2.47 \times 10^{-2} \qquad \bar{F} < 2.0 \times 10^{-2} \tag{94A}$$

$$\log \bar{T}_{1/3} = -1.136 + 0.283 \log \bar{F} \qquad 2 \times 10^{-2} < \bar{F} < 1.2 \times 10^{5} \tag{94B}$$

$$\bar{T}_{1/3} = 2.0 \qquad \bar{F} > 1.2 \times 10^{5} \tag{94C}$$

Significant Height

$$\bar{H}_{1/3} = 5.74 \times 10^{-4} \qquad \bar{F} < 1.6 \times 10^{-2} \tag{95A}$$

$$\log \overline{H}_{1/3} = -2.5 + 0.415 \log \overline{F} \qquad 1.6 \times 10^{-2} < \overline{F} < 5.0 \times 10^{4} \tag{95B}$$

$$\overline{H}_{1/3} = 2.82 \times 10^{-1} \qquad \overline{F} > 5.0 \times 10^{4} \;. \tag{95C}$$

Weigel[55] extends Bretschneider's dimensionless curves to the case of duration limited wind waves. These curves are approximated by

<u>Significant Period</u>

$$\log \overline{T}_{1/3} = -0.2 + 0.224 \log \overline{D} \;, \tag{96}$$

<u>Significant Height</u>

$$\log \overline{H}_{1/3} = -2.272 + 0.3282 \log \overline{D} \;, \tag{97}$$

where

$\overline{T}_{1/3} = \dfrac{g\, T_{1/3}}{2\pi W V}$, the dimensionless significant period

$\overline{H}_{1/3} = \dfrac{g\, H_{1/3}}{W V^2}$, the dimensionless significant height

$\overline{F} = \dfrac{g\, F}{W V^2}$, the fetch parameter

$\overline{D} = \dfrac{g\, D}{W V}$, the duration parameter

$T_{1/3}$ is the significant period

$H_{1/3}$ is the significant wave height

F is the fetch

D is the duration

g is the gravitational constant

WV is the wind velocity .

In order to determine if the waves are fetch or duration limited, the minimum duration for a given fetch must be determined. From Bretschneider's curves, the minimum duration is given by

$$\mathrm{LOG}\left(\frac{D_{min} \cdot WV}{F}\right) = 1.477 - 0.255 \ \mathrm{LOG}\ \overline{F} \quad . \tag{98}$$

If the duration (D) is less than the minimum duration (D_{min}) the waves are duration limited; if greater, the waves are fetch limited.

For a given wind speed, fetch, and duration, the significant wave height and period can be computed by using the above equations. Longuet-Higgins[56] and Bretschneider[52] have shown that the distributions of wave heights and squared periods can be represented by Rayleigh distributions. Thus, the wave height distribution is

$$p(H) = \frac{\pi H}{2 \bar{H}^2} e^{-\frac{\pi}{4}\frac{H^2}{\bar{H}^2}} , \tag{99}$$

and the wave period distribution is

$$p(T) = 2.7 \frac{T^3}{\bar{T}^4} e^{-0.675\left(\frac{T}{\bar{T}}\right)^4} . \tag{100}$$

The mean wave height and periods are

$$\bar{H} = 0.625 \, H_{1/3} \tag{101}$$

and

$$\bar{T} = 0.758 \, T_{1/3} . \tag{102}$$

Ocean wind wave amplitude spectra are of the form

$$S_{H^2}(\omega) = A \, \omega^m e^{-Bn} . \tag{103}$$

Pierson and Moskowitz[57] analyzed 54 data sets and evaluated A, B, m, and n . The exponent m was set equal to -5 and n was found to vary between 2 and 4 depending on the wind speed. Kettler[58] optimized the parameters by using a least-squares fit of each data set used by Pierson-Moskowitz and proposed the form

$$S_{H^2}(\omega) = 10 \cdot \omega^{-5.5} e^{(-b\omega^{-4.5})} + C \quad , \tag{104}$$

where

$$b = (1.75 \times 10^5)\, WV^{-4.305}$$

$$C = 0.03054\, e^{(0.154 \cdot WV)} \quad .$$

The Bretschneider spectrum, given by

$$S_{H^2}(\omega) = \alpha g^2 \omega^{-5} e^{-0.675\left(\frac{g}{WV\omega F_2}\right)^4} \quad , \tag{105}$$

where

$$F_1 = \frac{g\overline{H}}{WV^2}$$

$$F_2 = \frac{g\overline{T}}{2\pi WV}$$

$$\alpha = 3.437 \frac{F_1^2}{F_2^4} \quad ,$$

was chosen for this study since it closely resembles the optimized spectrum and is integrable.

St. Denis and Pierson[24] proposed a random wave height model in 1953 of the form

$$X_w(t) = \int_0^\infty \cos\left(\omega t + \epsilon(\omega)\right) \cdot \sqrt{S_{H^2}(\omega)\, d\omega} \quad , \tag{106}$$

where $\epsilon(\omega)$ is a random variable whose values are equally probable for any value between 0 and 2π. The integral is not an integral in the Riemann sense since the function is discontinuous because of the random variable. The expression indicates that the random wave heights can be represented as a finite number of cosine waves of different frequency, each having random phase. Let the spectral density $S_{H^2}(\omega)$ be partitioned into N frequency bands (figure 12) in such a manner that

$$0 < \omega_0 < \omega_1 < \omega_2 \cdots < \omega_N = \bar{W},$$

where the spectral density is essentially zero if ω is greater than $\bar{W}$. The width of the nth band is

$$\Delta\omega_n = \omega_n - \omega_{n-1}, \tag{107}$$

and the mean angular frequency of the nth band is

$$\bar{\omega}_n = \frac{1}{2}\left(\omega_n + \omega_{n-1}\right). \tag{108}$$

The random wave height model is now defined as

$$X_w(t) = \sum_{n=1}^{N} \sqrt{S_{H^2}(\bar{\omega}_n)\Delta\omega_n} \cos\left(\bar{\omega}_n t + \epsilon_n\right),$$

where ϵ_n, $n = 1, 2, 3, \ldots, N$ are independent random variables distributed uniformly over the interval 0 to 2π. Borgman[59] indicates that an equally spaced subdivision $\Delta\omega_n = \bar{W}/N$ will result in $X_w(t)$ repeating itself with period $2\pi/\bar{\omega}_1$. Borgman

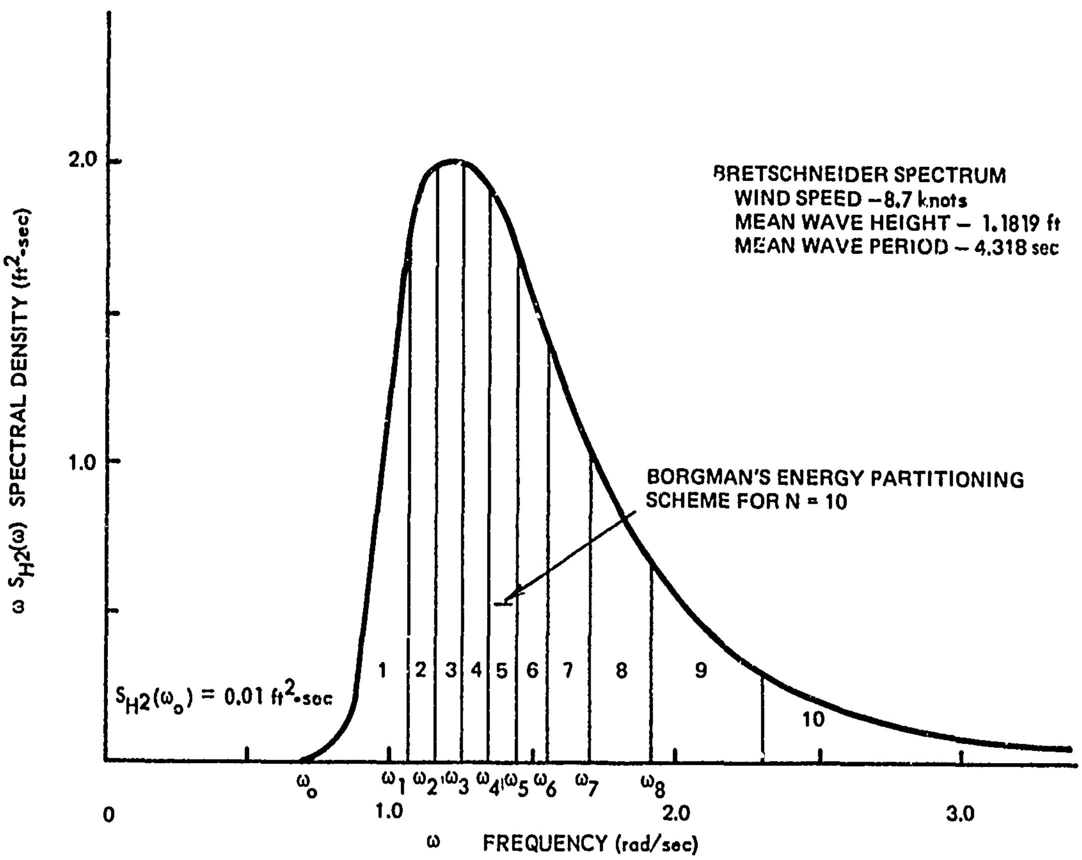

Figure 12. Borgman's Energy Partitioning in a Bretschneider Spectrum

partitions the spectrum on an energy basis using the cumulative spectrum given by

$$\bar{S}_{H^2}(\omega) = 2\int_0^{\omega} S_{H^2}(\omega)\, d\omega \quad ; \tag{109}$$

thus,

$$S_{H^2}(\bar{\omega}_n)\,\Delta\omega_n \cong \frac{1}{2}\left(\bar{S}_{H^2}(\omega_n) - \bar{S}_{H^2}(\omega_{n-1})\right) \quad ; \tag{110}$$

hence,

$$x_w(t) = \frac{1}{\sqrt{2}} \sum_{n=1}^{N} \sqrt{\bar{S}_{H^2}(\omega_n) - \bar{S}_{H^2}(\omega_{n-1})}\ \cos(\bar{\omega}_n t + \epsilon_n) . \tag{111}$$

The periodicity is avoided if the set of ω_n values are chosen to make $\bar{S}_{H^2}(\omega_n) - \bar{S}_{H^2}(\omega_{n-1})$ constant for all n . Let

$$\bar{S}_{H^2}(\omega_n) - \bar{S}_{H^2}(\omega_{n-1}) = h^2 \quad ; \tag{112}$$

then, the instantaneous wave height is

$$x_w(t) = \frac{h}{\sqrt{2}} \sum_{n=1}^{N} \cos(\bar{\omega}_n t + \epsilon_n) , \tag{113}$$

The frequencies, $\bar{\omega}_n$, are given by

$$S_{H^2}(\bar{\omega}_n) = \frac{n}{N}\, \bar{S}_{H^2}(\infty) \qquad n = 1, 2, \cdots, N \quad , \tag{114}$$

which corresponds to an equal subdivision of the energy coordinate axis for

$S_{H^2}(\omega)$.

Using the Bretschneider-Pierson spectral density of the form

$$S_{H^2}(\omega) = \frac{AB}{\omega^5}\, e^{-B/\omega^4} \quad , \tag{115}$$

which is directly integrable, we find that

$$\bar{S}_{H^2}(\omega) = 2\int_0^{\omega} \frac{AB}{s^5}\, e^{-B/s^4}\, ds \;=\; \frac{A}{2}\, e^{-B/\omega^4} \quad . \tag{116}$$

Integrating out to infinity, we find that

$$\bar{S}_{H^2}(\infty) = \frac{A}{2} \quad ,$$

and

$$\omega_n = \left[\frac{B}{\mathrm{LOG}_e (N/n)}\right]^{1/4} \quad , \tag{117}$$

where the coefficient is given by

$$B = -0.675 \left(\frac{g}{WV\ F_2}\right)^4 . \tag{118}$$

Next, we define the various elements of the random sea state model:

<u>Wave Height</u>

$$X_w(t) = \frac{1}{2} \sum_{n=1}^{N} - \sqrt{S_{H^2}(\bar{\omega}_n)\,\Delta\omega_n}\;\; \mathrm{SIN}\left(\bar{\omega}_n t + \epsilon_n\right) \tag{119}$$

Vertical Velocity Component

$$\dot{x}_w(t) = \frac{1}{2}\sum_{n=1}^{N} -\bar{\omega}_n \sqrt{S_{H^2}(\bar{\omega}_n)\Delta\omega_n}\ \cos(\bar{\omega}_n t + \epsilon_n) \tag{120}$$

Horizontal Velocity Component

$$\dot{z}_w(t) = \frac{1}{2}\sum_{n=1}^{N} -\bar{\omega}_n \sqrt{S_{H^2}(\bar{\omega}_n)\Delta\omega_n}\ \sin(\bar{\omega}_n t + \epsilon_n) \tag{121}$$

Vertical Acceleration Component

$$\ddot{x}_w(t) = \frac{1}{2}\sum_{n=1}^{N} \bar{\omega}_n^2 \sqrt{S_{H^2}(\bar{\omega}_n)\Delta\omega_n}\ \sin(\bar{\omega}_n t + \epsilon_n) \tag{122}$$

Horizontal Acceleration Component

$$\ddot{z}_w(t) = \frac{1}{2}\sum_{n=1}^{N} -\bar{\omega}_n^2 \sqrt{S_{H^2}(\bar{\omega}_n)\Delta\omega_n}\ \cos(\bar{\omega}_n t + \epsilon_n) \tag{123}$$

Wave Slope

$$\beta_w(t) = \frac{1}{2}\sum_{n=1}^{N} k_n \sqrt{S_{H^2}(\bar{\omega}_n)\Delta\omega_n}\ \cos(\bar{\omega}_n t + \epsilon_n) \tag{124}$$

Angular Velocity of Free Surface

$$\dot{\beta}_w(t) = \frac{1}{2}\sum_{n=1}^{N} -k_n \bar{\omega}_n \sqrt{S_{H^2}(\bar{\omega}_n)\Delta\omega_n}\ \sin(\bar{\omega}_n t + \epsilon_n) \tag{125}$$

Angular Acceleration of Free Surface

$$\ddot{\beta}_w(t) = \frac{1}{2}\sum_{n=1}^{N} -k_n \bar{\omega}_n^2 \sqrt{S_{H^2}(\bar{\omega}_n)\Delta\omega_n}\ \cos(\bar{\omega}_n t + \epsilon_n) \tag{126}$$

Again, the wave height, velocity components, and acceleration components must be transformed to body coordinates according to equations (92A), (92B), and (93).

A ten-component, random sea state model was programmed in FORTRAN for use with the UNIVAC 1108 digital computer at the Naval Underwater Systems Center, New London Laboratory. This program is shown in appendix B as subroutine "RWAVE." The ten-component model was found to truncate the low and high ends of the spectrum (the first and ninth frequency components). Since the low-frequency end of the spectrum is important in the computation of the response of mechanical systems, Borgman's frequency partition method was modified to include the low-frequency energy by the following numerical scheme:

1. Use a trial and error method to compute the frequency at which the value of the spectral density rises above some threshold value, for example, $S_{H^2}(\omega) > 0.01\ ft.^2$. Let this frequency be denoted ω_0 .

2. Thus,

$$\bar{\omega}_1 = \frac{1}{2}(\omega_1 - \omega_0)$$

and

$$\Delta\omega_1 = \omega_1 - \omega_0 \text{ ,}$$

3. Use the energy computed for the second partition $\bar{S}_{H^2}(\omega_2) - \bar{S}_{H^2}(\omega_1)$ to compute the component amplitude.

This method accounts for the energy in the low-frequency end of the spectrum.

3.1.6 Numerical Solution of the Equations of Motion

Having computed the wind wave displacements, velocities, and accelerations, we can now compute the hydrostatic and hydrodynamic forces acting on the buoy (terms B and H in equation (5)). The hydrostatic forces and moments depend on the position and orientation of the waterplane relative to the buoy. The wave height, given by equation (91A) for a sinusoidal wave model or by equation (119) for a random wave model, must be transformed to buoy coordinates. The transformation is

$$X_{W_Z} = X_W \cos\beta \cos\gamma - X_{OG} \cos\beta \cos\gamma \, , \tag{127}$$

where X_{OG} is the vertical height of the center of gravity of the buoy below the mean waterplane with no buoy pitch or roll. The transformed wave height must be subtracted from the heave motion of the buoy in order to apply equation (93), the location of the intersection of the waterplane and the "vertical" axis of the buoy. Restricting the study to waves traveling along the x axis of the coordinate system, the wave slope β_W in the inertial coordinate system is given by equation (91F), for sinusoidal waves and by equation (124) for the random wave model. The attitude of the waterplane, relative to the buoy coordinates, is described by the angles $\beta_S = \beta - \beta_W$ and $\gamma_S = \gamma$. The slope of the sea surface is

$$\beta' = \cos^{-1}(\cos\gamma_S \cos\beta_S). \tag{128}$$

With the location (equation (93)) and slope (equation (128)), the buoyant forces and moments for a sphere are given by equations (49), (55), and (56).

In a similar manner, the hydrodynamic forces are computed by considering water mass movements relative to the buoy. With the assumption that the buoy dimensions are small relative to the wavelength and applying the Froude-Kryloff hypothesis* for the viscous forces, we find that water mass velocities and accelerations are given by equations (91B), (91C), (91D), (91E), (91G), and (91H) for a sinusoidal wave model and by equations (120), (121), (122), (123), (125), and (126) for a random wave model. Water mass accelerations are simply transformed to buoy coordinates (equation (100B)) and subtracted from buoy accelerations to compute the motion of the buoy relative to the water mass. The relative acceleration is

$$\ddot{Q}' = \ddot{Q} - \Omega \cdot \ddot{Q}_w \quad , \tag{129}$$

where

$\ddot{Q}'$ is the acceleration vector relative to water mass

$\ddot{Q}$ is the buoy acceleration

$\ddot{Q}_w$ is the water mass acceleration.

Water mass velocities are more complex because ocean currents exist and must be included. There is a difference in reference frame that must be resolved since buoy velocities cause a reactive force (i.e., a positive buoy velocity

*The presence of the buoy does not appreciably change water mass movements in the vicinity of the buoy.

causes a negative force) while waves and currents cause active forces (positive velocities cause positive forces). The velocity vector of the buoy, relative to the water mass, is given by

$$\dot{Q}'' = \dot{Q} - \Omega \cdot \dot{Q}_w - \Omega \cdot \dot{Q}_c \quad , \tag{130}$$

where

$\dot{Q}$ is the buoy velocity vector

$\dot{Q}_w$ is the particle velocity vect r due to waves

$\dot{Q}_c$ is the current velocity vec e.

For current velocity components CV and CW acting in the positive y_o and z_o directions, respectively, the cu ent velocity vector is

$$\dot{Q}_c = \begin{bmatrix} 0 \\ CV \\ CW \end{bmatrix} \tag{131}$$

For viscous dissipative forces, which are functions of the velocity squared, the velocities are

$$\dot{Q}'^2 = \dot{Q}' \, |\dot{Q}'| \, . \tag{132}$$

The absolute value is used in order to preserve the sign convention.

If the buoy were free floating, not moored, the equations of motion for the buoy could now be integrated for a given set of environmental conditions to solve for the buoy response.

The equations of motion for a spherical buoy are summarized. Equation (5) is

$$M\ddot{Q} = MG - B - H - V - T.$$

In the R_2 coordinate system, the heave acceleration is given by

$$\ddot{x} = \frac{1}{m}\Big[mg\cos\gamma\cos\beta - B\cos\gamma\cos\beta$$

$$- m_{h_{xx}}\cdot\ddot{x}' - n_{xx}\cdot\dot{x}' - d_{xx}\cdot\dot{x}''|\dot{x}''| - W_{x_2}$$

$$+ T_x\cos\gamma\cos\beta + T_y\sin\gamma + T_z\cos\gamma\sin\beta \Big].$$

The sway acceleration is given by

$$\ddot{y} = \frac{1}{m}\Big[mg\sin\gamma\cos\beta - B\sin\gamma\cos\beta - m_{h_{yy}}\cdot\ddot{y}'$$

$$- m_{h_{y\gamma}}\cdot\ddot{\gamma}' - n_{yy}\cdot\dot{y}' - n_{y\gamma}\cdot\dot{\gamma}' - d_{yy}\cdot\dot{y}''|\dot{y}''|$$

$$- d_{y\gamma}\cdot\dot{\gamma}''|\dot{\gamma}''| - W_{y_2} - T_x\sin\gamma\cos\beta$$

$$+ T_y\cos\gamma - T_z\sin\gamma\sin\beta \Big].$$

The surge acceleration is given by

$$\ddot{z} = \frac{1}{m}\Big[-mg\sin\beta + B\sin\beta - m_{h_{zz}}\cdot\ddot{z}' - m_{h_{z\beta}}\cdot\ddot{\beta}'$$

$$- n_{zz}\cdot\dot{z}' - n_{z\beta}\cdot\dot{\beta}' - d_{zz}\cdot\dot{z}''|\dot{z}''| - d_{z\beta}\cdot\dot{\beta}''|\dot{\beta}''|$$

$$- W_{z_2} - T_x\sin\beta + T_z\cos\beta \Big].$$

The yaw acceleration is given by

$$\ddot{\alpha} = \frac{1}{I_{\alpha\alpha}} \left[- I_{h_{\alpha\alpha}} \cdot \ddot{\alpha} - d_{\alpha\alpha} \cdot \dot{\alpha} \cdot |\dot{\alpha}| \right].$$

The pitch acceleration is given by

$$\ddot{\beta} = \frac{1}{I_{\beta\beta}} \Big[-M_\beta - I_{h_{\beta\beta}} \cdot \ddot{\beta}' - m_{h_{\beta z}} \cdot \ddot{z}' - n_{\beta z} \cdot \dot{z}'$$

$$- d_{\beta\beta} \cdot \dot{\beta}'' |\dot{\beta}''| - d_{\beta z} \cdot \dot{z}'' |\dot{z}''| - W_{\beta_2}$$

$$- H_{ML} \left(-T_x \sin\beta + T_z \cos\beta \right) \Big].$$

The roll acceleration is given by

$$\ddot{\gamma} = \frac{1}{I_{\alpha\alpha}} \Big[-M_\gamma - I_{h_{\gamma\gamma}} \cdot \ddot{\gamma}' - m_{h_{\gamma y}} \cdot \ddot{y}' - n_{\gamma y} \cdot \dot{y}'$$

$$- d_{\gamma\gamma} \cdot \dot{\gamma}'' |\dot{\gamma}''| - d_{\gamma y} \cdot \dot{y}'' |\dot{y}''| - W_{\gamma_2}$$

$$- H_{ML} \left(-T_x \sin\gamma \cos\beta + T_y \cos\gamma - T_z \sin\gamma \sin\beta \right) \Big].$$

Hydrodynamic inertias and wave damping are computed for motions of the buoy relative to the water mass. Thus, for waves traveling along the z axis, we see that

$$\begin{array}{lll}
\ddot{x}' = \ddot{x} - \ddot{x}_{w_2} & \dot{x}' = \dot{x} - x_{w_2} & x' = x - x_{w_2} \\
\ddot{y}' = \ddot{y} & \dot{y}' = \dot{y} & y' = y \\
\ddot{z}' = \ddot{z} - z_{w_2} & \dot{z}' = \dot{z} - z_{w_2} & z' = z - z_{w_2} \\
\ddot{\alpha}' = \ddot{\alpha} & \dot{\alpha}' = \dot{\alpha} & \alpha' = \alpha \\
\ddot{\beta}' = \ddot{\beta} - \beta_{w_2} & \dot{\beta}' = \dot{\beta} - \dot{\beta}_{w_2} & \beta' = \beta - \beta_{w_2} \\
\ddot{\gamma}' = \ddot{\gamma} & \dot{\gamma}' = \dot{\gamma} & \gamma' = \gamma
\end{array}$$

where the subscript W_Z indicates that the computed wave induced water particle motions are transformed to the buoy coordinates. The viscous drag forces and moments must include a contribution due to the steady-state currents; thus,

$$\begin{aligned}
\dot{X}'' &= \dot{X}' \\
\dot{Y}'' &= \dot{Y}' - CV \\
\dot{Z}'' &= \dot{Z}' - CW \\
\dot{\alpha}'' &= \dot{\alpha}' \\
\dot{\beta}'' &= \dot{\beta}' \\
\dot{\gamma}'' &= \dot{\gamma}'
\end{aligned}$$

The draft of the buoy is $H_D = H_{CG} + X'$ where H_{CG} is the height of the center of gravity of the buoy from the bottom of the buoy hull. The buoyant force is

$$B = \rho g \pi A^3 \left[\frac{2}{3} + \frac{H_D}{A} \cos\beta' - \frac{H_D^3}{3A^3} \cos^3\beta' \right].$$

The pitch and roll buoyant moments are given by

$$M_\beta = B \cdot \left(Z_{CB} \cos\beta' + (H_{CG} - X_{CB}) \sin\beta' \right)$$

and

$$M_\gamma = B \cdot \left(Y_{CB} \cos\gamma' + (H_{CG} - X_{CB}) \sin\gamma' \right).$$

The hydrodynamic inertia coefficients are summarized in equation (85). Wave damping coefficients are summarized in equation (86). Viscous drag force coefficients are summarized in equation (87). Finally, wind forces are shown in equation (18).

With all the coefficients in the equations of motion defined and with the sea state model available as a forcing function, the dynamics of a free-floating buoy* (no mooring line) can be investigated by numerical solution of equation (5). The matrix equations of motion can be rewritten to yield six, coupled, second-order, ordinary differential equations with nonconstant coefficients — three force equations and three moment equations. They can be rewritten as twelve first-order equations.

These equations can be solved numerically in the time domain for the six buoy motions using a standard higher order numerical integration algorithm (usually Milne Predictor-Corrector methods or Runge-Kutta methods). In this study, a fourth-order, Runge-Kutta method was used to integrate the buoy equations of motion on a UNIVAC 1108 digital computer. Although a bit slower than Predictor-Corrector methods, the Gill's Method Runge-Kutta subroutine is available on the UNIVAC 1108 and was found to be easier to implement for large numbers of coupled, second-order differential equations.

Errors in the fourth-order, Runge-Kutta method are on the order of h^5, where h is the integration step size. For the smaller oceanographic buoys, it was found that a step size on the order of 10^{-2} sec was required for numerical stability. If a step size of 5×10^{-3} were used, the error would be on the order of 3.125×10^{-12}.

The computer programs used are described in detail in appendix B.

---

*The mooring line tension force will be developed in the next section on cable dynamics and the equations of motion for the buoy will be coupled with those for the cable.

3.2 Cable Dynamics

A study of the dynamics of cables in the ocean environment must include hydrodynamic forces acting on the cable and be capable of including nonlinear stress-strain properties for the cable. Since oceanic currents may flow in various directions at different depths and the excitation at the ends of the cable may be described by a three-dimensional force vector, the analysis must be conducted in three dimensions.

3.2.1 The Cable Equations

Consider a free body of a cable segment of length dS_o (figure 13) being acted upon by an external force per unit length, $\vec{Q}$, and assume perfect flexibility. The geometric center of the cable segment lies at a point (x_o, y_o, z_o) in a cartesian coordinate system. The external force $\vec{Q}\, dS_o$ acting on the cable segment can be resolved into components; they are

$$\vec{Q}\, dS_o = X\, dS_o \cdot \hat{i} + Y\, dS_o \cdot \hat{j} + Z\, dS_o \cdot \hat{k} \quad . \tag{133}$$

Writing Newton's Second Law, we see that in the x direction

$$\mu(S_o)\, dS_o \frac{\partial^2 x}{\partial t^2} = X\, dS_o + \left[\vec{T}(S_o + dS_o) - \vec{T}(S_o)\right] \cdot \hat{i} \quad ; \tag{134A}$$

in the y direction

$$\mu(S_o)\, dS_o \frac{\partial^2 y}{\partial t^2} = Y\, dS_o + \left[\vec{T}(S_o + dS_o) - \vec{T}(S_o)\right] \cdot \hat{j} \quad ; \tag{134B}$$

and in the z direction,

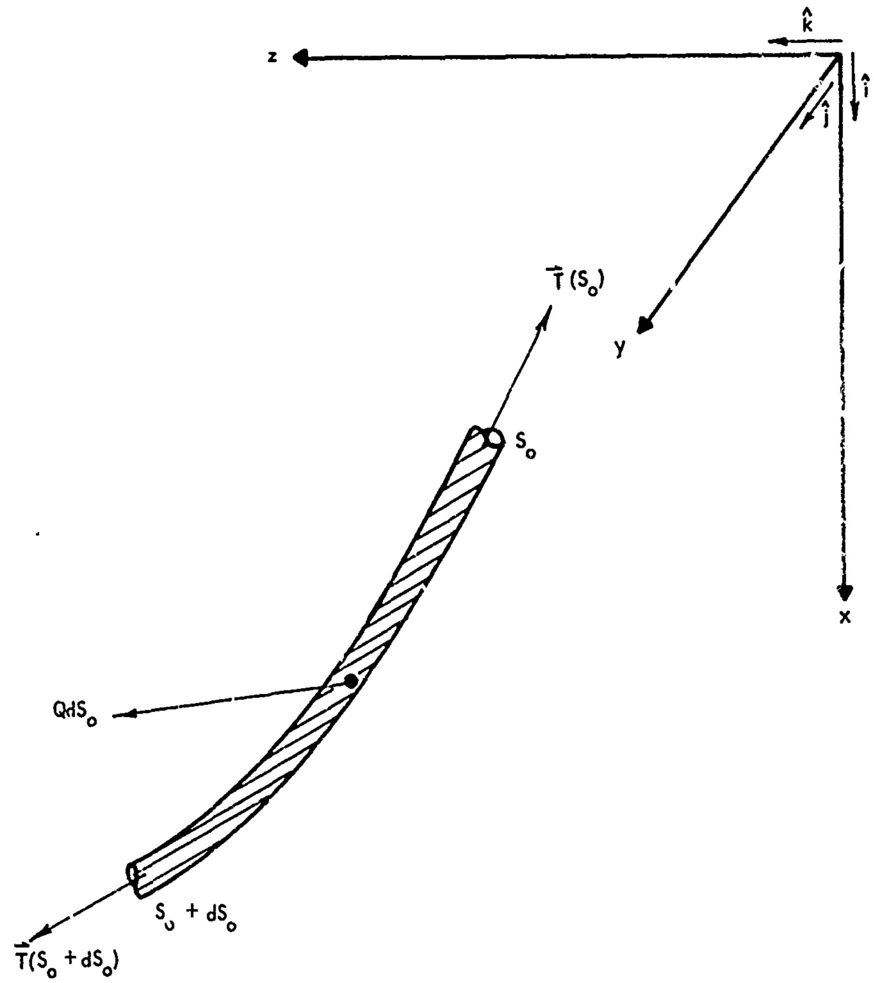

Figure 13. Free Body of a Cable Segment

$$\mu(S_o)\, dS_o \frac{\partial^2 z}{\partial t^2} = Z_1\, dS_o + \left[\vec{T}(S_o + dS_o) - \vec{T}(S_o)\right]\cdot\hat{k} \quad , \qquad \text{(134C)}$$

where $\mu(S_o)$ is the mass per unit length of the cable. Divide through by dS_o and let $dS_o \longrightarrow 0$. Taking the limit, we can write equation (134A) as

$$\mu(S_o)\frac{\partial^2 x}{\partial t^2} = \lim_{dS_o \to 0}\left(X + \frac{1}{dS_o}\left[\vec{T}(S_o + dS_o) - \vec{T}(S_o)\right]\cdot\hat{i}\right) ,$$

or

$$\mu(S_o)\frac{\partial^2 x}{\partial t^2} = X + \frac{\partial \vec{T}}{\partial S_o}\cdot\hat{i} \quad . \qquad \text{(135A)}$$

and, in a similar manner, equations (134B) and (134C) become

$$\mu(S_o)\frac{\partial^2 y}{\partial t^2} = Y + \frac{\partial \vec{T}}{\partial S_o}\cdot\hat{j} \qquad \text{(135B)}$$

and

$$\mu(S_o)\frac{\partial^2 z}{\partial t^2} = Z_1 + \frac{\partial \vec{T}}{\partial S_o}\cdot\hat{k} \quad . \qquad \text{(135C)}$$

Define the vector $\vec{r}$ from the origin to a point S_o on the cable segment. The vector is defined as

$$\vec{r} = x\cdot\hat{i} + y\cdot\hat{j} + z\cdot\hat{k} \quad .$$

A vector tangent to the cable is

$$\frac{\partial \vec{r}}{\partial S_o} = \frac{\partial x}{\partial S_o}\cdot\hat{i} + \frac{\partial y}{\partial S_o}\cdot\hat{j} + \frac{\partial z}{\partial S_o}\cdot\hat{k} \quad .$$

The unit vector tangent to the cable is

$$\frac{\frac{\partial \vec{r}}{\partial S_o}}{\left|\frac{\partial \vec{r}}{\partial S_o}\right|} = \frac{\frac{\partial \vec{r}}{\partial S_o}}{\sqrt{\left(\frac{\partial x}{\partial S_o}\right)^2 + \left(\frac{\partial y}{\partial S_o}\right)^2 + \left(\frac{\partial z}{\partial S_o}\right)^2}} \; .$$

At point S_o, the tension $\vec{T}$ is tangential to the cable if the cable is assumed to be perfectly flexible (i.e., the cable can not support bending moments). The tension is

$$\vec{T} = T \frac{\left(\frac{\partial \vec{r}}{\partial S_o}\right)}{\sqrt{\left(\frac{\partial x}{\partial S_o}\right)^2 + \left(\frac{\partial y}{\partial S_o}\right)^2 + \left(\frac{\partial z}{\partial S_o}\right)^2}} \; ,$$

where T is the magnitude of the tension. The x component of the change of tension along the cable is

$$\frac{\partial \vec{T}}{\partial S_o} \cdot \hat{i} = \frac{\partial}{\partial S_o}\left(\vec{T} \cdot \hat{i}\right) = \frac{\partial}{\partial S_o}\left(\frac{T}{\left|\frac{\partial \vec{r}}{\partial S_o}\right|} \cdot \frac{\partial x}{\partial S_o}\right) \; . \tag{136}$$

Substituting equation (136) into equation (135A), we find that

$$\mu(S_o) \frac{\partial^2 x}{\partial t^2} = X + \frac{\partial}{\partial S_o}\left(\frac{T}{\left|\frac{\partial \vec{r}}{\partial S_o}\right|} \cdot \frac{\partial x}{\partial S_o}\right) \; , \tag{137A}$$

and in a similar manner for the y and z forces, we find that

$$\mu(S_o) \frac{\partial^2 y}{\partial t^2} = Y + \frac{\partial}{\partial S_o}\left(\frac{T}{\left|\frac{\partial \vec{r}}{\partial S_o}\right|} \cdot \frac{\partial y}{\partial S_o}\right) \tag{137B}$$

and

$$\mu(S_o)\frac{\partial^2 z}{\partial t^2} = Z_1 + \frac{\partial}{\partial S_o}\left(\frac{T}{\left|\frac{\partial \vec{r}}{\partial S_o}\right|}\cdot\frac{\partial z}{\partial S_o}\right). \tag{137C}$$

The strain, (ϵ), is defined as

$$\epsilon \equiv \frac{dS - dS_o}{dS_o} = \left|\frac{\partial \vec{r}}{\partial S_o}\right| - 1 \quad , \tag{138}$$

where S is the strained length of the cable. Substituting equation (138) into equations (137A), (137B), and (137C), we can write the equations of motion as follows:

$$\mu(S_o)\frac{\partial^2 x}{\partial t^2} - \frac{\partial}{\partial S_o}\left(\frac{T}{1+\epsilon}\cdot\frac{\partial x}{\partial S_o}\right) - X = 0 \quad , \tag{139A}$$

$$\mu(S_o)\frac{\partial^2 y}{\partial t^2} - \frac{\partial}{\partial S_o}\left(\frac{T}{1+\epsilon}\cdot\frac{\partial y}{\partial S_o}\right) - Y = 0 \quad , \tag{139B}$$

and

$$\mu(S_o)\frac{\partial^2 z}{\partial t^2} - \frac{\partial}{\partial S_o}\left(\frac{T}{1+\epsilon}\cdot\frac{\partial z}{\partial S_o}\right) - Z_1 = 0 \quad . \tag{139C}$$

In addition, the auxiliary equation (138) becomes

$$\epsilon = \frac{dS}{dS_o} - 1 \quad .$$

A constitutive relation,

$$T = T(\epsilon) \quad , \tag{140}$$

must also be defined.

This set of equations is standard for cable systems and has been developed by Cristecu,[60] Schram,[61] Whicker,[62] Lindsay,[63] and others.

It is desirable to transform the equations of motion to a "natural" coordinate system (i.e.. a coordinate system aligned normal and tangential to the cable), because hydrodynamic forces are usually defined as normal and tangential to the cable. The coordinate systems are shown in figure 14. Rotating about the y axis, the transform is

$$A1 = \begin{bmatrix} \cos\theta & 0 & \sin\theta \\ 0 & 1 & 0 \\ -\sin\theta & 0 & \cos\theta \end{bmatrix} .$$

Rotating about the z axis, the transform is

$$A2 = \begin{bmatrix} \cos\phi & \sin\phi & 0 \\ -\sin\phi & \cos\phi & 0 \\ 0 & 0 & 1 \end{bmatrix} .$$

For both rotations, w‹ ‹hat

$$A = A2 \cdot A1 ;$$

thus,

$$A = \begin{bmatrix} \cos\phi\cos\theta & \sin\phi & \cos\phi\sin\theta \\ -\sin\phi\cos\theta & \cos\phi & -\sin\phi\sin\theta \\ -\sin\theta & 0 & \cos\theta \end{bmatrix} . \tag{141}$$

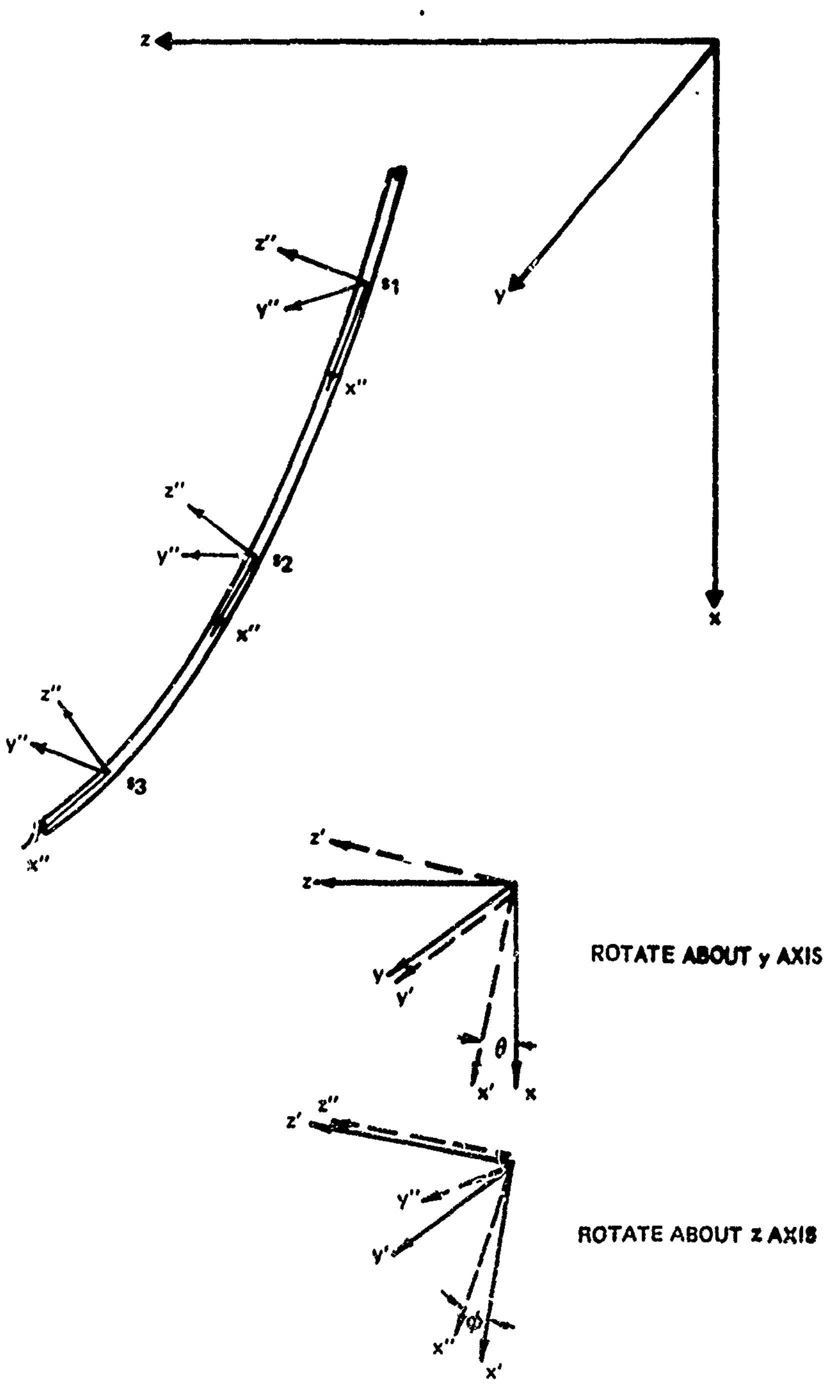

Figure 14. Cable Coordinates

A is the transform matrix from the x, y, z coordinate system to the x'', y'', z'' system. Since A is orthogonal, we see that $A^{-1} = A^t$; thus,

$$A^{-1} = \begin{bmatrix} \cos\phi\cos\theta & -\sin\phi\cos\theta & -\sin\theta \\ \sin\phi & & \\ \cos\phi\sin\theta & -\sin\phi\sin\theta & \cos\theta \end{bmatrix} . \tag{142}$$

In the double-primed system, let x'' be along the cable and z'' and y'' normal to each other and the cable. Since $\frac{1}{1+\epsilon}\left(\frac{\partial\vec{r}}{\partial S_o}\right)$ is a unit vector tangent to the cable, $\frac{1}{1+\epsilon}\left(\frac{\partial\vec{r}}{\partial S_o}\right)$ transforms to $\begin{bmatrix}1\\0\\0\end{bmatrix}$ in the double-primed coordinate system. This transformation is

$$\frac{1}{1+\epsilon}\left(\frac{\partial\vec{r}}{\partial S_o}\right) = A^{-1}\begin{bmatrix}1\\0\\0\end{bmatrix} ,$$

or

$$\left(\frac{1}{1+\epsilon}\right)\begin{bmatrix} \frac{\partial x}{\partial S_o} \\ \frac{\partial y}{\partial S_o} \\ \frac{\partial z}{\partial S_o} \end{bmatrix} = \begin{bmatrix} \cos\phi\cos\theta \\ \sin\phi \\ \cos\phi\sin\theta \end{bmatrix} . \tag{143}$$

The components of equation (143) are

$$\frac{\partial x}{\partial S_o} = (1+\epsilon)\cos\phi\cos\theta , \tag{144A}$$

$$\frac{\partial y}{\partial S_o} = (1+\epsilon)\sin\phi , \tag{144B}$$

and

$$\frac{\partial z}{\partial S_o} = (1+\epsilon)\cos\phi\,\sin\theta\ . \tag{144C}$$

Let H, G, and I be forces per unit length acting on the cable along the x'', y'', and z'' axes, respectively. In earth coordinates, the cable forces per unit length are

$$\begin{bmatrix} X \\ Y \\ Z \end{bmatrix} = A^{-1}\begin{bmatrix} H \\ G \\ I \end{bmatrix} . \tag{145}$$

Writing equations (139A), (139B), and (139C) in vector form (in the unprimed coordinate system), we see that

$$\begin{bmatrix} \frac{\partial}{\partial S_o}(T\cos\phi\cos\theta) \\ \frac{\partial}{\partial S_o}(T\sin\phi) \\ \frac{\partial}{\partial S_o}(T\cos\phi\sin\theta) \end{bmatrix} + A^{-1}\begin{bmatrix} H \\ G \\ I \end{bmatrix} = \mu(S_o)\begin{bmatrix} \frac{\partial u}{\partial t} \\ \frac{\partial v}{\partial t} \\ \frac{\partial w}{\partial t} \end{bmatrix} , \tag{146}$$

where u, v, and w are velocities in the x, y, and z directions, respectively. Transforming to the double-primed coordinate system, equation (146) becomes

$$A\begin{bmatrix} \frac{\partial}{\partial S_o}(T\cos\phi\cos\theta) \\ \frac{\partial}{\partial S_o}(T\sin\phi) \\ \frac{\partial}{\partial S_o}(T\cos\phi\sin\theta) \end{bmatrix} + \begin{bmatrix} H \\ G \\ I \end{bmatrix} = \mu(S_o)A\begin{bmatrix} \frac{\partial u}{\partial t} \\ \frac{\partial v}{\partial t} \\ \frac{\partial w}{\partial t} \end{bmatrix} . \tag{147}$$

The first term on the left is

$$\begin{bmatrix} \frac{\partial T}{\partial S_0}\left(\cos^2\phi\cos^2\theta+\sin^2\phi+\cos^2\phi\sin^2\theta\right) \\ \quad +T\frac{\partial\phi}{\partial S_0}\left(-\cos^2\theta\cos\phi\sin\phi+\sin\phi\cos\phi-\sin^2\theta\sin\phi\cos\phi\right) \\ \quad\quad +T\frac{\partial\theta}{\partial S_0}\left(-\cos^2\phi\sin\theta\cos\theta+\cos^2\phi\sin\theta\cos\theta\right) \\ \\ \frac{\partial T}{\partial S_0}\left(-\cos^2\theta\sin\phi\cos\phi+\cos\phi\sin\phi-\sin^2\theta\sin\phi\cos\phi\right) \\ \quad +T\frac{\partial\phi}{\partial S_0}\left(\cos^2\theta\sin^2\phi+\cos^2\phi+\sin^2\theta\sin^2\phi\right) \\ \quad\quad +T\frac{\partial\theta}{\partial S_0}\left(\sin\phi\cos\theta\sin\theta\cos\phi-\sin\phi\cos\theta\sin\theta\cos\phi\right) \\ \\ \frac{\partial T}{\partial S_0}\left(-\sin\theta\cos\phi\cos\theta+\sin\theta\cos\theta\cos\phi\right) \\ \quad +T\frac{\partial\phi}{\partial S_0}\left(\cos\theta\sin\theta\sin\phi-\cos\theta\sin\theta\sin\phi\right) \\ \quad\quad +T\frac{\partial\theta}{\partial S_0}\left(\cos\phi\sin^2\theta+\cos\phi\cos^2\theta\right) \end{bmatrix},$$

which can be reduced to

$$\begin{bmatrix} \frac{\partial T}{\partial S_0} \\ T\frac{\partial\phi}{\partial S_0} \\ T\cos\phi\,\frac{\partial\theta}{\partial S_0} \end{bmatrix}. \tag{148}$$

Now consider the term on the right side of equation (147),

$$\mu(S_0)A\begin{bmatrix} \frac{\partial u}{\partial t} \\ \frac{\partial v}{\partial t} \\ \frac{\partial w}{\partial t} \end{bmatrix}.$$

If U, V, and W are the velocity components along the x'', y'', and z'' axes, respectively, the velocity components in inertial coordinates are

$$\begin{bmatrix} u \\ v \\ w \end{bmatrix} = A^{-1} \begin{bmatrix} U \\ V \\ W \end{bmatrix} \quad ;$$

then, the acceleration components are

$$\begin{bmatrix} \frac{\partial u}{\partial t} \\ \frac{\partial v}{\partial t} \\ \frac{\partial w}{\partial t} \end{bmatrix} = \frac{\partial}{\partial t}(A^{-1}) \begin{bmatrix} U \\ V \\ W \end{bmatrix} + A^{-1} \begin{bmatrix} \frac{\partial U}{\partial t} \\ \frac{\partial V}{\partial t} \\ \frac{\partial W}{\partial t} \end{bmatrix} .$$

Multiply through by the mass density and the transformation matrix (A),

$$\mu(S_o) A \begin{bmatrix} \frac{\partial u}{\partial t} \\ \frac{\partial v}{\partial t} \\ \frac{\partial w}{\partial t} \end{bmatrix} = \mu(S_o) A \frac{\partial}{\partial t}(A^{-1}) \begin{bmatrix} U \\ V \\ W \end{bmatrix} + \mu(S_o) A A^{-1} \begin{bmatrix} \frac{\partial U}{\partial t} \\ \frac{\partial V}{\partial t} \\ \frac{\partial W}{\partial t} \end{bmatrix} . \tag{149}$$

Considering the first term on the right of equation (149), we see that

$$\frac{\partial}{\partial t}(A^{-1}) = \frac{\partial}{\partial t} \begin{bmatrix} \cos\phi\cos\theta & -\sin\phi\cos\theta & -\sin\theta \\ \sin\phi & \cos\phi & 0 \\ \cos\phi\sin\theta & -\sin\phi\sin\theta & \cos\theta \end{bmatrix}$$

or

$$
= \begin{bmatrix}
\left(\begin{array}{l} -\cos\theta\sin\phi\,\frac{\partial\phi}{\partial t} \\ \quad -\cos\phi\sin\theta\,\frac{\partial\theta}{\partial t}\end{array}\right) & \left(\begin{array}{l} -\cos\theta\cos\phi\,\frac{\partial\phi}{\partial t} \\ \quad +\sin\phi\sin\theta\,\frac{\partial\theta}{\partial t}\end{array}\right) & \left(-\cos\theta\,\frac{\partial\theta}{\partial t}\right) \\
\left(\cos\phi\,\frac{\partial\phi}{\partial t}\right) & \left(-\sin\phi\,\frac{\partial\phi}{\partial t}\right) & 0 \\
\left(\begin{array}{l} -\sin\theta\sin\phi\,\frac{\partial\phi}{\partial t} \\ \quad +\cos\phi\cos\theta\,\frac{\partial\theta}{\partial t}\end{array}\right) & \left(\begin{array}{l} -\sin\theta\cos\phi\,\frac{\partial\phi}{\partial t} \\ \quad -\sin\phi\cos\theta\,\frac{\partial\theta}{\partial t}\end{array}\right) & \left(-\sin\theta\,\frac{\partial\theta}{\partial t}\right)
\end{bmatrix}
$$

A further expansion of $A\,\frac{\partial}{\partial t}(A^{-1})$ gives

$$
\begin{bmatrix}
\left\{\begin{array}{l} -\cos^2\theta\cos\phi\sin\phi\,\frac{\partial\phi}{\partial t} \\ -\cos^2\phi\cos\theta\sin\theta\,\frac{\partial\theta}{\partial t} \\ +\sin\phi\cos\phi\,\frac{\partial\phi}{\partial t} \\ -\sin^2\theta\cos\phi\sin\phi\,\frac{\partial\phi}{\partial t} \\ +\cos^2\phi\cos\theta\sin\theta\,\frac{\partial\theta}{\partial t}\end{array}\right\} & \left\{\begin{array}{l} -\cos^2\theta\cos^2\phi\,\frac{\partial\phi}{\partial t} \\ +\sin\phi\sin\theta\cos\phi\cos\theta\,\frac{\partial\theta}{\partial t} \\ -\sin^2\phi\,\frac{\partial\phi}{\partial t} \\ -\sin^2\theta\cos^2\phi\,\frac{\partial\phi}{\partial t} \\ -\sin\phi\sin\theta\cos\phi\cos\theta\,\frac{\partial\theta}{\partial t}\end{array}\right\} & \left\{\begin{array}{l} -\cos\phi\cos^2\theta\,\frac{\partial\theta}{\partial t} \\ -\cos\phi\sin^2\theta\,\frac{\partial\theta}{\partial t}\end{array}\right\} \\
\left\{\begin{array}{l} \cos^2\theta\sin^2\phi\,\frac{\partial\phi}{\partial t} \\ +\sin\phi\sin\theta\cos\theta\cos\phi\,\frac{\partial\theta}{\partial t} \\ +\cos^2\phi\,\frac{\partial\phi}{\partial t} \\ +\sin^2\phi\sin^2\theta\,\frac{\partial\phi}{\partial t} \\ -\sin\phi\sin\theta\cos\theta\cos\phi\,\frac{\partial\theta}{\partial t}\end{array}\right\} & \left\{\begin{array}{l} \cos^2\theta\sin\phi\cos\phi\,\frac{\partial\phi}{\partial t} \\ -\sin^2\phi\cos\theta\sin\theta\,\frac{\partial\theta}{\partial t} \\ -\cos\phi\sin\phi\,\frac{\partial\phi}{\partial t} \\ +\sin^2\theta\sin\phi\cos\phi\,\frac{\partial\phi}{\partial t} \\ +\sin^2\phi\sin\theta\cos\theta\,\frac{\partial\theta}{\partial t}\end{array}\right\} & \left\{\begin{array}{l} \cos^2\theta\sin\phi\,\frac{\partial\theta}{\partial t} \\ +\sin^2\theta\sin\phi\,\frac{\partial\theta}{\partial t}\end{array}\right\} \\
\left\{\begin{array}{l} \sin\theta\cos\theta\sin\phi\,\frac{\partial\phi}{\partial t} \\ +\sin^2\theta\cos\phi\,\frac{\partial\theta}{\partial t} \\ -\sin\phi\cos\theta\sin\theta\,\frac{\partial\phi}{\partial t} \\ +\cos^2\theta\cos\phi\,\frac{\partial\theta}{\partial t}\end{array}\right\} & \left\{\begin{array}{l} \sin\theta\cos\theta\cos\phi\,\frac{\partial\phi}{\partial t} \\ -\sin^2\theta\sin\phi\,\frac{\partial\theta}{\partial t} \\ -\sin\theta\cos\theta\cos\phi\,\frac{\partial\phi}{\partial t} \\ -\cos^2\theta\sin\phi\,\frac{\partial\theta}{\partial t}\end{array}\right\} & \left\{\begin{array}{l} \sin\theta\cos\theta\,\frac{\partial\theta}{\partial t} \\ -\sin\theta\cos\theta\,\frac{\partial\theta}{\partial t}\end{array}\right\}
\end{bmatrix} .
$$

The above matrix can be reduced, and we find that

$$A\frac{\partial}{\partial t}(A^{-1}) = \begin{bmatrix} 0 & -\frac{\partial\phi}{\partial t} & -\cos\phi\frac{\partial\theta}{\partial t} \\ \frac{\partial\phi}{\partial t} & 0 & \sin\phi\frac{\partial\theta}{\partial t} \\ \cos\phi\frac{\partial\theta}{\partial t} & -\sin\phi\frac{\partial\theta}{\partial t} & 0 \end{bmatrix}. \tag{150}$$

Substituting into equation (149), the accelerations become

$$\mu(S_0)A\begin{bmatrix} \frac{\partial u}{\partial t} \\ \frac{\partial v}{\partial t} \\ \frac{\partial w}{\partial t} \end{bmatrix} = \mu(S_0)\begin{bmatrix} \frac{\partial U}{\partial t} - V\frac{\partial\phi}{\partial t} - W\cos\phi\frac{\partial\theta}{\partial t} \\ \frac{\partial V}{\partial t} + U\frac{\partial\phi}{\partial t} + W\sin\phi\frac{\partial\theta}{\partial t} \\ \frac{\partial W}{\partial t} + U\cos\phi\frac{\partial\theta}{\partial t} - V\sin\phi\frac{\partial\theta}{\partial t} \end{bmatrix}. \tag{151}$$

Substituting equations (148) and (151) into equation (147) and writing the component equations, we obtain the equations of motion:

$$\frac{\partial T}{\partial S_0} + H = \mu(S_0)\left(\frac{\partial U}{\partial t} - V\frac{\partial\phi}{\partial t} - W\cos\phi\frac{\partial\theta}{\partial t}\right) \tag{152}$$

$$T\frac{\partial\phi}{\partial S_0} + G = \mu(S_0)\left(\frac{\partial V}{\partial t} + U\frac{\partial\phi}{\partial t} + W\sin\phi\frac{\partial\theta}{\partial t}\right) \tag{153}$$

$$T\cos\phi\frac{\partial\theta}{\partial S_o}+I=\mu(S_o)\left(\frac{\partial W}{\partial t}+U\cos\phi\frac{\partial\theta}{\partial t}-V\sin\phi\frac{\partial\theta}{\partial t}\right). \tag{154}$$

In addition, we have the strain definition,

$$\frac{\partial S}{\partial S_o}=1+\epsilon \quad , \tag{155}$$

and the constitutive relation,

$$T=T(\epsilon) \tag{156}$$

Equations (152) through (156) give five equations in eight unknowns $(T,\phi,\theta,U,V,W,S\,\&\,\epsilon)$. Three more geometrical equations can be developed by considering the velocities. The velocities are

$$\begin{bmatrix}u\\v\\w\end{bmatrix}=A^{-1}\begin{bmatrix}U\\V\\W\end{bmatrix} ,$$

and the space derivative of the velocity vector is

$$\frac{\partial}{\partial S_o}\begin{bmatrix}u\\v\\w\end{bmatrix}=\frac{\partial}{\partial S_o}(A^{-1})\begin{bmatrix}U\\V\\W\end{bmatrix}+A^{-1}\begin{bmatrix}\frac{\partial U}{\partial S_o}\\\frac{\partial V}{\partial S_o}\\\frac{\partial W}{\partial S_o}\end{bmatrix}. \tag{157}$$

Consider the left-hand term of equation (157). The space derivative of the velocity, vector becomes

$$\frac{\partial}{\partial S_0}\begin{bmatrix} u \\ v \\ w \end{bmatrix} = \frac{\partial}{\partial S_0}\begin{bmatrix} \frac{\partial x}{\partial t} \\ \frac{\partial y}{\partial t} \\ \frac{\partial z}{\partial t} \end{bmatrix} = \frac{\partial}{\partial t}\begin{bmatrix} \frac{\partial x}{\partial S_0} \\ \frac{\partial y}{\partial S_0} \\ \frac{\partial z}{\partial S_0} \end{bmatrix} .$$

From equations (144A), (144B), and (144C), we see that

$$\frac{\partial}{\partial S_0}\begin{bmatrix} u \\ v \\ w \end{bmatrix} = \frac{\partial}{\partial t}\begin{bmatrix} (1+\epsilon)\cos\phi\cos\theta \\ (1+\epsilon)\sin\phi \\ (1+\epsilon)\cos\phi\sin\theta \end{bmatrix} . \tag{158}$$

Rewrite equation (157) and transform with A; thus

$$AA^{-1}\begin{bmatrix} \frac{\partial U}{\partial S_0} \\ \frac{\partial V}{\partial S_0} \\ \frac{\partial W}{\partial S_0} \end{bmatrix} = A\frac{\partial}{\partial S_0}\begin{bmatrix} u \\ v \\ w \end{bmatrix} - A\frac{\partial}{\partial S_0}(A^{-1})\begin{bmatrix} U \\ V \\ W \end{bmatrix}$$

and

$$\begin{bmatrix} \frac{\partial U}{\partial S_0} \\ \frac{\partial V}{\partial S_0} \\ \frac{\partial W}{\partial S_0} \end{bmatrix} = A\frac{\partial}{\partial t}\begin{bmatrix} (1+\epsilon)\cos\phi\cos\theta \\ (1+\epsilon)\sin\phi \\ (1+\epsilon)\cos\phi\sin\theta \end{bmatrix} - A\frac{\partial}{\partial S_0}(A^{-1})\begin{bmatrix} U \\ V \\ W \end{bmatrix} . \tag{159}$$

By analogy with the development of equation (148), the first term on the right-hand side of the above equation is

$$\begin{bmatrix} \frac{\partial \epsilon}{\partial t} \\ (1+\epsilon)\frac{\partial \phi}{\partial t} \\ (1+\epsilon)\cos\phi \frac{\partial \theta}{\partial t} \end{bmatrix} .$$

By analogy with the development of equation (150), the second term on the right-hand of equation (159) is

$$\begin{bmatrix} 0 & -\frac{\partial \phi}{\partial S_0} & -\cos\phi \frac{\partial \theta}{\partial S_0} \\ \frac{\partial \phi}{\partial S_0} & 0 & \sin\phi \frac{\partial \theta}{\partial S_0} \\ \cos\phi \frac{\partial \theta}{\partial S_0} & -\sin\phi \frac{\partial \theta}{\partial S_0} & 0 \end{bmatrix} .$$

Substituting into equation (159), and writing the component equations gives

$$\frac{\partial U}{\partial S_0} = \frac{\partial \epsilon}{\partial t} - \left(-V \frac{\partial \phi}{\partial S_0} - W \cos\phi \frac{\partial \theta}{\partial S_0}\right) , \tag{160A}$$

$$\frac{\partial V}{\partial S_0} = (1+\epsilon)\frac{\partial \phi}{\partial t} - \left(U \frac{\partial \phi}{\partial S_0} + W \sin\phi \frac{\partial \theta}{\partial S_0}\right), \tag{160B}$$

and

$$\frac{\partial W}{\partial S_0} = (1+\epsilon)\cos\phi \frac{\partial \theta}{\partial t} - \left(U \cos\phi \frac{\partial \theta}{\partial S_0} - V \sin\phi \frac{\partial \theta}{\partial S_0}\right) . \tag{160C}$$

Rewriting the constitutive relation, we obtain the time derivative of tension:

$$\frac{\partial T}{\partial t} = \frac{dT}{d\epsilon} \frac{\partial \epsilon}{\partial t} .$$

Finally, the equations are summarized as follows:

$$\frac{\partial T}{\partial S_o} - \mu(S_o)\left(\frac{\partial U}{\partial t} - V\frac{\partial \phi}{\partial t} - W\cos\phi\frac{\partial \theta}{\partial t}\right) + H = 0 \quad , \tag{161}$$

$$T\frac{\partial \phi}{\partial S_o} - \mu(S_o)\left(\frac{\partial V}{\partial t} + U\frac{\partial \phi}{\partial t} + W\sin\phi\frac{\partial \theta}{\partial t}\right) + G = 0 \quad , \tag{162}$$

$$T\cos\phi\frac{\partial \theta}{\partial S_o} - \mu(S_o)\left(\frac{\partial W}{\partial t} + U\cos\phi\frac{\partial \theta}{\partial t} - V\sin\phi\frac{\partial \theta}{\partial t}\right) + I = 0 \, , \tag{163}$$

$$\frac{\partial U}{\partial S_o} - \frac{\partial \epsilon}{\partial t} + \left(-V\frac{\partial \phi}{\partial S_o} - W\cos\phi\frac{\partial \theta}{\partial S_o}\right) = 0 \quad , \tag{164}$$

$$\frac{\partial V}{\partial S_o} - (1+\epsilon)\frac{\partial \phi}{\partial t} + \left(U\frac{\partial \phi}{\partial S_o} + W\sin\phi\frac{\partial \theta}{\partial S_o}\right) = 0 \quad , \tag{165}$$

$$\frac{\partial W}{\partial S_o} - (1+\epsilon)\cos\phi\frac{\partial \theta}{\partial t} + \left(U\cos\phi\frac{\partial \theta}{\partial S_o} - V\sin\phi\frac{\partial \theta}{\partial S_o}\right) = 0 \tag{166}$$

and

$$\frac{\partial T}{\partial t} - \frac{dT'}{d\epsilon}\frac{\partial \epsilon}{\partial t} = 0 \, . \tag{167}$$

We have seven, nonlinear, partial differential equations in seven unknowns. Using the constitutive relation equation (167), these reduce to six equations with six unknowns. Jeffrey and Taniuti[64] show that an analytic solution in the form of a power series for a single, nonlinear, hyperbolic, partial differential equation can only be obtained locally, or "in the small" for a point P on a noncharacteristic curve Γ in the time-space plane. Physically, it is known that the flexible cable can propagate both tensile stress waves and transverse flexural waves. It is also known that the characteristic velocity of the transverse waves is a function of the state of stress of the cable. Thus, the usual method of characteristics approach to solve nonlinear wave equations is not tractable because the characteristics diverge in the time-space domain. Solutions must be obtained simultaneously at the same locations in the time-space domain in order to continually update the transverse wave characteristic. A numerical method, which is an extension of Hartree's "hybrid" method,[65-70] will be employed to conduct simultaneous integrations at nodal points of a rectangular grid in the time-space domain. Because this method utilizes integration along characteristics in the immediate vicinity of the time-space grid nodal points, it is necessary to rewrite the cable equations in their "normal" form, i.e., characteristic equations.

First, the characteristics must be found. Assume a linear variation of tension with strain. Equation (167) reduces to

$$T = \frac{dT}{d\epsilon}\,\epsilon = K\epsilon \,.$$

Rewriting equations (161) through (166) in the form $A U_t + B U_s + G = 0$ (168)

gives

$$\begin{bmatrix} 0 & \mu V & \mu W\cos\phi & -\mu & 0 & 0 \\ 0 & -\mu U & -\mu W\sin\phi & 0 & -\mu & 0 \\ 0 & 0 & -\mu(U\cos\phi - V\sin\phi) & 0 & 0 & -\mu \\ -1 & 0 & 0 & 0 & 0 & 0 \\ 0 & -(1+\epsilon) & 0 & 0 & 0 & 0 \\ 0 & 0 & -(1+\epsilon)\cos\phi & 0 & 0 & 0 \end{bmatrix} \begin{bmatrix} \partial\epsilon/\partial t \\ \partial\phi/\partial t \\ \partial\theta/\partial t \\ \partial U/\partial t \\ \partial V/\partial t \\ \partial W/\partial t \end{bmatrix}$$

$$
+\begin{bmatrix} \frac{dT}{d\epsilon} & 0 & 0 & 0 & 0 & 0 \\ 0 & \epsilon\frac{dT}{d\epsilon} & 0 & 0 & 0 & 0 \\ 0 & 0 & \epsilon\frac{dT}{d\epsilon}\cos\phi & 0 & 0 & 0 \\ 0 & -V & -W\cos\phi & 1 & 0 & 0 \\ 0 & U & W\sin\phi & 0 & 1 & 0 \\ 0 & 0 & (U\cos\phi - V\sin\phi) & 0 & 0 & 1 \end{bmatrix} \begin{bmatrix} \partial\epsilon/\partial S_0 \\ \partial\phi/\partial S_0 \\ \partial\theta/\partial S_0 \\ \partial U/\partial S_0 \\ \partial V/\partial S_0 \\ \partial W/\partial S_0 \end{bmatrix} + \begin{bmatrix} H \\ G \\ I \\ 0 \\ 0 \\ 0 \end{bmatrix} = 0 \; .
$$

Rewriting equation (168), we see that

$$
A^{-1}AU_t + A^{-1}BU_s + A^{-1}G = 0 \quad ,
$$

or

$$
U_t + A^{-1}BU_s + A^{-1}G = 0 \; . \tag{169}
$$

The six characteristics are derived from equation (169). This derivation is shown in detail in appendix C. From appendix C the six equations (equations (161) through (166)) yield six characteristics:

$$
\lambda_1 = +\sqrt{\frac{1}{\mu(S_0)}\frac{dT}{d\epsilon}} \quad , \tag{170}
$$

$$
\lambda_2 = -\sqrt{\frac{1}{\mu(S_0)}\frac{dT}{d\epsilon}} \quad , \tag{171}
$$

$$
\lambda_3 = +\sqrt{\frac{1}{\mu(S_0)}\frac{\epsilon}{(1+\epsilon)}\frac{dT}{d\epsilon}} \quad , \tag{172}
$$

$$\lambda_4 = -\sqrt{\frac{1}{\mu(S_o)}\frac{\epsilon}{(1+\epsilon)}\frac{dT}{d\epsilon}} \quad , \tag{173}$$

$$\lambda_5 = +\sqrt{\frac{1}{\mu(S_o)}\frac{\epsilon}{(1+\epsilon)}\frac{dT}{d\epsilon}} \quad , \tag{174}$$

and

$$\lambda_6 = -\sqrt{\frac{1}{\mu(S_o)}\frac{\epsilon}{(1+\epsilon)}\frac{dT}{d\epsilon}} \quad . \tag{175}$$

Rewrite the cable equations in their normal form using the characteristics. To find the characteristic equations, we can write equation (161) in terms of ϵ using the constitutive relation (equation (167)) multiplied by $1/\mu$ and subtract from equation (164) multiplied by dS. This operation is

$$\left[\frac{1}{\mu}\frac{dT}{d\epsilon}\frac{\partial\epsilon}{\partial S}dt - \left(\frac{\partial U}{\partial t}dt - V\frac{\partial\phi}{\partial t}dt - W\cos\phi\frac{\partial\theta}{\partial t}dt\right) + \frac{1}{\mu}H\,dt\right]$$

$$+\left[\frac{\partial U}{\partial s}ds - \frac{\partial\epsilon}{\partial t}ds + \left(-V\frac{\partial\phi}{\partial s}ds - W\cos\phi\frac{\partial\theta}{\partial s}ds\right)\right] = 0 \quad . \tag{176}$$

Since there are only two independent variables, s and t, the total differential of any dependent variable, for example U, is

$$dU = \frac{\partial U}{\partial s}ds + \frac{\partial U}{\partial t}dt \quad . \tag{177}$$

The variables in equation (176) are expanded as follows:

$$-\frac{1}{\mu}\frac{dT}{d\epsilon}\frac{\partial\epsilon}{\partial s}dt - \frac{\partial\epsilon}{\partial t}ds + \frac{\partial U}{\partial t}dt + \frac{\partial U}{\partial s}ds - V\frac{\partial\phi}{\partial t}dt$$

$$-V\frac{\partial\phi}{\partial s}ds - W\cos\phi\frac{\partial\theta}{\partial t}dt - W\cos\phi\frac{\partial\theta}{\partial s}ds - \frac{1}{\mu}H\,dt = 0\,, \quad (178)$$

or

$$-\frac{1}{\mu}\frac{dT}{d\epsilon}\frac{\partial\epsilon}{\partial s}dt - \frac{\partial\epsilon}{\partial t}ds + dU - Vd\phi - W\cos\phi\,d\theta - \frac{1}{\mu}H\,dt = 0. \quad (179)$$

In terms of the characteristic values, λ, we see that

$$\left(-\lambda_{1,2}^2\frac{\partial\epsilon}{\partial s} - \frac{1}{\mu}H\right)dt - \frac{\partial\epsilon}{\partial t}ds + dU - Vd\phi - W\cos\phi\,d\theta = 0\,, \quad (180)$$

where $\lambda_{1,2} = \pm\sqrt{\frac{1}{\mu}\frac{dT}{d\epsilon}}$ are the axial wave characteristics in the t–s plane; hence, $\frac{ds}{dt} = \pm\sqrt{\frac{1}{\mu}\frac{dT}{d\epsilon}}$.

The characteristic equation becomes

$$-\sqrt{\frac{1}{\mu}\frac{dT}{d\epsilon}}\cdot d\epsilon + dU - Vd\phi - W\cos\phi\,d\theta - \frac{1}{\mu}H\,dt = 0. \quad (181)$$

This equation represents the motion of the cable in the axial direction (stretching). If we let the α characteristic be associated with $+\sqrt{\frac{1}{\mu}\frac{dT}{d\epsilon}}$ and represent disturbances traveling <u>down</u> the cable, we see that

$$\frac{dU}{d\alpha} - \sqrt{\frac{1}{\mu}\frac{dT}{d\epsilon}}\frac{d\epsilon}{d\alpha} - V\frac{d\phi}{d\alpha} - W\cos\phi\frac{d\theta}{d\alpha} - \frac{1}{\mu}H\frac{dt}{d\alpha} = 0 \quad (182)$$

Similarly, let β be associated with disturbances traveling <u>up</u> the cable,

$$-\sqrt{\frac{1}{\mu}\frac{dT}{d\epsilon}}$$; then,

$$\frac{dU}{d\beta}+\sqrt{\frac{1}{\mu}\frac{dT}{d\epsilon}}\frac{d\epsilon}{d\beta}-V\frac{d\phi}{d\beta}-W\cos\phi\frac{d\theta}{d\beta}-\frac{1}{\mu}H\frac{dt}{d\beta}=0 . \tag{183}$$

Again. equation (162) multiplied by $(1/\mu)\,dt$ is subtracted from equation (165) multiplied by ds to give

$$\frac{\partial V}{\partial s}ds+\frac{\partial V}{\partial t}dt+U\frac{\partial\phi}{\partial s}ds+U\frac{\partial\phi}{\partial t}dt+W\sin\phi\frac{\partial\theta}{\partial s}ds$$

$$+W\sin\phi\frac{\partial\theta}{\partial t}dt-(1+\epsilon)\frac{\partial\phi}{\partial t}ds-\frac{\epsilon}{\mu}\frac{dT}{d\epsilon}\frac{\partial\phi}{\partial s}dt-\frac{1}{\mu}G\,dt=0 .$$

Dividing through by $(1+\epsilon)$, we find that

$$-\left(\frac{1}{\mu}\frac{\epsilon}{(1+\epsilon)}\frac{dT}{d\epsilon}\frac{\partial\phi}{\partial s}dt+\frac{\partial\phi}{\partial t}ds\right)+\frac{1}{(1+\epsilon)}U\,d\phi+\frac{1}{(1+\epsilon)}dV$$

$$+\frac{1}{(1+\epsilon)}W\sin\phi\,d\theta-\frac{1}{\mu(1+\epsilon)}G\,dt=0 .$$

The transverse wave characteristics in the t-s plane are

$$\lambda_{3,4}=\pm\sqrt{\frac{1}{\mu}\frac{\epsilon}{(1+\epsilon)}\frac{dT}{d\epsilon}} ;$$

hence,

$$\frac{ds}{dt}=\pm\sqrt{\frac{1}{\mu}\frac{\epsilon}{(1+\epsilon)}\frac{dT}{d\epsilon}} ,$$

and

$$dV-(1+\epsilon)\sqrt{\frac{1}{\mu}\frac{\epsilon}{(1+\epsilon)}\frac{dT}{d\epsilon}}\,d\phi+U\,d\phi+W\sin\phi\,d\theta-\frac{1}{\mu}G\,dt=0 .$$

Let the α characteristic be associated with $+\sqrt{\frac{1}{\mu}\frac{\epsilon}{(1+\epsilon)}\frac{dT}{d\epsilon}}$ and represent disturbances traveling <u>down</u> the cable in the y'' - x'' plane:

$$\frac{dV}{d\alpha} - \left((1+\epsilon)\sqrt{\frac{1}{\mu}\frac{\epsilon}{(1+\epsilon)}\frac{dT}{d\epsilon}} + U\right)\frac{d\phi}{d\alpha} + W \sin\phi \frac{d\theta}{d\alpha} - \frac{1}{\mu} G \frac{dt}{d\alpha} = 0 . \quad (184)$$

Let the β characteristic be associated with $-\sqrt{\frac{1}{\mu}\frac{\epsilon}{(1+\epsilon)}\frac{dT}{d\epsilon}}$ and represent disturbances traveling up the cable in the y'' - x'' plane:

$$\frac{dV}{d\beta} + \left((1+\epsilon)\sqrt{\frac{1}{\mu}\frac{\epsilon}{(1+\epsilon)}\frac{dT}{d\epsilon}} - U\right)\frac{d\phi}{d\beta} + W \sin\phi \frac{d\theta}{d\beta} - \frac{1}{\mu} G \frac{dt}{d\beta} = 0 . \quad (185)$$

Finally, equation (163) multiplied by $(1/\mu)$dt is subtracted from equation (166) multiplied by ds to give

$$-(1+\epsilon)\cos\phi\left(\frac{\partial\theta}{\partial t} ds + \frac{1}{\mu}\frac{\epsilon}{(1+\epsilon)}\frac{dT}{d\epsilon}\frac{\partial\theta}{\partial s} dt\right) + dW$$

$$+ (U\cos\phi - V\sin\phi)\, d\theta - \frac{1}{\mu} I\, dt = 0 .$$

The transverse wave characteristic in the t-s plane is

$$\lambda_{5,6} = \pm\sqrt{\frac{1}{\mu}\frac{\epsilon}{(1+\epsilon)}\frac{dT}{d\epsilon}} ;$$

hence

$$\frac{ds}{dt} = \pm\sqrt{\frac{1}{\mu}\frac{\epsilon}{(1+\epsilon)}\frac{dT}{d\epsilon}} .$$

and

$$dW - (1+\epsilon)\cos\phi\sqrt{\frac{1}{\mu}\frac{\epsilon}{(1+\epsilon)}\frac{dT}{d\epsilon}} \cdot d\theta + (U\cos\phi - V\sin\phi)\, d\theta - \frac{1}{\mu} I\, dt = 0 .$$

Let the α characteristic be associated with $+\sqrt{\frac{1}{\mu}\frac{\epsilon}{(1+\epsilon)}\frac{dT}{d\epsilon}}$ and represent disturbances traveling down the cable in the z'' - x'' plane:

$$\frac{dW}{d\alpha} - \left((1+\epsilon)\cos\phi\sqrt{\frac{1}{\mu}\frac{\epsilon}{(1+\epsilon)}\frac{dT}{d\epsilon}} - (U\cos\phi - V\sin\phi)\right)\frac{d\theta}{d\alpha} - \frac{1}{\mu} I \frac{dt}{d\alpha} = 0 . \quad (186)$$

Let the β characteristic be associated with $-\sqrt{\frac{1}{\mu}\frac{\epsilon}{(1+\epsilon)}\frac{dT}{d\epsilon}}$ and represent disturbances traveling up the cable in the z'' - x'' plane:

$$\frac{dW}{d\beta}+\left((1+\epsilon)\cos\phi\sqrt{\frac{1}{\mu}\frac{\epsilon}{(1+\epsilon)}\frac{dT}{d\epsilon}}+(U\cos\phi-V\sin\phi)\right)\frac{d\theta}{d\beta}-\frac{1}{\mu}I\frac{dt}{d\beta}=0 \text{.} \tag{187}$$

The characteristic equations are now summarized. For tensile waves traveling down the cable with velocity $+\sqrt{\frac{1}{\mu(S_o)}\frac{dT}{d\epsilon}}$, we have

$$\frac{dU}{d\alpha}-\sqrt{\frac{1}{\mu(S_o)}\frac{dT}{d\epsilon}}\frac{d\epsilon}{d\alpha}-V\frac{d\phi}{d\alpha}-W\cos\phi\frac{d\theta}{d\alpha}-\frac{1}{\mu(S_o)}H\frac{dt}{d\alpha}=0 \text{.} \tag{188}$$

For tensile waves traveling up the cable with velocity $-\sqrt{\frac{1}{\mu(S_o)}\frac{dT}{d\epsilon}}$, we have

$$\frac{dU}{d\beta}+\sqrt{\frac{1}{\mu(S_o)}\frac{dT}{d\epsilon}}\frac{d\epsilon}{d\beta}-V\frac{d\phi}{d\beta}-W\cos\phi\frac{d\theta}{d\beta}-\frac{1}{\mu(S_o)}H\frac{dt}{d\beta}=0 \text{.} \tag{189}$$

For transverse waves in the y'' - x'' plane traveling down the cable with velocity $+\sqrt{\frac{1}{\mu(S_o)}\frac{\epsilon}{(1+\epsilon)}\frac{dT}{d\epsilon}}$, we have

$$\frac{dV}{d\alpha}-\left((1+\epsilon)\sqrt{\frac{1}{\mu(S_o)}\frac{\epsilon}{(1+\epsilon)}\frac{dT}{d\epsilon}}+U\right)\frac{d\phi}{d\alpha}+W\sin\phi\frac{d\theta}{d\alpha}-\frac{1}{\mu(S_o)}G\frac{dt}{d\alpha}=0 \text{.} \tag{190}$$

For transverse waves in the y'' - x'' plane traveling up the cable with velocity

$-\sqrt{\frac{1}{\mu(S_o)}\frac{\epsilon}{(1+\epsilon)}\frac{dT}{d\epsilon}}$, we have

$$\frac{dV}{d\beta}+\left((1+\epsilon)\sqrt{\frac{1}{\mu(S_o)}\frac{\epsilon}{(1+\epsilon)}\frac{dT}{d\epsilon}}-U\right)\frac{d\phi}{d\beta}+W\sin\phi\frac{d\theta}{d\beta}-\frac{1}{\mu(S_o)}G\frac{dt}{d\beta}=0 \text{.} \tag{191}$$

For transverse waves in the z'' - x'' plane traveling down the cable with velocity $+\sqrt{\frac{1}{\mu(S_o)}\frac{\epsilon}{(1+\epsilon)}\frac{dT}{d\epsilon}}$, we have

$$\frac{dW}{d\alpha} - \left((1+\epsilon)\cos\phi\sqrt{\frac{1}{\mu(S_o)}\frac{\epsilon}{(1+\epsilon)}\frac{dT}{d\epsilon}} - \left(U\cos\phi - V\sin\phi\right)\right)\frac{d\theta}{d\alpha} - \frac{1}{\mu(S_o)}I\frac{d\tau}{d\alpha} = 0 \quad (192)$$

For transverse waves in the z" - x" plane traveling up the cable with velocity

$-\sqrt{\frac{1}{\mu(S_o)}\frac{\epsilon}{(1+\epsilon)}\frac{dT}{d\epsilon}}$, we have

$$\frac{dW}{d\beta} + \left((1+\epsilon)\cos\phi\sqrt{\frac{1}{\mu(S_o)}\frac{\epsilon}{(1+\epsilon)}\frac{dT}{d\epsilon}} + \left(U\cos\phi - V\sin\phi\right)\right)\frac{d\theta}{d\beta} - \frac{1}{\mu(S_o)}I\frac{dt}{d\beta} = 0 \quad (193)$$

Equations (188) through (193) form the basis for a numerical solution of the three-dimensional equations of motion for a buoy mooring cable. The original set of six partial differential equations with six unknowns has been transformed to a set of six ordinary differential equations with six unknowns with the restriction that integration operations must be carried out along characteristic curves.

The solution of sets of coupled, nonlinear, partial differential equations with different characteristic velocities is usually accomplished by assuming that the equations can be decoupled. At best, they can then be linearized and a separation of variables method can be used to obtain an analytical solution. At worst, the normal forms can be integrated numerically along characteristics.

Examination of the functional form of the transverse wave characteristics show that they are dependent on the state of stress in the cable. Thus, the cable equations can not be decoupled if they are subject to time or space varying forces. Also, the particular cable system studied here is a combined initial value — boundary value system:

1. All the dependent parameters are known at time = 0.

2. The displacements at the lower bound (anchor) are constants for all time and their time derivations are zero.

3. The displacements at the upper bound (buoy motions) must be solved for simultaneously as are cable motions.

Buoy system cable motions, as posed here, can best be handled numerically with a modification of Hartree's method, i.e., solving for the values of the dependent variables at rectangular grid nodes in the time-space domain. Hartree's method, as described by Ames,[66] was developed for a single hyperbolic equation whose coefficients may be time or space dependent. In this study, the basic method will be extended for a set of coupled hyperbolic equations with variable coefficients.

3.2.2 Finite-Difference Methods

Consider a rectangular grid in the time-space plane (figure 15). Assume that the values of the six independent parameters are known at the nodal points on the jth time line. It is desired to advance the solution to the nodal points on the (j + 1)th time line; specifically, for the ith point R. If the characteristics are known at point R, characteristic lines can be drawn back from R to intersect the jth time line. The six parameter values at points B, A, and D can be linearly interpolated to find the values at each intersection point, P_1, P_2, Q_1, and Q_2. Now, the characteristic equations, (188) through (193), can be used to advance the solution to point R. For tensile waves, the length between point A and point P_1 in the grid is

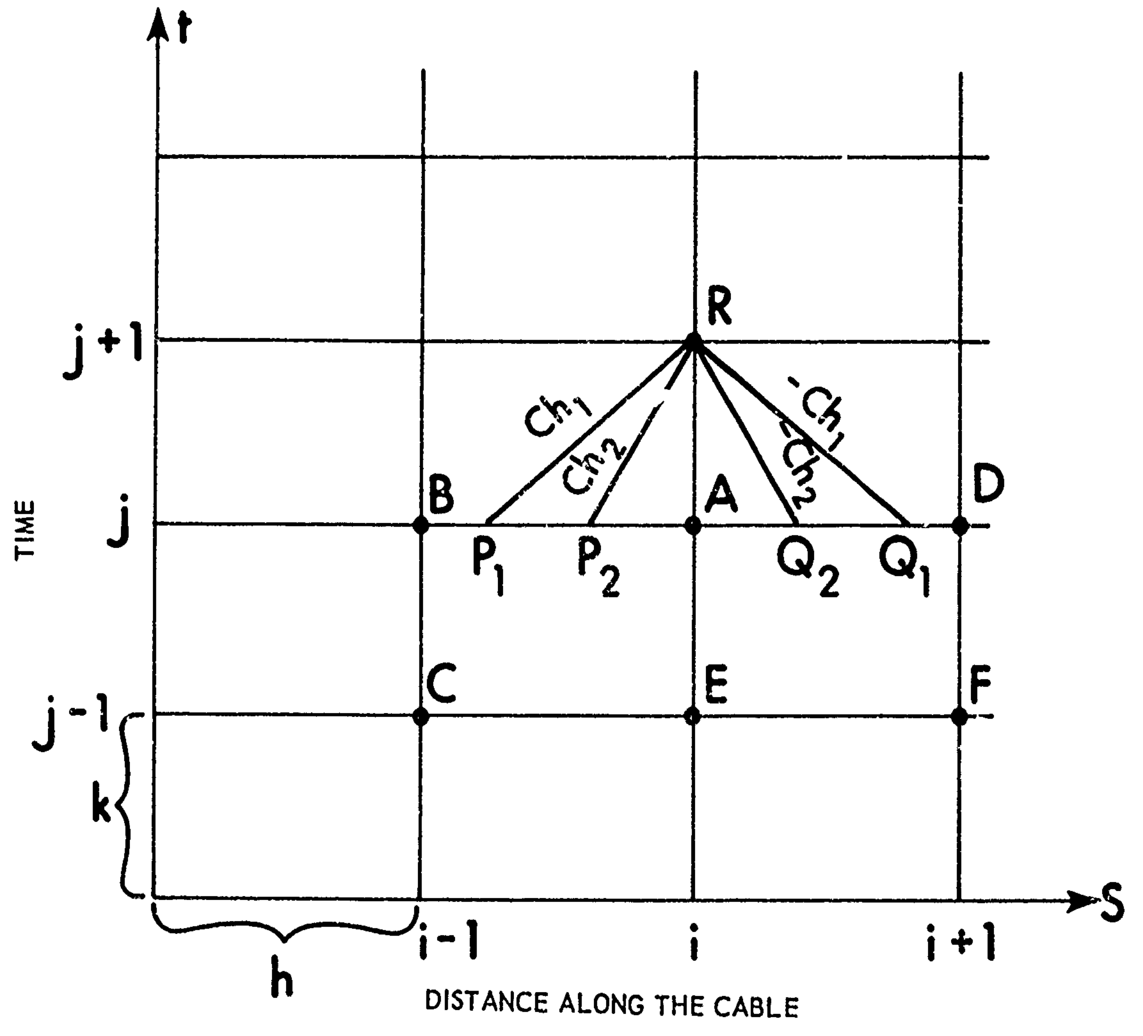

Figure 15. Grid for Adaptation of Hartree's Method

$$S_R - S_{P_1} = \frac{1}{2}\left(Ch_{1_R} + Ch_{1_{P_1}}\right) \cdot k \quad .$$

If constant cable mass and modulus is assumed, the tensile characteristic is independent of the tension; thus,

$$Ch_{1_R} = Ch_{1_{P_1}} = Ch_1 = \sqrt{\frac{1}{\mu}\frac{dT}{d\epsilon}} \quad .$$

The location of point P_1 is given by $S_R - S_{P_1} = Ch_1 \cdot k$; in a similar manner, point Q_1 (associated with tensile waves propagating up the cable) is given by $S_R - S_{Q_1} = -Ch_1 \cdot k$. For tensile waves traveling down the cable, the finite-difference equation is

$$\begin{aligned} U_R - U_{P_1} - \frac{1}{2}\left(Ch_{1_R} + Ch_{1_{P_1}}\right)\left(\epsilon_R - \epsilon_{P_1}\right) - \frac{1}{2}\left(V_R + V_{P_1}\right)\left(\phi_R - \phi_{P_1}\right) \\ - \frac{1}{2}\left(W_R + W_{P_1}\right)\left[\cos\left(\frac{1}{2}\left(\phi_R + \phi_{P_1}\right)\right)\right]\left(\theta_R - \theta_{P_1}\right) \\ - \frac{1}{\mu} \cdot \frac{1}{2}\left(H_R + H_{P_1}\right) \cdot k = 0 \quad . \end{aligned} \tag{194}$$

For tensile waves traveling up the cable, the finite-difference equation is

$$\begin{aligned} U_R - U_{Q_1} + \frac{1}{2}\left(Ch_{1_R} + Ch_{1_{Q_1}}\right)\left(\epsilon_R - \epsilon_{Q_1}\right) - \frac{1}{2}\left(V_R + V_{Q_1}\right)\left(\phi_R - \phi_{Q_1}\right) \\ - \frac{1}{2}\left(W_R + W_{Q_1}\right)\left[\cos\left(\frac{1}{2}\left(\phi_R + \phi_{Q_1}\right)\right)\right]\left(\theta_R - \theta_{Q_1}\right) \\ - \frac{1}{\mu} \cdot \frac{1}{2}\left(H_R + H_{Q_1}\right) \cdot k = 0 \quad . \end{aligned} \tag{195}$$

For transverse waves in the y" - x" plane traveling down the cable, point P_2 is located by

$$S_R - S_{P_2} = \frac{1}{2}\left(Ch_{2_R} + Ch_{2_{P_2}}\right) \cdot k \quad ,$$

where

$$Ch_{2_R} = \sqrt{\frac{1}{\mu}\frac{\epsilon}{(1+\epsilon)}\frac{dT}{d\epsilon}} \quad .$$

The finite-difference equation is

$$V_R - V_{P_2} - \frac{1}{2}\left(Ch_{2_R} + Ch_{2_{P_2}}\right)\left(\phi_R - \phi_{P_2}\right)$$
$$+ \frac{1}{2}\left(W_R + W_{P_2}\right)\left[\mathrm{SIN}\left(\frac{1}{2}\left(\phi_R + \phi_{P_2}\right)\right)\right]\left(\theta_R - \theta_{P_2}\right)$$
$$- \frac{1}{\mu}\cdot\frac{1}{2}\left(G_R + G_{P_2}\right)\cdot k = 0 \quad . \tag{196}$$

For transverse waves in the $y'' - x''$ plane traveling up the cable, point Q_2 is located by

$$S_R - S_{Q_2} = -\frac{1}{2}\left(Ch_{2_R} + Ch_{2_{Q_2}}\right)\cdot k \quad .$$

The finite-difference equation is

$$V_R - V_{Q_2} + \frac{1}{2}\left(Ch_{2_R} + Ch_{2_{Q_2}}\right)\left(\phi_R - \phi_{Q_2}\right)$$
$$+ \frac{1}{2}\left(W_R + W_{Q_2}\right)\left[\mathrm{SIN}\left(\frac{1}{2}\left(\phi_R + \phi_{Q_2}\right)\right)\right]\left(\theta_R - \theta_{Q_2}\right)$$
$$- \frac{1}{\mu}\cdot\frac{1}{2}\left(G_R + G_{Q_2}\right)\cdot k = 0 \quad . \tag{197}$$

For transverse waves in the $z'' - x''$ plane traveling down the cable (note that the characteristics for the transverse waves are the same), the finite-difference equation is

$$W_R - W_{P_2} - \left\{\frac{1}{2}\left[\left(1+\epsilon_R\right)Ch_{2_R} + \left(1+\epsilon_{P_2}\right)Ch_{2_{P_2}}\right]\mathrm{COS}\left(\frac{1}{2}\left(\phi_R + \phi_{P_2}\right)\right)\right.$$
$$\left. - \frac{1}{2}\left(U_R + U_{P_2}\right)\mathrm{COS}\left(\frac{1}{2}\left(\phi_R + \phi_{P_2}\right)\right) + \frac{1}{2}\left(V_R + V_{P_2}\right)\mathrm{SIN}\left(\frac{1}{2}\left(\phi_R + \phi_{P_2}\right)\right)\right\}\left(\theta_R - \theta_{P_2}\right)$$
$$- \frac{1}{\mu}\cdot\frac{1}{2}\left(I_R + I_{P_2}\right)\cdot k = 0 \quad . \tag{198}$$

For transverse waves in the $z'' - x''$ plane traveling up the cable, the finite-difference equation is

$$W_R - W_{Q_2} + \left\{ \frac{1}{2}\left[(1+\epsilon_R) Ch_{2_R} + (1+\epsilon_{Q_2}) Ch_{2_{Q_2}}\right] \cos\left(\tfrac{1}{2}(\phi_R + \phi_{Q_2})\right) \right.$$

$$\left. + \frac{1}{2}(U_R + U_{Q_2}) \cos\left(\tfrac{1}{2}(\phi_R + \phi_{Q_2})\right) - \frac{1}{2}(V_R + V_{Q_2}) \mathrm{SIN}\left(\tfrac{1}{2}(\phi_R + \phi_{Q_2})\right) \right\} (\theta_R - \theta_{Q_2})$$

$$- \frac{1}{\mu} \cdot \frac{1}{2}(I_R + I_{Q_2}) \cdot k = 0 \; . \qquad (199)$$

Rewriting the six finite-difference equations, we see that

$$U_R - \frac{1}{2}(Ch_{1_R} + Ch_{1_{P_1}})\epsilon_R - \frac{1}{2}(V_R + V_{P_1})\phi_R - \frac{1}{2}(W_R + W_{P_1})\left[\cos\left(\tfrac{1}{2}(\phi_R + \phi_{P_1})\right)\right]\theta_R$$

$$+ \left\{ -U_{P_1} + \frac{1}{2}(Ch_{1_R} + Ch_{1_{P_1}})\epsilon_{P_1} + \frac{1}{2}(V_R + V_{P_1})\phi_{P_1} + \frac{1}{2}(W_R + W_{P_1})\left[\cos\left(\tfrac{1}{2}(\phi_R + \phi_{P_1})\right)\right]\theta_{P_1} \right.$$

$$\left. - \frac{1}{\mu} \cdot \frac{1}{2}(H_R + H_{P_1}) \cdot k \right\} = 0 \quad , \qquad (200)$$

$$U_R + \frac{1}{2}(Ch_{1_R} + Ch_{1_{Q_1}})\epsilon_R - \frac{1}{2}(V_R + V_{Q_1})\phi_R - \frac{1}{2}(W_R + W_{Q_1})\left[\cos\left(\tfrac{1}{2}(\phi_R + \phi_{Q_1})\right)\right]\theta_R$$

$$+ \left\{ -U_{Q_1} - \frac{1}{2}(Ch_{1_R} + Ch_{1_{Q_1}})\epsilon_{Q_1} + \frac{1}{2}(V_R + V_{Q_1})\phi_{Q_1} + \frac{1}{2}(W_R + W_{Q_1})\left[\cos\left(\tfrac{1}{2}(\phi_R + \phi_{Q_1})\right)\right]\theta_{Q_1} \right.$$

$$\left. - \frac{1}{\mu} \cdot \frac{1}{2}(H_R + H_{Q_1}) \cdot k \right\} = 0 \quad , \qquad (201)$$

$$V_R - \frac{1}{2}\left((1+\epsilon_R) Ch_{2_R} + (1+\epsilon_{P_2}) Ch_{2_{P_2}}\right)\phi_R + \frac{1}{2}(W_R + W_{P_2})\left[\mathrm{SIN}\left(\tfrac{1}{2}(\phi_R + \phi_{P_2})\right)\right]\theta_R$$

$$+ \left\{ -V_{P_2} + \frac{1}{2}\left((1+\epsilon_R) Ch_{2_R} + (1+\epsilon_{P_2}) Ch_{2_{P_2}}\right)\phi_{P_2} \right.$$

$$\left. - \frac{1}{2}(W_R + W_{P_2})\left[\mathrm{SIN}\left(\tfrac{1}{2}(\phi_R + \phi_{P_2})\right)\right]\theta_{P_2} - \frac{1}{\mu}\,\frac{1}{2}(G_R + G_{P_2}) \cdot k \right\} = 0 \; , \qquad (202)$$

$$
\begin{aligned}
&V_R + \tfrac{1}{2}\left((1+\epsilon_R)Ch_{2_R} + (1+\epsilon_{Q_2})Ch_{2_{Q_2}}\right)\phi_R + \tfrac{1}{2}(W_R + W_{Q_2})\left[SIN\left(\tfrac{1}{2}(\phi_R+\phi_{Q_2})\right)\right]\theta_R \\
&\quad + \Big\{-V_{Q_2} - \tfrac{1}{2}\left((1+\epsilon_R)Ch_{2_R} + (1+\epsilon_{Q_2})Ch_{2_{Q_2}}\right)\phi_{Q_2} \\
&\qquad - \tfrac{1}{2}(W_R + W_{Q_2})\left[SIN\left(\tfrac{1}{2}(\phi_R+\phi_{Q_2})\right)\right]\theta_{Q_2} - \tfrac{1}{\mu}\tfrac{1}{2}(G_R + G_{Q_2})\cdot k\Big\} = 0 ,
\end{aligned}
\tag{203}
$$

$$
\begin{aligned}
&W_R - \Big\{\tfrac{1}{2}\left((1+\epsilon_R)Ch_{2_R} + (1+\epsilon_{P_2})Ch_{2_{P_2}}\right)COS\left(\tfrac{1}{2}(\phi_R+\phi_{P_2})\right) \\
&\qquad - \tfrac{1}{2}(U_R + U_{P_2})COS\left(\tfrac{1}{2}(\phi_R+\phi_{P_2})\right) + \tfrac{1}{2}(V_R+V_{P_2})SIN\left(\tfrac{1}{2}(\phi_R+\phi_{P_2})\right)\Big\}\theta_R \\
&\quad + \left[\left\{\begin{matrix}\text{SAME}\\ \text{COEFFICIENT}\end{matrix}\right\}\theta_{P_2} - \tfrac{1}{\mu}\cdot\tfrac{1}{2}(I_R + I_{P_2})\cdot k\right] = 0 ,
\end{aligned}
\tag{204}
$$

and

$$
\begin{aligned}
&W_R + \Big\{\tfrac{1}{2}\left((1+\epsilon_R)Ch_{2_R} + (1+\epsilon_{Q_2})Ch_{2_{Q_2}}\right)COS\left(\tfrac{1}{2}(\phi_R+\phi_{Q_2})\right) \\
&\qquad + \tfrac{1}{2}(U_R + U_{Q_2})COS\left(\tfrac{1}{2}(\phi_R+\phi_{Q_2})\right) - \tfrac{1}{2}(V_R+V_{Q_2})SIN\left(\tfrac{1}{2}(\phi_R+\phi_{Q_2})\right)\Big\}\theta_R \\
&\quad + \left[-\left\{\begin{matrix}\text{SAME}\\ \text{COEFFICIENT}\end{matrix}\right\}\theta_{Q_2} - \tfrac{1}{\mu}\cdot\tfrac{1}{2}(I_R + I_{Q_2})\cdot k\right] = 0.
\end{aligned}
\tag{205}
$$

In determinant form, they become

$$
\begin{aligned}
U_R + 0 + 0 + A_{14}\epsilon_R + A_{15}\phi_R + A_{16}\theta_R + A_{17} &= 0 \\
U_R + 0 + 0 + A_{24}\epsilon_R + A_{25}\phi_R + A_{26}\theta_R + A_{27} &= 0 \\
0 + V_R + 0 + 0 + A_{35}\phi_R + A_{36}\theta_R + A_{37} &= 0 \\
0 + V_R + 0 + 0 + A_{45}\phi_R + A_{46}\theta_R + A_{47} &= 0 \\
0 + 0 + W_R + 0 + 0 + A_{56}\theta_R + A_{57} &= 0 \\
0 + 0 + W_R + 0 + 0 + A_{66}\theta_R + A_{67} &= 0 ,
\end{aligned}
$$

where the A_{ij} are the coefficients in the preceding set of equations, (200) through (205). The six simultaneous equations are solved to give

$$\begin{array}{r} W_R + A_{56}\theta_R = -A_{57} \\ -(W_R + A_{66}\theta_R = -A_{67}) \\ \hline (A_{56} - A_{66})\theta_R = A_{67} - A_{57} \end{array}$$

$$\therefore \theta_R = \frac{(A_{67} - A_{57})}{(A_{56} - A_{66})} \ ,$$

$$W_R + A_{56}\theta_R = -A_{57} \qquad \therefore W_R = -A_{57} - A_{56}\theta_R \ ,$$

$$\begin{array}{r} V_R + A_{35}\phi_R = -A_{36}\theta_R - A_{37} \\ -(V_R + A_{45}\phi_R = -A_{46}\theta_R - A_{47}) \\ \hline (A_{35} - A_{45})\phi_R = (A_{46} - A_{36})\theta + A_{47} - A_{37} \end{array}$$

$$\therefore \phi_R = \frac{(A_{46} - A_{36})\theta + A_{47} - A_{37}}{(A_{35} - A_{45})} \ ,$$

$$V_R + A_{35}\phi_R = -A_{36}\theta_R - A_{37} \qquad \therefore V_R = -A_{35}\phi_R - A_{36}\theta_R - A_{37} \ ,$$

$$\begin{array}{r} U_R + A_{14}\epsilon_R = -A_{15}\phi_R - A_{16}\theta_R - A_{17} \\ -(U_R + A_{24}\epsilon_R = -A_{25}\phi_R - A_{26}\theta_R - A_{27}) \\ \hline (A_{14} - A_{24})\epsilon_R = (A_{25} - A_{15})\phi_R + (A_{26} - A_{16})\theta_R + A_{27} - A_{17} \end{array}$$

$$\therefore \epsilon_R = \frac{(A_{25} - A_{15})\phi_R + (A_{26} - A_{16})\theta_R + A_{27} - A_{17}}{(A_{14} - A_{24})} \ ,$$

and

$$U_R = -A_{14}\epsilon_R - A_{15}\phi_R - A_{16}\theta_R - A_{17} \ .$$

The numerical procedure within the time-space plane grid is as follows:

Step 1

Compute the coefficients of the six simultaneous equations using the values previously computed along the two preceding iso-time lines.

Parameters between grid points are estimated by linear interpolation along an iso-time line; for example,

$$U_{P_1} = U_A - (h_{P_1}/h)(U_A - U_B) ,$$

where

$$h_{P_1} = S_A - S_{P_1} .$$

Accelerations are needed to compute the hydrodynamic mass terms in the loading functions. Accelerations are estimated by using an Euler numerical approximation along an iso-space line, for example,

$$\dot{U}_R = (U_R - U_A)/k .$$

In order to begin the iteration, assume that the values of the parameters at point R are equal to the values at point A.

Step 2

Solve the simultaneous equations for the six parameters at point R.

Step 3

Go back to step 1 using the new values at R in the coefficients and recompute values at R.

Step 4

Repeat this procedure three times. *

*A more efficient method would be to specify an error and iterate until the computed parameter values converge within the error band. However, three iterations were found to give good convergence.

From the above scheme, it is obvious that solutions along two iso-time lines are needed to start the iteration. Use the initial conditions along the cable at $t = 0$ to fill in the parameter values at points C, E, and F. Assign these same values to points along the cable at $t = k$ to obtain parameter values at points B, A, and D. Begin iteration at grid point (1, 2); $S = h$, $t = 2k$, and iterate down the cable. At the lower end of the cable, set $S = h$ and $t = 3k$ and repeat.

Velocities along the upper boundary are described by the motion of the cable end. However, at the beginning of each new iso-time line, strain and angles must be computed at $S = 0$ for the previous time increment. Hartree's method can not be used here because parameter values at times less than 0 are not available. A linear extrapolation along the previous iso-time line is used to obtain the required values; for example,

$$@\, S = 0 \;;\; \epsilon_B = \epsilon_A - (\epsilon_D - \epsilon_A) \,.$$

The same problem exists along the lower boundary; only here the velocities are set to 0. Once again the values of strain and angles are determined by linear extrapolation along the previous iso-time line.

This method fails to converge if points P_1 or P_2 fall outside the space interval A-D. Since the locations of these points are determined by the characteristics, the minimum relative size of the space-to-time increment is equal to the value of the greatest characteristic. The tensile wave characteristic is always greater than the transverse wave characteristic; thus,

$$\left(\frac{h}{k}\right)_{min.} = Ch_1 \,.$$

The maximum space increment is determined by the size of the smallest wavelength in the cable. The transverse wave characteristic will determine the smallest wavelength. If the transverse wave characteristic is known to be 250 ft/sec and the cable is being excited by a sinusoid with a 2-sec period, the wavelength will be 500 ft in length. At least ten points are needed to describe a sinusoid; thus, the maximum size of the space increment is 50 ft. The time increment for a 3,000-ft/sec tensile wave characteristic is

$$K_{max.} = \frac{h}{Ch_1} = \frac{50 \text{ ft.}}{3000 \text{ ft./sec}} = 0.01667 \text{ sec} \quad .$$

Note that the characteristics must always be real, finite values. If the characteristics are zero or imaginary, the equations become ultrahyperbolic with multiple solutions for a given set of initial conditions. In this system, this is possible if the tensions are less than zero. Transverse wave characteristics are then imaginary and the problem is indeterminate. This study is further constrained by the requirement that the tension must be greater than zero at all times over the whole length of cable.

3.2.3 Cable Loading Functions

The loading functions H, G, and I (figure 16) in the cable equations are composed of the weight components in the double-primed coordinate system, the steady-state and dynamic drag components (viscous forces), and hydrodynamic inertia components (acceleration proportional forces).

The weight components are found by simply transforming the weight per unit length from the inertial coordinate system to the cable coordinates. The weight components are $W_c'' = A \cdot W_c$, or

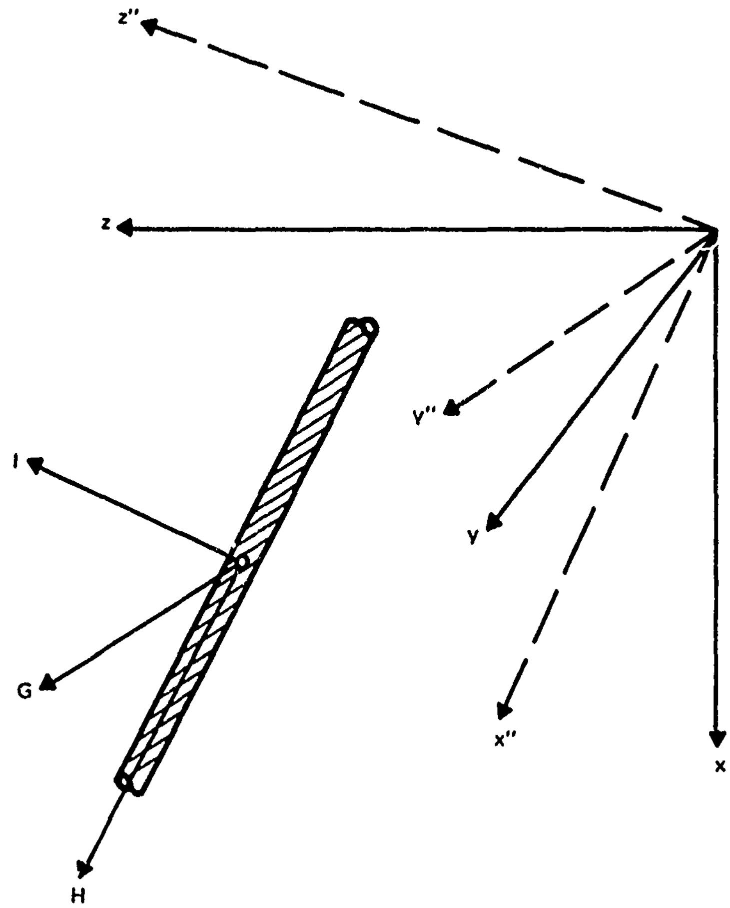

Figure 16. Cable Loading Functions

$$W_c'' = \begin{bmatrix} w_c \cos\phi \cos\theta \\ -w_c \sin\phi \cos\theta \\ -w_c \sin\theta \end{bmatrix}. \tag{206}$$

Drag forces are assumed to follow a velocity-squared drag law of the form:

$$D = \frac{1}{2}\rho C_D A V^2. \tag{207}$$

On a unit length basis, they become

$$D = \frac{1}{2}\rho C_D d V|V|, \tag{208}$$

where d is the cable diameter. In order to maintain a sign convention, equation (208) is rewritten as

$$D = \frac{1}{2}\rho C_D d V|V|. \tag{209}$$

Casarella and Parsons[71] have reviewed the state of the art for analysis of hydrodynamic forces on cable systems. Two approaches are described: the use of loading functions* to compute the normal and tangential drag force components, and the direct computation of normal and tangential drag using normal and tangential drag coefficients. The latter method, used by Wilson[11,12] for mooring problems, is employed in this study because it lends itself to three-dimensional cable problems and only requires a simple transformation of the relative velocity components to cable coordinates. The first method requires

*Loading functions are defined as the ratio of the hydrodynamic force component of interest to the drag force when the cable is oriented normal to the flow.

multiple transformations to define the normal and tangential forces and to resolve them into three force components.

If the current velocity components are given by

$$C_S = \begin{bmatrix} 0 \\ V_S \\ W_S \end{bmatrix}$$

(no vertical currents) and the velocity components of the cable element are

$$\begin{bmatrix} \dot{X} \\ \dot{Y} \\ \dot{Z} \end{bmatrix},$$

then the velocity components of the water relative to the cable are

$$\begin{bmatrix} U_R \\ V_R \\ W_R \end{bmatrix} = \begin{bmatrix} 0-\dot{X} \\ V_S-\dot{Y} \\ W_S-\dot{Z} \end{bmatrix}.$$

Transforming to cable coordinates gives

$$\begin{bmatrix} U_R'' \\ V_R'' \\ W_R'' \end{bmatrix} = \begin{bmatrix} -\dot{X}\cos\phi\cos\theta + (V_S-\dot{Y})\sin\phi + (W_S-\dot{Z})\cos\phi\sin\theta \\ \dot{X}\sin\phi\cos\theta + (V_S-\dot{Y})\cos\phi - (W_S-\dot{Z})\sin\phi\sin\theta \\ \dot{X}\sin\theta + (W_S-\dot{Z})\cos\theta \end{bmatrix}.$$

The drag force components are now written:

$$D_{x''} = \frac{1}{2}\rho C_{DT}\, d\, U_R''|U_R''| \ , \tag{210A}$$

$$D_{y''} = \frac{1}{2}\rho C_{DN}\, d\, V_R''|V_R''| \ , \tag{210B}$$

and

$$D_{z''} = \frac{1}{2}\rho C_{DN}\, d\, W_R''|W_R''| \ . \tag{210C}$$

Hoerner,[48] Wilson,[11] and others show plots of normal and tangential drag coefficients versus Reynolds number for stranded cables. Wilson's data were used in the G. S. A. program "CURFIT," and the following expressions for normal and tangential drag coefficients were developed:

$$C_{DN} = 1.32027 + 10.6962/Re \qquad 0 < Re < 100 \ ,$$

$$= 1.4 \qquad 100 < Re < 5\times10^5 \ , \tag{211A}$$

$$C_{DT} = 0.60546\cdot(Re^{-0.47588}) \qquad 0 < Re < 5\times10^5 \ , \tag{211B}$$

where $Re = \frac{Vd}{\nu}$; ν is the kinematic viscosity. These expressions are valid only in the subcritical Reynolds number region (Re 5×10^5). However, since this Reynolds number would apply to a 2-in.-diameter cable moving at 35 knots, it is felt that the range of Reynolds numbers covered is adequate.

Hydrodynamic inertia forces are defined normal and tangential to the cable. Transforming the accelerations to cable coordinates and assuming steady ocean currents, we find that the accelerations become

$$\begin{bmatrix} \ddot{x}'' \\ \ddot{y}'' \\ \ddot{z}'' \end{bmatrix} = \begin{bmatrix} \ddot{x}\cos\phi\cos\theta + \ddot{y}\sin\phi + \ddot{z}\cos\phi\sin\theta \\ -\ddot{x}\sin\phi\cos\theta + \ddot{y}\cos\phi - \ddot{z}\sin\phi\sin\theta \\ -\ddot{x}\sin\theta + \ddot{z}\cos\theta \end{bmatrix} .$$

The hydrodynamic inertia force vector is

$$\begin{bmatrix} F_{h_{mx}} \\ F_{h_{my}} \\ F_{h_{mz}} \end{bmatrix} = \begin{bmatrix} m_{h_{xx''}} & 0 & 0 \\ 0 & m_{h_{yy''}} & 0 \\ 0 & 0 & m_{h_{zz''}} \end{bmatrix} \cdot \begin{bmatrix} \ddot{x}'' \\ \ddot{y}'' \\ \ddot{z}'' \end{bmatrix} .$$

The hydrodynamic mass dyadic is a diagonal matrix due to the axisymmetry of the cable. Also, for a cylindrical object of infinite length, the tangential hydrodynamic mass ($m_{h_{xx''}}$) is zero. For a smooth, constant diameter cable, the normal hydrodynamic masses ($m_{h_{yy''}}, m_{h_{zz''}}$) are equal.

Lamb,[45] Basset,[72] and others have used potential flow theory to compute the normal hydrodynamic mass of a circular cylinder:

$$m_{h_N} = \pi \rho d^2/4 . \tag{212}$$

Miller[73] and Miller and Hagist[74] have investigated the frequency dependence of hydrodynamic mass for various bodies. Their data show a linear decrease in hydrodynamic mass with increasing frequency in the Stokes number region $0 < St. < 3 \times 10^5$. By using Miller's data for a 5:1 cylinder,[74] we can see that the slope is -1.62×10^{-6}. Equation (212) is modified to include the frequency dependence as follows:

$$m_{h_N} = \left(1.0 - (1.62 \times 10^{-6}) \cdot \frac{\omega d^2}{\nu}\right) \pi \rho d^2/4 \quad ; 0 < \frac{\omega d^2}{\nu} < 3 \times 10^5 . \tag{213}$$

The components of the hydrodynamic inertia force are

$$F_{h_{mx}} = 0 , \tag{214A}$$

$$F_{h_{my}} = m_{h_N} \cdot \ddot{y}'' , \tag{214B}$$

and

$$F_{h_{mz}} = m_{h_N} \cdot \ddot{z}'' . \tag{214C}$$

The loading functions are summarized by using equations (206), (210), and (214):

$$H = w_c \cos\phi \cos\theta + \left(0.60546 \cdot \left(Re_{U''}^{-0.4758}\right)\right) \frac{\rho}{2} d\, U_R'' \left| U_R'' \right| , \tag{215A}$$

$$G = -w_c \sin\phi \cos\theta + C_{DN_{V''}} \frac{\rho}{2} d\, V_R'' \left| V_R'' \right| + \left(1.0 - (1.62 \times 10^{-6}) \cdot \frac{\omega d^2}{\nu}\right) \pi \rho \frac{d^2}{4} \cdot \ddot{y}'' , \tag{215B}$$

and

$$I = -w_c \sin\theta + C_{DN_{W''}} \frac{\rho}{2} d\, W_R'' \left| W_R'' \right| + \left(1.0 - (1.62 \times 10^{-6}) \cdot \frac{\omega d^2}{\nu}\right) \pi \rho \frac{d^2}{4} \cdot \ddot{z}'' , \tag{215C}$$

where

$$Re_{U''} = \frac{U'' d}{\nu}$$

$$Re_{V''} = \frac{V'' d}{\nu}$$

$$Re_{W''} = \frac{W'' d}{\nu}$$

$$C_{DN_{v''}} = 1.32027 + 10.6962/Re_{v''} \qquad 0 < Re_{v''} < 100$$

$$= 1.4 \qquad 100 < Re_{v''} < 5 \times 10^5$$

$$C_{DN_{w''}} = 1.32027 + 10.6962/Re_{w''} \qquad 0 < Re_{w''} < 100$$

$$= 1.4 \qquad 100 < Re_{w''} < 5 \times 10^5 .$$

3.2.4 Lumped-Mass Model

The finite-difference analysis for cable dynamics can become very expensive in computer time and can require large amounts of computer "storage" because of the large arrays. A lumped-mass analysis can offer significant savings in computational time at the expense of simulation accuracy. In general, the lumped-mass analysis will truncate the high-frequency response of the system. However, for many engineering applications, the high-frequency, low-amplitude response is not of interest, and the cable can be represented as a small number of lumped masses.

Assume that a uniform cable of length L can be broken up into N segments of equal length (figure 17). The length of each segment is

$$\Delta L = L/N .$$

Assume that the properties (weight, mass, hydrodynamic forces, etc.) of the cable can be concentrated at points 2, 3, ..., N, which are located ΔL,

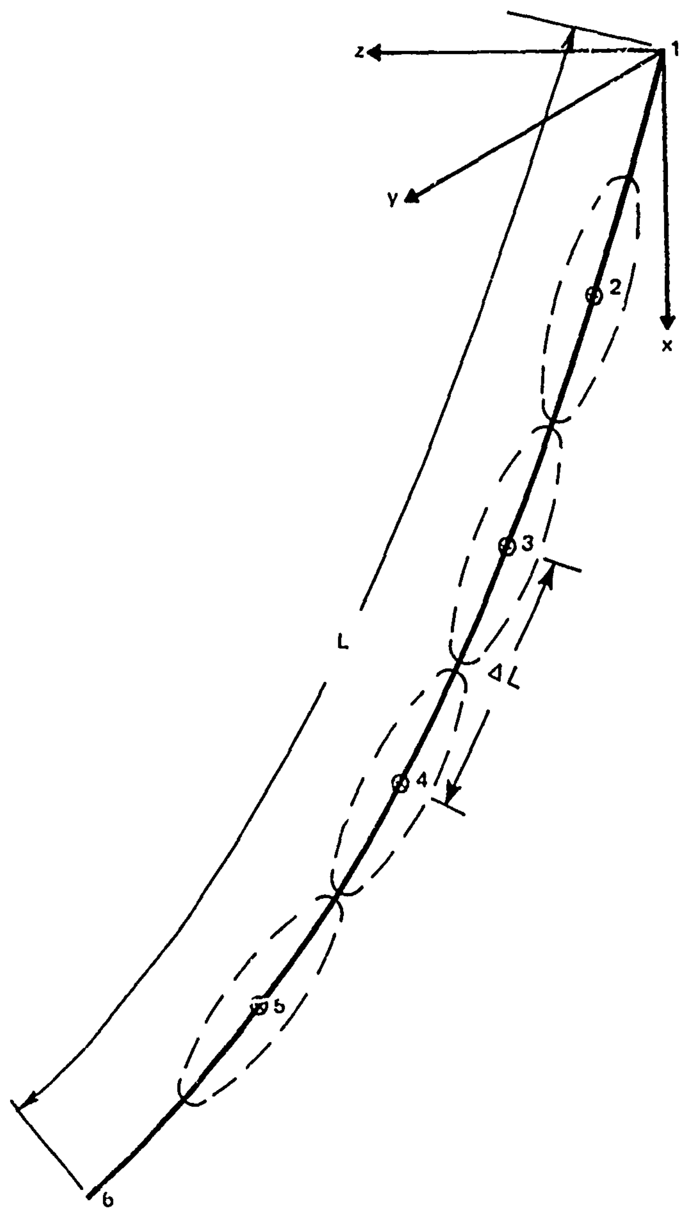

Figure 17. Segments for a Five-Element, Lumped-Mass Model

$2\Delta L, \ldots, (N-1)\Delta L$ from the upper end of the cable. All the forces acting on the cable span from $(N-1)\Delta L \pm \frac{\Delta L}{2}$ are concentrated at the nth mass point. Cristecu's cable equations, (135A), (135B), and (135C), are written for each mass point:

$$\mu(S_o)\Delta L \frac{d^2 X_n}{dt^2} = X_n \Delta L + \left(\vec{T}_n \cdot \hat{\imath} - \vec{T}_{n-1} \cdot \hat{\imath}\right) , \tag{216A}$$

$$\mu(S_o)\Delta L \frac{d^2 Y_n}{dt^2} = Y_n \Delta L + \left(\vec{T}_n \cdot \hat{\jmath} - \vec{T}_{n-1} \cdot \hat{\jmath}\right) , \tag{216B}$$

and

$$\mu(S_o)\Delta L \frac{d^2 Z_n}{dt^2} = Z_n \Delta L + \left(\vec{T}_n \cdot \hat{k} - \vec{T}_{n-1} \cdot \hat{k}\right) . \tag{216C}$$

This is equivalent to modeling the cable with a system of spring-mass elements as shown in figure 18. In order to compute the forces acting on each mass element, the cable angles (ϕ and θ) for each cable element must be defined. From the geometry between the nth and (N + 1)th mass element, we see that

$$\theta_n = \mathrm{SIN}^{-1}\left(\frac{(Z_{n+1} - Z_n)}{\sqrt{(X_{n+1} - X_n)^2 + (Z_{n+1} - Z_n)^2}}\right) \tag{217}$$

and

$$\phi_n = \mathrm{SIN}^{-1}\left(\frac{(Y_{n+1} - Y_n)}{\sqrt{(X_{n+1} - X_n)^2 + (Y_{n+1} - Y_n)^2 + (Z_{n+1} - Z_n)^2}}\right) . \tag{218}$$

Tensions between the lumped masses are computed by using the elastic properties of the cable and the deformation of the cable. If the effective cable

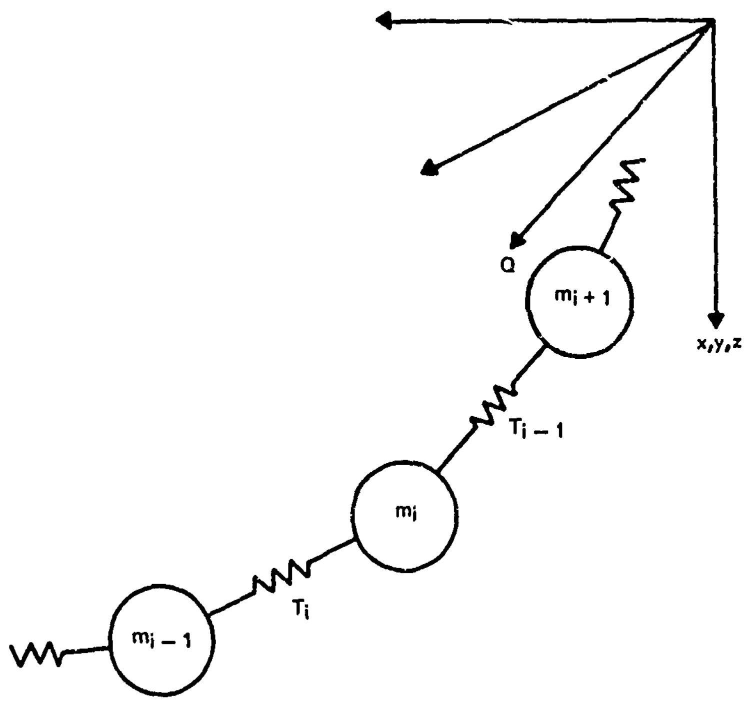

Figure 18. Lumped-Mass Model

modulus is E_c and the deformation of the cable of length ΔL is δ, the spring constant along the cable is

$$K_{x''} = \frac{F}{\delta} = \frac{\pi \frac{d^2}{4} \sigma}{\delta} = \pi \frac{d^2}{4} \frac{E_c}{\Delta L} , \tag{219}$$

The stretched length between the nth and (N + 1)th mass element is

$$\sqrt{(X_{n+1} - X_n)^2 + (Y_{n+1} - Y_n)^2 + (Z_{n+1} - Z_n)^2} .$$

If the difference between the stretched length of the cable and the unstretched length (Δ L) is less than zero, the tension is zero since the cable can not support compression. (This is analogous to the ultrahyperbolic equations that occur in the finite-difference analysis if tensions go to zero.) Otherwise, the tension in the nth cable segment is defined as

$$T_{n_{x''}} = K_{x''} \left(\sqrt{(X_{n+1} - X_n)^2 + (Y_{n+1} - Y_n)^2 + (Z_{n+1} - Z_n)^2} - \Delta L \right) . \tag{220}$$

Transforming to inertial coordinates, the tension becomes

$$T_n = A^{-1} \cdot \begin{bmatrix} T_{n_{x''}} \\ 0 \\ 0 \end{bmatrix} = \begin{bmatrix} T_{n_{x''}} \cos \phi_n \cos \theta_n \\ T_{n_{x''}} \sin \phi_n \\ T_{n_{x''}} \cos \phi_n \sin \theta_n \end{bmatrix} . \tag{221}$$

These tension components are used in equations (216) to compute the tension difference across the mass element.

As before, the forces $X_n \Delta L$, $Y_n \Delta L$ and $Z_n \Delta L$ acting on each mass element consist of weight, viscous drag, and hydrodynamic inertia forces. The weight force vector per unit length is

$$W_c = \begin{bmatrix} w_c \\ 0 \\ 0 \end{bmatrix},$$

where w_c is the weight per unit length in water of the cable. Again, if the current velocity components at the nth element are

$$C_S = \begin{bmatrix} 0 \\ V_{S_n} \\ W_{S_n} \end{bmatrix}$$

and the velocity components of the nth element are

$$\begin{bmatrix} \dot{X}_n \\ \dot{Y}_n \\ \dot{Z}_n \end{bmatrix},$$

then the relative velocity components are

$$\begin{bmatrix} U_{R_n} \\ V_{R_n} \\ W_{R_n} \end{bmatrix} = \begin{bmatrix} 0 - \dot{X}_n \\ V_{S_n} - \dot{Y}_n \\ W_{S_n} - \dot{Z}_n \end{bmatrix}, \tag{222}$$

If the mean cable angles at the nth mass element are computed, we find

$$\bar{\phi}_n = \frac{1}{2}(\phi_n + \phi_{n-1}) \tag{223A}$$

and

$$\bar{\theta}_n = \frac{1}{2}\left(\theta_n + \theta_{n-1}\right) . \tag{223B}$$

The relative velocity components are transformed to cable coordinates as follows:

$$U''_{R_n} = -\dot{X}_n \cos\bar{\phi}_n \cos\bar{\theta}_n + (V_{S_n} - \dot{Y}_n)\sin\bar{\phi}_n + (W_{S_n} - \dot{Z}_n)\cos\bar{\phi}_n \sin\bar{\theta}_n ,$$

$$V''_{R_n} = \dot{X}_n \sin\bar{\phi}_n \cos\bar{\theta}_n + (V_{S_n} - \dot{Y}_n)\cos\bar{\phi}_n - (W_{S_n} - \dot{Z}_n)\sin\bar{\phi}_n \sin\bar{\theta}_n ,$$

and

$$W''_{R_n} = \dot{X}_n \sin\bar{\theta}_n + (W_{S_n} - \dot{Z}_n)\cos\bar{\theta}_n .$$

The drag forces per unit length are

$$D''_{X_n} = \frac{1}{2}\rho C_{DT}\, d\, U''_{R_n} \left| U''_{R_n} \right| ,$$

$$D''_{Y_n} = \frac{1}{2}\rho C_{DN}\, d\, V''_{R_n} \left| V''_{R_n} \right| ,$$

and

$$D''_{Z_n} = \frac{1}{2}\rho C_{DN}\, d\, W''_{R_n} \left| W''_{R_n} \right| ,$$

where the drag coefficients are computed from equations (211A) and (211B).

The accelerations of the nth mass element in cable coordinates are

$$\ddot{X}''_n = \ddot{X}_n \cos\bar{\phi}_n \cos\bar{\theta}_n + \ddot{Y}_n \sin\bar{\phi}_n + \ddot{Z}_n \cos\bar{\phi}_n \sin\bar{\theta}_n ,$$

$$\ddot{Y}''_n = -\ddot{X}_n \sin\bar{\phi}_n \cos\bar{\theta}_n + \ddot{Y}_n \cos\bar{\phi}_n - \ddot{Z}_n \sin\bar{\phi}_n \sin\bar{\theta}_n ,$$

and

$$\ddot{Z}''_n = -\ddot{X}_n \sin\bar{\theta}_n + \ddot{Z}_n \cos\bar{\theta}_n .$$

The hydrodynamic inertia force components per unit length are

$$F''_{hm_{x_n}} = 0 \quad , \tag{224A}$$

$$F''_{hm_{y_n}} = -m_{h_n} \cdot \ddot{Y}''_n \quad , \tag{224B}$$

and

$$F''_{hm_{z_n}} = -m_{h_n} \cdot \ddot{Z}''_n \quad , \tag{224C}$$

where m_{h_n} is computed from equation (213). The drag and hydrodynamic inertia forces per unit length are summed and transformed back to inertial coordinates and added to the weight force; thus,

$$\begin{bmatrix} X_n \\ Y_n \\ Z_n \end{bmatrix} = \begin{bmatrix} W_c \\ 0 \\ 0 \end{bmatrix} + A^{-1} \cdot \begin{bmatrix} D''_{x_n} + 0 \\ D''_{y_n} + F''_{hm_{y_n}} \\ D''_{z_n} + F''_{hm_{z_n}} \end{bmatrix} . \tag{225}$$

All terms have been defined in the equations of motion for the cable elements. The three equations, (216A), (216B), and (216C), must be integrated simultaneously for each mass element. Thus, if the cable is broken up into ten segments, there will be nine mass elements, each having three degrees of freedom. Therefore, there will be 9 x 3 x 2 = 54 simultaneous first-order equations. Note that the upper half of the first cable length and the lower half of the last cable length are not included in these equations of motion. These cable segments are assumed to be moving with the upper and lower boundaries and their properties should be lumped in with the properties of the buoy and anchor. The computer program developed for the lumped-mass simulation of cable dynamics will be discussed in a later section.

3.3 Steady-State Buoy System Configurations

As an introduction to the coupling of the buoy and cable equations of motion and the resulting computer programs, the steady-state buoy system configuration (zeroth-order case of buoy system dynamics) will be investigated. The specification of the proper mooring line length for a moored buoy system is critical in the design of the system in order to avoid tow-under of the buoy, minimize the "watch circle" of the buoy, reduce steady-state tensions in the moor, etc. This analysis offers a method to select the proper mooring line length for a given buoy, water depth, and current.

If the time dependent terms in the cable equations (equations (161) through (167)) are allowed to go to zero, we find that

$$\frac{\partial T}{\partial S_0} + H = 0 \quad , \tag{226}$$

$$T \frac{\partial \phi}{\partial S_0} + G = 0 \quad , \tag{227}$$

$$T \cos\phi \frac{\partial \theta}{\partial S_0} + I = 0 \quad , \tag{228}$$

and

$$\epsilon = \frac{1}{K} T \ . \tag{229}$$

Letting cable velocities go to zero in the loading functions, we find that

$$H = w_c \cos\phi \cos\theta + \left(0.60546 \cdot \left(R_{e_{U_R''}}^{-0.4755}\right)\right)\frac{\rho}{2}\, d\, U_R''|U_R''| \ ,$$

$$G = -w_c \sin\phi \cos\theta + C_{DN_{V''}} \frac{\rho}{2}\, d\, V_R''|V_R''| \ ,$$

and

$$I = -w_c \sin\theta + C_{DN_{W''}} \frac{\rho}{2}\, d\, W_R''|W_R''| \ ,$$

where

$$U_R'' = V_s \sin\phi + W_s \cos\phi \sin\theta$$

$$V_R'' = V_s \cos\phi - W_s \sin\phi \sin\theta$$

$$W_R'' = W_s \cos\theta$$

$$C_{DN_{V''}} = 1.32027 + 10.6962/Re_{V''} \qquad 0 < Re_{V''} < 100$$

$$= 1.4 \qquad 100 < Re_{V''} < 5\times10^5$$

$$C_{DN_{W''}} = 1.32027 + 10.6962/Re_{W''} \qquad 0 < Re_{W''} < 100$$

$$= 1.4 \qquad 100 < Re_{W''} < 5\times10^5$$

$$Re_{U''} = \frac{U''d}{\nu}$$

$$Re_{V''} = \frac{V''d}{\nu}$$

$$Re_{W''} = \frac{W''d}{\nu} \ .$$

Expanding equations (226), (227), and (228) to include the loading functions and taking total derivatives, we find that the steady-state cable equations become

$$\frac{dT}{dS_o} = -W_c \cos\phi \cos\theta - \left(0.60546\left(Re_{U_R''}^{-0.4758}\right)\right)\frac{\rho}{2} d\, U_{R'}'' \left|U_R''\right| , \tag{230}$$

$$\frac{d\phi}{dS_o} = \frac{1}{T}\left(W_c \sin\phi \cos\theta - C_{DN_{V''}} \frac{\rho}{2} d\, V_R'' \left|V_R''\right|\right) , \tag{231}$$

$$\frac{d\theta}{dS_o} = \frac{1}{T\cos\phi}\left(W_c \sin\theta - C_{DN_{W''}} \frac{\rho}{2} d\, W_R'' \left|W_R''\right|\right) , \tag{232}$$

and

$$\frac{dS}{dS_o} = 1 + \epsilon = 1 + \frac{1}{K} T \ . \tag{233}$$

Before integrating these equations, the upper boundary conditions (at the buoy) must be determined. The tension at the buoy is

$$T_B = \sqrt{(Disp - W_B)^2 + Drag^2} \ , \tag{234}$$

where

Disp is the buoy displacement

Drag is the buoy drag force due to surface currents

W_B is the buoy weight.

For convenience, let the z axis of the inertial coordinate system be aligned with the surface current. Then, the initial buoy moor angle is

$$\theta_o = \tan^{-1}\left(\frac{Drag}{(Disp - W_B)}\right) , \tag{235}$$

and the initial moor transverse angle is

$$\phi_o = 0 \ . \tag{236}$$

Unfortunately, the displacement and drag of the buoy are functions of the cable tension at the buoy. Thus, a trial and error solution must be used. For a given current profile, $V_s = f_1(x)$; $W_s = f_2(x)$, the depth of water is the controlling parameter. When the vertical projection of the cable is equal to the depth of water, the correct solution has been obtained. The differential equations defining the cable shape (equations (230) to (233)) are controlled by the unstressed cable length S_o . Each iteration must take into account the stretch in the segment before the x component of segment is computed. Thus, if the integration step size is dS_o and the tension and angles for that segment are T, θ , and ϕ, the stretched length is

$$dS = (1+\epsilon)\, dS_o \,. \tag{237}$$

From the cable properties, we see that

$$\epsilon = \frac{\sigma}{E_c} = \frac{4T}{\pi d^2 E_c} \,.$$

Rewriting equation (237), we see that the stretched length increment is

$$dS = \left(1 + \frac{4T}{\pi d^2 E_c}\right) dS_o \,. \tag{238}$$

The components of the cable incremental length dS are

$$dx = dS \cos\phi \cos\theta \,,$$

$$dy = dS \sin\phi \,,$$

and

$$dz = dS \cos\phi \sin\theta \,.$$

Since both the displacement and drag of the buoy are functions of the draft of the buoy (equations (52) and (95) developed for an oblate spheroid — similar equations can be developed for buoys of different shape), the draft H is incremented upward from its "free-floating" value, i.e., as if the buoy were floating on a calm surface with no mooring. The configuration of the cable is then computed using a fourth-order, Runge-Kutta numerical integration algorithm for the given current structure. which may vary in magnitude and direction as a function of depth. The components of the incremental length dS are computed and summed. The x component of the end of the cable is tested logically to see if it falls within a specified error band about the water depth. If the computed vertical projection is less than the water depth, the buoy draft is incremented upward and the process is repeated. If the computed vertical projection falls within the error band, the solution can be accepted or the width of the error band can be reduced and the process repeated until the solution achieves the desired accuracy. This process is shown schematically in figure 19.

This method has been programmed in FORTRAN IV and is shown in appendix B. Subroutines are included for the displacement and drag of oblate spheroids, spherical buoys, cylindrical buoys (cans or spars), torroidal buovs ("donut" buoys), and discus buoys ("monster" buoys). The user must input the buoy characteristics (weight, dimensions, etc.) the cable characteristics (diameter. length. cable modulus, and weight per foot in water - negative if buoyant), and the environmental characteristics (water depth, current structure, etc.). The output includes unstretched length, stretched length, tensions,

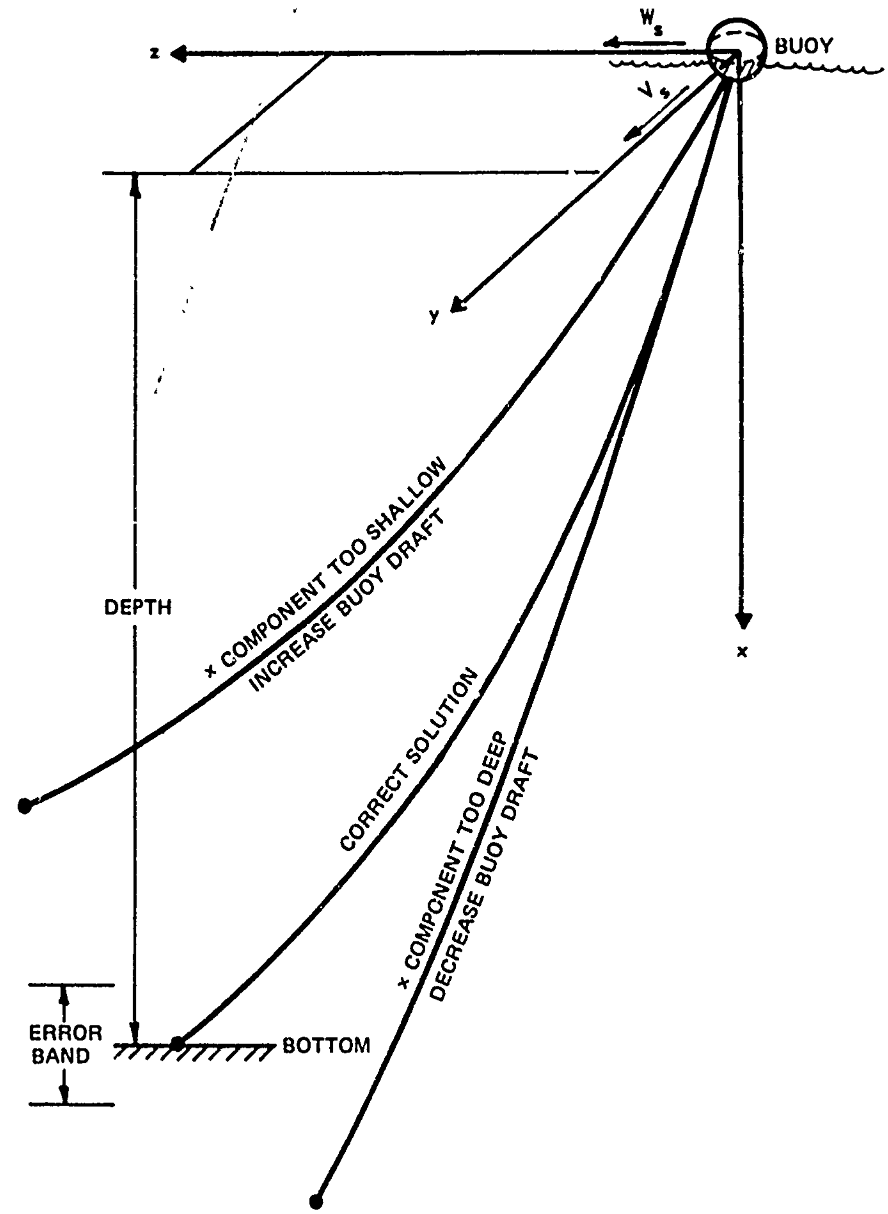

Figure 19. Buoy System Configuration Computation Procedures

the cable angles, and the x, y, z coordinates of each integration step. The step size of the buoy draft is incremented upward as some percentage of the total buoy draft (as if it were fully submerged). Downward buoy draft increments are taken as half the prior upward increments to avoid a lock-step situation where the solution swings between two values and never converges. Subsequent draft increments are halved to avoid the same situation. If the initial error band specified is too narrow and the solution overshoots the error band, the solution may converge too slowly. A limiter is built in to stop the program after 15 configurations are computed. The user should then open up the initial error band. If the buoy draft is increased to its maximum value, the program prints out a statement that the buoy sinks and the computation stops. This indicates that the buoy tows under either because it has insufficient excess buoyancy or the system drag is too high.

If the mooring line is made up of more than one type of cable, rope, or chain, logical "IF" statements are used to change the cable properties at the proper cable lengths. The writer has found that at the transition of cable to chain, the integration step size must be reduced to ensure numerical stability.

Also, if the mooring line has objects (instruments, buoys, weights, etc.) attached to it, the change in tension and angles across the discontinuity must be computed from the free body of the object (figure 20). If the cable parameters just above the discontinuity are T_H , ϕ_H and θ_H , the tension components at that point are

$$T_{H_x} = T_H \cos\phi_H \cos\theta_H , \tag{239A}$$

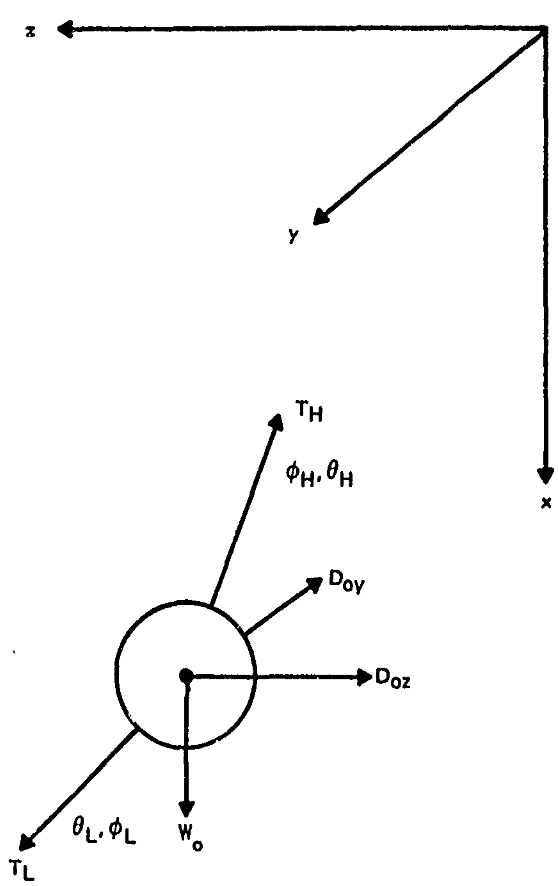

Figure 20. Free Body of an Object on the Mooring Line

$$T_{H_y} = T_H \; SIN \, \phi_H \;, \tag{239B}$$

and

$$T_{H_z} = T_H \; COS \, \phi_H \; SIN \, \theta_H \;. \tag{239C}$$

By summing the forces on the free body, we can determine the tension components below the discontinuity. The tension components are

$$T_{L_x} = T_{H_x} - W_0 \;,$$

$$T_{L_y} = T_{H_y} + D_{0y} \;,$$

and

$$T_{L_z} = T_{H_z} + D_{0z} \;,$$

where

W_0 is the in-water weight of the object

D_{0y} is the drag of the object in the minus y direction

D_{0z} is the drag of the object in the minus z direction .

The cable tension just below the discontinuity is

$$T_L = \sqrt{T_{L_x}^2 + T_{L_y}^2 + T_{L_z}^2} \;, \tag{240}$$

and the cable angles become

$$\theta_L = TAN^{-1}\left(T_{L_z} / T_{L_x} \right) , \tag{241}$$

and

$$\phi_L = TAN^{-1}\left(T_{Ly} / \sqrt{T_{Lx}^2 + T_{Lz}^2} \right) . \tag{242}$$

The integration down the cable can resume using the new tension and angles. The process can be repeated for other objects along the mooring line.

Computer programs developed for buoy system statics and dynamics are shown and discussed in appendix B. The experimental data taken and the validation of the analytical models will now be discussed.

IV. EXPERIMENTAL MEASUREMENTS AND COMPARISON WITH MODELS

4.1 Steady-State Buoy System Configurations

The steady-state analysis of the buoy system configuration is important since it serves as the set of initial conditions for the dynamic analysis. Also, the steady-state analysis is the first step for the buoy system designer to ensure that his system will not tow-under or have other undesirable static characteristics. The analysis for both shallow and deep water oceanographic buoy systems are compared with data taken at sea to validate the steady-state analysis.

4.1.1 Torroid and Current Meter Array at Station BRAVO

On 22 August 1967, the writer installed a buoy-supported, current meter array at station BRAVO (41° 51.15'N, 71° 46.50'W) at the Block Island — Fishers Island (BIFI) Oceanographic and Acoustic Range in Block Island Sound. This array was recovered on 19 September 1967, and the current meter data were analyzed. The components of the array are shown in figure 21. The three Braincon type 316 current meters were suspended below the buoy at cable lengths of 15, 60, and 105 ft. The buoy and array were moored with a 70-lb Danforth anchor and a 100-lb lead weight to keep the line pull horizontal. The buoy used in this experiment is shown in figure 22.

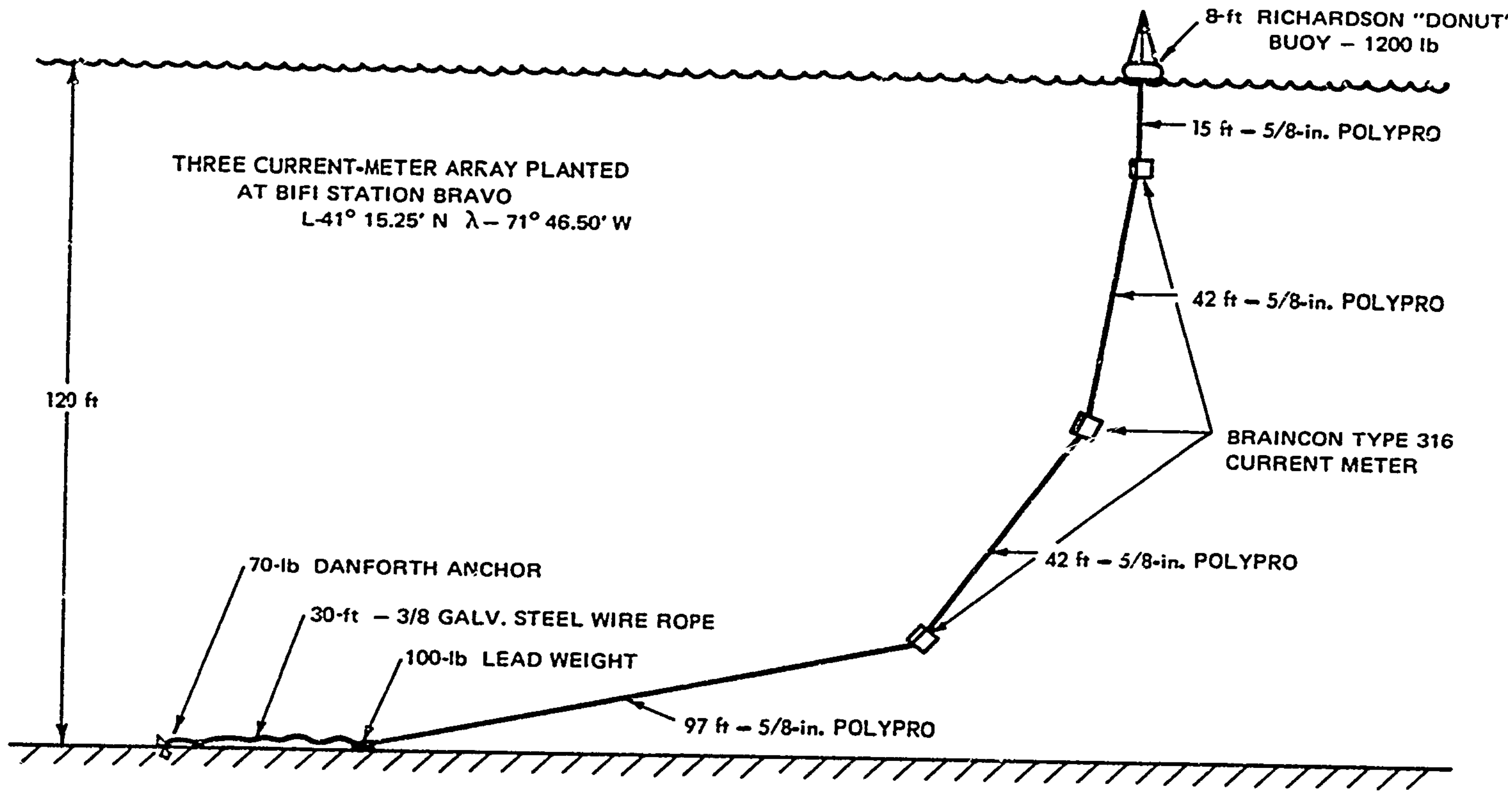

Figure 21. Current Meter Array at Station BRAVO

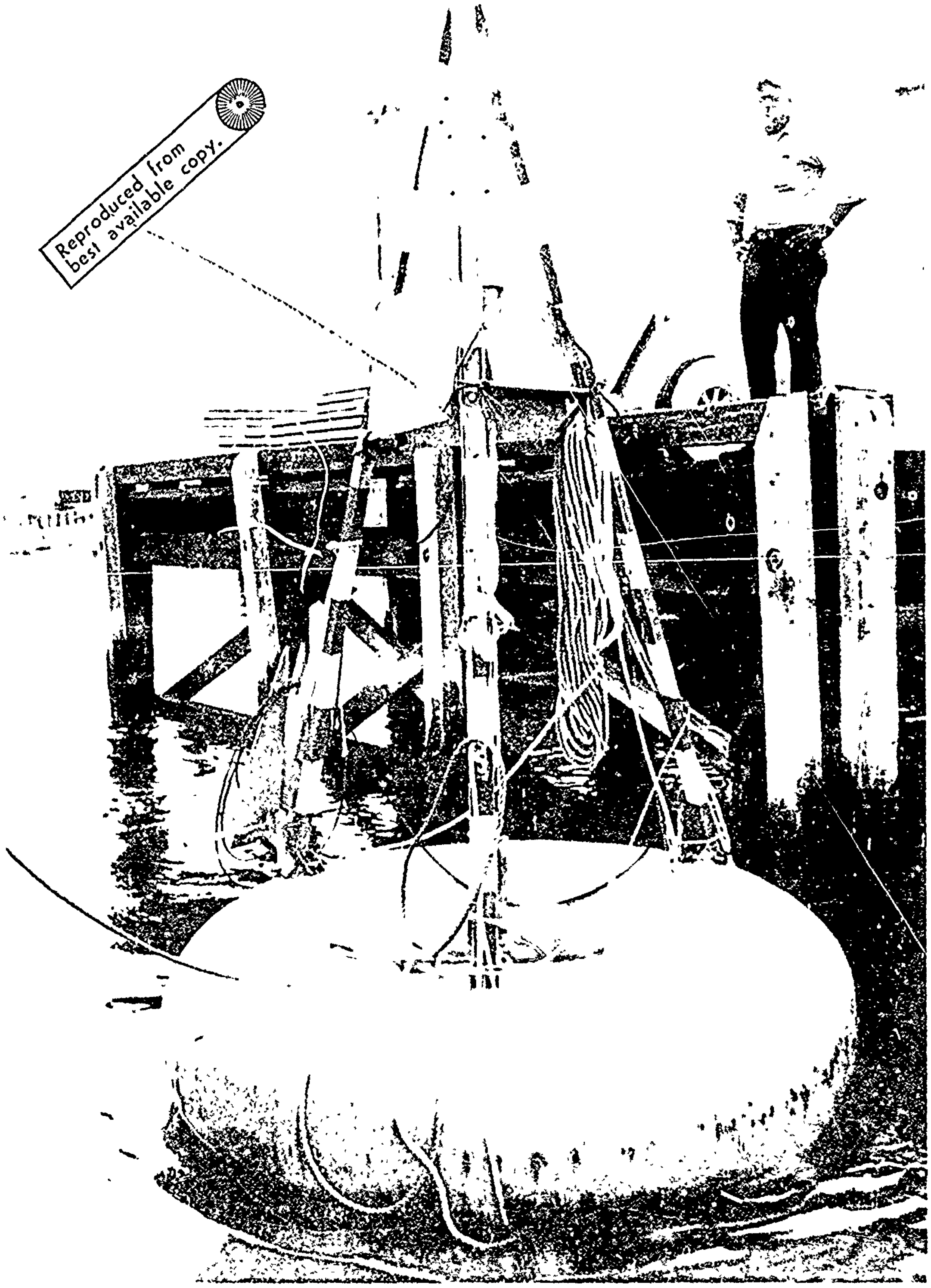

Figure 22. Torroidal Buoy Used for the Three-Current-Meter Array

Twenty-eight samples of the current meter data were selected and are shown in table 1. Data from the bottom current meter were highly variable and erratic and were not regarded as reliable. The data shown are 10-min time averages due to the photographic method used to record data. The instruction manual for the type 316 current meter[75] gives the following ranges and accuracies:

	Range	Accuracy
Current speed	0.5 - 5 knots	$\pm$ 0.15 knot
Current direction	0 - 360 deg	$\pm$ 5 deg
Current meter tilt	0 40 deg	$\pm$ 1 deg
Timing mechanism	5 months	$\pm$ 10 sec/day.

The weight in sea water of the current meter is given in the instruction manual as 67 lb. The cylindrical body of the current meter is $8\frac{1}{2}$ in. in diameter by $38\frac{3}{4}$ in. long with a 36-in. vertical vane attached to align it with the flow. Sunblad[76] gives a normal drag coefficient of 0.59 based on frontal area derived from tow tank data for the type 316 current meter.

The torroidal buoy has an 8-ft outer diameter and a 3-ft hole through the center. The buoy weighed 1200 lb in air. The mooring line was 5/8-in.-diameter polypropylene rope having 0.02 lb/ft buoyancy. The 3/8-in.-diameter wire rope at the anchor weighed 0.2 lb/ft. The cable modulus of elasticity for the polypropylene rope was taken as 1.67×10^5 lb/in.^{2} (50° F) and for the steel cable as 12.0×10^6 lb/in.^{2}.

Williams[77] and Nalwalk et al.[78] have made current measurements at station BRAVO and have found a two-layer current structure. On an ebb tide

TABLE 1. CURRENT METER DATA — STATION BRAVO

Time (hr)	Speed (knots)			Direction (deg) Reference to Magnetic North			Observed Tilt Angle (deg ± 1 deg)		
	15	60	105	15	60	105	15	60	105
.333	1.177	1.27	.701	278	270	301	10	22	40
.666	1.205	1.16	1.04	276	276	310	10	20	40
1.000	1.079	1.08	1.11	281	277	300	7	18	40
1.333	1.099	1.07	1.84	284	283	257	6	14	40
1.666	.945	.928	.498	292	282	217	6	11	18
2.000	.836	.713	.777	290	276	206	5	7	41
2.333	.717	.578	1.031	286	273	119	4	7	40
2.666	.538	.497	4.688	298	284	115	4	5	40
3.000	.509	.341	3.92	316	302	171	3	3	10
3.333	.378	.214	.110	335	316	160	2	4	17
3.666	.420	.159	.069	27	188	151	3	1	7
49.0	1.253	1.086	.764	290	280	215	15	25	18
50.0	1.169	1.088	1.386	298	275	202	15	25	40
51.0	.940	.943	.697	291	272	246	10	20	40
52.0	.748	.516	.523	308	289	110	6	11	40
53.0	.617	.265	1.472	21	91	109	5	5	9
54.0	.790	.578	.687	83	89	17	5	5	0
55.0	.908	.666	.901	93	86	56	4	10	40
56.0	.824	.814	1.964	90	100	1	5	5	19
20.0	.632	.699	.756	71	96	1	5	5	40
21.0	.578	.345	.859	41	104	5	5	5	5
22.0	.630	.363	1.394	283	242	312	6	15	40
23.0	.910	.845	4.539	[illegible]	267	305	10	23	40
24.0	1.178	1.108	2.141	278	268	309	16	30	41
25.0	1.219	.985	[illegible].545	283	260	306	14	30	40
26.0	1.158	1.05[illegible]	1.283	288	257	306	15	26	18
27.0	.893	[illegible]	1.894	298	257	201	9	20	18
28.0	.691	[illegible]42	.832	347	254	111	6	6	40

(current setting to the east) the bottom layer appears to set to the northeast. On a flood tide (current setting to the west) the bottom layer sets to the northwest. Williams and Nalwalk never observed bottom currents greater than 1.5 knots. which make the data from the bottom current meter questionable. Also, the high tilt angles of the bottom current meter preclude proper response of the Savonius rotor to the ambient currents. In the following study, which was made to compare predicted current meter tilt angles with observed tilt angles, the current is modeled as an upper layer having a thickness of 70 ft and a bottom layer with a thickness of 50 ft. The current speed and direction of the upper layer is approximated by the mean of the speeds and directions from the two upper current meters. The speed and direction of the lower layer is assumed to be equal to the speed and direction from the bottom current meter. Bottom currents greater than 1.5 knots were set equal to the value of the upper layer current.

The computer program for steady-state buoy configurations shown in appendix B was modified to include the effects of the current meters and lead weight by solving the free body at each object (equations (239A) through (242)). The torroidal buoy subroutine was used and cable configurations were integrated with a fourth-order, Runge-Kutta algorithm using a 1-ft step size. Current meter tilt angles were computed by balancing moments on each current meter. The program was run on the GSA-360 time sharing computer and results for the first ten cases are shown in table 2 and in figure 23. Average tilt angle errors for the ten cases are as follows:

TABLE 2. COMPARISON OF OBSERVED CURRENT METER TILT ANGLES WITH DATA COMPUTED BY INTEGRATION OF CABLE EQUATIONS

Time (hr)	Observed Tilt Angle (deg ± 1 deg)			Computed Tilt Angle (deg)			Tilt Angle Error (deg)		
	15	60	105	15	60	105	15	60	105
.333	10	22	40	10.59	20.62	49.86	.59	-1.38	—
.666	10	20	40	9.91	19.39	48.82	-.09	- .61	—
1.000	7	18	40	8.38	16.69	44.87	1.38	-1.31	—
1.333	6	14	40	8.31	16.33	49.00	2.31	2.33	—
1.866	6	11	18	6.46	13.27	34.32	.46	2.27	16.32
2.000	5	7	41	4.45	9.25	25.82	-.55	2.25	—
2.333	4	7	40	3.11	6.50	13.50	-.89	- .50	—
2.666	4	5	40	1.99	4.17	10.92	-2.01	- .83	—
3.000	3	3	10	1.34	2.81	8.49	-1.66	- .19	-1.51
3.333	2	4	17	.65	1.37	5.38	-1.35	-2.63	-11.62
						Average error	0.22	0.20	1.06
						Overall average error	-0.49		

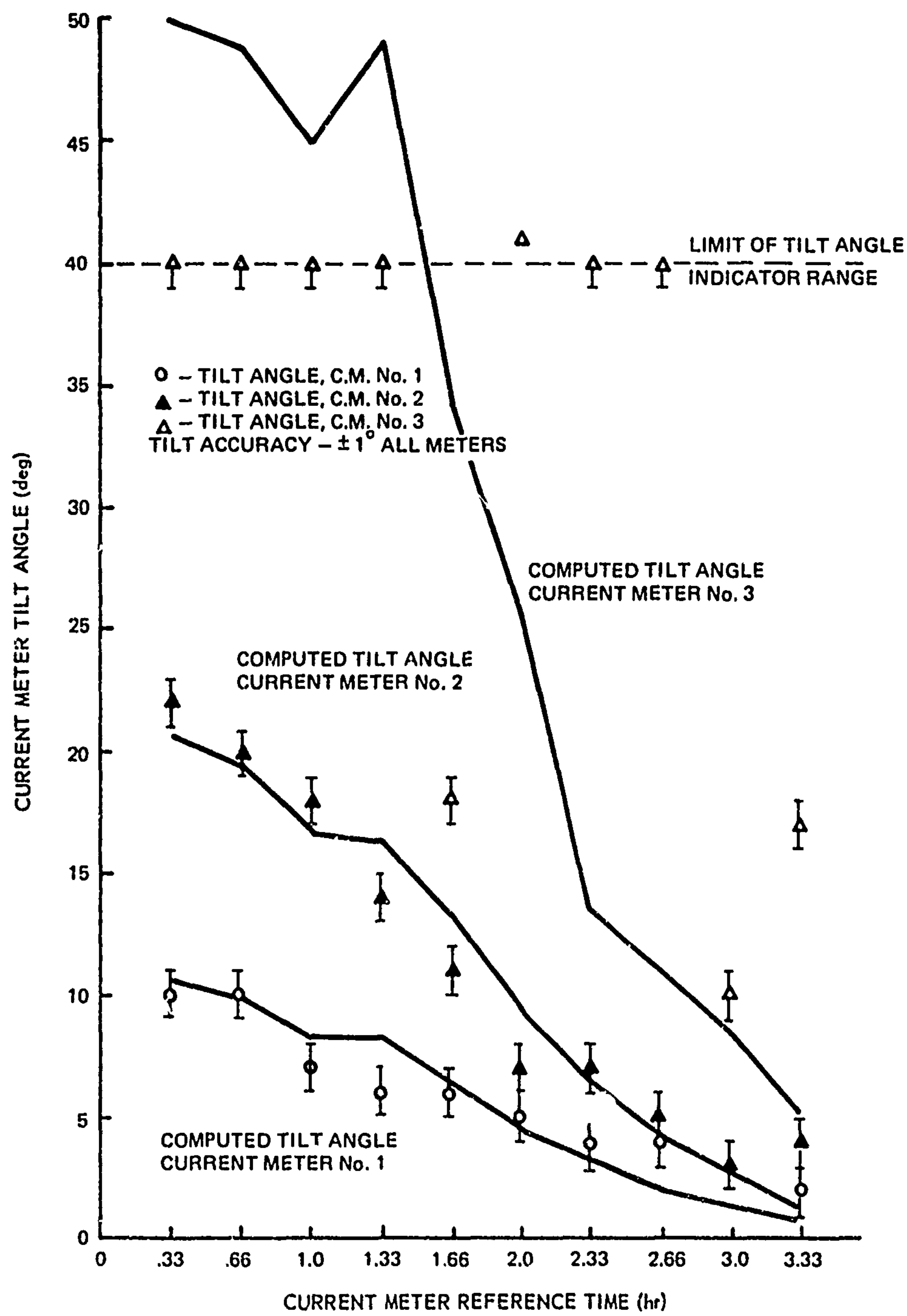

Figure 23. Current Meter Tilt Angles Computed by Integrating Down the Cable Compared With Observed Data

Upper current meter	+ 0.22 deg
Middle current meter	+ 0.2 deg
Lower current meter*	+ 1.06 deg
Overall average error	+ 0.49 deg.

With the exception of the lower current meter, these errors fall within the ± 1 deg accuracy of the tilt indicator indicating good agreement of the computer model with observed data. The computer study indicated that the 100-lb weight was never picked up off the bottom by the strongest currents and that the weight and drag of the current meters control the buoy system configuration to a greater degree than the weight and drag of the polypropylene rope. With this in mind, a simple statics model of the buoy system was developed; it was assumed that the rope was not deflected between current meters and that half of the drag force acting on each rope span could be assumed to be concentrated at the end of the current meter to which it was attached. Since the tensions in the integrated cable configurations were observed to be very small, the buoy draft was computed for the buoy weight and the weight of the current meters only. Thus, the vertical force component is equal to the weight of the current meters. The simplified model is shown on figure 24. Lateral deflections computed by the integrated configurations were very small; thus, the simplified model was restricted to two dimensions. Drag forces on the rope spans and on the current meters were computed as if the currents were acting normal to the rope or current meter. The small buoyancy and the stretch of the rope were neglected.

---

*The errors of the lowest current meter were not computed for data where the observed tilt angle was 40 deg.

$$\tan \theta_{CM_1} = \frac{3 \cdot (D_B + D_{C1} + D_{CM}) - 1.5 \cdot D_{CM}}{3 \cdot (2_1 \cdot W_{CM}) + 1.5 \cdot W_{CM}}$$

$$\tan \theta_{CM_2} = \frac{3 \cdot (D_B + D_{C2} + 2_1 D_{CM}) - 1.5 \cdot D_{CM}}{3 \cdot W_{CM} + 1.5 \cdot W_{CM}}$$

$$\tan \theta_{CM_3} = \frac{3 \cdot (D_B + D_{C1} + D_{C2} + 3 \cdot D_{CM}) - 1.5 \cdot D_{CM}}{1.5 \cdot W_{CM}}$$

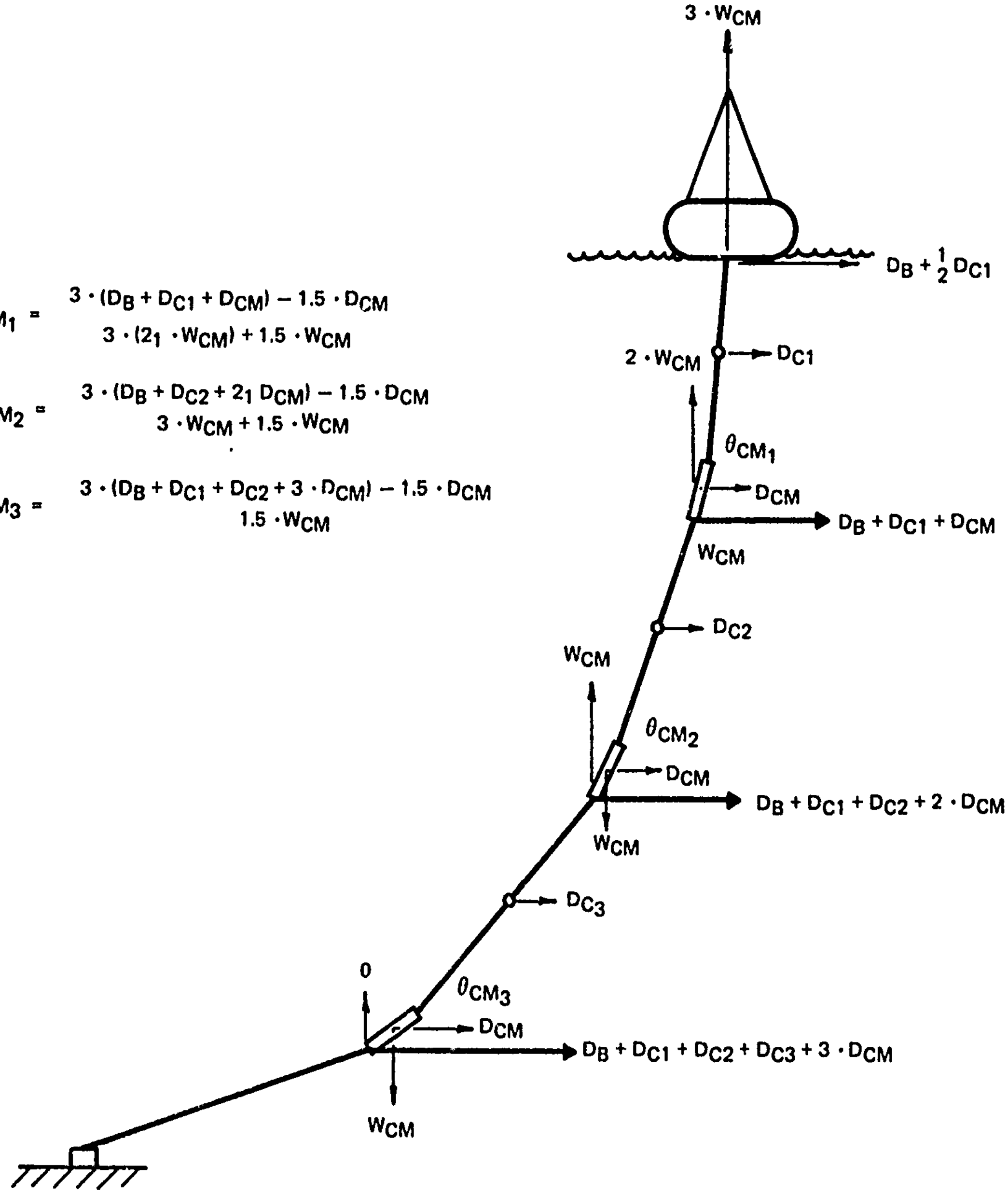

Figure 24. A Simple Statics Model of the Current Meter Array

Buoy system configurations for the case at current meter reference time of 0.333 hr are shown in figure 25 and are quite similar. Computed current meter tilt angles were compared with the observed tilt angles. The angles were computed by using a uniform current equal to the mean value of the current speeds from the upper two current meters. The angles are shown in table 3 and on figure 26. The average errors for the first ten data sets are as follows:

Upper current meter	- 2.15 deg
Middle current meter	- 0.26 deg
Lower current meter	+ 7.64 deg
Overall average error	+ 1.74 deg.

These errors indicate that the simple statics model is about three times less accurate than integration down the cable but may be adequate for engineering applications. The average errors for 28 data sets are as follows:

Upper current meter	- 3.77 deg
Middle current meter	- 2.69 deg
Lower current meter	16.66 deg
Overall average error	3.4 deg.

The preceding study indicates that the steady-state buoy system configuration model can predict current meter inclination angles to within $\frac{1}{2}$ deg on the average. No tension data were recorded; thus, the steady-state tension errors were not computed. The shallow water buoy system described above is most heavily influenced by the weight and drag of the current meters. In most deep water buoy systems, the weight and drag of the mooring cables are the predominant forces.

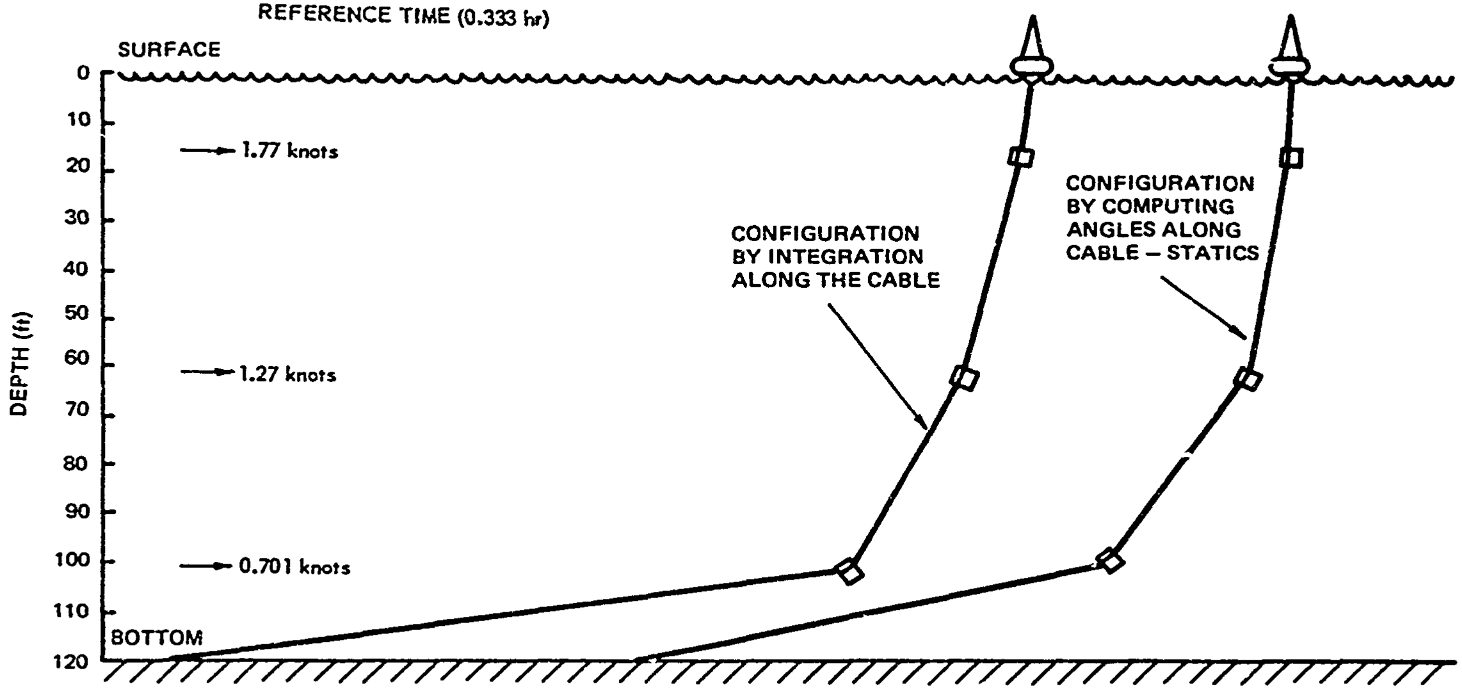

Figure 25. Comparison of Computed Buoy System Configurations

TABLE 3. COMPARISON OF OBSERVED CURRENT METER TILT ANGLES WITH DATA COMPUTED BY ASSUMING NO CABLE CURVATURE

Time (hr)	Speed (knots)		Observed Tilt Angle (deg ± 1 deg)			Computed Tilt Angle (deg)			Tilt Angle Error (deg)		
	15	60	15	60	105	15	60	105	15	60	105
.33	1.177	1.27	10	22	40	6.90	20.77	62.53	-3.10	-1.12	-
.66	1.205	1.16	10	20	40	6.45	19.50	60.90	-3.55	- .50	-
1.00	1.079	1.08	7	18	40	5.38	16.45	56.27	-1.62	-1.55	-
1.33	1.099	1.07	6	14	40	5.43	16.59	56.51	- .57	2.59	-
1.66	.945	.928	6	11	18	4.06	12.53	48.42	-1.94	1.53	30.42
2.00	.836	.713	5	7	40	2.78	8.64	37.62	-2.22	1.64	-
2.33	.717	.578	4	7	40	1.94	6.06	28.31	-2.06	-.94	-
2.66	.538	.497	4	5	40	1.24	3.88	18.99	-2.76	-1.12	-
3.00	.509	.341	3	3	10	.84	2.62	13.07	-2.16	- .38	3.07
3.33	.378	.214	2	4	17	.41	1.27	6.42	-1.59	-2.73	10.58
3.66	.420	.159	3	1	7	.39	1.22	6.15	-2.61	.22	-.85
49.0	1.253	1.086	15	25	18	6.31	19.11	60.36	-8.69	-5.89	42.36
50.0	1.169	1.088	15	25	40	5.88	17.88	58.57	-9.12	-7.12	-
51.0	.940	.943	10	20	40	4.10	12.66	48.72	-5.90	-7.34	-
52.0	.748	.516	6	11	40	1.85	5.78	27.17	-4.15	-5.22	-
53.0	.617	.265	5	5	9	.90	2.82	14.03	-4.10	-2.18	5.03
54.0	.790	.578	5	5	10	2.17	6.76	31.01	-2.83	1.76	21.01
55.0	.908	.666	4	10	40	2.87	8.92	38.51	-1.13	-1.08	-
56.0	.824	.814	5	5	19	3.10	9.64	40.76	-1.90	4.64	21.76
20.0	.632	.699	5	5	40	2.05	6.40	29.64	-2.95	1.40	-
21.0	.578	.345	5	5	5	.99	3.09	15.31	-4.01	-1.91	10.31
22.0	.630	.363	6	15	40	1.14	3.57	17.58	-4.86	- 11.43	-
23.0	.910	.845	10	23	40	3.56	11.04	44.70	-6.44	-11.96	-
24.0	1.178	1.108	16	30	41	6.03	18.31	59.22	-9.97	-11.69	-
[illegible]	1.219	.985	14	30	40	5.61	17.10	57.35	-8.39	-12.90	-
[illegible]	1.158	1.056	15	26	18	5.66	17.25	57.58	-9.34	-8.75	39.58
27.0	.893	699	9	20	18	2.93	9.12	39.15	-6.07	-10.88	21.15
28.0	.691	.342	6	6	40	1.24	3.87	18.92	-4.76	-2.13	

28 Set average error -3.77 -2.69 16.66

Overall average error 3.4

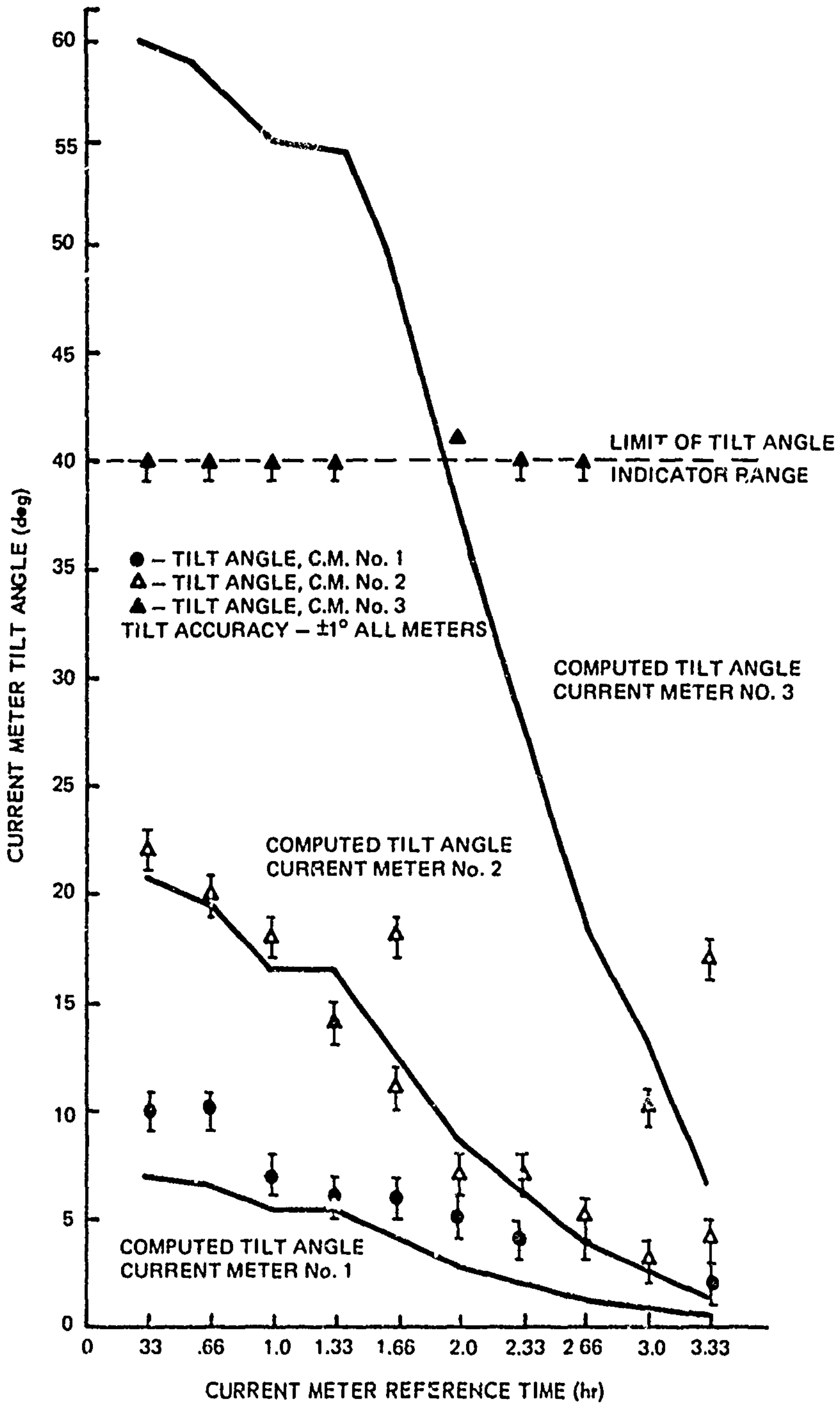

Figure 26. Current Meter Tilt Angles Computed by Simple Statistics Model Compared With Observed Data

4.1.2 WHOI Mooring No. 279

Millard[37] describes tension measurements made on a taut-moored buoy system. The buoy system (figure 27) was installed in water 2685 m deep at Woods Hole Oceanographic Institution Site D. Tensions were recorded at four locations along the mooring line, and currents were recorded at a depth of 12 m for the $2\frac{1}{2}$ months that the buoy system was on station. Berteaux and Walden[79] describe the properties of the wire rope and plaited nylon rope used in this buoy system as follows:

	Diameter (in.)	Weight/ft in Sea Water (lb/ft)
1/4-in. 1 × 50 wire rope	0.25	0.090
5/8-in. plaited nylon	0.625	0.01047.

The cable modulus for the wire rope was taken as 1.682×10^7 lb/in.^{2}. Nylon rope is subject to both elastic and inelastic deformation when loaded. New rope, when first loaded, will acquire a permanent deformation, the amount of which depends on the initial load. Furthermore, if the load is left on the rope, the rope is subject to creep and the permanent deformation increases with time. Martin[14] discusses the various mechanisms for the deformation of nylon rope. Using Martin's curve for the percent stretch versus load for the 5/8-in.-diameter plaited nylon rope, the rope modulus is computed as follows:

$$E = 3.52 \times 10^5 \text{ lb/in.}^2 \; ; \; 0 < T < 1000 \text{ lb}$$

$$E = 6.79 \times 10^5 \text{ lb/in.}^2 \; ; \; 1000 < T < 2000 \text{ lb}$$

$$E = 1.041 \times 10^6 \text{ lb/in.}^2 \; ; \; 2000 < T .$$

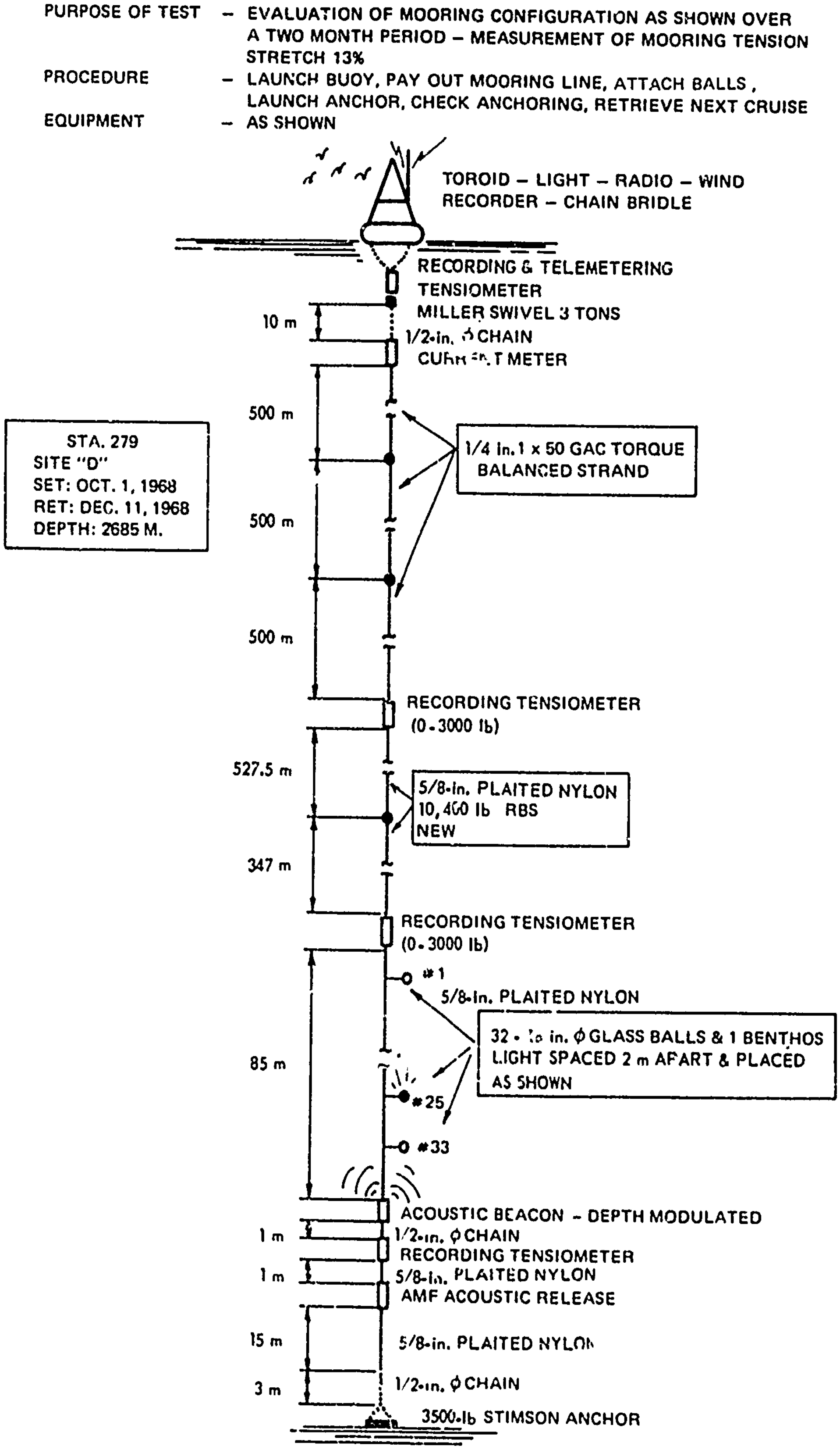

Figure 27. Woods Hole Oceanographic Institution Mooring No. 279

Webster[80] measured currents for a 2-month period at site D . Webster's data were curve-fitted using the program CURFIT on the GSA time-sharing computer, and the following function for the current strength as a function of depth was developed:

$$C = 2.6 \cdot Cs \cdot D^{-0.418} ,$$

where

C is the current (ft/sec)

Cs is the surface current (ft/sec)

D is the depth (meters).

The steady-state buoy system configuration computer program was modified to include Webster's current profile, Martin's elastic properties for the nylon rope. and the cable properties given by Berteaux and Walden. Since information on the variations of current direction with depth was not available, the currents were assumed to be acting in the same direction at all depths. Furthermore, the initial inelastic stretch due to the emplantment and the dynamic wave loads is not known. The no-current elastic stretch of the nylon rope was assumed, and the tensions in the system were computed while currents acted on the system. Tensions at the junction of the wire rope and nylon rope are shown in figure 28 as functions of the surface current and of the no-current elastic stretch. Data taken by Millard at the same location on the mooring line are also shown on figure 28. Because of the creep properties of the nylon rope, the inelastic stretch will increase and the no-current elastic stretch will decrease as time increases. The shape of the tension curve will remain roughly the same, but the tension bias will decrease with time. Since the

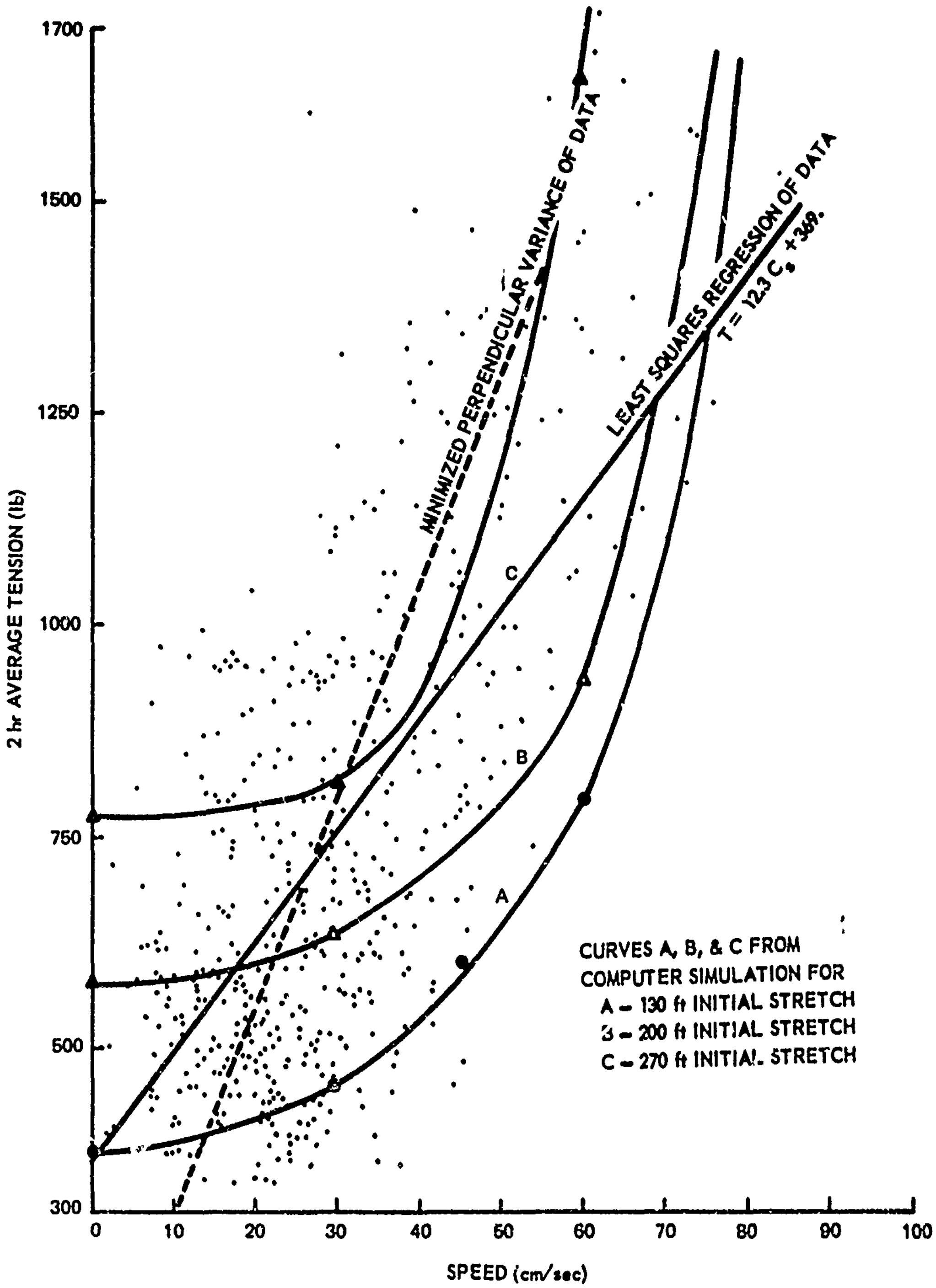

Figure 28. Comparisons of WHOI Data With Computed Mean Mooring Line Tensions

creep properties of the nylon rope are not known, computation of errors between observed and computed tensions in this case is of little value.

Millard analyzed the tension versus surface current data shown on figure 28 and least-squares fitted the linear function:

$$T = 12.3 \cdot Cs + 369 \ .$$

Least-squares linear fits to the computed curves A, B, and C are

$$T = 12.59 \cdot Cx + 608 \ ,$$

$$T = 12.25 \cdot Cs + 381 \ ,$$

and

$$T = 12.10 \cdot Cs + 203 \ .$$

Slopes of the computed linearized functions are in very close agreement, which indicates that the functional form of the computed tensions is accurate.

From this comparison, it is obvious that more experimentation on the elastoplastic properties of nylon rope is needed in order to predict the steady-state configurations of deep ocean, taut-moored buoy systems. Also, a deep ocean buoy system should be installed with both recording tensiometers and inclinometers to better validate the steady-state computer model.

4.2 Experimental Measurements of Buoy System Dynamics

In order to validate the computer simulation of buoy system dynamics, buoy motions as measured at sea will be correlated with computer simulated buoy system response to the same environmental conditions.

Two oceanographic buoys were equipped with motion sensing instrumentation and installed in Block Island Sound. The smaller of the two buoys, a

$3\frac{1}{2}$-ft-diameter sphere, was installed in March 1970 off Great Salt Pond entrance, Block Island, Rhode Island. The larger buoy, an 8-ft-diameter torroid was installed at station BRAVO during May 1970. A description of the instrumentation and a discussion of the measurements taken are presented in reference 81.

4.2.1 Spherical Buoy at Station D

The $3\frac{1}{2}$-ft-diameter spherical buoy is shown in figure 29. This buoy was loaned to the writer by Dr. A. Nalwalk, of the Marine Sciences Institute of the University of Connecticut. The buoy was equipped with the following instrumentation:

Heave motion statistical accelerometers

Current meter

Heave accelerometer

Surge Accelerometer

Sway accelerometer

Pitch pendulous potentiometer

Roll pendulous potentiometer

Cable pitch pendulous potentiometer

Cable roll pendulous potentiometer

Cable tension gage

Thermistor.

The buoy system was installed in 62 ft of water, west of Great Salt Pond entrance at Block Island by the Research Vessel, UCONN, on 2 March 1970. The $1\frac{1}{2}$-in.-diameter, 14-conductor armored cable was laid along the bottom to

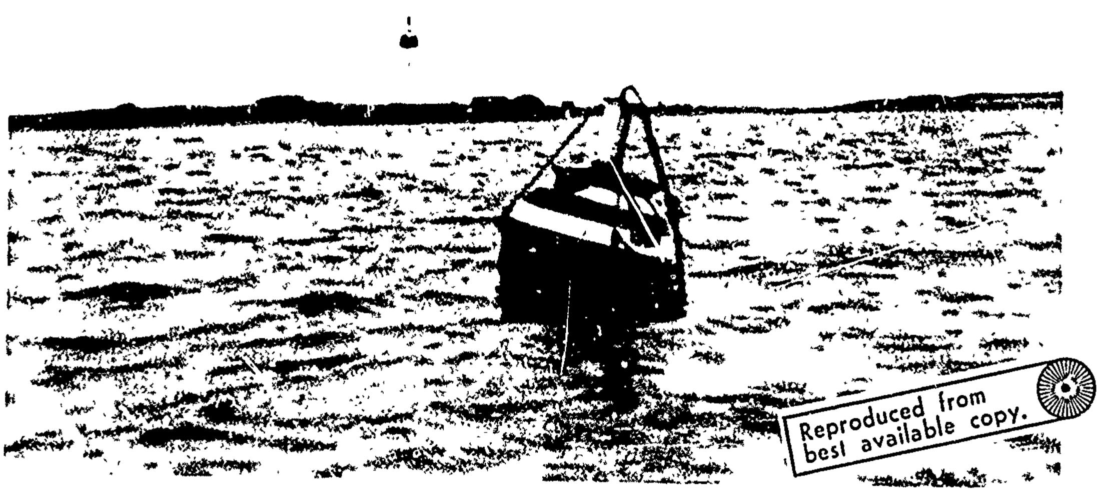

Figure 29. Spherical Buoy at Block Island Station D

the beach and was carried over the beach to the BIFI field station: A Snodgrass wave sensor was also installed off the beach in 25 ft of water. The arrangement of cables and instruments is shown schematically in figure 30.

Two weeks of statistical heave accelerometer data were collected. Some buoy motion data were also recorded. The electrical conductors in the cable began to fail after a month of use and a number of attempts were made to repair the cable in order to continue collecting data. The buoy broke loose during a storm in early November 1970 and is missing.

The statistical accelerometers were designed to count at 0.35-, 0.50-, 0.65-, 0.80-, 1.20-, 1.35-, 1.50-, and 1.65-g heave acceleration levels. The pulses from the accelerometers actuated counters in the van at the BIFI Field Station, and the total count was recorded daily. Sea state data were based on estimates by the resident engineer (Carl T. Milner) and by Coast Guard observations reported by the ESSA Marine Weather Service. Data were recorded during the period 4 March to 12 March 1970.

Data from the 22 observations of positive acceleration counts were used to generate figure 31, a plot of the counts per hour versus acceleration level for various sea states. The negative acceleration counters did not work, because of the failure of leads in the cable. Figure 31 indicates that for any sea state greater than sea state 0, the buoy will always undergo 1.2-g accelerations at a rate of 1,000/hr. The number of cycles per hour for higher acceleration levels will increase with increasing sea state. Figure 32 is the conditional probability of the buoy exceeding various positive acceleration levels given that the buoy exceeds 1.2-g level accelerations. Figure 33 shows the buoy heave acceleration

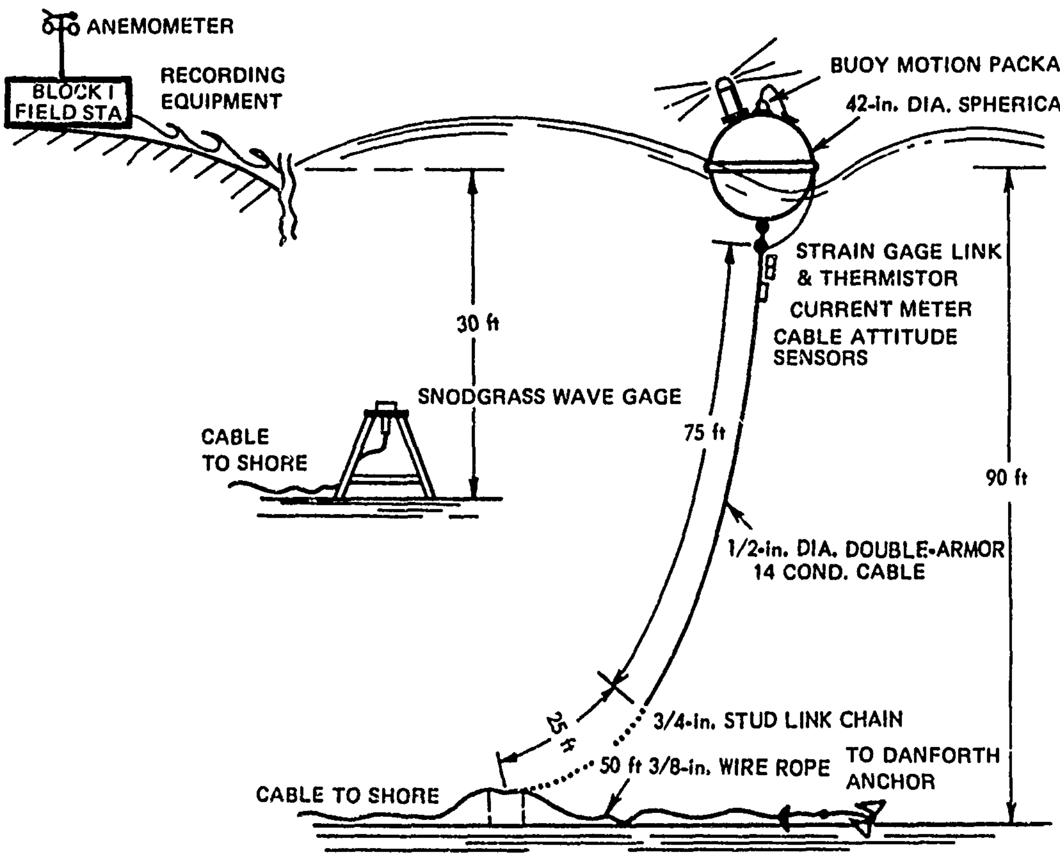

Figure 30. Spherical Buoy System at Block Island

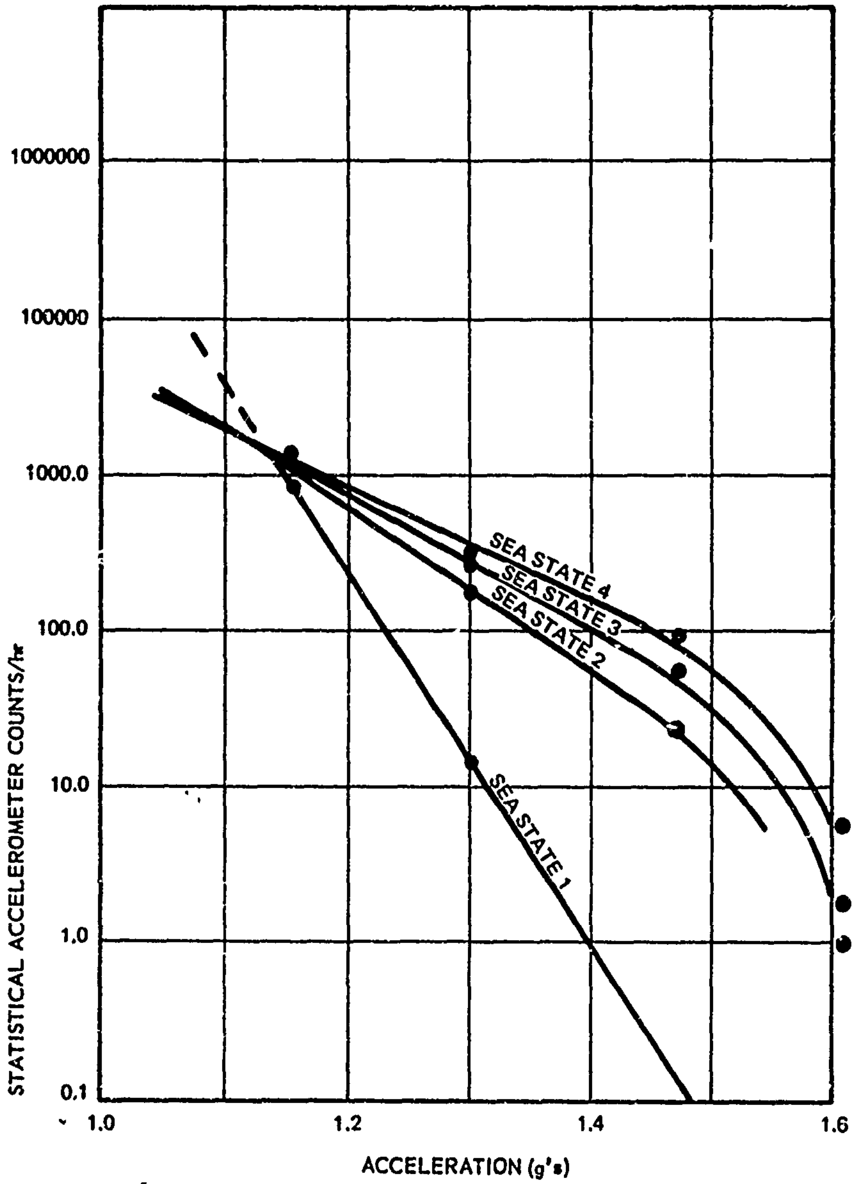

Figure 31. Statistical Accelerometer Data for Heave Motions

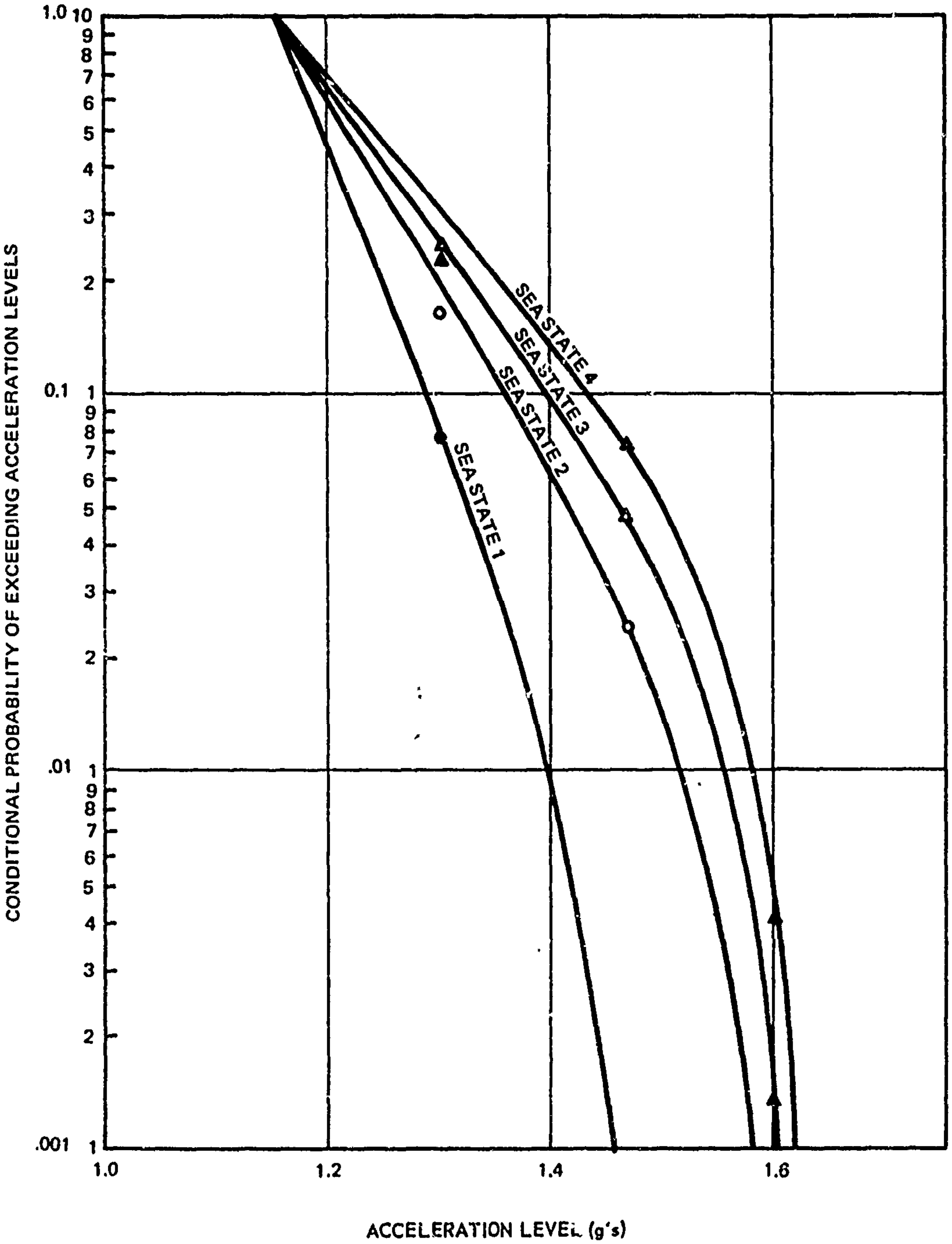

Figure 32. Conditional Probabilities for Heave Motions

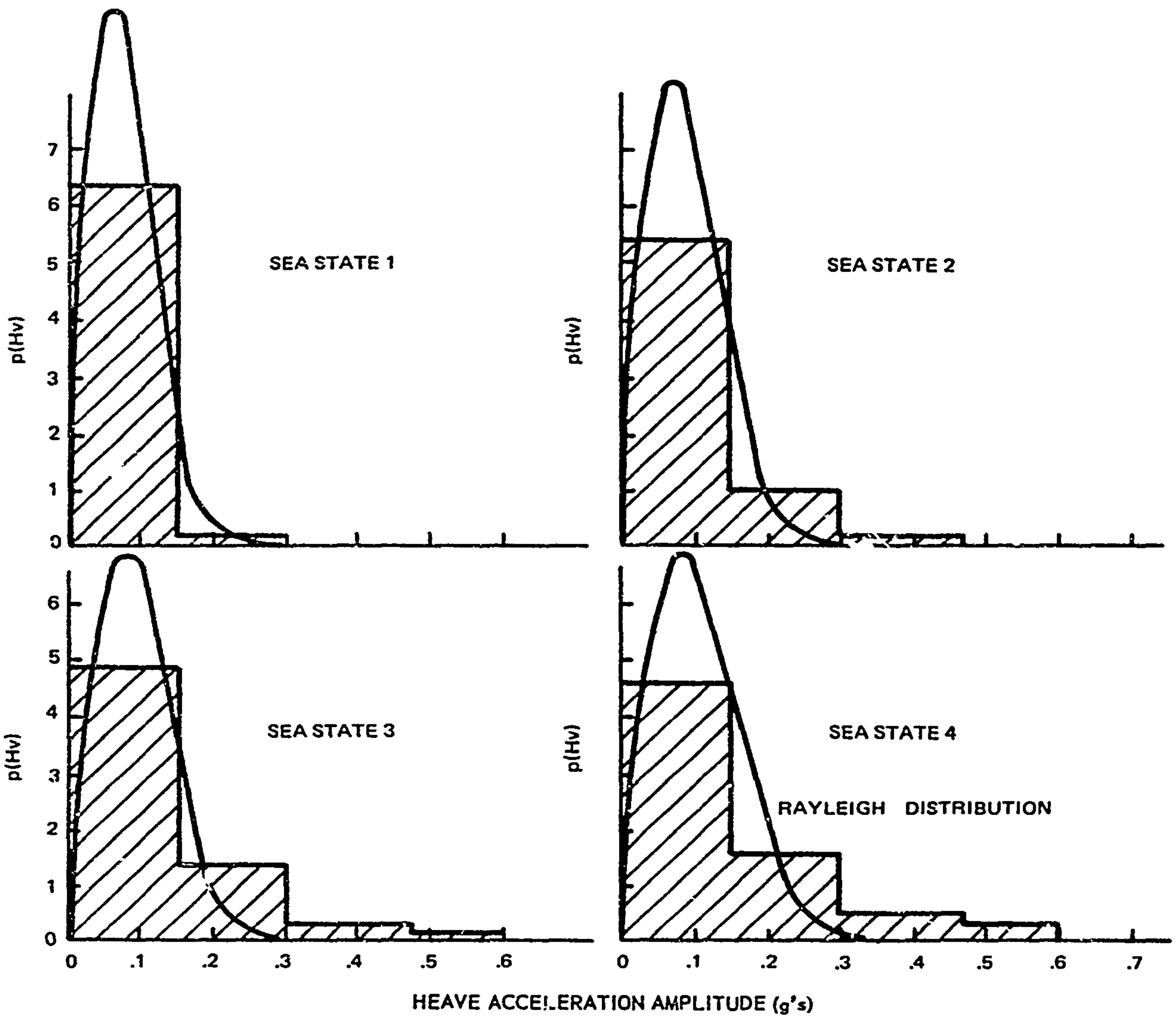

Figure 33. Spherical Buoy Heave Acceleration Amplitude Distributions

amplitude histogram for various sea state conditions. Rayleigh distributions are plotted over the histograms and were computed by using the mean of the histograms. Longuet-Higgins[55] and Bretschneider[51] have shown that the distribution of wave heights is given by the Rayleigh distribution.

Analog data of the spherical buoy motions were also recorded. On 16 March 1970, the following records were obtained on a two-channel strip chart recorder:

Wave height (20 min)

Buoy heave and buoy surge (15 min)

Buoy heave and buoy pitch (10 min)

Buoy heave and buoy roll (10 min)

Buoy heave and cable pitch (10 min)

Buoy heave and cable roll (10 min).

Winds were 15 to 20 knots, northeast, with an estimated sea state 3 at the buoy. Results of a simple "quick look" analysis are shown in figures 34 through 37.

One-hundred samples of each record were digitized and analyzed on the GSA-440 time sharing computer. Figure 34 shows means, variances, and standard deviations for each parameter. In addition, the correlation matrix for simple product-moment correlations is shown. Parameters that should be coupled appear to be coupled, and parameters that should be decoupled appear to be decoupled. For example, heave-surge, heave-pitch, and surge-pitch are coupled, and heave-roll, surge-roll, and pitch-roll are decoupled. Also, cable angles are mildly coupled to buoy displacements but decoupled from buoy angles.

VARIABLE	MEAN	VARIANCE	STANDARD DEVIATION
HEAVE ACCELERATION	0 g	0.0242 g^2	0.1555 g
SURGE ACCELERATION	0 g	0.00978 g^2	0.0991 g
PITCH ANGLE	1.1 deg BOW DOWN	104.2 deg^2	10.20 deg
ROLL ANGLE	14.3 deg PORT	55.3 deg^2	7.58 deg
CABLE PITCH	-27.1 deg	24.0 deg^2	4.90 deg
CABLE ROLL	-7.3 deg	16.2 deg^2	4.01 deg

THE CORRELATION MATRIX

	HEAVE	SURGE	PITCH	ROLL	CABLE PITCH	CABLE ROLL
HEAVE	1.0	0.4806	0.6050	-0.0706	0.2435	0.0454
SURGE		1.0	-0.4199	0.0054	-0.1605	0.1975
PITCH			1.0	-0.1021	0.0063	-0.0946
ROLL				1.0	0.2121	-0.3813
CABLE PITCH					1.0	-0.2282
CABLE ROLL						1.0

Figure 34. Spherical Buoy Motion Parameter Statistics

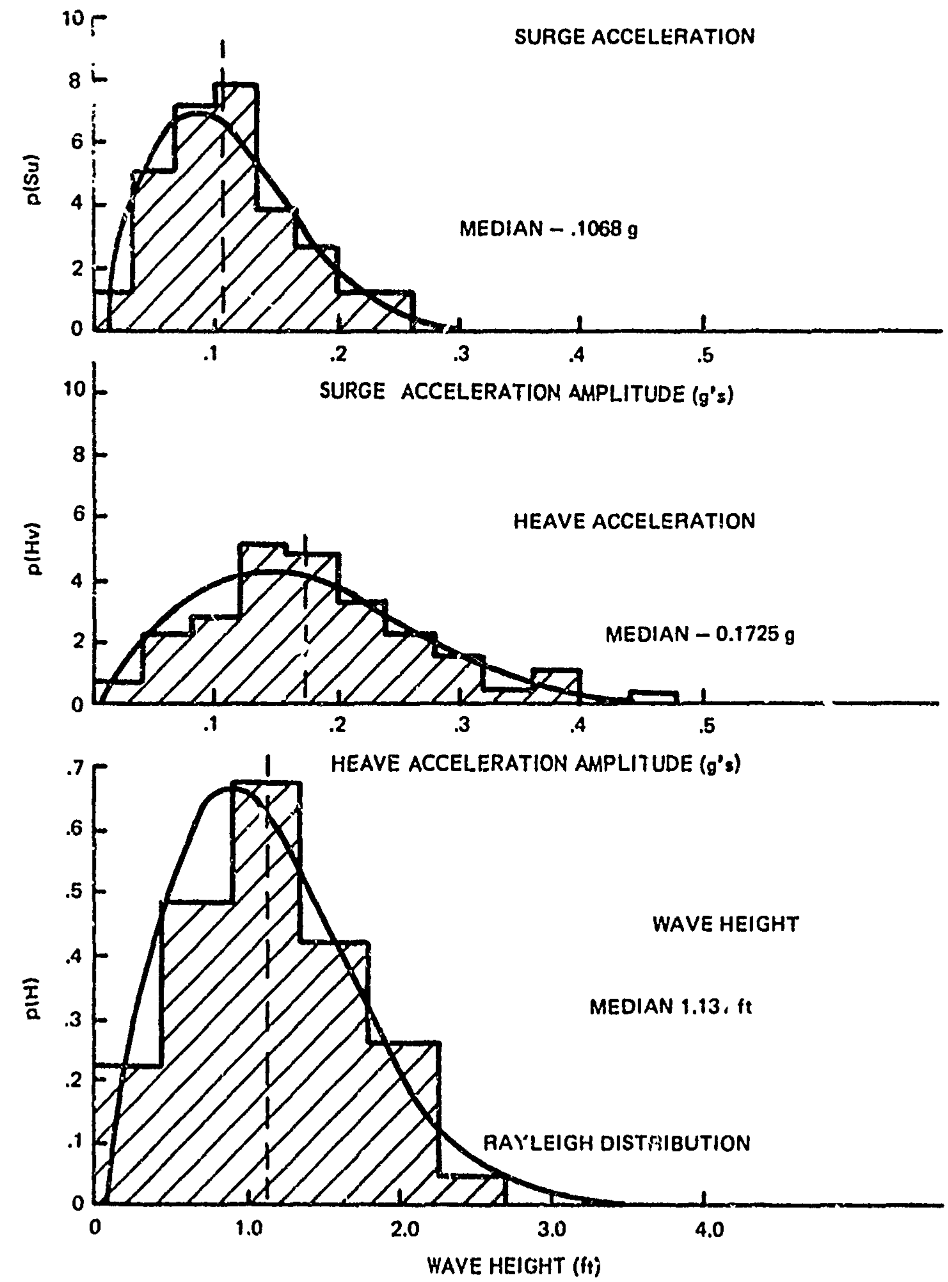

Figure 35. Spherical Buoy Motion Amplitude Histograms — Wave Height, Heave, and Surge

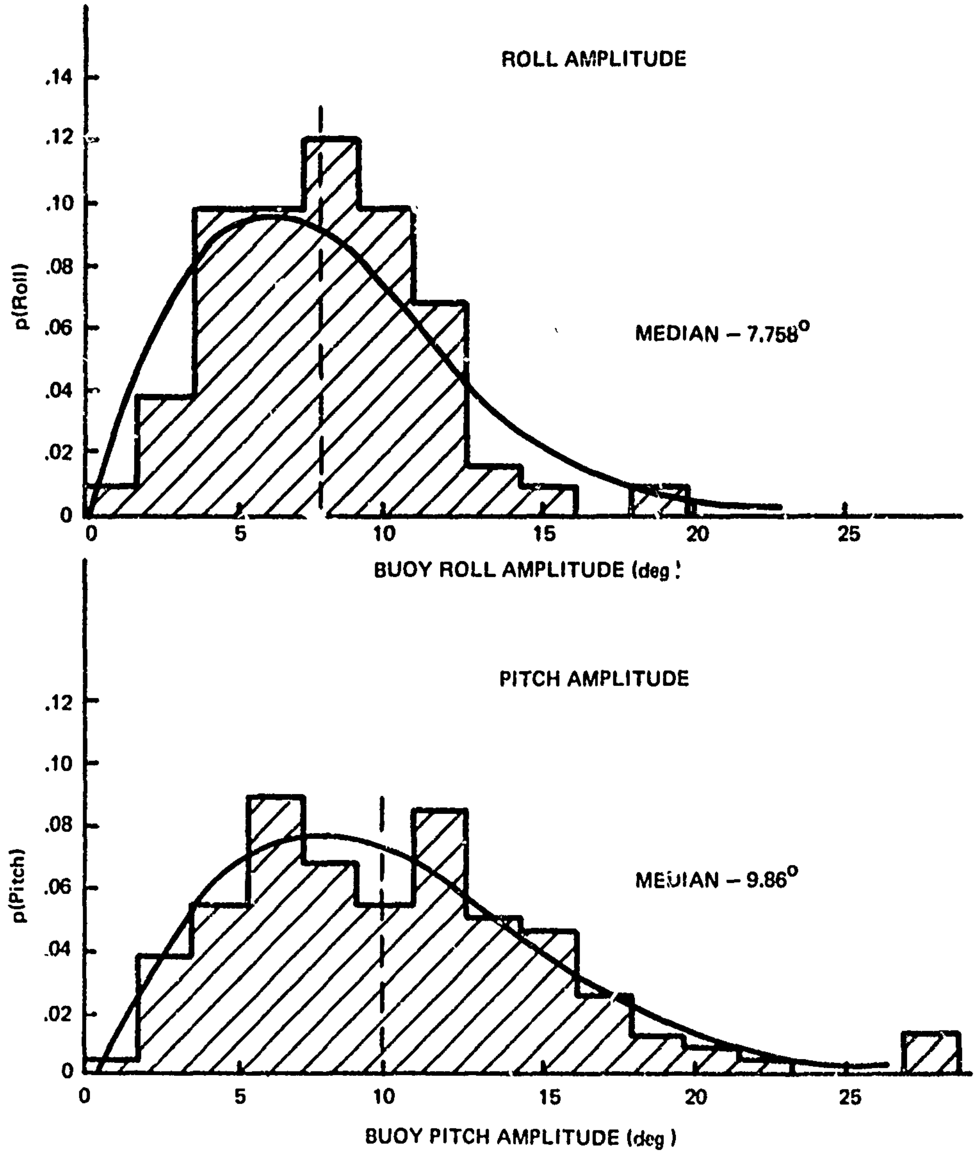

Figure 36. Spherical Buoy Motion Amplitude Histograms — Pitch and Roll

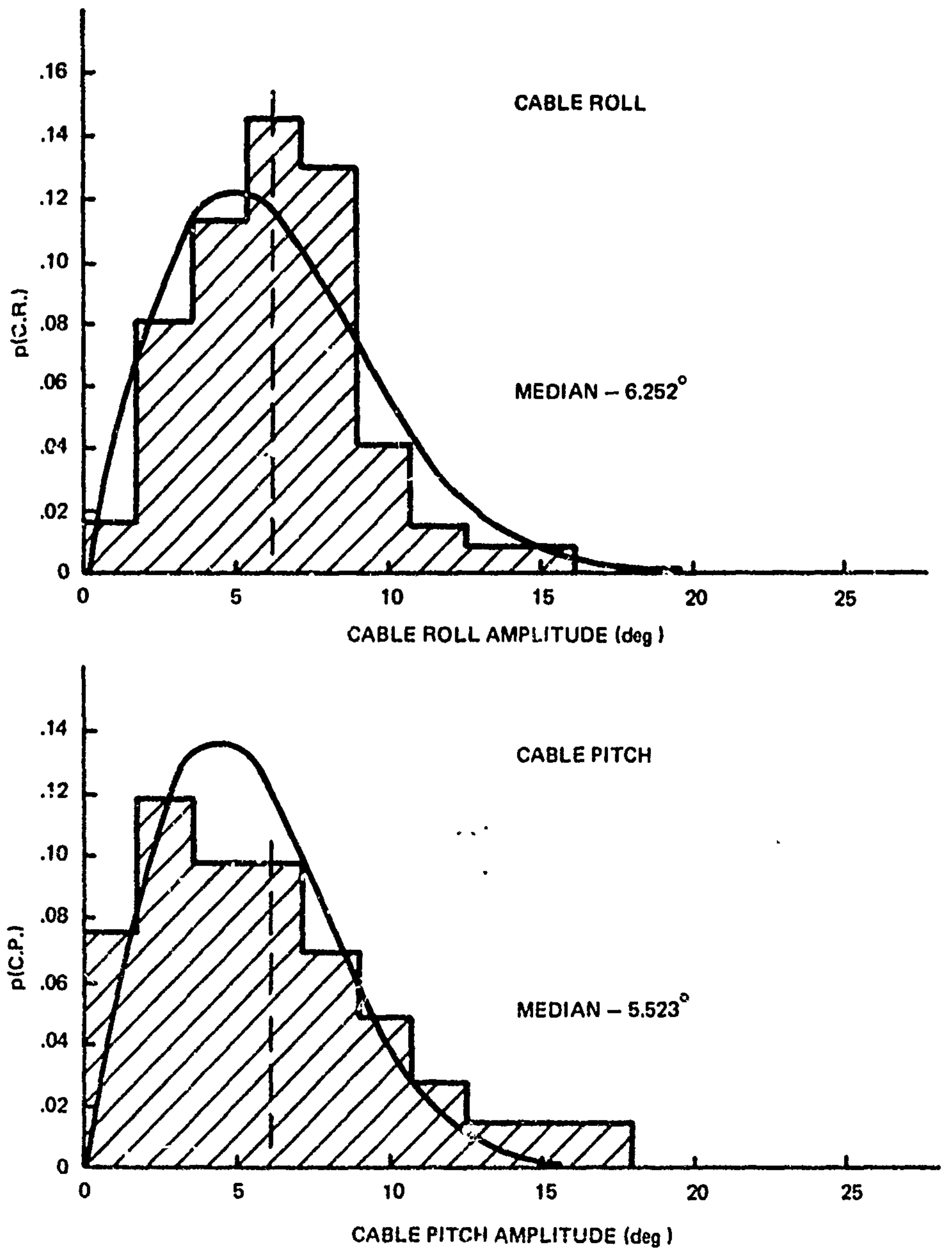

Figure 37. Spherical Buoy Motion Amplitude Histograms — Cable Pitch and Roll

One hundred amplitudes from each parameter record were digitized and were used to generate parameter amplitude histograms. These probability distributions are shown in figures 35 and 37. The median amplitudes were computed and were used to compute Rayleigh distributions, which are plotted over the histograms. The Rayleigh distributions of the form

$$p(H) = \frac{\pi}{2}\frac{H}{\overline{H}^2} e^{-\frac{\pi}{4}\frac{H^2}{\overline{H}^2}} ,$$

where

p(H) is the probability of parameter H

H is the parameter

$\overline{H}$ is the mean value of the parameter,

were found to match the histograms quite well. The fact that the amplitude probability distributions all appear to fit a Rayleigh distribution indicates a linear transform from wave height to buoy response.

If the functions relating the mean buoy motion amplitude parameters to sea state were known, the probability distribution for any parameter in any sea state can be computed from the Rayleigh distribution.

From the statistical accelerometer data, the mean heave acceleration amplitude can be plotted versus mean wave height (using Vine and Volkman's[80] relations for sea state and mean wave height). This curve, shown in figure 38, can be approximated in the region H = 1 to 10 ft with the linear function:

$$\overline{H_V} = 0.11 + 0.0086\,\overline{H} .$$

Assuming a linear transform for the other motion parameters and averaging pitch and roll amplitude means, we can write a set of linear equations for the

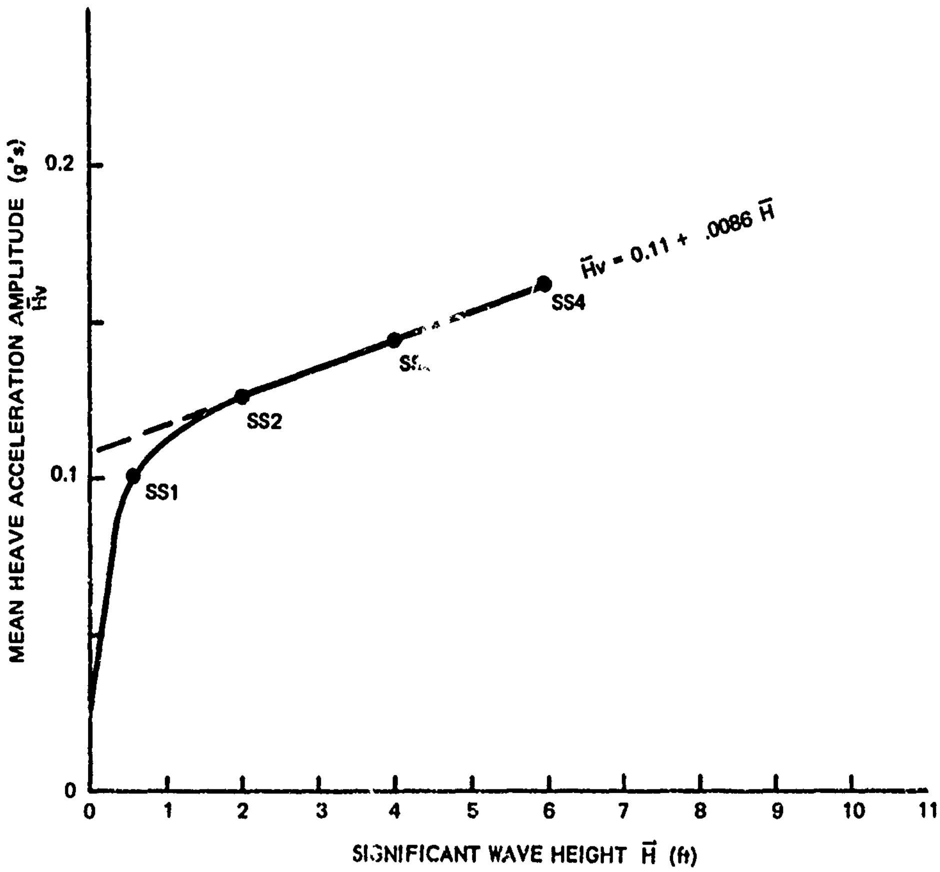

Figure 38. Heave Response of the Spherical Buoy

mean motion amplitudes. In addition, these equations can be substituted into the Rayleigh equation to find the amplitude probability distribution for any parameter. The linear equations and their amplitude distributions are as follows:

For $1 < H < 10$ ft, the mean heave acceleration amplitude is

$$\overline{Hv} = 0.11 + 0.0086\,\overline{H} .$$

The amplitude probability distribution is

$$p(Hv) = \frac{\pi}{2}\frac{Hv}{\overline{Hv}^2} e^{-\frac{\pi}{4}\frac{Hv^2}{\overline{Hv}^2}} .$$

The mean surge acceleration amplitude is

$$\overline{Su} = 0.0688 + 0.00537\,\overline{H} ,$$

and the probability distribution is

$$p(Su) = \frac{\pi}{2}\frac{Su}{\overline{Su}^2} e^{-\frac{\pi}{4}\frac{Su^2}{\overline{Su}^2}} .$$

The mean sway acceleration amplitude is

$$\overline{Sw} = 0.0688 + 0.00537\,\overline{H} ,$$

and the probability distribution is

$$p(Sw) = \frac{\pi}{2}\frac{Sw}{\overline{Sw}^2} e^{-\frac{\pi}{4}\frac{Sw^2}{\overline{Sw}^2}} .$$

The mean pitch angle amplitude is

$$\overline{Pt} = 5.59 + 0.436\,\overline{H} ,$$

and the probability distribution is

$$p(Pt) = \frac{\pi}{2}\frac{Pt}{\overline{Pt}^2} e^{-\frac{\pi}{4}\frac{Pt^2}{\overline{Pt}^2}} .$$

The mean roll angle amplitude is

$$\overline{Rl} = 5.59 + 0.436\,\overline{H} ,$$

and the probability distribution is

$$p(RL) = \frac{\pi}{2}\frac{RL}{\overline{RL}^2}e^{-\frac{\pi}{4}\frac{RL^2}{\overline{RL}^2}}.$$

The mean cable pitch angle amplitude is

$$\overline{CPt} = 3.41 + 0.294\,\overline{H},$$

and the probability distribution is

$$p(CPt) = \frac{\pi}{2}\frac{CPt}{\overline{CPt}^2}e^{-\frac{\pi}{4}\frac{CPt^2}{\overline{CPt}^2}}.$$

The mean cable roll angle amplitude is

$$\overline{CRL} = 3.41 + 0.294\,\overline{H},$$

and the probability distribution is

$$p(CRL) = \frac{\pi}{2}\frac{CRL}{\overline{CRL}^2}e^{-\frac{\pi}{4}\frac{CRL^2}{\overline{CRL}^2}}.$$

The preceding empirical equations will serve as a first-order approximation to the buoy motion parameters for the spherical buoy and can be used for design purposes.

4.2.2 Torroidal Buoy at Station BRAVO

An 8-ft-diameter, torroidal oceanographic buoy was outfitted with buoy motion sensing instrumentation and telemetry and was installed in Block Island Sound during May-June 1970. The buoy (figure 39) was installed by the USCGC MARIPOSA on 30 April 1970 at station BRAVO in 120 ft of water. A telemetry receiving station was established in the generator building at the Watch Hill Lighthouse, Watch Hill, Rhode Island (figures 40 and 41). A schematic of the instrumentation arrangement is shown in figures 42 and 43. A detailed description of the instrumentation, circuitry, and calibrations is described in reference 81.

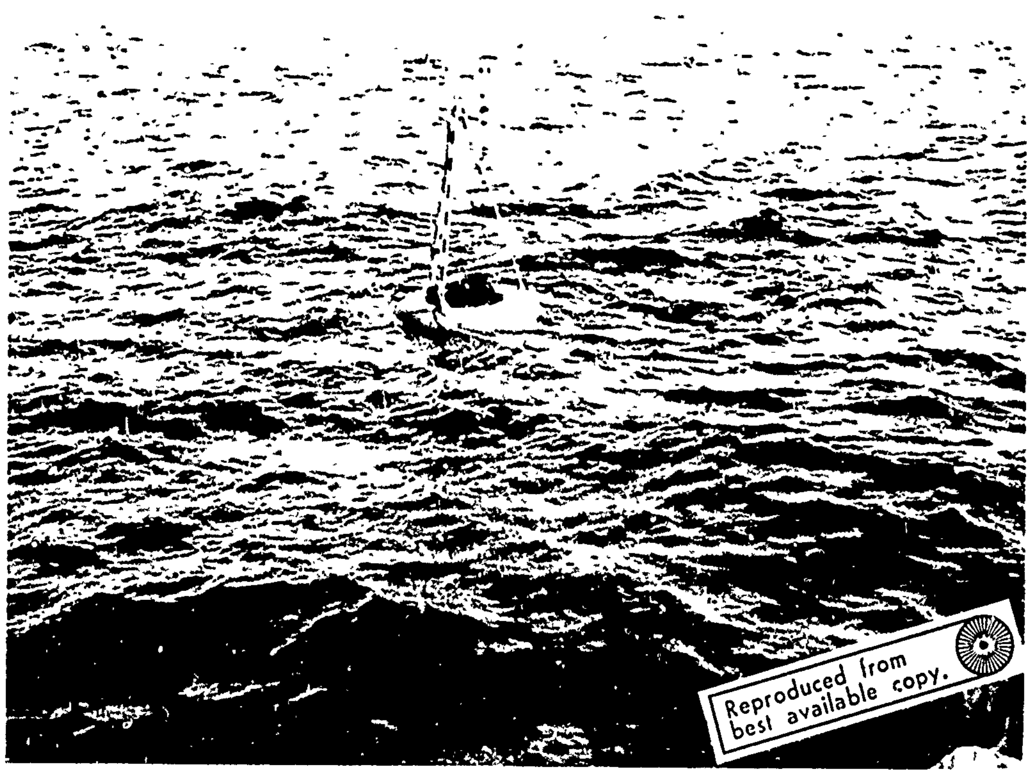

Figure 39. Torroidal Buoy at Station BRAVO

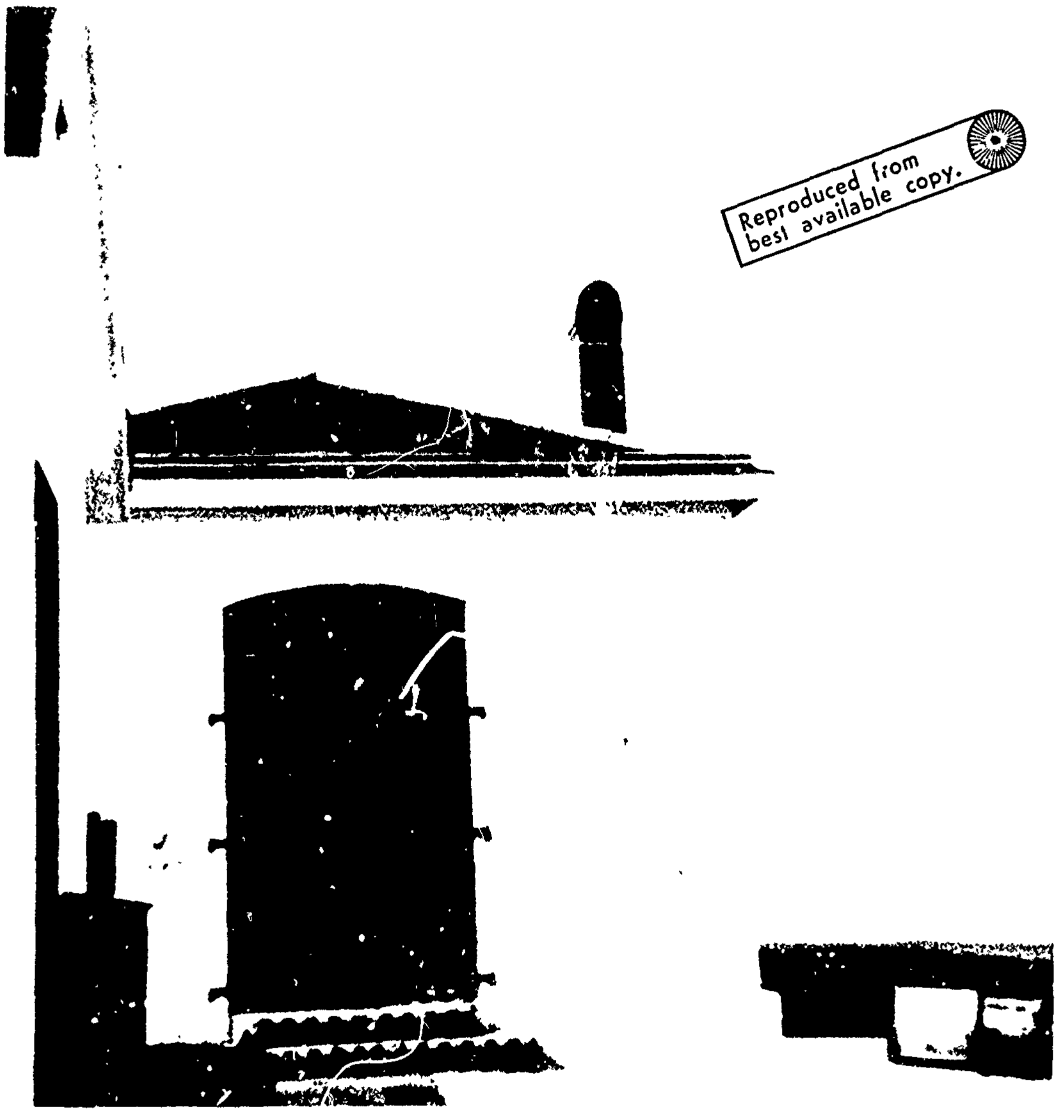

Figure 40. The Shore Station at Watch Hill Lighthouse

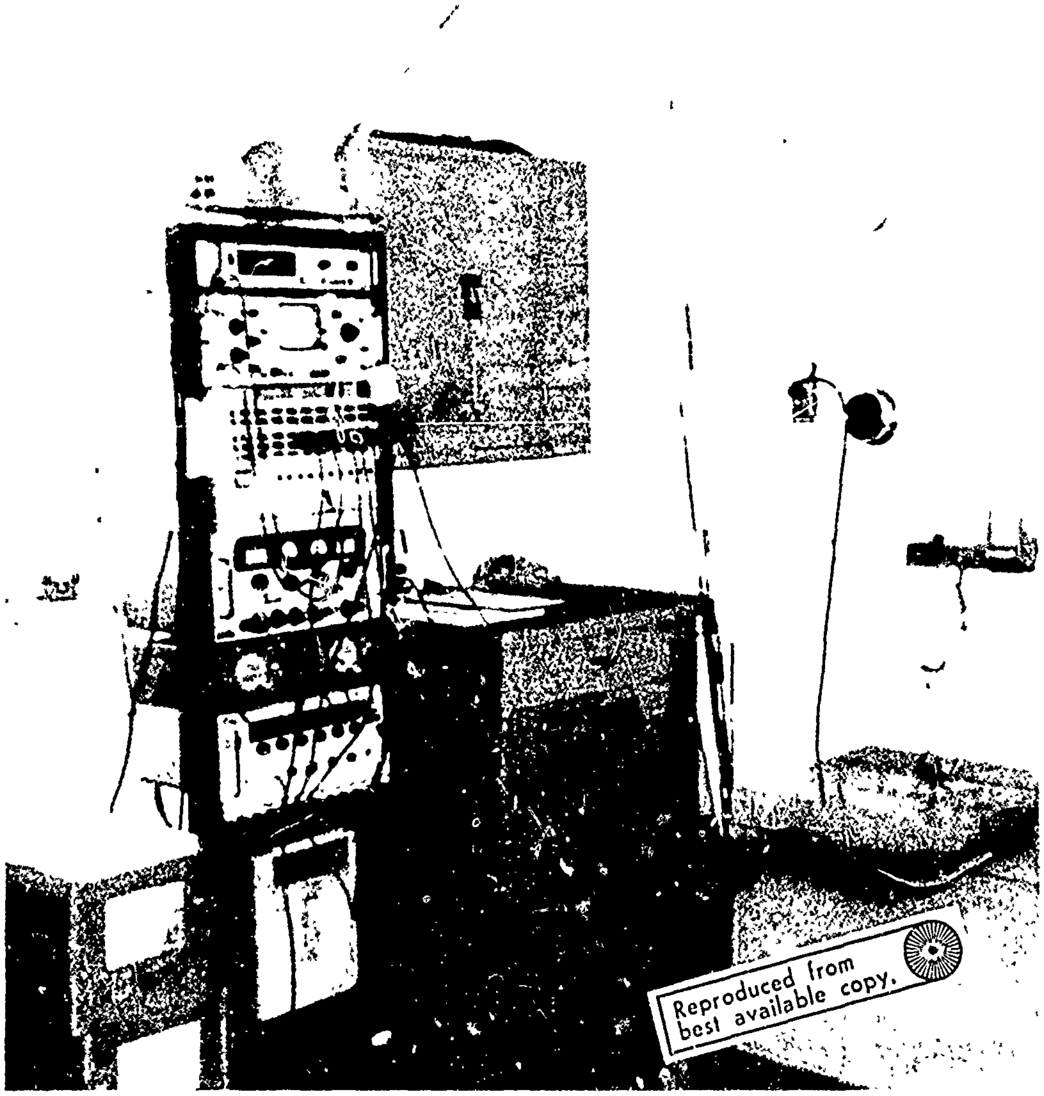

Figure 41. Telemetry Receiver and Recording Equipment

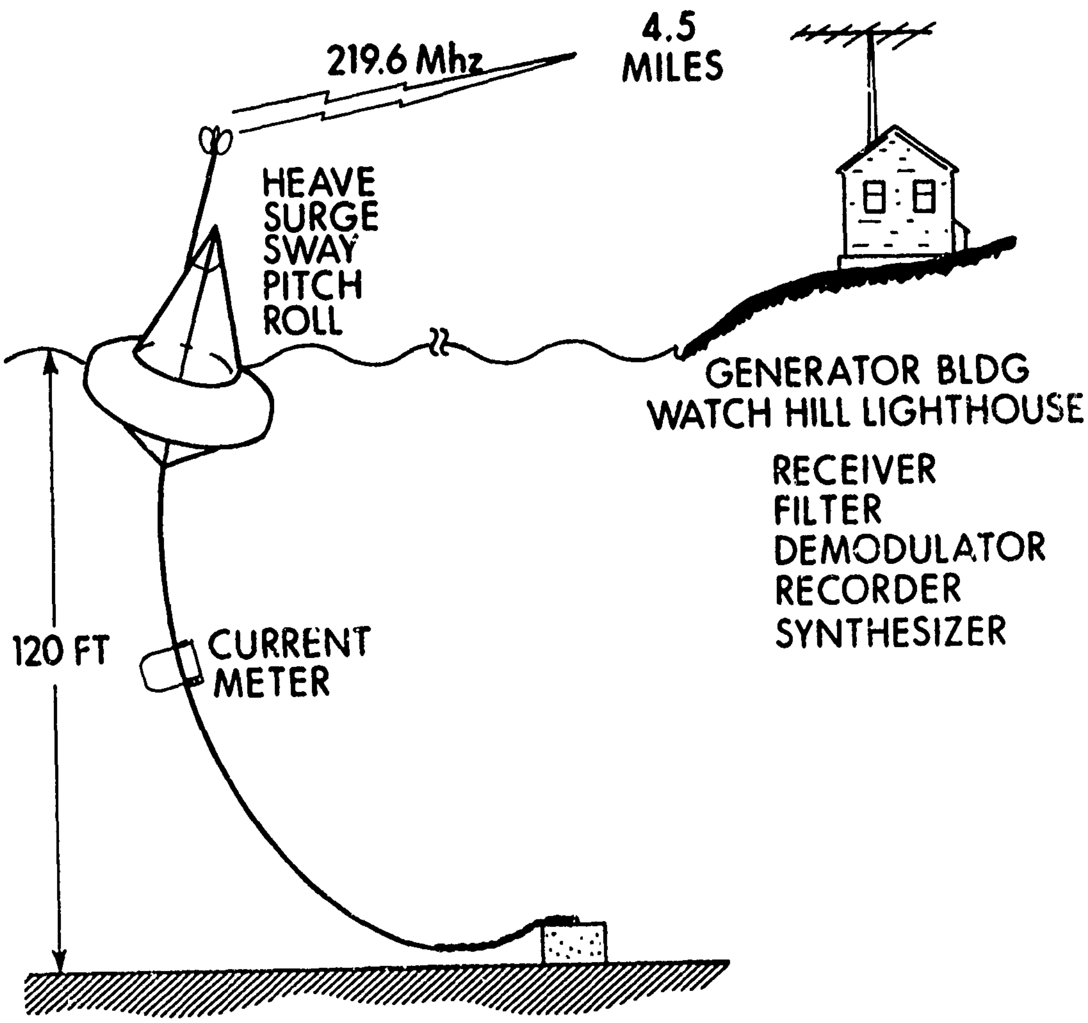

Figure 42. Torroidal Buoy Motion Experiment Setup

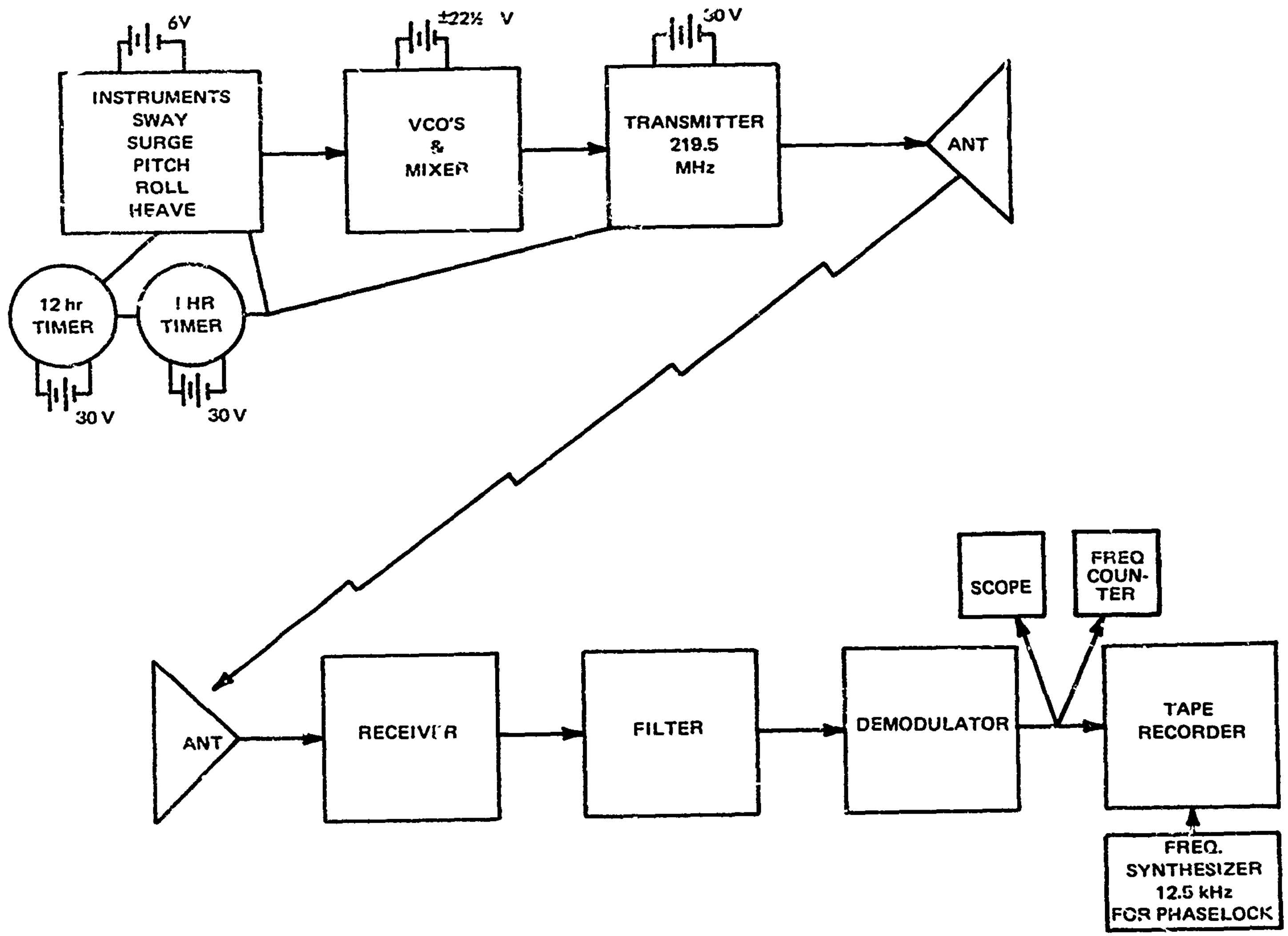

Figure 43. Buoy Motion Telemetry System

The buoy contained the following motion sensing instrumentation:

Heave accelerometer

Surge accelerometer

Sway accelerometer

Pitch angle potentiometer

Roll angle potentiometer.

In addition, a self-recording current meter was attached to the mooring cable at a depth of 60 ft. Wind speeds were recorded on a paper tape recorder at the Watch Hill Lighthouse. Wind directions were logged every 4 hr by the duty personnel at the Lighthouse. Also, the ESSA weather reports on 163.5 kHz were monitored during each data run, and reported conditions at Coast Guard Stations bordering Block Island Sound were logged on the data sheets.

The buoy transmitted data every 12 hr for a ½-hr time period. Each data transmission was preceded by a calibration sequence consisting of two voltage levels from the potentiometer sensors. The FM signals from the buoy containing the five mixed frequencies were demodulated and recorded on an FM tape recorder. The composite signal and a 12.5-kHz phase-lock signal were also recorded on two AM channels.

During the 51 days the buoy was on station, 55 data transmissions were recorded. The only major problem encountered was the failure of the operational amplifier that mixed the five frequencies from the voltage controlled oscillators in the buoy. This component was replaced and tests continued. Structurally, the only failure was the loss of a cotter pin on a shackle holding one of the three chain bridle legs under the buoy. The loss of this pin allowed the shackle to come undone in such a manner that the buoy bridle had only two active legs. The buoy was recovered on 19 June 1970 by the USCGC REDWOOD.

Because of the large amount of recorded data, a simple "quick look" analysis of the data was performed by playing back the recorded data for each of the five motion parameters on a "memoscope." A 2-min sample of each parameter for each run was traced out. The mean width of the band trace-out was measured, and the value of the parameter double amplitude (in volts) was logged. This value was assumed to be the "significant" amplitude, i.e., the mean of the highest one-third of the amplitudes. It was found that the data on the pitch channel were too noisy to be used in this fashion; thus, pitch was not included in this analysis. The logged values of buoy heave, surge, and sway acceleration amplitudes along with buoy roll angle amplitude are shown in table 4. The environmental conditions are also shown for each run.

The statistics of the measured parameters are shown in figure 44. The matrix of simple product-moment correlation coefficients is also shown. These statistics were computed on the GSA-440 time sharing computer. Inspection of the correlation matrix indicates that all the significant buoy motions are well correlated. In addition, they correlate well with wind speed and, to a lesser extent, with computed wind wave height. A similar analysis was conducted with current speed. The elements of that correlation matrix are as follows:

	Heave	Sway	Surge	Roll
Current	0.1537	-0.00572	0.1040	-0.0237.

Thus, it appears that buoy motion amplitudes are not correlated with current speed. Buoy motions are not significantly affected by current speed.

TABLE 4. SUMMARY OF OBSERVED ENVIRONMENTAL AND BUOY RESPONSE DATA FOR THE TORROIDAL BUOY BRAVO

Date (1967)	Time (hr)	Wind			Computed Depth & Current			Computed Wind Waves		Observed Waves		Parameter Double Amplitude from Memoscope (V)					Mean Pitch (V)	Mean Roll (V)
		Speed (knots)	Direction (deg)	Duration (hr)	Water Depth (ft)	Surface Current (knots)	Set (deg)	$H_{1/3}$ (ft)	$T_{1/3}$ (sec)	Swell (ft)	Wind (ft)	Heave	Sway	Surge	Pitch	Roll		
4/30	2230	-	-	-	120.0	1.00	065	-	-	-	-	-	-	0.3	-	-	-	-
5/1	1030	8.0	135.0	2.0	120.1	0.66	065	1.597	5.270	1.0	-	0.5	0.45	0.5	-	-	-	-0.55
5/1	2230	-	-	-	120.3	0.615	065	-	-	-	-	-	-	-	-	-	-	-
5/2	1030	6.3	130.0	2.0	120.4	0.234	065	1.719	5.467	1.5	1	0.5	0.55	0.65	-	0.25	-	-0.5
5/3	2230	0	-	-	123.2	0.456	265	-	-	2.0	0	0.25	0.15	0.2	-	0.18	-	-0.5
5/4	2230	3.5	22.5	2.0	121.7	1.04	265	0.306	2.31	1.5	0	0.25	0.2	0.15	0.15	0.25	-0.45	-0.35
5/5	1033	4.3	202.5	1.0	122.1	1.26	265	0.472	2.87	1.0	0	0.18	0.15	0.14	-	0.2	-	-0.55
5/5	2100	6.0	180.0	3.0	123.6	1.30	265	1.600	5.27	3.0	1.0	0.5	0.55	0.55	-	0.2	-	-0.5
5/6	0900	14.8	292.5	5.0	122.6	0.95	265	1.717	3.459	2.5	1.5	0.5	0.5	0.45	-	0.2	-	-0.5
5/6	2100	34.5	292.5	10.0	123.5	0.93	265	4.670	5.01	2.0	1.5	0.85	0.6	0.65	-	0.2	-	-0.5
5/7	0900	16.9	292.5	12.0	122.1	0.50	265	2.006	3.66	1.0	1.75	0.55	0.45	0.52	-	0.28	-	-0.52
5/7	2100	17.0	292.5	12.0	122.8	0.36	265	2.019	3.67	0.5	0	0.56	0.58	0.52	-	0.32	-	-0.52
5/8	0900	10.4	281.0	4.0	121.8	0	-	1.136	2.97	0.75	0.5	0.52	0.75	0.65	-	0.28	-	-0.5
5/8	2100	10.0	225.0	3.5	122.1	0	-	2.169	4.68	1.5	0	0.5	0.55	0.4	-	0.25	-	-0.55
5/9	0900	0	225.0	-	121.3	0.41	065	-	-	1.0	0	0.2	0.25	0.1	-	0.15	-	-0.5
5/10	0900	0.87	225.0	-	121.0	0.68	065	-	-	1.5	0	0.45	0.35	0.32	-	0.32	-	-0.52
5/10	2100	10.0	225.0	1.0	120.6	0.58	065	2.495	6.59	1.0	1.0	0.65	0.5	0.55	-	0.40	-	-0.60
5/11	0900	3.9	292.5	1.0	121.1	0.73	065	0.380	2.57	2.0	0	0.40	0.37	0.45	-	0.40	-	-0.55
5/11	2100	0	-	-	120.7	0.66	065	-	-	1.25	0	-	-	-	-	-	-	-
5/12	0900	0	270.0	-	120.7	0.75	065	-	-	1.0	0	0.6	0.5	0.5	-	0.45	-	-0.52
5/12	2100	12.2	90.0	1.5	120.9	0.66	065	3.714	8.04	1.0	1.0	0.3	0.35	0.36	-	0.40	-	-0.62
5/14	2100	8.7	45.0	4.0	120.9	0.39	065	0.698	2.27	-	1.5	0.65	0.7	0.65	-	0.45	-	-0.6
5/15	0900	7.8	45.0	1.0	120.7	0.23	065	1.519	4.96	1.5	0.5	0.65	0.5	0.4	-	0.20	-	-0.5
5/16	0900	11.3	90.0	3.0	120.8	0	-	3.186	7.44	2.5	1.0	0.25	0.25	0.21	-	0.11	-	-0.26
5/17	0900	20.9	135.0	10.0	121.2	0.46	265	9.097	9.66	-	4.5	0.8	0.65	0.75	-	0.50	-	-0.6
5/18	0900	20.9	67.5	10.0	120.7	0.78	265	4.562	5.94	2.5	4.0	-	-	-	-	-	-	-
5/25	0830	18.2	90.0	3.0	120.9	0.88	065	8.265	11.989	-	2.5	0.8	0.65	0.65	-	0.5	-	-0.75
5/25	2030	17.3	135.0	12.0	121.1	0.87	065	6.41	8.022	-	1.75	0.4	0.55	0.4	-	0.25	-	-0.65
5/26	0830	0	-	-	120.5	1.08	065	-	-	1.0	0	0.45	0.4	0.3	-	0.2	-	-0.65
5/26	2020	21.7	202.5	3.0	120.6	0.99	065	3.73	5.106	2.25	0.5	0.8	0.5	0.7	0.25	0.25	0.4	-0.5

TABLE 4. (Cont'd) SUMMARY OF OBSERVED ENVIRONMENTAL AND BUOY RESPONSE DATA FOR THE TORROIDAL BUOY BRAVO

Date (1967)	Time (hr)	Wind			Computed Depth & Current			Computed Wind Waves		Observed Waves		Parameter Double Amplitude from Memoscope (V)					Mean Pitch (V)	Mean Roll (V)
		Speed (knots)	Direction (deg)	Duration (hr)	Water Depth (ft)	Surface Current (knots)	Set (deg)	$H_{1/3}$ (ft)	$T_{1/3}$ (sec)	Swell (ft)	Wind (ft)	Heave	Sway	Surge	Pitch	Roll		
5/27	0830	4.8	315.0	6.0	120.2	1.05	065	0.348	1.754	2.5	0.3	-	-	-	-	-	-	-
5/27	2030	13.0	315.0	11.0	120.3	0.92	065	1.116	2.703	2.0	0.5	0.8	0.6	0.5	-	0.2	-	-0.55
5/28	0830	4.4	315.0	0.5	120.1	0.74	065	0.483	2.899	2.0	0	0.25	0.3	0.35	-	0.2	-	-0.55
5/28	2030	4.4	225.0	6.0	120.3	0.65	065	0.463	2.814	1.5	0.3	0.45	0.5	0.24	-	0.2	-	-0.6
5/29	2030	3.5	135.0	5.0	120.7	0.23	065	0.306	2.306	1.0	0.5	0.25	0.2	0.25	-	0.15	-	-0.6
5/30	2030	8.7	135.0	6.0	121.9	0.90	265	1.888	5.731	-	1.5	0.45	0.4	0.35	-	0.2	-	-0.6
5/31	2030	10.4	270.0	4.0	122.1	0.82	265	1.136	2.968	-	2.0	0.6	0.7	0.75	-	0.4	-	-0.7
6/1	0830	7.4	270.0	0.5	122.7	1.15	265	1.366	4.874	-	1.5	0.55	0.55	0.55	-	0.25	-	-0.52
6/1	2030	4.3	225.0	2.5	123.2	1.29	265	0.461	2.83	-	2.0	0.48	0.5	0.55	-	0.2	-	-0.65
6/2	0830	2.2	225.0	2.0	122.2	1.28	265	0.121	1.449	1.0	1.0	0.45	0.5	0.45	-	0.25	-	-0.65
6/2	2030	7.8	225.0	2.0	123.4	1.32	265	1.518	5.138	2.0	0	0.75	0.6	0.55	-	0.25	-	-0.64
6/3	0830	4.3	225.0	3.0	122.4	1.12	265	0.461	2.832	1.0	1.5	0.55	0.44	0.45	-	0.24	-	-0.6
6/3	2030	4.8	225.0	8.0	123.5	1.02	265	0.430	2.026	-	1.5	0.54	0.58	0.6	-	0.25	-	-0.55
6/4	0830	4.3	315.0	7.0	123.3	0.72	265	0.306	1.672	-	0.5	0.3	0.35	0.3	-	0.25	-	-0.65
6/4	2030	0	180.0	-	123.3	0.70	265	-	-	1.0	0	0.35	0.35	0.3	-	0.32	-	-0.65
6/5	0830	8.7	90.0	2.5	122.2	0.22	265	.888	5.731	1.5	0	0.28	0.2	0.25	-	0.18	-	-0.6
6/5	2030	0	135.0	-	122.9	0.22	265	-	-	1.0	0	0.25	0.2	0.25	-	0.15	-	-0.6
6/7	2030	2.6	225.0	0.5	122.2	0.47	265	0.168	1.713	3.0	0	-	-	-	-	-	-	-
6/8	0830	0	270.0	-	[illegible]	0.45	065	-	-	2.5	0	-	-	-	-	-	-	-
6/8	2030	4.3	225.0	9.0	121.3	0.375	065	0.341	1.800	1.5	0	0.4	0.55	0.4	-	0.25	-	-0.6
6/9	0830	0	225.0	-	120.8	0.756	065	-	-	1.0	0	0.3	0.45	0.3	-	0.25	-	-0.6
6/9	2030	5.7	225.0	8.0	121.0	0.72	065	1.159	3.210	0	-	-	-	-	-	-	-	-
6/10	0830	0	-	-	120.6	0.78	065	-	-	1.0	0	-	-	-	-	-	-	-
6/10	2030	5.0	180.0	-	120.9	0.72	065	0.624	3.294	1.0	0.33	1.47	-	-	-	-	-	-
6/11	0830	0	-	-	120.6	0.72	065	-	-	1.0	0	-	-	-	-	-	-	-
6/11	2030	8.7	225.0	1.0	120.9	0.636	065	1.888	5.732	1.0	1.0	-	-	-	-	-	-	-
6/12	0830	0	225.0	-	120.5	0.483	065	-	-	1.0	0	-	-	-	-	-	-	-
Means -		[illegible]			120.0	0.70138						0.4773	0.45386	0.43431		0.26465		0.5625

VARIABLE	MEAN	VARIANCE	STANDARD DEVIATION
WIND	8.198 (knots)	52.72 (knots^2)	7.261 (knots)
SIGNIFICANT WAVE HEIGHT	1.62 ft	4.44 ft^2	2.10 ft
SIGNIFICANT HEAVE ACCELERATION AMPLITUDE	0.197 g	0.00574 g^2	0.0758 g
SIGNIFICANT SWAY ACCELERATION AMPLITUDE	0.1397 g	0.0024 g^2	0.049 g
SIGNIFICANT SURGE ACCELERATION AMPLITUDE	0.135 g	0.00284 g^2	0.0532 g
SIGNIFICANT ROLL AMPLITUDE	14 deg	25.9 deg^2	5.09 deg
CURRENT	0.7022 (knots)	0.1435 (knots^2)	0.3787 (knots)

THE CORRELATION MATRIX

	WIND	WAVE	HEAVE	SWAY	SURGE	ROLL
WIND	1.0	0.7699	0.6418	0.4839	0.5802	0.1997
WAVE		1.0	0.4989	0.3765	0.4553	0.4134
HEAVE			1.0	0.8058	0.8448	0.4671
SWAY				1.0	0.8642	0.4885
SURGE					1.0	0.5571
ROLL						1.0

Figure 44. Torroidal Buoy Motion Statistics for 6-week Period

The GSA-440 computer was also used to fit curves to the observed parameter significant amplitudes. Six curves were fitted using least-squares methods.

In general, the linear plot had the best index of determination when fitted to the data. Figures 45 through 50 show the observed buoy motion significant amplitudes plotted versus wind speed, computed significant wave height, and buoy heave acceleration. The least-mean-squares linear curve is shown on each plot. The least-mean-squares linear functions were transformed to engineering units and are summarized in figure 51. If the buoy motion amplitudes are assumed to be distributed by the Rayleigh distribution, the mean amplitude is $62\frac{1}{2}$ percent of the significant amplitude. The empirical equations shown in figure 51 were again transformed in such a manner that they are in terms of mean amplitudes. They are shown in figure 52.

The cumulative probability distributions for wind, current, observed and computed wave height, and buoy motion amplitudes are shown in figures 53 through 55 for the time period that the buoy was on station.

A complete spectral analysis was performed on two runs of buoy motion data taken on 10 and 11 June 1970. A Fast Fourier Transform method that is programmed and is available on the NUSC UNIVAC 1108 computer was used to compute power spectra and cross correlations. The data were digitized at a rate of 64 samples per second on automatic data processing equipment by the Data Analysis Branch at NUSC. A set of buoy motion spectra for the second data run, which was taken at 2030 EDST, on 11 June 1970, is shown in figures 56 through 61. The wind was at 10 knots from the southwest and had been blowing

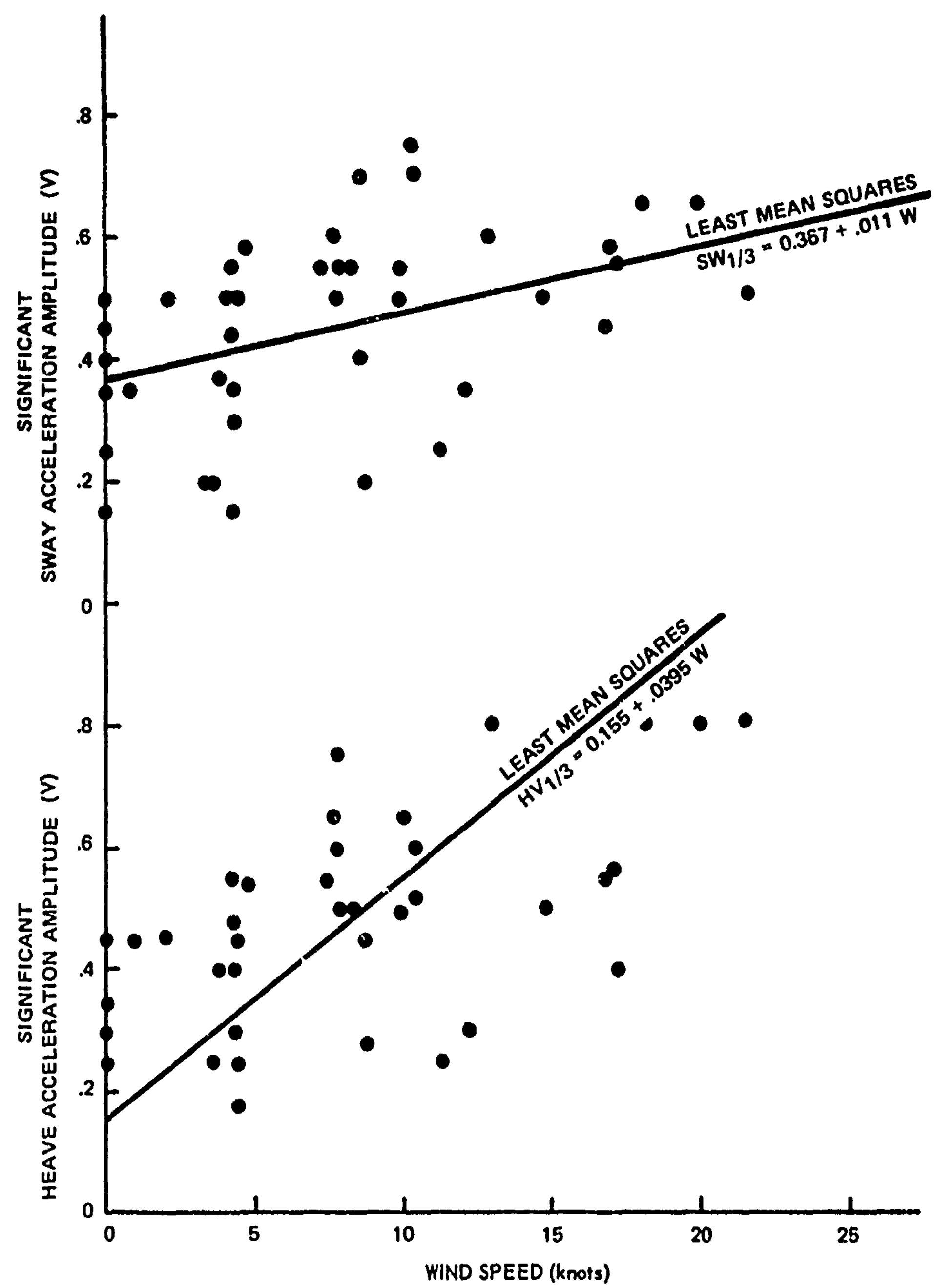

Figure 45. Buoy Motions versus Wind Speed — Heave and Sway

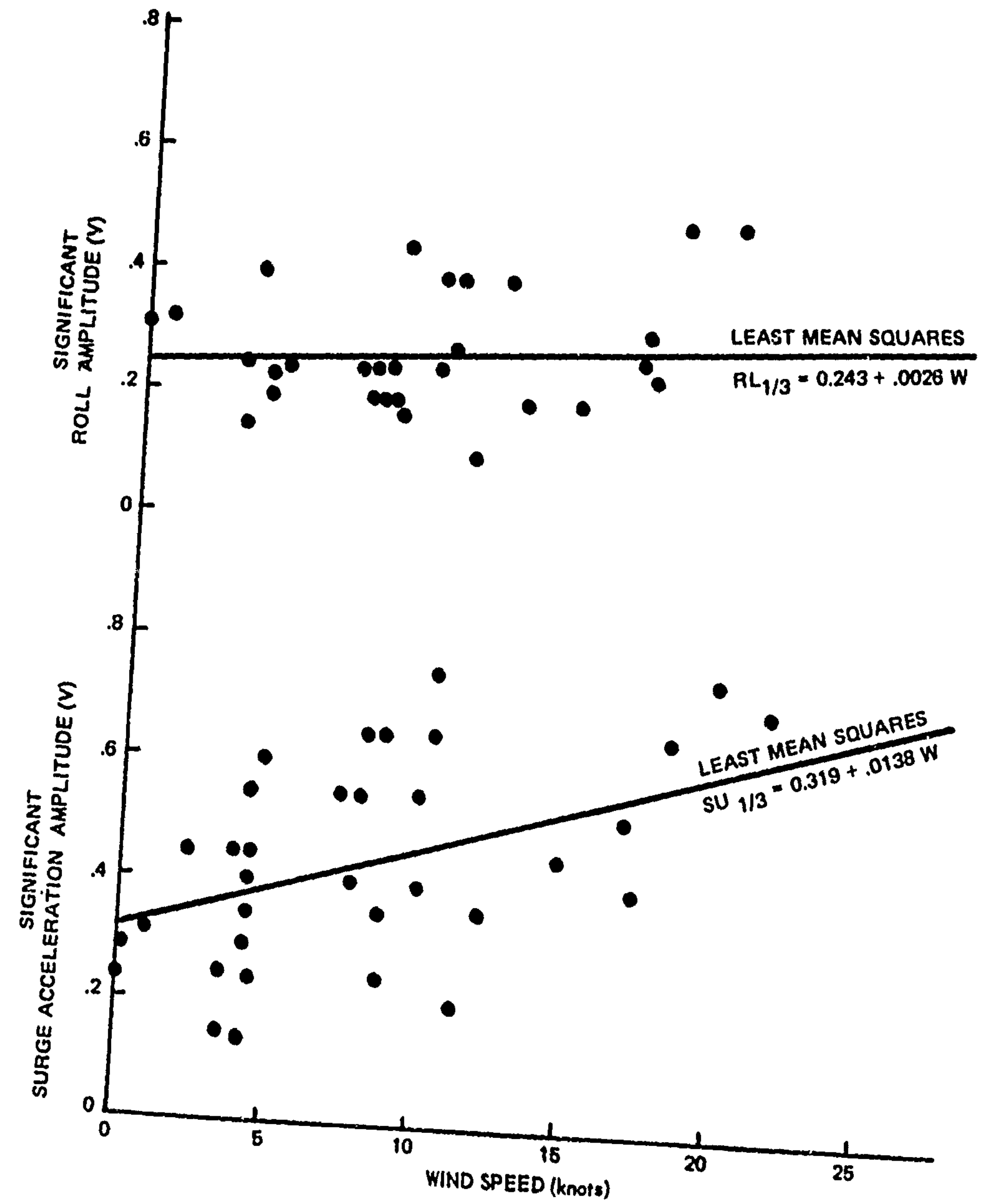

Figure 46. Buoy Motions versus Wind Speed — Surge and Roll

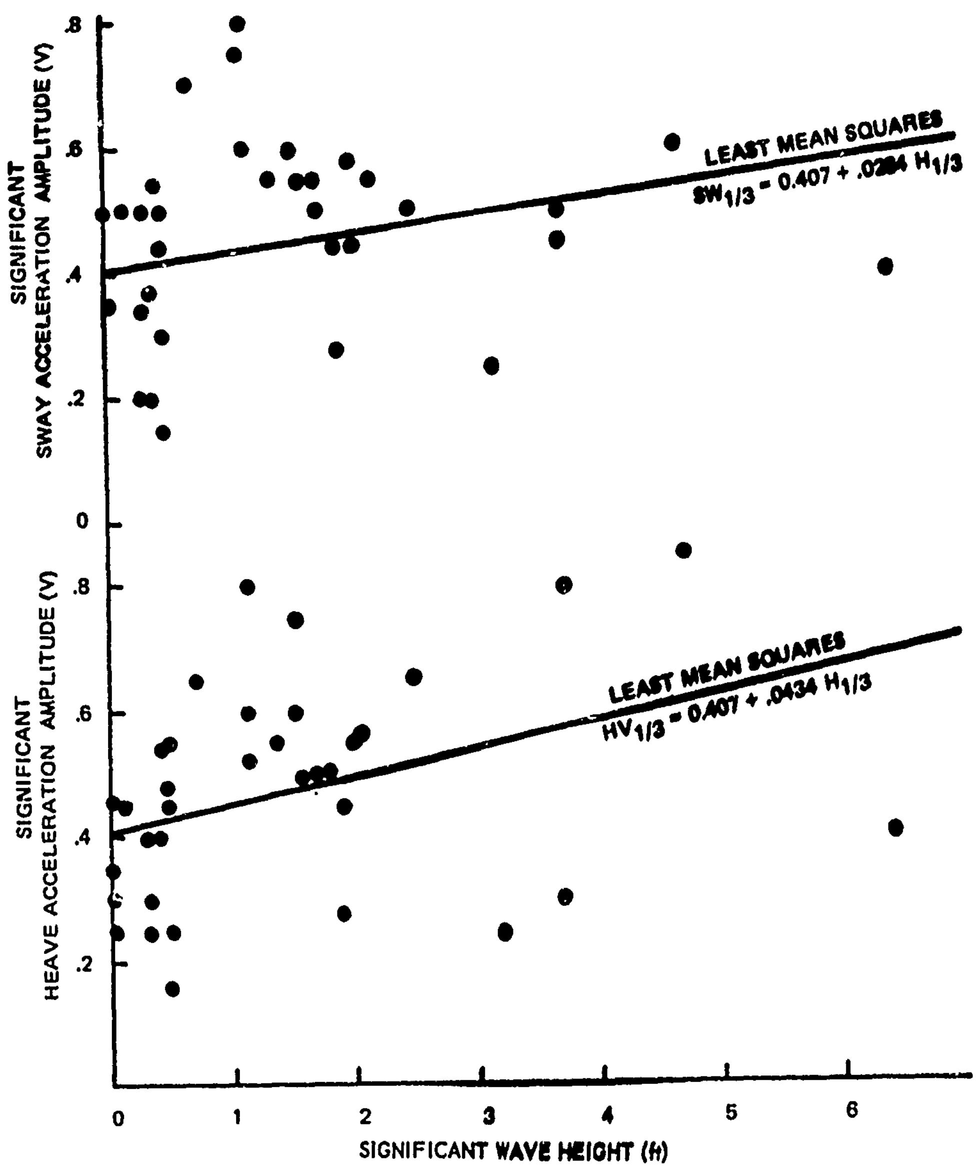

Figure 47. Buoy Motions versus Wave Height — Heave and Sway

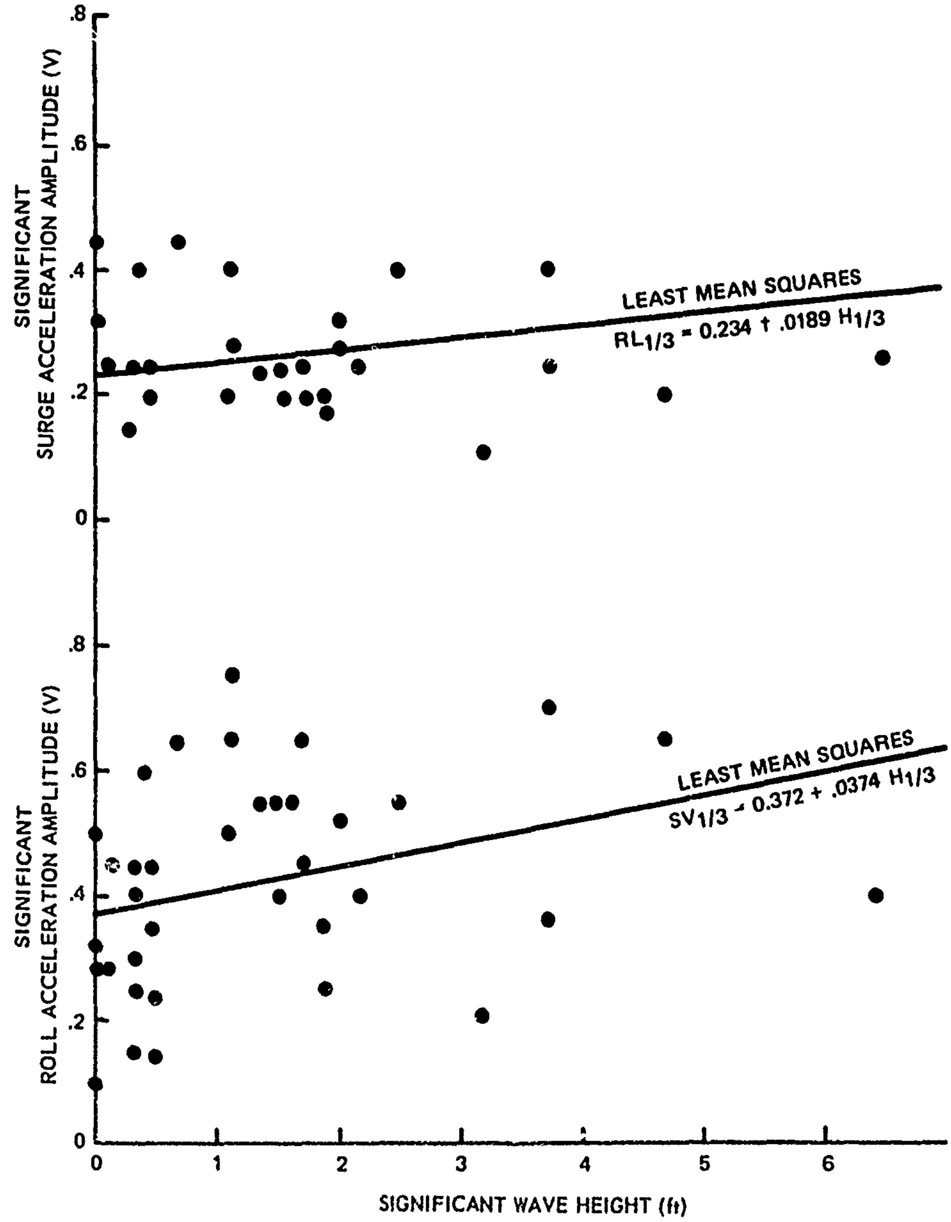

Figure 48. Buoy Motions versus Wave Height — Surge and Roll

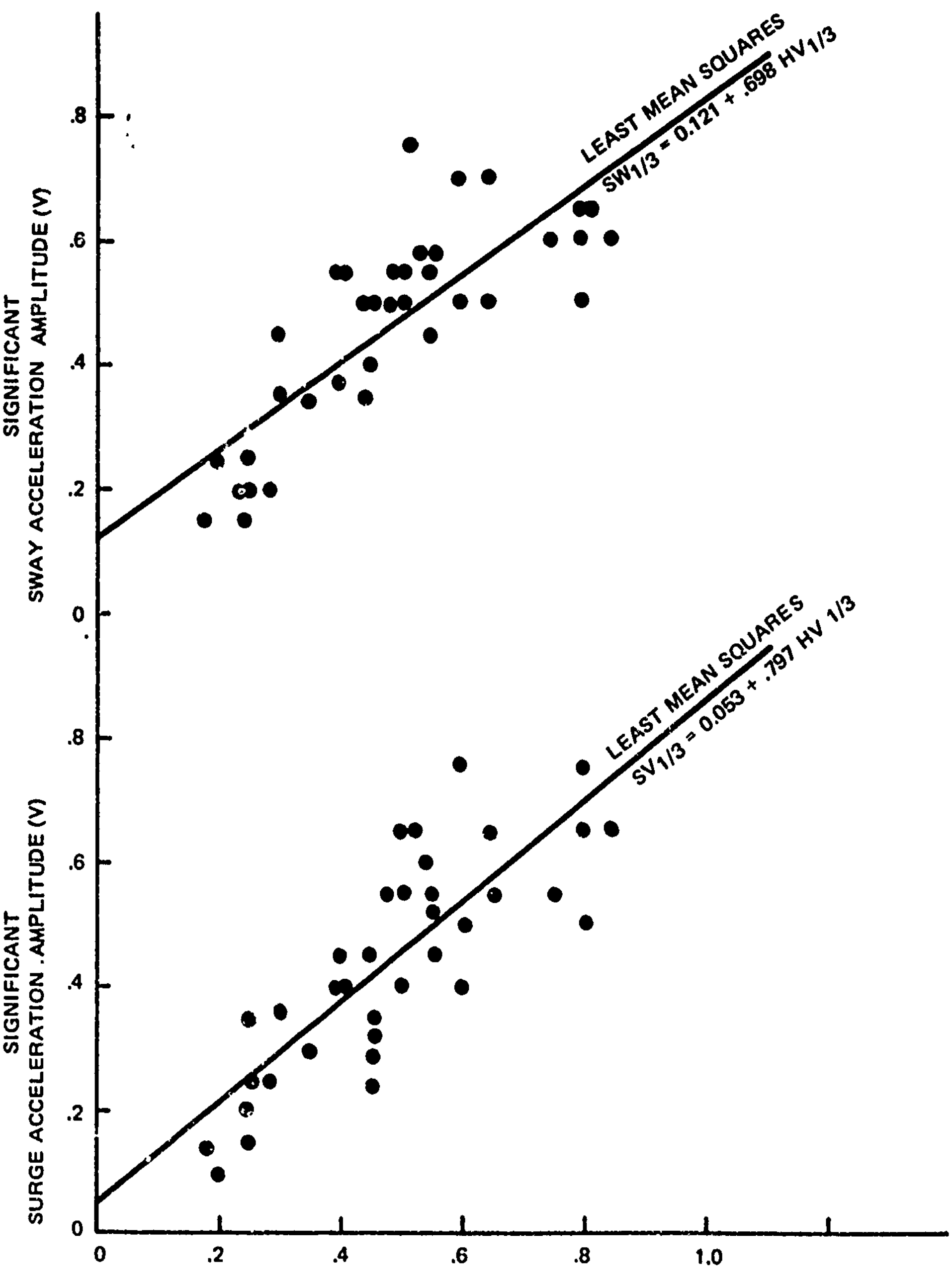

Figure 49. Surge and Sway Motions versus Heave Motion

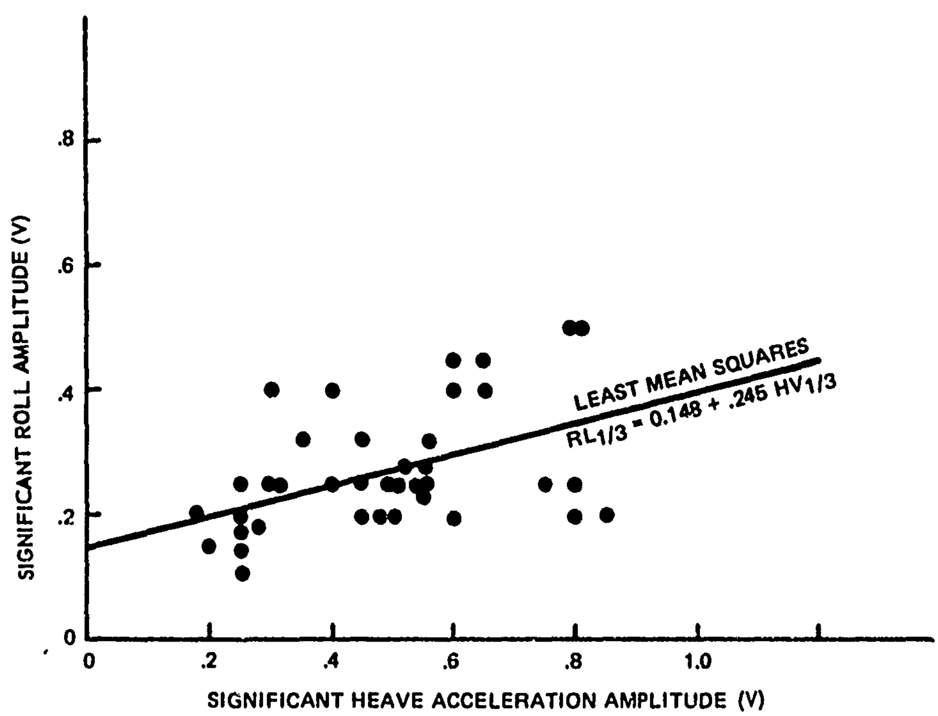

Figure 50. Roll Motion versus Heave Motion

1. ON WIND (W in knots)

HEAVE ACCELERATION	$Hv_{1/3} = 0.0064 + 0.0163 \bullet W$ (g's)
SWAY-SURGE ACCELERATION	$Su_{1/3} = Sw_{1/3} = 0.1056 + 0.003825 \bullet W$ (g's)
PITCH-ROLL ANGLE	$Pi_{1/3} = Rl_{1/3} = 12.83° + 0.1373 \bullet W$ (deg)

2. ON SIGNIFICANT WAVE HEIGHT ($H_{1/3}$ in ft)

HEAVE ACCELERATION	$Hv_{1/3} = 0.168 + 0.01792 \bullet H_{1/3}$ (g's)
SWAY-SURGE ACCELERATION	$Su_{1/3} = Sw_{1/3} = 0.120 + 0.01015 \bullet H_{1/3}$ (g's)
PITCH-ROLL ANGLE	$Pi_{1/3} = Rl_{1/3} = 12.36 + 1.0 \bullet H_{1/3}$ (deg)

3. ON HEAVE ACCELERATION AMPLITUDE ($Hv_{1/3}$ in g's)

SWAY-SURGE ACCELERATION	$Su_{1/3} = Sw_{1/3} = 0.0268 + 0.557 \bullet Hv_{1/3}$ (g's)
PITCH-ROLL ANGLE	$Pi_{1/3} = Rl_{1/3} = 7.82 + 31.35 \bullet Hv_{1/3}$ (deg)

Figure 51. Empirical Equations for Significant Buoy Motion Amplitudes (Based on Linear, Least-Mean-Squares Equations)

1. ON WIND (W in knots)

HEAVE ACCELERATION $\overline{Hv} = 0.004 + 0.0102 \bullet W$ (g's)

SWAY-SURGE ACCELERATION $\overline{Su} = \overline{Sw} = 0.066 + 0.002394 \bullet W$ (g's)

PITCH-ROLL ANGLE $\overline{Pi} = \overline{Rl} = 8.03 + 0.086 \bullet W$ (deg)

$$p(Hv) = \frac{\pi}{2} \bullet \frac{Hv}{\overline{Hv}^2} \bullet e^{-\left(\frac{\pi}{4} \bullet \frac{Hv^2}{\overline{Hv}^2}\right)} \qquad p(Sw) = p(Su) = \frac{\pi}{2} \bullet \frac{Su}{\overline{Su}^2} \bullet e^{-\left(\frac{\pi}{4} \bullet \frac{Su^2}{\overline{Su}^2}\right)}$$

$$p(Pi) = p(Rl) = \frac{\pi}{2} \bullet \frac{Rl}{\overline{Rl}^2} \bullet e^{-\left(\frac{\pi}{4} \bullet \frac{Rl^2}{\overline{Rl}^2}\right)}$$

2. ON MEAN WAVE HEIGHT ($\overline{H}$ in ft)

HEAVE ACCELERATION $\overline{Hv} = 0.105 + 0.01792 \bullet \overline{H}$ (g's)

SWAY-SURGE ACCELERATION $\overline{Sw} = \overline{Su} = 0.075 + 0.01015 \bullet \overline{H}$ (g's)

PITCH-ROLL ANGLE $\overline{Pi} = \overline{Rl} = 7.72° + 1.0 \bullet \overline{H}$ (deg)

(NOTE THAT THE PROBABILITY DISTRIBUTIONS ARE THE SAME AS ABOVE.)

3. ON MEAN HEAVE ACCELERATION AMPLITUDE ($\overline{Hv}$ in g's)

SWAY-SURGE ACCELERATION $\overline{Sw} = \overline{Su} = 0.01674 + 0.557 \bullet \overline{Hv}$ (g's)

PITCH-ROLL ANGLE $\overline{Pi} = \overline{Rl} = 4.89 + 31.35 \bullet \overline{Hv}$ (deg)

Figure 52. Empirical Equations for Mean Buoy Motion Amplitudes

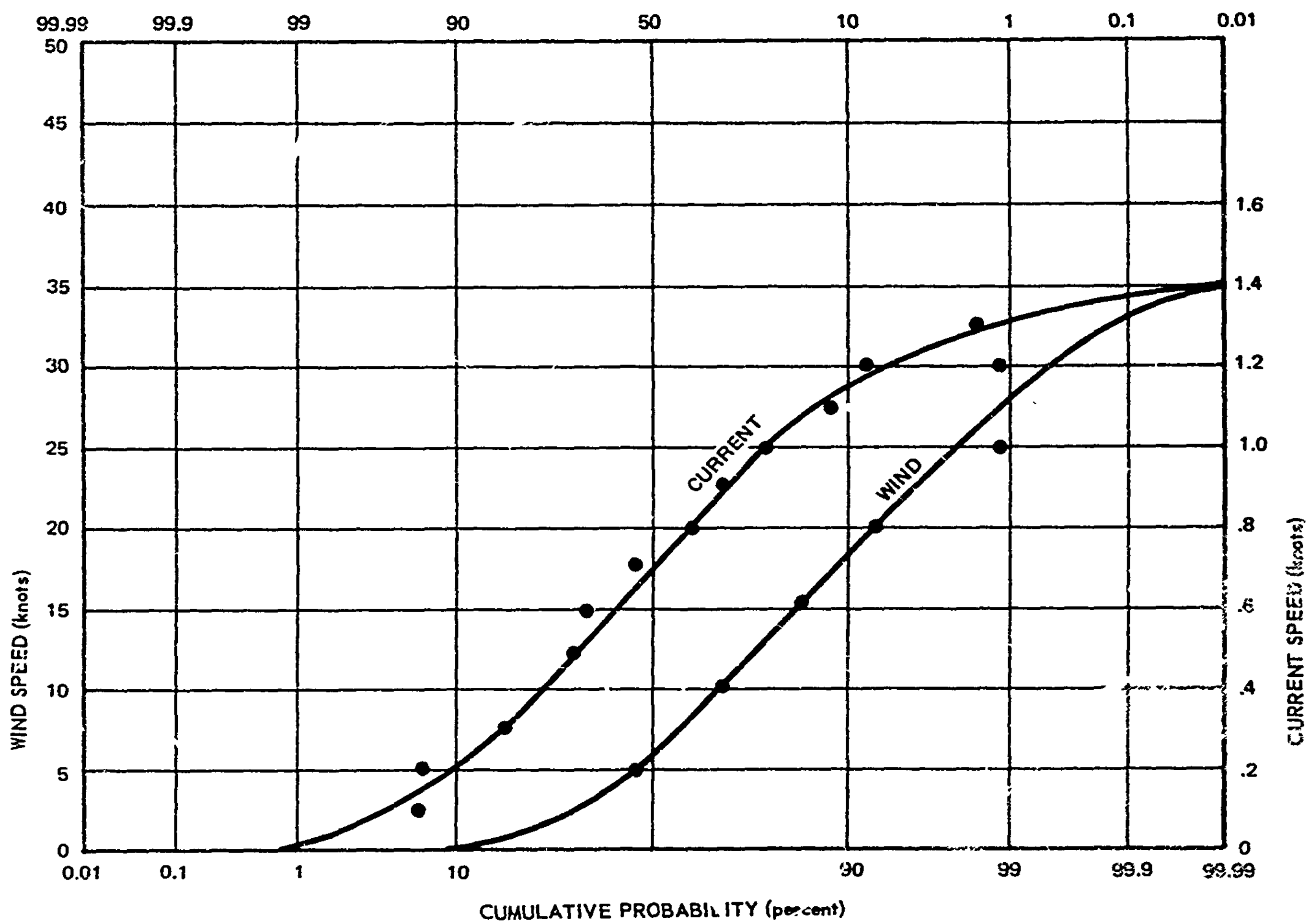

Figure 53. Wind and Current Cumulative Distributions

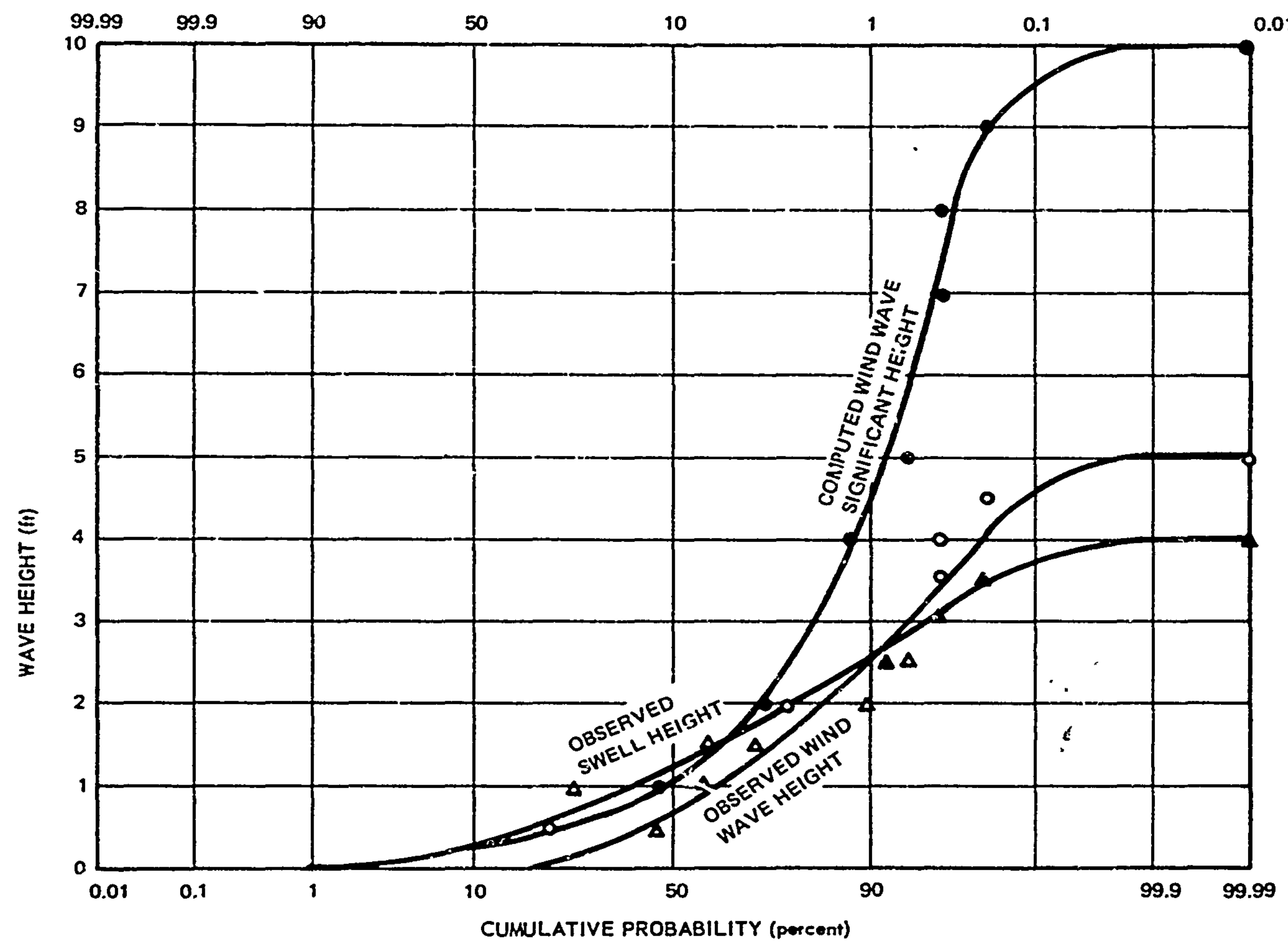

Figure 54. Significant Wave Height Cumulative Distributions

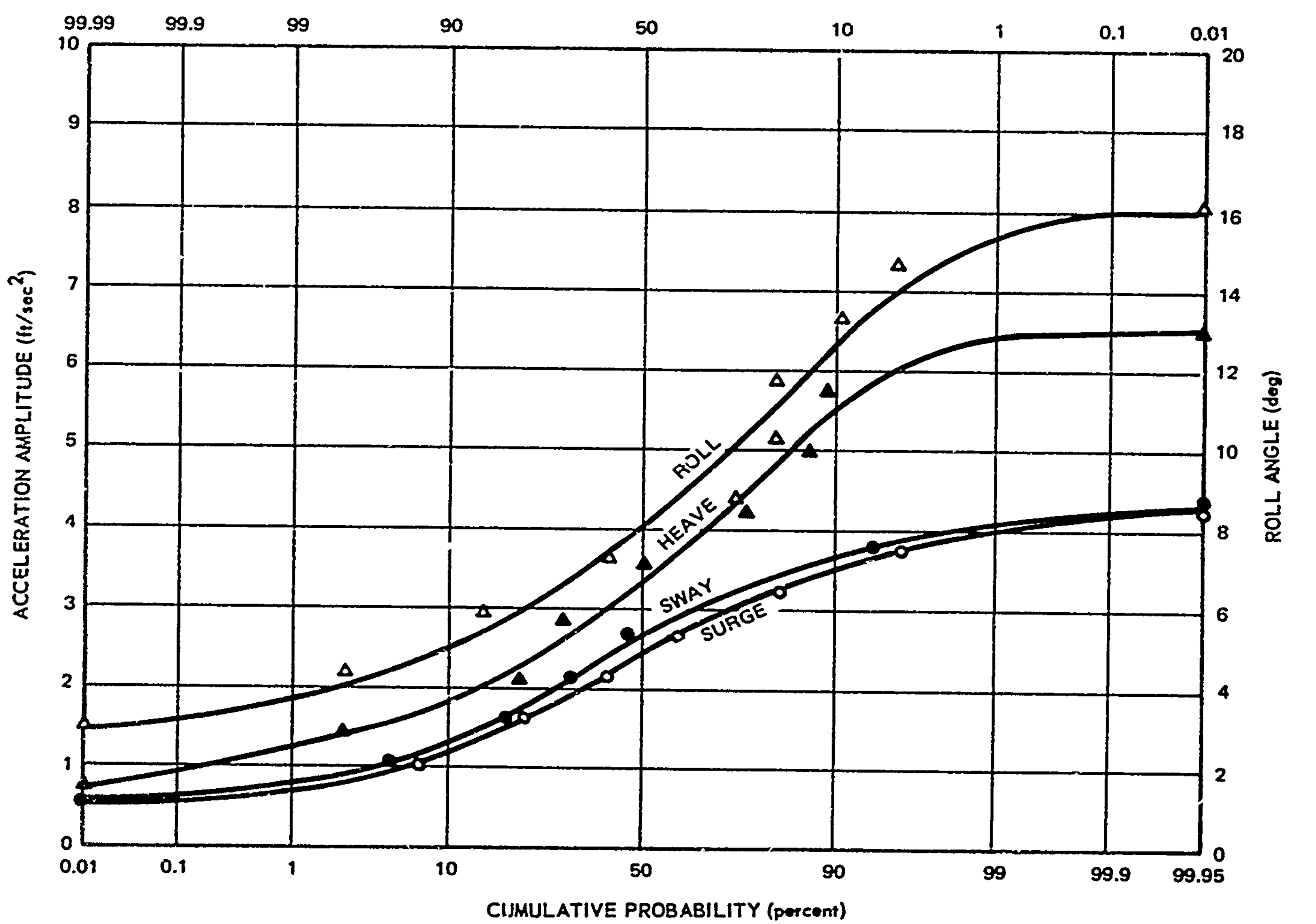

Figure 55. Significant Buoy Motion Cumulative Distributions

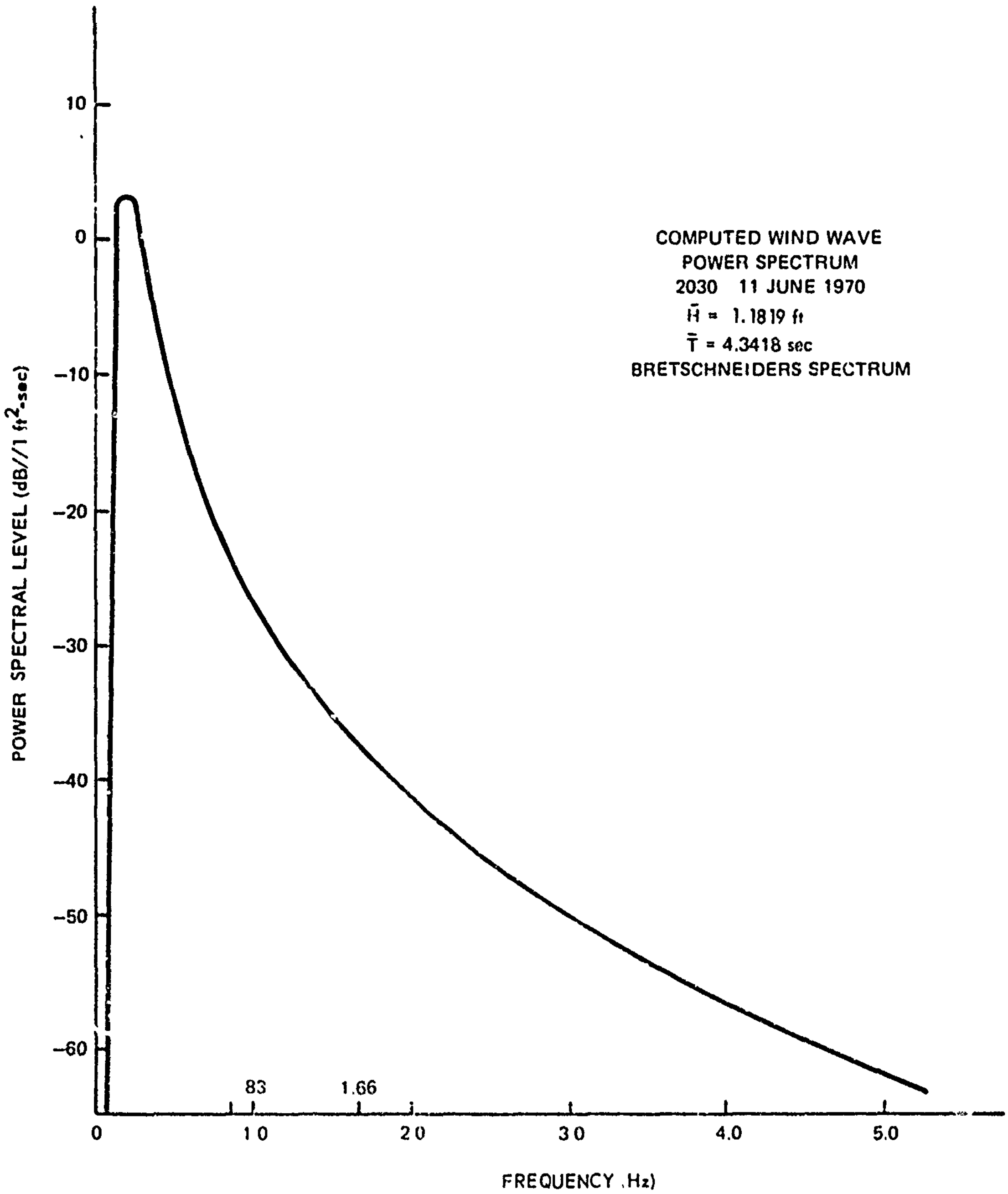

Figure 56. Computed Wind Wave Spectral Levels — 2030 hr, 11 June 1970

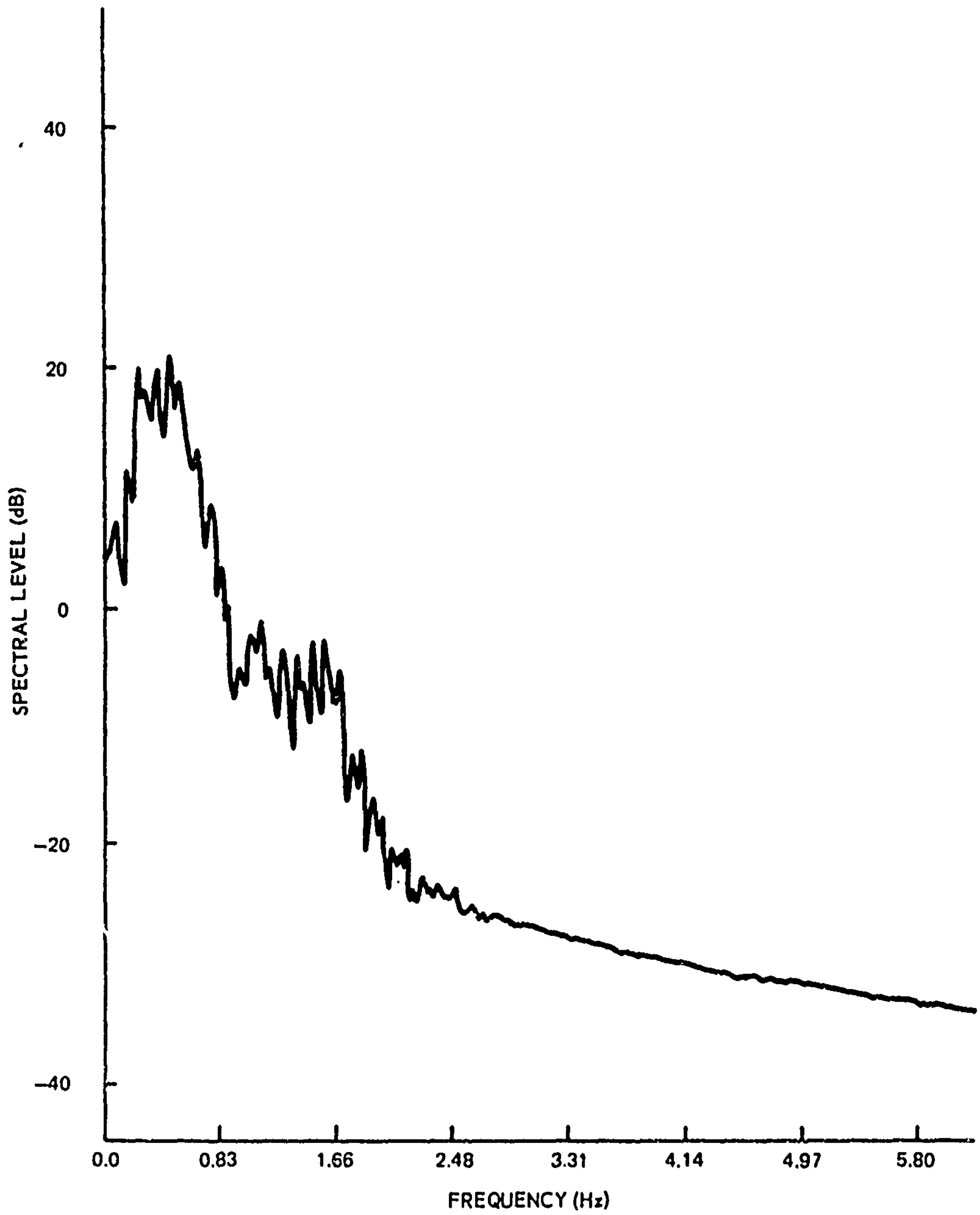

Figure 57. Observed Heave Spectral Levels

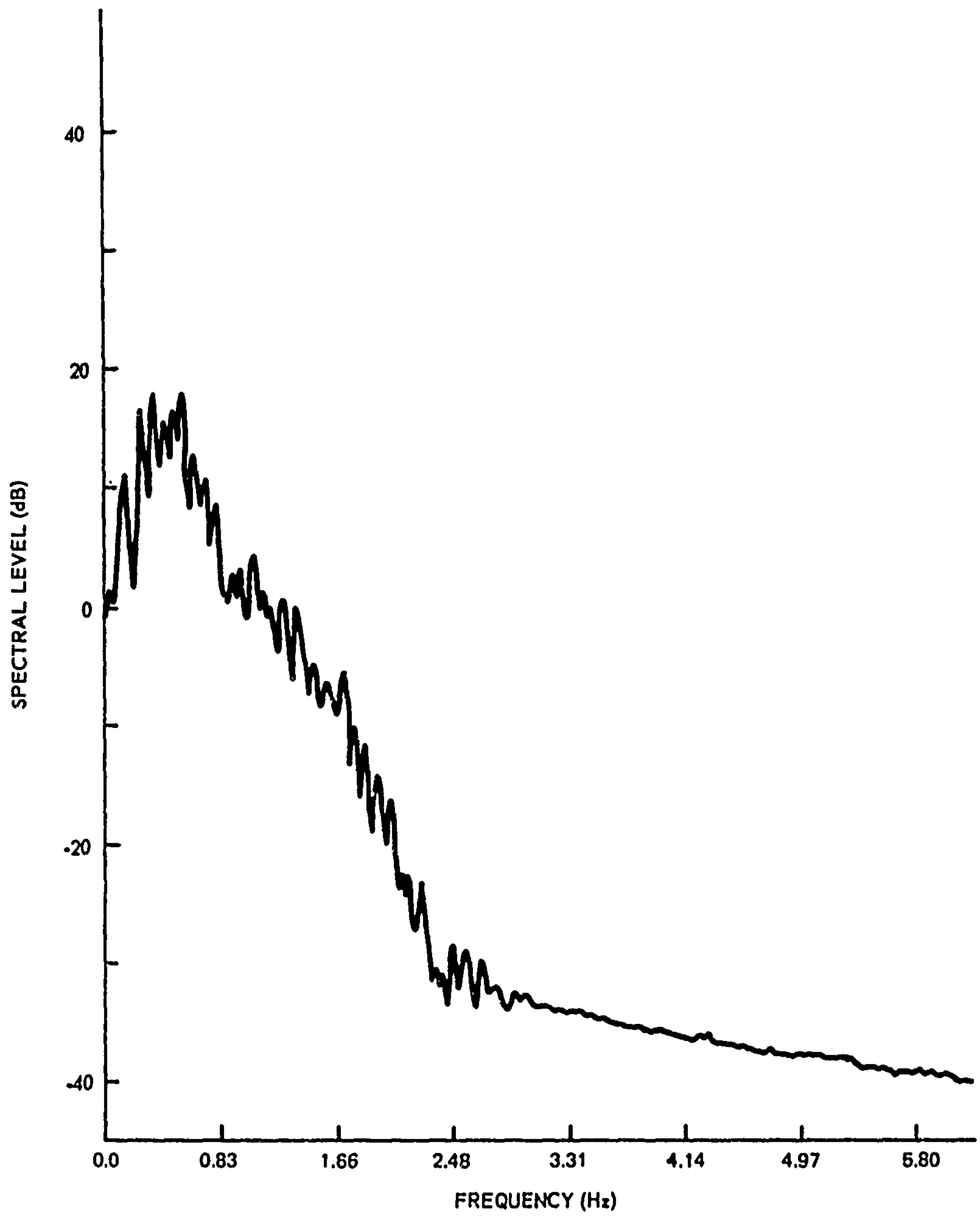

Figure 58. Observed Surge Spectral Levels

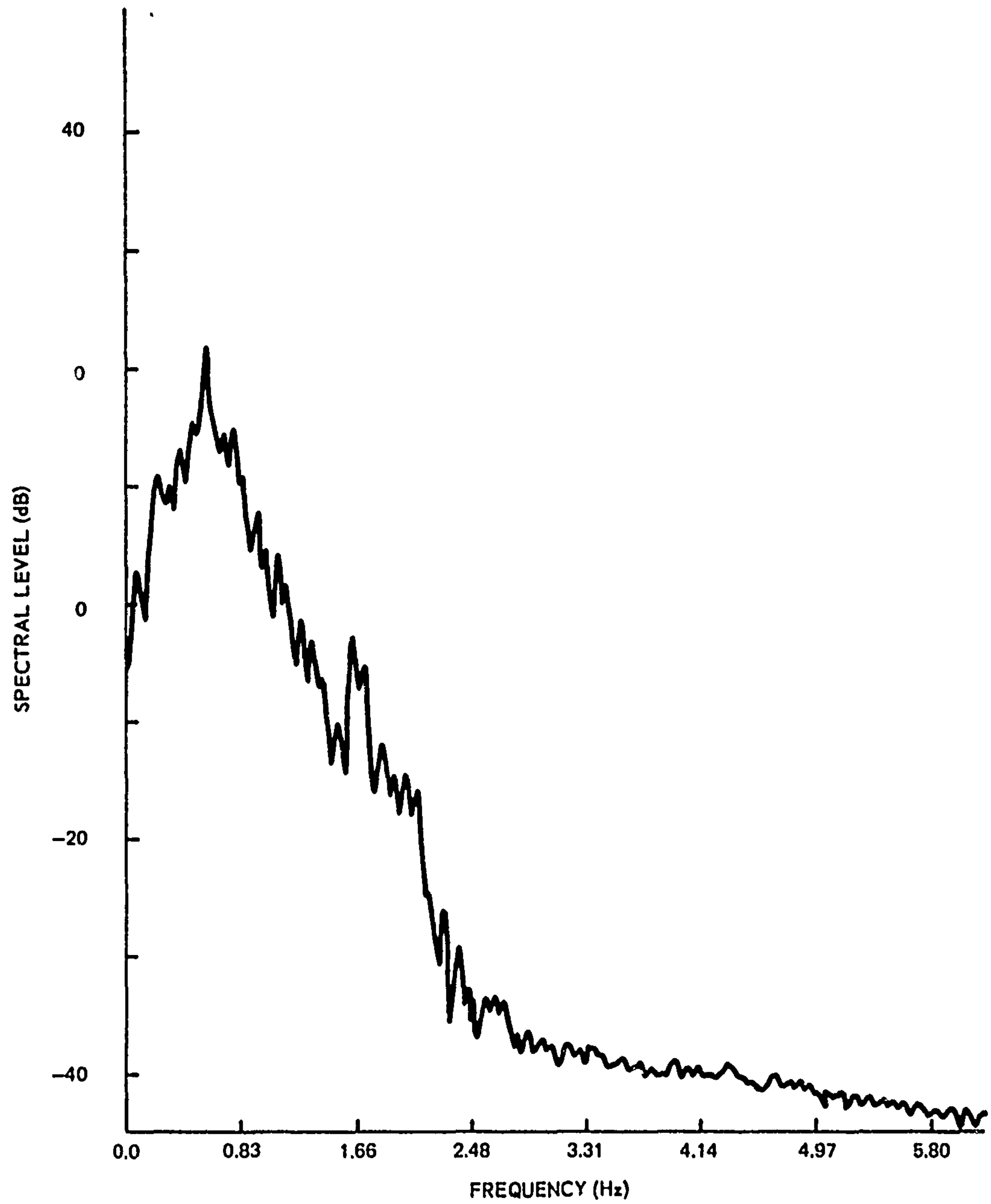

Figure 59. Observed Sway Spectral Levels

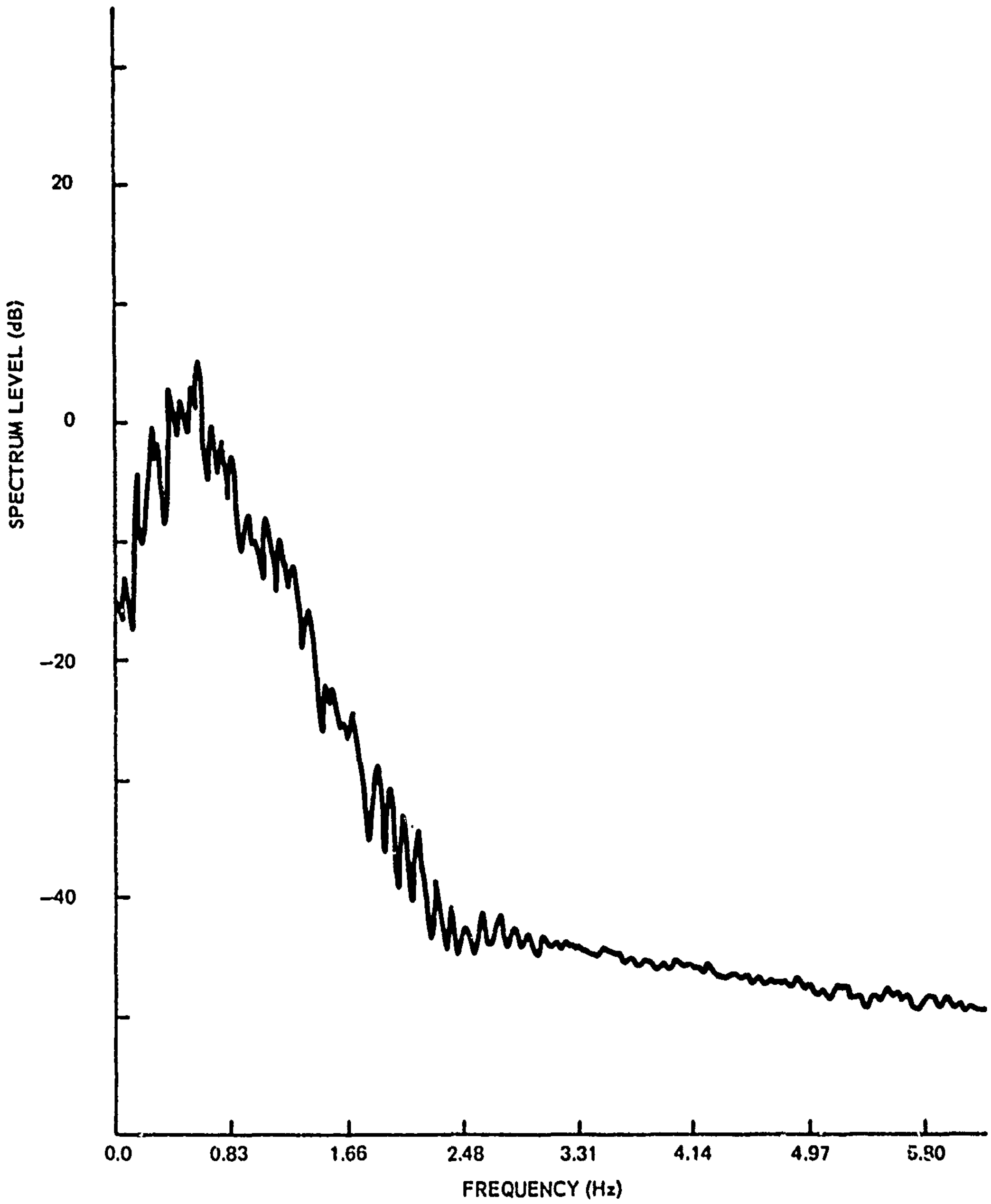

Figure 60. Observed Pitch Spectral Levels

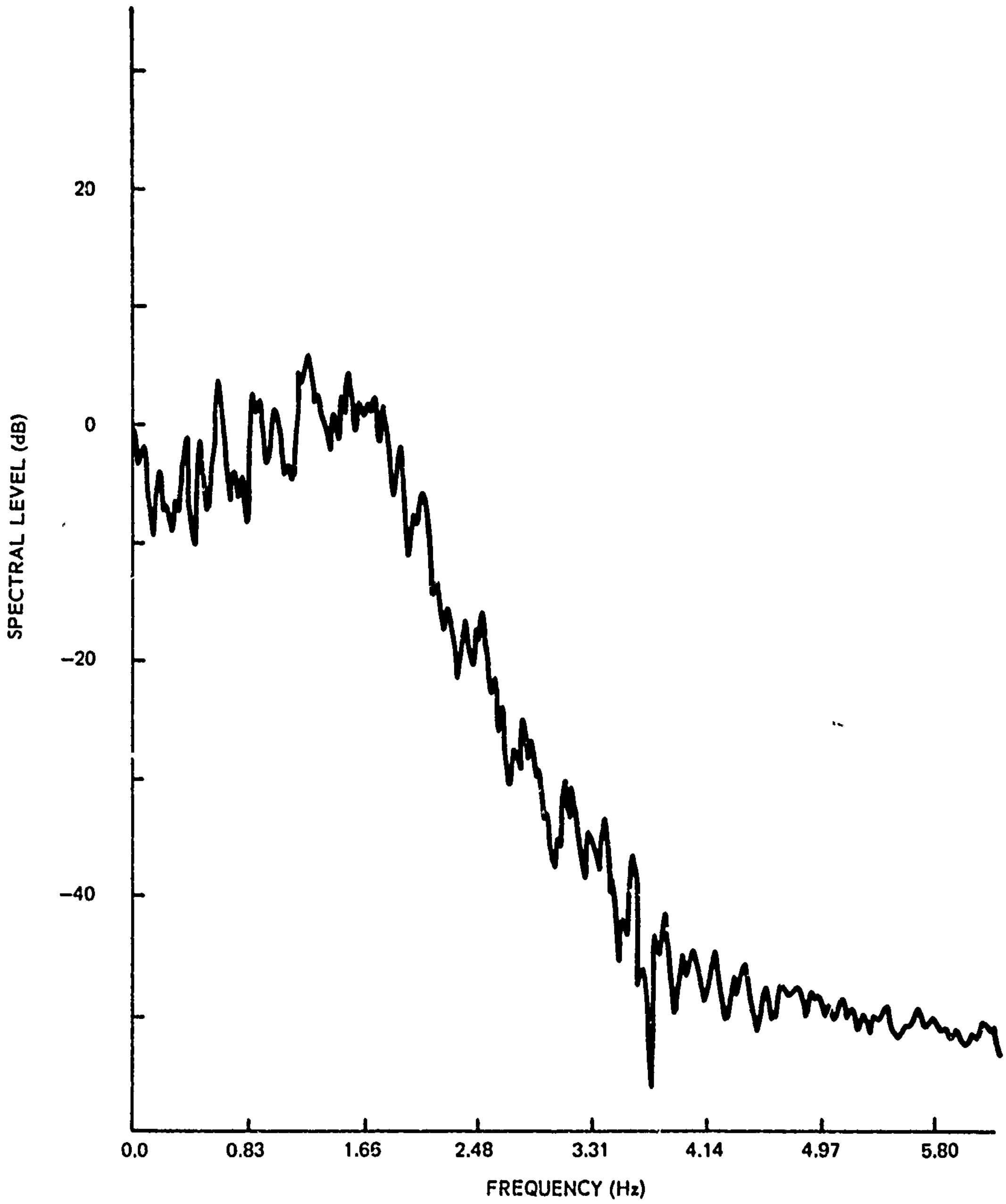

Figure 61. Observed Roll Spectral Levels

steady at that strength for 1 hr. The wind wave spectrum was computed by using a two-parameter Bretschneider spectrum. Figure 56 shows the computed wind wave power spectrum. Figures 57 through 61 show the buoy motion power spectra. Figure 57, the buoy heave acceleration power spectra, shows a peak in the energy around 0.5 rad/sec (T = 12.5 sec). There is also a peak around 1.5 rad/sec, which corresponds to the peak of the computed wind wave power spectrum.

The peak at the lower frequency may be caused by swell; a 1-ft swell from the south was observed visually during the data run. The same type of energy distribution is seen in the other spectra. Buoy roll angle and sway acceleration spectra indicate relatively more energy at wind wave frequencies; thus, it is concluded that the buoy was oriented in such a manner that the sway-heave plane was close to a southwest-northeast orientation.

Buoy motion parameters were cross-correlated with buoy heave acceleration and are shown in figures 62 through 65. These plots indicate the existence of two modes with rather strong coupling between motion parameters. If a linear system is assumed, the input and output spectra can be related by the transfer function:

$$S_{A^2}(\omega) = H(\omega)^2 \cdot S_{H^2}(\omega) \; ,$$

where

$S_{A^2}(\omega)$ is the buoy motion power spectrum

$S_{H^2}(\omega)$ is the wave height power spectrum

$H(\omega)$ is the transfer function .

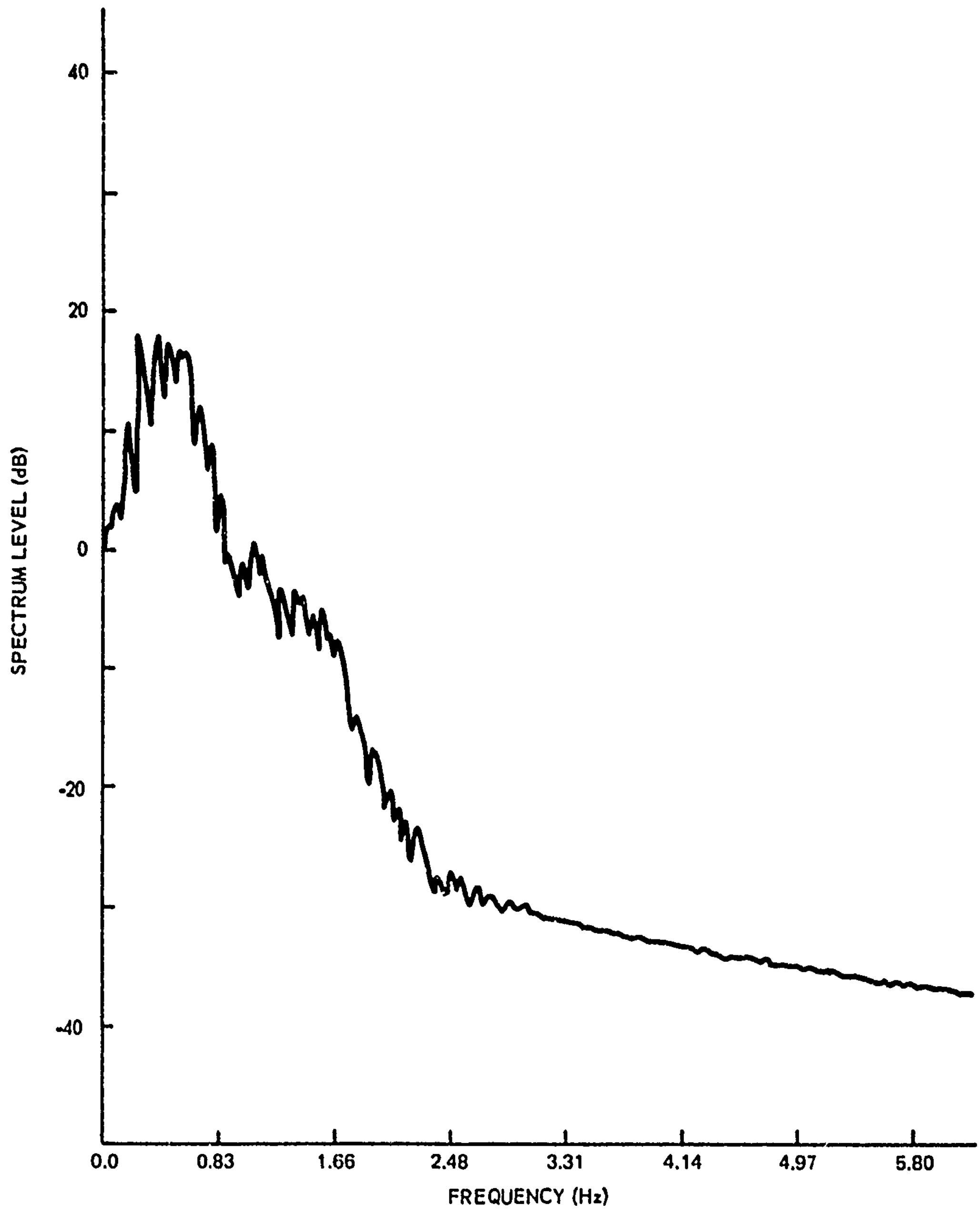

Figure 62. Cross-Spectral Levels of Surge and Heave

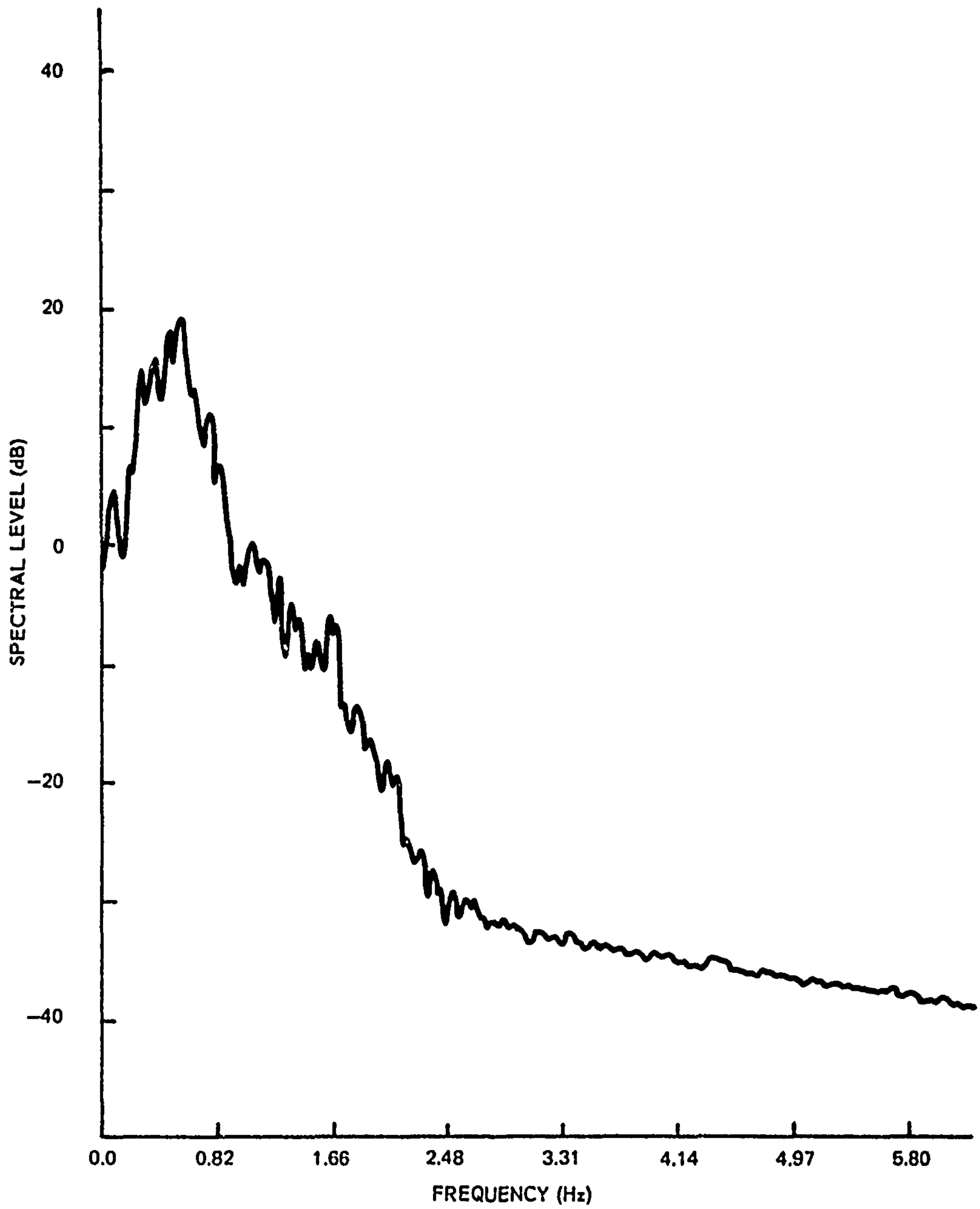

Figure 63. Cross-Spectral Levels of Sway and Heave

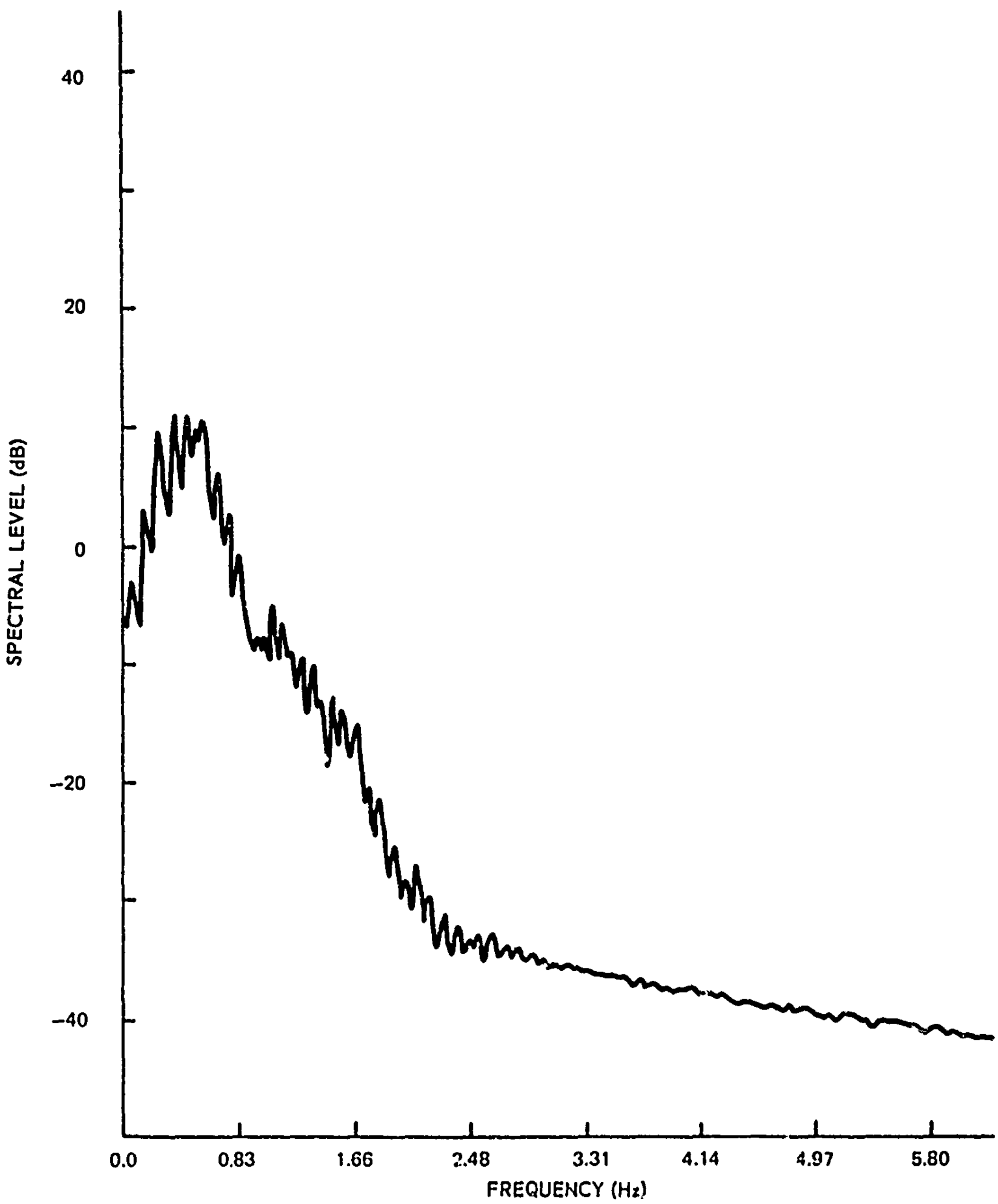

Figure 64. Cross-Spectral Levels of Pitch and Heave

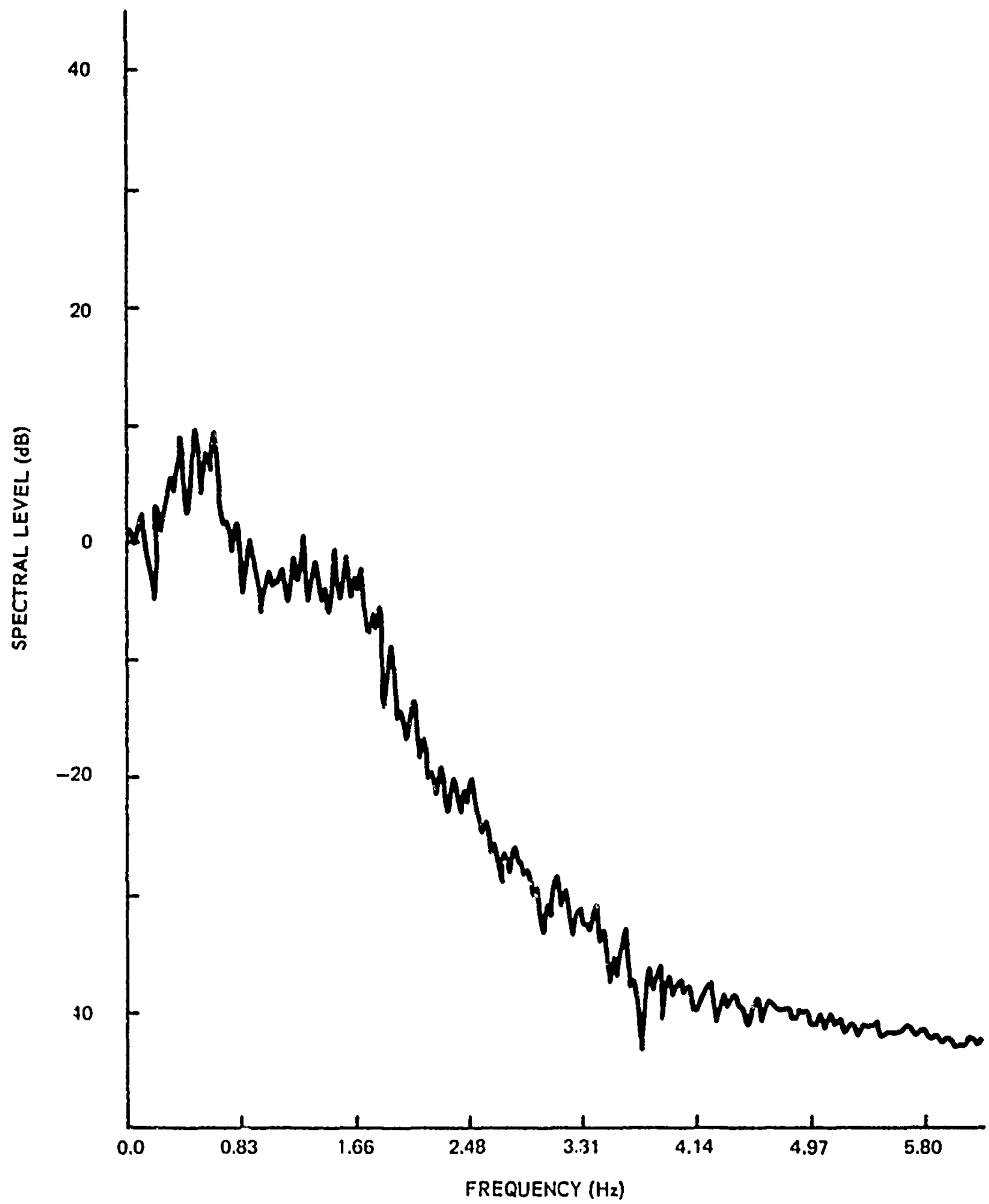

Figure 65. Cross-Spectral Levels of Roll and Heave

Wave spectra determined by Williams[77] for similar conditions in Block Island Sound indicate that swell appears in the wave spectrum as a horizontal line to the left of the wind wave peak and is about 5 dB down from the peak. Figure 56 was modified to include swell. The buoy motion power spectra were smoothed and the difference in decibels between them and the wave spectrum (including swell) were plotted as the square of the absolute value of the transfer function in decibels. Figures 66 through 70 show the transfer functions and indicate the existence of two modes. The relative magnitudes of the peaks indicate that the modes are a heave mode (low frequency) and a roll mode (high frequency). Observations made by the writer while servicing the buoy at sea indicate that the sway-surge mode has the lowest frequency, the heave mode has the next highest frequency, and the pitch-roll mode has the highest frequency.

These spectra indicate that the heave, surge, and sway motions of the buoy are primarily excited by the sea swell, whereas buoy pitch and roll are excited by the higher frequency wind waves.

Analysis of measured buoy motion data for the $3\frac{1}{2}$-ft spherical buoy and for the 8-ft torroidal buoy have yielded sets of empirical equations that can be used to predict mean buoy motions and amplitude distributions for various sea states. Buoy motion amplitude distributions appear to follow a Rayleigh distribution, which indicates that the dynamic system is linear or near-linear.

Spectra for the torroidal buoy indicate the existence of a heave mode and a pitch-roll mode within the range of wave frequencies. In general, both buoys are hard-coupled to the sea surface in heave. The torroidal buoy appears to respond in pitch-roll motions to a greater extent than does the spherical buoy.

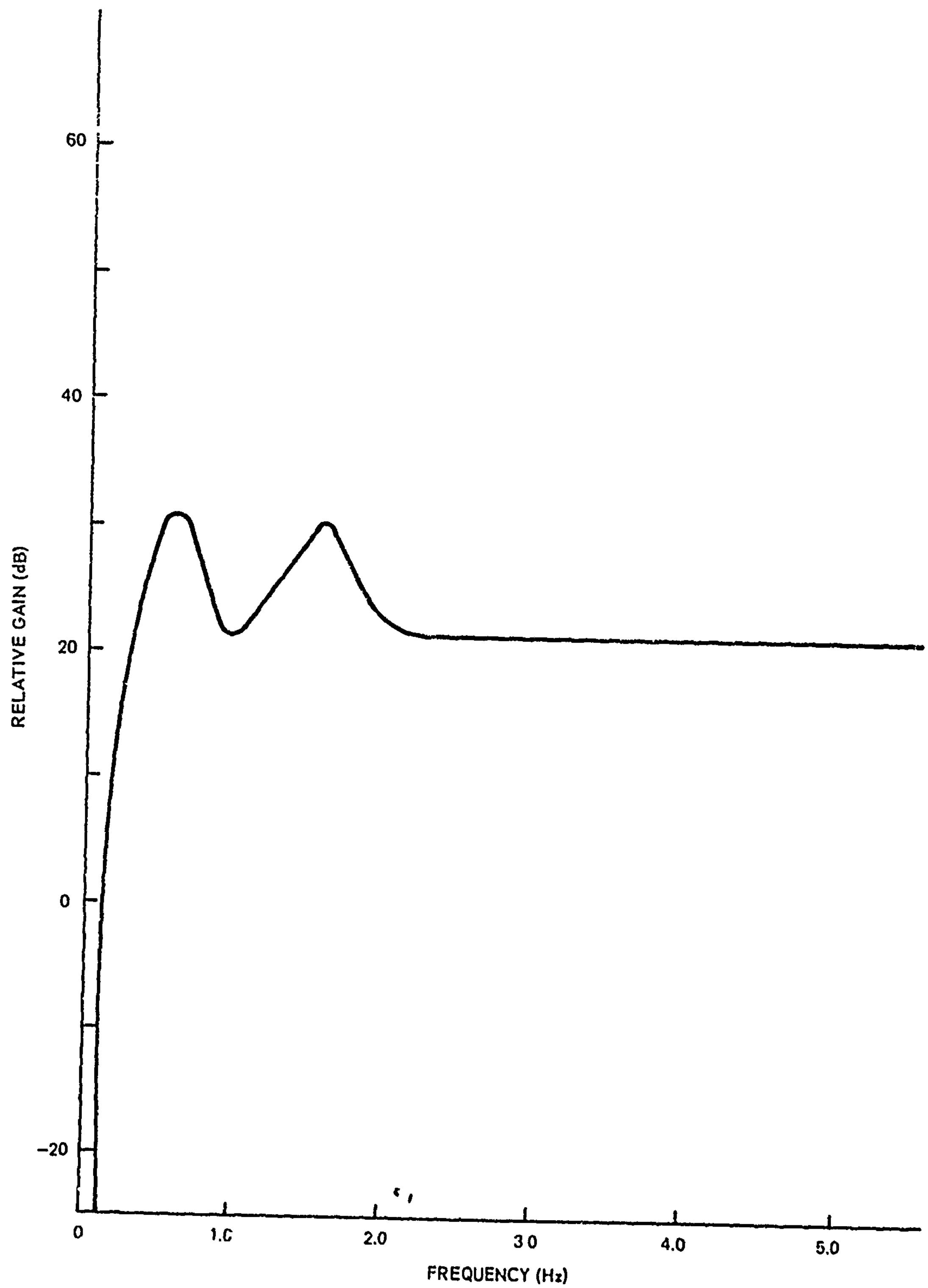

Figure 66. Gain Function for Heave and Wave Height

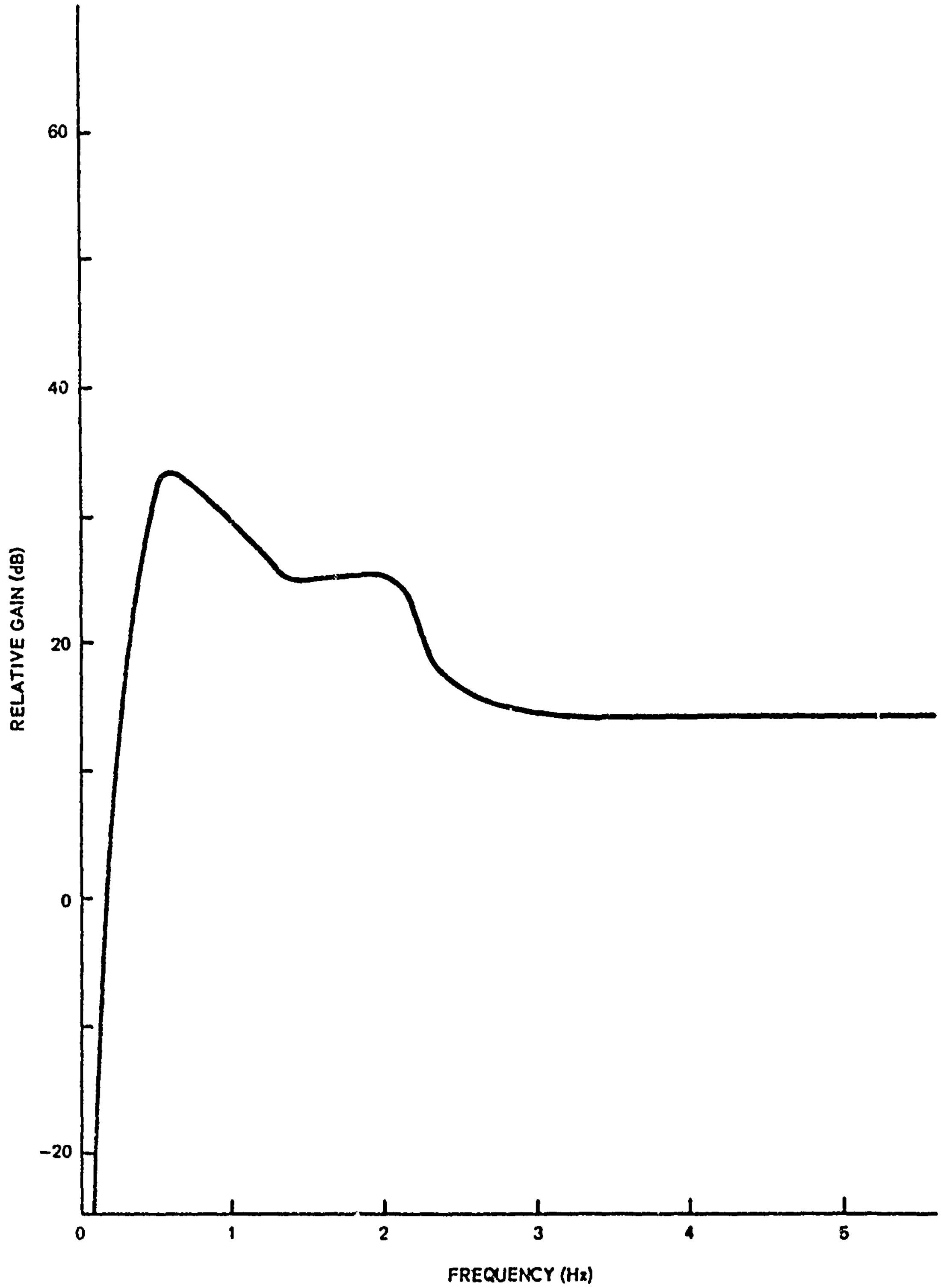

Figure 67. Gain Function for Sway and Wave Height

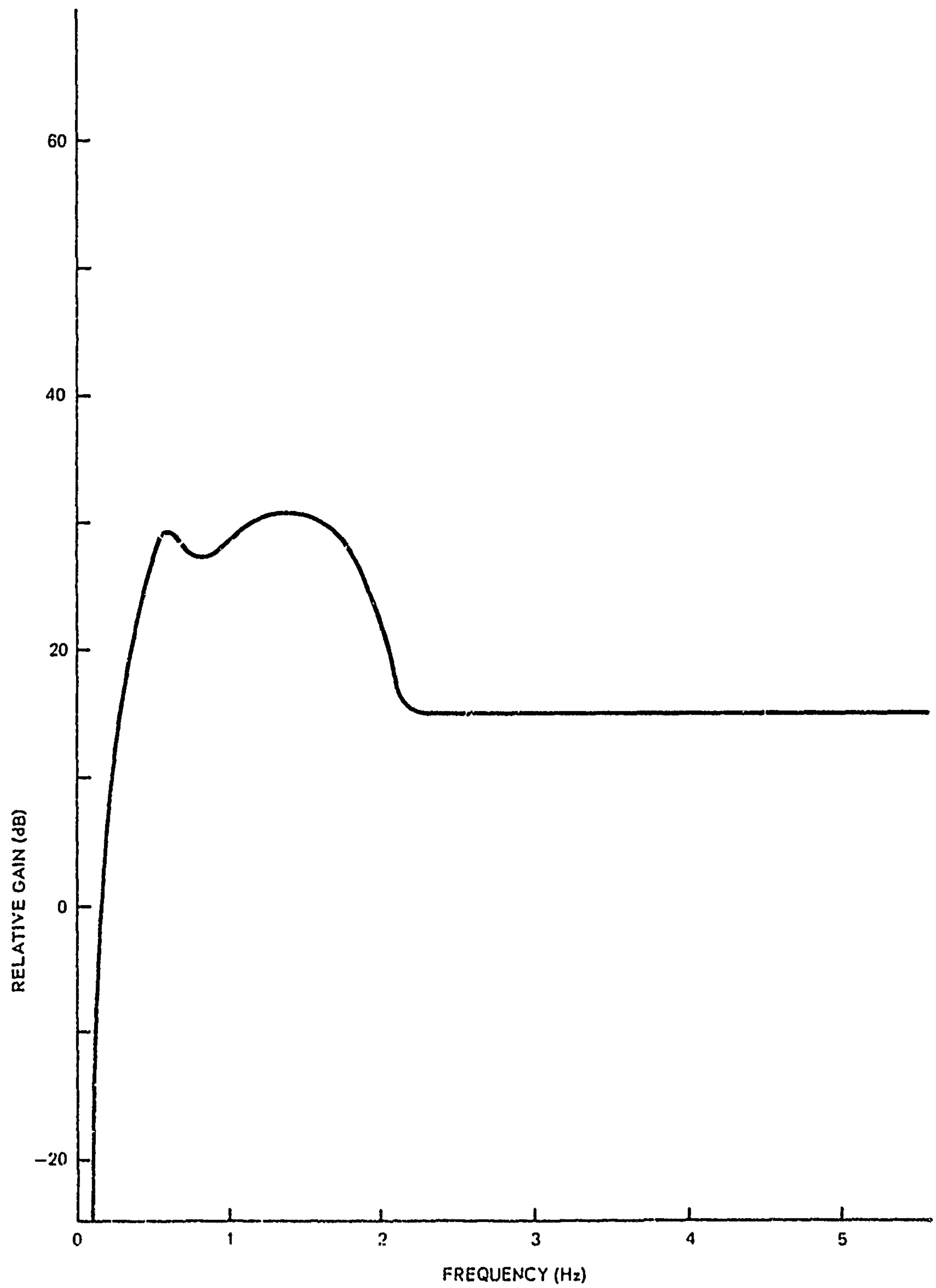

Figure 68. Gain Function for Surge and Wave Height

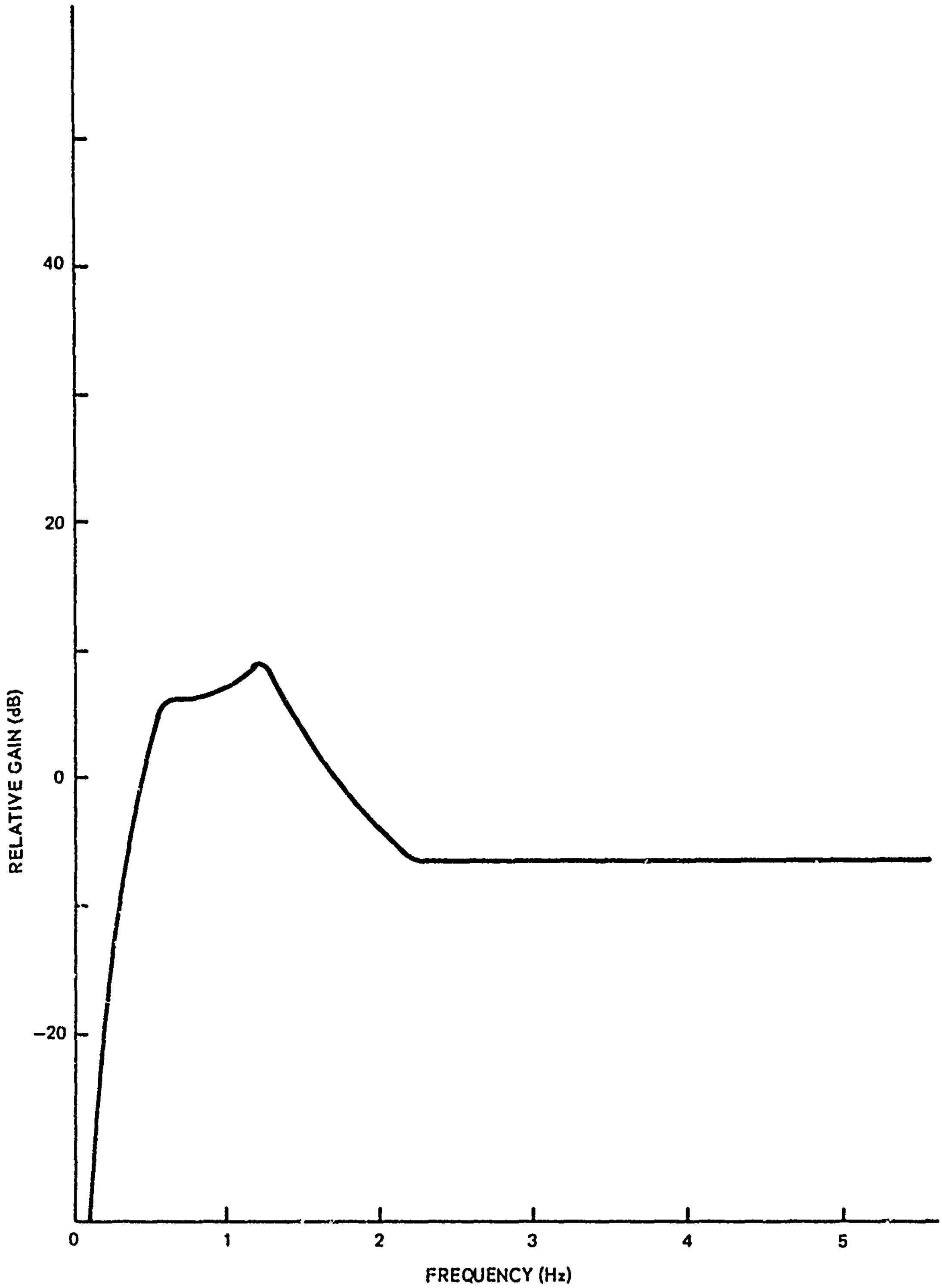

Figure 69. Gain Function for Pitch and Wave Height

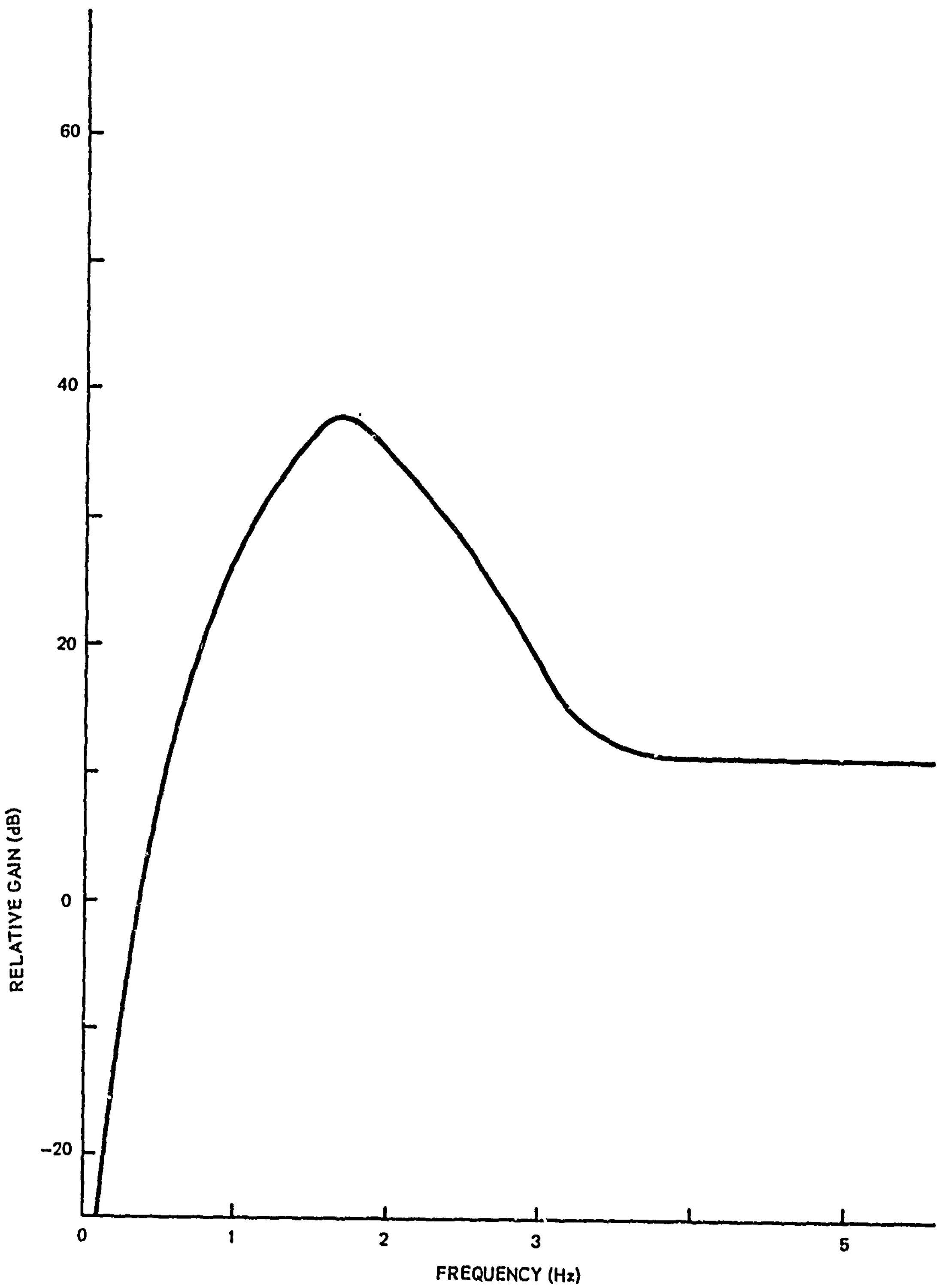

Figure 70. Gain Function for Roll and Wave Height

4.3 Simulation and Comparison of Buoy System Dynamics

4.3.1 Spherical Buoy at Station D

Steady-state configurations of the spherical buoy system, installed at Station D, are shown in figure 71 for various uniform currents. Very little of the 3/4-in. DiLock chain is picked up off the bottom even under the worst current conditions — 1 knot. Steady-state tensions never go over 100 lb, and the watch circle radius can vary from 38 ft at 0 knot to 62 ft at 1 knot. These configurations were computed on the GSA time-sharing computer using the steady-state buoy system configuration program shown in appendix B. The Savonius rotor current meter used in the spherical buoy system failed 3 days after emplantment, thus; cable angles can not be correlated with current strength for this buoy system. However, the computed configurations are used as initial conditions for the buoy system dynamics simulation when current strength and direction are computed from the Coast and Geodetic Survey current tables.[83]

The lumped-mass dynamic equations of motion for the cable and the equations of motion for the spherical buoy were programmed and solved numerically in the time domain using a fourth-order,Runge-Kutta numerical integration scheme. Five mooring line mass elements were used — three for the cable and two for the chain. The buoy was allowed six degrees of freedom (heave, surge, sway, yaw, pitch, and roll), and each mooring line mass element was allowed three degrees of freedom (x_i , y , and z). The program shown in appendix B can accept wind and current vectors coming from any

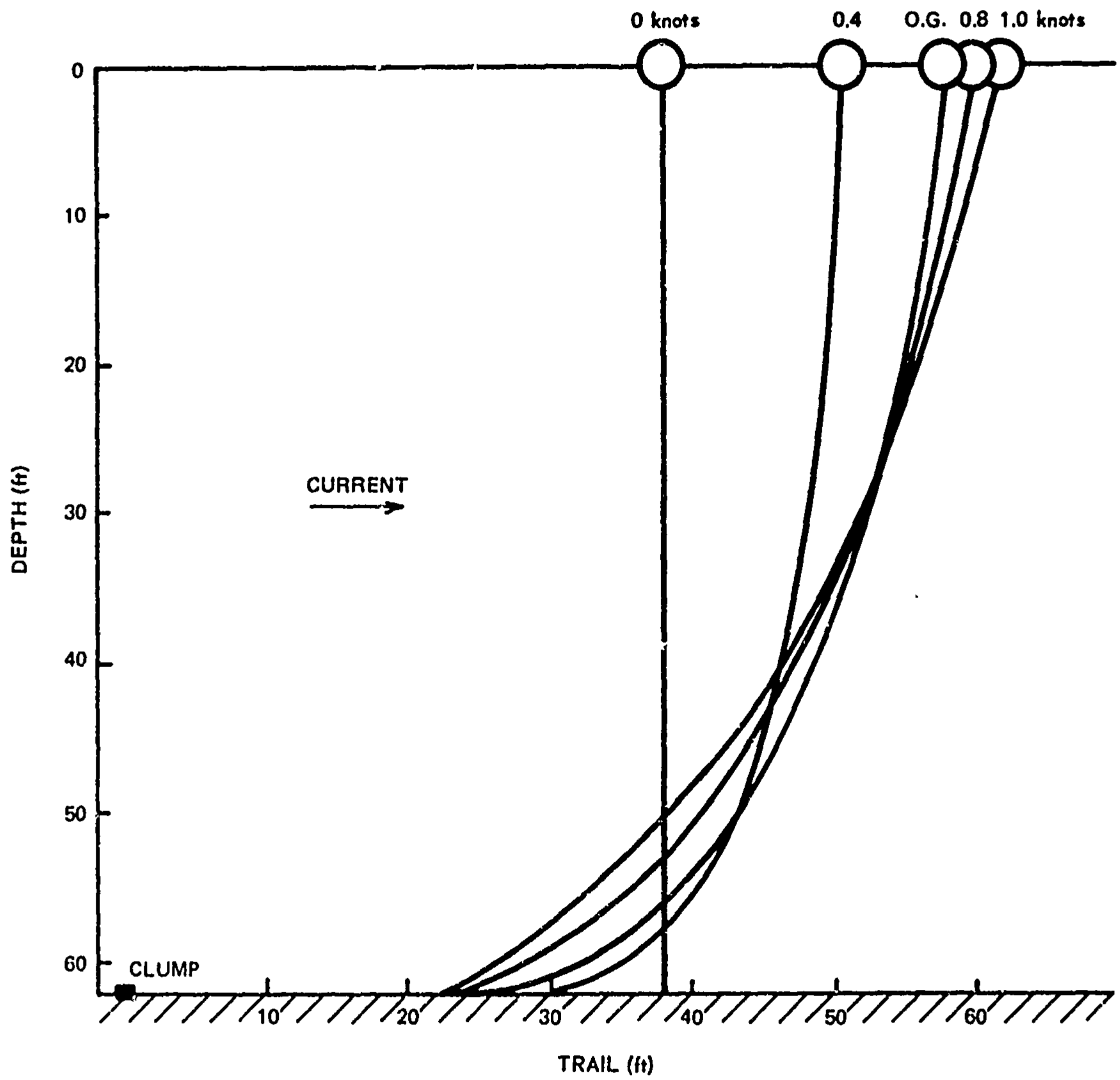

Figure 71. Computed Steady-State Configurations of the Spherical Buoy System

direction; however, the waves are assumed to be two-dimensional and are constrained to come in on the z axis of the inertial coordinate system. A complete listing of the input data needed to describe the spherical buoy system is shown in appendix D. Mean wave heights and periods were computed from reference 82 for various sea state conditions. The spherical buoy system dynamics model was excited with the ten-component random wave model based upon a two-parameter Bretschneider spectrum having the mean wave height and period for each sea state. The average wind strength and direction and the average current strength over the time period in which the statistical accelerometers were in operation were also used to force the model. The wave amplitudes for each component were allowed to build linearly over two component wave periods. This procedure minimized transient motions. The solution was allowed to proceed in time as transients decayed. Finally, buoy heave accelerations were sampled over a time period, and the mean heave acceleration amplitude was computed.

These computed amplitudes are shown in figure 72 and are compared with the amplitudes derived from the statistical accelerometer data. The computer model overestimates the heave acceleration amplitudes at the lower sea states and agrees quite well at the higher sea states. Since the observed sea states are based upon the Block Island resident engineer's visual observations, a plus or minus one sea state error band is shown in figure 72 for the observed data. It is concluded that the computer model provides a conservative estimate of buoy accelerations for design purposes.

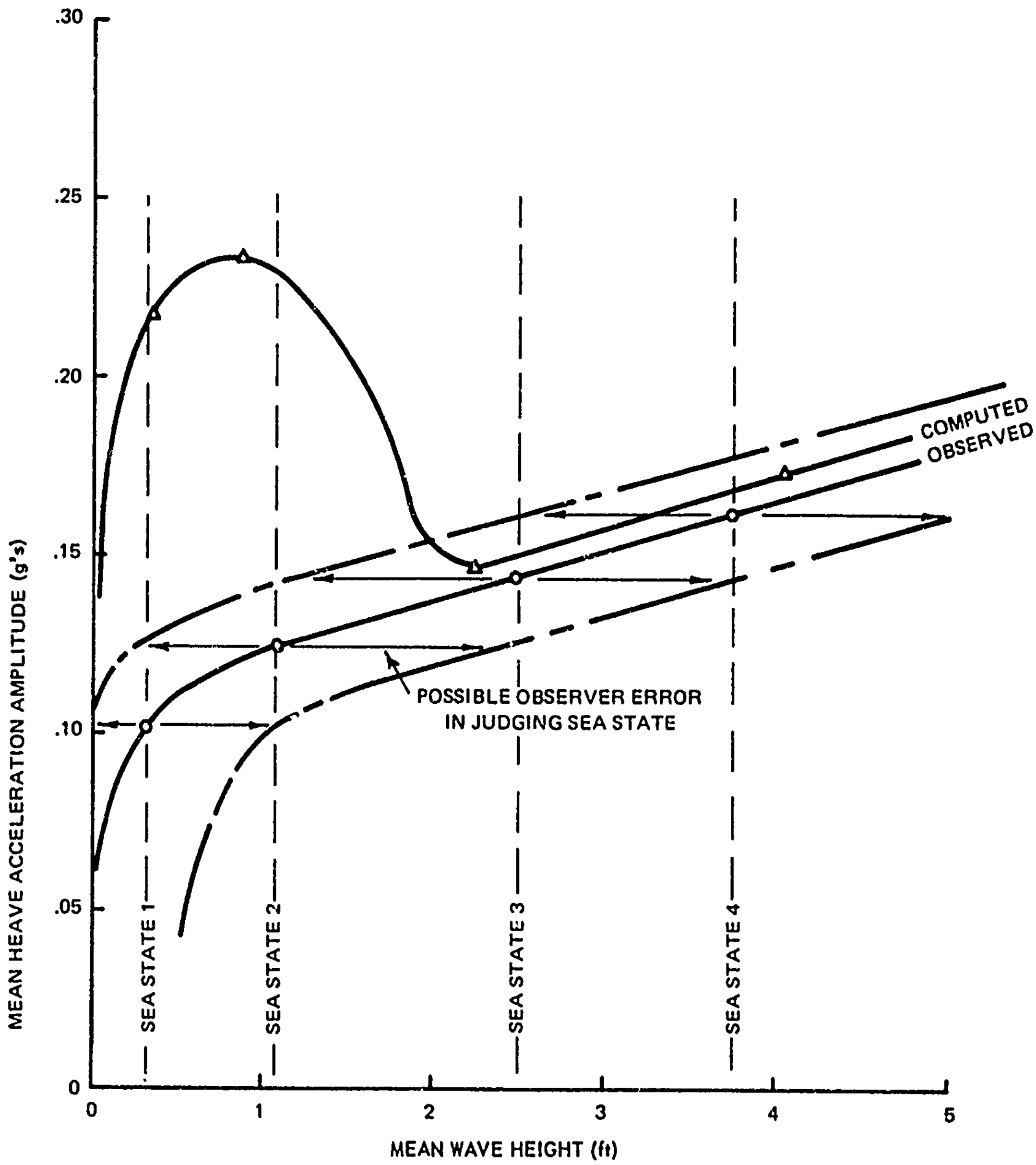

Figure 72. Observed and Simulated Heave Motions of the Spherical Buoy

On 16 March 1970. strip chart recordings of the buoy motion instrumentation were made. The computed Bretschneider wind wave spectrum for that location, date, and time based upon the observed wind speed, direction, and duration is shown in figure 73. This spectrum was used to determine component amplitudes for the random sea forcing function. The observed wind and the current as computed from the tidal current tables were also used to force the model on the UNIVAC 1108. Computed buoy heave, sway,and surge accelerations, pitch, roll, cable pitch, and cable roll were sampled in the same manner as the observed data and were analyzed on the GSA time-sharing computer.

The reduced spherical buoy motion parameters based upon computed motions and observed motions are shown on figures 74 and 75, respectively. Since the spherical buoy was not equipped with a yaw sensing device, the motions designated surge and sway and pitch and roll are not known relative to the z axis, along which the waves are traveling. Visual observations made from the beach while the data were being recorded indicated that the buoy was aligned in one direction with little or no yaw motion. A comparison of figures 34 and 75 indicates that the observed sway may really have been surge and that pitch and roll should be interchanged. Figure 75 reflects these changes.

A comparison of figures 74 and 75 indicates that the computer model predicts buoy heave accelerations with good engineering accuracy (-9.5 percent error for heave acceleration standard deviation), underestimates buoy sway accelerations (-71 percent error for sway acceleration standard deviation), and overestimates buoy pitch and roll motion (+54 percent error for pitch angle and

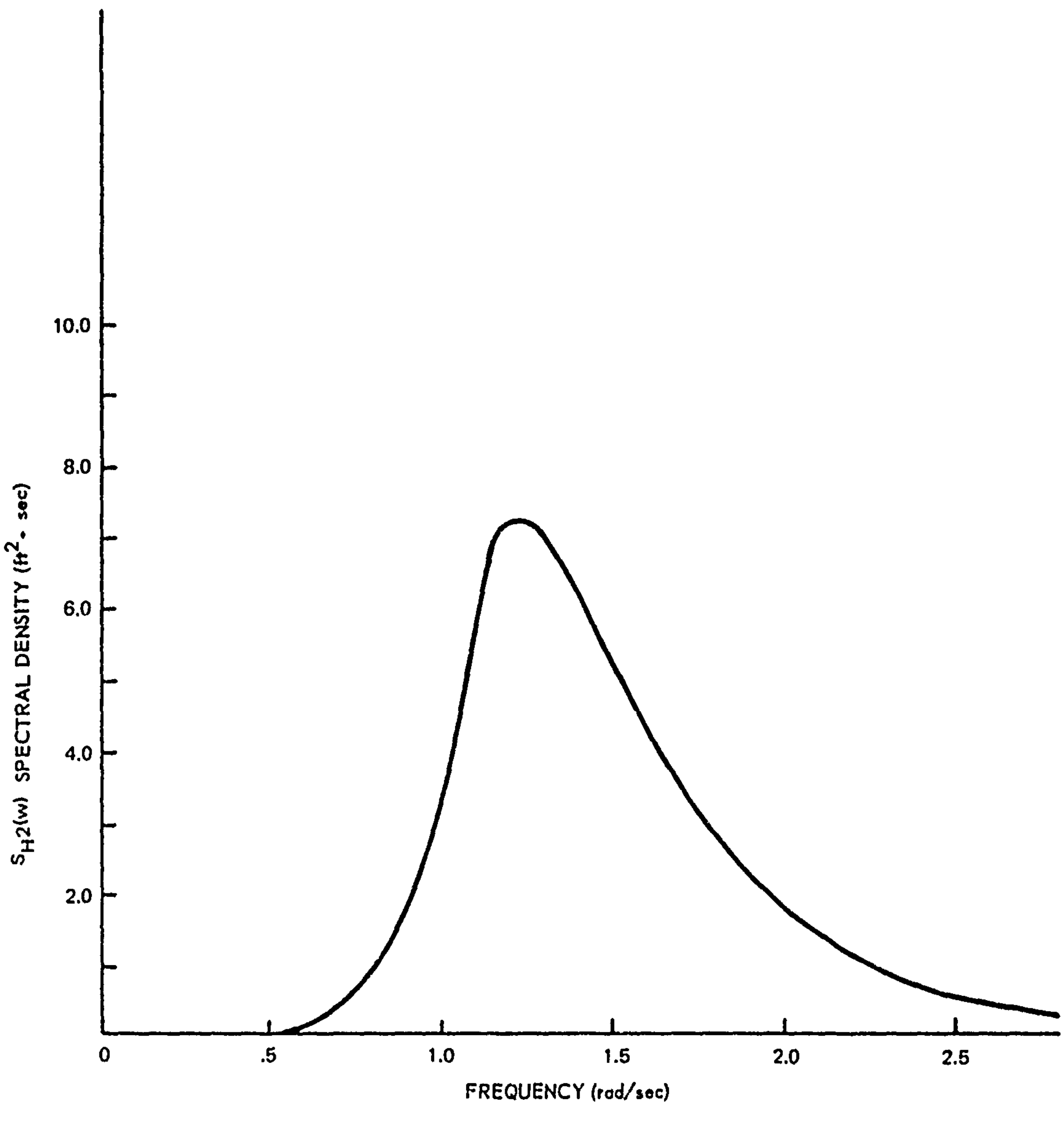

Figure 73. Bretschneider Spectrum — 1200 hr; 16 March 1970 Station D

VARIABLE	MEAN	VARIANCE	STANDARD DEVIATION
HEAVE ACCELERATION	0 g	0.0198 g^2	0.1408 g
SWAY ACCELERATION	0 g	0.0009 g^2	0.0288 g
SURGE ACCELERATION	0 g	0.0015 g^2	0.0390 g
PITCH	-1.37 deg	137.00 deg^2	11.70 deg
ROLL	-1.01 deg	315.07 deg^2	17.75 deg
CABLE PITCH	-19.37 deg	13.38 deg^2	3.66 deg
CABLE ROLL	38.29 deg	15.72 deg^2	3.97 deg

THE CORRELATION MATRIX

	HEAVE	SWAY	SURGE	PITCH	ROLL	CABLE PITCH	CABLE ROLL
HEAVE	1.0	0.4774	-0.2632	-0.1251	-0.0410	0.2660	-0.3602
SWAY		1.0	-0.6762	-0.6023	-0.5559	0.1582	-0.2172
SURGE			1.0	0.1980	0.3751	0.1502	0.1979
PITCH				1.0	0.7363	-0.3377	0.2582
ROLL					1.0	-0.1546	0.3268
CABLE PITCH						1.0	0.0388
CABLE ROLL							1.0

Figure 74. Simulated Spherical Buoy Motion Parameter Statistics

VARIABLE	MEAN	VARIANCE	STANDARD DEVIATION
HEAVE ACCELERATION	0 g	0.0242 g^2	0.1555 g
SWAY ACCELERATION	0 g	0.0098 g^2	0.0991 g
SURGE ACCELERATION	—	—	—
PITCH	14.3 deg	55.3 deg^2	7.58 deg
ROLL	1.1 deg	104.2 deg^2	10.20 deg
CABLE PITCH	-7.3 deg	16.2 deg^2	4.01 deg
CABLE ROLL	-27.1 deg	24.0 deg^2	4.90 deg

THE CORRELATION MATRIX

	HEAVE	SWAY	SURGE	PITCH	ROLL	CABLE PITCH	CABLE ROLL
HEAVE	1.0	0.4806	—	-0.0706	0.6050	0.0454	0.2435
SWAY		1.0	—	0.0054	-0.4199	0.1975	-0.1605
SURGE			1.0	—	—	—	—
PITCH				1.0	-0.1021	-0.3813	-0.2121
ROLL					1.0	-0.0946	0.0063
CABLE PITCH						1.0	-0.2282
CABLE ROLL							1.0

Figure 75. Observed Spherical Buoy Motion Parameter Statistics

+74 percent error for roll angle standard deviations). Mooring line pitch and roll angle standard deviations are underestimated by -33.6 percent and -19.0 percent, respectively.

The simple product-moment correlation matrix for the observed data indicates moderate coupling for heave-sway, heave-roll, sway-roll, and pitch-cable pitch. Because of the axial symmetry of the buoy, it is expected that heave-pitch and surge-pitch would also be coupled. The simulated buoy motion correlation matrix indicates coupling between heave-sway, sway-surge, sway-pitch, sway-roll, and pitch-roll. The modal coupling indicated by the two correlation matrices do not agree. This poor agreement is probably due to the rather short sample time used to compute the product moment correlations. An error estimate based upon an assumed bandpass white noise sea spectrum with a bandwidth of 1 Hz indicates normalized errors of about 22 percent in the standard deviations and about 48 percent in the product-moment correlations. The comparison of simulated buoy motions with observed buoy motions for this case indicates reasonable agreement for parameter standard deviations but poorer agreement for product moment correlations. In view of the limited amount of data and its relatively poor quality, this particular comparison will not be extended.

4.3.2 Torroidal Buoy at Station BRAVO

The buoy motion computer model with lumped-mass cable elements was modified and input values were changed in order to simulate motions of the torroidal buoy BRAVO. A subroutine to compute the buoyant forces and moments by polar integration around the torroid as a function of its draft and tilt angle was incorporated in the program (appendix E). A subroutine to compute simple statistical properties (mean, variance, and standard deviation) of the input wave height and output buoy motions (heave, surge, and sway accelerations and pitch and roll angles) was also incorporated in the program.

Winds were assumed to act from the southwest (the predominant wind direction during May and June), and an average ebb current of 0.7 knot was assumed (uniform in depth, setting to the east). Thus, the buoy system coordinate system has the z axis pointing southwest and the y axis pointing southeast (figure 76). The S-M-B method was used to compute the mean wave height and period for winds of 5, 10, 15, 20, and 25 knots for the southwest winds with an assumed duration of 4 hr. The computed mean wind wave heights and periods for station BRAVO are shown in figure 77. Resulting Bretschneider spectra for these conditions are shown in figure 78. These spectra were used to compute random wave component amplitudes and frequencies which,in turn, forced the buoy motion computer model.

Initial runs with a five-element cable model were found to be very time-consuming in machine time since the relatively low mass and high elastic modulus of the cable elements required that numerical integration step sizes on the order of 0.001 sec be used for numerical stability. A step size of 0.0005 sec was used for accuracy. The program was rewritten, and inputs were recomputed for a three-element mooring line model. Cable masses were concentrated at the current meter in the middle of the cable, and the lengths of heavy anchor chain were broken up to form the other two mooring line lumped masses. This

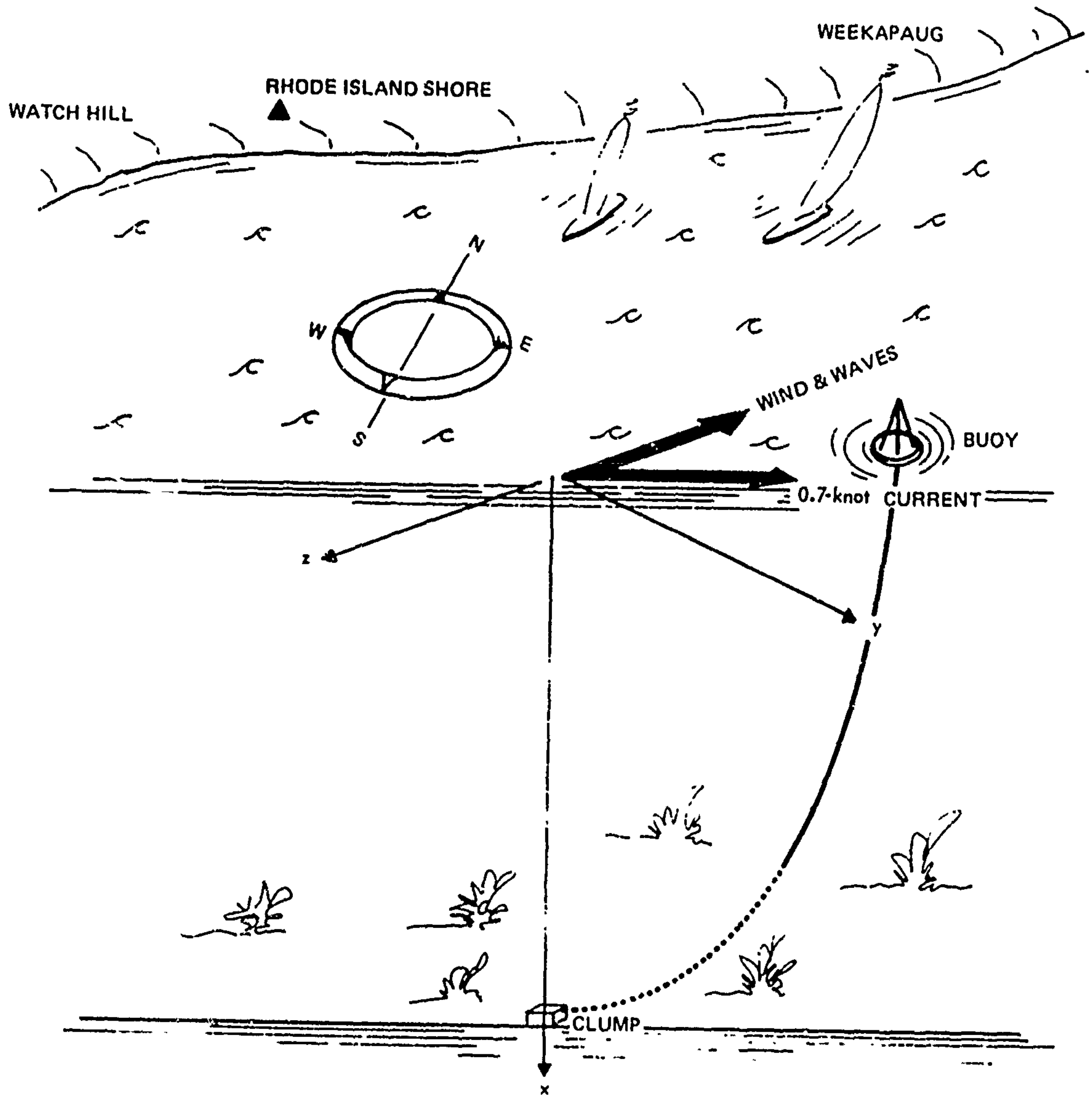

Figure 76. Torroidal Buoy BRAVO with Ebb Current and Southwest Winds

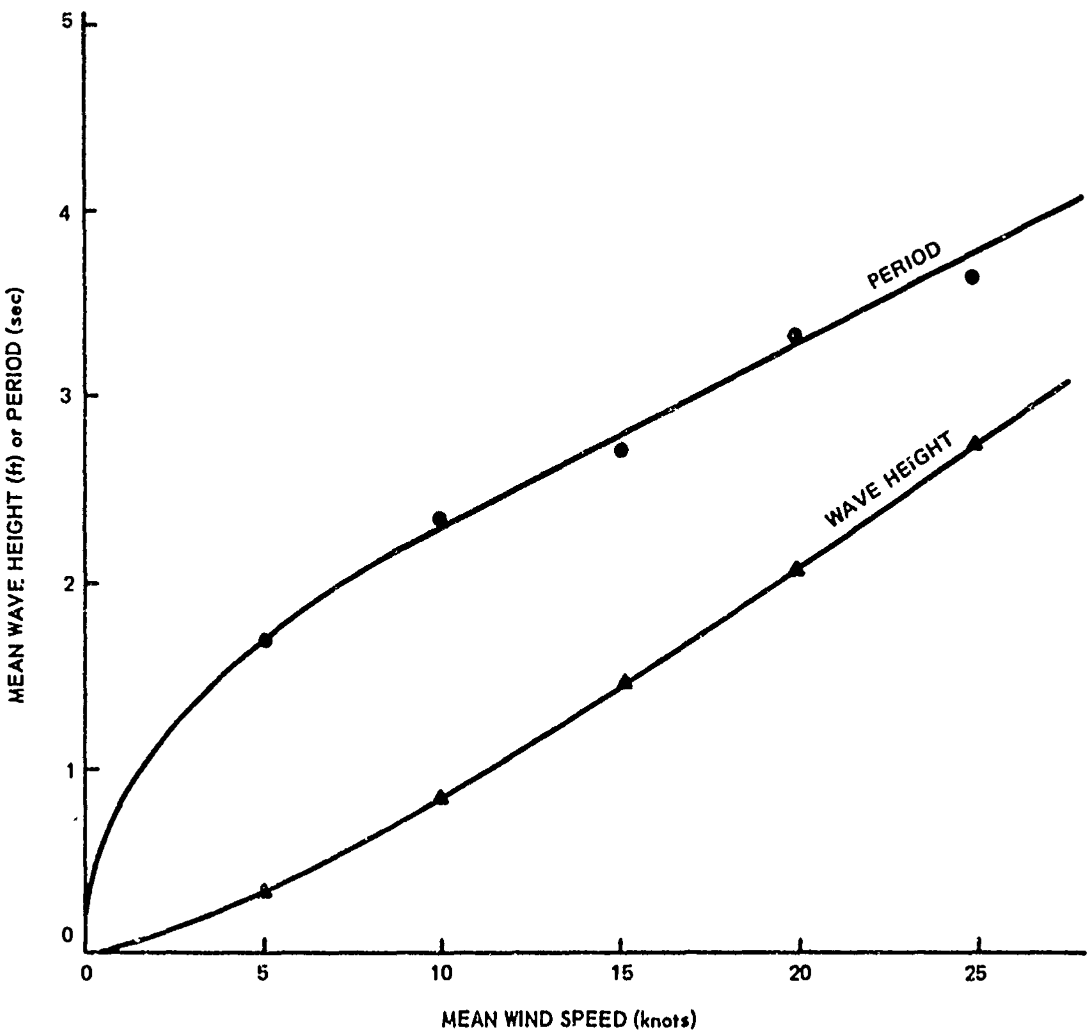

Figure 77. Computed Mean Wave Heights and Periods at Station BRAVO

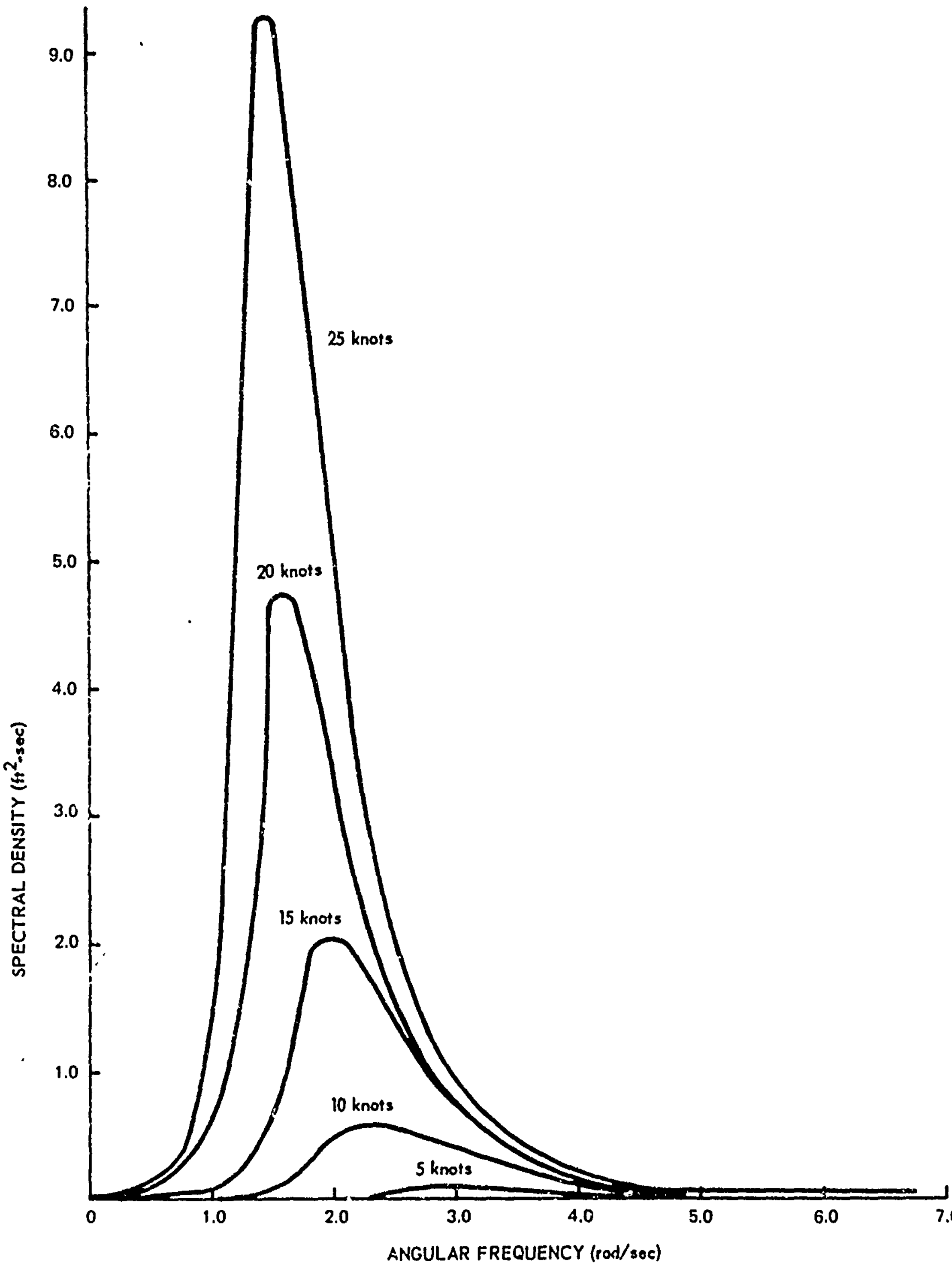

Figure 78. Computed Wind Wave Spectra

procedure greatly reduced the highest natural frequency of the system and the step size could be increased to 0.01 sec before numerical instability occurred. A step size of 0.005 sec, which allowed an order of magnitude increase in computational speed, was used. No significant difference was seen in computed buoy motions when using the three-lump or five-lump cable model.

The run procedure is as follows. First, the model is acted upon by the mean wind and current components (no waves) and allowed to converge to its steady-state configuration. Then, the random wave components are introduced and buoy motions sampled at every integration for 60 sec. Each run required about 20 min of computer time on the UNIVAC 1108. The ratio of computer time to solution time was 9.15:1.

The results of four runs with mean wind speeds of 5, 10, 15, and 20 knots are shown in figures 79, 80, and 81. The least-mean-squares plots of the observed data, as shown in figures 45 through 50 and as summarized in figure 51, are also shown in figures 79, 80, and 81. Since the yaw orientation of the buoy was not known during the at-sea measurements, the coefficients of the surge and sway empirical functions and of the pitch and roll empirical functions were averaged. Also, since the winds and waves in the computer model are acting along the z axis, only heave, surge, and pitch motions are compared with observed data. The average error indicated in the simulation over the range of wind speeds considered are as follows:

1. <u>On Mean Wind Speed</u>

Mean heave acceleration amplitude	+14.45 percent
Mean surge acceleration amplitude	-63.6 percent

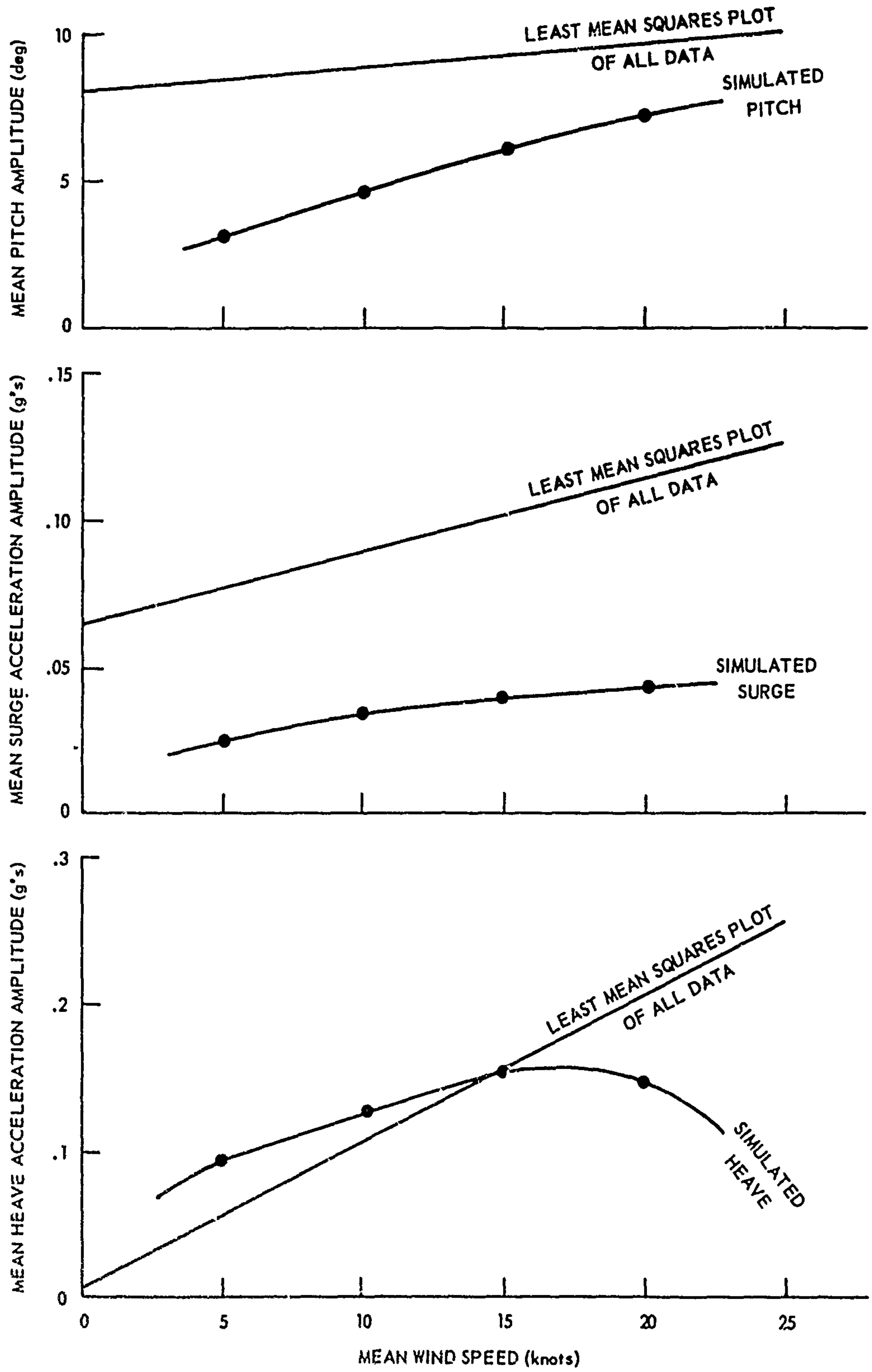

Figure 79. Simulated and Observed Buoy Motions versus Wind Speed

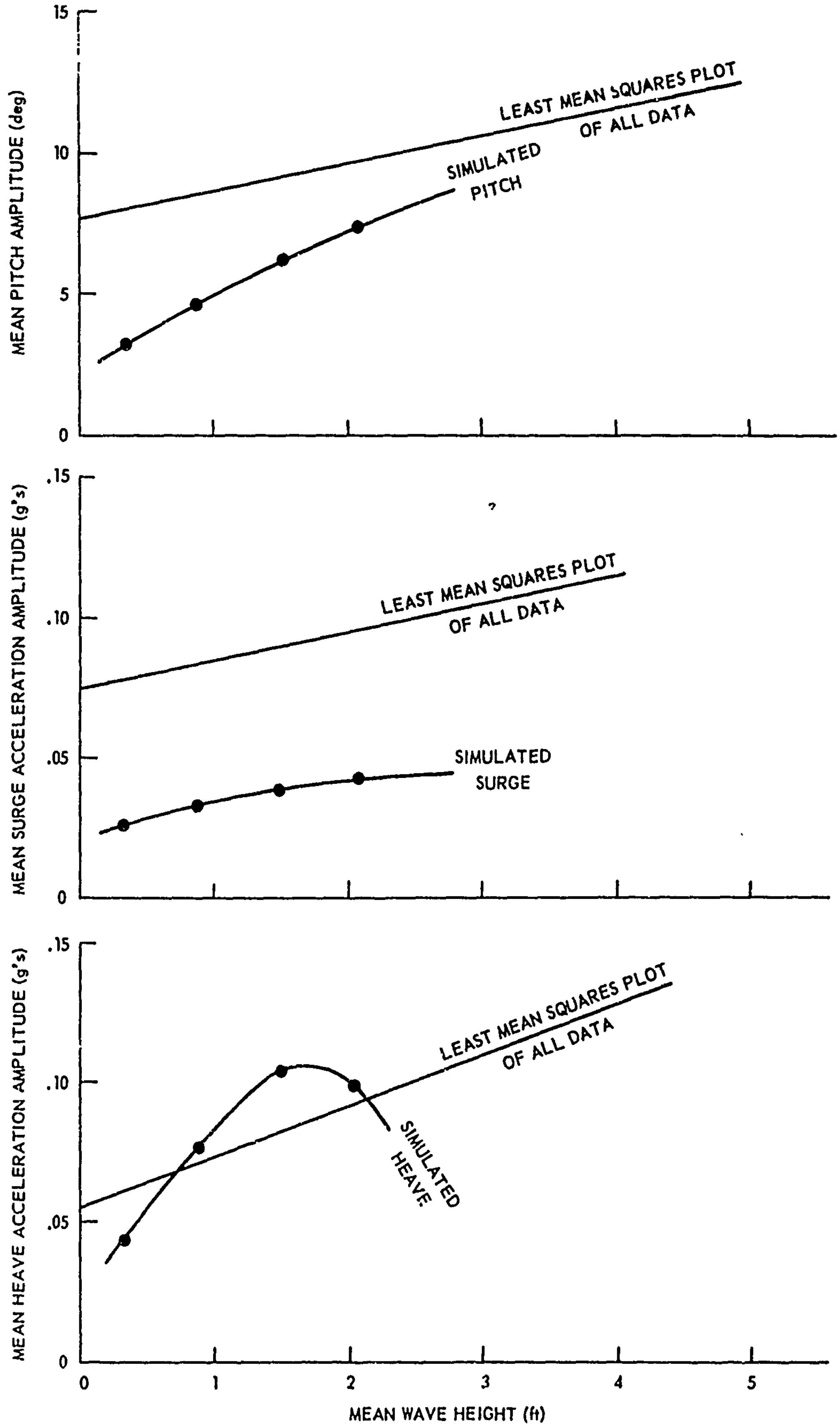

Figure 80. Simulated and Observed Buoy Motions versus Wave Height

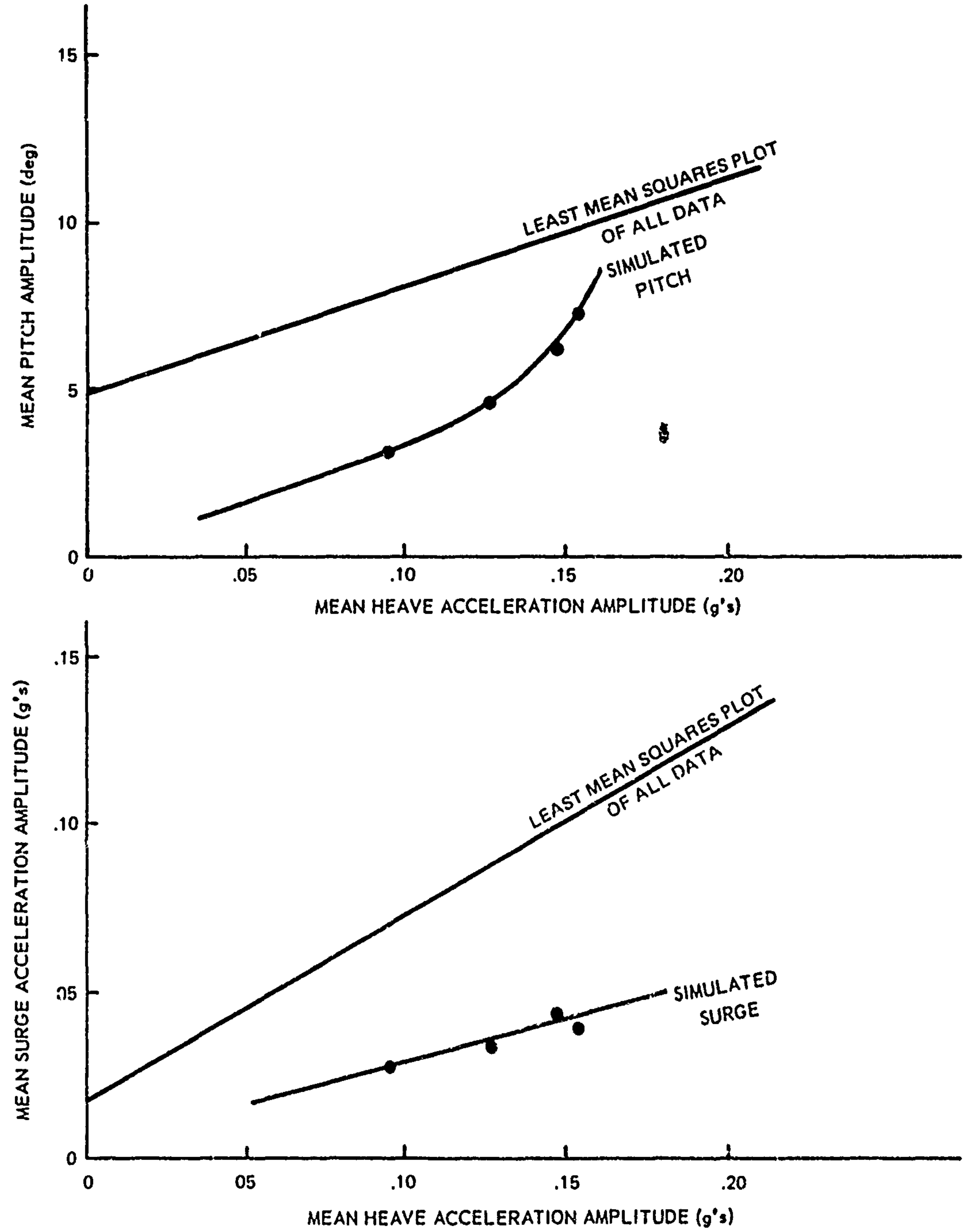

Figure 81. Simulated and Observed Surge and Pitch versus Heave

Mean pitch angle amplitude -42.4 percent

2. <u>On Mean Wave Height*</u>

Mean heave acceleration amplitude +2.22 percent

Mean surge acceleration amplitude -60.15 percent

Mean pitch angle amplitude -41.43 percent

3. <u>On Mean Heave Acceleration Amplitude</u>

Mean surge acceleration amplitude -60.4 percent

Mean pitch angle amplitude -42.3 percent.

Again, assuming bandpass-limited white noise spectra of about 1-Hz bandwidth, note that the error in the standard deviations of the simulated buoy motion is about ±13 percent. Also, known and estimated errors in the sensors and instrumentation (including possible observer error in reading the memoscope) indicate an overall error of ±20.13 percent in the observed data.

The differences in observed and computed mean heave acceleration amplitudes fall within these error bands and thus indicate that the computer model offers reasonable accuracy for this motion. However, even if these error bands are taken into account, the model is systematically underestimating surge and pitch motions. Since surge and sway motions are underestimated with both the spherical buoy and with the torroidal buoy, it is suspected that the transverse hydrodynamic mass and damping used in the model may be in error. Recent

*Note that wave heights for the observed data were based upon visual observations while wave heights for the simulated buoy motions were computed by the S-M-B method.

communications with E. Geller and R. Canada, who are affiliated with the National Data Buoy Project, have indicated that the results of their model buoy tests in towing basins do not agree with present theory because surge and sway hydrodynamic forces are less than predicted analytically. This communication confirms the above suspicion, but judgment is reserved until more test tank data are published.

The environmental conditions as measured during the data run of 11 June 1970 at 2030 EDST were used as input to the computer model, and buoy motions were computed. Power spectra for wave height, buoy heave accelerations, buoy sway acceleration, buoy surge acceleration, buoy pitch motions, and buoy roll motions were computed by a Fast Fourier Transform method.[84-86] A total of 1,024 samples, sampled at 0.06-sec intervals for each parameter, were transformed. The samples were smoothed by averaging over a 0.3-sec interval to prevent aliasing in the spectra. Eight ensemble averages were used, and they resulted in 64 statistical degrees of freedom and a standard error of 17.66 percent. The frequency resolution is 0.0163 Hz. Williams[87] states that a resolution on the order of 0.02 Hz is adequate to define ocean swell spectral peaks in his study of ocean wave spectra in Block Island Sound.

The input wave spectrum is shown in figure 82 along with the frequencies of the components that form the "random" wave forcing function. Figure 83 shows the computed spectrum level of the "random" wave model compared with the theoretical spectrum level. As expected, the "random" wave model exhibits characteristics of narrow-band white noise, which is reasonable since it is made up of a finite number of sine wave components close to one another in

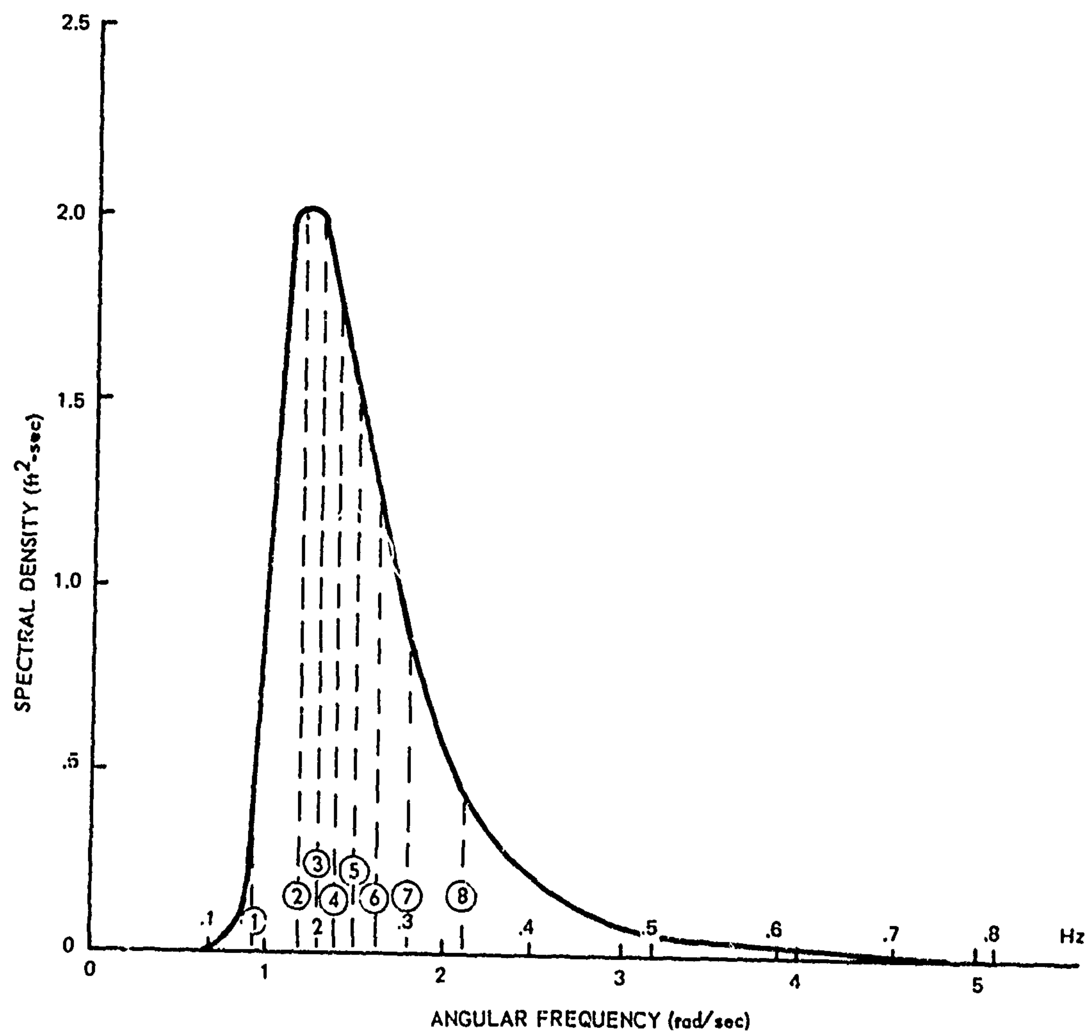

Figure 82. Wave Height Spectrum — 2030 hr, 11 June 1970

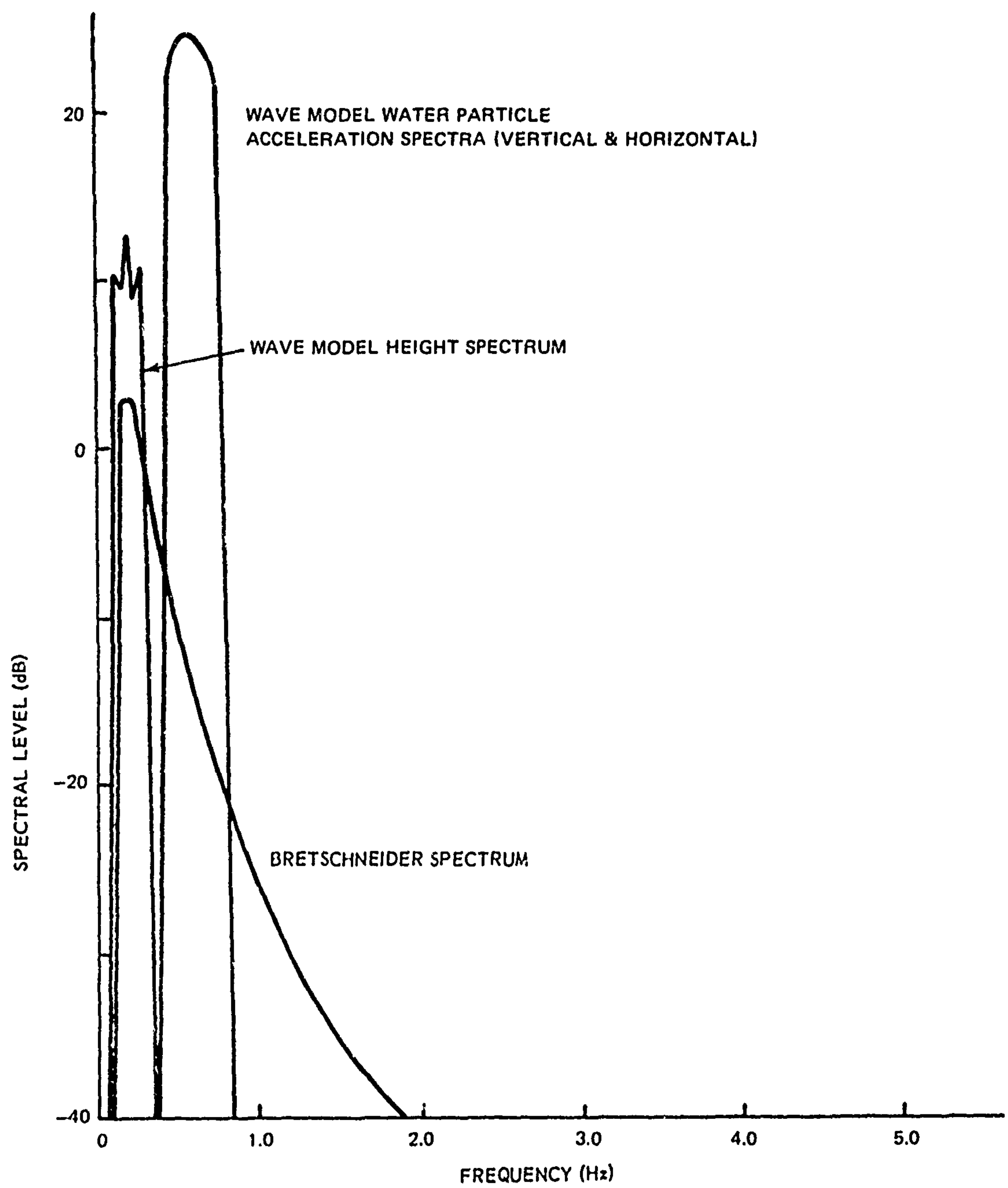

Figure 83. Simulated Wave Height Spectral Levels

the frequency domain.

The standard deviations for the input wave height and the output buoy motions are as follows:

Wave height	0.4807 ft
Heave acceleration	1.9321 ft/sec^2
Sway acceleration	0.4217 ft/sec^2
Surge acceleration	0.4974 ft/sec^2
Pitch angle	2.98 deg
Roll angle	4.437 deg.

Output spectral levels are shown in figures 84 through 88. In general, the spectra exhibit more deterministic properties than the buoy motion spectra from the at-sea data. More smoothing was done on the at-sea spectra than on the simulated spectra, but the at-sea spectra do not appear to have the narrow-band characteristics of the simulated spectra, especially in heave, surge, and pitch. This indicates that the model may be inadequately damped. The natural frequency of the buoy in heave when at middraft is computed to be 0.36 Hz. The heave, surge, and pitch spectra exhibit peaks at about this frequency. Since surge and pitch are decoupled from heave hydrodynamically, the coupling must be effected through the cable tensions acting on the buoy.

The second peak in the heave spectrum is located at about the same frequency as the peak of the water particle acceleration spectra. The forcing function component due to the heave hydrodynamic inertia force caused by water particle acceleration is driving the buoy in this frequency range. The surge spectrum also indicates that this forcing mechanism is active in that mode.

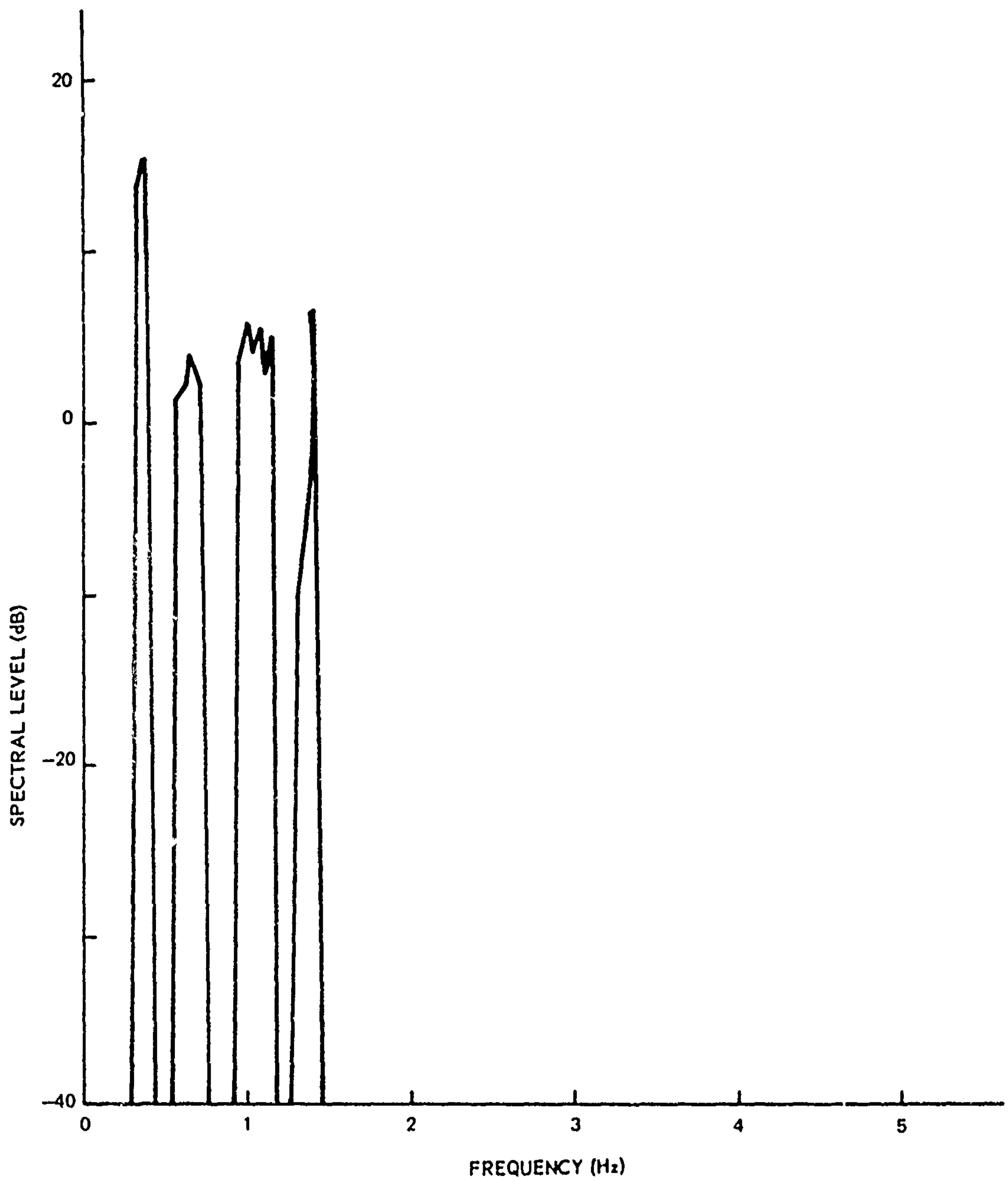

Figure 84. Simulated Heave Spectral Levels

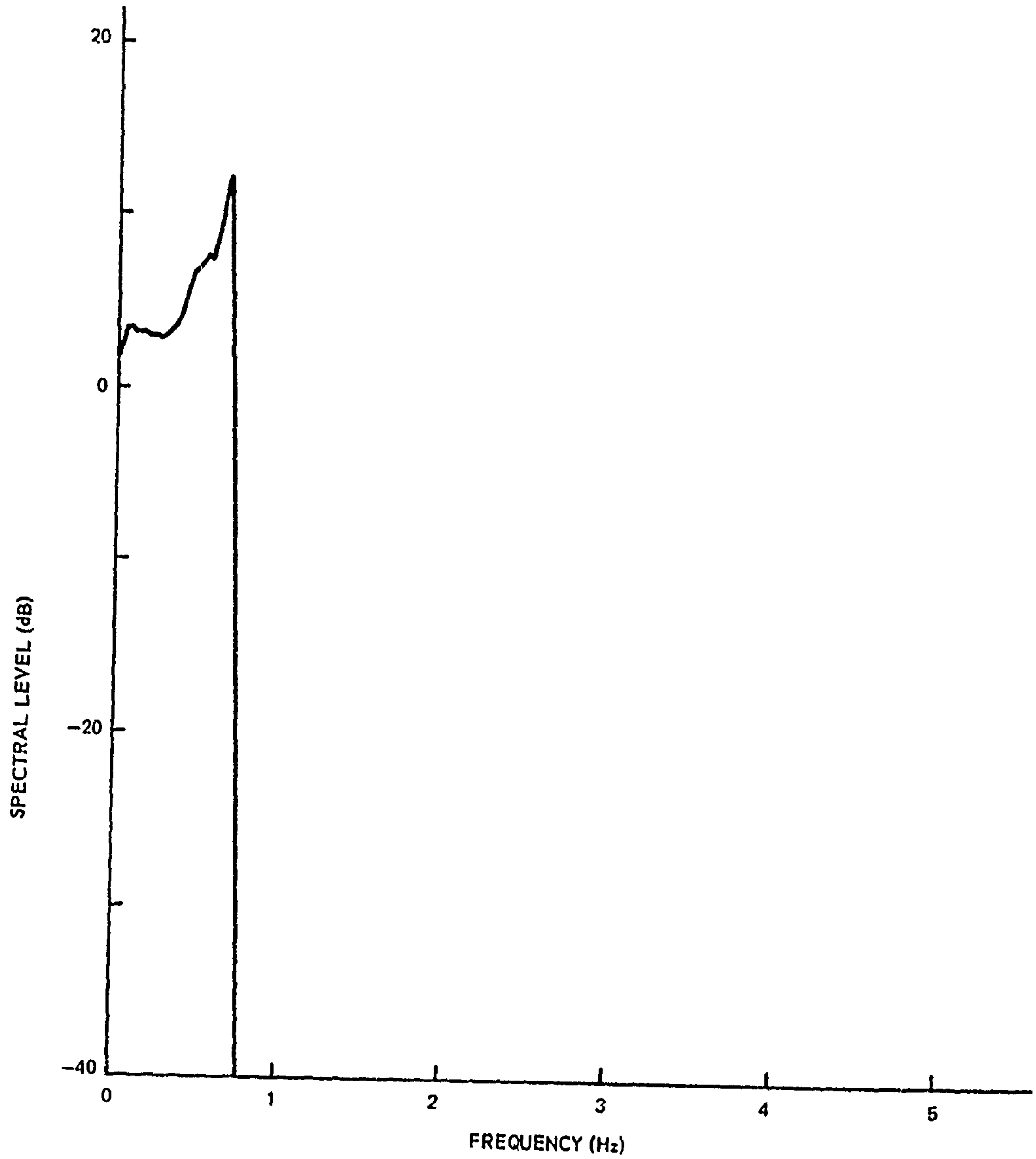

Figure 35. Simulated Sway Spectral Levels

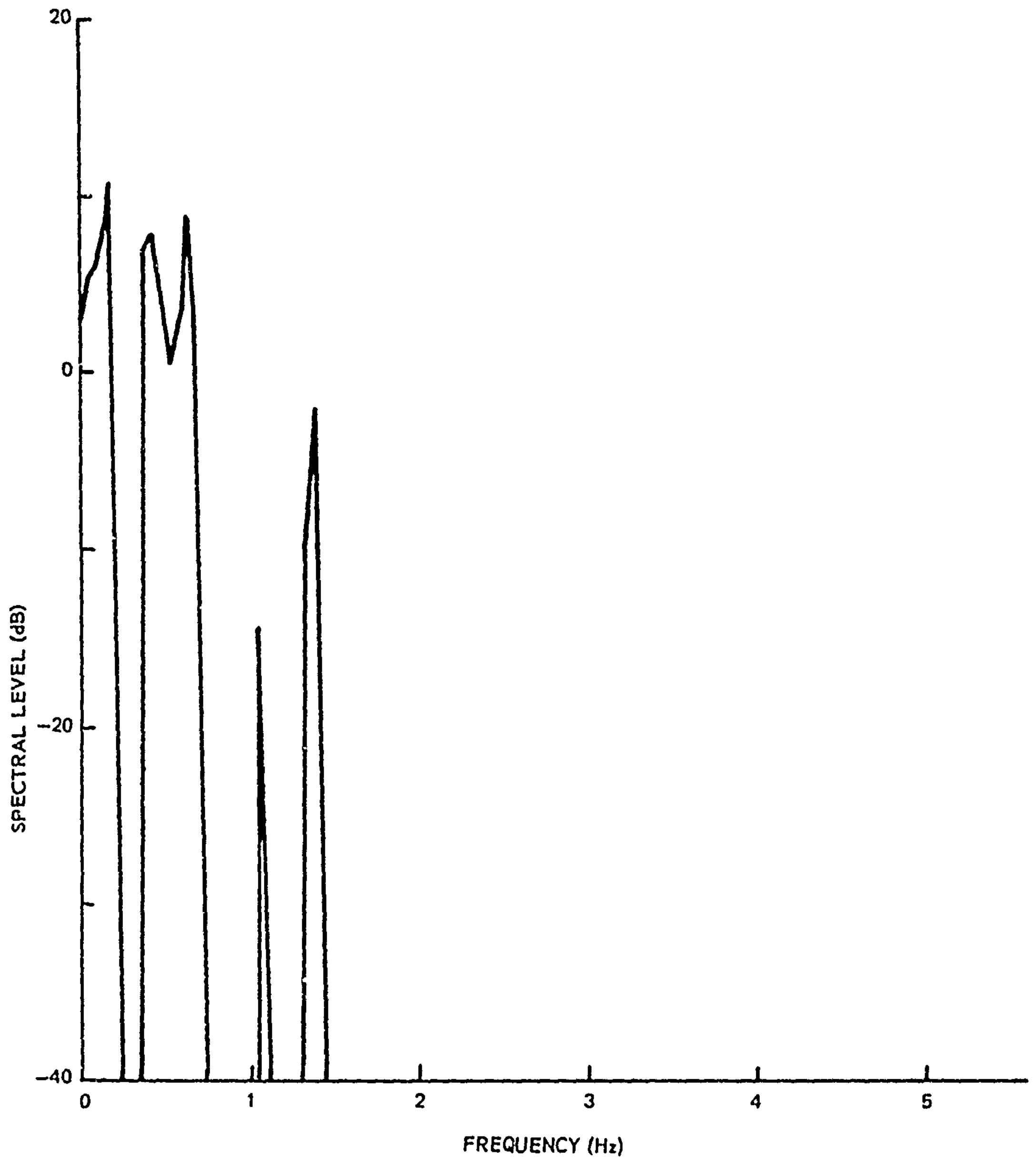

Figure 86. Simulated Surge Spectral Levels

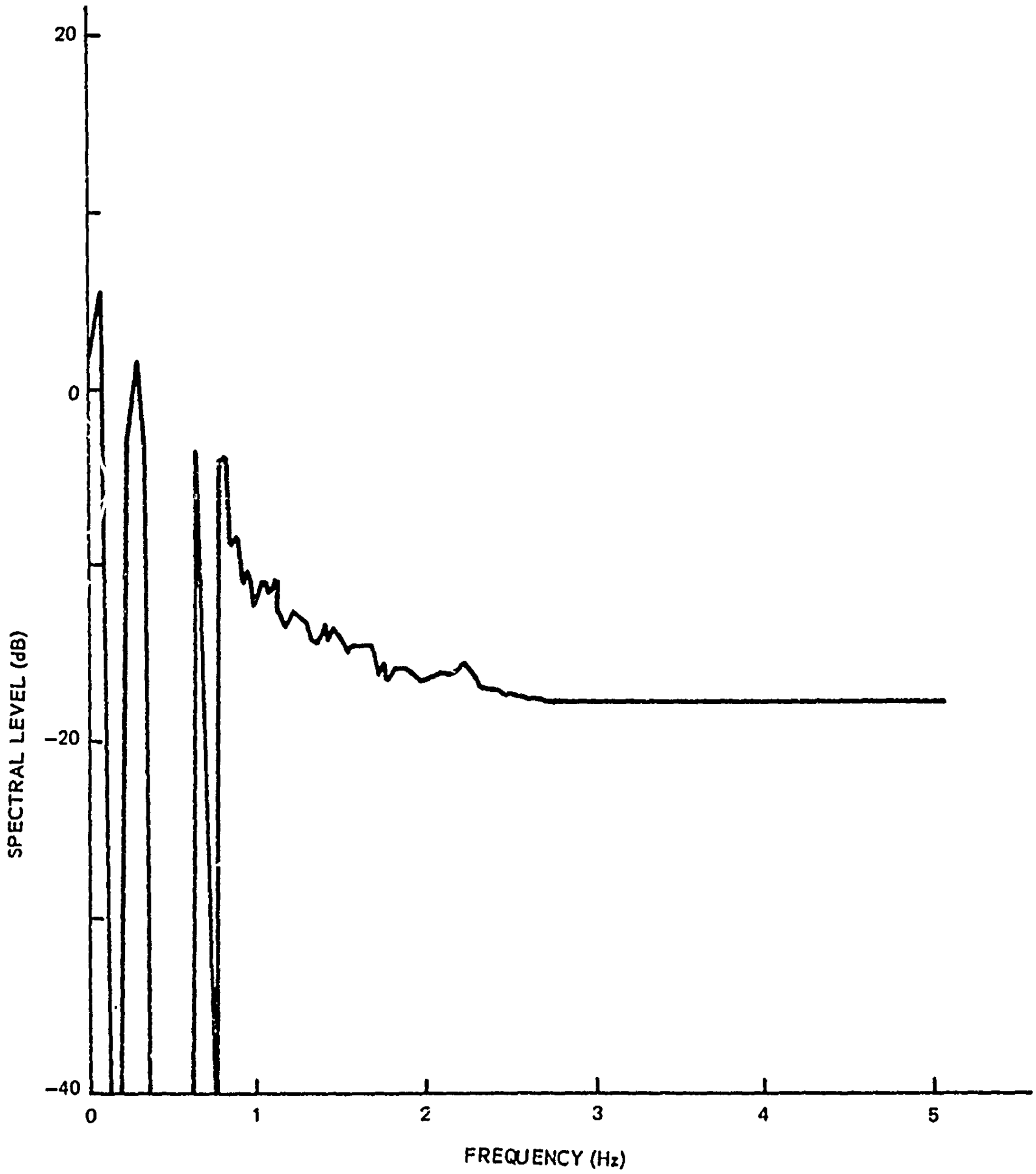

Figure 87. Simulated Pitch Spectral Levels

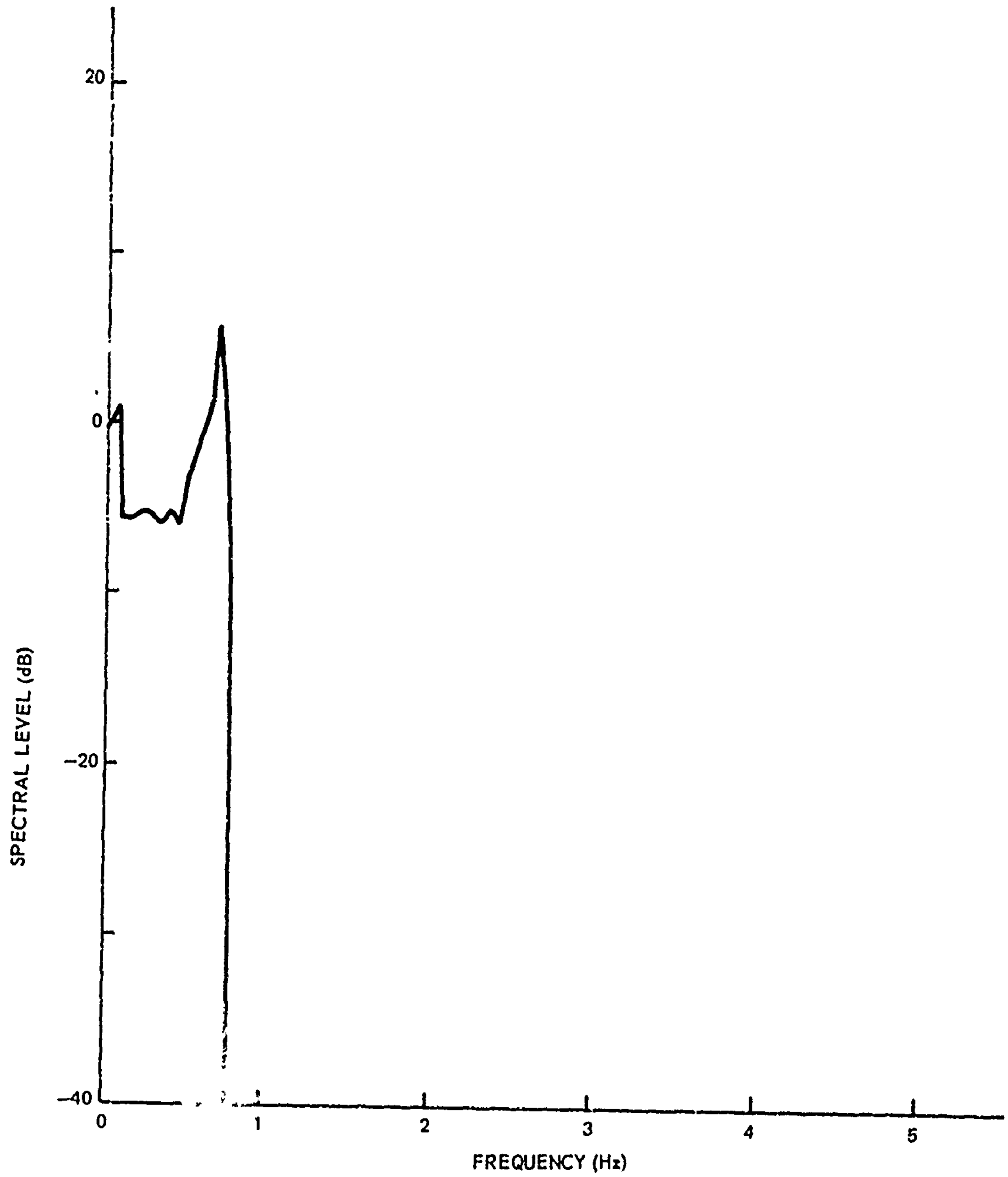

Figure 88. Simulated Roll Spectral Levels

Both pitch and roll spectra show peaks at this frequency. Pitch and roll motions have computed natural frequencies at about 0.7 Hz and would tend to respond to this forcing mechanism through coupling from surge and sway motions. Since the water particle motions are constrained to the x - z plane, one would not expect a response out of plane. However, the current vector has an out-of-plane component; thus, the mooring line tension force will have an out-of-plane component. Heave and surge motions will couple into sway and roll motions because of the mooring line tension. This coupling also illustrates another unusual feature of this dynamic system in that the response of the system is strongly dependent on the mean values of the system element spatial locations — a strong argument against linearized, decoupled models of buoy systems.

Both heave and surge show peaks at higher frequencies (1.05 and 1.4 Hz). These peaks are probably due to natural frequencies for the lumped-mass cable model. Sway and roll spectra have nearly the same shape and thus indicate a strong coupling in these modes. Surge and sway (also, pitch and roll through coupling) indicate some response at very low frequencies. This is due to the lowest natural frequency of the buoy system in a horizontal mode. If the analogy is made with a pendulum having a length order of magnitude with the water depth, the natural frequency of this motion would be quite low.

The heave spectrum computed from the experimental data (figure 57) indicates a peak at 0.4 Hz, which agrees well with the peak in the simulated heave spectrum due to the buoys natural frequency in heave. Surge, sway, pitch, and roll spectra all have spikes at 0.6 Hz. This is in agreement with the peaks in the simulated sway, surge, pitch, and roll spectra. All the spectra, especially in roll, indicate energy at frequencies out to 2 Hz. This energy may be due to vibration in the mooring line coupling into the buoy.

This comparison of simulated buoy motions with observed buoy motions for the torroid buoy at station BRAVO on 11 June 1970 indicates that the computer model is distributing energy in its response in about the same way as the actual buoy system. However, the model is apparently underdamped and is filtering out some energy between natural frequencies. Again, more test tank data are needed for buoy hulls to determine their hydrodynamic characteristics.

The simulations of buoy system dynamics for the spherical and torroidal buoys moored in Block Island Sound have used the lumped-mass model of cable dynamics. In the course of this research, it was found that if mean tensions in the cable are very low or if a number of force discontinuities are present along the cable (both conditions common to shallow water moorings), the finite-difference method is usually not suitable. With very low tensions, the cable equations can go ultrahyperbolic, which could cause the numerical method to break down. When many force discontinuities are in the line, a large number of nodes are needed in the cable segments between the discontinuities in addition to equation of motion for each discontinuity. The resulting computational time becomes prohibitive.

4.3.3 WHOI Mooring No. 238

In order to validate the buoy dynamics simulatation using the finite-difference cable model, mooring line tension data taken with WHOI mooring No. 238 (reference 37) is compared with simulated tension data for the same buoy system. WHOI mooring No. 238 is essentially the same as WHOI mooring No. 279 (figure 27) and was moored at the same location. Tensions were measured just below the torroidal surface buoy and were telemetered ashore. Computed inputs for the simulation of WHOI mooring No. 279 are shown in appendix D, and the buoy system dynamics program incorporating the finite-difference cable model is shown in appendix B. Since the WHOI data are shown against wind speed, the primary input is wind speed. The fetch was assumed to be 100 miles for this location in the North Atlantic, and wind durations were taken to be 24 hr. The Webster current profile, with a surface current of 1.5 ft/sec, was assumed to act in the direction of the wind for all cases.

Strains and cable angles at each node must be read in as initial conditions. The steady-state buoy system configuration program was used to compute these parameters for each wind speed and the given current profile. The initial cable angles are shown in figures 89 and 90. The standard deviation for the cable tension just below the buoy was computed for each run. Millard[37] presents a "scattergram" of "dynamic tension amplitude" versus 2-hr mean wind speed. Tensions were recorded on a Rustrak recorder, which has a very slow chart speed — on the order of centimeters per day. Thus, this "amplitude" was read by measuring the breadth of a very thick line. This actually represents the tension difference between the highest and lowest tension that occurred in a 2-hr period. It is assumed that these "amplitudes" correspond to the highest 1/10th wave heights found in wind-wave height distributions. The WHOI data of "dynamic tension amplitude" versus wind speed is shown in figure 91.

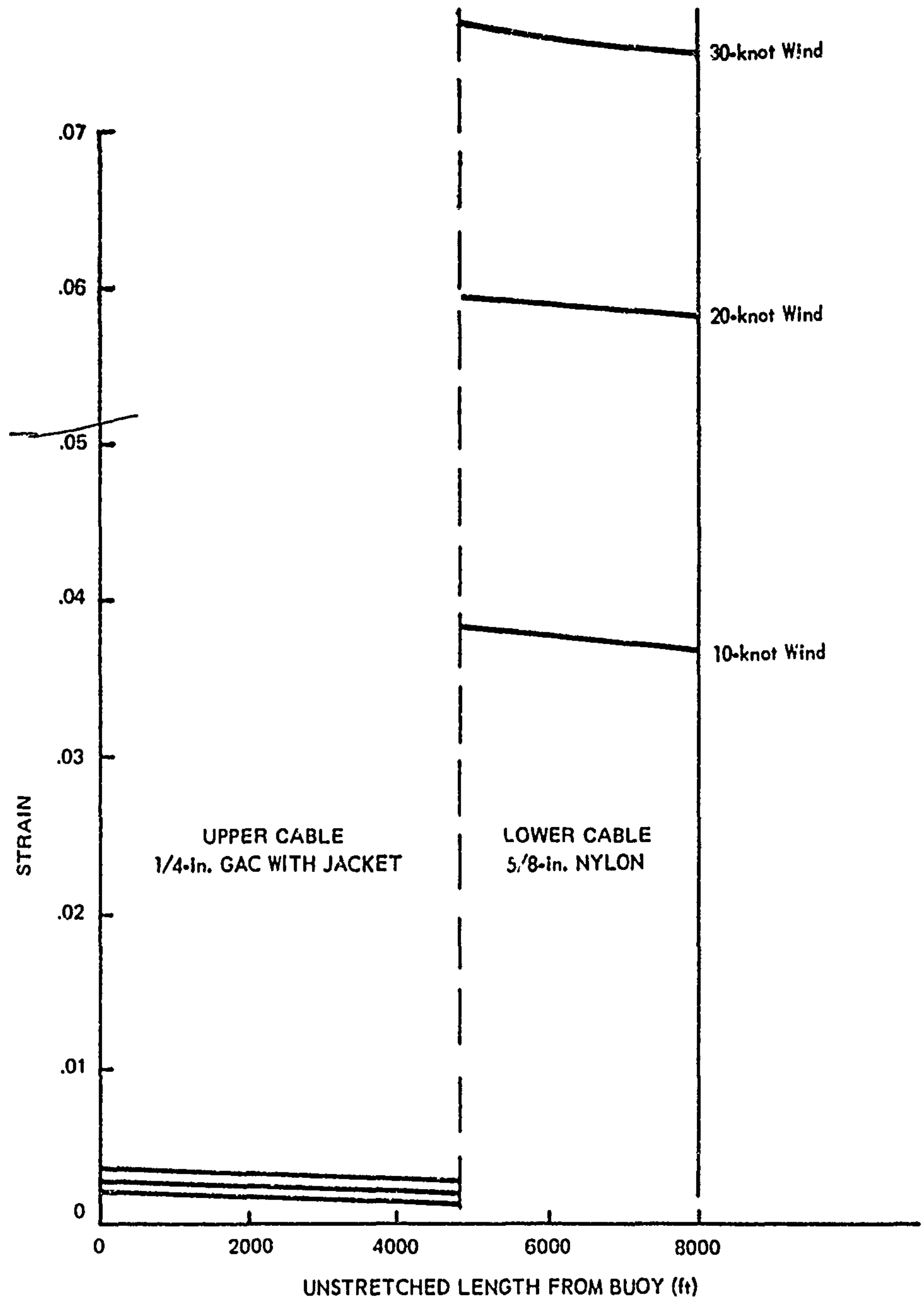

Figure 89. Initial Strains for WHOI Mooring No. 238

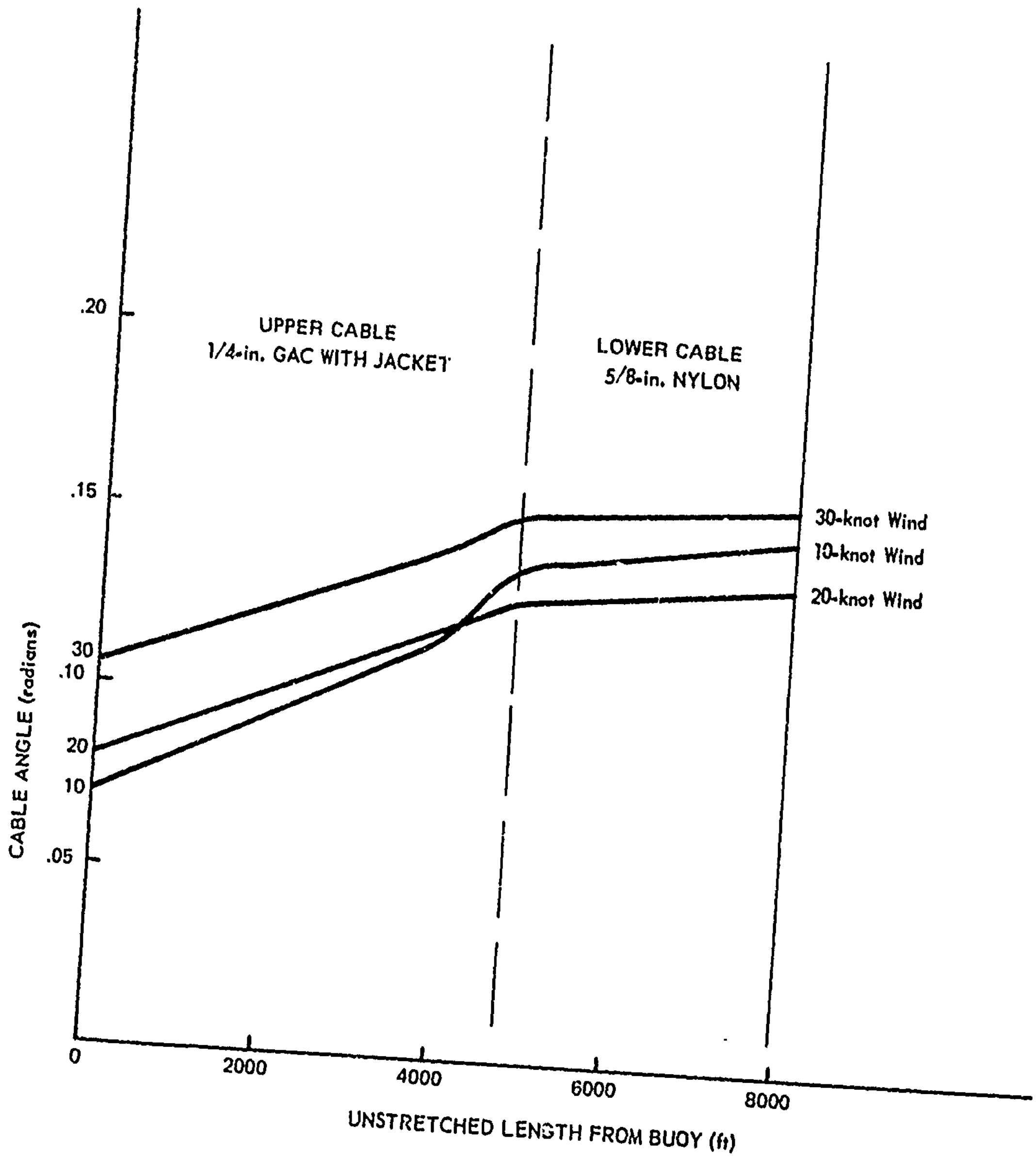

Figure 90. Initial Angles for WHOI Mooring No. 238

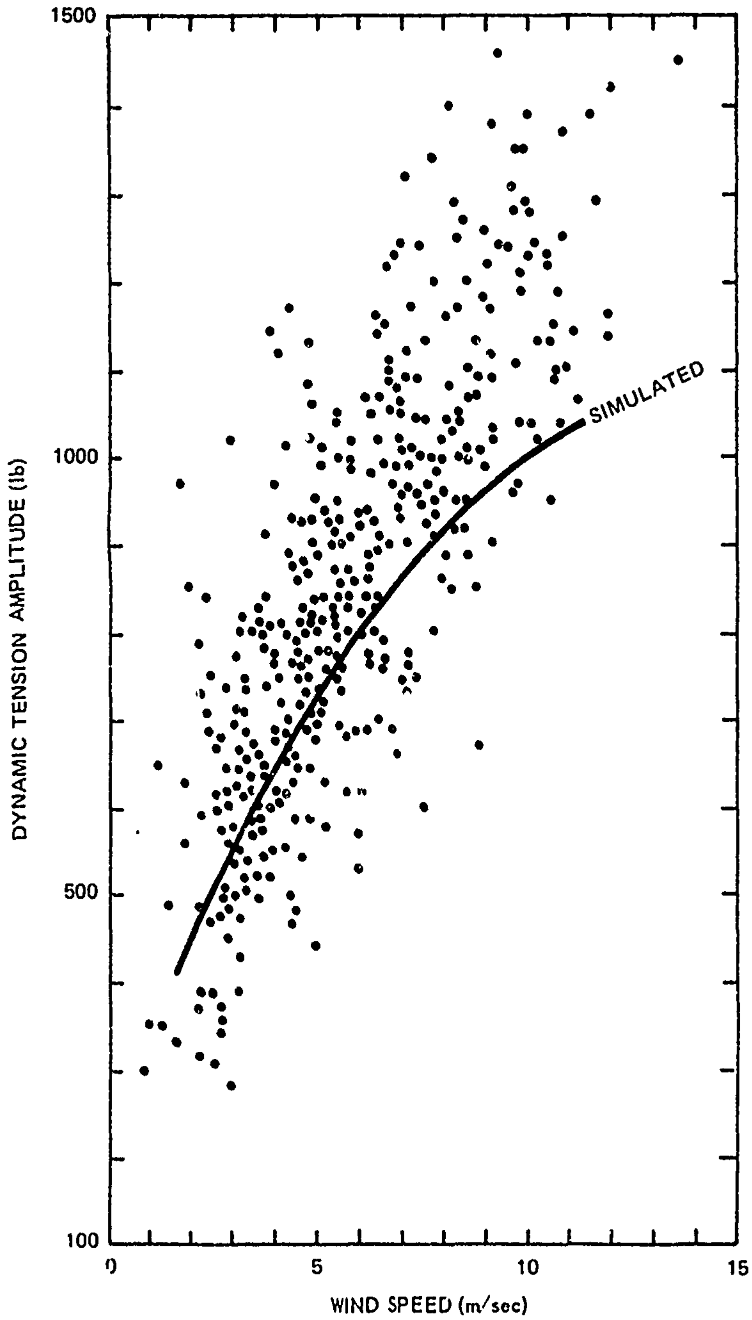

Figure 91. Computed and Observed Tension Amplitudes at 12 m for WHOI Mooring No. 238

Tension standard deviations for each run were first converted to mean amplitudes by assuming sinusoidal variations, converted to highest 1/10th amplitudes by assuming a Rayleigh distribution, and finally converted to double amplitudes. The resulting expression is

$$T_{WHOI} = (1.57)(2.03)(2.0) \cdot T_{SD} \; .$$

The simulated "dynamic tension amplitudes" are plotted in figure 91. Errors for the simulation were not computed in this case since the meaning of the WHOI "dynamic tension amplitude" is not clear. However, the simulation computes dynamic tensions that are order of magnitude and that increase with increasing wind speed. A better set of buoy motion and tension measurements are needed for deep sea buoy systems in order to fully validate the buoy motion dynamic simulation with the finite-difference cable model.

V. SUMMARY

5.1 Restatement of the Problem

The object of this investigation was to evaluate the forces acting on the components of a simple buoy system exposed to the oceanic environment and to develop a numerical model of buoy system dynamics to simulate buoy system response. Axisymmetric buoy hull shapes were considered in general, and hydrostatic and hydrodynamic forces and moments on oblate spheroids were studied. The set of integro-differential equations of motion for the buoy were reduced to a set of ordinary differential equations with nonconstant coefficients by using frequency dependent hydrodynamic force coefficients published in the literature.

A "quasi-random" wind wave model was developed to simulate the motions of the water masses in the immediate vicinity of the buoy. Wind wave properties were computed with the S-M-B method from the mean wind speed, fetch, and duration. Borgman's energy partitioning method was applied to a two-component Bretschneider spectrum, and sinusoidal wave component amplitudes and frequencies were computed. The random phase components were summed to compute instantaneous water particle motions.

Major assumptions made in the investigation of buoy dynamics include the following:

1. Dissipative forces can be separated into those due to surface wave generation and those due to viscous drag.

2. Infinitesimal buoy motions exist; this assumption was made by John[22,23] in the derivation of the hydrodynamic force and moment integrals and subsequently by Kim,[42] who evaluated the integrals for oblate spheroids.

3. The Haskind hypothesis is valid; i.e., it is assumed that the general problem of an object moving on a free surface in response to gravity waves on that free surface can be linearized to the extent that the velocity potential for that motion is the sum of

a. the linearized velocity potential of the gravity waves alone,

b. the velocity potential of the object moving on the free surface with no waves, and

c. the velocity potential due to the waves generated by the motion of the body.

The Haskind hypothesis was used in order to apply Kim's coefficients for oblate spheroids, which were derived for objects oscillating on a free surface, to the case of objects oscillating on a free surface with gravity waves.

4. The St. Denis-Pierson hypothesis is valid, i.e., it was assumed that the sea can be represented as the linear sum of elementary waves of random phase.

5. Body dimensions are small compared with a wavelength. This assumption was made in order to use the computed water particle motions as the motions of the mass of water in the immediate vicinity of the buoy hull.

Equations of motion for an elastic cable capable of supporting both axial and transverse waves simultaneously were written. A unique finite-difference numerical technique, an extension of Hartree's method for hyperbolic partial differential equations, was developed for the solution of sets of coupled hyperbolic equations. A lumped-mass cable model was also developed. Major assumptions made in the development of the cable dynamics model are that the cable is homogeneous and perfectly flexible and that hysterisis damping is negligible compared with viscous damping. The equations of motion for the buoy and cable were programmed and solved numerically on a UNIVAC 1108 digital computer in the time domain. Two types of buoy hulls were considered — a spherical buoy and a torroidal buoy. Both shallow water and deep water moorings were simulated using the lumped-mass and finite-difference cable models. Simulated data were compared with observed data in two steady-state cases and in three dynamics cases.

5.2 Conclusions

Steady-state buoy system configurations were simulated using the method described in chapter III for a shallow water buoy system and for a deep water buoy system. Comparison of simulated to observed configuration parameters (current meter tilt angles for the shallow water mooring and mean tensions for the deep water mooring) indicate good agreement between the computer model configurations and the configurations of the actual buoy systems. Although this comparison of a few bits of data from two buoy systems does not constitute a full validation of the steady-state buoy system configuration model (angles and tensions all along the mooring line for many current profiles and winds and for many different buoy systems should be simulated and correlated for a full validation), it does indicate that the simulation errors are on the order of 5 percent, which is adequate for engineering analysis.

Buoy system dynamics were simulated for three cases (two shallow water moorings where the lumped-mass cable model was used and one deep water mooring where the finite-difference cable model was used), and simulated buoy motion parameters were compared with observed parameters. In general, the lumped-mass cable model is more adaptable to shallow water buoy systems, which, if slack-moored, tend to have very low tensions at the bottom and cable angles that approach $\pi/2$ and, if taut-moored, tend to have very high dynamic strain levels, which can cause slack cable. The lumped-mass cable model can handle these cases easily (if tensions on an element go to zero, the element simply free falls through the water), whereas the finite-difference cable model breaks down with slack cable conditions since the equations of motion are ultrahyperbolic and possess an infinite number of equally valid solutions. Also, the lumped-mass model is more adaptable when the mooring line contains a number of mass or force discontinuities, i.e., instruments, subsurface buoys, sentinels, etc.

The comparison for both shallow water cases, one a spherical buoy and the other a Richardson torroid, indicate that the surge and sway hydrodynamic forces were underestimated in the simulation. Also, the comparison of observed to simulated shallow water torroidal buoy motion spectral levels indicates that the simulation is underdamped in all modes. There is good agreement in simulated and observed heave motions, the most important motion parameter for the buoy system designer. In general, the simulation appears to predict heave motions within ± 15 percent and the other motions within ± 50 percent. Since the environmental conditions were not monitored at either buoy during the motion measurements but were inferred from wind speeds measured ashore, from computed tidal currents based upon previous current measurements, and from visual observations of sea conditions, it is impossible to draw conclusions on the validity of the model, except that it computes buoy system motions that are order of magnitude with observed motions.

The comparison of simulated deep sea buoy system dynamics using the finite-difference model is inconclusive because of uncertainties in monitoring the environment and in the statistical meaning of the tension data collected.

5.2 Suggestions for Further Study

Future research in the area of buoy system dynamics should involve the emplantment and the fitting of motion sensing instrumentation to a wide spectrum of oceanic buoy system types — both shallow and deep water. The environment at each site should be adequately monitored (winds, waves, and currents), and a complete set of buoy system motions should be recorded. The measurements should include angles and tensions along the mooring line as well.

Another key area that should be investigated involves the hydrodynamic forces acting on a body on the free surface of a fluid when the free surface is subjected to random gravity waves. John's analysis assumed infinitesimal body motions in order to linearize the free surface boundary conditions. Kim's analysis assumed sinusoidal body motions in order to evaluate the hydrodynamic force and moment integrals. An investigation of the validity of these assumptions should be made in order to better understand the nature of the body-fluid interaction. Also, test tank data are needed to validate theoretical force and moment coefficients.

Extension of the analysis presented in this dissertation to nonaxisymmetric buoy hulls to include cross-coupled hydrodynamic forces and moments in the other modes would be of significance as a more general study of buoy system dynamics.

Finally, more research on the behavior of wire ropes and synthetic lines that are used in the ocean environment is needed for the prediction of buoy system performance.

REFERENCES

1. J. D. Isaacs et al., Development and Testing of Taut-Nylon Moored Instrument Stations, Scripps Institution of Oceanography, Report 65-5, San Diego, Calif., 15 April 1965. 86 pp.

2. W. S. Richardson et al., "Current Measurements from Moored Buoys," Deep Sea Research, Vol. 10, No. 4, October 1963, pp. 369-388.

3. G. H. Volkman, Mooring Summary 1967, Woods Hole Oceanographic Institution, Report 68-80, Woods Hole, Mass., 1968, 69 pp.

4. G. H. Volkman, Mooring Summary 1968, Woods Hole Oceanographic Institution, Report 69-35, Woods Hole, Mass. 1968, 70 pp.

5. J. E. Smith, Structures in Deep Ocean Engineering — Manual for Underwater Construction, U. S. Naval Civil Engineering Laboratory Report 284-7, Port Hueneme, Cal., October 1965, Ch. 7.

6. F. Webster, "Some Perils of Measurement from Moored Ocean Buoys," Transcript of the 1964 Buoy Technology Symposium, Marine Technology Symposium, Marine Technology Society, Washington, D. C., 25 March 1964, pp. 33-48.

7. F. Webster, "A scheme for Sampling Deep-Sea Currents from Moored Buoys," Transcript of the Second International Buoy Technology Symposium, Marine Technology Society, Washington, D. C., 20 September 1967, pp. 419-431.

8. S. O. Marcus, "Evaluation of NOMAD-II Data in Their Meteorological and Oceanographic Applications," Transcript of the Second International Buoy Technology Symposium, Marine Technology Society, Washington, D. C., 20 September 1967, pp. 395-408.

9. L. C. Huff, "Evaluation of the NOMAD Wind Measurement Subsystem," Transcript of the Second International Buoy Technology Symposium, Marine Technology Society, Washington, D. C., 20 September 1967, pp. 395-408.

10. G. C. Day, "Wind Measurements from Moored Buoys," Woods Hole Oceanographic Institution Reference No. 70-19, Woods Hole, Mass., May 1970.

11. B. W. Wilson, Characteristics of Anchor Cables in Uniform Ocean Currents, Texas A & M Report TR No. 204-1, Texas A & M University, College Station, Texas, April 1960.

12. B. W. Wilson, Characteristics of Deep-Sea Anchor Cables in Strong Ocean Currents, Texas A & M Report 204-3, Texas A & M University, College Station, Texas, 3 February 1961.

13. K. T. Patton, "On the Equilibrium Configuration of Moored Surface Buoys in Currents," U.S. Navy Underwater Sound Laboratory Technical Memorandum No. 2212-212-68, U.S. Navy Underwater Sound Laboratory, New London, Conn., 25 October 1968.

14. W. D. Martin, "Tension and Geometry of Single Point Moored Surface Buoy System." M.S. Thesis, Dept. of Naval Architecture and Marine Engineering, Massachusetts Institute of Technology, Cambridge, Mass., 8 November 1968.

15. L. Euler, Scientia Navalis, 1749.

16. The Papers of William Froude, ed. by A. D. Duckworth, The Institution of Naval Architects, London, 1955, 359 pp.

17. A. Kriloff, "A General Theory of the Oscillations of a Ship on Waves," Transactions of the Institution of Naval Architects, Vol. 40, 1898, pp. 135-212.

18. F. M. Lewis, "The Inertia of Water Surrounding a Vibrating Ship," Transactions of the Society of Naval Architects and Marine Engineers, Vol. 37, 1929, pp. 1-20.

19. M. D. Haskind, "Oscillation of a Ship on a Calm Sea," Izvestia Akademii Nauk, S.S.S.R., Otdelenie Techinicheskikh Nauk, No. 1, 1946. 23-24, English Translation: Technical and Research Bulletin No. 1-12, The Society of Naval Architects and Marine Engineering 1953.

20. M. D. Haskind and I. S. Riman, "A Method of Determining the Pitching and Heaving Characteristics of Ships," Izvestia Akedemii Nauk, S.S.S.R., Otdelenie Techinicheskikh Nauk, No. 10 (1946) 1373-1383, English Translation: David Taylor Model Basin, Translation No. 253, 1955.

21. M. D. Haskind, "The Exciting Forces and Wetting of Ships." Izvestia Akademii Nauk, S.S.S.R., Otdelenie Techinicheskikh Nauk, No. 7, 1957, pp. 65-79, English Translation: David Taylor Model Basin Translation No. 307, March 1962.

22. F. John, "On the Motion of Floating Bodies, I," Communications on Pure and Applied Mathematics, Vol. 2, 1949.

23. F. John, "On the Motion of Floating Bodies. II. Simple Harmonic Motions," Communications on Pure and Applied Mathematics. Vol. 3, 1950. pp. 45-101.

24. M. St. Denis and W. J. Pierson, "On the Motions of Ships in Confused Seas," Transactions of the Society of Naval Architects and Marine Engineers, Vol. 61, (1953) pp. 280-332.

25. B. V. Korvin-Kroukovsky, "Investigation of Ships Motions in Regular Waves," Transactions of the Society of Naval Architects and Marine Engineers, Vol. 65, 1957.

26. B. V. Korvin-Kroukovsky, "Pitching and Heaving Motions of a Ship in Regular Waves," Transactions of the Society of Naval Architects and Marine Engineers, Vol. 65, 1957.

27. B. V. Korvin-Kroukovsky, "Theory of Seakeeping," The Society of Naval Architects and Marine Engineers, 1961, New York.

28. J. K. Lunde and S. W. Doroff, Proceedings of the Fifth Symposium on Naval Hydrodynamics - Ship Motion, Drag Reduction, Office of Naval Research Publication ACR-112, Dept. of the Navy, Washington, D. C., September, 1964, 1154 pp.

29. R. F. Devereux, Development of an Ocean Data Telemetering Buoy, General Dynamics/Convair Division Report GD/C-65-018, San Diego, Calif., May 1965, 255 pp.

30. R. F. Devereux, et al., Some Observations from a Prototype Ocean Data Station Buoy in Hurricane Betsy 6-8 Sept., 1965, General Dynamics/Convair Division Report GDIC-65-203, San Diego, Calif., 1 October 1965, 57 pp.

31. S. T. Uyeda, et al., "Two Experimental Moorings of a Large Oceanographic Buoy in 13,000 feet of Water Near Bermuda," Transactions of the Second International Buoy Technology Symposium, Marine Technology Society, Washington, D.C., 20 September 1967, pp. 85-104.

32. R. D. Gaul and N. L. Brown, "A Comparison of Wave Measurements from a Free-Floating Wave Meter and the Monster Buoy," Transactions of the Second International Buoy Technology Symposium, Marine Technology Society, Washington, D.C., 20 September 1967, pp. 473-494.

33. R. G. Paquette, et al., The Dynamics of Simple Deep-Sea Buoy Moorings, General Motors Defense Research Corp., Report No. TR-65-79, Santa Barbara, Calif., November 1965, 167 pp.

34. L. E. Bivens and B. R. Swann, "Moored Buoy Performance Measurement," Transactions of the Second International Buoy Technology Symposium, Marine Technology, Washington, D.C., 20 September 1967, pp. 245-267.

35. P. Rudnick, "Motion of a Large Spar Buoy in Sea Waves," Journal of Ship Research, Vol. 11, No. 4, December 1967, pp. 257-260.

36. R. Blumberg and C. D. Osborn, "Computer Aided Design of Submerged Ocean Buoy Systems," Proceedings of the 1969 Offshore Technology Conference, Houston, Texas, 18 May 1969, Paper No. OTC-1133, pp. 497-504.

37. R. C. Millard, Jr., "Observations of Static and Dynamic Tension Variations from Surface Moorings," Woods Hole Oceanographic Institution Reference No. 69-29, Woods Hole, Mass., May 1969, 23 pp.

38. J. H. Nath, Dynamics of Single Point Ocean Moorings of a Buoy — A Numerical Model for Solution by Computer, Oregon State University, Department of Oceanography Report No. 69-10, Corvallis, Oregon, July 1969, 109 pp.

39. F. H. Hsu and K. A. Blenkarn, "Analysis of Peak Mooring Force Caused by Slow Vessel Drift Oscillation in Random Seas," Proceedings of the 1970 Offshore Technology Conference, Houston, Texas, Paper No. OTC 1159, 22 April 1970, pp. 135-147.

40. B. G. Burke, "The Analysis of Drilling Vessel Motions in a Random Sea," Proceedings of the 1970 Offshore Technology Conference, Houston, Texas, Paper No. OTC 1219, 22 April 1970, pp. 701-716.

41. The Collected Papers of Sir Thomas Havelock on Hydrodynamics, ed. by C. Wigley, Office of Naval Research, Dept. of the Navy Report ONR/ACR-103, Washington, D.C. 11 March 1963, pp. 627.

42. W. D. Kim, "Oscillations of a Rigid Body on a Free Surface," Journal of Fluid Mechanics, Vol. 21, 1965, pp. 427-451.

43. R. Barakat, "Vertical Motion of a Floating Sphere in a Sine-Wave Sea," Journal of Fluid Mechanics, Vol. 13, 1962, pp. 540-569.

44. G. Birkhoff, Hydrodynamics, Princeton University Press, Princeton, N. J. 1960.

45. H. Lamb, Hydrodynamics, 6th ed., Dover Publications, New York, 1932, 738 pp.

46. M. Martin, "Roll Damping Due to Bilge Keels," PhD dissertation, State University of Iowa, Iowa City, Iowa, 1959.

47. H. Schlicting, Boundary Layer Theory, 4th ed., McGraw-Hill Book Co., Inc., New York, 1960, 644 pp.

48. S. F. Hoerner, Fluid Dynamic Drag, published by author, Midland Park, N. J., 1958.

49. J. F. Dalzell, Cross-Spectral Analysis of Ship Model Motions: A Destroyer Model in Irregular Long-Crested Head Seas, Stevens Institute of Technology — Davidson Laboratory Report No. 810, 1962.

50. J. F. Dalzell, Some Further Experiments on the Application of Linear Superposition Techniques to the Responses of a Destroyer Model in Extreme Long-Crested Head Seas, Stevens Institute of Technology — Davidson Laboratory Report No. 918, 1962.

51. J. Gerritsma, Ship Motions in Longitudinal Waves, International Ship Building Progress, No. 7, 1960, pp. 49-76.

52. C. L. Bretschneider, "Wave Variability and Wave Spectra for Wind-Generated Gravity Waves," Technical Memorandum No. 118, Beach Erosion Board, U. S. Army Corps of Engineers, 1959.

53. H. U. Sverdrup and W. H. Munk, Wind Sea and Swell: Theory of Relations for Forecasting, Hydrographic Office, Pub. No. 601, U. S. Department of the Navy, 1947.

54. K. T. Patton, "Prediction of Wind Waves in Block Island Sound," U. S. Navy Underwater Sound Laboratory Technical Memorandum No. 2212-78-69, 8 April 1969.

55. R. L. Weigel, Some Engineering Aspects of Wave Spectra: Ocean Wave Spectra-Proceedings of a Conference, Prentice-Hall, Inc., Englewood Cliffs, N. J., 1963.

56. M. S. Longuet-Higgins, "On the Statistical Distribution of the Heights of Sea Waves," Journal of Marine Research, Vol. 11, No. 3, 1952, pp. 345-366.

57. W. J. Pierson and L. Moskowitz, "A Proposed Spectral Form for Fully Developed Wind Seas Based on the Similarity Theory of S. A. Kitaigorodskii," Journal of Geophysical Research, Vol. 69, No. 24, 1964, pp. 5181-5190.

58. C. F. Kottler, Jr., "A Wind Wave Co-Cumulative Spectral Model," Journal of Ship Research, Vol. 14, No. 4, December 1970, pp. 277-296.

59. L. E. Borgman, Ocean Wave Simulation for Engineering Design, Hydraulic Engineering Laboratory — University of California Technical Report HEL-9-13, October 1967, 44 pp.

60. N. Cristecu, "Rapid Motions of Extensible Strings," Journal of Mechanics of Physics and Solids, 1964, Vol. 12, pp. 269-273.

61. J. W. Schram, "A Three-Dimensional Analysis of a Towed System," PhD. dissertation, Rutgers — The State University, New Brunswick, N. J., 1968.

62. L. F. Whicker, "The Oscillatory Motion of Cable Towed Bodies," PhD. dissertation, University of California, 1957.

63. R. B. Lindsay, Mechanical Radiation, McGraw-Hill Book Company, Inc., New York, 1960, 415 pp.

64. A. Jeffrey and T. Taniuti, Non-Linear Wave Propagation, Academic Press, New York, 1964, 369 pp.

65. D. R. Hartree, Numerical Analysis, 2nd ed., Oxford University Press, London, 1958.

66. W. F. Ames, Nonlinear Partial Differential Equations in Engineering, Academic Press, New York, 1965, 512 pp.

67. Nonlinear Partial Differential Equations — A Symposium on Methods of Solution, ed. by W. F. Ames, Academic Press, New York, 1967, 316 pp.

68. D. Greenspan, Introduction to Partial Differential Equations, McGraw-Hill Book Company, Inc., New York, 1961, 195 pp.

69. L. Fox, Numerical Solution of Ordinary and Partial Differential Equations, Pergamon Press, Oxford, G. B., 1962, 509 pp.

70. G. F. D. Duff and D. Naylor, Differential Equations of Applied Mathematics, John Wiley & Sons, Inc., New York, 1966, 423 pp.

71. M. Casarella and M. Parsons, "Cable Systems Under Hydrodynamic Loading," Marine Technology Society Journal, Vol. 4, No. 4, July-August 1970.

72. A. B. Basset, A Treatise on Hydrodynamics, 2 vols., Dover Publications, Inc., New York, 1961 (first published 1888).

73. R. R. Miller, The Effects of Frequency and Amplitude of Oscillation on the Hydrodynamic Mass of Irregular Shaped Bodies," M.S. Thesis, University of Rhode Island, Kingston, R.I., 1965.

74. R. R. Miller and W. M. Hagist, Experimental Determination of the Hydrodynamic Mass, University of Rhode Island, Division of Engineering Research and Development Report to U. S. Navy Underwater Sound Laboratory, Kingston, R. I., 1965.

75. "Instruction Bulletin — Type 316 Histogram Current Meter," Braincon Corp., Marion, Mass. April 1965.

76. R. L. Sunblad. "The Histogram Current Meter," Instrument Society of America, Conference Preprint, date unknown.

77. R. G. Williams, Physical Oceanography of Block Island Sound, U. S. Navy Underwater Sound Laboratory Report No. 966, New London, Conn., 1 July 1969.

78. A. J. Nalwalk et al., Final Report of Oceanographic Measurements Along the Block Island-Fishers Island (BIFI) Range in Block Island Sound from January 1969 through June 1970., University of Connecticut—Marine Research Laboratory Report to Navy Underwater Sound Laboratory, Noank, Conn., December 1970.

79, H. O. Berteaux and R. G. Walden, Analysis and Experimental Evaluation of Single Point Moored Buoy Systems, Woods Hole Oceanographic Institution Report No. 69-36, Woods Hole, Mass., May 1969.

80. F. Webster, "Vertical Profiles of Horizontal Ocean Currents," Deep Sea Research, Vol. 16, No. 1, 1969, pp 85-98.

81. Patton, K. T., "Buoy Motions in Block Island Sound — Preliminary Data," NUSC Technical Memorandum No. 2212-29-71, Naval Underwater Systems Center, New London Laboratory, New London, Conn., March 1971, 87 pp.

82. A. Vine and C. H. Volkman, "Nomogram for Wind Waves at Sea," Undersea Technology, Vol. 5, No. 5, May 1964, p. 37.

83. "1970 Tidal Current Tables — Atlantic Coast of North America," U. S. Dept. of Commerce, Environmental Science Services Administration, Coast and Geodetic Survey, Rockville, Md., 1959.

84. J. S. Bendat and A. G. Piersol, Measurement and Analysis of Random Data, John Wiley & Sons, Inc., New York, 1966.

85. J. F. Ferrie and A. H. Nuttall, "Availability of Fisher's FFT Algorithm," NUSC Technical Memorandum No. 2070-21-71, Naval Underwater Systems Center, New London Laboratory, New London, Conn., January 1971, 11 pp.

86. A. H. Nuttall, Spectral Estimation by Means of Overlapped Fast Fourier Transform Processing of Windowed Data, NUSC Report No. 4169, Naval Underwater Systems Center, New London Laboratory, New London, Conn., October 1971, 40 pp.

87. R. G. Williams, "Estimating Ocean Wind Wave Spectra by Means of Underwater Sound," PhD. dissertation, New York University — Dept. of Meteorology and Oceanography, New York, 1971, 186 pp.

Appendix A

ANGULAR STABILITY OF AXISYMMETRIC BUOYS

It is known from visual observation and from collected motion data that buoys do not become unstable in the sense of Liapunov; i.e., buoy motions will not build to infinity. However, buoys will undergo large excursions and can be upset. For example, a buoy that undergoes gross heaving motions in the sea so that it is alternately awash and then rises out of water to fall over on its side would be deemed unstable by the casual observer; however, the buoy would actually be stable since its motions are bounded and do not tend to infinity with time. Of course, if this buoy housed meteorologic or oceanographic instrumentation, it would be of little value because of its wild motions.

The "stability" of this type of motion is best described in the pitch (or roll) phase plane, i.e., a plot of pitch angular velocity versus pitch. However, pitching (and rolling) motions are heavily influenced by the draft of the buoy, i.e., the location of the center of buoyancy relative to the center of gravity. Thus, the heave motions and resulting buoy draft must be considered. Because the righting moment depends on the location of the center of buoyancy relative to the center of gravity, the pitch (or roll) equations of motion are similar to the nonlinear equations of motion for a pendulum.

A wide spectrum of axisymmetric buoy shapes will be considered, ranging from a spar buoy with a high draft-to-beam ratio to a discus buoy with a low draft-to-beam ratio (figure A-1). First, consider the spar buoy. In the absence of external forces (mooring line tensions, etc.), static stability is maintained only if the center of gravity is below the center of buoyancy:

$$L_{CG} < H/2 .$$

This is obvious from the undamped pitch equation of motion for the spar buoy:

$$I_\beta \ddot{\beta} + \rho g \frac{\pi}{4} B^2 H\left(\frac{H}{2} - L_{CG}\right) \sin\beta = 0 .$$

Also, if the buoy is tilted at extreme angles, we see that

$$\beta > \pi \qquad \text{or} \qquad \beta < -\pi .$$

The spar buoy will not return to its initial equilibrium position but will undergo a complete revolution and seek equilibrium at either 2π or -2π. A typical pitch phase plane for the spar buoy is shown on figure A-2 for two possible conditions:

1. $L_{CG} < H/2$
2. $L_{CG} > H/2$.

Note that if the buoy is initially unstable, $L_{CG} > H/2$, it is stable at $\pm\pi$; i.e., it is stable upside down.

A cable attached to the bottom of the spar buoy will tend to stabilize the buoy. Adding a restoring moment due to the cable tension in the equation of motion yields

$$I_\beta \ddot{\beta} + \rho g \frac{\pi}{4} B^2 H\left(H/2 - L_{CG}\right) \sin\beta$$
$$+ K L_{CG} (1 - \cos\beta) L_{CG} \sin\beta = 0 ,$$

where K is a cable spring constant. For a stable system, the sum of the two restoring moment terms must be positive. Solving for L_{CG}, we see that

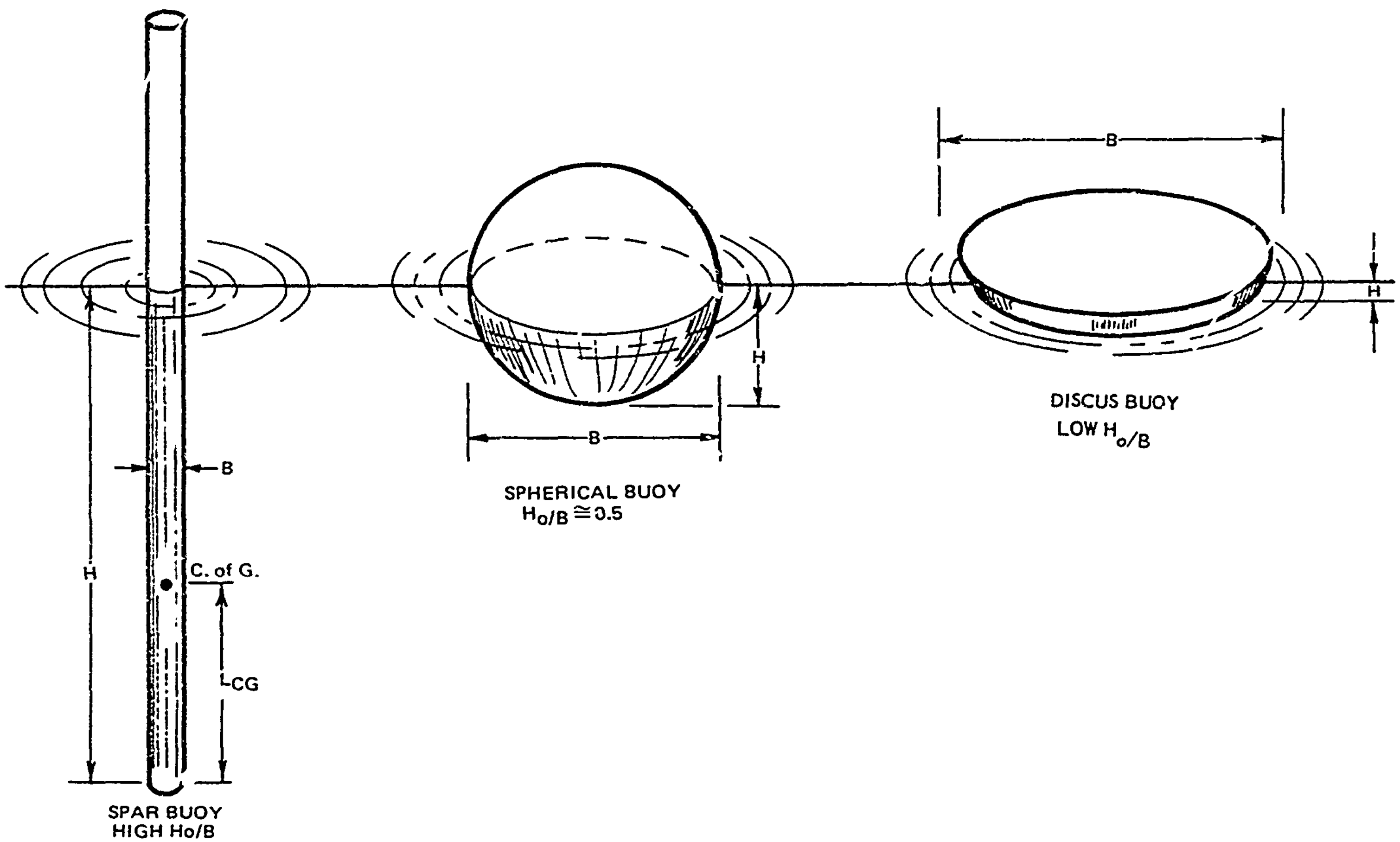

Figure A-1. Axisymmetric Buoy Shapes

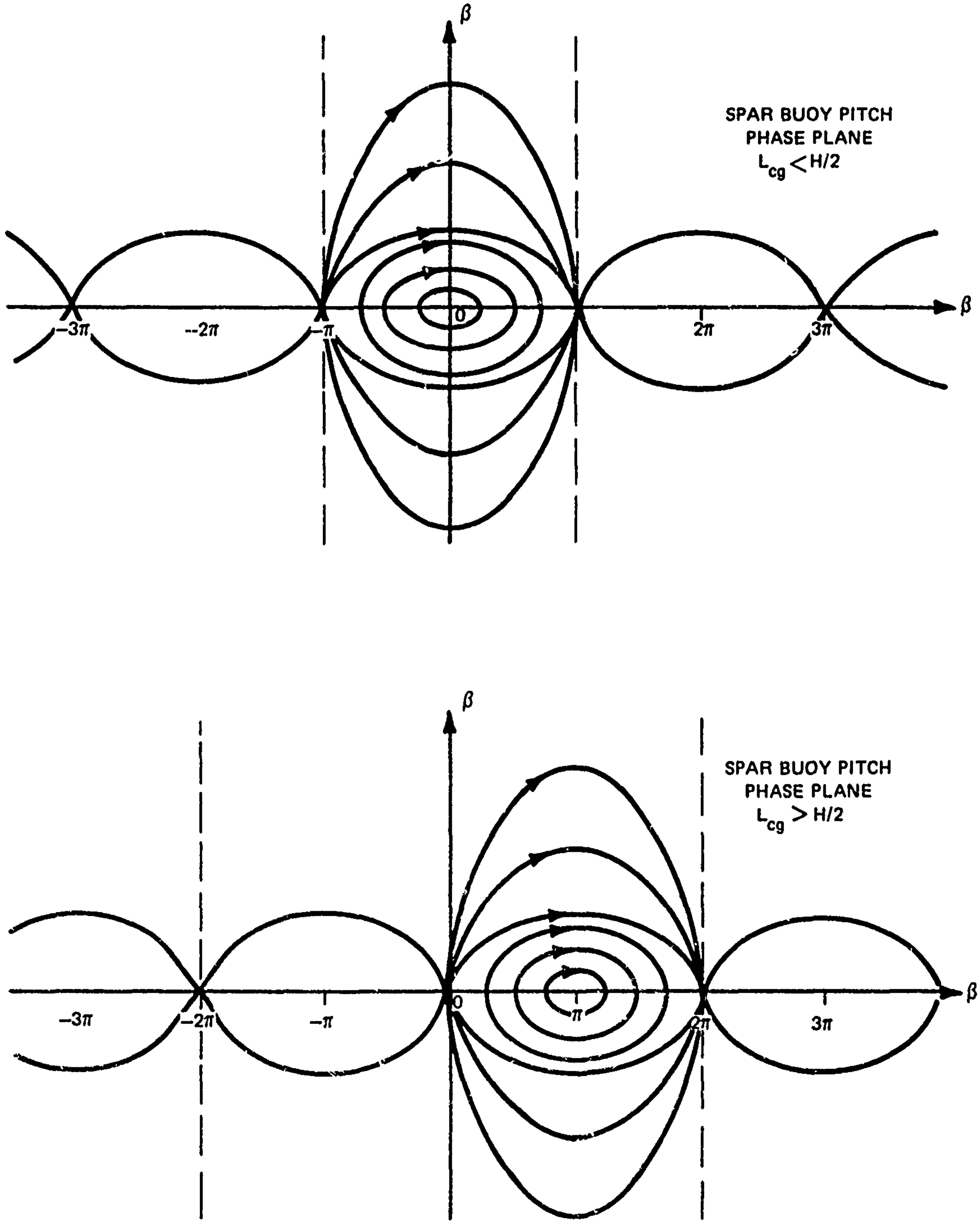

Figure A-2. Spar Buoy Phase Planes

$$L_{CG} = \frac{C}{2} + \frac{1}{2}\sqrt{C}\cdot\sqrt{C-2H} \quad ,$$

where

$$C = \frac{\rho g \pi B^2 H}{4K(1-\cos\beta)} \quad .$$

In general, a spar buoy is designed to minimize heave response. Thus, the shallowest buoy draft would be the static draft of the buoy minus one-half the largest wave height:

$$H_{MIN} = H_0 - \frac{1}{2}\eta_{MAX} \quad .$$

For a stable buoy, we see that

$$L_{CG} < \frac{H_{MIN}}{2} = \frac{H_0 - \frac{1}{2}\eta_{MAX}}{2} .$$

The spherical buoy shape is subject to the same types of moments, but the study is complicated by the fact that the center of buoyancy will deviate from the vertical axis of the buoy as the buoy pitches. If the center of gravity lies below the center of buoyancy (5/8 H from the bottom), the buoy is positively stable and will have a phase plane representation similar to that shown in figure A-2 for the spar buoy. The upper phase plane applies if $L_{CG} < 5/8\ H$, and the lower phase plane applies if $L_{CG} > H$. However, the buoy is neutrally stable if $5/8\ H < L_{CG} < H$, since the center of buoyancy is always directly below the center of gravity. In this situation there is no definite stable position, because there is no restoring moment. Again, the tension of a mooring line attached below the center of buoyancy will stabilize the buoy.

Any buoy with a draft-to-beam ratio less than 0.5 and a hull height-to-beam ratio less than 1 can be bistable; i.e., it can be stable right side up or upside down. Torroid and discus buoys are of this class. If the center of gravity is located far below the buoy hull (achieved by means of ballast weights on a boom or tripod), the phase plane is similar to the upper curve for the spar buoy. If the center of gravity is far above the buoy hull (due to heavy instruments or equipment), the lower curve for the spar buoy phase plane would apply — the buoy is stable when upside down. If the center of gravity is near the geometric center of the buoy hull, the buoy is equally stable right side up or upside down. The phase plane for this situation is shown on figure A-3. Inspection of figure A-3 indicates that the width of the stable (in the sense that the buoy is right-side-up) region in the phase plane can vary from 2π to 0 depending on the vertical location of the center of gravity.

This simple discussion of buoy stability did not consider other modes of possible unstable motion since they have never been observed to offer serious problems. Cross-coupled moments due to the hydrodynamic forces acting on the buoy and the horizontal tension components were neglected in this discussion. Even with these restrictions, a few design guides are apparent. The buoy should be designed with the center of gravity below the center of buoyancy if at all possible. Also, the mooring line attachment point should be as low as possible to offer the greatest righting moment if the buoy does capsize.

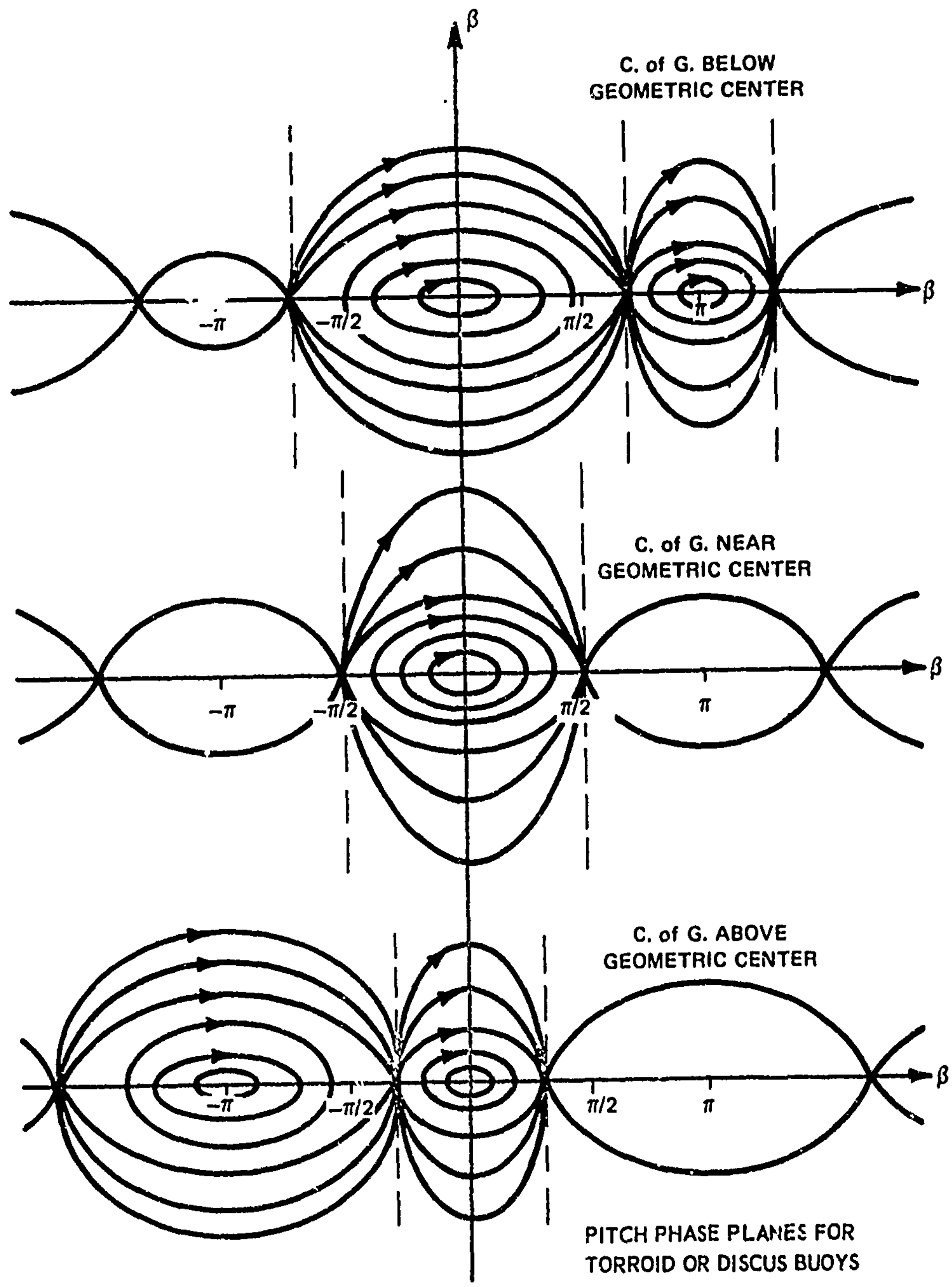

Figure A-3. Torroid or Discus Buoy Phase Planes

Appendix B

COMPUTER PROGRAMS FOR THE MODELS

Steady-State Buoy System Configurations

This program computes the three-dimensional spatial configuration, tensions, and strains of either an elastic or inelastic buoy system mooring line. Winds from any compass direction can act on the buoy, and currents that vary in strength and direction as a function of depth can act on the buoy and mooring line. The mooring line can be composed of segments having different properties (weight in water, mass, drag, elasticity, etc.). Point mass discontinuities (to simulate current meters, hydrophones, etc.) can also be accounted for.

The basic cable equations (equations (230) to (233)) and a discussion of the development of this program are included in chapter III of the main text. The logic employed in this program is shown in figure B-1, which generally illustrates the computational operations.

The input data are as follows:

1. Buoy major diameter (ft)
2. Buoy minor diameter (ft)
    a. Vertical diameter for an oblate spheroid
    b. Hole diameter for a torroid

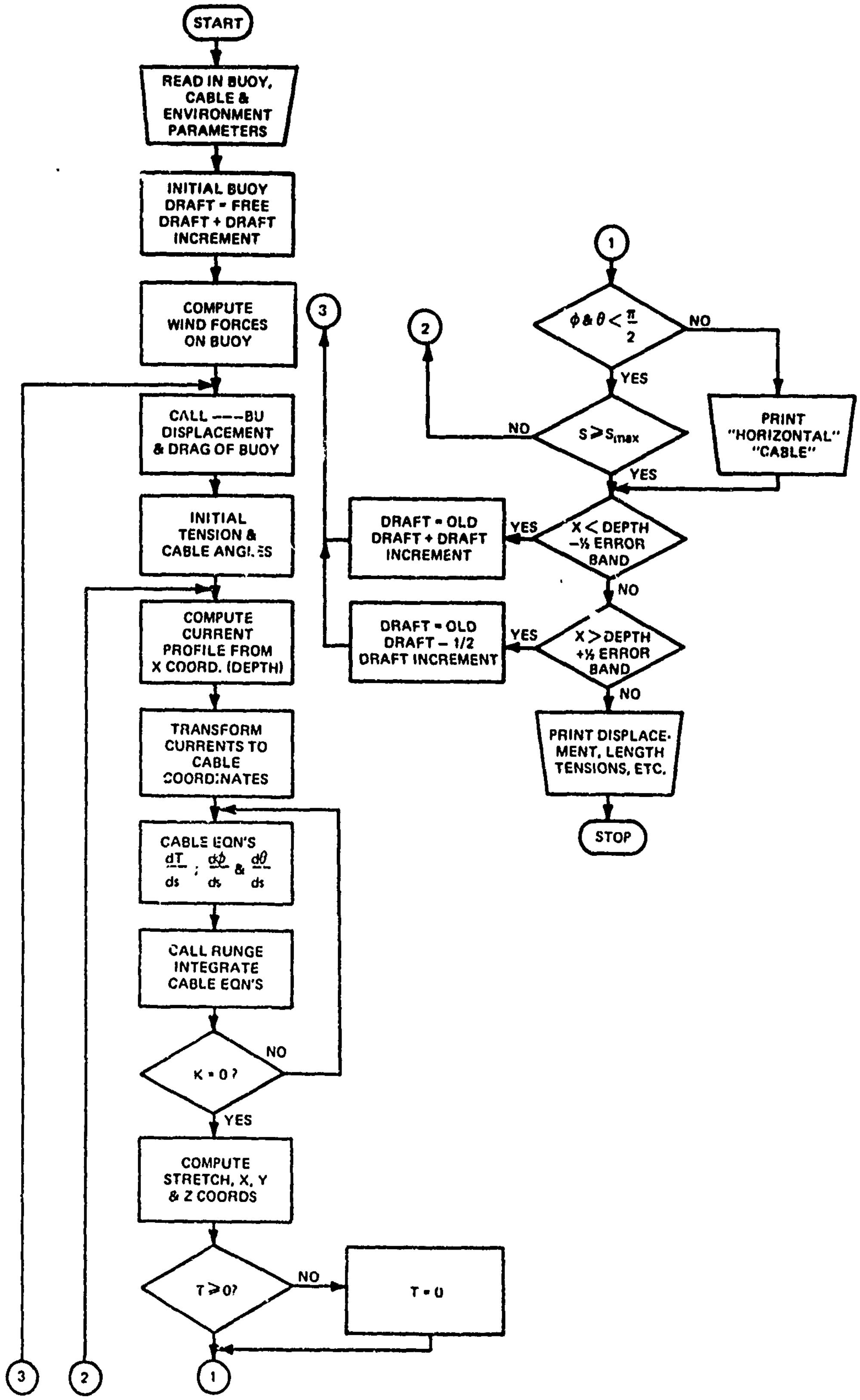

Figure B-1. Steady-State Buoy System Configuration Flow Chart

c. 0 for a cylinder

d. 0 for a sphere

3. Buoy weight (lb)

4. Maximum draft of hull (ft)

5. Free draft with no mooring line (ft)

6. Buoy windage (ft^2)

7. Wind drag coefficient

8. Cable diameter (in.)

9. Cable weight in water per unit length (lb/ft)

10. Effective cable modulus of elasticity ($lb/in.^2$)

11. Unstretched cable length (ft)

12. Surface current (knots)

13. Water depth (ft)

14. Wind speed component in y direction (ft/sec)

15. Wind speed components in z direction (ft/sec).

The integration step size "B" is normally set at 1/100th of the total cable length. However, if the cable properties are changed from a lightweight line to a very heavy line (for example, anchor chain), the step size should be changed in inverse proportion to the in-water weights. Also, the normal and tangential drag coefficients ("DRGON" and "DRGCT") should be changed accordingly if the mooring line section is not circular, for example, hair-faired cable and chain. Occasionally, the solution will not converge into the depth error band. This occurs if the first draft increment is too large and the computed x dimension of the mooring line "overshoots" the depth. With each overshoot, the buoy draft increment is halved; thus, convergence may be very slow. The initial buoy draft increment should be halved if this occurs.

```
PATTON                                                              DATE 060372 PAGE    3

BI FOR S1279,S:279
UNIVAC 1108 FORTRAN V LEVEL 2206 0023                                                          10:12:56.278
THIS COMPILATION WAS DONE ON 06 MAR 72 AT 10:12:56

   MAIN PROGRAM

   STORAGE USED (BLOCK, NAME, LENGTH)

         0001    *CODE    000645
         0000    *DATA    000617
         0002    *BLANK   000000

   EXTERNAL REFERENCES (BLOCK, NAME)

         0003    DBLBU
         0004    RUNGE
         0005    NRDCS
         0006    NI02S
         0007    SQRT
         0010    ATAN
         0011    SIN
         0012    COS
         0013    NEXP6S
         0014    NERR2S
         0015    NWDUS
         0016    NSTOPS

   STORAGE ASSIGNMENT FOR VARIABLES (BLOCK, TYPE, RELATIVE LOCATION, NAME)

 0001     000453 10L     0000     000547 100F    0000     000551 101F    000n     000553 1n2F    n000     0nn455 104F
 0000     000557 106F    0000     000563 107F    0001     000475 12L     0001     000470 18L     0001     000522 2710
 0001     000275 3L      0001     000355 4L      0001     000203 5L      0001     000116 7L      0001     000440 9L
 0000 R 000503 B         0000 R 000462 BO1       0000 R 000463 BO2       0000 R 000512 C         0000 R 000540 CRENT
 0000 R 000475 CUR       0000 R 000535 CWXC      0000 R 000536 CWYC      0000 R 000537 CWZC      0000 R 000000 D
 0000 R 000511 DC        0000 R 000515 DDP       0000 R 000476 DEEP      0000 R 000516 DH        0000 R 000471 DIA
 0000 R 000521 DISP      0000 R 000522 DRB       0000 R 000542 DRGCN     0000 R 000541 DRGCT     0000 R 000543 DS
 0000 R 000544 DX        0000 R 000545 DY        0000 R 000546 DZ        0000 R 000510 E         0000 R 000473 EC
 0000 R 000517 H         0000 R 000466 HFREE     0000 R 000465 HM        0000 I 000507 J         0000 I 000506 K
 0000 I 000520 L         0000 I 000505 M         0000 I 000504 N         0000 R 000152 PHI       0000 R 000003 R
 0000 R 000502 RHO       0000 R 000526 S         0000 R 000474 SM        0000 R 000527 STR       0000 R 000006 TEN
 0000 R 000316 THE       0000 R 000532 UC        0000 R 000530 V         0000 R 000533 VC        0000 R 000501 VIS
 0000 R 000531 W         0000 R 000467 WAREA     0000 R 000464 WB        0000 R 000534 WC        0000 R 000470 WCD
 0000 R 000513 WFY       0000 R 000514 WFZ       0000 R 000477 WINDY     0000 R 000500 WINDZ     0000 R 000472 WTC
 0000 R 000523 X         0000 R 000524 Y         0000 R 000525 Z

 00100      1*      C
 00100      2*      C
 00100      3*      C
 00100      4*      C
 00100      5*      C
```

PATTON   DATE 060372 PAGE   4

```
00100   C
00100   C
00100   C
00100   C
00100   C
00100   C
00100   C
00100   C
00100   C      THIS PROGRAM COMPUTES STEADY STATE BUOY SYSTEM CONFIGURATIONS.
00100   C      THE DRAFT OF THE BUOY CONTROLS THE BUOY'S DISPLACEMENT AND
00100   C      DRAG WHICH DETERMINE THE UPPER BOUNDARY CONDITIONS ON THE CABLE.
00100   C      THE CABLE CONFIGURATION IS COMPUTED AND ITS VERTICAL PROJECTION
00100   C      IS TESTED AGAINST THE WATER DEPTH - IF SHALLOW,THE BUOY DRAFT
00100   C      IS INCREASED - IF TOO DEEP, THE BUOY DRAFT IS DECREASED.
00100   C
00100   C      UNITS ARE IN FEET,POUNDS,SECONDS
00100   C
00100   C      COORDINATE SYSTEM
00100   C
00100   C
00100   C                  Z -----------------------------O BUOY
00100   C                       SURFACE CURRENT          /I
00100   C                     TOWARD BUOY ALONG Z AXIS  /*I
00100   C                                             /   I
00100   C                                            / *  I
00100   C                                           /     I
00100   C                                          /  *   I
00100   C                                         /       I
00100   C                                        /  *     I
00100   C                                       /         I
00100   C                                      /  *       I
00100   C                                     Y           I
00100   C                                      *          I
00100   C                                                 I
00100   C                                     *           I
00100   C                                                 I
00100   C                                   *             I
00100   C                                                 I
00100   C                         ANCHOR O****            I
00100   C                                                 X
00100   C
00100   C      BEGIN ITERATION AT THE FREE FLOATING DRAFT OF THE BUOY, I.E. - AS
00100   C      IF THERE WERE NO MOORING CABLE.
00101          DIMENSION D(3),R(3)
00103          DIMENSION TEN(100),PHI(100),THE(100)
00103   C
00103   C      READ IN THE BUOY PARAMETERS - MAJOR DIAMETER. MINOR DIAMETER.
00103   C      WEIGHT. MAXIMUM HULL DRAFT ANDFREE DRAFT
00104          READ 100,BD1,BD2,WB,HM,HFREE
00104   C
00104   C      READ IN THE BUOY WINDAGE AND WIND DRAG COEFFICIENT
00113          READ 102,WAREA,WCD
00113   C      READ IN THE CABLE PARAMETERS - DIAMETER(INCHES), WEIGHT PER FOOT
00113   C      IN WATER, CABLE MODULUS(LB/SQ. IN.), LENGTH
00117          READ 101,DIA,WTC,EC,SM
00117   C
```

```
00117    C    READ IN THE ENVRIONMENTAL PARAMETERS - SURFACE CURRENT(KTS.)
00117    C    WATER DEPTH AND WIND COMPONENTS
00125         READ 102,CUR,DEEP
00131         READ 102,WINDY,WINDZ
00131    C
00131    C    THE KINEMATIC VISCOSITY AND DENSITY FOR SALT WATER AT 10 DEG. C
00135         VIS=1.45E-5
00136         RHO=1.992
00137     100 FORMAT(3F10.3)
00140     101 FORMAT(4F15.4)
00141     102 FORMAT(2F10.3)
00142     104 FORMAT(8F8.2)
00142    C    THE INTEGRATION STEP SIZE IS .01 OF THE CABLE LENGTH
00143         B=.01*SM
00144         N=3
00145         M=0
00146         K=0
00147         J=1
00150         E=144.*EC
00151         DC=DIA/12.0
00152         C=1.69*CUR
00152    C    WIND FORCES ON THE BUOY
00153         WFY=0.0034*WCD*WAREA*WINDY*ABS(WINDY)
00154         WFZ=0.0034*WCD*WAREA*WINDZ*ABS(WINDZ)
00154    C
00154    C    INITIAL ERROR BAND  WIDTH = DEEP/20
00155         DGP=DEEP/20.0
00155    C    THE INITIAL BUOY DRAFT INCREMENT
00156         DH=HM/20.
00157         H=HFREE+DH
00160       7 CONTINUE
00161         L=1
00162         CALL ORLBU(BD1,BD2,H,HM,RHO,C,DISP,DRB)
00163         X=0.0
00164         Y=0.0
00165         Z=0.0
00166         S=0.0
00167         STR=0.0
00170         R(1)=SQRT(((DISP-WB)**2)+((DRB+WFZ)**2)+WFY**2)
00171         R(2)=ATAN(WFY/SQRT(((DRB+WFZ)**2)+((DISP-WB)**2)))
00172         R(3)=ATAN((DRB+WFZ)/(DISP-WB))
00173       5 CONTINUE
00173    C    COMPUTE THE CURRENT PROFILE - DIRECTION AND MAGNITUDE - AS A
00173    C    FUNCTION OF DEPTH, RELATIVE TO THE SURFACE CURRENT. EXPRESS AS Y
00173    C    AND Z COMPONENTS GOING IN THE NEGATIVE DIRECTIONS.
00173    C
00173    C    FOR A UNIFORM CURRENT
00174         V=0.0
00175         W=C
00176         UC=V*SIN(R(2))+W*COS(R(2))*SIN(R(3))
00177         VC=V*COS(R(2))-W*SIN(R(2))*SIN(R(3))
00200         WC=W*COS(R(3))
00200    C
00200    C    IF MORE THAN ONE TYPE OF CABLE IS USED IN THE MOOR, CHANGE CABLE
00200    C    CHARACTERISTICS HERE. USE A LOGICAL IF AT THE PROPER LENGTH
00200    C    REMEMBER TO CHANGE THEM BACK BEFORE THE NEXT CONFIGURATION IS
00200    C    COMPUTED
00200    C
```

```
00200   C     IF INSTRUMENTS,SINKERS,OR OTHER CONCENTRATED FORCES ARE ACTING ON
00200   C     THE MOORING LINE,CHANGE THE TENSIONS AND ANGLES BY USING A
00200   C     LOGICAL IF AT THE PROPER LENGTH(S) AND THEN SOLVING FOR THE
00200   C     STATIC FORCES ON THE FREEBODY OF THE ITEM.
00200   C
00201         CWXC=WTC*COS(R(2))*COS(R(3))
00202         CWYC=-WTC*SIN(R(2))*COS(R(3))
00203         CWZC=-WTC*SIN(R(3))
00204         CRENT=UC*DC/VIS
00205         DRGCT=.6055*(CRENT**-.4759)
00206         DRGCN=1.4
00207       3 CONTINUE
00207   C     DTEN/DS
00210         D(1)=-CWXC+0.5*RHO*DRGCT*DC*UC*ABS(UC)
00210   C     DPHI/DS
00211         D(2)=(-CWYC+0.5*RHO*DRGCN*DC*VC*ABS(VC))/R(1)
00211   C     DTHE /DS
00212         D(3)=(-CWZC+0.5*RHO*DRGCN*DC*WC*ABS(WC))/(R(1)*COS(R(2)))
00213         CALL RUNGE(N,R,D,S,B,M,K)
00214         GO TO(3,4),K
00215       4 DS=B*(1.0+1.272*R(1)/(E*(DC**2)))
00216         DX=DS*COS(R(2))*COS(R(3))
00217         X=X+DX
00220         TEN(L)=R(1)
00221         PHI(L)=R(2)
00222         THE(L)=R(3)
00223         L=L+1
00224         IF(S-SM)5,6,6
00224   C     TEST THE X COORDINATE AGAINST THE WATER DEPTH
00227       6 IF(X-(DEEP-DDP))8,9,9
00232       8 H=H+DH
00233         J=J+1
00234         IF(J-15)17,18,18
00237      17 GO TO 7
00240       9 IF(X-(DEEP+DDP))10,11,11
00243      11 DH=DH/2.
00244         H=H-DH
00245         GO TO 7
00246      10 DDP=DDP/2.0
00247         DH=DH/2.
00247   C     ERROR BAND HALF WIDTH MUST BE GREATER THAN THE STEP SIZE
00250         IF(DDP-B/2.)12,7,7
00253      18 WRITE(4,106)
00255     106 FORMAT(15H NO CONVERGENCE)
00256      12 WRITE(4,107)
00260     107 FORMAT(21H  DRAFT  DISPLACEMENT)
00261         WRITE(4,102)H,DISP
00265         X=0.0
00266         Y=0.0
00267         Z=0.0
00270         DO 82 L=1,100
00273         S=B*L
00274         DS=B*(1.0+1.272*TEN(L)/(E*(DC**2)))
00275         DX=DS*COS(PHI(L))*COS(THE(L))
00276         DY=DS*SIN(PHI(L))
00277         DZ=DS*COS(PHI(L))*SIN(THE(L))
00300         STR=STR+DS
00301         X=X+DX
```

```
         PATTON                                              DATE 060372  PAGE   7

00302   180*        Y=Y+DY
00303   181*        Z=Z+DZ
00304   182*        PHI(L)=57.4*PHI(L)
00305   183*        THE(L)=57.4*THE(L)
00306   184*     *2 WRITE(6,104)S,STR,TEN(L),PHI(L),THE(L),X,Y,Z
00321   185*        STOP
00322   186*        END

    END OF UNIVAC 1108 FORTRAN V COMPILATION.     0 *DIAGNOSTIC* MESSAGE(S)
```

```
                    PATTON                                              DATE  060372  PAGE    8
      QI FOR OBLBU,OBLBU
      UNIVAC 1108 FORTRAN V LEVEL 2206 0023                                                          10:12:58.591
      THIS COMPILATION WAS DONE ON 06 MAR 72 AT 10:12:58

         SUBROUTINE OBLBU     ENTRY POINT 000126

         STORAGE USED (BLOCK, NAME, LENGTH)

              0001   *CODE   000142
              0000   *DATA   000034
              0002   *BLANK  000000

         EXTERNAL REFERENCES (BLOCK, NAME)

              0003   SQRT
              0004   ASIN
              0005   NERR3$

         STORAGE ASSIGNMENT FOR VARIABLES (BLOCK, TYPE, RELATIVE LOCATION, NAME)

          0000 R 000000 A           0000 R 000004 AD         0000 R 000001 B         0000 R 000005 CD         0000 R 000002 HD
          0000   000016 INJP$       0000 R 000003 VOL

      00101      1*          SUBROUTINE OBLBU(BD1,BD2,H,HM,RHO,C,DISP,DRB)
      00101      2*      C   DISPLACEMENT AND DRAG FOR AN OBLATE SPHEROIDAL BUOY
      00103      3*          A=BD2/2.
      00104      4*          B=BD1/2.
      00105      5*          HD=H-A
      00106      6*          IF(HD.GE.A)HD=A
      00110      7*          VOL=3.1416*A*(B**2)*(.666+(H/A)-.333*((H/A)**3))
      00111      8*          AD=1.571*A*B+(B/A)*HD*SQRT(A**2-HD**2)+A*B*ASIN(HD/ABS(A))
      00112      9*          DISP=32.2*RHO*VOL
      00113     10*          CD=.354*A/B
      00114     11*          DRB=0.5*RHO*CD*AD*C*ABS(C)
      00115     12*          RETURN
      00116     13*          END

           END OF UNIVAC 1108 FORTRAN V COMPILATION.      0 *DIAGNOSTIC* MESSAGE(S)
```

```
          PATTON                                              DATE  060372  PAGE     9

QI FOR TORBU,TORBU                                                                          10:12:59.698
UNIVAC 1108 FORTRAN V LEVEL 2206 0023
THIS COMPILATION WAS DONE ON 06 MAR 72 AT 10:12:59

   SUBROUTINE TORE       ENTRY POINT 000166

   STORAGE USED (BLOCK, NAME, LENGTH)

         0001    *CODE    000207
         0000    *DATA    000033
         0002    *BLANK   000000

   EXTERNAL REFERENCES (BLOCK, NAME)

         0003    SQRT
         0004    ATAN
         0005    NERR3$

   STORAGE ASSIGNMENT FOR VARIABLES (BLOCK, TYPE, RELATIVE LOCATION, NAME)

    0001   000124 3L          0001   000046 5L         0001   000130 6L         0000 R 000000 ARG       0000 R 000001 AI
    0000 R 000002 B           0000   000014 INJP$

  00101      1*              SUBROUTINE TORBU(R,E,F,H,C,DRB,DISP)
  00101      2*     C        DISPLACEMENT AND DRAG FOR A TORROIDAL BUOY WITH CANS
  00101      3*     C        E IS TORROID DIA. (OD) - F IS CAN XSECT AREA
  00103      4*              IF(H-R)4,4,5
  00106      5*            4 CONTINUE
  00107      6*              ARG=(R-H)/R
  00110      7*              AI=(R**2)*(1.572-ATAN(ARG/SQRT(1.0-ARG)))
  00110      8*            1 -(R-H)*SQRT((R**2)-((R-H)**2))
  00111      9*              GO TO 6
  00112     10*            5 CONTINUE
  00113     11*              IF(H-2.0*R)2,3,3
  00116     12*            2 ARG=(R-(2.0*R-H))/R
  00117     13*              AI=3.1416*(R**2)-(R**2)*(1.572-ATAN(ARG/SQRT(1.0-ARG)))
  00117     14*            1 +(H-R)*SQRT((R**2)-((R-H)**2))
  00120     15*              GO TO 6
  00121     16*            3 AI=3.1416*(R**2)
  00122     17*            6 CONTINUE
  00123     18*              B=(E-2.0*R)/2.0
  00124     19*              DRB=(AI+2.0*B*H)*0.6*(C**2)
  00125     20*              DRB=2.0*DRB
  00126     21*              DISP=(6.2832*B*AI+F*H)*64.0
  00127     22*              RETURN
  00130     23*              END

      END OF UNIVAC 1108 FORTRAN V COMPILATION.       0 *DIAGNOSTIC* MESSAGE(S)
```

```
                    PATTON                                          DATE  080372  PAGE   10
   @I FOR CYLBU,CYLBU
   UNIVAC 1108 FORTRAN V LEVEL 2206 0023                                                      10:13: 0.910
   THIS COMPILATION WAS DONE ON 06 MAR 72 AT 10:13:01

      SUBROUTINE CYLBU     ENTRY POINT 000041

      STORAGE USED (BLOCK, NAME, LENGTH)

           0001   *CODE    000054
           0000   *DATA    000014
           0002   *BLANK   000000

      EXTERNAL REFERENCES (BLOCK, NAME)

           0003   NERR3$

      STORAGE ASSIGNMENT FOR V/°IABLES (BLOCK, TYPE, RELATIVE LOCATION, NAME)

       0000   000004 INJP$

 00101     1*          SUBROUTINE CYLBU(BD1,BD2,H,L,RHO,C,DISP,DRB)
 00101     2*    C     DISPLACEMENT AND DRAG OF A CYLINDRICAL BUOY (CAN OR SPAR)
 00103     3*          IF(H.GE.L)H=L
 00105     4*          DISP=25.3*(BD1**2)*RHO*H
 00106     5*          DRB=0.5*RHO*1.4*BD1*H*C*ABS(C)
 00107     6*          RETURN
 00110     7*          END

      END OF UNIVAC 1108 FORTRAN V COMPILATION.      0 *DIAGNOSTIC* MESSAGE(S)
```

```
                    PATTON                                              DATE 060372  PAGE    11
  9I FOR DISBU,DISBU
  UNIVAC 1108 FORTRAN V LEVEL 2206 0023                                                                     10:13: 1.936
  THIS COMPILATION WAS DONE ON 06 MAR 72 AT 10:13:02

     SUBROUTINE DISBU      ENTRY POINT 000134

     STORAGE USED (BLOCK, NAME, LENGTH)

          0001    *CODE    000171
          0000    *DATA    000026
          0002    *BLANK   000000

     EXTERNAL REFERENCES (BLOCK, NAME)

          0003    NERR3$

     STORAGE ASSIGNMENT FOR VARIABLES (BLOCK, TYPE, RELATIVE LOCATION, NAME)

       0001   000046 3L          0001   000057 4L          0001   000124 9L          0000 R 000000 AI          0000   000007 INJP$
       0000 R 000001 RAD

  00101       1*            SUBROUTINE DISBU(R,E,F,L,H,C,DRB,DISP)
  00101       2*      C     DISPLACEMENT AND DRAG FOR A DISC BUOY
  00101       3*      C     E IS HEIGHT OF BEVEL - F IS WIDTH OF BEVEL
  00103       4*            IF(H-E)2,3,3
  00106       5*          2 AI=2.0*R*H-(H**2)*F/E
  00107       6*            DRB=1.2*AI*(C**2)
  00110       7*            RAD=R-F+H*F/E
  00111       8*            DISP=64.0*1.0472*H*((RAD**2)+RAD*(R-F)+((R-F)**2))
  00112       9*            GO TO 9
  00113      10*          3 IF(H-L)4,5,5
  00116      11*          5 H=L
  00117      12*          4 AI=2.0*R*E-E*F+2.0*(H-E)*R
  00120      13*            DRB=1.2*AI*(C**2)
  00121      14*            DISP=64.0*1.0472*E*((R**2)+R*(R-F)+((R-F)**2))+3.1416*(R**2)*(H-E)
  00122      15*          9 RETURN
  00123      16*            END

      END OF UNIVAC 1108 FORTRAN V COMPILATION.       0 *DIAGNOSTIC* MESSAGE(S)
```

```
PATTON                                                              DATE  0F0372  PAGE    12
QI FOR SPHBU,SPHBU
UNIVAC 1108 FORTRAN V LEVEL 2206 0023                                                    10:13: 3.106
THIS COMPILATION WAS DONE ON 06 MAR 72 AT 10:13:03

    SUBROUTINE SPHBU      ENTRY POINT 000075

    STORAGE USED (BLOCK, NAME, LENGTH)

         0001   *CODE   000116
         0000   *DATA   000024
         0002   *BLANK  000000

    EXTERNAL REFERENCES (BLOCK, NAME)

         0003   SQRT
         0004   ATAN
         0005   NERR3$

    STORAGE ASSIGNMENT FOR VARIABLES (BLOCK, TYPE, RELATIVE LOCATION, NAME)

    0001   000010 2L        0000 R 000000 ARG      0000 R 000001 AI        0000    000011 INJP$

 00101      1*          SUBROUTINE SPHBU(R,H,C,DRB,DISP)
 00101      2*     C    DISPLACEMENT AND DRAG FOR A SPHERICAL BUOY
 00103      3*          IF(H-2.0*R)2,3,3
 00106      4*        3 H=2.0*R
 00107      5*        2 ARG=(R-H)/R
 00110      6*          AI=(R**2)*(1.572-ATAN(ARG/SQRT(1.0-ARG)))
 00110      7*         1-(R-H)*SQRT((R**2)-((R-H)**2))        )
 00111      8*          DRB=0.4*AI*(C**2)
 00112      9*          DISP=64.0*3.1416*(R-H/3.0)*(H**2)
 00113     10*          RETURN
 00114     11*          END

      END OF UNIVAC 1108 FORTRAN V COMPILATION.      0 *DIAGNOSTIC* MESSAGE(S)
```

```
PATTON                                                  DATE 060372  PAGE   13

QI FOR RUNGE,RUNGE
UNIVAC 1108 FORTRAN V LEVEL 2206 0023                                         10:13: 4.230
THIS COMPILATION WAS DONE ON 06 MAR 72 AT 10:13:04

    SUBROUTINE RUNGE      ENTRY POINT 000134

    STORAGE USED (BLOCK, NAME, LENGTH)

        0001   *CODE   000163
        0000   *DATA   000053
        0002   *BLANK  000000

    EXTERNAL REFERENCES (BLOCK, NAME)

        0003   NERR2$
        0004   NERR3$

    STORAGE ASSIGNMENT FOR VARIABLES (BLOCK, TYPE, RELATIVE LOCATION, NAME)

    0001    000021 1L        0001   000121 10L       0001   000023 107G      0001   000054 120G      0001   000102 130G
    0001    000030 3L        0001   000032 4L        0001   000036 5L        0001   000074 7L        0001   000117 9L
    0000 R  000021 A         0000 I 000020 I         0000   000033 INJP$     0000 R 000000 G

 00101     1*        SUBROUTINE RUNGE(N,Y,F,X,H,M,K)
 00101     2*  C     THIS ROUTINE PERFORMS RUNGE KUTTA CALCULATIONS BY GILLIS METHOD
 00103     3*        DIMENSION Y(16),F(16),Q(16)
 00104     4*        M=M+1
 00105     5*        GO TO (1,4,5,3,7),M
 00106     6*      1 DO 2 I=1,N
 00111     7*      2 Q(I)=0.0
 00113     8*        A=0.5
 00114     9*        GO TO 9
 00115    10*      3 A=1.707107
 00115    11*  C     IF YOU NEED MORE ACCURACY USE A=1.7071067811865475244
 00116    12*      4 X=X+0.5*H
 00117    13*      5 DO 6 I=1,N
 00122    14*        Y(I)=Y(I)+A*(F(I)*H-Q(I))
 00123    15*      6 Q(I)=2.0*A*H*F(I)+(1.0-3.0*A)*Q(I)
 00125    16*        A=0.2928932
 00125    17*  C     IF YOU NEED MORE ACCURACY USE A=0.2928932188134524756
 00126    18*        GO TO 9
 00127    19*      7 DO 8 I=1,N
 00132    20*      8 Y(I)=Y(I)+H*F(I)/6.0-Q(I)/3.0
 00134    21*        M=0.0
 00135    22*        K=2.0
 00136    23*        GO TO 10
 00137    24*      9 K=1.0
 00140    25*     10 RETURN
 00141    26*        END
```

Buoy System Dynamics for the Spherical Buoy

This program simulates the motions of a spherical buoy exposed to winds, currents, and a random sea. The mooring line is simulated as five, elastically connected, lumped masses. Cable weights, drag forces, and inertia forces are concentrated at each mass. The buoy is allowed six degrees of freedom, and each mooring line mass element is allowed three translational degrees of freedom. With a total of 21 degrees of freedom, 42 first-order differential equations are integrated simultaneously in the time domain.

The equations of motion for the buoy and the development of the forces acting on the buoy are presented in chapter III of the main text. The lumped-mass cable equations are also shown in that chapter.

Major computational procedures in this program are shown in figure B-2. The input data are as follows:

1. Buoy hull radius (ft)
2. Height of the center of gravity of the buoy above the mooring line connection point on the buoy (ft)
3. Height of the mooring line connection point below the buoy hull (ft)
4. Buoy weight (lb)
5. Buoy structural and floodwater mass (lb-sec^2/ft)
6. Yaw mass moment of inertia (lb-sec^2/ft)
7. Pitch mass moment of inertia (lb-sec^2/ft)
8. Roll mass moment of inertia (lb-sec^2/ft)
9. Effective buoy wind drag coefficient (dimensionless)

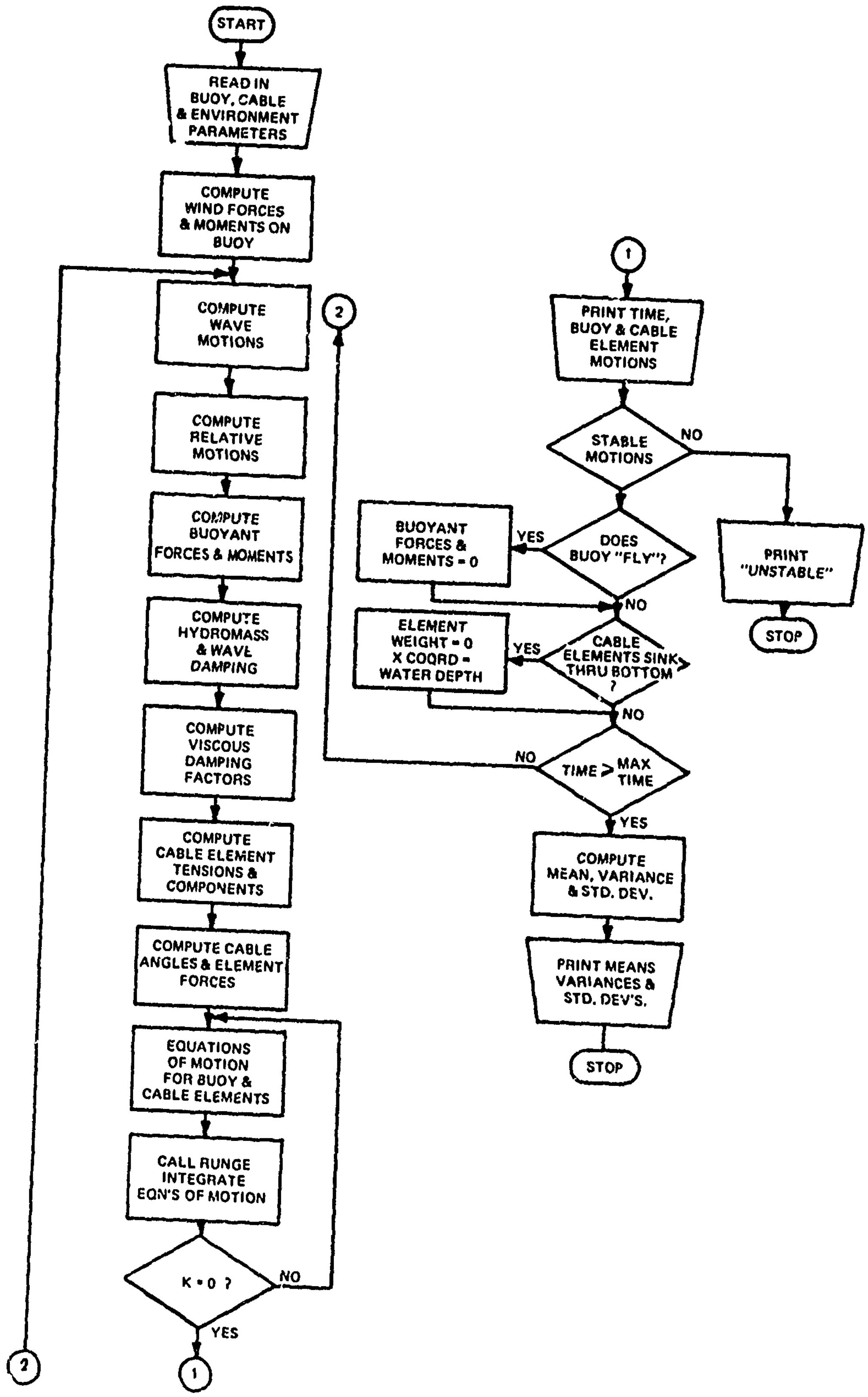

Figure B-2. Spherical Buoy Dynamics Simulation Flow Chart

10. Effective buoy wind lift coefficient (dimensionless)

11. Buoy windage (profile area) (ft^2)

12. Buoy plan area (ft^2)

13. Height of the wind center of pressure above the center of gravity of the buoy (ft)

14. Mean wave height (ft)

15. Mean wave period (sec)

16. The unstretched cable lengths between mass elements (ft) (6 required)

17. Upper mooring line segment diameter (ft)

18. Upper mooring line segment weight in water per unit length (lb/ft)

19. Upper mooring line segment mass per unit length ($lb\text{-}sec^2/ft$)

20. Lower mooring line segment diameter (ft)

21. Lower mooring line segment weight in water per unit length (lb/ft)

22. Lower mooring line segment mass per unit length ($lb\text{-}sec^2/ft$)

23. Surface current y component (ft/sec)

24. Surface current z component (ft/sec)

25. Wind speed y component (ft/sec)

26. Wind speed z component (ft/sec)

27. Initial buoy displacements x, y, and z (ft)

28. Initial cable element displacements (including the anchor clump) x, y, and z for each of 6 sets (ft).

The user of this program should first estimate the highest natural frequency in the system. In general, the upper mooring line segment will be lightest and the highest natural frequencies are in the axial mode along the cable. Using the same variable names as those in the program we can estimate the highest natural frequency:

$$f_{HI} = \frac{1}{2\pi}\sqrt{\frac{2\ EA}{DCSM1 \cdot CLO(2)}} ,$$

where

EA is the cable modulus* (lb)

DCSM1 is the mass per unit length of the upper mooring line segment ($lb\text{-}sec^2/ft^2$)

CLO(2) is the unstretched cable length between the first and second cable mass elements (ft).

It the cable lengths were very short or the cable modulus were very high in the lower mooring line segment, an estimate should be made of its highest natural frequency also.

For numerical stability, the integration step size should be about 1/20th the shortest period present. Thus, the step size is computed:

$$R = 0.05(1/f_{HI}) .$$

In this program, the wave component amplitudes, frequencies, and phase angles are computed externally and are listed in the body of the program (MOMEG, AMP, and PHS). The water depth (DEEP) is also listed, and the x coordinate of the mooring anchor clump should be set equal to the water depth. The total time of the simulation is controlled by a logical "IF" statement (statement

---

*The cable modulus is the product of the cable material elastic modulus and the actual cable cross-sectional area.

no. 491), which shifts to the "STOP" control if the maximum simulated time is exceeded.

In this program, buoy motion output data are not printed for the first 6 sec of simulation as initial transients decay. After this time, the following buoy system outputs are printed every 800 time steps:

Simulation time (sec)

Water particle vertical acceleration (ft/sec^2)

Buoy heave acceleration (ft/sec^2)

Buoy sway acceleration (ft/sec^2)

Buoy surge acceleration (ft/sec^2)

Buoy pitch angle (deg)

Buoy roll angle (deg).

```
BUOY DYNAMICS                                              DATE 100172 PAGE   3

@ FOR S1676,S1676                                                                              15: 8:15.750
UNIVAC 1108 FORTRA' ' LEVEL 2206 0023
THIS COMPILATION W.. DONE ON 10 JAN 72 AT 15:08:15

   MAIN PROGRAM

   STORAGE USED (BLOCK, NAME, LENGTH)

         0001   *CODE    003023
         0000   *DATA    001021
         0002   *BLANK   000000

   EXTERNAL REFERENCES (BLOCK, NAME)

         0003   RUNGE
         0004   NRDC$
         0005   NIO2$
         0006   SIN
         0007   COS
         0010   NWDU$
         0011   SQRT
         0012   HEXP6$
         0013   EXP
         0014   ATAN
         0015   NERR2$
         0016   NSTOP$

   STORAGE ASSIGNMENT FOR VARIABLES (BLOCK, TYPE, RELATIVE LOCATION, NAME)

   0000     000640 102F     0000     000642 103F     0000     000645 105F     0000     000647 106F     0000     000652 107F
   0000     000654 108F     0000     000656 109F     0001     000645 21L      0001     000707 22L      0001     000674 24L
   0001     000725 25L      0001     000753 26L      0001     001003 27L      0001     000325 2716     0001     001023 28L
   0001     001057 30L      0001     000344 3076     0001     001116 31L      0001     001132 32L      0001     001134 33L
   0001     001146 34L      0001     001154 35L      0001     000434 3536     0001     002723 40L      0001     001243 41L
   0001     001253 42L      0001     001303 43L      0001     001273 44L      0001     001455 46L      0001     001442 47L
   0001     001517 49L      0001     000354 5L       0001     002327 50L      0001     002744 51L      0001     002755 52L
   0001     001761 6406     0001     002026 72L      0001     002044 7276     0001     002044 73L      0001     002761 7626
   0001     002773 7706     0001     003017 88L      0001     003012 92L      0000 R   000450 A        0000 R   000635 ALFA
   0000 R   000373 ALIN     0000 R   000465 ALW      0000 R   000305 AMP      0000 R   000505 ANG      0000 R   000555 ARXX
   0000 R   000557 ARYY     0000 R   000560 ARZZ     0000 R   000546 BA       0000 R   000534 BBB      0000 R   000542 BBX
   0000 R   000636 BETA     0000 R   000537 BGG      0000 R   000543 BGX      0000 R   000545 BLAMB    0000 R   000367 BR
   0000 R   000374 BTIN     0000 R   000466 BTW      0000 R   000507 BT1      0000 R   000540 BXB      0000 R   000541 BXG
   0000 R   000530 BXX      0000 R   000502 CABK     0000 R   000576 CHMN     0000 R   000427 CHMN1    0000 R   000430 CHMN2
   0000 R   000575 CHMT     0000 R   000425 CHMT1    0000 R   000426 CHMT2    0000 R   000606 CL       0000 R   000226 CLF
   0000 R   000257 CLO      0000 R   000175 CN       0000 R   000550 CMX      0000 R   000551 CMY      0000 R   000552 CMZ
   0000 R   000553 CNXX     0000 R   000554 CNYY     0000 R   000624 CPHI     0000 R   000615 CPIT     0000 R   000616 CROLL
   0000 R   000574 CSM      0000 R   000423 CSM1     0000 R   000424 CSM2     0000 R   000622 CTHE     0000 R   000625 CUR
   0000 R   000626 CVR      0000 R   000627 CWR      0000 R   000434 CY       0000 R   000432 CYS      0000 R   000435 CZ
   0000 R   000433 CZS      0000 R   000000 D.       0000 R   000473 DALW     0000 R   000514 DAL1     0000 R   000522 DAL2
   0000 R   000474 DBTW     0000 R   000516 DBT1     0000 R   000523 DBT2     0000 R   000407 DCSM1    0000 R   000412 DCSM2
   0000 R   000501 DDALW    0000 R   000502 DDBYW    0000 R   000633 DDBT1    0000 R   000503 DDGMW    0000 R   000634 DDGM1
   0000 R   000476 DDXW     0000 R   000630 DDX1     0000 R   000477 DDYW     0000 R   000631 DDY1     0000 R   000500 DDZW
   0000 R   000632 DDZ1     0000 R   000431 DEEP     0000 R   000564 DGAA     0000 R   000565 DGBB     0000 R   000571 DGBZ
```

```
0000 R 000566 DGGG     0000 R 000572 DGGY     0000 R 000475 DGMW     0000 R 00051- DGM1     0000 R 000524 DGM2
0000 R 000600 DGN      0000 R 000421 DGN1     0000 R 000422 DGN2     0000 R 000577 DGT      0000 R 000417 DGT1
0000 R 000420 DGT2     0000 R 000561 DGXX     0000 R 000567 DGYG     0000 R 000562 DGYY     0000 R 000570 DGZB
0000 R 000563 DGZZ     0000 R 000405 DIA1     0000 R 000410 DIA2     0000 R 000406 DWC1     0000 R 000411 DWC2
0000 R 000470 DXW      0000 R 000511 DX1      0000 R 000517 DX2      0000 R 000471 DYW      0000 R 000512 DY1
0000 R 000520 DY2      0000 R 000472 DZW      0000 R 000513 DZ1      0000 R 000521 DZ2      0000 R 000601 EA
0000 R 000413 EA1      0000 R 000414 EA2      0000 R 000556 ETA      0000 R 000612 FAL      0000 R 000613 FBT
0000 R 000614 FGM      0000 R 000544 FR       0000 R 000607 FX       0000 R 000610 FY       0000 R 000611 FZ
0000 R 000637 GAMMA    0000 R 000375 GMIN     0000 R 000467 GMW      0000 R 000510 GM1      0000 R 000525 H
0000 R 000526 HBT      0000 R 000533 HBTP     0000 R 000527 HGM      0000 R 000536 HGMP     0000 R 000531 HP
0000 I 000453 I        0000 I 000445 J        0000 I 000451 K        0000 I 000617 KI       0000 I 000452 M
0000 R 000347 MB       0000 R 000336 MHAA     0000 R 000334 MHBB     0000 R 000345 MHBX     0000 R 000343 MHBZ
0000 R 000335 MHGG     0000 R 000346 MHGX     0000 R 000344 MHGY     0000 R 000337 MHXB     0000 R 000340 MHXG
0000 R 000331 MHXX     0000 R 000341 MHYG     0000 R 000332 MHYY     0000 R 000342 MHZB     0000 R 000333 MHZZ
0000 R 000273 MOMEG    0000 R 000350 MU       0000 I 000446 N        0000 R 000354 NAA      0000 R 000355 NBB
0000 R 000360 NBX      0000 R 000366 NBZ      0000 R 000356 NGG      0000 R 000362 NGX      0000 R 000364 NGY
0000 I 000620 NT       0000 R 000357 NXB      0000 R 000361 NXG      0000 R 000351 NXX      0000 R 000363 NYG
0000 R 000352 NYY      0000 R 000365 NZB      0000 R 000353 NZZ      0000 R 000404 PER      0000 R 000317 PHS
0000 R 000447 P        0000 R 000623 SPHI     0000 R 000621 STHE     0000 R 000144 T        0000 R 000265 TEN
0000 R 000532 VBB      0000 R 000460 VELBB    0000 R 00046I VELGB    0000 R 000455 VELXG    0000 R 000456 VELYB
0000 R 000457 VELZB    0000 R 000335 VGG      0000 R 000400 WAREA    0000 R 000401 WAREL    0000 R 000372 WB
0000 R 000573 WC       0000 R 000376 WCD      0000 R 000377 WCL      0000 R 000402 WCPHT    0000 R 000415 WC1
0000 R 000416 WC2      0000 R 000443 WFBT     0000 R 000444 WFGM     0000 R 000440 WFX      0000 R 000441 WFY
0000 R 000442 WFZ      0000 R 000454 WHT      0000 R 000403 WHTM     0000 R 000436 WINDY    0000 R 000437 WINDZ
0000 R 000504 WK       0000 R 000370 XCG      0000 R 000547 XHM      0000 R 000371 XML      0000 R 000603 XMPT
0000 R 000462 XW       0000 R 000506 X1       0000 R 000062 Y        0000 R 000604 YMPT     0000 R 000463 YW
0000 R 000605 ZMPT     0000 R 000464 ZW
```

```
00100   C   THIS PROGRAM COMPUTES THE RESPONSE OF AN AXI-SYMMETRIC BUOY
00100   C   EXPOSED TO THE OCEAN ENVRIONMENT
00100   C   UNITS ARE IN FT',LB,SEC
00100   C
00101       DIMENSION D(50),Y(50),T(25),CM(25),CLF(25),CLO(6),TEN(6)
00103       DIMENSION MOMEG(10),AMP(10),PHS(10)
00104       REAL MOMEG
00105       REAL MHXX,MHYY,MHZZ,MHBB,MHGG,MHAA,MHXB,MHXG,MHYG,MHZB,MHBZ
00106       REAL MHGY,MHBX,MHGX,MB,MU,NXX,NYY,NZZ,NAA,NBB,NGG,NXB,NBX
00107       REAL NXG,NGX,NYG,NGY,NZB,NBZ
00107   C   THE COORDINATE SYSTEM
00107   C
00107   C
00107   C
00107   C
00107   C      Z --------   -----------------------------------
00107   C                                                    /I
00107   C                                                   / I
00107   C                                                  /  I
00107   C                                                 /   I
00107   C                                                /    I
00107   C                                               /     I
00107   C                                              /      I
00107   C                                             /       I
00107   C                                            Y        I
00107   C                                                     I
```

```
            BUOY DYNAMICS                                            DATE  100172  PAGE     5
00107    C                                                      I
00107    C                                                      I
00107    C                                                      I
00107    C                                                      I
00107    C                                                      I
00107    C                                                      I
00107    C                                                      I
00107    C                                                      I
00107    C                                                      X
00107    C
0107     C
00110       102 FORMAT(8F10.2)
00111       103 FORMAT(11H BUOY SINKS)
00112       105 FORMAT(6F10.2)
00113       106 FORMAT(9H UNSTABLE)
00114       107 FORMAT(5F10.4)
00115       108 FORMAT(2F10.4)
00116       109 FORMAT(3F10.4)
00116    C      READ IN THE BUOY PARAMETERS
00116    C      BUOY RADIUS, HT. OF C.OF G. FROM MOOR POINT AND THE LENGTH OF THE
00116    C      MOOR POINT BELOW THE BOTTOM OF THE BUOY
00117           READ 109,BR,XCG,XML
00117    C      INERTIAS
00124           READ 107,WB,MB,ALIN,BTIN,GMIN
00124    C      WIND LIFT AND DRAG COEFFICIENTS AND AREAS
00133           READ 107,WCD,WCL,WAREA,WAREL,WCPHT
00133    C
00133    C      THE VISCOSITY OF THE WATER AT 40 DEG F
00142           MU=2.735E-5
00142    C
00142    C      THE WAVE PARAMETERS
00143           READ 108,WHTM,PER
00147           MOMEG(1)=1.7337
00150           MOMEG(2)=2.2326
00151           MOMEG(3)=2.3953
00152           MOMEG(4)=2.5665
00153           MOMEG(5)=2.7613
00154           MOMEG(6)=3.0013
00155           MOMEG(7)=3.3310
00156           MOMEG(8)=3.8899
00157           MOMEG(9)=682.07
00160           AMP(1)=0.3046
00161           AMP(2)=0.1565
00162           AMP(3)=0.1563
00163           AMP(4)=0.1562
00164           AMP(5)=0.1561
00165           AMP(6)=0.1559
00166           AMP(7)=0.1555
00167           AMP(8)=0.1537
00170           AMP(9)=0.0
00171           PHS(1)=0.657
00172           PHS(2)=0.435
00173           PHS(3)=5.545
00174           PHS(4)=3.220
00175           PHS(5)=0.575
00176           PHS(6)=5.20
00177           PHS(7)=4.655
00200           PHS(8)=6.255
```

```
      PHS(9)=0.306
C
C     THE CABLE PARAMETERS
C     THE CABLE LENGTHS BETWEEN ELEMENTS
      READ 105,CLO(1),CLO(2),CLO(3),CLO(4),CLO(5),CLO(6)
C     THE UPPER CABLE PROPERTIES
      READ 109,DIA1,DWC1,DCSM1
C     THE LOWER CABLE PROPERTIES
      READ 109,DIA2,DWC2,DCSM2
      EA1=2.16E5
      EA2=EA1
      WC1=DWC1*CLO(1)
      WC2=DWC2*CLO(5)
      DGT1=0.05*DIA1*CLO(1)
      DGT2=0.2*DIA2*CLO(5)
      DGN1=1.2*DIA1*CLO(1)
      DGN2=1.2*DIA2*CLO(5)
      CSM1=DCSM1*CLO(1)
      CSM2=DCSM2*CLO(5)
      CHMT1=0.0
      CHMT2=0.753*(DIA2**2)*CLO(5)
      CHMN1=1.56*(DIA1**2)*CLO(1)
      CHMN2=1.56*(DIA2**2)*CLO(5)
C     THE WATER DEPTH
      DEEP=62.0
C
C     THE CURRENTS IN THE WATER COLUMN
C     READ THE Y AND Z COMPONENTS OF THE  SURFACE CURRENT
      READ 108,CYS,CZS
C     IF THE CURRENT VARIES WITH DEPTH, INSERT THE FUNCTIONS FOR
C     STRENGTH AND DIRECTION
C
C     FOR A UNIFORM CURRENT
      CY=CYS
      CZ=CZS
C
C     THE WIND ACTING ON THE BUOY
C     READ THE Y AND Z COMPONENTS OF THE MEAN WIND
      READ 108,WINDY,WINDZ
      WFX=-0.0034*WCL*WAREL*(WINDY**2+WINDZ**2)
      WFY=0.0034*WCD*WAREA*WINDY*ABS(WINDY)
      WFZ=0.0034*WCD*WAREA*WINDZ*ABS(WINDZ)
      WFBT=-WFZ*WCPHT
      WFGM=-WFY*WCPHT
      J=1
      N=42
      R=0.0005
      A=0.0
      K=0
      M=0
C     THE INITIAL CONDITIONS
C     ALL ACCELERATIONS AND VELOCITIES ARE ZERO
      DO 58 I=1,41,2
      D(I)=0.0
   58 Y(I)=0.0
C     READ THE INITIAL BUOY DISPLACEMENTS - X,Y,Z
      READ 109,Y(2),Y(4),Y(6)
C     THE INITIAL BUOY ANGLES ARE ZERO
```

```
00303          Y(8)=0.0
00304          Y(10)=0.0
00305          Y(12)=0.0
00305    C     READ THE INITIAL CABLE DISPLACEMENTS
00306          DO 53 I=14,44,6
00311       53 READ 109,Y(I),Y(I+2),Y(I+4)
00317        5 CONTINUE
00320          WHT=A*WHTM/(2.0*PER)
00321          IF(A.GE.(2.0*PER))WHT=WHTM
00323          VELXB=Y(1)
00324          VELYB=Y(3)
00325          VELZB=Y(5)
00326          VELBB=Y(9)
00327          VELGB=Y(11)
00327    C     THE WAVES
00327    C     FOR A SINGLE TRAIN OF WAVES, ASSUME THEY ARE COMING IN ON THE
00327    C     Z AXIS
00330          XW=0.0
00331          YW=0.0
00332          ZW=0.0
00333          ALW=0.0
00334          BTW=0.0
00335          GMW=0.0
00336          DXW=0.0
00337          DYW=0.0
00340          DZW=0.0
00341          DALW=0.0
00342          DBTW=0.0
00343          DGMW=0.0
00344          DDXW=0.0
00345          DDYW=0.0
00346          DDZW=0.0
00347          DDALW=0.0
00350          DDBTW=0.0
00351          DDGMW=0.0
00352          DO 14 I=1,9
00355          WK=(MOMEG(I)**2)/32.2
00356          ANG=A*MOMEG(I)+PHS(I)
00357          XW=XW-AMP(I)*SIN(ANG)
00360          ZW=ZW+AMP(I)*COS(ANG)
00361          BTW=BTW+WK*AMP(I)*COS(ANG)
00362          DXW=DXW-MOMEG(I)*AMP(I)*COS(ANG)
00363          DZW=DZW-MOMEG(I)*AMP(I)*SIN(ANG)
00364          DBTW=DBTW-WK*MOMEG(I)*AMP(I)*SIN(ANG)
00365          DDXW=DDXW+(MOMEG(I)**2)*AMP(I)*SIN(ANG)
00366          DDZW=DDZW-(MOMEG(I)**2)*AMP(I)*COS(ANG)
00367       14 DDBTW=DDBTW-WK*(MOMEG(I)**2)*AMP(I)*COS(ANG)
00367    C
00367    C     THE BUOY MOTIONS RELATIVE TO THE WATER MASS
00367    C     DISPLACEMENTS
00371          X1=Y(2)-XW
00372          BT1=Y(10)-BTW
00373          GM1=Y(12)-GMW
00373    C     VELOCITIES
00374          DX1=Y(1)-DXW
00375          DY1=Y(3)-DYW
00376          DZ1=Y(5)-DZW
00377          DAL1=Y(7)-DALW
```

```
00400          DGM1=Y(11)-DGMW
00401          DBT1=Y(9)-DBTW
00402          UGM1=Y(11)
00402     C
00402     C    WATER MASS VELOCITIES RELATIVE TO THE BUOY INCLUDING CURRENTS
00403          UX2=UX1
00404          UY2=UY1-CY
00405          UZ2=UZ1-CZ
00406          UAL2=UAL1
00407          UBT2=UBT1
00410          DGM2=DGM1
00410     C
00410     C    THE COEFFICIENTS FOR A SPHERICAL BUOY
00410     C
00410     C    THE BUOYANCY FORCES AND MOMENTS
00411          H=XCG+X1-XML
00412          IF(H.LE.0.0)H=0.0
00414          HBT=H+(BR+XML-XCG)*(1.0-COS(BT1))
00415          HGM=H+(BR+XML-XCG)*(1.0-COS(GM1))
00415     C    HEAVE BUOYANT FORCE,BXX
00416          IF(H.GE.BR)GO TO 21
00420          BXX=67.1*(H**2)*(3.0*BR-H)
00421          GO TO 22
00422       21 IF(H.GE.(2.0*BR))GO TO 24
00424          HP=2.0*BR-H
00425          BXX=268.4*(BR**3)-67.1*(HP**2)*(3.0*BR-HP)
00426          GO TO 22
00427       24 BXX=268.4*(BR**3)
00430          WRITE(4,103)
00432          GO TO 30
00432     C    PITCH BUOYANT MOMENT,BBB
00433       22 IF(HBT.GE.BR)GO TO 25
00435          VBB=67.1*(HBT**2)*(3.0*BR-HBT)
00436          GO TO 26
00437       25 IF(HBT.GE.(2.0*BR))GO TO 30
00441          HBTP=2.0*BR-HBT
00442          VBB=268.4*(BR**3)-67.1*(HBTP**2)*(3.0*BR-HBTP)
00443       26 BBB=VBB*(BR+XML-XCG)*SIN(BT1)
00443     C    ROLL BUOYANT MOMENT
00444          IF(HGM.GE.BR)GO TO 27
00446          VGG=67.1* (HGM**2)*(3.0*BR-HGM)
00447          GO TO 28
00450       27 HGMP=2.0*BR-HGM
00451          VGG=268.4*(BR**3)-67.1*(HGMP**2)*(3.0*BR-HGMP)
00452       28 BGG=VGG*(BR+XML-XCG)*SIN(GM1)
00452     C    HEAVE-PITCH BUOYANT FORCE  ,BXB
00453          BXB=VBB-BXX
00453     C    HEAVE-ROLL BUOYANT FORCE, BXG
00454          BXG=VGG-BXX
00454     C    PITCH-HEAVE BUOYANT MOMENT,BBX
00455          BBX=BXB*(BR+XML-XCG)*SIN(BT1)
00455     C    ROLL-HEAVE BUOYANT MOMENT,BGX
00456          BGX=BXG*(BR+XML-XCG)*SIN(GM1)
00457       30 CONTINUE
00457     C
00457     C    THE HYDRODYNAMIC MASSES AND MOMENTS OF INERTIA
00457     C
00457     C    THE DIMENSIONLESS FREQUENCY
```

```
      FR=((6.2832/PER)**2)*BR/32.2
      BLAMB=SQRT(6.25/(PER*MU))
      BA=BLAMB*BR
C     HYDRODYNAMIC FORCE MOMENT ARM
      XHM=XLG-XML-0.625*H
C     HEAVE
      IF(FR.GE.0.1)GO TO 31
      CMX=1.85
      GO TO 33
   31 IF(FR.GE.3.4)GO TO 32
      CMX=1.02*(FR**(-.256))
      GO TO 33
   32 CMX=1.0
C     SWAY-SURGE
   33 IF(FR.GE.0.74)GO TO 34
      CMY=1.069+0.529*FR
      GO TO 35
   34 CMY=1.0/(-0.0318+0.954*FR)
   35 CMZ=CMY
      MHXX=1.988*(BR**3)*CMX
      MHYY=1.988*(BR**3)*CMY
      MHZZ=1.988*(BR**3)*CMZ
C     YAW
      MHAA=16.65*(BR**5)*(1.0+BA)/(1.0+2.0*BA+2.0*(BA**2))
C     PITCH AND ROLL
      MHBB=MHZZ*(XHM**2)
      MHGG=MHBB
C     CROSS-COUPLED HYDROMASSES
      MHBX=0.0
      MHGX=0.0
      MHXB=0.0
      MHXG=0.0
      MHYG=-MHYY*XHM
      MHZB=-MHYG
      MHBZ=MHZB
      MHGY=MHYG
C
C     THE DAMPING DUE TO WAVE GENERATION
C
C     HEAVE
      IF(FR.GE.0.4)GO TO 41
      CNXX=0.126+0.17*FR
      GO TO 42
   41 CNXX=1.18*EXP(-0.83*FR)
   42 IF(FR.LE.0.1)CNYY=0.0
      IF(FR.GE.1.37)GO TO 44
      CNYY=-0.069+0.71*FR
      GO TO 43
   44 CNYY=1.595*EXP(-0.415*FR)
   43 NXX=1.988*FR*(BR**3)*CNXX
      NYY=1.988*FR*(BR**3)*CNYY
      NZZ=NYY
C     PITCH AND ROLL
      NAA=4.195*MU*(BR**3)*(3.0+6.0*BA+6.0*(BA**2)+2.0*(BA**3))
     1 /(1.0+2.0*BA+2.0*(BA**2))
      NBB=NAA+NZZ*(XHM**2)
      NGG=NBB
C     CROSS COUPLED WAVE DAMPING
```

```
00543           NXB=0.0
00544           NBX=0.0
00545           NXG=0.0
00546           NGX=0.0
00547           NYG=-NYY*XHM
00550           NZB=-NYG
00551           NBZ=NZB
00552           NGY=NYG
00552     C
00552     C     THE VISCOUS DAMPING AND DRAG
00552     C     AREAS
00553           ARXX=3.1416*(BR**2)
00554           IF(H.GT.(0.95*BR))GO TO 47
00556           ETA=2.0*ATAN((SQRT(2.0*H*BR-(H**2)))/(BR-H))
00557           ARYY=0.5*(BR**2)*(ETA-SIN(ETA))
00560           GO TO 49
00561        47 IF(H.GT.(1.05*BR))GO TO 46
00563           ARYY=1.5708*(BR**2)
00564           GO TO 49
00565        46 HP=2.0*BR-H
00566           ETA=2.0*ATAN((SQRT(2.0*HP*BR-(HP**2)))/(BR-HP))
00567           ARYY=(BR**2)*(3.1416-0.5*(ETA-SIN(ETA)))
00570        49 ARZZ=ARYY
00571           IF(H.GE.(2.0*BR))ARYY=3.1416*(BR**2)
00573           DGXX=0.497*ARXX
00574           DGYY=0.497*ARZZ
00575           DGZZ=0.497*ARZZ
00576           DGAA=0.0
00577           DGBB=0.0
00600           DGGG=0.0
00600     C     CROSS-COUPLED VISCOUS DRAG
00601           DGYG=-DGYY*(XHM**2)
00602           DGZB=-DGYG
00603           DGBZ=DGZB
00604           DGGY=DGYG
00604     C
00604     C     TENSIONS AND FORCES FOR THE 5 ELEMENT LUMP MASSCABLE MODEL
00604     C     THE FIRST THREE ELEMENTS ARE CABLE. THE LAST TWO ARE CHAIN
00605           WC=WC1
00606           CSM=CSM1
00607           CHMT=CHMT1
00610           CHMN=CHMN1
00611           DGT=DGT1
00612           DGN=DGN1
00613           EA=EA1
00614           CABK=EA/CLO(1)
00615           XMPT=Y(2)+XCG*COS(Y(10))*COS(Y(12))
00616           YMPT=Y(4)-XCG*COS(Y(10))*SIN(Y(12))
00617           ZMPT=Y(6)+XCG*SIN(Y(10))*COS(Y(12))
00620           CL=SQRT(((XMPT-Y(14))**2)+((YMPT-Y(16))**2)+((ZMPT-Y(18))**2))
00621           TEN(1)=CABK*(CL-CLO(1))
00622           IF(TEN(1).LE.0.0)TEN(1)=0.0
00624           T(4)=TEN(1)*(Y(14)-XMPT)/CL
00625           T(5)=TEN(1)*(Y(16)-YMPT)/CL
00626           T(6)=TEN(1)*(Y(18)-ZMPT)/CL
00626     C     ADD 30 LBS. TO ACCOUNT FOR THE INSTRUMENT PACKAGE UNDER THE BUOY
00627           FX=T(4)+30.0
00630           FY=T(5)
```

```
00631          FZ=T(6)
00632          FAL=0.0
00633          FBT=-XCG*(-FZ*COS(Y(10))*COS(Y(12))+FX*SIN(Y(10))*COS(Y(12)))
00634          FGM=-XCG*(FY*COS(Y(10))*COS(Y(12))+FX*SIN(Y(12))*COS(Y(10)))
00635          CPIT=57.4*ATAN((Y(18)-ZMPT)/(Y(14)-XMPT))
00636          CROLL=57.4*ATAN((Y(16)-YMPT)/SQRT((Y(14)-XMPT)**2+(Y(18)-ZMPT)
00636         1 **2))
00637          DO 71 I=13,37,6
00642          KI=((I-1)/2)-2
00643          NT=((I-1)/6)
00644          CL=SQRT(((Y(I+1)-Y(I+7))**2)+((Y(I+3)-Y(I+9))**2)+
00644         1 ((Y(I+5)-Y(I+11))**2))
00645          IF(NT.GE.4)GO TO 72
00647          GO TO 73
00647    C     CHARACTERISTICS OF THE LOWER PART OF THE MOORING LINE
00650       72 WC=WC2
00651          CSM=CSM2
00652          CHMT=CHMT2
00653          CHMN=CHMN2
00654          DGT=DGT2
00655          DGN=DGN2
00656          EA=EA2
00657       73 CABK=EA/CLO(NT)
00660          TEN(NT)=CABK*(CL-CLO(NT))
00661          IF(TEN(NT).LE.0.0)TEN(NT)=0.0
00661    C     THE TENSION COMPONENTS
00663          T(KI+3)=TEN(NT)*(Y(I+7)-Y(I+1))/CL
00664          T(KI+4)=TEN(NT)*(Y(I+9)-Y(I+3))/CL
00665          T(KI+5)=TEN(NT)*(Y(I+11)-Y(I+5))/CL
00665    C     THE SINES AND COSINES OF THE CABLE ANGLES
00666          STHE=(Y(I+11)-Y(I+5))/SQRT(((Y(I+1)-Y(I+7))**2)
00666         1 +((Y(I+5)-Y(I+11))**2))
00667          CTHE=(Y(I+7)-Y(I+1))/SQRT(((Y(I+1)-Y(I+7))**2)
00667         1 +((Y(I+5)-Y(I+11))**2))
00670          SPHI=(Y(I+9)-Y(I+3))/CL
00671          CPHI=SQRT(((Y(I+1)-Y(I+7))**2)+((Y(I+5)-Y(I+11))**2))/CL
00672          CM(KI)=CSM+CHMT*CPHI*CTHE
00673          CM(KI+1)=CSM+CHMN*CPHI
00674          CM(KI+2)=CSM+CHMN*CTHE
00675          CUR=Y(I)*CPHI*CTHE+(Y(I+2)-CY)*SPHI+(Y(I+4)-CZ)*CPHI*STHE
00676          CVR=-Y(I)*SPHI*CTHE+(Y(I+2)-CY)*CPHI-(Y(I+4)-CZ)*SPHI*STHE
00677          CWR=-Y(I)*STHE+(Y(I+4)-CZ)*CTHE
00700          CLF(KI)=DGT*CPHI*CTHE*CUR*ABS(CUR)-DGN*SPHI*CTHE*CVR*ABS(CVR)
00700         1 -DGN*STHE*CWR*ABS(CWR)
00701          CLF(KI+1)=DGT*SPHI*CUR*ABS(CUR)+DGN*CPHI*CVR*ABS(CVR)
00702       71 CLF(KI+2)=DGT*CPHI*STHE*CUR*ABS(CUR)-DGN*SPHI*STHE*CVR*ABS(CVR)
00702         1 +DGN*CTHE*CWR*ABS(CWR)
00704       50 CONTINUE
00705          DDX1=(Y(1)-VELXB)/R
00706          DDY1=(Y(3)-VELYB)/R
00707          DDZ1=(Y(5)-VELZB)/R
00710          DDBT1=(Y(9)-VELBB)/R
00711          DDGM1=(Y(11)-V'LGB)/R
00711    C
00711    C     THE EQUATIONS OF MOTION FOR THE BUOY
00711    C
00711    C     HEAVE -X MOTION
00712          D(1)=(WB-BXX-BXB-BXG+MHXX*DDXW-MHXB*DDBT1-MHXG*DDGM1-NXX*DX1
```

```
00712          1 -NXB*DBT1-NXG*DGM1-DGXX*DX2*ABS(DX2)+WFX+FX)/(MB+MHXX)
00713            D(2)=Y(1)
00713      C
00713      C     SWAY - Y MOTION
00714            D(3)=(MHYY*DDYW-MHYG*DDGM1-NYY*DY1-NYG*DGM1-DGYY*DY2*ABS(DY2)
00714          1 -DGYG*DGM2*ABS(DGM2)+WFY+FY)/(MB+MHYY)
00715            D(4)=Y(3)
00715      C
00715      C     SURGE - Z MOTION
00716            D(5)=(MHZZ*DDZW-MHZB*DDBT1-NZZ*DZ1-NZB*DBT1-DGZZ*DZ2*ABS(DZ2)
00716          1 -DGZB*DBT2*ABS(DBT2)+WFZ+FZ)/(MB+MHZZ)
00717            D(6)=Y(5)
00717      C
00717      C     YAW - ALFA MOTION
00720            D(7)=(MHAA*DDALW-NAA*DAL1-DGAA*DAL2*ABS(DAL2)+FAL)/(ALIN+MHAA)
00721            D(8)=Y(7)
00721      C
00721      C     PITCH - BETA MOTION
00722            D(9)=(-BBX-BBB-MHBX*DDX1-MHBZ*DDZ1+MHBB*DDBTW-NBX*DX1-NBB*DBT1
00722          1 -NBZ*DZ1-DGBZ*DZ2*ABS(DZ2)-DGBB*DBT2*ABS(DBT2)+WFBT+FBT)/
00722          2 (BTIN+MHBB)
00723            D(10)=Y(9)
00723      C
00723      C     ROLL- GAMMA MOTION
00724            D(11)=(-BGX-BGG-MHGX*DDX1-MHGY*DDY1+MHGG*DDGMW-NGX*DX1-NGY*DY1
00724          1 -NGG*DGM1-DGGY*DY2*ABS(DY2)-DGGG*DGM2*ABS(DGM2)+WFGM+FGM)/
00724          2 (GMIN+MHGG)
00725            D(12)=Y(11)
00725      C     EQUATIONS OF MOTION FOR A 5 LUMP MODEL
00726            DO 81 I=13,37,6
00731            KI=((I-1)/2)-2
00731      C     ELEMENT X MOTION
00732            D(I)=(-T(KI)+T(KI+3)-CLF(KI))/CM(KI)
00733            D(I+1)=Y(I)
00733      C     ELEMENT Y MOTION
00734            D(I+2)=(-T(KI+1)+T(KI+4)-CLF(KI+1))/CM(KI+1)
00735            D(I+3)=Y(I+2)
00735      C     ELEMENT Z MOTION
00736            D(I+4)=(-T(KI+2)+T(KI+5)-CLF(KI+2))/CM(KI+2)
00737         81 D(I+5)=Y(I+4)
00737      C
00741            CALL RUNGE(N,Y,D,A,R,M,K)
00742            GO TO (50,40),K
00743         40 ALFA=57.4*Y(8)
00744            BETA=57.4*Y(10)
00745            GAMMA=57.4*Y(12)
00746            IF(J.EQ.200)GO TO 51
00750            J=J+1
00751            GO TO 52
00752         51 CONTINUE
00753            WRITE(4,108)A,D(1)
00757            J=1
00760         52 CONTINUE
00760      C     INSTABILITY LIMITER
00761            DO 60 I=1,N
00764         60 IF(Y(I).GE.10000.0)GO TO 92
00764      C     THE CABLE ELEMENTS CANT SINK THRU THE BOTTOM
00767            DO 218 I=14,38,6
```

```
00772   492*     218 IF(Y(1).GE.DEEP)Y(I)=DEEP
00775   493*         IF(A.GE.26.0)GO TO 88
00777   494*         GO TO 5
01000   495*      92 WRITE(4,106)
01002   496*      88 STOP
01003   497*         END

       END OF UNIVAC 1106 FORTRAN V COMPILATION.     0 *DIAGNOSTIC* MESSAGE(S)
```

```
                BUOY DYNAMICS                                          DATE  100172  PAGE    14

GI FOR RUNGE,RUNGE                                                                                      15: 8:22.132
UNIVAC 1108 FORTRAN V LEVEL 2206 0023
THIS COMPILATION WAS DONE ON 10 JAN 72 AT 15:08:22

   SUBROUTINE RUNGE      ENTRY POINT 000134

   STORAGE USED (BLOCK, NAME, LENGTH)

         0001   *CODE   000163
         0000   *DATA   000115
         0002   *BLANK  000000

   EXTERNAL REFERENCES (BLOCK, NAME)

         0003   NERR2$
         0004   NERR3$

   STORAGE ASSIGNMENT FOR VARIABLES (BLOCK, TYPE, RELATIVE LOCATION, NAME)

    0001    000021 1L         0001    000121 10L        0001    000023 107G       0001    000054 120G       0001    000102 130G
    0001    000030 3L         0001    000032 4L         0001    000036 5L         0001    000074 7L         0001    000117 9L
    0000 R  000063 A          0000 I  000062 I          0000    000075 INJP$      0000 R  000000 Q

00101       1*             SUBROUTINE RUNGE(N,Y,F,X,H,M,K)
00101       2*     C       THIS ROUTINE PERFORMS RUNGE KUTTA CALCULATIONS BY GILL'S METHOD
00103       3*             DIMENSION Y(50),F(50),Q(50)
00104       4*             M=M+1
00105       5*             GO TO (1,4,5,3,7),M
00106       6*           1 DO 2 I=1,N
00111       7*           2 Q(I)=0.0
00113       8*             A=0.5
00114       9*             GO TO 9
00115      10*           3 A=1.707107
00115      11*     C       IF YOU NEED MORE ACCURACY USE A=1.7071067811865475244
00116      12*           4 X=X+0.5*H
00117      13*           5 DO 6 I=1,N
00122      14*             Y(I)=Y(I)+A*(F(I)*H-Q(I))
00123      15*           6 Q(I)=2.0*A*H*F(I)+(1.0-3.0*A)*Q(I)
00125      16*             A=0.2928932
00125      17*     C       IF YOU NEED MORE ACCURACY USE A=0.29289321881345247 56
00126      18*             GO TO 9
00127      19*           7 DO 8 I=1,N
00132      20*           8 Y(I)=Y(I)+H*F(I)/6.0-Q(I)/3.0
00134      21*             M=0.0
00135      22*             K=2
00136      23*             GO TO 10
00137      24*           9 K=1
00140      25*          10 RETURN
00141      26*             END
```

Buoy System Dynamics for the Torroidal Buoy at Station BRAVO

The previous program, developed for the spherical buoy, was modified to simulate the torroidal buoy dynamics. As indicated in figure B-3, the basic computational procedures remain the sàme as for the spherical buoy. However, the wave component amplitudes, frequencies, and phase angles are computed in a subroutine (RWAVE) in the program and do not have to be listed in the program. The buoyant forces and moments for the torroidal buoy are also computed in a subroutine (TORBU) using an integration method developed in appendix E. Finally, since the output motions were to be displayed as spectrum, subroutines using Fast Fourier Transform (FFT) methods were employed to compute the spectra.

Buoy hull hydrodynamic force functions in the program were modified according to Kim's data for a half-beam to draft ratio of 3.2:1. Terms are included to account for the hydrodynamic mass and drag of the three-leg chain bridle under the buoy, and the effective hydrodynamic centers are modified to account for the bridle. The computed inputs for the torroidal buoy are shown in appendix D.

A three-element, lumped-mass cable model was used in this simulation since the actual masses in the system were concentrated at three places along the mooring line (the current meter, the sentinel, and halfway down the 3/4-in. chain). Initial runs using a five-lump cable model were compared with runs using a three-lump cable model, and no significant difference in buoy motions was noted. However, there was an order of magnitude increase in computational speed since the two, high-natural-frequency cable lumps were summed into the

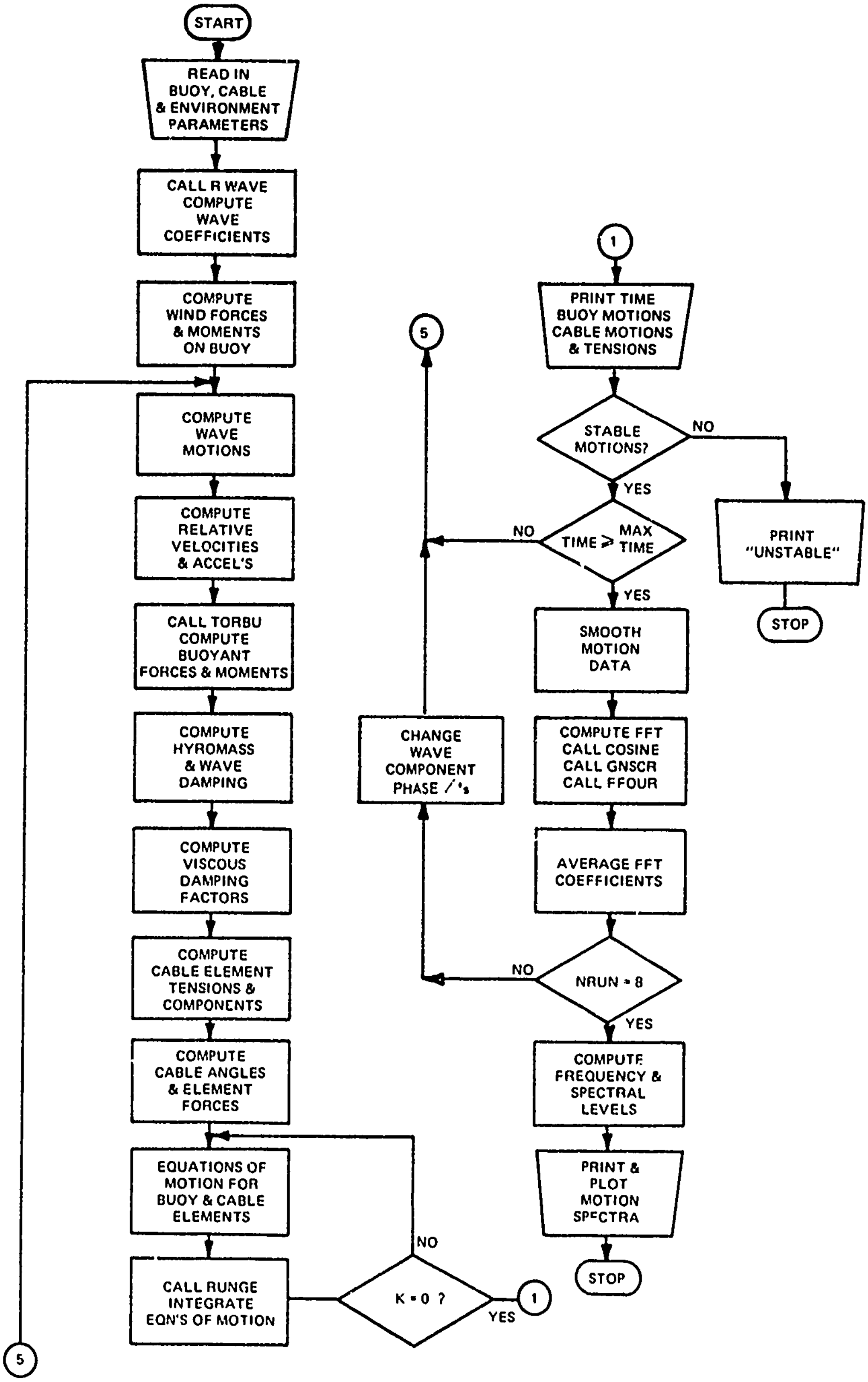

Figure B-3. Torroidal Buoy BRAVO Dynamics Simulation Flow Chart current meter lump.

Input data for this program are as follows:

1. Buoy hull radius (ft)

2. Height of the center of gravity of the buoy above the mooring line connection point on the buoy (ft)

3. Height of the mooring line connection point below the buoy hull (ft)

4. Buoy weight (lb)

5. Buoy structural and floodwater mass (lb-sec^2/ft)

6. Yaw mass moment of inertia (lb-sec^2/ft)

7. Pitch mass moment of inertia (lb-sec^2/ft)

8. Roll mass moment of inertia (lb-sec^2/ft)

9. Effective buoy wind drag coefficient (dimensionless)

10. Effective buoy wind lift coefficient (dimensionless)

11. Buoy windage (profile area) (ft^2)

12. Buoy plan area (ft^2)

13. Height of the wind center of pressure above the center of gravity of the buoy (ft)

14. Mean wind speed causing the wind waves (ft/sec)

15. Wind duration (hr)

16. Surface current y component (ft/sec)

17. Surface current z component (ft/sec)

18. Wind y component (ft/sec)

19. Wind z component (ft/sec)

20. Initial displacements of the buoy x, y, and z (ft)

21. Initial cable displacements (including the anchor clump) x, y, and z for each of four sets (ft)

Again, the user should estimate the highest natural frequency in the system and adjust the integration step size as required. Computed buoy motions are sampled every 12th time step, and 1024, or 2^{10}, samples are stored. Simple statistical estimates (mean, variance, and standard deviation) of the output motions are computed. Each data point is smoothed to reduce aliasing by averaging with the four data points closest to it in time. Spectra are computed using FFT subroutines and are smoothed for plotting. Statements 557 through 595 plot the spectral levels in dB. A Stromberg Datagraphics, Inc. integrated graphics system peripheral to the Naval Underwater Systems Center UNIVAC 1108 computer was used for this procedure.

```
                 BUOY DYNAMICS                                          DATE  230272  PAGE     3

@ FOR S1676,S1676                                                                                            12:43:57. 53
UNIVAC 1108 FORTRAN V LEVEL 2206 0023
THIS COMPILATION WAS DONE ON 23 FEB 72 AT 12:43:57

  MAIN PROGRAM

  STORAGE USED (BLOCK, NAME, LENGTH)

       0001    *CODE    003731
       0000    *DATA    045324
       0002    *BLANK   000000


  EXTERNAL REFERENCES (BLOCK, NAME)

       0003    R#AVE
       0004    TORBU
       0005    RUNGE
       0006    DSTAT
       0007    COSINE
       0010    GNSCR
       0011    FFOUR
       0012    MODESG
       0013    OBJCTG
       0014    SUBJEG
       0015    GRIDG
       0016    LABELG
       0017    TITLEG
       0020    LINESG
       0021    PAGEG
       0022    EXITG
       0023    NRDC$
       0024    NIO2$
       0025    SIN
       0026    COS
       0027    SQRT
       0030    NEXP6$
       0031    EXP
       0032    NERR2$
       0033    NWDU$
       0034    ALOG10
       0035    NSTOP$


  STORAGE ASSIGNMENT FOR VARIABLES (BLOCK, TYPE, RELATIVE LOCATION, NAME)

 0001    002501 1003G      0001    002567 1021G      0000    015022 103F       0001    002604 1030G      0001    002640 1042G
 0000    015025 105F       0000    015027 106F       0000    015032 107F       0000    015034 108F       0000    015036 109F
 0000    015040 112F       0000    015042 116F       0000    015045 117F       0000    01505* 120F       0000    015052 121F
 0000    015054 122F       0000    015056 123F       0000    015060 124F       0000    015062 127F       0001    003405 130L
 0001    003503 131L       0001    003531 132L       0001    003557 133L       0001    003605 134L       0001    003633 135L
 0001    003661 136L       0001    000217 262G       0001    000230 274G       0001    000576 31L        0001    000247 312G
 0001    000612 32L        0001    000264 326G       0001    000614 33L        0001    000355 374G       0001    002117 40L
 0001    000707 41L        0001    000717 42L        0001    002601 450L       0001    000275 5L         0001    001513 50L
 0001    000257 500L       0001    002145 51L        0001    002167 52L        0001    001173 556G       0001    002040 641G
```

```
0001     002171 701G     0001     002203 707G     0001     002330 757G     0001     002221 88L      0001     003725 89L
0001     003712 92L      0000 R 014612 A          0000 R 021160 ACX        0000 R 015007 ACXC       0000 R 025160 ACY
0000 R 015010 ACYC       0000 R 031160 ACZ        0000 R 015011 ACZC       0000 R 014756 ALFA       0000 R 014552 ALIN
0000 R 014626 ALW        0000 R 000305 AMP        0000 R 014646 ANG        0000 R 014707 ARXX       0000 R 014764 AXMN
0000 R 014766 AXSD       0000 R 014765 AXVR       0000 R 014767 AYMN       0000 R 014771 AYSD       0000 R 014770 AYVR
0000 R 014772 AZMN       0000 R 014774 AZSD       0000 R 014773 AZVR       0000 R 014700 BA         0000 R 014670 BBB
0000 R 014672 BBX        0000 R 014757 BETA       0000 R 014673 BGG        0000 R 014675 BGX        0000 I 014507 BIN
0000 R 014677 BLAMB      0000 R 035160 BPIT       0000 R 015012 BPITC      0000 R 014775 BPMN       0000 R 014777 BPSD
0000 R 014776 BPVR       0000 R 014546 BR         0000 R 015000 BRMN       0000 R 041160 BROL       0000 R 015013 BROLC
0000 R 015002 BRSD       0000 R 015001 BRVR       0000 R 014553 BTIN       0000 R 014627 BTW        0000 R 014650 BT1
0000 R 014671 BXB        0000 R 014674 BXG        0000 R 014667 BXX        0000 R 014724 CABK       0000 R 000343 CHMN
0000 R 000336 CHMT       0000 R 014730 CL         0000 R 000226 CLF        0000 R 000257 CLO        0000 R 000175 CM
0000 R 014702 CMX        0000 R 014703 CMY        0000 R 014704 CMZ        0000 R 014705 CNXX       0000 R 014706 CNYY
0000 R 000367 COSI       0000 R 014745 CPHI       0000 R 000331 CSM        0000 R 014743 CTHE       0000 R 014746 CUR
0000 R 014747 CVR        0000 R 014750 CWR        0000 R 014573 CY         0000 R 014571 CYS        0000 R 014574 CZ
0000 R 014572 CZS        0000 R 000000 D          0000 R 014634 DALW       0000 R 014655 DAL1       0000 R 014663 DAL2
0000 C 015160 DATA       0000 R 005356 DATAS      0000 C 021160 DATB       0000 R 006522 DATBS      0000 C 025160 DATC
0000 R 007666 DATCS      0000 C 031160 DATD       0000 R 011032 DATDS      0000 C 035160 DATE       0000 R 012176 DATES
0000 C 041160 DATF       0000 R 013342 DATFS      0000 R 014635 DBTW       0000 R 014657 DBT1       0000 R 014664 DBT2
0000 R 014642 DDALW      0000 R 014643 DCBTW      0000 R 014754 DDBT1      0000 R 014644 DDGMW      0000 R 014755 DDGM1
0000 R 014637 DDXW       0000 R 014751 DDX1       0000 R 014640 DDYW       0000 R 014752 DDY1       0000 R 014641 DDZW
0000 R 014753 DDZ1       0000 R 014570 DEEP       0000 R 014713 DGAA       0000 R 014714 DGBB       0000 R 014721 DGBZ
0000 R 014715 DGGS       0000 R 014722 DGGY       0000 R 014636 DGMW       0000 R 014656 DGM1       0000 R 014665 DGM2
0000 R 000362 DGN        0000 R 000355 DGT        0000 R 014710 DGXX       0000 R 014717 DGYG       0000 R 014711 DGYY
0000 R 014720 DGZB       0000 R 014712 DGZZ       0000 R 015014 DPAX       0000 R 015015 DPAY       0000 R 015016 DPAZ
0000 R 015017 DPPT       0000 R 015020 DPHL       0000 R 014563 DUR        0000 R 014631 DXW        0000 R 014652 DX1
0000 R 014660 DX2        0000 R 014632 DYW        0000 R 014653 DY1        0000 R 014661 DY2        0000 R 014633 DZW
0000 R 014654 DZ1        0000 R 014662 DZ2        0000 R 014723 EA         0000 R 014566 EA1        0000 R 014567 EA2
0000 R 014734 FAL        0000 R 014735 FBT        0000 R 014736 FGM        0000 R 014676 FR         0000 R 004615 FRQ
0000 R 014731 FX         0000 R 014732 FY         0000 R 014733 FZ         0000 R 014760 GAMMA      0000 R 014554 GMIN
0000 R 014630 GMA        0000 R 014651 GM1        0000 R 014666 H          0000 I 014611 I          0000 I 015005 IP
0000 I 000767 ISCR       0000 I 014613 J          0000 I 014606 K          0000 I 014737 KI         0000 I 014614 L
0000 I 014607 M          0000 R 014526 MB         0000 R 014515 MHAA       0000 R 014513 MHBB       0000 R 014524 MHBX
0000 R 014522 MHBZ       0000 R 014514 MHGG       0000 R 014525 MHGX       0000 R 014523 MHGY       0000 R 014516 MHXB
0000 R 014517 MHXG       0000 R 014510 MHXX       0000 R 014520 MHYG       0000 R 014511 MHYY       0000 R 014521 MHZB
0000 R 014512 MHZZ       0000 R 000273 MOMEG      0000 R 014527 MU         0000 I 014604 N          0000 R 014533 NAA
0000 R 014534 NBB        0000 R 014537 NBX        0000 R 014545 NBZ        0000 R 014535 NGG        0000 R 014541 NGX
0000 R 014543 NGY        0000 I 015004 NL         0000 I 015003 NN         0000 I 014741 NP         0000 I 015021 NPLT
0000 I 014610 NRUN       0000 I 014740 NT         0000 R 014536 NXB        0000 R 014540 NXG        0000 R 014530 NXX
0000 R 014542 NYG        0000 R 014531 NYY        0000 R 014544 NZB        0000 R 014532 NZZ        0000 R 003220 PAX
0000 R 003451 PAY        0000 R 003702 PAZ        0000 R 014565 PER        0000 R 000317 PHS        0000 R 004133 PPT
0000 R 004364 PRL        0000 R 002767 PWV        0000 I 014506 Q          0000 R 014605 R          0000 R 014744 SPHI
0000 R 014742 STHE       0000 R 000144 T          0000 R 000265 TEN        0000 R 014621 VELBB      0000 R 014622 VELGB
0000 R 014616 VELXB      0000 R 014617 VELYB      0000 R 014620 VELZB      0000 R 014557 WAREA      0000 R 014560 WAREL
0000 R 014551 WB         0000 R 000350 WC         0000 R 014555 WCD        0000 R 014556 WCL        0000 R 014561 WCPHT
0000 R 014602 WFBT       0000 R 014603 WFGM       0000 R 014577 WFX        0000 R 014600 WFY        0000 R 014601 WFZ
0000 R 014615 WHT        0000 R 014564 WHTM       0000 R 014562 WINDS      0000 R 014575 WINDY      0000 R 014576 WINDZ
0000 R 014645 WK         0000 R 014761 WVMN       0000 R 014763 WVSD       0000 R 014762 WVVR       0000 R 014547 XCG
0000 R 014716 XCPRS      0000 R 014701 XHM        0000 R 014550 XML        0000 R 014725 XMPT       0000 R 014623 XW
0000 R 015160 XWV        0000 R 015006 XWVC       0000 R 014647 X1         0000 R 000062 Y          0000 R 014726 YMPT
0000 R 014624 YW         0000 R 005046 Z          0000 R 014727 ZMPT       0000 R 014625 ZW


00100       1*    C      THIS PROGRAM COMPUTES THE RESPONSE OF AN AXI-SYMMETRIC BUOY
00100       2*    C      EXPOSED TO THE OCEAN ENVRIONMENT
00100       3*    C      UNITS ARE IN FT',LB,SEC
```

```
00100      C
00101            DIMENSION D(50),Y(50),T(25),CM(25),CLF(25),CLO(6),TEN(6)
00103            DIMENSION MOMEG(10),AMP(10),PHS(10)
00104            DIMENSION CSM(5),CHMT(5),CHMN(5),WC(5),DGT(5),DGN(5)
00105            DIMENSION XWV(2048),COSI(256),ISCR(1024)
00105            DIMENSION ACX(2048),ACY(2048),ACZ(2048),BPIT(2048),BROL(2048)
00107            DIMENSION PWV(153),PAX(153),PAY(153),PAZ(153),PPT(153),PRL(153)
00110            DIMENSION FRQ(153),Z(200)
0.111            DIMENSION DATAS(612),DATBS(612),DATCS(612),DATDS(612),DATES(612)
00112            DIMENSION DATFS(612)
00113            INTEGER Q,BIN
00114            COMPLEX DATA(1024)
00115            COMPLEX DATB(1024)
00116            COMPLEX DATC(1024)
00117            COMPLEX DATD(1024)
00120            COMPLEX DATE(1024)
00121            COMPLEX DATF(1024)
00122            EQUIVALENCE(DATA,XWV)
00123            EQUIVALENCE(DATB,ACX)
00124            EQUIVALENCE(DATC,ACY)
00125            EQUIVALENCE(DATD,ACZ)
00126            EQUIVALENCE(DATE,BPIT)
00127            EQUIVALENCE(DATF,BROL)
00130            REAL MHXX,MHYY,MHZZ,MHBB,MHGG,MHAA,MHXB,MHXG,MHYG,MHZB,MHBZ
00131            REAL MHGY,MHBX,MHGX,MB,MU,NXX,NYY,NZZ,NAA,NBB,NGG,NXB,NBX
00132            REAL NXG,NGX,NYG,NGY,NZB,NBZ
00133            REAL MOMEG
00133      C     THE COORDINATE SYSTEM
00133      C
00133      C
00133      C
00133      C
00133      C       Z ---------------------------------------------
00133      C                                                    /I
00133      C                                                   / I
00133      C                                                  /  I
00133      C                                                 /   I
00133      C                                                /    I
00133      C                                               /     I
00133      C                                              /      I
00133      C                                             /       I
00133      C                                            /        I
00133      C                                           Y         I
00133      C                                                     I
00133      C                                                     I
00133      C                                                     I
00133      C                                                     I
00133      C                                                     I
00133      C                                                     I
00133      C                                                     I
00133      C                                                     I
00133      C                                                     X
00133      C
00133      C
00133      C
00134       103 FORMAT(11H BUOY SINKS)
00135       105 FORMAT(6F10.2)
00136       106 FORMAT(9H UNSTABLE)
```

```
      BUOY DYNAMICS                                        DATE  230272  PAGE    6
00137        107 FORMAT(5F10.4)
00140        108 FORMAT(2F10.4)
00141        109 FORMAT(3F10.4)
00142        112 FORMAT(8F8.2)
00143        116 FORMAT(1F10.4,6F8.2)
00144        117 FORMAT(1F8.4,11F8.2)
00145        120 FORMAT(1F10.4)
00146        121 FORMAT(1F20.4)
00147        122 FORMAT(1F30.4)
00150        123 FORMAT(1F40.4)
00151        124 FORMAT(1F50.4)
00152        127 FORMAT(6F10.4)
00152      C     READ IN THE BUOY PARAMETERS
00152      C     BUOY RADIUS, HT. OF C.OF G. FROM MOOR POINT AND THE LENGTH OF THE
00152      C     MOOR POINT BELOW THE BOTTOM OF THE BUOY
00153            READ 109,BR,XCG,XML
00153      C     INERTIAS
00160            READ 107,WB,MB,ALIN,BTIN,GMIN
00160      C     WIND LIFT AND DRAG COEFFICIENTS AND AREAS
00167            READ 107,WCD,WCL,WAREA,WAREL,WCPHT
00167      C
00167      C     THE VISCOSITY OF THE WATER AT 40 DEG F
00176            MU=2.735E-5
00176      C
00176      C     READ THE MEAN WIND SPEED AND DURATION CAUSING THE WIND WAVES
00177            READ 108,WINDS,DUR
00203            CALL RWAVE(WINDS,DUR,WHTM,PER,MOMEG,AMP,PHS)
00203      C
00203      C     THE CABLE PARAMETERS
00203      C     THE CABLE LENGTHS BETWEEN ELEMENTS
00204            CLO(1)=53.0
00205            CLO(2)=47.0
00206            CLO(3)=50.0
00207            CLO(4)=145.0
00210            CSM(1)=2.08
00211            CSM(2)=8.54
00212            CSM(3)=20.96
00213            CHMT(1)=0.1975
00214            CHMT(2)=0.0
00215            CHMT(3)=0.666
00216            CHMN(1)=1.5362
00217            CHMN(2)=1.228
00220            CHMN(3)=2.908
00221            WC(1)=34.51
00222            WC(2)=254.2
00223            WC(3)=624.5
00224            DGT(1)=0.5942
00225            DGT(2)=0.940
00226            DGT(3)=1.10
00227            DGN(1)=3.142
00230            DGN(2)=8.75
00231            DGN(3)=6.49
00232            EA1=2.16E5
00233            EA2=EA1
00233      C     THE WATER DEPTH
00234            DEEP=120.9
00234      C
00234      C     THE CURRENTS IN THE WATER COLUMN
```

```
00234   C      READ THE Y AND Z COMPONENTS OF THE  SURFACE CURRENT
00235          READ 108,CYS,CZS
00235   C      IF THE CURRENT VARIES WITH DEPTH, INSERT THE FUNCTIONS FOR
00235   C      STRENGTH AND DIRECTION
00235   C
00235   C      FOR A UNIFORM CURRENT
00241          CY=CYS
00242          CZ=CZS
00242   C
00242   C      THE WIND ACTING ON THE BUOY
00242   C      READ THE Y AND Z COMPONENTS OF THE MEAN WIND
00243          READ 108,WINDY,WINDZ
00247          WFX=-0.0034*WCL*WAREL*(WINDY**2+WINDZ**2)
00250          WFY=0.0034*WCD*WAREA*WINDY*ABS(WINDY)
00251          WFZ=0.0034*WCD*WAREA*WINDZ*ABS(WINDZ)
00252          WFBT=-WFZ*WCPHT
00253          WFGM=-WFY*WCPHT
00254          N=30
00255          R=0.005
00256          K=0
00257          M=0
00260          NRUN=1
00261          DO 440 I=1,612
00264          DATAS(I)=0.0
00265          DATBS(I)=0.0
00266          DATCS(I)=0.0
00267          DATDS(I)=0.0
00270          DATES(I)=0.0
00271      440 DATFS(I)=0.0
00271   C      THE INITIAL CONDITIONS
00271   C      ALL ACCELERATIONS AND VELOCITIES ARE ZERO
00273          DO 58 I=1,41,2
00276          D(I)=0.0
00277       58 Y(I)=0.0
00277   C      READ THE INITIAL BUOY DISPLACEMENTS - X,Y,Z
00301          READ 109,Y(2),Y(4),Y(6)
00301   C      THE INITIAL BUOY ANGLES ARE ZERO
00306          Y(8)=0.0
00307          Y(10)=0.0
00310          Y(12)=0.0
00310   C      READ THE INITIAL CABLE DISPLACEMENTS
00311          DO 53 I=14,32,6
00314       53 READ 109,Y(I),Y(I+2),Y(I+4)
00314   C
00314   C      INPUTS AND OPERATIONS FOR THE POWER SPECTRA COMPUTATIONS
00322      500 CONTINUE
00323          A=0.0
00324          J=1
00325          DO 59 L=1,2048
00330          ACX(L)=0.0
00331          ACY(L)=0.0
00332          ACZ(L)=0.0
00333          BPIT(L)=0.0
00334          BROL(L)=0.0
00335       59 XWV(L)=0.0
00337          L=1
00340        5 CONTINUE
00341          WHT=A*WHTM/(2.0*PER)
```

```
00342          IF(A.GE.(2.0*PER))WHT=WHTM
00344          VELXB=Y(1)
00345          VELYB=Y(3)
00346          VELZB=Y(5)
00347          VELBB=Y(9)
00350          VELGB=Y(11)
00350     C    THE WAVES
00350     C    FOR A SINGLE TRAIN OF WAVES, ASSUME THEY ARE COMING IN ON THE
00350     C    Z AXIS
00351          XW=0.0
00352          YW=0.0
00353          ZW=0.0
00354          ALW=0.0
00355          BTW=0.0
00356          GMW=0.0
00357          DXW=0.0
00360          DYW=0.0
00361          DZW=0.0
00362          DALW=0.0
00363          DBTW=0.0
00364          DGMW=0.0
00365          DDXW=0.0
00366          DDYW=0.0
00367          DDZW=0.0
00370          DDALW=0.0
00371          DDBTW=0.0
00372          DDGMW=0.0
00373          DO 14 I=1,9
00376          WK=(MOMEG(I)**2)/32.2
00377          ANG=A*MOMEG(I)+PHS(I)
00400          XW=XW-AMP(I)*SIN(ANG)
00401          ZW=ZW+AMP(I)*COS(ANG)
00402          BTW=BTW+WK*AMP(I)*COS(ANG)
00403          DXW=DXW-MOMEG(I)*AMP(I)*COS(ANG)
00404          DZW=DZW-MOMEG(I)*AMP(I)*SIN(ANG)
00405          DBTW=DBTW-WK*MOMEG(I)*AMP(I)*SIN(ANG)
00406          DDXW=DDXW+(MOMEG(I)**2)*AMP(I)*SIN(ANG)
00407          DDZW=DDZW-(MOMEG(I)**2)*AMP(I)*COS(ANG)
00410       14 DDBTW=DDBTW-WK*(MOMEG(I)**2)*AMP(I)*COS(ANG)
00410     C
00410     C    THE BUOY MOTIONS RELATIVE TO THE WATER MASS
00410     C    DISPLACEMENTS
00412          X1=Y(2)-XW
00413          BT1=Y(10)-BTW
00414          GM1=Y(12)-GMW
00414     C    VELOCITIES
00415          DX1=Y(1)-DXW
00416          DY1=Y(3)-DYW
00417          DZ1=Y(5)-DZW
00420          DAL1=Y(7)-DALW
00421          DGM1=Y(11)-DGMW
00422          DBT1=Y(9)-DBTW
00423          DGM1=Y(11)
00423     C
00423     C    WATER MASS VELOCITIES RELATIVE TO THE BUOY INCLUDING CURRENTS
00424          DX2=DX1
00425          DY2=DY1-CY
00426          DZ2=DZ1-CZ
```

```
00427         DAL2=DAL1
00430         DBT2=DBT1
00431         DGM2=DGM1
00431   C
00431   C
00431   C     THE BUOYANCY FORCES AND MOMENTS
00432         H=XCG+X1-XHL
00433         CALL TORBU(H,BT1,BXX,BBB,BXB,BBX)
00434         CALL TORBU(H,GM1,BXX,BGG,BXG,BGX)
00435      30 CONTINUE
00435   C
00435   C     THE HYDRODYNAMIC MASSES AND MOMENTS OF INERTIA
00435   C
00435   C     THE DIMENSIONLESS FREQUENCY
00436         FR=((6.2832/PER)**2)*BR/32.2
00437         BLAMB=SQRT(6.25/(PER*MU))
00440         BA=BLAMB*BR
00440   C     HYDRODYNAMIC FORCE MOMENT ARM
00441         XHM=4.16
00441   C     HEAVE
00442         IF(FR.GE.0.2)GO TO 31
00444         CMX=2.31
00445         GO TO 33
00446      31 IF(FR.GE.2.4)GO TO 32
00450         CMX=1.35725*(FR**(-.330597))
00451         GO TO 33
00452      32 CMX=1.0
00452   C     SWAY-SURGE
00453      33 CMY=0.215
00454      35 CMZ=CMY
00455         MHXX=1.988*(BR**3)*CMX
00456         MHYY=1.988*((BR**3)*CMY+0.8045)
00457         MHZZ=MHYY
00457   C     YAW
00460         MHAA=16.65*(BR**5)*(1.0+BA)/(1.0+2.0*BA+2.0*(BA**2))
00460   C     PITCH AND ROLL
00461         MHBB=MHZZ*(XHM**2)
00462         MHGG=MHBB
00462   C     CROSS-COUPLED HYDROMASSES
00463         MHBX=0.0
00464         MHGX=0.0
00465         MHXB=0.0
00466         MHXG=0.0
00467         MHYG=-MHYY*XHM
00470         MHZB=-MHYG
00471         MHBZ=MHZB
00472         MHGY=MHYG
00472   C
00472   C     THE DAMPING DUE TO WAVE GENERATION
00472   C
00472   C     HEAVE
00473         IF(FR.GE.0.8)GO TO 41
00475         CNXX=FR/(0.132617+0.873644*FR)
00476         GO TO 42
00477      41 CNXX=1.2476*EXP(-0.37376*FR)
00500      42 CNYY=0.14
00501      43 NXX=1.988*FR*(BR**3)*CNXX
00502         NYY=1.988*FR*(BR**3)*CNYY
```

```
00503          NZZ=NYY
00503     C    PITCH AND ROLL
00504          NAA=4.195*RU*(BR**3)*(3.0+6.0*BA+6.0*(BA**2)+2.0*(BA**3))
00504         1 /(1.0+2.0*BA+2.0*(BA**2))
00505          NBB=NAA+NZZ*((1.282-0.5*H)**2)
00506          NGG=NBB
00506     C    CROSS COUPLED WAVE DAMPING
00507          NXB=0.0
00510          NBX=0.0
00511          NXG=0.0
00512          NGX=0.0
0051           NYG=-NYY*(1.282-0.5*H)
00514          NZB=-NYG
00515          NBZ=NZB
00516          NGY=NYG
00516     C
00516     C    THE VISCOUS DAMPING AND DRAG
00516     C    AREAS
00517          ARXX=3.1416*(BR**2)
00520          DGXX=1.2*ARXX
C0521          DGYY=15.5
00522          DGZZ=15.6
00523          DGAA=0.0
00524          DGBB=0.0
00525          DGGG=0.0
00526          XCPRS=3.25
00526     C    CROSS-COUPLED VISCOUS DRAG
00527          DGYG=-DGYY*(XCPRS**2)
00530          DGZB=-DGYG
00531          DGBZ=DGZB
00532          DGGY=DGYG
00532     C
00532     C    TENSIONS AND FORCES FOR THE 3 LUMP MASS CABLE MODEL
00532     C    THE FIRST ELEMENT IS CABLE , THE LAST TWO ARE CHAIN
00533          EA=EA1
00534          CABK=EA/CLO(1)
00535          XMPT=Y(2)+XCG*COS(Y(10))*COS(Y(12))
00536          YMPT=Y(4)-XCG*COS(Y(10))*SIN(Y(12))
00537          ZMPT=Y(6)+XCG*SIN(Y(10))*COS(Y(12))
00540          CL=SQRT(((XMPT-Y(14))**2)+((YMPT-Y(16))**2)+((ZMPT-Y(18))**2))
00541          TEN(1)=CABK*(CL-CLO(1))
00542          IF(TEN(1).LE.0.0)TEN(1)=0.0
00544          T(4)=TEN(1)*(Y(14)-XMPT)/CL
00545          T(5)=TEN(1)*(Y(16)-YMPT)/CL
00546          T(6)=TEN(1)*(Y(18)-ZMPT)/CL
00546     C    ADD 165 LBS. TO ACCOUNT FOR THE CHAINS UNDER THE BUOY
00547          FX=T(4)+165.0
00550          FY=T(5)
00551          FZ=T(6)
00552          FAL=0.0
00553          FBT=-XCG*(-FZ*COS(Y(10))*COS(Y(12))+FX*SIN(Y(10))*COS(Y(12)))
00554          FGM=-XCG*(FY*COS(Y(10))*COS(Y(12))+FX*SIN(Y(12))*COS(Y(10)))
00555          DO 71 I=13,25,6
00560          KI=((I-1)/2)-2
00561          NT=((I-1)/6)
00562          NP=NT-1
00563          CL=SQRT(((Y(I+1)-Y(I+7))**2)+((Y(I+3)-Y(I+9))**2)+
00563         1 ((Y(I+5)-Y(I+11))**2))
```

```
00564       73 CABK=EA/CLO(NT)
00565          TEN(NT)=CABK*(CL-CLO(NT))
00566          IF(TEN(NT).LE.0.0)TEN(NT)=0.0
00566     C    THE TENSION COMPONENTS
00570          T(KI+3)=TEN(NT)*(Y(I+7)-Y(I+1))/CL
00571          T(KI+4)=TEN(NT)*(Y(I+9)-Y(I+3))/CL
00572          T(KI+5)=TEN(NT)*(Y(I+11)-Y(I+5))/CL
00572     C    THE SINES AND COSINES OF THE CABLE ANGLES
00573          STHE=(Y(I+11)-Y(I+5))/SQRT(((Y(I+1)-Y(I+7))**2)
00573         1 +((Y(I+5)-Y(I+11))**2))
00574          CTHE=(Y(I+7)-Y(I+1))/SQRT(((Y(I+1)-Y(I+7))**2)
00574         1 +((Y(I+5)-Y(I+11))**2))
00575          SPHI=(Y(I+9)-Y(I+3))/CL
00576          CPHI=SQRT(((Y(I+1)-Y(I+7))**2)+((Y(I+5)-Y(I+11))**2))/CL
00577          CUR=Y(I)*CPHI*CTHE+(Y(I+2)-CY)*SPHI+(Y(I+4)-CZ)*CPHI*STHE
00600          CVR=-Y(I)*SPHI*CTHE+(Y(I+2)-CY)*CPHI-(Y(I+4)-CZ)*SPHI*STHE
00601          CWR=-Y(I)*STHE+(Y(I+4)-CZ)*CTHE
00601     C    CABLE MASSES
00602          CM(KI)=CSM(NP)+CHMT(NP)*CPHI*CTHE
00603          CM(KI+1)=CSM(NP)+CHMN(NP)*CPHI
00604          CM(KI+2)=CSM(NP)+CHMN(NP)*CTHE
00604     C    CABLE LOADING FUNCTIONS
00605          CLF(KI)=DGT(NP)*CPHI*CTHE*CUR*ABS(CUR)-DGN(NP)*SPHI*CTHE*CVR*
00605         1 ABS(CVR)-DGN(NP)*STHE*CWR*ABS(CWR)-WC(NP)
00606          CLF(KI+1)=DGT(NP)*SPHI*CUR*ABS(CUR)+DGN(NP)*CPHI*CVR*ABS(CVR)
00607       71 CLF(KI+2)=DGT(NP)*CPHI*STHE*CUR*ABS(CUR)-DGN(NP)*SPHI*STHE
00607         1 *CVR*ABS(CVR)+DGN(NP)*CTHE*CWR*ABS(CWR)
00611       50 CONTINUE
00612          DDX1=(Y(1)-VELXB)/R
00613          DDY1=(Y(3)-VELYB)/R
00614          DDZ1=(Y(5)-VELZB)/R
00615          DDBT1=(Y(9)-VELBB)/R
00616          DDGM1=(Y(11)-VELGB)/R
00617          DDX1=0.0
00620          DDY1=0.0
00621          DDZ1=0.0
00622          DDBT1=0.0
00623          DDGM1=0.0
00623     C
00623     C    THE EQUATIONS OF MOTION FOR THE BUOY
00623     C
00623     C    HEAVE -X MOTION
00624          D(1)=(WB-BXX-BXB-BXG+MHXX*DDXW-MHXB*DDBT1-MHXG*DDGM1-NXX*DX1
00624         1 -NXB*DBT1-NXG*DGM1-DGXX*DX2*ABS(DX2)+WFX+FX)/(MB+MHXX)
00625          D(2)=Y(1)
00625     C
00625     C    SWAY - Y MOTION
00626          D(3)=(MHYY*DDYW-MHYG*DDGM1-NYY*DY1-NYG*DGM1-DGYY*DY2*ABS(DY2)
00626         1 -DGYG*DGM2*ABS(DGM2)+WFY+FY)/(MB+MHYY)
00627          D(4)=Y(3)
00627     C
00627     C    SURGE - Z MOTION
00630          D(5)=(MHZZ*DDZW-MHZB*DDBT1-NZZ*DZ1-NZB*DBT1-DGZZ*DZ2*ABS(DZ2)
00630         1 -DGZB*DBT2*ABS(DBT2)+WFZ+FZ)/(MB+MHZZ)
00631          D(6)=Y(5)
00631     C
00631     C    YAW - ALFA MOTION
00632          D(7)=(MHAA*DDALW-NAA*DAL1-DGAA*DAL2*ABS(DAL2)+FAL)/(ALIN+MHAA)
```

```
00633       D(8)=Y(7)
00633 C
00633 C     PITCH - BETA MOTION
00634       D(9)=(-BBX-BBB-MHBX*DDX1-MHBZ*DDZ1+MHBB*DDBTW-NBX*DX1-NBB*DBT1
00634      1 -NBZ*DZ1-DGBZ*DZ2*ABS(DZ2)-DGBB*DBT2*ABS(DBT2)+WFBT+FBT)/
00634      2 (BTIN+MHBB)
00635       D(10)=Y(9)
00635 C
00635 C     ROLL- GAMMA MOTION
00636       D(11)=(-BGX-BGG-MHGX*DDX1-MHGY*DDY1+MHGG*DDGMW-NGX*DX1-NGY*DY1
00636      1 -NGG*DGM1-DGGY*DY2*ABS(DY2)-DGGG*DGM2*ABS(DGM2)+WFGM+FGM)/
00636      2 (GMIN+MHGG)
00637       D(12)=Y(11)
00637 C     EQUATIONS OF MOTION FOR A 3 LUMP MODEL OF THE CABLE
00640       DO 81 I=13,25,6
00643       KI=((I-1)/2)-2
00643 C     ELEMENT X MOTION
00644       D(I)=(-T(KI)+T(KI+3)-CLF(KI))/CM(KI)
00645       D(I+1)=Y(I)
00645 C     ELEMENT Y MOTION
00646       D(I+2)=(-T(KI+1)+T(KI+4)-CLF(KI+1))/CM(KI+1)
00647       D(I+3)=Y(I+2)
00647 C     ELEMENT Z MOTION
00650       D(I+4)=(-T(KI+2)+T(KI+5)-CLF(KI+2))/CM(KI+2)
00651    81 D(I+5)=Y(I+4)
00651 C
00653       CALL RUNGE(N,Y,D,A,R,M,K)
00654       GO TO (50,40),K
00655    40 ALFA=57.4*Y(8)
00656       BETA=57.4*Y(10)
00657       GAMMA=57.4*Y(12)
00657 C
00660       IF(A.LE.5.0)GO TO 52
00662       IF(J.EQ.12)GO TO 51
00664       J=J+1
00665       GO TO 52
00666    51 CONTINUE
00667       J=1
00670       XWV(L)=XW
00671       ACX(L)=D(1)
00672       ACY(L)=D(3)
00673       ACZ(L)=D(5)
00674       BPIT(L)=Y(10)
00675       BROL(L)=Y(12)
00676       L=L+2
00677    52 CONTINUE
00677 C
00677 C     INSTABILITY LIMITER
00700       DO 60 I=1,30
00703    60 IF(Y(I).GT.10000.0)GO TO 92
00703 C     THE CABLE ELEMENTS CANT SINK THRU THE BOTTOM
00706       DO 218 I=14,26,6
00711   218 IF(Y(I).GE.DEEP)Y(I)=DEEP
00714       IF(L.EQ.2049)GO TO 88
00716       GO TO 5
00717    88 CONTINUE
00717 C
00717 C     COMPUTE SIMPLE STATISTICAL PROPERTIES
```

```
00720          CALL DSTAT(XWV,WVMN,WVVR,WVSD)
00721          CALL DSTAT(ACX,AXMN,AXVR,AXSD)
00722          CALL DSTAT(ACY,AYMN,AYVR,AYSD)
00723          CALL DSTAT(ACZ,AZMN,AZVR,AZSD)
00724          CALL DSTAT(BPIT,BPMN,BPVR,BPSD)
00725          CALL DSTAT(BROL,BRMN,BRVR,BRSD)
00726          WRITE(4,127)WVMN,AXMN,AYMN,AZMN,BPMN,BRMN
00736          WRITE(4,127)WVSD,AXSD,AYSD,AZSD,BPSD,BRSD
00746          WRITE(4,127)WVVR,AXVR,AYVR,AZVR,BPVR,BRVR
00746    C     SMOOTH THE MOTION DATA TO MINIMIZE ALIASING
00756          DO 433 L=5,2043,2
00761          XWV(L)=(XWV(L-4)+XWV(L-2)+XWV(L)+XWV(L+2)+XWV(L+4))/5.0
00762          ACX(L)=(ACX(L-4)+ACX(L-2)+ACX(L)+ACX(L+2)+ACX(L+4))/5.0
00763          ACY(L)=(ACY(L-4)+ACY(L-2)+ACY(L)+ACY(L+2)+ACY(L+4))/5.0
00764          ACZ(L)=(ACZ(L-4)+ACZ(L-2)+ACZ(L)+ACZ(L+2)+ACZ(L+4))/5.0
00765          BPIT(L)=(BPIT(L-4)+BPIT(L-2)+BPIT(L)+BPIT(L+2)+BPIT(L+4))/5.0
00766      433 BROL(L)=(BROL(L-4)+BROL(L-2)+BROL(L)+BROL(L+2)+BROL(L+4))/5.0
00766    C     COMPUTE POWER SPECTRA
00770          BIN=1024
00771          Q=BIN
00772          CALL COSINE(COSI,BIN)
00773          CALL GNSCR(ISCR,Q)
00773    C
00773    C     WAVE HEIGHT
00774          CALL FFOUR(DATA,COSI,ISCR,Q,BIN,-1)
00775          CALL FFOUR(DATB,COSI,ISCR,Q,BIN,-1)
00776          CALL FFOUR(DATC,COSI,ISCR,Q,BIN,-1)
00777          CALL FFOUR(DATD,COSI,ISCR,Q,BIN,-1)
01000          CALL FFOUR(DATE,COSI,ISCR,Q,BIN,-1)
01001          CALL FFOUR(DATF,COSI,ISCR,Q,BIN,-1)
01001    C     USE 8 ENSEMBLE AVERAGES
01001    C     AVERAGE THE COEFFICIENTS OVER 8 RUNS
01002          DO 410 I=1,306
01005          DATAS(I)=DATAS(I)+DATA(I)
01006          DATBS(I)=DATBS(I)+DATB(I)
01007          DATCS(I)=DATCS(I)+DATC(I)
01010          DATDS(I)=DATDS(I)+DATD(I)
01011          DATES(I)=DATES(I)+DATE(I)
01012      410 DATFS(I)=DATFS(I)+DATF(I)
01014          IF(NRUN.EQ.8)GO TO 450
01016          NRUN=NRUN+1
01017          PHS(10)=PHS(1)
01020          DO 404 NN=1,9
01023          NL=NN+1
01024      404 PHS(NN)=PHS(NL)
01026          GO TO 500
01027      450 DO 411 I=1,306
01032          DATA(I)=DATAS(I)/8.0
01033          DATB(I)=DATBS(I)/8.0
01034          DATC(I)=DATCS(I)/8.0
01035          DATD(I)=DATDS(I)/8.0
01036          DATE(I)=DATES(I)/8.0
01037      411 DATF(I)=DATFS(I)/8.0
01041          DO 164 I=4,306,2
01044          IP=I/2
01045          FRQ(IP)=I/61.44
01046          XWVC=(DATA(I-3)+DATA(I-2)+DATA(I-1)+DATA(I)
01046         1 +DATA(I+1)+DATA(I+2)+DATA(I+3))/7.0
```

```
01047          ACXC=(DATB(I-3)+DATB(I-2)+DATB(I-1)+DATB(I)
01047         1 +DATB(I+1)+DATB(I+2)+DATB(I+3))/7.0
01050          ACYC=(DATC(I-3)+DATC(I-2)+DATC(I-1)+DATC(I)
01050         1 +DATC(I+1)+DATC(I+2)+DATC(I+3))/7.0
01051          ACZC=(DATD(I-3)+DATD(I-2)+DATD(I-1)+DATD(I)
01051         1 +DATD(I+1)+DATD(I+2)+DATD(I+3))/7.0
01052          BPITC=(DATE(I-3)+DATE(I-2)+DATE(I-1)+DATE(I)
01052         1 +DATE(I+1)+DATE(I+2)+DATE(I+3))/7.0
01053          BROLC=(DATF(I-3)+DATF(I-2)+DATF(I-1)+DATF(I)
01053         1 +DATF(I+1)+DATF(I+2)+DATF(I+3))/7.0
01054          IF(XWVC.LE.0.0001)XWVC=0.0001
01056          IF(ACXC.LE.0.0001)ACXC=0.0001
01060          IF(ACYC.LE.0.0001)ACYC=0.0001
01062          IF(ACZC.LE.0.0001)ACZC=0.0001
01064          IF(BPITC.LE.0.0001)BPITC=0.0001
01066          IF(BROLC.LE.0.0001)BROLC=0.0001
01070          PWV(IP)=10.0*ALOG10(XWVC)
01071          PAX(IP)=10.0*ALOG10(ACXC)
01072          PAY(IP)=10.0*ALOG10(ACYC)
01073          PAZ(IP)=10.0*ALOG10(ACZC)
01074          PPT(IP)=10.0*ALOG10(BPITC)
01075          PRL(IP)=10.0*ALOG10(BROLC)
01076          DPAX=PAX(IP)-PWV(IP)
01077          DPAY=PAY(IP)-PWV(IP)
01100          DPAZ=PAZ(IP)-PWV(IP)
01101          DPPT=PPT(IP)-PWV(IP)
01102          DPRL=PRL(IP)-PWV(IP)
01103      164 WRITE(4,117)FRQ(IP),PWV(IP),PAX(IP),PAY(IP),PAZ(IP),PPT(IP),
01103         1 PRL(IP),DPAX,DPAY,DPAZ,DPPT,DPRL
01103     C
01103     C    PLOT THE SPECTRA
01122          NPLT=0
01123          CALL MODESG(Z,0)
01124      130 NPLT=NPLT+1
01125          CALL OBJCTG(Z,500.,500.,3600.,3000.)
01126          CALL SUBJEG(Z,0.,-40.,5.,40.)
01127          CALL GRIDG(Z,1.,10.,0.,0.)
01130          CALL LABELG(Z,0,1.,0.,2)
01131          CALL LABELG(Z,1,10.,0.,4)
01132          IF(NPLT.EQ.1)GO TO 131
01134          IF(NPLT.EQ.2)GO TO 132
01136          IF(NPLT.EQ.3)GO TO 133
01140          IF(NPLT.EQ.4)GO TO 134
01142          IF(NPLT.EQ.5)GO TO 135
01144          IF(NPLT.EQ.6)GO TO 136
01146      131 CALL TITLEG(Z,9,9HFREQUENCY,8,8HDB LEVEL,13,13HWAVE SPECTRUM)
01147          CALL LINESG(Z,153,FRQ,PWV)
01150          CALL PAGEG(Z,0,1,1)
01151          GO TO 130
01152      132 CALL TITLEG(Z,9,9HFREQUENCY,8,8HDB LEVEL,14,14HHEAVE SPECTRUM)
01153          CALL LINESG(Z,153,FRQ,PAX)
01154          CALL PAGEG(Z,0,1,1)
01155          GO TO 130
01156      133 CALL TITLEG(Z,9,9HFREQUENCY,8,8HDB LEVEL,13,13HSWAY SPECTRUM)
01157          CALL LINESG(Z,153,FRQ,PAY)
01160          CALL PAGEG(Z,0,1,1)
01161          GO TO 130
01162      134 CALL TITLEG(Z,9,9HFREQUENCY,8,8HDB LEVEL,14,14HSURGE SPECTRUM)
```

```
                     BUOY DYNAMICS                                                DATE  230272  PAGE    15
01163    584*              CALL LINESG(Z,153,FRQ,PAZ)
01164    585*              CALL PAGEG(Z,0,1,1)
01165    586*              GO TO 130
01166    587*          135 CALL TITLEG(Z,9,9HFREQUENCY,8,8HDB LEVEL,14,14HPITCH SPECTRUM)
01167    588*              CALL LINESG(Z,153,FRQ,PPT)
01170    589*              CALL PAGEG(Z,0,1,1)
01171    590*              GO TO 130
01172    591*          136 CALL TITLEG(Z,9,9HFREQUENCY,8,8HDB LEVEL,13,13HROLL SPECTRUM)
01173    592*              CALL LINESG(Z,153,FRQ,PRL)
01174    593*              CALL PAGEG(Z,0,1,1)
01175    594*              CALL EXITG(Z)
01176    595*              GO TO 89
01177    596*           92 WRITE(4,105)
01201    597*              WRITE(4,120)A
01204    598*           89 STOP
01205    599*              END

        END OF UNIVAC 1108 FORTRAN V COMPILATION.      0 *DIAGNOSTIC* MESSAGE(S)
```

```
                    BUOY DYNAMICS                                                        DATE  230272  PAGE    16
WI FOR RWAVE,RWAVE
UNIVAC 1108 FORTRAN V LEVEL 2206 0023
THIS COMPILATION WAS DONE ON 23 FEB 72 AT 12:44:04                                                                   12:44: 4,826

  SUBROUTINE RWAVE      ENTRY POINT 000417

  STORAGE USED (BLOCK, NAME, LENGTH)

       0001    *CODE    000452
       0000    *DATA    000173
       0002    *BLANK   000000

  EXTERNAL REFERENCES (BLOCK, NAME)

       0003    ALOG10
       0004    NEXP6$
       0005    ALOG
       0006    EXP
       0007    SQRT
       0010    NERR3$

  STORAGE ASSIGNMENT FOR VARIABLES (BLOCK, TYPE, RELATIVE LOCATION, NAME)

  0001    000207 143G      0001    000303 161G      0001    000321 167G      0001    000061 304L      0001    000235 402L
  0000 R 000052 APAR      0000 R 000053 BPAR      0000 R 000012 DOMEG     0000 R 000042 DURMIN    0000 R 000036 FETCH
  0000 R 000037 FPAR      0000 R 000043 FPARL     0000 R 000050 FP1       0000 R 000051 FP2       0000 R 000055 G
  0000 R 000047 H3PAR     0000 R 000046 H3PARL    0000    000134 INJP$    0000 I 000054 IS        0000 R 000056 OM
  0000 R 000000 OMEG      0000 R 000045 P3PAR     0000 R 000044 P3PARL    0000 R 000024 SPEC      0000 R 000057 SPECT
  0000 R 000041 TPAR      0000 R 000040 TPARL

00101      1*           SUBROUTINE RWAVE(WINDS,DUR,WHTM,PER,MOMEG,AMP,PHS)
00101      2*     C     USE THE BRETTSCHNEIDER WAVE METHOD TO COMPUTE THE MEAN WAVE
00101      3*     C     HEIGHT AND PERIOD
00101      4*     C     USE A 15 MILE FETCH AT STATION BRAVO
00103      5*           DIMENSION OMEG(10),MOMEG(10),DOMEG(10),SPEC(10),PHS(10),AMP(10)
00104      6*           REAL MOMEG
00105      7*           FETCH=9.12E4
00105      8*     C     FETCH LIMITED CASE
00106      9*           FPAR=32.2*FETCH/(WINDS**2)
00107     10*           TPARL=1.477-0.225*ALOG10(FPAR)
00110     11*           TPAR=10.0**TPARL
00111     12*           DURMIN=TPAR*FETCH/(WINDS*3600.0)
00112     13*           IF(DUR-DURMIN)303,304,304
00112     14*     C     DURATION LIMITED CASE
00115     15*       303 TPAR=DUR*WINDS*3600.0/FETCH
00116     16*           FPARL=5.78-3.915*ALOG10(TPAR)
00117     17*           FPAR=10.0**FPARL
00120     18*       304 P3PARL=-1.136+0.283*ALOG10(FPAR)
00121     19*           P3PAR=10.0**P3PARL
00122     20*           IF(FPAR.LT.0.02)P3PAR=0.0247
```

```
                    BUOY DYNAMICS                                  DATE  230272  PAGE    17
00124                  IF(FPAR.GT.1.2E5)P3PAR=2.0
00126                  PER=0.148*P3PAR*WINDS
00127                  H3PARL=-2.5+0.415*ALOG10(FPAR)
00130                  H3PAR=10.0**H3PARL
00131                  IF(FPAR.LT.0.016)H3PAR=0.00057
00133                  IF(FPAR.GT.5.0E4)H3PAR=0.282
00135                  WHTM=0.01942*H3PAR*(WINDS**2)
00135          C       COMPUTE FREQUENCIES AND AMPLITUDES FOR A 9 COMPONENT WAVE MODEL
00136                  FP1=32.2*WHTM/(WINDS**2)
00137                  FP2=32.2*PER/(6.2832*WINDS)
00140                  APAR=3.437*(FP1**2)/(FP2**4)
06141                  BPAR=-0.675*((32.2/(WINDS*FP2))**4)
00142                  DO 401 IS=1,9
00145                  G=10.0/IS
00146              401 OMEG(IS)=(-BPAR/(ALOG(G)))**0.25
00150                  OMEG(10)=500.0
00151                  OM=0.0
00152              402 OM=OM+0.05
00153                  SPECT=(1037.0*APAR/(OM**5))*EXP(BPAR/(OM**4))
00154                  IF(SPECT.LE.0.001)GO TO 402
00156                  MOMEG(1)=OM+0.5*(OMEG(1)-OM)
00157                  DOMEG(1)=OMEG(1)-OM
00160                  DO 403 IS=2,9
00163                  MOMEG(IS)=(OMEG(IS)+OMEG(IS+1))/2.0
00164              403 DOMEG(IS)=OMEG(IS+1)-OMEG(IS)
00166                  DO 404 IS=1,8
00171                  SPEC(IS)=(1037.0*APAR/((MOMEG(IS))**5))
00171                 1 *EXP(BPAR/((MOMEG(IS))**4))
00172              404 AMP(IS)=0.5*SQRT(SPEC(IS)*DOMEG(IS))
00174                  AMP(9)=0.0
00174          C       USE A RANDOM NUMBER TABLE TO SELECT RANDOM PHASE ANGLES FR
00174          C       EACH COMPONENT
00175                  PHS(1)=0.306
00176                  PHS(2)=6.255
00177                  PHS(3)=4.655
00200                  PHS(4)=5.20
00201                  PHS(5)=0.575
00202                  PHS(6)=3.220
00203                  PHS(7)=5.545
00204                  PHS(8)=0.435
00205                  PHS(9)=0.657
00206                  RETURN
00207                  END

         END OF UNIVAC 1108 FORTRAN V COMPILATION.      0 *DIAGNOSTIC* MESSAGE(S)
```

BUOY DYNAMICS   DATE 230272 PAGE 18

```
@I FOR TORBU,TORBU
UNIVAC 1108 FORTRAN V LEVEL 2206 0023                                                      12:44: 6.542
THIS COMPILATION WAS DONE ON 23 FEB 72 AT 12:44:06

   SUBROUTINE TORBU      ENTRY POINT 000340

   STORAGE USED (BLOCK, NAME, LENGTH)

        0001    *CODE    000363
        0000    *DATA    000061
        0002    *BLANK   000000


   EXTERNAL REFERENCES (BLOCK, NAME)

        0003    SIN
        0004    COS
        0005    SQRT
        0006    ATAN
        0007    NERR3$


   STORAGE ASSIGNMENT FOR VARIABLES (BLOCK, TYPE, RELATIVE LOCATION, NAME)

   0001     000145 10L     0001     000225 11L     0001     000220 16L     0001     000231 18L     0001     000245 19L
   0001     000275 20L     0001     000236 3L      0001     000132 8L      0001     000016 9L      0000 R 000012 ALF
   0000 R 000013 AH        0000 R 000011 ART      0000 R 000014 ARTY     0000 R 000016 BXTIL    0000 R 000002 OGAM
   0000 R 000001 GAM       0000 R 000010 HB       0000     000041 INJP$   0000 I 000000 J        0000 R 000004 RS
   0000 R 000003 RT        0000     000006 VOL     0000 R 000007 VOLX     0000 R 000015 X        0000 R 000017 XM
   0000 R 000005 ZGBH


 00101            SUBROUTINE TORBU(H,TIL,BXX,BTT,BXT,BTX)
 00101      C     THIS SUBROUTINE COMPUTES THE DISPLACEMENT AND RIGHTING MOMENT
 00101      C     FOR THE 8 FOOT DIA, RICHARDSON BUOY USED IN THE BUOY MOTION
 00101      C     EXPERIMENT
 00103            J=1
 00104            GAM=-1.5708
 00105            OGAM=0.1
 00106            RT=2.75
 00107            RS=1.25
 00110            ZGBH=1.282
 00111            VOL=0.0
 00112            VOLX=0.0
 00113          9 CONTINUE
 00114            HB=H-(ZGBH-H)*(1.0-COS(TIL))+RT*SIN(TIL)*SIN(GAM)
 00115            IF(J.EQ.1)HB=H
 00117            IF(HB.LE.0.0)HB=0.0
 00121            IF(HB.GT.(0.99*RS))GO TO 8
 00123            IF(HB.GE.(1.99*RS))GO TO 11
 00125            ART=SQRT(((RS**2)/((RS-HB)**2))-1.0)
 00126            IF(ART.GE.25.0)GO TO 16
 00130            ALF=2.0*ATAN(ART)
```

```
      AR=0.5*(RS**2)*(ALF-SIN(ALF))
      GO TO 18
    8 CONTINUE
      IF(HB.GT.(1.01*RS))GO TO 10
      AR=1.5708*RS*RS
      GO TO 18
   10 ARTY=((RS**2)/((RS-(2.0*RS-HB))**2))-1.0
      IF(ARTY.LE.0.0)ARTY=0.0
      ART=SQRT(ARTY)
      IF(ART.GE.25.0)GO TO 16
      ALF=2.0*ATAN(ART)
      AR=3.1416*(RS**2)-0.5*(RS**2)*(ALF-SIN(ALF))
      GO TO 18
   16 AR=1.5708*(RS**2)
      GO TO 18
   11 AR=3.1416*(RS**2)
   18 IF(J.EQ.1)GO TO 3
      GO TO 19
    3 BXX=402.124*RT*AR
      J=2
      GO TO 9
   19 VOL=VOL+UGAM*RT*AR
      X=RT*SIN(GAM)
      VOLX=VOLX+X*UGAM*RT*AR
      GAM=GAM+UGAM
      IF(GAM.GE.1.57)GO TO 20
      GO TO 9
   20 BXTIL=128.0*VOL
      BXT=BXTIL-BXX
C     THE RIGHTING ARM
      XM=(VOLX/VOL)*COS(TIL)-(ZGBH-H)*SIN(TIL)
      BTT=BXTIL*XM
      BTX=BXT*XM
      RETURN
      END
```

END OF UNIVAC 1108 FORTRAN V COMPILATION.   0 *DIAGNOSTIC* MESSAGE(S)

```
            BUOY DYNAMICS                                          DATE  230272  PAGE    20
@I FOR RUNGE,RUNGE                                                                                      12:44: 8.128
UNIVAC 1108 FORTRAN V LEVEL 2206 0023
THIS COMPILATION WAS DONE ON 23 FEB 72 AT 12:44:08

  SUBROUTINE RUNGE     ENTRY POINT 000134

  STORAGE USED (BLOCK, NAME, LENGTH)

      0001   *CODE   000163
      0000   *DATA   000115
      0002   *BLANK  000000


  EXTERNAL REFERENCES (BLOCK, NAME)

      0003   NERR2$
      0004   NERR3$


  STORAGE ASSIGNMENT FOR VARIABLES (BLOCK, TYPE, RELATIVE LOCATION, NAME)

   0001    000021 1L          0001    000121 10L         0001    000023 107G        0001    000054 120G        0001    000102 130G
   0001    000030 3L          0001    000032 4L          0001    000036 5L          0001    000074 7L          0001    000117 9L
   0000 R  000063 A           0000 I  000062 I           0000    000075 INJP$       0000 R  000000 Q


00101      1*          SUBROUTINE RUNGE(N,Y,F,X,H,M,K)
00101      2*    C     THIS ROUTINE PERFORMS RUNGE KUTTA CALCULATIONS BY GILL'S METHOD
00103      3*          DIMENSION Y(50),F(50),Q(50)
00104      4*          M=M+1
00105      5*          GO TO (1,4,5,3,7),M
00106      6*        1 DO 2 I=1,N
00111      7*        2 Q(I)=0.0
00113      8*          A=0.5
00114      9*          GO TO 9
00115     10*        3 A=1.707107
00115     11*    C     IF YOU NEED MORE ACCURACY USE A=1.7071067811865475244
00116     12*        4 X=X+0.5*H
00117     13*        5 DO 6 I=1,N
00122     14*          Y(I)=Y(I)+A*(F(I)*H-Q(I))
00123     15*        6 Q(I)=2.0*A*H*F(I)+(1.0-3.0*A)*Q(I)
00125     16*          A=0.2928932
00125     17*    C     IF YOU NEED MORE ACCURACY USE A=0.29289321881345524756
00126     18*          GO TO 9
00127     19*        7 DO 8 I=1,N
00132     20*        8 Y(I)=Y(I)+H*F(I)/6.0- (I)/3.0
00134     21*          M=0.0
00135     22*          K=2
00136     23*          GO TO 10
00137     24*        9 K=1
00140     25*       10 RETURN
00141     26*          END
```

```
                BUOY DYNAMICS                                           DATE  230272  PAGE    22
@I FOR DSTAT.DSTAT
UNIVAC 1108 FORTRAN V LEVEL 2206 0023                                                                              12:44: 9.365
THIS COMPILATION WAS DONE ON 23 FEB 72 AT 12:44:09

  SUBROUTINE DSTAT      ENTRY POINT 000045

  STORAGE USED (BLOCK, NAME, LENGTH)

        0001    *CODE    000062
        0000    *DATA    000017
        0002    *BLANK   000000

  EXTERNAL REFERENCES (BLOCK, NAME)

        0003    SQRT
        0004    NERR3$

  STORAGE ASSIGNMENT FOR VARIABLES (BLOCK, TYPE, RELATIVE LOCATION, NAME)

   0001   000012 110G        0000    000005 INJP$      0000 I 000003 J        0000 I 000000 N        0000 R 000001 S
   0000 R 000002 S1

00101      1*          SUBROUTINE DSTAT(PAR,PRMN,PRVR,PRSD)
00103      2*          DIMENSION PAR(2048)
00104      3*          N=1024
00105      4*          S=0.0
00106      5*          S1=0.0
00107      6*          DO 3 J=1,2047,2
00112      7*          S=S+PAR(J)
00113      8*        3 S1=S1+PAR(J)*PAR(J)
00115      9*          PRMN=S/N
00116     10*          PRVR=(S1-PRMN*S)/N
00117     11*          PRSD=SQRT(PRVR)
00120     12*          RETURN
00121     13*          END

       END OF UNIVAC 1108 FORTRAN V COMPILATION.      0 *DIAGNOSTIC* MESSAGE(S)
```

```
                 BUOY DYNAMICS                                          DATE  230272  PAGE     23
@A     FOR    FFOUR,FFOUR                                                                          12:44:10.490
UNIVAC 1108 FORTRAN V LEVEL 2206 0023
THIS COMPILATION WAS DONE ON 23 FEB 72 AT 12:44:10

   SUBROUTINE FFOUR      ENTRY POINT 000322

   STORAGE USED (BLOCK, NAME, LENGTH)

        0001    *CODE    000357
        0000    *DATA    000051
        0002    *BLANK   000000


   EXTERNAL REFERENCES (BLOCK, NAME)

        0003    UNSCR
        0004    NERR3$


   STORAGE ASSIGNMENT FOR VARIABLES (BLOCK, TYPE, RELATIVE LOCATION, NAME)

    0001     000021 10L        0001     000175 153G       0001     000257 170G       0001     000143 30L        0001     000304 4L
    0001     000023 40L        0001     000041 60L        0001     000024 80L        0001     000153 91L        0001     000166 93L
    0001     000223 94L        0000 C 000001 A           0000 R 000013 CSE         0000 C 000013 E           0000 I 000012 I
    0000 I 000006 INDEX       0000     000021 INJP$      0000 I 000011 I2          0000 I 000005 LINC        0000 I 000000 LOC
    0000 I 000007 LOC1        0000 I 000004 THTA        0000 I 000003 TINC        0000 R 000010 Y


00101       1*            SUBROUTINE FFOUR(X,C,ISCR,T,BIN,J)
00103       2*            COMPLEX E,X(1),A
00104       3*            INTEGER T,TINC,THTA,BIN
00105       4*            DIMENSION CSE(2),C(1),ISCR(1)
00106       5*            EQUIVALENCE (E,CSE)
00107       6*          2 TINC=BIN/T
00110       7*            LINC=T/2                                                  FF8
00111       8*         10 LOC=LINC                                                  FF9
00112       9*         40 THTA=0                                                    FF10
00113      10*         80 CSE(1)=C(THTA+1)                                          FF11
00114      11*            INDEX=BIN/4+1-THTA
00115      12*            CSE(2)=-C(INDEX)
00116      13*         60 LOC=LOC+1                                                 FF13
00117      14*            LOC1=LOC-LINC                                             FF14
00120      15*            E=E*(X(LOC1)-X(LOC))                                      FF15
00121      16*            X(LOC1)=X(LOC1)+X(LOC)                                    FF16
00122      17*            X(LOC)=E                                                  FF17
00123      18*            THTA=THTA+TINC                                            FF18
00124      19*            IF(THTA-BIN/2) 20,30,30                                   FF19
00127      20*         20 IF(THTA-BIN/4) 80,50,50                                   FF20
00132      21*         50 INDEX=BIN/2+1-THTA
00133      22*            CSE(1)=-C(INDEX)
00134      23*            INDEX=THTA-(BIN/4-1)
00135      24*            CSE(2)=-C(INDEX)
00136      25*            GO TO 60                                                  FF23
```

```
                 BUOY DYNAMICS                                          DATE  230272  PAGE    24

00137          30 IF.LOC-T) 90,91,91
00142          90 LOC=LOC+LINC                                                  FF24
00143             GO TO 40                                                      FF25
00144          91 IF(2-LINC) 92,93,94                                           FF26
00147          92 LINC=LINC/2                                                   FF27
00150             TINC=TINC+TINC                                                FF28
00151             GO TO 10                                                      FF29
00152          93 DO 100 LOC=2,T,2                                              FF30
00155             LOC1=LOC-1                                                    FF31
00156             E=X(LOC1)-X(LOC)                                              FF32
00157             X(LOC1)=X(LOC1)+X(LOC)                                        FF33
00160         100 X(LOC)=E                                                      FF34
00162          94 CALL UNSCR(X,ISCR,T)                                          FF35
00163             IF(J.EQ.-1) GO TO 4
00165             Y=1.0/T
00166             I2=T/2+1
00167             DO 3 I=2,I2
00172             A=X(I)
00173             X(I)=CMPLX(REAL(X(T+2-I))*Y,AIMAG(X(T+2-I))*Y)
00174           3 X(T+2-I)=CMPLX(REAL(A)*Y,AIMAG(A)*Y)
00176             X(1)=CMPLX(REAL(X(1))*Y,AIMAG(X(1))*Y)
00177           4 RETURN
00200             END
                                                                                FF38

      END OF UNIVAC 1108 FORTRAN V COMPILATION.      0 *DIAGNOSTIC* MESSAGE(S)
```

```
                BUOY DYNAMICS                                    DATE  230272  PAGE    25
@A    FOR   GNSCR,GNSCR
UNIVAC 1108 FORTRAN V LEVEL 2206 0023                                                        12:44:12. 93
THIS COMPILATION WAS DONE ON 23 FEB 72 AT 12:44:12

  SUBROUTINE GNSCR      ENTRY POINT 000062

  STORAGE USED (BLOCK, NAME, LENGTH)

        0001    *CODE    000075
        0000    *DATA    000024
        0002    *BLANK   000000

  EXTERNAL REFERENCES (BLOCK, NAME)

        0003    NERR3$

  STORAGE ASSIGNMENT FOR VARIABLES (BLOCK, TYPE, RELATIVE LOCATION, NAME)

   0001   000013 11L        0001   000020 111G        0001   000046 8L          0000   00000_ INJP$       0000 I 000003 J
   0000 I 000001 M          0000 I 000002 N          0000 I 000000 TM

00101      1*           SUBROUTINE GNSCR(SCR,T)
00103      2*           INTEGER T,TM,SCR(1)
00104      3*           SCR(1)=1
00105      4*           M=1                                                      FF44
00106      5*           N=1                                                      FF45
00107      6*           TM=T/2                                                   FF46
00110      7*        11 DO 9 J=1,M                                               FF47
00113      8*           N=N+1                                                    FF48
00114      9*         9 SCR(N)=TM+SCR(J)                                         FF49
00116     10*           IF(T-SCR(N)) 8,8,10                                      FF50
00121     11*        10 M=M+M                                                    FF51
00122     12*           TM=TM/2                                                  FF52
00123     13*           GO TO 11                                                 FF53
00124     14*         8 RETURN                                                   FF54
00125     15*           END                                                      FF55
                                                                                 FF56

  END OF UNIVAC 1108 FORTRAN V COMPILATION.     0 *DIAGNOSTIC* MESSAGE(S)
```

```
                    BUOY DYNAMICS                                    DATE  230272  PAGE    26
@A    FOR   UNSCR,UNSCR
UNIVAC 1108 FORTRAN V LEVEL 2206 0023                                                                 12:44:13.208
THIS COMPILATION WAS DONE ON 23 FEB 72 AT 12:44:13

  SUBROUTINE UNSCR      ENTRY POINT 000047

  STORAGE USED (BLOCK, NAME, LENGTH)

       0001    *CODE    000061
       0000    *DATA    000023
       0002    *BLANK   000000

  EXTERNAL REFERENCES (BLOCK, NAME)

       0003    NERR3$

  STORAGE ASSIGNMENT FOR VARIABLES (BLOCK, TYPE, RELATIVE LOCATION, NAME)

   0001    000012 106G      0001    000030 9L       0000 C 000000 E        0000 I 000003 I      0000    000004 INJP$
   0000 I 000002 J

00101      1*          SUBROUTINE UNSCR(X,SCR,T)
00103      2*          COMPLEX E,X(1)
00104      3*          INTEGER T,SCR(1)
00105      4*          DO 9 J=1,T
00110      5*          I=SCR(J)                                               FF62
00111      6*          IF(J-I) 9,9,10                                          FF63
00114      7*       10 E=X(J)                                                  FF64
00115      8*          X(J)=X(I)                                               FF65
00116      9*          X(I)=E
00117     10*        9 CONTINUE                                                FF67
00121     11*          RETURN                                                  FF68
00122     12*          END                                                     FF69
                                                                               FF70
     END OF UNIVAC 1108 FORTRAN V COMPILATION.     0 *DIAGNOSTIC* MESSAGE(S)
```

```
               BUOY DYNAMICS                                          DATE  230272  PAGE    27

BA    FOR   COSINE,COSINE                                                                                      12:44:14.245
UNIVAC 1108 FORTRAN V LEVEL 2206 0023
THIS COMPILATION WAS DONE ON 23 FEB 72 AT 12:44:14


   SUBROUTINE COSINE    ENTRY POINT 000126

   STORAGE USED (BLOCK, NAME, LENGTH)

         0001    *CODE    000141
         0000    *DATA    000053
         0002    *BLANK   000000


   EXTERNAL REFERENCES (BLOCK, NAME)

         0003    RND
         0004    DCOS
         0005    DSIN
         0006    NERR3$


   STORAGE ASSIGNMENT FOR VARIABLES (BLOCK, TYPE, RELATIVE LOCATION, NAME)

    0001   000060 120G        0000 D 000000 ANG        0000 D 000002 CS         0000 D 000006 CSJ        0000 I 000013 INDEX
    0000   000030 INJP$       0000 I 000012 INTB       0000 I 000014 J          0003 R 000000 RND        0000 D 000004 SN
    0000 D 000010 SNJ


00100       1*    C *** SUBROUTINE COSINE *** 10/14/70 *** A.H.NUTTALL
00101       2*          SUBROUTINE COSINE(C,BIN)                                  FF80
00103       3*          DOUBLE PRECISION ANG,CS,SN,CSJ,SNJ
00104       4*          INTEGER BIN                                               FF82
00105       5*          DIMENSION C(1)
00106       6*          ANG=6.283185307179586480D0/BIN
00107       7*          INTB=BIN/8                                                FF84
00110       8*          INDEX=2*INTB+1
00111       9*          CS=DCOS(ANG)
00112      10*          SN=DSIN(ANG)
00113      11*          CSJ=1.0D0
00114      12*          SNJ=0.0D0
00115      13*          C(1)=1.0                                                  FF87
00116      14*          C(INDEX)=0.0
00117      15*          DO 9 J=1,INTB                                             FF89
00122      16*          ANG=CSJ*CS-SNJ*SN
00123      17*          SNJ=CSJ*SN+SNJ*CS
00124      18*          CSJ=ANG
00125      19*          C(J+1)=RND(CSJ)
00126      20*        9 C(INDEX-J)=RND(SNJ)
00130      21*          RETURN                                                    FF92
00131      22*          END                                                       FF93

        END OF UNIVAC 1108 FORTRAN V COMPILATION.      0 *DIAGNOSTIC* MESSAGE(S)
```

```
                 BUOY DYNAMICS                                                     DATE  230272  PAGE   28
@I ASM RND,RND
ASSEMBLER  BL3D  2404 0007                                                                                              12:44:15.517
THIS ASSEMBLY WAS DONE ON 23 FEB 72 AT 12:44:15
                                                                   REGNAM                          . ASSOCIATE REG'S WITH MNEM'S
                                                          $(1)                                     . GENERATE CODE UNDER L.C.1
                                                          RND*                                     . ENTRY POINT FOR X=RND(DX)
         01     000000  71 13 00 13 1 000000                       DL       A0,*0,X11              . A0,A1 <-- DX
                000001  76 17 04 00 0 000014                       FCL      A4,A0                  . A4 <-- SINGL(DX)
                000002  01 00 04 00 0 000000                       SA       A4,SPDX                . SPDX <-- A4
                000003  73 13 03 00 0 000011                       LDSL     A3,9                   . A3 <-- C,A4 <-- M XXX
                000004  73 02 04 00 0 000011                       SSL      A4,9                   . A4 <-- M
                000005  74 03 00 00 0 000017                       JN       A0,NEG                 . JUMP IF DX < 0
                000006  45 00 01 00 0 000001                       TOP      A1,(0040000,0)         . SKIP NI IF ROUND UP
                000007  74 04 00 00 0 000030                       J        FIN                    . NO  UND UP, EXIT
                000010  10 00 02 00 0 000002                       LA       A2,(000777777777)      . A0 <-- 000777777777
                000011  52 00 02 00 0 000020                       TE       A2,A4                  . SKIP NI IF M = 7'S
                000012  74 04 00 00 0 000033                       J        FIN1                   . NO, JUST INCREMENT
                000013  14 16 03 00 0 000001                       AA,U     A3,1                   . C <-- C+1
                000014  10 00 04 00 0 000003                       LA       A4,(0400000,0)         . M <-- 400000000000
                000015  73 03 03 00 0 000011                       DSL      A3,9                   . A4 <-- C,M
                000016  74 04 00 00 0 000031                       J        FIN2                   . EXIT
                000017  44 00 01 00 0 000001      NEG              TEP      A1,(0040000,0)         . SKIP NI IF ROUND UP
                000020  74 04 00 00 0 000030                       J        FIN                    . NO ROUND UP, EXIT
                000021  05 00 00 00 0 000016                       SZ       A2                     . A2 <-- 0
                000022  52 00 02 00 0 000020                       TE       A2,A4                  . SKIP NI IF M = 0'S
                000023  74 04 00 00 0 000037                       J        FIN3                   . NO, JUST DECREMENT
                000024  15 16 03 00 0 000001                       ANA,U    A3,1                   . C <-- C - 1
                000025  10 00 04 00 0 000004                       LA       A4,(0377777777777)     . M <-- 377777777777
                000026  73 03 03 00 0 000011                       DSL      A3,9                   . A4 <-- C,M
                000027  74 04 00 00 0 000031                       J        FIN2                   . EXIT
                000030  10 00 04 00 0 000000      FIN              LA       A4,SPDX                . A4 <-- SPDX
                000031  01 00 04 00 0 000014      FIN2             SA       A4,A0                  . A0 <-- A4
                000032  74 04 00 13 0 000002                       J        2,X11                  . RETURN
                000033  10 00 04 00 0 000000      FIN1             LA       A4,SPDX                . A4 <-- SPDX
                000034  14 16 04 00 0 000001                       AA,U     A4,1                   . A4 <-- A4+1
                000035  01 00 04 00 0 000014                       SA       A4,A0                  . A0 <-- A4
                000036  74 04 00 13 0 000002                       J        2,X11                  . RETURN
                000037  10 00 04 00 0 000000      FIN3             LA       A4,SPDX                . A4 <-- SPDX
                000040  15 16 04 00 0 000001                       ANA,U    A4,1                   . A4 <-- A4-1
                000041  01 00 04 00 0 000014                       SA       A4,A0                  . A0 <-- A4
                000042  74 04 00 13 0 000002                       J        2,X11                  . RETURN
                                                  $(0)                                             . GENERATE DATA UNDER L.C.0
         00     000000  000000000000              SPDX             +        0                      . SINGLE PRECISION DX
                                                                   END                             .
                000001  040000 000000
                000002  000777777777
                000003  400000 000000
                000004  377777777777
```

Buoy System Dynamics for the Torroidal Buoy Used in WHOI Mooring No. 238

This program (figure B-4) is basically the same as the previous program except that the mooring line forces and dynamics are simulated with the finite-difference method described in chapter III of the main text. Subroutine "MOOR" (figure B-5) takes the spatial values of the six variables (strain, two angles, and the velocity components) describing the cable motions and updates them for the next time step. The tension and angles at the top of the cable are then used to compute the mooring line forces acting on the buoy.

For numerical stability, the value of the tensile wave characteristic should never exceed the quotient of the nodal spacing, H, and the time step, K, in the subroutine:

$$Ch_1 < H/K.$$

The list of input values is the same as that for the previous program. In this particular program, the mooring line is composed of two segments, and the cable weights, masses, etc. are changed at a cable length of 4800 ft. There are 20 nodes spaced 400 ft apart to simulate dynamics of an 8,000-ft mooring line.

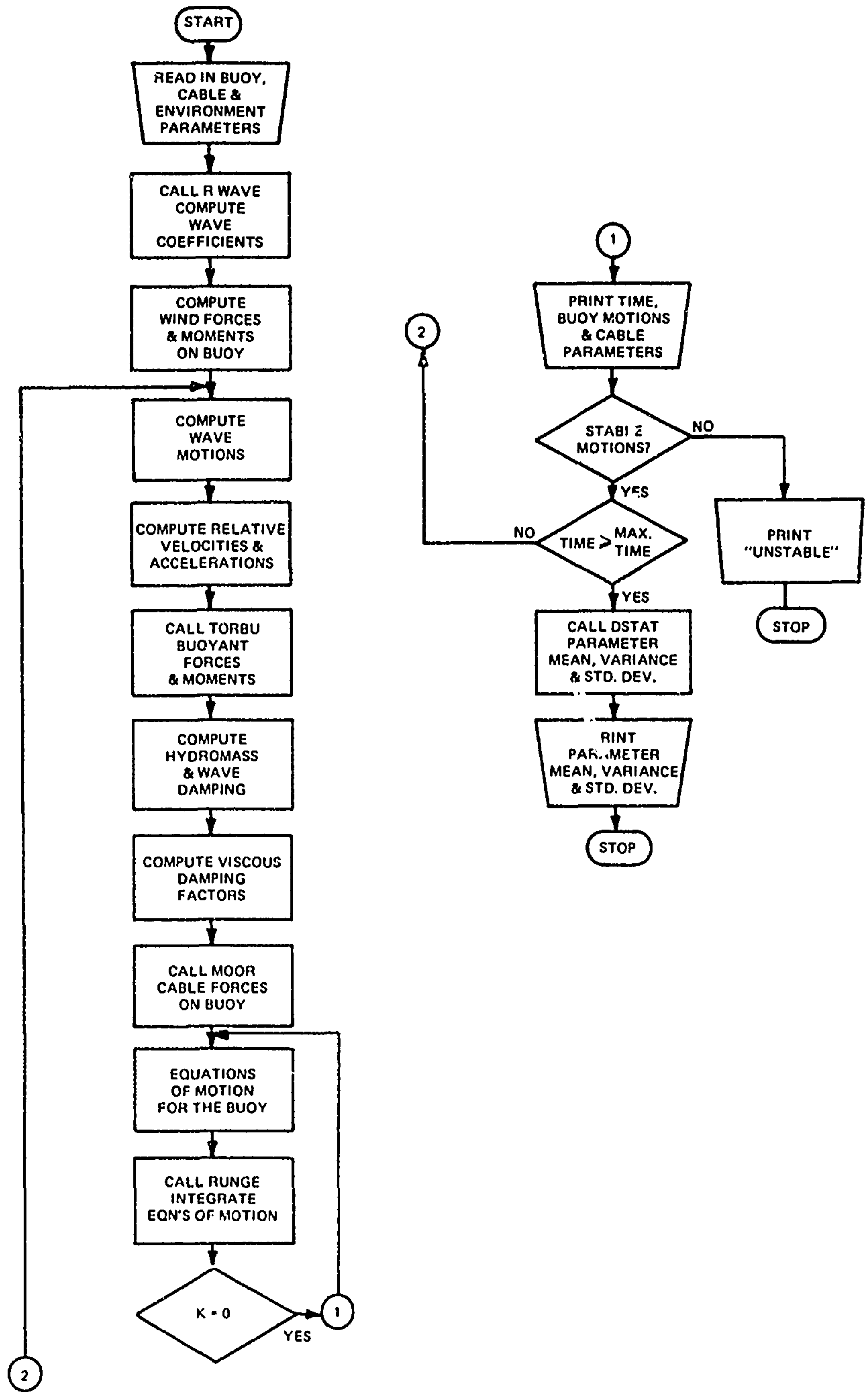

Fi. ure B-4. Torroidal Buoy WHOI Mooring No. 238
Dynamics Simulation Flow Chart

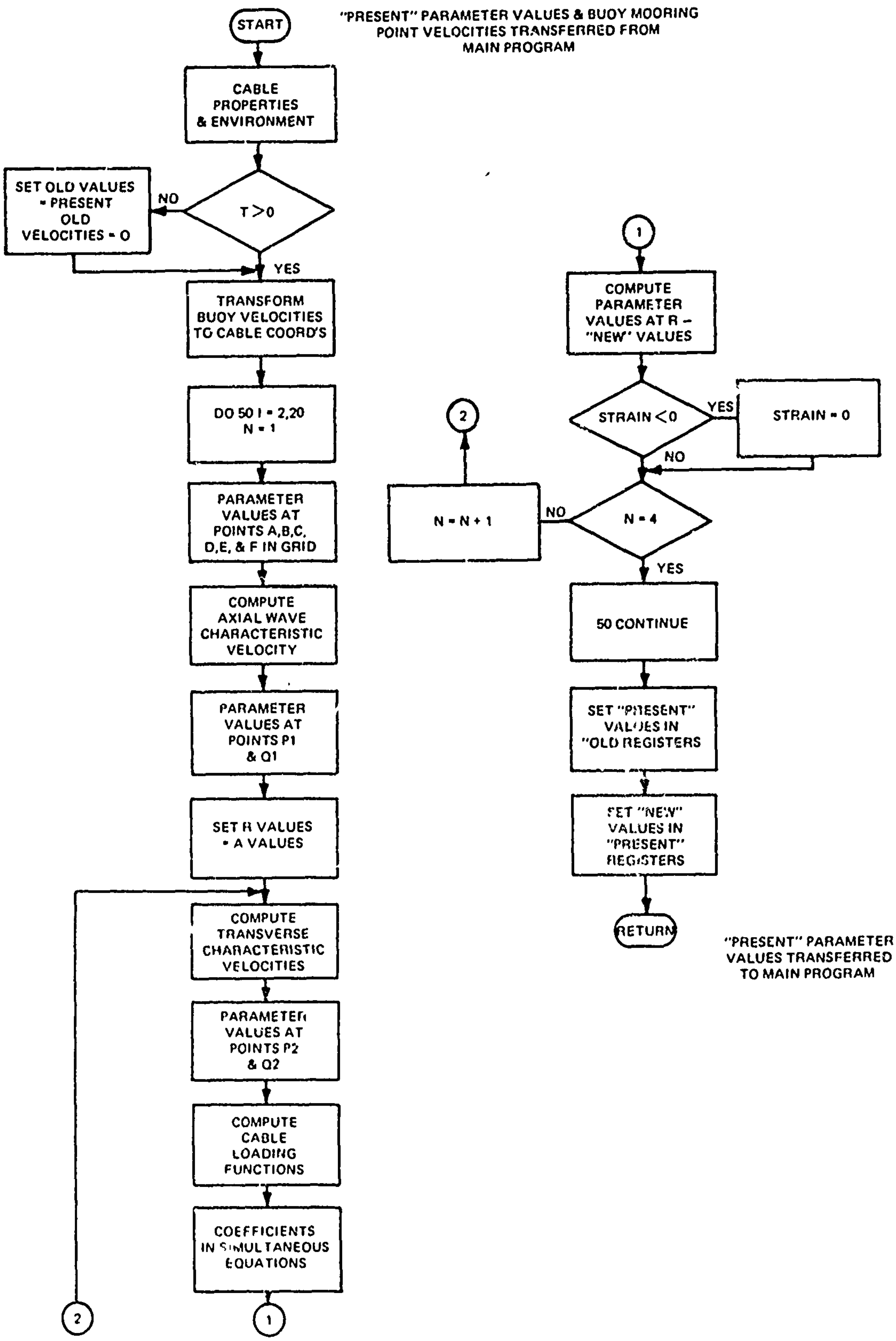

Figure B-5. Finite-Difference Cable Dynamics Simulation Flow Chart

```
                BUOY DYNAMICS                                          DATE  010572  PAGE     3
G FOR S1279,S1279                                                                                   10:50:52.667
UNIVAC 1108 FORTRAN V LEVEL 2206 0023
THIS COMPILATION WAS DONE ON 01 MAY 72 AT 10:50:52

  MAIN PROGRAM

  STORAGE USED (BLOCK, NAME, LENGTH)

       0001    *CODE    001735
       0000    *DATA    010637
       0002    *BLANK   000000

  EXTERNAL REFERENCES (BLOCK, NAME)

       0003    RWAVE
       0004    TORBU
       0005    MOOR
       0006    RUNGE
       0007    DSTAT
       0010    NRDU$
       0011    NI02$
       0012    SQRT
       0013    NEXP6$
       0014    EXP
       0015    COS
       0016    SIN
       0017    NERR2$
       0020    NWDU$
       0021    NSTOP$

  STORAGE ASSIGNMENT FOR VARIABLES (BLOCK, TYPE, RELATIVE LOCATION, NAME)

  0000      010515 103F      0000      010520 105F      0000      010522 106F      0000      010525 107F      0000      010527 108F
  0000      010531 109F      0000      010533 112F      0000      010535 120F      0000      010537 121F      0000      010541 122F
  0000      010543 123F      0000      010545 124F      0000      010547 129F      0000      010551 131F      0000      000145 211G
  0001      000164 227G      0001      000225 31L       0001      000241 32L       0001      000243 33L       0001      000551 371G
  0001      001431 40L       0001      000336 41L       0001      000346 42L       0001      000774 441G      0001      000452 5L
  0001      001065 50L       0001      001520 542G      0001      001452 72L       0001      001514 73L       0001      001535 87L
  0001      001731 88L       0001      001716 92L       0000 R 010327 A          0000 R 003232 ACX        0000 R 004232 ACY
  0000 R 005232 ACZ        0000 R 010462 ALFA       0000 R 010274 ALIN       0000 R 010373 ALW        0000 R 000206 AMP
  0000 R 010413 ANG        0000 R 010345 ARXX       0000 R 010470 AWMN       0000 R 010472 AWSD       0000 R 002232 AWV
  0000 R 010471 AWVR       0000 R 010476 AXMN       0000 R 010500 AXSD       0000 R 010477 AXVR       0000 R 010501 AYMN
  0000 R 010503 AYSD       0000 R 010502 AYVR       0000 R 010504 AZMN       0000 R 010506 AZSD       0000 R 010505 AZVR
  0000 R 010336 BA         0000 R 010434 BBB        0000 R 010436 BBX        0000 R 010463 BETA       0000 R 010437 BGG
  0000 R 010441 BGX        0000 R 010335 BLAMB      0000 R 006232 BPIT       0000 R 010507 BPMN       0000 R 010511 BPSD
  0000 R 010510 BPVR       0000 R 010270 BR         0000 R 010512 BRMN       0000 R 007232 BROL       0000 R 010514 BRSD
  0000 R 010513 BRVR       0000 R 010275 BTIN       0000 R 010374 BTW        0000 R 010415 BT1        0000 R 010435 BXB
  0000 R 010440 BXG        0000 R 010433 BXX        0000 R 010340 CMX        0000 R 010341 CMY        0000 R 010342 CMZ
  0000 R 010343 CNXX       0000 R 010344 CNYY       0000 R 010312 CY         0000 R 010310 CYS        0000 R 010313 CZ
  0000 R 010311 CZS        0000 R 000000 D          0000 R 010401 DALW       0000 R 010422 DAL1       0000 R 010430 DAL2
  0000 R 010402 DBTW       0000 R 010424 DBT1       0000 R 010431 DBT2       0000 R 010407 DDALW      0000 R 010410 DDBTW
  0000 R 010460 DDBT1      0000 R 010411 DDGMW      0000 R 010461 DDGM1      0000 R 010404 DDXW       0000 R 010455 DDX1
  0000 R 010405 DDYW       0000 R 010456 DDY1       0000 R 010406 DDZW       0000 R 010457 DDZ1       0000 R 010351 DGAA
```

```
0000 R 010352 DGBB     0000 R 010357 DGBZ     0000 R 010353 DGGG     0000 R 010360 DGGY     0000 R 010403 DGMW
0000 R 010423 DGM1     0000 R 010432 DGM2     0000 R 010346 DGXX     0000 R 010355 DGYG     0000 R 010347 DGYY
0000 R 010356 DGZB     0000 R 010350 DGZZ     0000 R 010446 DTDE     0000 R 010376 DXW      0000 R 010417 DX1
0000 R 010425 DX2      0000 R 010377 DYW      0000 R 010420 DY1      0000 R 010426 DY2      0000 R 010400 DZW
0000 R 010421 DZ1      0000 R 010427 DZ2      0000 R 010452 FAL      0000 R 010453 FBT      0000 R 010454 FGM
0000 R 010334 FH       0000 R 010447 FX       0000 R 010450 FY       0000 R 010451 FZ       0000 R 010464 GAMMA
0000 R 010276 GMIN     0000 R 010375 GMW      0000 R 010416 GM1      0000 R 010361 H        0000 I 010332 I
0000 I 010323 J        0000 I 010330 K        0000 I 010333 L        0000 I 010331 M        0000 R 010250 MB
0000 R 010237 MHAA     0000 R 010235 MHBB     0000 R 010246 MHBX     0000 R 010244 MHBZ     0000 R 010236 MHGG
0000 R 010247 MHGX     0000 R 010245 MHGY     0000 R 010240 MHXB     0000 R 010241 MHXG     0000 R 010232 MHXX
0000 R 010242 MHYG     0000 R 010233 MHYY     0000 R 010243 MHZB     0000 R 010234 MHZZ     0000 R 000174 MOMEG
0000 R 010251 MU       0000 I 010324 N        0000 R 010255 NAA      0000 R 010256 NBB      0000 R 010261 NBX
0000 R 010267 NBZ      0000 R 010257 NGG      0000 R 010263 NGX      0000 R 010265 NGY      0000 I 010325 NN
0000 R 010260 NXB      0000 R 010262 NXG      0000 R 010252 NXX      0000 R 010264 NYG      0000 R 010253 NYY
0000 R 010266 NZB      0000 R 010254 NZZ      0000 R 010307 PER      0000 R 000122 PHI      0000 R 000220 PHS
0000 R 010326 R        0000 R 010442 RCAB     0000 R 000075 STRN     0000 R 010465 TBMN     0000 R 010467 TBSD
0000 R 010466 TBVP     0000 R 000050 TEN      0000 R 000232 TENB     0000 R 000147 THE      0000 R 010443 UBY
0000 R 010444 VBY      0000 R 010366 VELBB    0000 R 010367 VELGB    0000 R 010363 VELXB    0000 R 010364 VELYB
0000 R 010365 VELZB    0000 R 010301 WAREA    0000 R 010302 WAREL    0000 R 010273 WB       0000 R 010445 WBY
0000 R 010277 WCD      0000 R 010300 WCL      0000 R 010303 WCPHT    0000 R 010305 WDUR     0000 R 010321 WFBT
0000 R 010322 WFGM     0000 R 010316 WFX      0000 R 010317 WFY      0000 R 010320 WFZ      0000 R 010362 WHT
0000 R 010306 WHTM     0000 R 010304 WINDS    0000 R 010314 WINDY    0000 R 010315 WINDZ    0000 R 010412 WK
0000 R 010473 WVMN     0000 R 010475 WVSD     0000 R 010474 WVVR     0000 R 010271 XCG      0000 R 010354 XCPRS
0000 R 010337 XHP      0000 R 010272 XML      0000 R 010370 XW       0000 R 001232 XWV      0000 R 010414 X1
0000 R 000024 Y        0000 R 010371 YW       0000 R 010372 ZW

00100      C      THIS PROGRAM COMPUTES THE RESPONSE OF AN AXI-SYMMETRIC BUOY
00100      C      EXPOSED TO THE OCEAN ENVRIONMENT
00100      C      UNITS ARE IN FT',LB,SEC
00100      C
00101             DIMENSION D(20),Y(20)
00103             DIMENSION TEN(21),STRN(21),PHI(21),THE(21)
00104             DIMENSION MOMEG(10),AMP(10),PHS(10)
00105             DIMENSION TENB(512),XWV(512),AWV(512),ACX(512),ACY(512)
00106             DIMENSION ACZ(512),BPIT(512),BROL(512)
00107             REAL MHXX,MHYY,MHZZ,MHBB,MHGG,MHAA,MHXB,MHXG,MHYG,MHZB,MHBZ
00110             REAL MHGY,MHBX,MHGX,MB,MU,NXX,NYY,NZZ,NAA,NBB,NGG,NXB,NBX
00111             REAL NXG,NGX,NYG,NGY,NZB,NBZ
00112             REAL MOMEG
00112      C      THE COORDINATE SYSTEM
00112      C
00112      C
00112      C
00112      C
00112      C        Z -----------------------------------------------
00112      C                                                      /I
00112      C                                                     / I
00112      C                                                    /  I
00112      C                                                   /   I
00112      C                                                  /    I
00112      C                                                 /     I
00112      C                                                /      I
00112      C                                               /       I
00112      C                                              Y        I
```

```
00112        C                                             I
00112        C                                             I
00112        C                                             I
00112        C                                             I
00112        C                                             I
00112        C                                             I
00112        C                                             I
00112        C                                             I
00112        C                                             X
00112        C
00112        C
00112        C
00113         103 FORMAT(11H BUOY SINKS)
00114         105 FORMAT(6F10.2)
00115         106 FORMAT(9H UNSTABLE)
00116         107 FORMAT(5F10.4)
00117         108 FORMAT(2F10.4)
00120         109 FORMAT(3F10.4)
00121         112 FORMAT(8F8.2)
00122         120 FORMAT(1F10.4)
00123         121 FORMAT(1F20.4)
00124         122 FORMAT(1F30.4)
00125         123 FORMAT(1F40.4)
00126         124 FORMAT(1F50.4)
00127         129 FORMAT(3F10.5)
00130         131 FORMAT(8F8.5)
00130        C    READ IN THE BUOY PARAMETERS
00130        C    BUOY RADIUS, HT. OF C.OF G. FROM MOOR POINT AND THE LENGTH OF THE
00130        C    MOOR POINT BELOW THE BOTTOM OF THE BUOY
00131             READ 109,BR,XCG,XML
00131        C    INERTIAS
00136             READ 107,WB,MB,ALIN,BTIN,GMIN
00136        C    WIND LIFT AND DRAG COEFFICIENTS AND AREAS
00145             READ 107,WCD,WCL,WAREA,WAREL,WCPHT
00145        C
00145        C    THE VISCOSITY    THE WATER AT 40 DEG F
00154             MU=2.735E-5
00154        C
00154        C    READ THE MEAN WIND CAUSING THE SEA STATE (WHICH MAY BE DIFFERENT
00154        C    THAN THE WIND  ACTING DURING THE SIMULATION) AND ITS DURATION
00155             READ 108,WINDS,WDUR
00161             CALL RWAVE(WINDS,WDUR,WHTM,PER,MOMEG,AMP,PHS)
00161        C
00161        C
00161        C    THE CURRENTS IN THE WATER COLUMN
00161        C    READ THE Y AND Z COMPONENTS OF THE  SURFACE CURRENT
00162             READ 108,CYS,CZS
00162        C    IF THE CURRENT VARIES WITH DEPTH, INSERT THE FUNCTIONS FOR
00162        C    STRENGTH AND DIRECTION
00162        C
00162        C    FOR A UNIFORM CURRENT
00166             CY=CYS
00167             CZ=CZS
00167        C
00167        C    THE WIND ACTING ON THE BUOY
00167        C    READ THE WIND COMPONENTS ACTING ON THE BUOY AT THE TIME OF THE
00167        C    SIMULATION
00170             READ 108,WINDY,WINDZ
```

```
00174          WFX=-0.0034*WCL*WAREL*(WINDY**2+WINDZ**2)
00175          WFY=0.0034*WCD*WAREA*WINDY*ABS(WINDY)
00176          WFZ=0.0034*WCD*WAREA*WINDZ*ABS(WINDZ)
00177          WFBT=-WFZ*WCPHT
00200          WFGM=-WFY*WCPHT
00201          J=1
00202          N=12
00203          NN=1
00204          R=0.0025
00205          A=0.0
00206          K=0
00207          M=0
00207    C     THE INITIAL CONDITIONS
00207    C     ALL ACCELERATIONS AND VELOCITIES ARE ZERO
00210          DO 56 I=1,41,2
00213          D(I)=0.0
00214       56 Y(I)=0.0
00214    C     READ THE INITIAL BUOY DISPLACEMENTS - X,Y,Z
00216          READ 109,Y(2),Y(4),Y(6)
00216    C     THE INITIAL BUOY ANGLES ARE ZERO
00223          Y(8)=0.0
00224          Y(10)=0.0
00225          Y(12)=0.0
00225    C     THE INITIAL CONDITIONS FOR THE CABLE
00226          DO 2 L=1,21
00231        2 READ 129,STRN(L),PHI(L),THE(L)
00237       30 CONTINUE
00237    C
00237    C     THE HYDRODYNAMIC MASSES AND MOMENTS OF INERTIA
00237    C
00237    C     THE DIMENSIONLESS FREQUENCY
00240          FR=((6.2832/PER)**2)*BR/32.2
00241          BLAMB=SQRT(6.25/(PER*MU))
00242          BA=BLAMB*BR
00242    C     HYDRODYNAMIC FORCE MOMENT ARM
00243          XHM=4.16
00243    C     HEAVE
00244          IF(FR.GE.0.2)GO TO 31
00246          CMX=2.31
00247          GO TO 33
00250       31 IF(FR.GE.2.4)GO TO 32
00252          CMX=1.35725*(FR**(-.330597))
00253          GO TO 33
00254       32 CMX=1.0
00254    C     SWAY-SURGE
00255       33 CMY=0.215
00256          [illegible]Z=CMY
00257          MHXX=1.988*(BR**3)*CMX
00260          M[illegible]YY=1.988*((BR**3)*CMY+0.0045)
00261          MHZZ=MHYY
00261    C
00262          MH[illegible]=16.65*(BR**5)*(1.0+BA)/(1.0+2.0*BA+2.0*(BA**2))
00262    C     PITC[illegible]D ROLL
00263          MHBB=[illegible]*(XHM**2)
00264          MHGG=MHBB
00264    C     CROSS-COUPLED HYDROMASSES
00265          MHBX=0.0
00266          MHGX=0.0
```

```
00267          MHXB=0.0
00270          MHXG=0.0
00271          MHYG=-MHYY*XHf
00272          MHZB=-MHYG
00273          MHBZ=MHZB
00274          MHGY=MHYG
00274     C
00274     C    THE DAMPING DUE TO WAVE GENERATION
00274     C
00274     C    HEAVE
00275          IF(FR.GE.0.8)GO TO 41
00277          CNXX=FR/(0.132617+0.873644*FR)
00300          GO TO 42
00301       41 CNXX=1.2476*EXP(-0.37376*FR)
00302       42 CNYY=0.14
00303       43 NXX=1.988*FR*(BR**3)*CNXX
00304          NYY=1.988*FR*(BR**3)*CNYY
00305          NZZ=NYY
00305     C    PITCH AND ROLL
00306          NAA=4.195*MU*(BR**3)*(3.0+6.0*BA+6.0*(BA**2)+2.0*(BA**3))
00306         1 /(1.0+2.0*BA+2.0*(BA**2))
00307          NGG=NBB
00307     C    CROSS COUPLED WAVE DAMPING
00310          NXB=0.0
00311          NBX=0.0
00312          NXG=0.0
00313          NGX=0.0
00314          NZB=-NYG
00315          NBZ=NZB
00316          NGY=NYG
00316     C
00316     C    THE VISCOUS DAMPING AND DRAG
00316     C    AREAS
00317          ARXX=3.1416*(BR**2)
00320          DGXX=1.2*ARXX
00321          DGYY=15.6
00322          DGZZ=15.6
00323          DGAA=0.0
00324          DGBB=0.0
00325          DGGG=0.0
00326          XCPRS=3.25
00326     C    CROSS-COUPLED VISCOUS DRAG
00327          DGYG=-DGYY*(XCPRS**2)
00330          DGZB=-DGYG
00331          DGBZ=DGZB
00332          DGGY=DGYG
00332     C
00333        5 CONTINUE
00334          NYG=-NYY*(1.282-0.5*H)
00335          NBB=NAA+NZZ*((1.282-0.5*H)**2)
00336          WHT=A*WHTM/(2.0*PER)
00337          IF(A.GE.(2.0*PER))WHT=WHTM
00341          VELXB=Y(1)
00342          VELYB=Y(3)
00343          VELZB=Y(5)
00344          VELBB=Y(9)
00345          VELGB=Y(11)
00345     C    THE WAVES
```

```
00345   C      FOR A SINGLE TRAIN OF WAVES, ASSUME THEY ARE COMING IN ON THE
00345   C      Z AXIS
00346          XW=0.0
00347          YW=0.0
00350          ZW=0.0
00351          ALW=0.0
00352          BTW=0.0
00353          GMW=0.0
00354          DXW=0.0
00355          DYW=0.0
00356          DZW=0.0
00357          DALW=0.0
00360          DBTW=0.0
00361          DGMW=0.0
00362          DDXW=0.0
00363          DDYW=0.0
00364          DDZW=0.0
00365          DDALW=0.0
00366          DDBTW=0.0
00367          DDGMW=0.0
00370          DO 14 I=1,9
00373          WK=(MOMEG(I)**2)/32.2
00374          ANG=A*MOMEG(I)+PHS(I)
00375          XW=XW-AMP(I)*SIN(ANG)
00376          ZW=ZW+AMP(I)*COS(ANG)
00377          BTW=BTW+WK*AMP(I)*COS(ANG)
00400          DXW=DXW-MOMEG(I)*AMP(I)*COS(ANG)
00401          DZW=DZW-MOMEG(I)*AMP(I)*SIN(ANG)
00402          DBTW=DBTW-WK*MOMEG(I)*AMP(I)*SIN(ANG)
00403          DDXW=DDXW+(MOMEG(I)**2)*AMP(I)*SIN(ANG)
00404          DDZW=DDZW-(MOMEG(I)**2)*AMP(I)*COS(ANG)
00405       14 DDBTW=DDBTW-WK*(MOMEG(I)**2)*AMP(I)*COS(ANG)
00405   C
00405   C      THE BUOY MOTIONS RELATIVE TO THE WATER MASS
00405   C      DISPLACEMENTS
00407          X1=Y(2)-XW
00410          BT1=Y(10)-BTW
00411          GM1=Y(12)-GMW
00411   C      VELOCITIES
00412          DX1=Y(1)-DXW
00413          DY1=Y(3)-DYW
00414          DZ1=Y(5)-DZW
00415          DAL1=Y(7)-DALW
00416          DGM1=Y(11)-DGMW
00417          DBT1=Y(9)-DBTW
00420          DGM1=Y(11)
00420   C
00420   C      WATER MASS VELOCITIES RELATIVE TO THE BUOY INCLUDING CURRENTS
00421          DX2=DX1
00422          DY2=DY1-CY
00423          DZ2=DZ1-CZ
00424          DAL2=DAL1
00425          DBT2=DBT1
00426          DGM2=DGM1
00426   C
00426   C
00426   C      THE BUOYANCY FORCES AND MOMENTS
00427          H=XCG+X1-XML
```

```
00430         CALL TORBU(H,BT1,BXX,BBB,BXB,BBX)
00431         CALL TORBU(H,GM1,BXX,BGG,BXG,BGX)
00431   C     MOORING LINE TENSIONS ACTING ON THE BUOY
00431   C     VELOCITY COMPONENTS AT THE END OF THE MOORING LINE
00432      84 RCAB=5.0*R
00433         UBY=Y(1)
00434         VBY=Y(3)-XCG*Y(11)
00435         WBY=Y(5)+XCG*Y(9)
00436         CALL MOOR(A,RCAB,UBY,VBY,WBY,STRN,PHI,THE)
00437         DTDE=6.87E5
00440         DO 83 I=1,21
00443         IF(I.GE.14)DTDE=3.06E4
00445      83 TEN(I)=DTDE*STRN(I)
00447         FX=TEN(1)*COS(PHI(1))*COS(THE(1))
00450         FY=TEN(1)*SIN(PHI(1))
00451         FZ=TEN(1)*COS(PHI(1))*SIN(THE(1))
00452         FAL=0.0
00453         FBT=-XCG*(-FZ*COS(Y(10))*COS(Y(12))+FX*SIN(Y(10))*COS(Y(12)))
00454         FGM=-XCG*(FY*COS(Y(10))*COS(Y(12))+FX*SIN(Y(12))*COS(Y(10)))
00455      50 CONTINUE
00456         DDX1=(Y(1)-VELXB)/R
00457         DDY1=(Y(3)-VELYB)/R
00460         DDZ1=(Y(5)-VELZB)/R
00461         DDBT1=(Y(9)-VELBB)/R
00462         DDGM1=(Y(11)-VELGB)/R
00463         DDX1=0.0
00464         DDY1=0.0
00465         DDZ1=0.0
00466         DDBT1=0.0
00467         DDGM1=0.0
00467   C
00467   C     THE EQUATIONS OF MOTION FOR THE BUOY
00467   C
00467   C     HEAVE -X MOTION
00470         D(1)=(WB-BXX-BXB-BXG+MHXX*DDXW-MHXB*DDBT1-MHXG*DDGM1-NXX*DX1
00470        1 -NXB*DBT1-NXG*DGM1-DGXX*DX2*ABS(DX2)+WFX+FX)/(MB+MHXX)
00471         D(2)=Y(1)
00471   C
00471   C     SWAY - Y MOTION
00472         D(3)=(MHYY*DDYW-MHYG*DDGM1-NYY*DY1-NYG*DGM1-DGYY*DY2*ABS(DY2)
00472        1 -DGYG*DGM2*ABS(DGM2)+WFY+FY)/(MB+MHYY)
00473         D(4)=Y(3)
00473   C
00473   C     SURGE - Z MOTION
00474         D(5)=(MHZZ*DDZW-MHZB*DDBT1-NZZ*DZ1-NZB*DBT1-DGZZ*DZ2*ABS(DZ2)
00474        1 -DGZB*DBT2*ABS(DBT2)+WFZ+FZ)/(MB+MHZZ)
00475         D(6)=Y(5)
00475   C
00475   C     YAW - ALFA MOTION
00476         D(7)=(MHAA*DDALW-NAA*DAL1-DGAA*DAL2*ABS(DAL2)+FAL)/(ALIN+MHAA)
00477         D(8)=Y(7)
00477   C
00477   C     PITCH - BETA MOTION
00500         D(9)=(-BBX-BBB-MHBX*DDX1-MHBZ*DDZ1+MHBB*DDBTW-NBX*DX1-NBB*DBT1
00500        1 -NBZ*DZ1-DGBZ*DZ2*ABS(DZ2)-DGBB*DBT2*ABS(DBT2)+WFBT+FBT)/
00500        2 (BTIN+MHBB)
00501         D(10)=Y(9)
00501   C
```

```
00501    C      ROLL- GAMMA MOTION
00502           D(11)=(-BGX-BGG-MHGX*DDX1-MHGY*DDY1+MHGG*DDGMW-NGX*DX1-NGY*DY1
00502          1 -NGG*DGM1-DGGY*DY2*ABS(DY2)-DGGG*DGM2*ABS(DGM2)+WFGM+FGM)/
00502          2 (GMIN+MHGG)
00503           D(12)=Y(11)
00503    C
00504           CALL RUNGE(N,Y,D,A,R,M,K)
00505           GO TO (50,40),K
00506        40 ALFA=57.4*Y(8)
00507           BETA=57.4*Y(10)
00510           GAMMA=57.4*Y(12)
00511           J=J+1
00512           IF(J.EQ.20)GO TO 72
00514           GO TO 73
00515        72 TENB(NN)=TEN(1)/1000.0
00516           XWV(NN)=XW
00517           AWV(NN)=DDXW
00520           ACX(NN)=D(1)
00521           ACY(NN)=D(3)
00522           ACZ(NN)=D(5)
00523           BPIT(NN)=Y(10)
00524           BROL(NN)=Y(12)
00525           WRITE(4,131)A,XW,DDXW,D(1),TENB(NN),STRN(1),PHI(1),THE(1)
00537           NN=NN+1
00540        73 CONTINUE
00540    C
00540    C      INSTABILITY LIMITER
00541           DO 60 I=1,N
00544        60 IF(Y(I).GE.10000.0)GO TO 92
00547           IF(NN.EQ.512)GO TO 87
00551           GO TO 5
00552        87 CALL DSTAT(TENB,TBMN,TBVR,TBSD)
00553           CALL DSTAT(AWV,AWMN,AWVR,AWSD)
00554           CALL DSTAT(XWV,WVMN,WVVR,WVSD)
00555           CALL DSTAT(ACX,AXMN,AXVR,AXSD)
00556           CALL DSTAT(ACY,AYMN,AYVR,AYSD)
00557           CALL DSTAT(ACZ,AZMN,AZVR,AZSD)
00560           CALL DSTAT(BPIT,BPMN,BPVR,BPSD)
00561           CALL DSTAT(BROL,BRMN,BRVR,BRSD)
00562           WRITE(4,109)TBMN,TBVR,TBSD
00567           WRITE(4,109)WVMN,WVVR,WVSD
00574           WRITE(4,109)AWMN,AWVR,AWSD
00601           WRITE(4,109)AXMN,AXVR,AXSD
00606           WRITE(4,109)AYMN,AYVR,AYSD
00613           WRITE(4,109)AZMN,AZVR,AZSD
00620           WRITE(4,109)BPMN,BPVR,BPSD
00625           WRITE(4,109)BRMN,BRVR,BRSD
00632           GO TO 88
00633        92 WRITE(4,106)
00635           WRITE(4,120)A
00640        88 STOP
00641           END

     END OF UNIVAC 1108 FORTRAN V COMPILATION.     0 *DIAGNOSTIC* MESSAGE(S)
```

```
                    BUOY DYNAMICS                                        DATE  010572  PAGE    11
Q1 FOR RWAVE,RWAVE                                                                                     10:50:57. 61
UNIVAC 1108 FORTRAN V LEVEL 2206 0023
THIS COMPILATION WAS DONE ON 01 MAY 72 AT 10:50:57

   SUBROUTINE RWAVE      ENTRY POINT 000417

   STORAGE USED (BLOCK, NAME, LENGTH)

         0001    *CODE    000452
         0000    *DATA    000173
         0002    *BLANK   000000

   EXTERNAL REFERENCES (BLOCK, NAME)

         0003    ALOG10
         0004    NEXP6$
         0005    ALOG
         0006    EXP
         0007    SQRT
         0010    NERR3$

   STORAGE ASSIGNMENT FOR VARIABLES (BLOCK, TYPE, RELATIVE LOCATION, NAME)

    0001   000207 143G      0001   000303 161G      0001   000321 167G      0001   000061 304L      0001   000235 402L
    0000 R 000052 APAR      0000 R 000053 BPAR      0000 R 000012 DOMEG     0000 R 000042 DURMIN    0000 R 000036 FETCH
    0000 R 000037 FPAR      0000 R 000043 FPARL     0000 R 000050 FP1       0000 R 000051 FP2       0000 R 000055 G
    0000 R 000047 H3PAR     0000 R 000046 H3PARL    0000   000134 INJPS     0000 I 000054 IS        0000 R 000056 OM
    0000 R 000000 OMEG      0000 R 000045 P3PAR     0000 R 000044 P3PARL    0000 R 000024 SPEC      0000 R 000057 SPECT
    0000 R 000041 TPAR      0000 R 000040 TPARL

00101      1*         SUBROUTINE RWAVE(WINDS,DUR,WHTM,PER,MOMEG,AMP,PHS)
00101      2*   C     USE THE BRETTSCHNEIDER WAVE METHOD TO COMPUTE THE MEAN WAVE
00101      3*   C     HEIGHT AND PERIOD
00101      4*   C     ASSUME A 100 MILE FETCH FOR DEEP SEA BUOYS
00103      5*         DIMENSION OMEG(10),MOMEG(10),DOMEG(10),SPEC(10),PHS(10),AMP(10)
00104      6*         REAL MOMEG
00105      7*         FETCH=6.08E5
00105      8*   C     FETCH LIMITED CASE
00106      9*         FPAR=32.2*FETCH/(WINDS**2)
00107     10*         TPARL=1.477-0.225*ALOG10(FPAR)
00110     11*         TPAR=10.0**TPARL
00111     12*         DURMIN=TPAR*FETCH/(WINDS*3600.0)
00112     13*         IF(DUR-DURMIN)303,304,304
00112     14*   C     DURATION LIMITED CASE
00115     15*     303 TPAR=DUR*WINDS*3600.0/FETCH
00116     16*         FPARL=5.78-3.915*ALOG10(TPAR)
00117     17*         FPAR=10.0**FPARL
00120     18*     304 P3PARL=-1.136+0.283*ALOG10(FPAR)
00121     19*         P3PAR=10.0**P3PARL
00122     20*         IF(FPAR.LT.0.02)P3PAR=0.0247
```

```
                 BUOY DYNAMICS                                          DATE  010572  PAGE    12
00124    21*          IF(FPAR.GT.1.2E5)P3PAR=2.0
00126    22*          PER=0.148*P3PAR*WINDS
00127    23*          H3PARL=-2.5+0.415*ALOG10(FPAR)
00130    24*          H3PAR=10.0**H3PARL
00131    25*          IF(FPAR.LT.0.016)H3PAR=0.00057
00133    26*          IF(FPAR.GT.5.0E4)H3PAR=0.282
00135    27*          *HTM=0.01942*H3PAR*(WINDS**2)
00135    28*    C     COMPUTE FREQUENCIES AND AMPLITUDES FOR A 9 COMPONENT WAVE MODEL
00136    29*          FP1=32.2**HTM/(WINDS**2)
00137    30*          FP2=32.2*PER/(6.2832*WINDS)
00140    31*          APAR=3.437*(FP1**2)/(FP2**4)
00141    32*          BPAR=-0.675*((32.2/(WINDS*FP2))**4)
00142    33*          DO 401 IS=1,9
00145    34*          G=10.0/IS
00146    35*      401 OMEG(IS)=(-BPAR/(ALOG(G)))**0.25
00150    36*          OMEG(10)=500.0
00151    37*          OM=0.0
00152    38*      402 OM=OM+0.05
00153    39*          SPECT=(1037.0*APAR/(OM**5))*EXP(BPAR/(OM**4))
00154    40*          IF(SPECT.LE.0.001)GO TO 402
00156    41*          MOMEG(1)=OM+0.5*(OMEG(1)-OM)
00157    42*          DOMEG(1)=OMEG(1)-OM
00160    43*          DO 403 IS=2,9
00163    44*          MOMEG(IS)=(OMEG(IS)+OMEG(IS+1))/2.0
00164    45*      403 DOMEG(IS)=OMEG(IS+1)-OMEG(IS)
00166    46*          DO 404 IS=1,8
00171    47*          SPEC(IS)=(1037.0*APAR/((MOMEG(IS))**5))
00171    48*         1 *EXP(BPAR/((MOMEG(IS))**4))
00172    49*      404 AMP(IS)=0.5*SQRT(SPEC(IS)*DOMEG(IS))
00174    50*          AMP(9)=0.0
00174    51*    C     USE A RANDOM NUMBER TABLE TO SELECT RANDOM PHASE ANGLES FR
00174    52*    C     EACH COMPONENT
00175    53*          PHS(1)=0.306
00176    54*          PHS(2)=6.255
00177    55*          PHS(3)=4.655
00200    56*          PHS(4)=5.20
00201    57*          PHS(5)=0.575
00202    58*          PHS(6)=3.220
00203    59*          PHS(7)=5.545
00204    60*          PHS(8)=0.435
00205    61*          PHS(9)=0.657
00206    62*          RETURN
00207    63*          END

      END OF UNIVAC 1108 FORTRAN V COMPILATION*     0 *DIAGNOSTIC* MESSAGE(S)
```

```
              BUOY DYNAMICS                                              DATE  010572  PAGE    13
QI FOR TORBU,TORBU                                                                                          10:50:58.774
UNIVAC 1108 FORTRAN V LEVEL 2206 0023
THIS COMPILATION WAS DONE ON 01 MAY 72 AT 10:50:58

   SUBROUTINE TORBU     ENTRY POINT 000340

   STORAGE USED (BLOCK, NAME, LENGTH)

        0001    *CODE    000363
        0000    *DATA    000061
        0002    *BLANK   000000


   EXTERNAL REFERENCES (BLOCK, NAME)

        0003    SIN
        0004    COS
        0005    SQRT
        0006    ATAN
        0007    NERR3$


   STORAGE ASSIGNMENT FOR VARIABLES (BLOCK, TYPE, RELATIVE LOCATION, NAME)

    0001     000145 10L         0001     000225 11L         0001     000220 16L         0001     000231 18L         0001     000245 19L
    0001     000275 20L         0001     000236 3L          0001     000132 8L          0001     000016 9L          0000 R 000012 ALF
    0000 R 000013 AK            0000 R 000011 ART           0000 R 000014 ARTY          0000 R 000016 BXTIL       0000 R 000002 DGAM
    0000 R 000001 GAM           0000 R 000010 HB            0000     000041 INJP$       0000 I 000000 J           0000 R 000004 RS
    0000 R 000003 RT            0000 R 000006 VOL           0000 R 000007 VOLX          0000 R 000015 X           0000 R 000017 XM
    0000 R 000005 ZGBH


00101      1*         SUBROUTINE TORBU(H,TIL,BXX,BTT,BXT,BTX)
00101      2*    C    THIS SUBROUTINE COMPUTES THE DISPLACEMENT AND RIGHTING MOMENT
00101      3*    C    FOR THE 8 FOOT DIA. RICHARDSON BUOY USED IN THE BUOY MOTION
00101      4*    C    EXPERIMENT
00103      5*         J=1
00104      6*         GAM=-1.5708
00105      7*         DGAM=0.1
00106      8*         RT=2.75
00107      9*         RS=1.25
00110     10*         ZGBH=1.282
00111     11*         VOL=0.0
00112     12*         VOLX=0.0
00113     13*       9 CONTINUE
00114     14*         HB=H-(ZGBH-H)*(1.0-COS(TIL))+RT*SIN(TIL)*SIN(GAM)
00115     15*         IF(J.EQ.1)HB=H
00117     16*         IF(HB.LE.0.0)HB=0.0
00121     17*         IF(HB.GT.(0.99*RS))GO TO 8
00123     18*         IF(HB.GE.(1.99*RS))GO TO 11
00125     19*         ART=SQRT(((RS**2)/((RS-HB)**2))-1.0)
00126     20*         IF(ART.GE.25.0)GO TO 16
00130     21*         ALF=2.0*ATAN(ART)
```

```
00131    22*          AR=0.5*(RS**2)*(ALF-SIN(ALF))
00132    23*          GO TO 18
00133    24*        8 CONTINUE
00134    25*          IF(HB.GT.(1.01*RS))GO TO 10
00136    26*          AR=1.5708*RS*RS
00137    27*          GO TO 18
00140    28*       10 ARTY=((RS**2)/((RS-(2.0*RS-HB))**2))-1.0
00141    29*          IF(ARTY.LE.0.0)ARTY=0.0
00143    30*          ART=SQRT(ARTY)
00144    31*          IF(ART.GE.25.0)GO TO 16
00146    32*          ALF=2.0*ATAN(ART)
00147    33*          AR=3.1416*(RS**2)-0.5*(RS**2)*(ALF-SIN(ALF))
00150    34*          GO TO 18
00151    35*       16 AR=1.5708*(RS**2)
00152    36*          GO TO 18
00153    37*       11 AR=3.1416*(RS**2)
00154    38*       18 IF(J.EQ.1)GO TO 3
00156    39*          GO TO 19
00157    40*        3 BXX=402.124*RT*AR
00160    41*          J=2
00161    42*          GO TO 9
00162    43*       19 VOL=VOL+DGAM*RT*AR
00163    44*          X=RT*SIN(GAM)
00164    45*          VOLX=VOLX+X*DGAM*RT*AR
00165    46*          GAM=GAM+DGAM
00166    47*          IF(GAM.GE.1.57)GO TO 20
00170    48*          GO TO 9
00171    49*       20 BXTIL=128.0*VOL
00172    50*          BXT=BXTIL-BX
00172    51*    C     THE RIGHTING ARM
00173    52*          XM=(VOLX/VOL)*COS(TIL)-(ZGBH-H)*SIN(TIL)
00174    53*          BTT=BXTIL*XM
00175    54*          BTX=BXT*XM
00176    55*          RETURN
00177    56*          END

   END OF UNIVAC 1108 FORTRAN V COMPILATION.      0 *DIAGNOSTIC* MESSAGE(S)
```

```
                BUOY DYNAMICS                                              DATE  010572  PAGE    15

GI FOR MOOR,MOOR                                                                                          10:51: 0.349
UNIVAC 1108 FORTRAN V LEVEL 2206 0023
THIS COMPILATION WAS DONE ON 01 MAY 72 AT 10:51:00

  SUBROUTINE MOOR        ENTRY POINT 002352

  STORAGE USED (BLOCK, NAME, LENGTH)

      0001   *CODE    002412
      0000   *DATA    000760
      0002   *BLANK   000000

  EXTERNAL REFERENCES (BLOCK, NAME)

      0003   COS
      0004   SIN
      0005   NEXP6$
      0006   SQRT
      0007   NERR3$

  STORAGE ASSIGNMENT FOR VARIABLES (BLOCK, TYPE, RELATIVE LOCATION, NAME)

   0001     000065 130G     0001     000215 146G     0001     000577 2L       0001     000074 3L       0001     000363 41L
   0001     000351 42L      0001     002267 462G     0001     002306 471G     0000 R 000374 A        0000 R 000540 ACUA
   0000 R 000541 ACUB     0000 R 000542 ACUD     0000 R 000612 ACUP1    0000 R 000613 ACUQ1    0000 R 000551 ACUR
   0000 R 000543 ACVA     0000 R 000544 ACVB     0000 R 000545 ACVD     0000 R 000614 ACVP2    0000 R 000615 ACVQ2
   0000 R 000552 ACVR     0000 R 000546 ACWA     0000 R 000547 ACWB     0000 R 000550 ACWD     0000 R 000616 ACWP2
   0000 R 000617 ACWQ2    0000 R 000553 ACWR     0000 R 000455 CDN      0000 R 000454 CDT      0000 R 000626 CGP2
   0000 R 000627 CGQ2     0000 R 000625 CGR      0000 R 000457 CHMCN    0000 R 000456 CHMCT    0000 R 000623 CHP1
   0000 R 000624 CHQ1     0000 R 000622 CHR      0000 R 000520 CHI      0000 R 000560 CH2P2    0000 R 000561 CH2Q2
   0000 R 000557 CH2R     0000 R 000631 CIP2     0000 R 000632 CIQ2     0000 R 000630 CIR      0000 R 000453 CMU
   0000 R 000451 DIA      0000 R 000621 DRAGN    0000 R 000620 DRAGT    0000 R 000460 DTDE     0000 R 000506 EA
   0000 R 000507 EB       0000 R 000510 ED       0000 R 000151 EN       0000 R 000527 EP1      0000 R 000531 EP2
   0000 R 000530 EQ1      0000 R 000532 EQ2      0000 R 000526 ER       0000 R 000462 H        0000 R 000524 HP1
   0000 R 000564 HP2      0000 R 000525 HQ1      0000 R 000565 HQ2      0000 I 000463 I        0000     000667 INJP$
   0000 I 000517 N        0000 R 000511 PHIA     0000 R 000512 PHIB     0000 R 000513 PHID     0000 R 000077 PHIN
   0000 R 000602 PHIP1    0000 R 000604 PHIP2    0000 R 000603 PHIQ1    0000 R 000605 PHIQ2    0000 R 000536 PHIR
   0000 R 000461 RHO      0000 R 000450 SMAX     0000 R 000522 SP1      0000 R 000562 SP2      0000 R 000523 SQ1
   0000 R 000563 SQ2      0000 R 000521 SR       0000 R 000514 THEA     0000 R 000515 THEB     0000 R 000516 THED
   0000 R 000124 THEN     0000 R 000606 THEP1    0000 R 000610 THEP2    0000 R 000607 THEQ1    0000 R 000611 THEQ2
   0000 R 000537 THER     0000 R 000464 UA       0000 R 000465 UB       0000 R 000466 UC       0000 R 000467 UD
   0000 R 000470 UE       0000 R 000471 UF       0000 R 000000 UN       0000 R 000275 UO       0000 R 000176 UP
   0000 R 000566 UP1      0000 R 000570 UP2      0000 R 000567 UQ1      0000 R 000571 UQ2      0000 R 000533 UR
   0000 R 000554 USS      0000 R 000472 VA       0000 R 000473 VB       0000 R 000474 VC       0000 R 000475 VD
   0000 R 000476 VE       0000 R 000477 VF       0000 R 000025 VN       0000 R 000322 VO       0000 R 000223 VP
   0000 R 000572 VP1      0000 R 000574 VP2      0000 R 000573 VQ1      0000 R 000575 VQ2      0000 R 000534 VR
   0000 R 000446 VSM      0000 R 000555 VSS      0000 R 000500 WA       0000 R 000501 WB       0000 R 000502 WC
   0000 R 000503 WD       0000 R 000504 WE       0000 R 000505 WF       0000 R 000052 WN       0000 R 000347 WO
   0000 R 000250 WP       0000 R 000576 WP1      0000 R 000600 WP2      0000 R 000577 WQ1      0000 R 000601 WQ2
   0000 R 000535 WR       0000 R 000447 WSM      0000 R 000556 WSS      0000 R 000452 WTC
```

```
00101        SUBROUTINE MOOR(T,K,UBY,VBY,WBY,EP,PHIP,THEP)
00101   C    THIS SUBROUTINE COMPUTES THE RESPONSE OF A MOORING LINE IN THE
00101   C    OCEAN ENVRIONMENT TO THE MOTIONS OF A BUOY. THREE DIMENSIONAL
00101   C    MOTIONS ARE CONSIDERED. COUPLED TENSILE WAVES AND TRANSVERSE WAVES
00101   C    ARE PROPOGATING UP AND DOWN THE MOORING LINE. THE MOORING CLUMP
00101   C    IS ASSUMED TO BE OF INFINITE MASS AND RIGIDITY CAUSING 100 PCT
00101   C    REFLECTION OF WAVES. THE SOLUTION OF THE SET OF PARTIAL
00101   C    DIFFERENTIAL EQUATIONS IS EFFECTED WITH A METHOD OF CHARACTERISTIC
00101   C    TECHNIQUE CALLED HARTREES METHOD.
00101   C    THE MOORING LINE HAS 4800 FT. OF 1/4 INCH WIRE ROPE AND 3200 FT.
00101   C    OF 5/8 NYLON ROPE
00101   C
00103        DIMENSION UN(21),VN(21),WN(21),PHIN(21),THEN(21),EN(21)
00104        DIMENSION UP(21),VP(21),WP(21),PHIP(21),THEP(21),EP(21)
00105        DIMENSION UO(21),VO(21),WO(21)
00106        DIMENSION A(6,7)
00107        REAL K
00107   C    THE CABLE PROPERTIES, INITIAL CONDITIONS AND COEFFICIENTS
00110        VSM=0.0
00111        WSM=-1.5
00112        SMAX=8000.0
00112   C    THE WIRE ROPE PROPERTIES
00113        DIA=0.0312
00114        WTC=0.125
00114   C    CABLE MASS PER UNIT LENGTH X 100
00114   C    DISTRIBUTE THE MASS OF THE INSTRUMENTS OVER THE CABLE
00115        CMU=0.672
00116        CDT=0.05
00117        CDN=1.4
00120        CHMCT=0.0
00121        CHMCN=0.00153
00122        DTDE=6.87E5
00123        RHO=1.987
00124        H=0.05*SMAX
00124   C
00124   C    AMES CRITERIA - H/K GREATER THAN ANY CHARACTERISTIC
00124   C
00125        IF(T.GT.0.0)GO TO 3
00127        DO 4 I=1,21
00132        UP(I)=0.0
00133        VP(I)=0.0
00134        WP(I)=0.0
00135        UO(I)=0.0
00136        VO(I)=0.0
00137      4 WO(I)=0.0
00141      3 CONTINUE
00141   C
00141   C    TRANSFORM THE BUOY VELOCITIES TO CABLE COORDINATES
00142        UN(1)=UBY*COS(PHIP(1))*COS(THEP(1))+VBY*SIN(PHIP(1))
00142       1 +WBY*COS(PHIP(1))*SIN(THEP(1))
00143        VN(1)=-UBY*SIN(PHIP(1))*COS(THEP(1))+VBY*COS(PHIP(1))
00143       1 -WBY*SIN(PHIP(1))*SIN(THEP(1))
00144        WN(1)=-UBY*SIN(THEP(1))+WBY*COS(THEP(1))
00145        DO 50 I=2,20
00150        UA=UP(I)
00151        UB=UP(I-1)
00152        UC=UO(I-1)
```

```
00153          UD=UP(I+1)
00154          UE=UO(I)
00155          UF=UO(I+1)
00156          VA=VP(I)
00157          VB=VP(I-1)
00160          VC=VO(I-1)
00161          VD=VP(I+1)
00162          VE=VO(I)
00163          VF=VO(I+1)
00164          WA=WP(I)
00165          WB=WP(I-1)
00166          WC=WO(I-1)
00167          WD=WP(I+1)
00170          WE=WO(I)
00171          WF=WO(I+1)
00172          EA=EP(I)
00173          EB=EP(I-1)
00174          ED=EP(I+1)
00174     C    STRAINS ARE DISCONTINUOUS BETWEEN TWO DIFFERENT CABLES
00174     C    USE AN EULER APPROXIMATION TO ESTIMATE THE STRAINS ACROSS THE
00174     C    DISCONTINUITY
00175          IF(I.EQ.13)ED=2.0*EP(13)-EP(12)
00177          IF(I.EQ.14)EB=2.0*EP(14)-EP(15)
00201          PHIA=PHIP(I)
00202          PHIB=PHIP(I-1)
00203          PHID=PHIP(I+1)
00204          THEA=THEP(I)
00205          THEB=THEP(I-1)
00206          THED=THEP(I+1)
00206     C    CHANGE THE CABLE PROPERTIES AT 4800 FT.
00207          IF(I.GE.14)GO TO 42
00211          GO TO 41
00211     C    THE NYLON ROPE PROPERTIES
00212       42 DIA=0.052
00213          WTC=0.0105
00214          CMU=0.455
00215          CHMCN=0.00425
00216          DTDE=3.06E4
00217       41 CONTINUE
00217     C
00217     C    THIS SECTION PERFORMS QUADRATURE IN THE T-S PLANE USING HARTREE'S
00217     C    METHOD (A HYBRID METHOD)
00217     C    ARRANGEMENT OF POINTS IN GRID FOR HARTREE'S METHOD
00217     C
00217     C    J+1            R
00217     C                  ---
00217     C                 - - -
00217     C    J          B--A--D
00217     C               -  -  -
00217     C               -  -  -
00217     C    J-1        C--E--F
00217     C
00217     C               I-1 I I+1
00217     C
00220          N=0
00221          CH1=11300.0
00222          IF(I.GE.14)CH1=2600.0
00224          SR=H*(I-1)
```

```
      SP1=SR-CH1*K
      SQ1=SR+CH1*K
      HP1=SR-SP1
      HQ1=HP1
      ER=EA
      EP1=EA-(HP1/H)*(EA-EB)
      EQ1=EA+(HQ1/H)*(ED-EA)
      EP2=EP1
      EQ2=EQ1
      UR=UA
      VR=VA
      WR=WA
      PHIR=PHIA
      THER=THEA
      ACUA=(UA-UE)/K
      ACUB=(UB-UC)/K
      ACUD=(UD-UF)/K
      ACVA=(VA-VE)/K
      ACVB=(VB-VC)/K
      ACVD=(VD-VF)/K
      ACWA=(WA-WE)/K
      ACWB=(WB-WC)/K
      ACWD=(WD-WF)/K
      ACUR=ACUA
      ACVR=ACVA
      ACWR=ACWA
C     WEBSTER CURRENT PROFILE
      WSM=3.9/((SR/3.2802)**0.418)
      WSM=-WSM
      USS=VSM*SIN(PHIA)-WSM*COS(PHIA)*SIN(THEA)
      VSS=VSM*COS(PHIA)-WSM*SIN(PHIA)*SIN(THEA)
      WSS=WSM*COS(THEA)
    2 CONTINUE
      CH2R=CH1*SQRT(ER/(1.0+ER))
      CH2P2=CH1*SQRT(EP2/(1.0+EP2))
      CH2Q2=CH1*SQRT(EQ2/(1.0+EQ2))
      SP2=SR-0.5*(CH2R+CH2P2)*K
      SQ2=SR+0.5*(CH2R+CH2Q2)*K
      HP2=SR-SP2
      HQ2=SQ2-SR
      EP2=EA-(HP2/H)*(EA-EB)
      EQ2=EA+(HQ2/H)*(ED-EA)
      UP1=UA-(HP1/H)*(UA-UB)
      UQ1=UA+(HQ1/H)*(UD-UA)
      UP2=UA-(HP2/H)*(UA-UB)
      UQ2=UA+(HQ2/H)*(UD-UA)
      VP1=VA-(HP1/H)*(VA-VB)
      VQ1=VA+(HQ1/H)*(VD-VA)
      VP2=VA-(HP2/H)*(VA-VB)
      VQ2=VA+(HQ2/H)*(VD-VA)
      WP1=WA-(HP1/H)*(WA-WB)
      WQ1=WA+(HQ1/H)*(WD-WA)
      WP2=WA-(HP2/H)*(WA-WB)
      WQ2=WA+(HQ2/H)*(WD-WA)
      PHIP1=PHIA-(HP1/H)*(PHIA-PHIB)
      PHIQ1=PHIA+(HQ1/H)*(PHID-PHIA)
      PHIP2=PHIA-(HP2/H)*(PHIA-PHIB)
      PHIQ2=PHIA+(HQ2/H)*(PHID-PHIA)
```

```
00316         THEP1=THEA-(HP1/H)*(THEA-THEB)
00317         THEQ1=THEA+(HQ2/H)*(THED-THEA)
00320         THEP2=THEA-(HP2/H)*(THEA-THEB)
00321         THEQ2=THEA+(HQ2/H)*(THED-THEA)
00322         ACUR=(UR-UA)/K
00323         ACVR=(VR-VA)/K
00324         ACWR=(WR-WA)/K
00325         ACUP1=ACUA-(HP1/H)*(ACUA-ACUB)
00326         ACUQ1=ACUA+(HQ1/H)*(ACUD-ACUA)
00327         ACVP2=ACVA-(HP2/H)*(ACVA-ACVB)
00330         ACVQ2=ACVA+(HQ2/H)*(ACVD-ACVA)
00331         ACWP2=ACWA-(HP2/H)*(ACWA-ACWB)
00332         ACWQ2=ACWA+(HQ2/H)*(ACWD-ACWA)
00332   C
00332   C     THE CABLE LOADING FUNCTIONS
00333         DRAGT=0.5*RHO*CDT*DIA
00334         DRAGN=0.5*PHO*CDN*DIA
00335         CHR=WTC*COS(PHIR)*COS(THER)-DRAGT*(USS+UR)*ABS(USS+UR)
00335        1 -ACUR*CHMCT
00336         CHP1=WTC*COS(PHIP1)*COS(THEP1)-DRAGT*(USS+UP1)*ABS(USS+UP1)
00336        1 -ACUP1*CHMCT
00337         CHQ1=WTC*COS(PHIQ1)*COS(THEQ1)-DRAGT*(USS+UQ1)*ABS(USS+UQ1)
00337        1 -ACUQ1*CHMCT
00340         CGR=-WTC*SIN(PHIR)*COS(THER)-DRAGN*(VSS+VR)*ABS(VSS+VR)
00340        1 -ACVR*CHMCN
00341         CGP2=-WTC*SIN(PHIP2)*COS(THEP2)-DRAGN*(VSS+VP2)*ABS(VSS+VP2)
00341        1 -ACVP2*CHMCN
00342         CGQ2=-WTC*SIN(PHIQ2)*COS(THEQ2)-DRAGN*(VSS+VQ2)*ABS(VSS+VQ2)
00342        1 -ACVQ2*CHMCN
00343         CIR=-WTC*SIN(THER)-DRAGN*(WSS+WR)*ABS(WSS+WR)-ACWR*CHMCN
00344         CIP2=-WTC*SIN(THEP2)-DRAGN*(WSS+WP2)*ABS(WSS+WP2)-ACWP2*CHMCN
00345         CIQ2=-WTC*SIN(THEQ2)-DRAGN*(WSS+WQ2)*ABS(WSS+WQ2)-ACWQ2*CHMCN
00346         CH2R=CH1*SQRT(ER/(1.0+ER))
00347         CH2P2=CH1*SQRT(EP2/(1.0+EP2))
00350         CH2Q2=CH1*SQRT(EQ2/(1.0+EQ2))
00350   C
00350   C     COEFFICIENTS IN THE MATRIX OF SIMULTANEOUS EQUATIONS
00350   C
00351         A(1,1)=1.0
00352         A(1,2)=0.0
00353         A(1,3)=0.0
00354         A(1,4)=-CH1
00355         A(1,5)=-0.5*(VR+VP1)
00356         A(1,6)=-0.5*(WR+WP1)*COS(0.5*(PHIR+PHIP1))
00357         A(1,7)=-UP1+CH1*EP1+0.5*(VR+VP1)*PHIP1-A(1,6)*THEP1
00357        1 -100.0*0.5*(CHR+CHP1)*K/CMU
00357   C
00360         A(2,1)=1.0
00361         A(2,2)=0.0
00362         A(2,3)=0.0
00363         A(2,4)=CH1
00364         A(2,5)=-0.5*(VR+VQ1)
00365         A(2,6)=-0.5*(WR+WQ1)*COS(0.5*(PHIR+PHIQ1))
00366         A(2,7)=-UQ1-CH1*EQ1+0.5*(VR+VQ1)*PHIQ1-A(2,6)*THEQ1
00366        1 -100.0*0.5*(CHR+CHQ1)*K/CMU
00366   C
00367         A(3,1)=0.0
00370         A(3,2)=1.0
```

```
00371            A(3,3)=0.0
00372            A(3,4)=0.0
00373            A(3,5)=-0.5*(((1.0+ER)*CH2R)+((1.0+EP2)*CH2P2))
00374            A(3,6)=0.5*(WR+WP2)*SIN(0.5*(PHIR+PHIP2))
00375            A(3,7)=-V ^+0.5*(((1.0+ER)*CH2R)+((1.0+EP2)*CH2P2))*PHIP2
00375           1 -A(3,6)*THEP2-100.0*0.5*(CGR+CGP2)*K/CMU
00375       C
00376            A(4,1)=0.0
00377            A(4,2)=1.0
00400            A(4,3)=0.0
00401            A(4,4)=0.0
00402            A(4,5)=0.5*(((1.0+ER)*CH2R)+((1.0+EQ2)*CH2Q2))
00403            A(4,6)=0.5*(WR+WQ2)*SIN(0.5*(PHIR+PHIQ2))
00404            A(4,7)=-VQ2-0.5*(((1.0+ER)*CH2R)+((1.0+EQ2)*CH2Q2))*PHIQ2
00404           1 -A(4,6)*THEQ2-100.0*0.5*(CGR+CGQ2)*K/CMU
00404       C
00405            A(5,1)=0.0
00406            A(5,2)=0.0
00407            A(5,3)=1.0
00410            A(5,4)=0.0
00411            A(5,5)=0.0
00412            A(5,6)=-(0.5*(((1.0+ER)*CH2R)+((1.0+EP2)*CH2P2))*COS(0.5*(PHIR
00412           1 +PHIP2))-(0.5*(UR+UP2)*COS(0.5*(PHIR+PHIP2))
00412           2 -0.5*(VR+VP2)*SIN(0.5*(PHIR+PHIP2))))
00413            A(5,7)=-WP2-A(5,6)*THEP2-100.0*0.5*(CIR+CIP2)*K/CMU
00413       C
00414            A(6,1)=0.0
00415            A(6,2)=0.0
00416            A(6,3)=1.0
00417            A(6,4)=0.0
00420            A(6,5)=0.0
00421            A(6,6)=(0.5*(((1.0+ER)*CH2R)+((1.0+EQ2)*CH2Q2))*COS(0.5*(PHIR
00421           1 +PHIQ2))+(0.5*(UR+UQ2)*COS(0.5*(PHIR+PHIQ2))
00421           2 -0.5*(VR+VQ2)*SIN(0.5*(PH R+PHIQ2))))
00422            A(6,7)=-WQ2-A(6,6)*THEQ2-100.0*0.5*(CIR+CIQ2)*K/CMU
00422       C
00422       C    SOLUTION OF THE SIX SIMULTANEOUS EQUATIONS
00422       C
00423            THER=(A(6,7)-A(5,7))/(A(5,6)-A(6,6))
00424            WR=-A(5,7)-A(5,6)*THER
00425            PHIR=(A(4,7)-A(3,7)+(A(4,6)-A(3,6))*THER)/(A(3,5)-A(4,5))
00426            VR=-A(3,7)-A(3,6)*THER-A(3,5)*PHIR
00427            ER=(A(2,7)-A(1,7)+(A(2,5)-A(1,5))*PHIR+(A(2,6)-A(1,6))*THER)
00427           1 /(A(1,4)-A(2,4))
00430            UR=-A(1,7)-A(1,5)*PHIR-A(1,6)*THER-A(1,4)*ER
00430       C    THE CABLE CAN'T SUPPORT COMPRESSION THUS STRAIN CAN NEVER BE NE
00431            IF(ER.LE.0.0001)ER=0.0001
00433         78 CONTINUE
00433       C    REPEAT THE PROCESS
00434            N=N+1
00435            IF(N-3)2,13,13
00440         13 THEN(I)=THER
00441            PHIN(I)=PHIR
00442            EN(I)=ER
00443            VN(I)=VR
00444            UN(I)=UR
00445            WN(I)=WR
00446         50 CONTINUE
```

```
                     BUCY DYNAMICS                                   DATE  010572  PAGE    21
00446    290*   C     THE LOWER BOUNDARY - VELOCITIES ARE ZERO
00450    291*         UN(21)=0.0
00451    292*         VN(21)=0.0
00452    293*         WN(21)=0.0
00452    294*   C     USE AN EULER APPROXIMATION FOR ANGLES AND STRAIN
00453    295*         EN(21)=2.0*EN(20)-EN(19)
00454    296*         PHIN(21)=2.0*PHIN(20)-PHIN(19)
00455    297*         THEN(21)=2.0*THEN(20)-THEN(19)
00456    298*         EN(1)=2.0*EN(2)-EN(3)
00457    299*         PHIN(1)=2.0*PHIN(2)-PHIN(3)
00460    300*         THEN(1)=2.0*THEN(2)-THEN(3)
00460    301*   C     SET JTH VALUES INTO THE (J-1)TH REGISTERS
00461    302*         DO 51 I=1,21
00464    303*         UO(I)=UP(I)
00465    304*         VO(I)=VP(I)
00466    305*      51 WO(I)=WP(I)
00466    306*   C     SET THE (J+1)TH VALUES INTO THE JTH REGISTERS
00470    307*         DO 52 I=1,21
00473    308*         UP(I)=UN(I)
00474    309*         VP(I)=VN(I)
00475    310*         WP(I)=WN(I)
00476    311*         EP(I)=EN(I)
00477    312*         PHIP(I)=PHIN(I)
00500    313*      52 THEP(I)=THEN(I)
00502    314*         RETURN
00503    315*         END

      END OF UNIVAC 1108 FORTRAN V COMPILATION.      0 *DIAGNOSTIC* MESSAGE(S)
```

```
                BUOY DYNAMICS                                        DATE  010572  PAGE    22

WI FOR RUNGE,RUNGE                                                                              10:51: 5.197
UNIVAC 1108 FORTRAN V LEVEL 2206 0023
THIS COMPILATION WAS DONE ON 01 MAY 72 AT 10:51:05

   SUBROUTINE RUNGE      ENTRY POINT 000134

   STORAGE USED (BLOCK, NAME, LENGTH)

         0001   *CODE    000163
         0000   *DATA    000115
         0002   *BLANK   000000

   EXTERNAL REFERENCES (BLOCK, NAME)

         0003   NERR2$
         0004   NERR3$

   STORAGE ASSIGNMENT FOR VARIABLES (BLOCK, TYPE, RELATIVE LOCATION, NAME)

    0001   000021 1L        0001   000121 10L     0001   000023 107G     0001   000054 120G     0001   000102 130G
    0001   000030 3L        0001   000032 4L      0001   000036 5L       0001   000074 7L       0001   000117 9L
    0000 R 000063 A         0000 I 000062 I       0000   000075 INJP$    0000 R 000000 Q

00101      SUBROUTINE RUNGE(N,Y,F,X,H,M,K)
00101   C  THIS ROUTINE PERFORMS RUNG  KUTTA CALCULATIONS BY GILL'S METHOD
00103      DIMENSION Y(50),F(50),Q(50)
00104      M=M+1
00105      GO TO (1,4,5,3,7),M
00106    1 DO 2 I=1,N
00111    2 Q(I)=0.0
00113      A=0.5
00114      GO TO 9
00115    3 A=1.707107
00115   C  IF YOU NEED MORE ACCURACY USE A=1.7071067811865475244
00116    4 X=X+0.5*H
00117    5 DO 6 I=1,N
00122      Y(I)=Y(I)+A*(F(I)*H-Q(I))
00123    6 Q(I)=2.0*A*H*F(I)+(1.0-3.0*A)*Q(I)
00125      A=0.2928932
00125   C  IF YOU NEED MORE ACCURACY USE A=0.2928932188134524756
00126      GO TO 9
00127    7 DO 8 I=1,N
00132    8 Y(I)=Y(I)+H*F(I)/6.0-Q(I)/3.0
00134      M=0.0
00135      K=2
00136      GO TO 10
00137    9 K=1
00140   10 RETURN
00141      END
```

```
            BUOY DYNAMICS
                                                            DATE  010572  PAGE    24
QI FOR DSTAT,DSTAT
UNIVAC 1108 FORTRAN V LEVEL 2206 0023                                               10:51: 6.415
THIS COMPILATION WAS DONE ON 01 MAY 72 AT 10:51:06

   SUBROUTINE DSTAT      ENTRY POINT 000045

   STORAGE USED (BLOCK, NAME, LENGTH)

        0001   *CODE    000062
        0000   *DATA    000017
        0002   *BLANK   000000

   EXTERNAL REFERENCES (BLOCK, NAME)

        0003   SQRT
        0004   NERR3$

   STORAGE ASSIGNMENT FOR VARIABLES (BLOCK, TYPE, RELATIVE LOCATION, NAME)

    0001   000012 110G        0000   000005 INJPS      0000 I 000003 J          0000 I 000000 N        0000 R 000001 S
    0000 R 000002 S1

00101       1*          SUBROUTINE DSTAT(PAR,PRMN,PRVR,PRSD)
00103       2*          DIMENSION PAR(2048)
00104       3*          N=512
00105       4*          S=0.0
00106       5*          S1=0.0
00107       6*          DO 3 J=1,512
00112       7*          S=S+PAR(J)
00113       8*        3 S1=S1+PAR(J)*PAR(J)
00115       9*          PRMN=S/N
00116      10*          PRVR=(S1-PRMN*S)/N
00117      11*          PRSD=SQRT(PRVR)
00120      12*          RETURN
00121      13*          END

     END OF UNIVAC 1108 FORTRAN V COMPILATION.      0 *DIAGNOSTIC* MESSAGE(S)
```

Appendix C

DERIVATION OF THE CABLE CHARACTERISTICS

In order to rewrite the cable equations in their "normal" form, the characteristic roots of the cable equations must be determined. From equation (168) of the main text, we see that $AU_t + BU_s + C = 0$,

$$
\begin{bmatrix}
0 & \mu V & \mu W\cos\phi & -\mu & 0 & 0 \\
0 & -\mu U & -\mu W\sin\phi & 0 & -\mu & 0 \\
0 & 0 & -\mu(U\cos\phi - V\sin\phi) & 0 & 0 & -\mu \\
-1 & 0 & 0 & 0 & 0 & 0 \\
0 & -(1+\epsilon) & 0 & 0 & 0 & 0 \\
0 & 0 & 0 & 0 & 0 & 0
\end{bmatrix}
\begin{bmatrix}
\partial\epsilon/\partial t \\
\partial\phi/\partial t \\
\partial\theta/\partial t \\
\partial U/\partial t \\
\partial V/\partial t \\
\partial W/\partial t
\end{bmatrix}
$$

$$
+\begin{bmatrix}
\frac{dT}{d\epsilon} & 0 & 0 & 0 & 0 & 0 \\
0 & \epsilon\frac{dT}{d\epsilon} & 0 & 0 & 0 & 0 \\
0 & 0 & \epsilon\frac{dT}{d\epsilon}\cos\phi & 0 & 0 & 0 \\
0 & -V & -W\cos\phi & 1 & 0 & 0 \\
0 & U & W\sin\phi & 0 & 1 & 0 \\
0 & 0 & (U\cos\phi - V\sin\phi) & 0 & 0 & 1
\end{bmatrix}
\begin{bmatrix}
\partial\epsilon/\partial s_0 \\
\partial\phi/\partial s_0 \\
\partial\theta/\partial s_0 \\
\partial U/\partial s_0 \\
\partial V/\partial s_0 \\
\partial W/\partial s_0
\end{bmatrix}
+
\begin{bmatrix}
H \\ G \\ I \\ 0 \\ 0 \\ 0
\end{bmatrix}
= 0 .
$$

Multiplying through by the inverse of the A matrix yields

$$A^{-1}AU_t + A^{-1}BU_s + A^{-1}C = 0\ ,$$

or

$$U_t + A^{-1}BU_s + A^{-1}C = 0 .$$

To find the inverse of the A matrix, partition the A matrix into four 3-by-3 matrices:

$$A = \begin{bmatrix} D & -\mu I \\ E & 0 \end{bmatrix}$$

$$D = \begin{bmatrix} 0 & \mu V & \mu W\cos\phi \\ 0 & -\mu U & -\mu W\sin\phi \\ 0 & 0 & -\mu(U\cos\phi - V\sin\phi) \end{bmatrix}$$

$$E = \begin{bmatrix} -1 & 0 & 0 \\ 0 & -(1+\epsilon) & 0 \\ 0 & 0 & -(1+\epsilon)\cos\phi \end{bmatrix} .$$

Let A^{-1} be partitioned in the same way,

$$A^{-1} = \begin{bmatrix} K_1 & K_2 \\ K_3 & K_4 \end{bmatrix} ;$$

then

$$\begin{bmatrix} D & -\mu I \\ E & 0 \end{bmatrix}\begin{bmatrix} K_1 & K_2 \\ K_3 & K_4 \end{bmatrix} = \begin{bmatrix} I & 0 \\ 0 & I \end{bmatrix} ,$$

$$DK_1 - \mu K_3 = I$$

$$DK_2 - \mu K_4 = 0$$

$$EK_1 + 0 = 0 \qquad E \text{ nonsingular} \quad \therefore K_1 = 0$$

$$EK_2 + 0 = I \quad \therefore K_2 = E^{-1} .$$

Substituting into the first equation, we see that

$$K_3 = \frac{1}{\mu} I .$$

From the second equation, we see that

$$K_4 = \frac{1}{\mu} DK_2 = \frac{1}{\mu} DE^{-1} .$$

$$\therefore \quad K_1 = 0$$

$$K_2 = \begin{bmatrix} -1 & 0 & 0 \\ 0 & -\frac{1}{(1+\epsilon)} & 0 \\ 0 & 0 & -\frac{1}{(1+\epsilon)\cos\phi} \end{bmatrix}$$

$$K_3 = \begin{bmatrix} -1/\mu & 0 & 0 \\ 0 & -1/\mu & 0 \\ 0 & 0 & -1/\mu \end{bmatrix}$$

$$K_4 = \begin{bmatrix} 0 & -\frac{V}{(1+\epsilon)} & -\frac{W}{(1+\epsilon)} \\ 0 & \frac{U}{(1+\epsilon)} & \frac{W \sin\phi}{(1+\epsilon)\cos\phi} \\ 0 & 0 & \frac{(U\cos\phi - V\sin\phi)}{(1+\epsilon)\cos\phi} \end{bmatrix} .$$

The A^{-1} matrix is written

$$A^{-1} = \begin{bmatrix} 0 & 0 & 0 & -1 & 0 & 0 \\ 0 & 0 & 0 & 0 & -\frac{1}{(1+\epsilon)} & 0 \\ 0 & 0 & 0 & 0 & 0 & -\frac{1}{(1+\epsilon)\cos\phi} \\ -\frac{1}{\mu} & 0 & 0 & 0 & -\frac{V}{(1+\epsilon)} & -\frac{W}{(1+\epsilon)} \\ 0 & -\frac{1}{\mu} & 0 & 0 & \frac{U}{(1+\epsilon)} & \frac{W\sin\phi}{(1+\epsilon)\cos\phi} \\ 0 & 0 & -\frac{1}{\mu} & 0 & 0 & \frac{(U\cos\phi - V\sin\phi)}{(1+\epsilon)\cos\phi} \end{bmatrix}.$$

<u>$A^{-1}B$</u>

$$A^{-1} \cdot \begin{bmatrix} \frac{dT}{d\epsilon} & 0 & 0 & 0 & 0 & 0 \\ 0 & \epsilon\frac{dT}{d\epsilon} & 0 & 0 & 0 & 0 \\ 0 & 0 & \epsilon\frac{dT}{d\epsilon}\cos\phi & 0 & 0 & 0 \\ 0 & -V & -W\cos\phi & 1 & 0 & 0 \\ 0 & U & W\sin\phi & 0 & 1 & 0 \\ 0 & 0 & (U\cos\phi - V\sin\phi) & 0 & 0 & 1 \end{bmatrix} =$$

$$\begin{bmatrix} 0 & V & W\cos\phi & -1 & 0 & 0 \\ 0 & -\frac{U}{(1+\epsilon)} & -\frac{W\sin\phi}{(1+\epsilon)} & 0 & -\frac{1}{(1+\epsilon)} & 0 \\ 0 & 0 & -\frac{(U\cos\phi - V\sin\phi)}{(1+\epsilon)\cos\phi} & 0 & 0 & -\frac{1}{(1+\epsilon)\cos\phi} \\ -\frac{1}{\mu}\frac{dT}{d\epsilon} & -\frac{UV}{(1+\epsilon)} & -\frac{UW\cos\phi}{(1+\epsilon)} & 0 & -\frac{V}{(1+\epsilon)} & -\frac{W}{(1+\epsilon)} \\ 0 & \left(-\frac{\epsilon}{\mu}\frac{dT}{d\epsilon} + \frac{U^2}{(1+\epsilon)}\right) & \left(\frac{2UW\sin\phi}{(1+\epsilon)} - \frac{VW\sin^2\phi}{(1+\epsilon)\cos\phi}\right) & 0 & \frac{U}{(1+\epsilon)} & \frac{W\sin\phi}{(1+\epsilon)\cos\phi} \\ 0 & 0 & \left(-\frac{\epsilon}{\mu}\frac{dT}{d\epsilon}\cos\phi + \frac{(U\cos\phi - V\sin\phi)^2}{(1+\epsilon)\cos\phi}\right) & 0 & 0 & \frac{(U\cos\phi - V\sin\phi)}{(1+\epsilon)\cos\phi} \end{bmatrix}.$$

$\underline{A^{-1}G}$

$$\begin{bmatrix} 0 & 0 & 0 & -1 & 0 & 0 \\ 0 & 0 & 0 & 0 & -\frac{1}{(1+\epsilon)} & 0 \\ 0 & 0 & 0 & 0 & 0 & -\frac{1}{(1+\epsilon)\cos\phi} \\ -\frac{1}{\mu} & 0 & 0 & 0 & -\frac{V}{(1+\epsilon)} & -\frac{W}{(1+\epsilon)} \\ 0 & -\frac{1}{\mu} & 0 & 0 & \frac{U}{(1+\epsilon)} & \frac{W\sin\phi}{(1+\epsilon)\cos\phi} \\ 0 & 0 & -\frac{1}{\mu} & 0 & 0 & \frac{(U\cos\phi - V\sin\phi)}{(1+\epsilon)\cos\phi} \end{bmatrix} \begin{bmatrix} H \\ G \\ I \\ 0 \\ 0 \\ 0 \end{bmatrix} = \begin{bmatrix} 0 \\ 0 \\ 0 \\ -H/\mu \\ -G/\mu \\ -I/\mu \end{bmatrix} .$$

To find the characteristics. λ , use $|A^{-1}B - \lambda I| = 0$:

$$\begin{vmatrix} 0-\lambda & V & W\cos\phi & -1 & 0 & 0 \\ 0 & -\frac{U}{(1+\epsilon)}-\lambda & -\frac{W\sin\phi}{(1+\epsilon)} & 0 & -\frac{1}{(1+\epsilon)} & 0 \\ 0 & 0 & -M-\lambda & 0 & 0 & -\frac{1}{(1+\epsilon)\cos\phi} \\ -\frac{1}{\mu}\frac{dT}{d\epsilon} & -\frac{UV}{(1+\epsilon)} & -\frac{UW\cos\phi}{(1+\epsilon)} & -\lambda & -\frac{V}{(1+\epsilon)} & -\frac{W}{(1+\epsilon)} \\ 0 & \left(-\frac{\epsilon}{\mu}\frac{dT}{d\epsilon}+\frac{V^2}{(1+\epsilon)}\right) & N & 0 & \left(\frac{U}{(1+\epsilon)}-\lambda\right) & \frac{W\sin\phi}{(1+\epsilon)\cos\phi} \\ 0 & 0 & \left(-\frac{\epsilon}{\mu}\frac{dT}{d\epsilon}\cos\phi+M(U\cos\phi-V\sin\phi)\right) & 0 & 0 & M-\lambda \end{vmatrix} = 0 ,$$

where

$$M = \frac{U\cos\phi - V\sin\phi}{(1+\epsilon)\cos\phi}$$

$$N = \frac{2UW\sin\phi}{(1+\epsilon)} - \frac{VW\sin^2\phi}{(1+\epsilon)\cos\phi} .$$

The first reduction is

$$
-\lambda \begin{bmatrix}
-\frac{U}{(1+\epsilon)}-\lambda & -\frac{W\sin\phi}{(1+\epsilon)} & 0 & -\frac{1}{(1+\epsilon)} & 0 \\
0 & -M-\lambda & 0 & 0 & -\frac{1}{(1+\epsilon)\cos\phi} \\
-\frac{UV}{(1+\epsilon)} & -\frac{UW\cos\phi}{(1+\epsilon)} & -\lambda & -\frac{V}{(1+\epsilon)} & -\frac{W}{(1+\epsilon)} \\
\left(-\frac{\epsilon}{\mu}\frac{dT}{d\epsilon}+\frac{U^2}{(1+\epsilon)}\right) & N & 0 & \left(\frac{U}{(1+\epsilon)}-\lambda\right) & \frac{W\sin\phi}{(1+\epsilon)\cos\phi} \\
0 & \left(-\frac{\epsilon}{\mu}\frac{dT}{d\epsilon}\cos\phi+M(U\cos\phi-V\sin\phi)\right) & 0 & 0 & M-\lambda
\end{bmatrix}
$$

$$
+\frac{1}{\mu}\frac{dT}{d\epsilon} \begin{bmatrix}
V & W\cos\phi & -1 & 0 & 0 \\
-\frac{U}{(1+\epsilon)}-\lambda & -\frac{W\sin\phi}{(1+\epsilon)} & 0 & -\frac{1}{(1+\epsilon)} & 0 \\
0 & -M-\lambda & 0 & 0 & -\frac{1}{(1+\epsilon)\cos\phi} \\
-\frac{\epsilon}{\mu}\frac{dT}{d\epsilon}+\frac{U^2}{(1+\epsilon)} & N & 0 & \left(\frac{U}{(1+\epsilon)}-\lambda\right) & \frac{W\sin\phi}{(1+\epsilon)\cos\phi} \\
0 & \left(-\frac{\epsilon}{\mu}\frac{dT}{d\epsilon}\cos\phi+M(U\cos\phi-V\sin\phi)\right) & 0 & 0 & M-\lambda
\end{bmatrix} = 0 .
$$

The second reduction is

$$
\lambda^2 \begin{bmatrix}
-\frac{U}{(1+\epsilon)}-\lambda & -\frac{W\sin\phi}{(1+\epsilon)} & -\frac{1}{(1+\epsilon)} & 0 \\
0 & -M-\lambda & 0 & -\frac{1}{(1+\epsilon)\cos\phi} \\
-\frac{\epsilon}{\mu}\frac{dT}{d\epsilon}+\frac{U^2}{(1+\epsilon)} & N & \frac{U}{(1+\epsilon)}-\lambda & \frac{W\sin\phi}{(1+\epsilon)\cos\phi} \\
0 & -\frac{\epsilon}{\mu}\frac{dT}{d\epsilon}\cos\phi+M(U\cos\phi-V\sin\phi) & 0 & M-\lambda
\end{bmatrix}
$$

$$
-\frac{1}{\mu}\frac{dT}{d\epsilon}\begin{bmatrix} -\frac{U}{(1+\epsilon)}-\lambda & -\frac{W\sin\phi}{(1+\epsilon)} & -\frac{1}{(1+\epsilon)} & 0 \\ 0 & -M-\lambda & 0 & -\frac{1}{(1+\epsilon)\cos\phi} \\ -\frac{\epsilon}{\mu}\frac{dT}{d\epsilon}+\frac{U^2}{(1+\epsilon)} & N & \frac{U}{(1+\epsilon)}-\lambda & \frac{W\sin\phi}{(1+\epsilon)\cos\phi} \\ 0 & -\frac{\epsilon}{\mu}\frac{dT}{d\epsilon}\cos\phi+M(V\cos\phi-V\sin\phi) & 0 & M-\lambda \end{bmatrix} = 0 \, .
$$

Note that these two matrices are the same. Since they must be nonsingular, we see that

$$
\lambda^2-\frac{1}{\mu}\frac{dT}{d\epsilon}=0 \quad ;
$$

thus,

$$
\lambda = \pm\sqrt{\frac{1}{\mu}\frac{dT}{d\epsilon}} \, .
$$

The third reduction is

$$
-\frac{1}{(1+\epsilon)}\begin{bmatrix} 0 & -M-\lambda & -\frac{1}{(1+\epsilon)\cos\phi} \\ -\frac{\epsilon}{\mu}\frac{dT}{d\epsilon}+\frac{U^2}{(1+\epsilon)} & N & \frac{W\sin\phi}{(1+\epsilon)\cos\phi} \\ 0 & -\frac{\epsilon}{\mu}\frac{dT}{d\epsilon}\cos\phi+M(V\cos\phi-V\sin\phi) & M-\lambda \end{bmatrix}
$$

$$+\left(\frac{U}{(1+\epsilon)}-\lambda\right)\begin{bmatrix} -\frac{U}{(1+\epsilon)}-\lambda & -\frac{W\sin\phi}{(1+\epsilon)} & 0 \\ 0 & -M-\lambda & -\frac{1}{(1+\epsilon)\cos\phi} \\ 0 & -\frac{\epsilon}{\mu}\frac{dT}{d\epsilon}\cos\phi+M(U\cos\phi-V\sin\phi) & M-\lambda \end{bmatrix}=0 .$$

The fourth reduction is

$$-\frac{1}{(1+\epsilon)}\left(\frac{\epsilon}{\mu}\frac{dT}{d\epsilon}-\frac{U^2}{(1+\epsilon)}\right)\begin{bmatrix} -M-\lambda & -\frac{1}{(1+\epsilon)\cos\phi} \\ -\frac{\epsilon}{\mu}\frac{dT}{d\epsilon}\cos\phi+M(U\cos\phi-V\sin\phi) & M-\lambda \end{bmatrix}$$

$$+\left(\frac{U}{(1+\epsilon)}-\lambda\right)\left(-\frac{U}{(1+\epsilon)}-\lambda\right)\begin{bmatrix} -M-\lambda & -\frac{1}{(1+\epsilon)\cos\phi} \\ -\frac{\epsilon}{\mu}\frac{dT}{d\epsilon}\cos\phi+M(U\cos\phi-V\sin\phi) & M-\lambda \end{bmatrix}=0 .$$

Again. the matrices are the same; since they must be nonsingular, we see that

$$-\frac{1}{(1+\epsilon)}\left(\frac{\epsilon}{\mu}\frac{dT}{d\epsilon}-\frac{U^2}{(1+\epsilon)}\right)+\left(\frac{U}{(1+\epsilon)}-\lambda\right)\left(-\frac{U}{(1+\epsilon)}-\lambda\right)=0 ,$$

or

$$\lambda=\pm\sqrt{\frac{1}{\mu}\frac{\epsilon}{(1+\epsilon)}\frac{dT}{d\epsilon}} .$$

The fifth reduction is

$$(-M-\lambda)(M-\lambda)-\left(\frac{\epsilon}{\mu}\frac{dT}{d\epsilon}\cos\phi+M(U\cos\phi-V\sin\phi)\right)\left(\frac{-1}{(1+\epsilon)\cos\phi}\right)=0 ,$$

or

$$\lambda = \pm\sqrt{\frac{1}{\mu}\frac{\epsilon}{(1+\epsilon)}\frac{dT}{d\epsilon}} .$$

Summarizing, the six characteristics are

$$\lambda_1 = +\sqrt{\frac{1}{\mu(S_0)}\frac{dT}{d\epsilon}}$$

$$\lambda_2 = -\sqrt{\frac{1}{\mu(S_0)}\frac{dT}{d\epsilon}}$$

$$\lambda_3 = +\sqrt{\frac{1}{\mu(S_0)}\frac{\epsilon}{(1+\epsilon)}\frac{dT}{d\epsilon}}$$

$$\lambda_4 = -\sqrt{\frac{1}{\mu(S_0)}\frac{\epsilon}{(1+\epsilon)}\frac{dT}{d\epsilon}}$$

$$\lambda_5 = +\sqrt{\frac{1}{\mu(S_0)}\frac{\epsilon}{(1+\epsilon)}\frac{dT}{d\epsilon}}$$

$$\lambda_6 = -\sqrt{\frac{1}{\mu(S_0)}\frac{\epsilon}{(1+\epsilon)}\frac{dT}{d\epsilon}} .$$

Appendix D

COMPUTED INPUT DATA FOR THE SIMULATIONS

This appendix provides computed input data for the following:

1. Steady-state configurations of the 8-ft torroidal buoy and current meter array at Block Island Sound station BRAVO.

2. Steady-state configurations of the 8-ft torroidal buoy and cable used for WHOI Mooring No. 279.

3. Dynamics of the $3\frac{1}{2}$-ft spherical buoy and cable at station DELTA off New Harbor, Block Island.

4. Dynamics of the 8-ft torroidal buoy and cable at station BRAVO in Block Island Sound.

5. Dynamics of the 8-ft torroidal buoy and cable used for WHOI Mooring No. 238.

Inputs for the Simulation of Steady-State Configurations of the 8-ft Torroid and Current Meter Array at BRAVO

The components used in the buoy system are shown in figure 21 and are described in chapter IV of the main text. The input data are as follows:

1.	Buoy diameter BD1	8.0 ft
2.	Torroid section diameter BD2	2.5 ft
3.	Buoy weight WB	1200.0 lb
4.	Maximum hull draft HM	2.5 ft

5. Free draft (when displacement equals buoy weight) HFREE — 0.7 ft

6. Buoy windage WAREA — 1[illegible].84 ft^2

7. Wind drag coefficient WCD — 0.971

8. Cable diameter DIA:

   Upper line - 5/8-in. polypropylene — 0.625 in.

   Lower line - 3/8-in. wire rope — 0.375 in.

9. Cable weight in water per unit length WTC:

   Upper line - — -0.02 lb/ft

   Lower line - — 0.2 lb/ft

10. Cable modulus of elasticity EC:

    Upper line - — 1.67×10^5 lb/in.^{2}

    Lower line - — 1.20×10^7 lb/in.^{2}

11. Mooring line length SM — 235.0 ft

12. Current speeds at three depths: CUR1, CUR2, and CUR3 — 1.0 to 1.77 knots

13. Current directions at three depths: DIR 1, DIR 2, and DIR 3 — 0-360 deg

14. Water depth DEEP — 120.0 ft

15. Wind speed y component — 0.0 ft/sec

16. Wind speed x component — 0.0 ft/sec.

The cable properties DIA, WTC, and EC are changed at a cable length of 230.0 ft from the values for the 5/8-in. polypropylene to the values for 3/8-in.

wire rope. Changes in tension and angles across the current meters were found by inserting the following procedures in the program:

1. Use and IF statement to locate the current meters along the mooring line.

2. Use the computed tension and angles to compute the force components acting on the top of the current meter.

3. Solve the statics equations for the current meter by using the current meter in-water weight and computed drag force components to find the force components acting on the bottom of the current meter.

4. Compute the current meter tilt angle.

5. Transform back to cable coordinates to find the new cable tension and angles.

6. Increase the cable length by 3 ft, i.e., the length of the current meter.

7. Continue integration down the cable.

The following data were required to accomplish the above:

Current meter weight in water WCM	67 lb
Current meter drag coefficient CDCM	0.59
Current meter frontal area ARCM	2.285 ft^2.

Current strengths and directions as functions of depth were computed as follows:

1. Average strengths and directions from current meters 1 and 2.

2. For depths of 0 to 70 ft, set the upper layer strength and direction equal to these values.

3. Test current meter 3 strength against mean strength of meters 1 and 2. If greater, set the lower layer current equal to the mean strength in the upper layer.

4. Current strength and direction in the lower layer (70 to 120 ft) set equal to current meter 3 strength and direction.

Integration step size (B) was set equal to 1.0 ft, and the limiting depth error bandwidth DDP was set equal to 1 ft.

Inputs for the Simulation of Steady-State Configurations of the 8-ft Torroid and Cable Used for WHOI Mooring No. 279

The components used in this mooring are shown in figure 27 and are described in chapter IV of the main text. Buoy dimensions are the same but the buoy weight is increased to account for the instruments in the buoy, the chain bridle, and instruments directly beneath the buoy. The input data are listed as follows:

1. Buoy diameter BD1	8.0 ft
2. Torroid section diameter BD2	2.5 ft
3. Buoy weight WB	2100.0 lb
4. Maximum hull draft HM	2.5 ft
5. Free draft HFREE	1.04 ft
6. Buoy windage WAREA	19.84 ft^2
7. Buoy wind drag coefficient	0.971
8. Cable diameter DIA:	
Upper cable - 1/4-in. GAC	0.25 in.

Lower cable - 5/8-in. plaited nylon 0.625 in.

9. Cable weight in sea water per unit length WTC:

Upper cable -	0.090 lb/ft
Lower cable -	0.0105 lb/ft

10. Cable modulus of elasticity EC:

Upper cable -	1.682×10^{7} lb/in.^{2}	
Lower cable -	3.52×10^{5} lb/in.^{2}	$0 < T < 1000$ lb
	6.79×10^{5} lb/in.^{2}	1000 lb $< T <$ 2000 lb
	1.041×10^{6} lb/in.^{2}	2000 lb $< T$

11. Mooring line length SM 8000.0 ft

12. Surface current CUR 0-1.46 knots

13. Water depth DEEP 8800.0 ft

14. Wind speed y component 0.0 ft/sec

15. Wind speed z component 0.0 ft/sec.

Cable properties were changed at a length of 4800 ft from the buoy and the changes in tension and angles were computed across the instruments in the line as before. The input data for the current meter and tensiometers are listed as follows:

Current meter:

Weight in water	120.0 lb
Drag coefficient	1.4
Frontal area	2.92 ft^{2}

Tensiometer:

Weight in water	50.0 lb
Drag coefficient	1.4
Frontal area	0.875 ft^2 .

The drag force acting on the buoy was increased to account for the chain bridle and the instruments directly below the buoy. An effective area-drag coefficient product of 22.18 ft^2 was added to the area-drag coefficient product of the buoy to account for the instruments and chains.

Inputs for the Simulation of Buoy System For the Spherical Buoy

The spherical buoy dimensions were measured and the buoy and its instrumentation were weighed. The center of gravity and mass moments of inertia were calculated from the known weights and dimensions. The cable and chain were weighed in air and the mass and weight in sea water of each were computed. Mean wind wave heights and periods and the frequencies, amplitudes, and phases were computed on the GSA computer by using program RWAVE (see subroutine RWAVE in appendix A) for a given wind speed, a 10-hr duration, and a 15-mile fetch. Input data are listed as follows:

1. Buoy hull radius BR	1.75 ft
2. Center of gravity height XML	0.208 ft
3. Mooring line connection height XML	0.208 ft
4. Buoy weight WB	440.0 lb
5. Buoy mass MB	13.66 lb-sec^2/ft
6. Yaw mass moment of inertia ALIN	11.967 lb-sec^2/ft

7.	Pitch mass moment of inertia BTIN	17.46 lb-sec^2/ft
8.	Roll mass moment of inertia GMIN	19.875 lb-sec^2/ft
9.	Wind drag coefficient WCD	0.5
10.	Windage (profile area) WAREA	5.435 ft^2
11.	Wind lift coefficient WCL	0.25
12.	Plan area WAREL	4.81 ft^2
13.	Wind center of pressure height	1.068 ft
14.	Mean wave height WHTM	0.5 to 4.05 ft
15.	Mean wave period PER	2.2 to 6.0 sec
16.	Unstretched cable lengths CLO(I)	18.75 ft
		18.75 ft
		18.75 ft
		18.75 ft
		12.5 ft
		12.5 ft
17.	Upper cable diameter DIA1	0.0416 ft
18.	Upper cable weight in sea water DWC1	0.35 lb/ft
19.	Upper cable mass per unit length DCSM1	0.0124 lb-sec^2/ft^2
20.	Lower cable diameter DIA2	0.125 ft
21.	Lower cable weight in sea water DWC2	7.3 lb/ft
22.	Lower cable mass per unit length DCSM2	0.233 lb-sec^2/ft^2
23.	Surface current y component CYS	0.0 ft/sec
24.	Surface current z component CZS	0.845 ft/sec
25.	Wind y component	-30.0 ft/sec

26.	Wind z component		-8.0 ft/sec
27.	Initial buoy displacements	y(2)	-0.21 ft
		y(4)	-41.1 ft
		y(6)	62.35 ft
28.	Initial cable element displacements	y(I)	15.04 ft
			27.54 ft
			38.76 ft
			49.46 ft
			55.95 ft
			62.00 ft
		y(I + 2)	-29.79 ft
			-20.54 ft
			-13.06 ft
			-6.86 ft
			-3.31 ft
			0.00 ft
		y(I + 4)	55.86 ft
			46.06 ft
			34.47 ft
			20.48 ft
			10.43 ft
			0.00 ft.

The highest natural frequency of the system was estimated by using the method described in appendix A, and a time step size (δ) of 5×10^{-4} sec was used. The currents were uniform over the 62-ft water depth. A 30-lb force was added to the vertical cable force component acting on the buoy to account for the instrument package just below the buoy.

Inputs for the Simulation of Buoy System Dynamics for Torroidal Buoy BRAVO

Again, buoy dimensions and weights were measured or taken from the manufacturers' drawings, and the properties of the buoy were calculated. The chain bridle below the buoy was assumed to be rigid, and its mass and drag were included in the computations. In this case, each cable element weight, mass, and drag were listed directly in the program since the mooring line was composed of many elements (cable chains, current meter, sentinel, etc.). Input data are listed as follows:

1.	Buoy hull radius RR	4.0 ft
2.	Center of gravity height XCG	13.064 ft
3.	Mooring line connection height XML	11.782 ft
4.	Buoy weight WB	2100.0 lb
5.	Buoy mass MB	65.25 lb
6.	Yaw mass moment of inertia ALIN	283.44 lb-sec^2/ft
7.	Pitch mass moment of inertia BTIN	445.12 lb-sec^2/ft
8.	Roll mass moment of inertia GMIN	445.12 lb-sec^2/ft
9.	Wind drag coefficient	0.971
10.	Wind lift coefficient	0.25
11.	Windage (profile area)	19.84 ft^2
12.	Plan area	50.3 ft^2

13.	Wind center of pressure height		6.19 ft
14.	Wind speed causing the waves		
	(11 June 1970)		16.9 ft/sec
15.	Wind duration		
16.	Surface current y component		
	(11 June 1970)		-0.21 ft/sec
17.	Surface current z component		
	(11 June 1970)		-0.597 ft/sec
18.	Wind y component		0.0 ft/sec
19.	Wind z component		
	(11 June 1970)		-16.9 ft/sec
20.	Initial buoy displacements	y(2)	-0.25 ft
		y(4)	-0.7 ft
		y(6)	208.6 ft
21.	Initial cable element displacements	y(I)	64.18 ft
			110.45 ft
			120.91 ft
			120.9 ft
		y(I + 2)	-0.8358 ft
			-0.7416 ft
			-0.6817 ft
			0.0 ft
		y(I + 4)	200.84 ft
			193.35 ft

144.95 ft

0.0 ft.

In this case, the time step size was taken to be 5×10^{-3} sec. Because of the chain bridle, the hydrodynamic force moment arm was computed to be 4.16 ft below the center of gravity. The surge and sway area-drag coefficient products include the effects of the steel bracing and chain bridle under the buoy.

Inputs for the Simulation of Buoy System Dynamics for the Torroidal Buoy and Cables Used in WHOI Mooring No. 238

Buoy dimensions, weights, masses, etc. are the same as those for the torroidal buoy at station BRAVO. The wind fetch length in subroutine RWAVE was changed to 100 miles to better simulate deep-sea wind wave conditions. Cable dynamics were simulated with subroutine MOOR, and the six dependent cable properties (tension, two angles, and three velocity components) were calculated at 20 points along the cable. Total unstretched mooring line length was 8000 ft: 4800 ft of 1/4-in. galvanized steel aircraft cable (polyolefin jacketed to 3/8-in. diameter) and 3200 ft of 5/8-in. plaited nylon.

The upper cable properties are listed as follows:

1.	Diameter	0.0312 ft
2.	Weight per unit length in sea water	0.125 lb/ft
3.	Mass per unit length	0.0054 lb-sec^2/ft^2
4.	Characteristic velocity	11,300.0 ft/sec
5.	Elastic modulus-cross section product	6.87×10^5 lb

The lower cable properties are listed as follows:

1.	Diameter	0.052 ft
2.	Weight per unit length in sea water	0.0105 lb/ft
3.	Mass per unit length	0.00455 lb-sec^2/ft
4.	Characteristic velocity	2600.0 ft/sec
5.	Elnetic modulus-cross section product	3.06 x 10^4 lb.

Cable properties were changed from wire rope to nylon rope at 4800 ft (I = 14). The Webster current profile was used to compute steady drag forces on the cable. Numerical stability was maintained by using a time step (d) of 0.02 sec. The H/K quotient is equal to 20,000 ft/sec, which is larger than the tensile wave speed in the upper cable (11,300 ft/sec). Initial strains and cable angles were computed with the steady-state, buoy system configuration program with the same current profile and a surface current of 1.5 knots. Winds of 10, 20, and 30 knots were used. and the computed steady-state strains and cable angles served as input (initial conditions) ´ e dynamics model.

Appendix E

BUOYANT FORCES AND MOMENTS FOR A TORROIDAL BUOY

In order to simulate the dynamics of the torroidal buoy, a method to compute the buoyant force and righting moment for a given buoy draft and tilt angle was developed. This computation was included in the program as subroutine TORBU, and it updated the buoyant force and moment for each integration time step.

Consider a torroid with major radius R and minor radius r, partially immersed in a fluid with a mean draft H and a tilt angle θ (figure E-1. The area of an immersed circular segment with draft H_s is given by

$$A_s = \frac{1}{2} r^2 (\alpha - \sin\alpha) , \tag{E-1}$$

where

$$\alpha = 2 \tan^{-1} \sqrt{\frac{r^2}{(r - H_s)^2} - 1} .$$

If $H_s > r$, we can redefine the draft

$$H_s' = 2r - H_s , \tag{E-2}$$

and

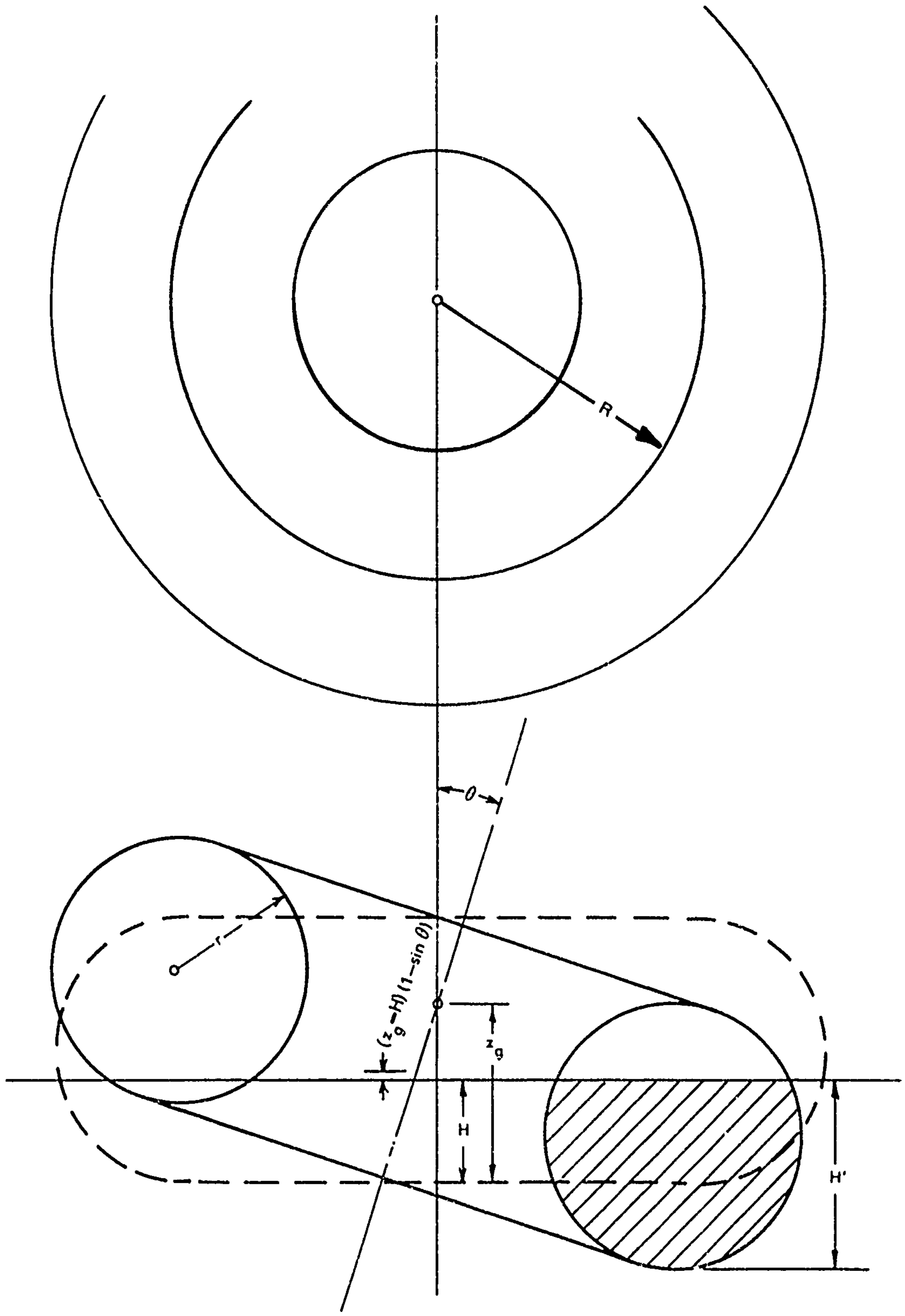

Figure E-1. Torroid Section

$$\alpha' = 2\ \mathrm{TAN}^{-1}\sqrt{\frac{r^2}{(r-H_s')^2} - 1}\ .$$

Thus, the area becomes

$$A_s = \pi r^2 - \frac{1}{2} r^2(\alpha' - \mathrm{SIN}\,\alpha') \tag{E-3}$$

Define the section draft, H_s, as a function of ϕ, the radial angle about the torroid axis. The maximum draft in the direction of the tilt angle θ $(\phi = \pi/2)$ is

$$H_{S_{MAX}} = H + R\,\mathrm{SIN}\,\theta\ ,$$

and the minimum draft is

$$H_{S_{MIN}} = H - R\,\mathrm{SIN}\,\theta\ .$$

For any angle ϕ around the torroid,

$$H_S = H + R\,\mathrm{SIN}\,\phi\,\mathrm{SIN}\,\theta + (Z_G - H)(1 - \mathrm{SIN}\,\theta)\ . \tag{E-4}$$

The last term represents the small change in the mean draft H due to the fact that the tilt is about the center of gravity and not about the waterplane center.

By using the draft for any section as defined above, we can compute the immersed area of any section from equation (E-1) or (E-3). The immersed volume is found by integrating around the torroid,

$$V = 2 \cdot \int_{-\pi/2}^{\pi/2} A_S\, R\, d\phi\ , \tag{E-5}$$

and the buoyant force

$$B = 2 \cdot \gamma \cdot R \int_{-\pi/2}^{\pi/2} A_s \, d\phi \, , \tag{E-6}$$

where γ is the weight density of the fluid. The centroid of the submerged volume V is computed in order to find the righting moment:

$$\bar{X} = \frac{2 \cdot \int_{-\pi/2}^{\pi/2} R \sin\phi \, A_s \, R \, d\phi}{2 \int_{-\pi/2}^{\pi/2} A_s \, R \, d\phi} \, . \tag{E-7}$$

The righting arm is

$$X_{RA} = \bar{X} \cos\theta - (z_G - H) \sin\theta \, , \tag{E-8}$$

and the righting moment is

$$M = X_{RA} \cdot B \, . \tag{E-9}$$

The above equations were programmed for subroutine TORBU, and the differential volumes were summed in 2-deg steps around the torroid. Buoy draft and tilt angle are the inputs, and the heave buoyant force, tilt righting moment, cross-coupled tilt-heave buoyant force, and cross-coupled heave-tilt righting moment are the outputs. Plots of the displacement, righting moment, and the cross-coupled force and moment for the Richardson torroid used at station BRAVO are shown in figures (E-2) through (E-5).

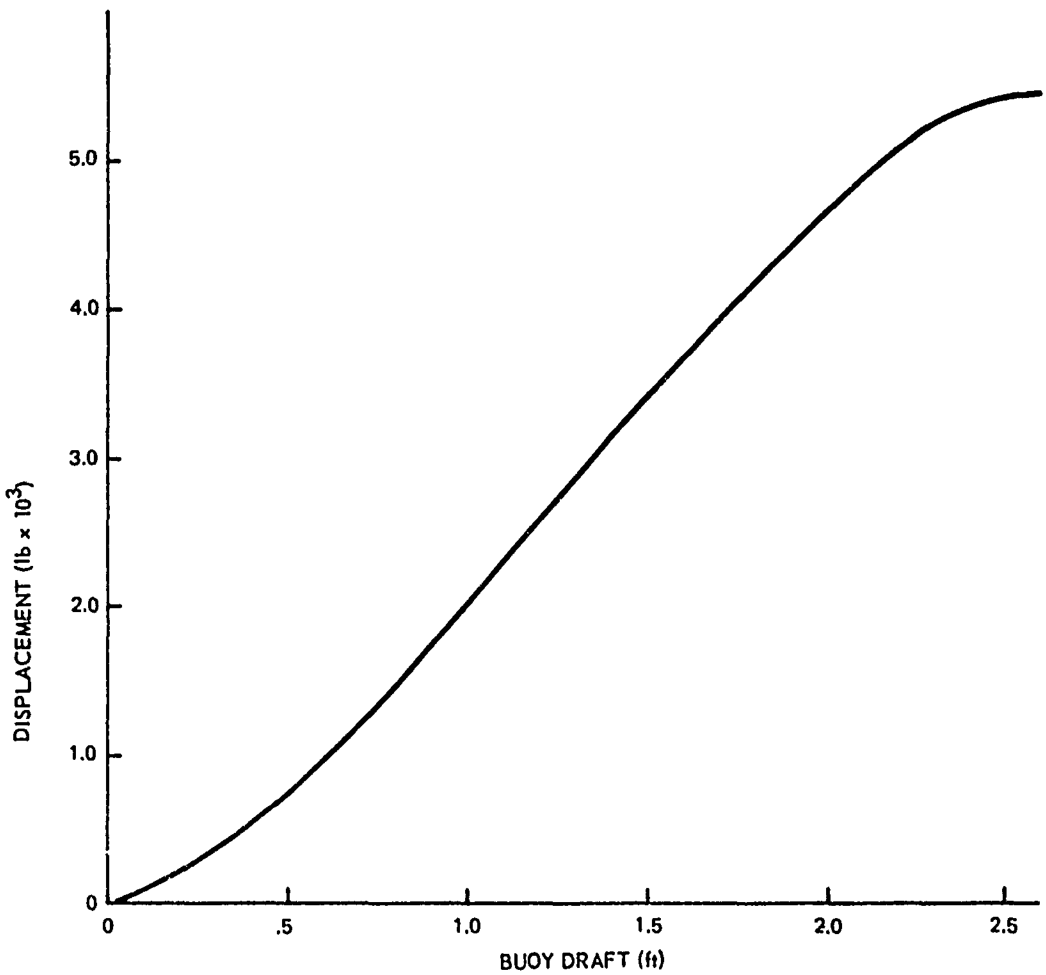

Figure E-2. Torroid (8-ft) Displacement versus Draft

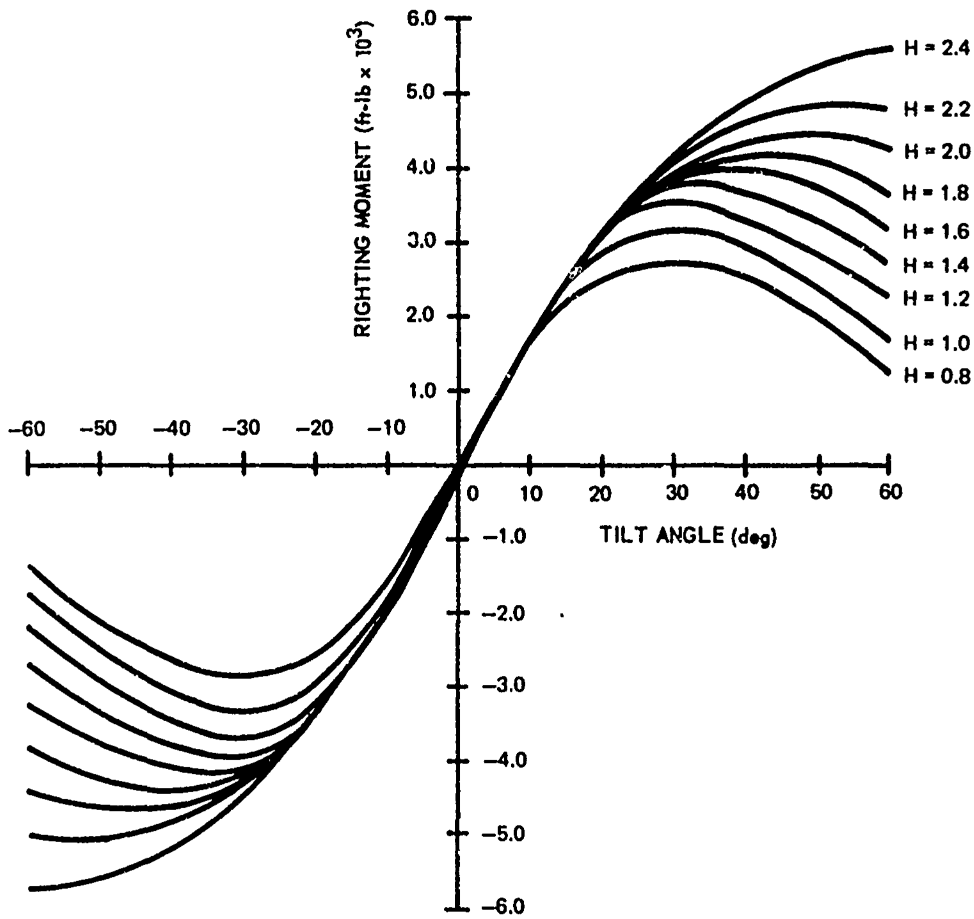

Figure E-3. Torroid (8-ft) Righting Moment versus Tilt Angle

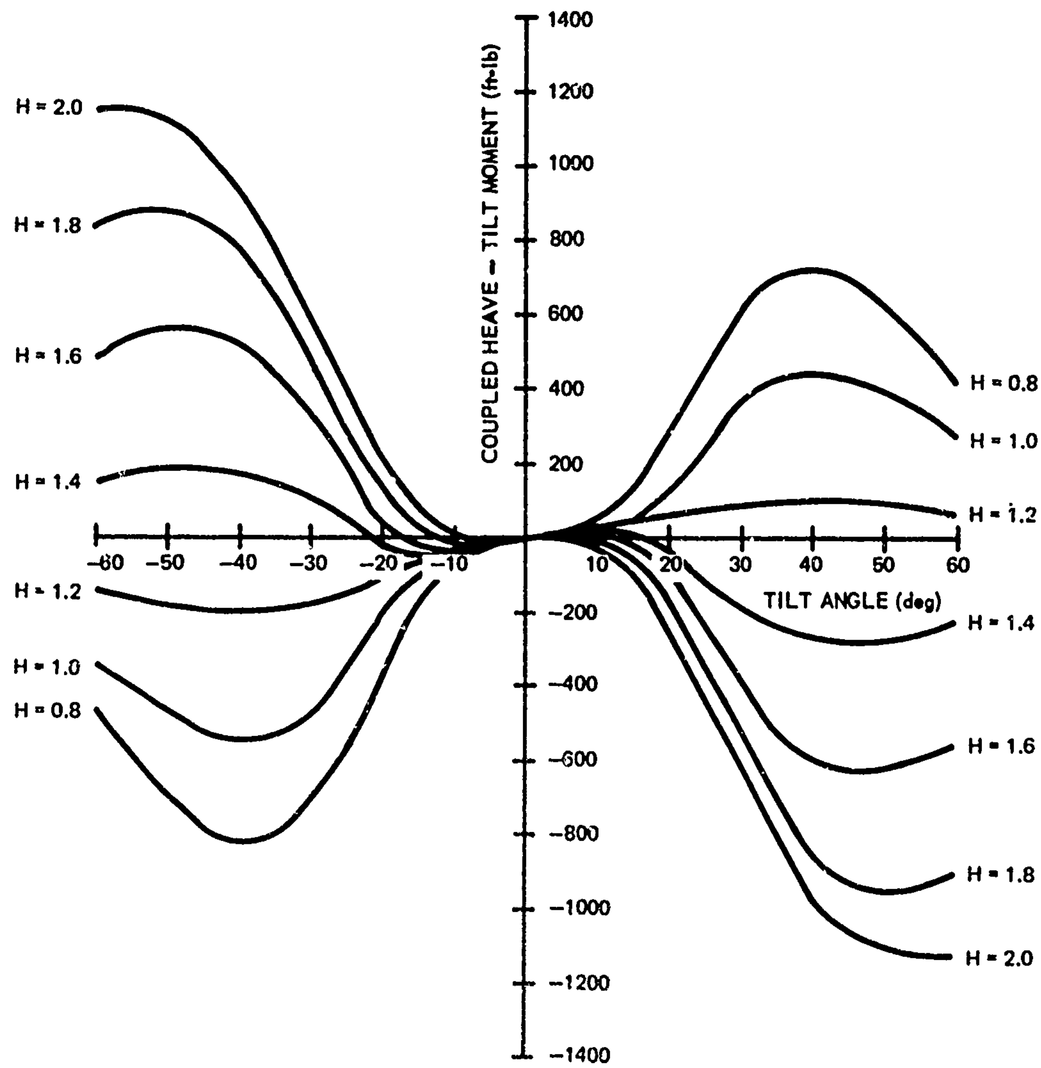

Figure E-4. Torroid (8-ft) Coupled Moment versus Tilt Angle

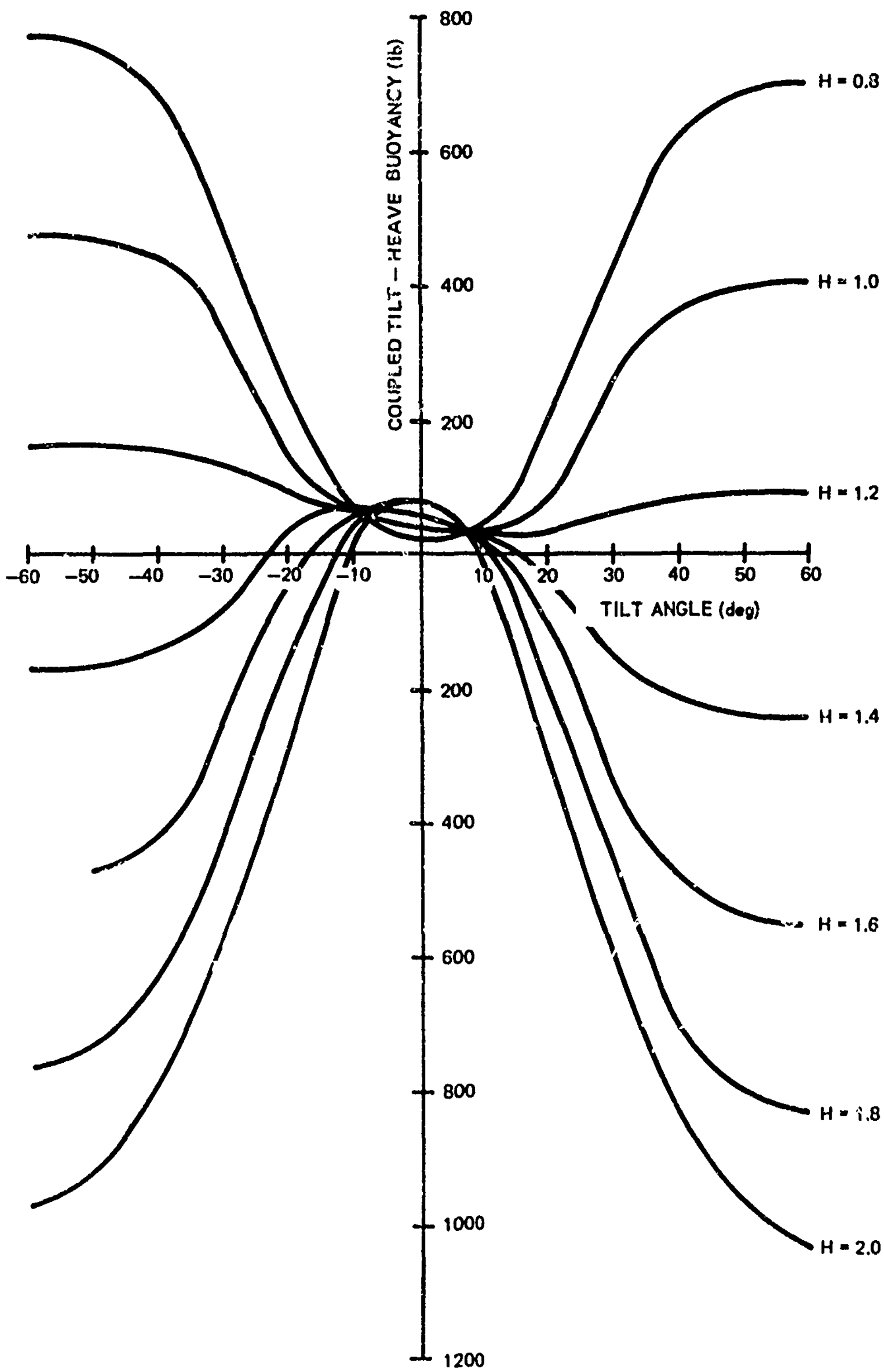

Figure E-5. Torroid (8-ft) Coupled Buoyancy versus Tilt Angle